REDUCED INDENYL AND CYCLOPENTADIENYL GROUP 4 COMPLEXES: FUNDAMENTAL REACTIVITY STUDIES AND DINITROGEN ACTIVATION

A Dissertation

Presented to the Faculty of the Graduate School

of Cornell University

In Partial Fulfillment of the Requirements for the Degree of

Doctor of Philosophy

by

Doris Pun

February 2010

REDUCED INDENYL AND CYCLOPENTADIENYL GROUP 4 COMPLEXES: FUNDAMENTAL REACTIVITY STUDIES AND DINITROGEN ACTIVATION

Doris Pun, Ph. D.

Cornell University 2010

Indenyl zirconocene dinitrogen complexes were synthesized from the direct activation of N_2 by isolable cyclopentadienyl η^9 indenyl zirconocene sandwich complexes, $(\eta^5\text{-}C_5Me_5)(\eta^9\text{-}C_9H_5\text{-}1\text{-}R\text{-}3\text{-}Me)Zr$ (R = Me, $CHMe_2$, CMe_3), or from the alkali metal reduction of the corresponding zirconocene dihalide under dinitrogen. In the former, dimeric weakly activated end-on dinitrogen complexes with η^5,η^2 indenyl ligands, $[(\eta^5\text{-}C_5Me_5)Zr]_2\,[\mu_2\text{-}\eta^2,\eta^2\text{-}\{4,5\text{-}(\eta^5\text{-}C_9H_5\text{-}1\text{-}R\text{-}3\text{-}Me)\}_2](\mu_2\text{-}\eta^1,\eta^1\text{-}N_2)$, were synthesized. In the latter, dimeric modestly activated side-on, end-on dinitrogen complexes with an η^5,η^4 indenyl ligand, $[(\eta^5\text{-}C_5Me_5)Zr]_2\,[\mu_2\text{-}\eta^5,\eta^4\text{-}(\eta^5\text{-}C_9H_5\text{-}1\text{-}R\text{-}3\text{-}Me)](\mu_2\text{-}\eta^2,\eta^1\text{-}N_2)\,(\mu_2\text{-}\eta^1,\eta^1\text{-}Cl)$, were isolated. The alkali metal reduction of a series of bis(indenyl) zirconocene dihalides under N_2 furnished dimeric strongly activated end-on dinitrogen dianions, $[(\eta^5\text{-}C_9H_5\text{-}1\text{-}CHMe_2\text{-}3\text{-}Me)(\eta^5\text{-}C_9H_5\text{-}1\text{-}CHMe_2\text{-}3\text{-}Me)Zr(NaX)]_2(\mu_2\text{-}\eta^1,\eta^1\text{-}N_2)$ (X = Cl, Br, I), which readily hydrogenate yielding the corresponding zirconocene hydrazido hydride complexes with a side-on bound hydrazide, $[(\eta^5\text{-}C_9H_5\text{-}1\text{-}CHMe_2\text{-}3\text{-}Me)(\eta^5\text{-}C_9H_5\text{-}1\text{-}CHMe_2\text{-}3\text{-}Me)ZrH]_2(\mu_2\text{-}\eta^2,\eta^2\text{-}N_2H_2)$. Due to the propensity of hafnium to attain its highest oxidation state, dinitrogen activation chemistry was not observed for indenyl hafnocene complexes, although several η^6,η^5 bis(indenyl)hafnium (II), along with hafnocene (III) species were isolated. The reduction of a series of *ansa*-zirconocene complexes with $[CH_2CH_2]$, $[Me_2Si]$ and $[Me_2C]$ bridges was also explored. Zirconocene diiodide compounds with $Me_2E(\eta^5\text{-}C_5H_3\text{-}3\text{-}R')_2$ (E = Si, R' = CMe_3; E = C, R' = $SiMe_3$, CMe_3)

ligands furnished strongly activated side-on bound dinitrogen complexes when treated with excess 0.5 % sodium amalgam under an atmosphere of N_2. Exposure of dihydrogen furnished the expected zirconocene hydrazido hydride complexes. However, the hydrazide readily underwent dehydrogenation, even under one atmosphere of H_2, affording hydrido zirconocene dinitrogen complexes $Me_2E(\eta^5\text{-}C_5H_3\text{-}3\text{-}R')_2ZrH]_2(\mu_2\text{-}\eta^2,\eta^2\text{-}N_2)$.

In the course of developing zirconium-promoted Pauson-Khand chemistry, the addition of ketones to η^9 indenyl zirconocene complexes showed divergent product formation: either yielding a zirconocene enolate hydride or insertion of the carbonyl into the indenyl ligand. In the former, a haptotropic rearrangement of the indenyl ligand from η^9 coordination to η^5 occurred, while in the latter rearrangement to η^1, η^3, η^5 or η^6. Mechanistic studies demonstrated that pK_a, steric bulk and concentration of the ketone reagent are important to the reactivity.

BIOGRAPHICAL SKETCH

Doris (Sau-Wah) Pun was born December 20, 1983 in New York, New York. She graduated from Brooklyn Technical High School majoring in Chemistry before attending New York University, where she also majored in Chemistry, double minoring in Computer Science and Computer Applications. During her undergraduate studies, she used Resonance Raman spectroscopy to study both the DNA repair enzyme DNA photolyase and the FAD containing glucose oxidase under the supervision of Professor Johannes Schelvis. In 2005, she started graduate school at Cornell University and joined the Chirik group, where she has worked on dinitrogen activation with indenyl and *ansa*-linked cyclopentadienyl group 4 complexes, following the work of both Chris and Tammy Bradley.

Wai Ming Lau & Chun Tim Pun

Julia S. Pun

Scott M. Gruenbaum

ACKNOWLEDGMENTS

I am truly indebted to my advisor, Paul Chirik, for taking a chance on me by allowing me to join his group and guiding me throughout my years at graduate school. Before joining his group, I had little experience with synthetic chemistry and lacked the ability to critically analyze my data. Thank you for not letting me stray when I needed guidance, in the laboratory and intellectually. To my committee members, Pete Wolczanski and Geoff Coates, and Dave Collum, thanks for lending your expertise and insightful criticisms. I believe I have matured as a professional scientist.

Both Chris and Tammy initiated my research projects, figuring out a lot of the difficult chemistry. I also have to thank them both, along with Marco, for training me to do air sensitive organometallic chemistry, allowing me to synthesize their truly unique complexes. To the other members of the Group 4 Dinitrogen Fixation project, Wes, Hannah, Don, David and Scott L., thank you for the insightful conversions. Don, your generous collaboration in synthesizing the Dp and Gp ligands have been especially appreciated. Thank you Mandy and Ryan for being there with me these past years when we were the oldest. Looking back it was scary, especially regenerating the hydrogen column and the Toepler pump (thank you Elliott for your assistance there). My fellow box mates, Ryan, Aaron, Jon, Marco, Scott and Chantal, I appreciate all the help with maintaining our box. I still remember having to overhaul our box vacuum pump and changing our catalyst. Thank you Jon and Aaron for help setting up our laboratory in G54. I am indebted to Kevin for synthesizing some of the 1,6 diene substrates. I also thank the rest of the members of the Chirik group, past and present – Suzanne, Sarah, Helen, Brad, Ignacio, Crisita, Andrew, etc. – for all the support, laughter, candy and cookies. Thank you to everyone who edited my dissertation.

I also need to especially thank both the Wolczanski and Collum groups for chemicals, air sensitive handling techniques and kinetic data collection, especially Emily, Elliott, Brenda and Alex. Emily and Nina were also wonderful roommates and friends.

This dissertation would also not be possible without the help of Emil for solving all my crystal structures, several of which were key to characterizing the compounds. Ivan has been especially helpful in teaching me to solve my indenyl zirconium complexes by a combination of 1D and 2D NMR spectroscopy. Thank you Dave Wise for being an excellent glass blower and helping us with our new labs and teaching us about glass maintenance.

Finally, this thesis is dedicated to my parents, my sister and Scott for all their support over the last four and a half years. Without my parents I would not have made it this far, academically, nor would I have been short on rice. To my sister, I thank her for being my guiding light, for helping to make myself better in order to reach her standards and for hauling rice to me from home. Scott has made my transition to graduate school, away from my family for the first time, a lot smoother. Thank you for carrying the rice.

TABLE OF CONTENTS

Biographical Sketch	iii
Dedication	iv
Acknowledgements	v
Table of Contents	vii
List of Figures	x
List of Tables	xiv

Chapter 1: Activation of Dinitrogen with Indenyl Zirconium Complexes: Different Modes of N_2 and Indenyl Coordination

Abstract	1
Introduction	2
Results and Discussion	7
Conclusions	40
Experimental	40
References	70

Chapter 2: Synthesis and Reactivity of Reduced Bis(Indenyl) Hafnium Compounds

Abstract	75
Introduction	75
Results and Discussion	78
Conclusions	101

Experimental 102

References 120

Chapter 3: C-C Bond Formation with η^9 Indenyl Zirconium Sandwiches: Cycloaddition of Dienes and Insertion of Ketones

Abstract 124

Introduction 125

Results and Discussion 127

Conclusions 158

Experimental 159

References 194

Chapter 4: Fundamental Studies of Dinitrogen Activation and Reduction with *ansa*-Zirconocene Complexes

Abstract 198

Introduction 199

Results and Discussion 202

Conclusions 220

Experimental 221

References 238

Chapter 5: Catalytic Dehydrogenation of Substituted Amine-Boranes with Isolable Titanocene and Zirconocene Sandwich and Titanocene Dinitrogen Complexes

Abstract	242
Introduction	242
Results and Discussion	244
Conclusions	253
Experimental	254
References	259
Appendix A: EPR Data	262
Appendix B: Kinetic Data	264
Appendix C: Crystal Structure Data	265
Appendix D: Permissions for Figure Reproduction	350

LIST OF FIGURES

1.1. Modes of dinitrogen coordination. 2

1.2. Reactivity similarity and differences between a weakly and a strongly activated zirconocene dinitrogen complexes. 3

1.3. Preparation of η^9, η^5 bis(indenyl) zirconocene sandwich complexes via reductive elimination (top left) or alkali metal reduction (top right). η^9, η^5 to η^5, η^9 ring interconversion via an η^5, η^5 intermediate (bottom). 4

1.4. Proposed catalytic cycle for the hydrogenation of dinitrogen with bis(indenyl) zirconium compounds. 5

1.5. Examples of N_2 activation from (left) isolable reduced complexes and (right) the reductive elimination of metal hydride precursors. 7

1.6. The Cp* indenyl zirconocene dihalides reduced in this study. 8

1.7. Isolable Cp* indenyl zirconocene sandwiches prepared. 8

1.8. Molecular structure for **8** at 30 % probability elipsoids. Hydrogen atoms omitted for clarity. 10

1.9. Molecular structure of $\mathbf{6_2N_2}$ at 30 % probability ellipsoids top view (top), side view (bottom). 13

1.10. Possible resonance structures for $\mathbf{3_2}$-$\mathbf{N_2}$, $\mathbf{6_2}$-$\mathbf{N_2}$ or $\mathbf{7_2}$-$\mathbf{N_2}$. 14

1.11. NOESY NMR spectrum of 6_2-N_2 in benzene-d_6. 16

1.12. Molecular structures of the major (left) and minor (right) isomers of **16-N_2Cl** at 30 % probability ellipsoids. 19

1.13. Possible resonance structures for **16-N_2Cl** and **17-N_2Cl**. 20

1.14. Possible mechanism for the formation of **6-THI-(H)I** from the reduction of **6-THI-I_2**. 22

1.15. Bis(indenyl) zirconocene dihalides reduced in this study. 23

1.16. Isolable bis(indenyl) zirconocene sandwich complexes prepared. 24

1.17. Molecular structure of ***meso*-13** with 30 % probability elipsoids. 25

1.18. Molecular structures of **[13-NaCl]$_2$$N_2$** (top) and **[13-NaI]$_2$$N_2$** (bottom) at 30 % probability elipsoids. Hydrogen atoms removed for clarity. 28

1.19. Different possible isomers of **[13-H]$_2$(N_2H_2)**. 32

1.20. ^{1}H, ^{15}N HSQC (top) and ^{1}H, ^{15}N HMBC (bottom) NMR spectra of the hydrogenation products of **[13-NaX]$_2$$N_2$**. The top spectrum depicts ten different isomers. 33

1.21. Molecular structures of dianion (top) and cation x 2 (bottom) for **[13-Cl]$_2$(N_2)(Na){Na(crown-ether)}$_{1.5}$**. 37

1.22. Categorizing of indenyl ligands that only formed stable sandwiches, activated N_2 or none of the above. 38

2.1. Formation of unique η^9, η^5 (center) and η^6, η^5 bis(indenyl) zirconocene sandwich complexes. 77

2.2. The indenyl hafnocene dihalides reduced in this study. 78

2.3. The bottom row consists of the hafnocene dicarbonyls prepared for this study. (The top row is included to designate some Zr shorthand naming.) 81

2.4. Respresentation of the two molecules of **5-THF** with the side views on the left and the top views on the right at 30 % probability elipsoids. 84

2.5. Depiction of **5-THF** with an L_2X_2 type benzo ligand and a Hf(IV) center. 85

2.6. Side (top) and top (bottom) views of **[5-Cl]$_2$Na{Na(DME)$_3$}** at 30 % probability ellipsoids. 88

2.7. Views of the two molecules of **5-Cl** with the side views on the left and the top views on the right. 91

2.8. Toluene glass EPR spectrum of **5-Cl** collected at 77 K. $g_x = 1.98$, $g_y = 1.96$ and $g_z = 1.70$. 93

2.9. NOESY NMR spectrum of **5-DHID-H** which depicts a *syn* isomer. Circles and ovals denote assignment of the dihydroindenediyl ring, while bold squares the orientation of the Hf-*H* over H_1 and H_3. 97

3.1. Formation of zirconacyclopentane derivatives and subsequent functionalization to afford cyclic compounds. 126

3.2. Molecular structure of **1-(CH$_2$CHCH$_2$)$_2$N^{t}Bu** at 30 % probability ellipsoids. 129

3.3. Stack plot of the ^{1}H NMR spectra of a toluene-d_8 solution of **1-(OCH$_2$CHCH$_2$)(CH$_2$CHCH$_2$)** at variable temperatures. 130

3.4. Molecular structures of **1-(O^{c}Pent)$_2$-1,4** (left) and **3-(O^{c}Pent)$_2$-1,4** (right) at 30 % probability elipsoids. 135

3.5. Divergent product formation upon two equivalents of various ketones to a pentane or benzene solution of 1 at 22 °C. 143

3.6. Molecular structure of **1-(OMe$_2$)$_2$-4,7** at 30 % probability ellipsoids. 145

3.7. pKas of the ketones utilized in this study. The ones on the left column form a 1,4 double insertion product, while the ones on the right an enolate hydride compound upon addition of excess ketone to a solution of 1. 147

3.8. Side (left) and top (right) views of **1-(Ofluorenyl)$_2$** at 30 % probability elipsoids. 151

3.9. Proposed mechanisms for both enolate hydride formation and ketone insertion. 157

4.1. Activation of dinitrogen with isolable group 4 complexes. 200

4.2. Molecular structure of **[*meso*-3]$_2$N$_2$** at 30 % probability ellipsoids. Hydrogen atoms omitted for clarity. 206

4.3. Molecular structure of **[*meso*-3]$_2$(H)I** at 30 % probability ellipsoids. 208

4.4. Different possible isomers of **3$_2$-N$_2$**, which demonstrate only 5 will be observable by ^{1}H NMR spectroscopy. 209

4.5. Views of both molecules of **[*rac*-4]$_2$N$_2$** at 30 % probability ellipsoids. Hydrogen atoms omitted for clarity. 213

4.6. NOESY NMR spectrum of a benzene-d_6 solution of the four diastereomers of **[*rac*-4-H$_2$]$_2$**. The squares denote exchange between the hydrides of two homochiral dimers, while the ovals the hydrides of the two heterochiral dimers. 217

4.7. Possible C_2 symmetric products arising from the heating of either **[*rac*-4]$_2$-N$_2$H$_4$** or **[*rac*-4]$_2$-H$_2$N$_2$** to 65 ºC. 220

5.1. The titanocene and zirconocene compounds explored in this study for competency as amine-borane dehydrogenation catalysts 245

5.2. Proposed mechanism for the dehydrogenation of Me_2NHBH_2 with titanocene sandwich and dinitrogen complexes. 250

5.3. Molecular structure of **14** at 30 % probability ellipsoids. 252

LIST OF TABLES

1.1. Comparison of selected crystallographic data for **8** and (η^9-C_9H_5-1,3-$(CHMe_2)_2$)(η^5-C_9H_5-1,3-$(CHMe_2)_2$)Zr. 10

1.2. Comparison of selected crystallographic data for **6_2-N_2** and **16-N_2Cl**. 14

1.3. Comparison of selected crystallographic data for ***meso*-13**, **[13-NaCl]$_2$$N_2$**, **[13-NaI]$_2$$N_2$** and **[13-Cl]$_2$$N_2$(Na){Na(18-crown-6)$_{1.5}$}**. 26

1.4. Comparison of carbonyl stretching frequencies for the corresponding dicarbonyl complexes of all zirconocene dihalides reduced. 39

2.1. Comparison of carbonyl stretching frequencies for the corresponding dicarbonyl complexes of all hafnocene dihalides reduced, along with their zirconium congeners. 82

2.2. Comparision of select metrical parameters of the two molecules of **5-THF** and the zirconium congener, **2-THF**. 85

2.3. Comparision of select metrical parameters of **[5-Cl]$_2$Na{Na(DME)$_3$}**. 89

2.4. Select metrical parameters of the two molecules of **5-Cl**. 92

3.1. Diastereoselectivity of each zirconacycle formed. 128

3.2. Comparison of metrical parameters of **1-(O^{c}Pent)$_2$-1,4** and **3-(O^{c}Pent)$_2$-1,4**. 134

3.3. Comparison of ^{1}H NMR resonances (ppm) of 1,4 cyclopentanone insertion products in benzene-d_6. 136

3.4. Comparison of ^{13}C NMR resonances (ppm) of 1,4 cyclopentanone insertion products in benzene-d_6. 136

3.5. Quantity of each compound with time (or upon addition of excess

ketone) when 3 is treated with 0.5 equivalents of cyclopentanone. 142

3.6. Selected metrical parameters of 1-(Ofluorenyl)$_2$. 151

4.1. Infrared carbonyl stretching frequencies for zirconocene dicarbonyl complexes. 201

4.2. Comparison of selected metrical parameters for *ansa*-zirconocene dinitrogen complexes. 214

5.1. Results of catalytic metallocene catalyzed dehydrogenation. 245

5.2. Comparison of selected metrical parameters for **14** and $(\eta^5\text{-}C_5H_5)_2Zr(BH_4)H$. 251

Chapter 1

Activation of Dinitrogen with Indenyl Zirconium Complexes: Different Modes of N_2 and Indenyl Coordination*

Abstract

Reduction of the cyclopentadienyl indenyl zirconium dihalide compounds, (η^5-C_5Me_5)(η^5-C_9H_5-1-R,3-Me)ZrX_2, (R = Me, $CHMe_2$, CMe_3) with excess 0.5 % sodium amalgam under argon resulted in the isolation of (η^5-C_5Me_5)(η^9-C_9H_5-1-R,3-Me)Zr sandwich complexes. In contrast, reduction under a dinitrogen atmosphere yielded rare examples of dimeric side-on, end-on bound dinitrogen compounds with bridging η^5, η^4 indenyl rings. Exposure of the zirconocene sandwich complexes to dinitrogen resulted in dimeric end-on coordination of N_2 where each indenyl is not only bound η^5 to a zirconium but also η^2 to the other zirconium center. Similar divergent product formation was observed upon reduction of the homoleptic bis(indenyl) zirconium compounds, (η^5-C_9H_5-1-$CHMe_2$,3-Me)$_2ZrX_2$ (X = Cl, Br, I). Sandwich complex was isolated from reduction under argon while dinitrogen complexes were obtained when the reaction was performed under N_2. Interestingly, the latter dimeric complexes exhibit a highly activated end-on bound N_2 ligand. The compound is dianionic and countered with two sodium cations, which coordinate to an indenyl from each zirconium in an η^2 fashion. The hydrogenation of all dinitrogen complexes was also explored, with the first example of hydrogenation from a set of strongly activated end-on dinitrogen complexes.

* Reproduced in part with permission from a) Pun, D.; Lobkovsky, E.; Chirik, P. J. *J. Am. Chem. Soc.* **2008**, *130*, 6047. Copyright 2008 American Chemical Society. b) Pun, D.; Bradley, C. A.; Lobkovsky, E.; Keresztes, I.; Chirik, P. J. *J. Am. Chem. Soc.* **2008**, *130*, 14046. Copyright 2008 American Chemical Society.

Introduction

Since the synthesis of the first transition metal dinitrogen complex, $[(NH_3)_5 RuN_2]^{2+}$ in 1965,[1] great interest has followed in developing more reactive N_2 complexes for functionalizing the inert dinitrogen molecule and for making nitrogen-containing molecules. Emphasis has revolved, in particular, around studying and mimicking the Haber-Bosch cycle or nitrogenase enzymes, both of which convert N_2 to NH_3.[2,3] Over the past forty-five years, many more transition metal dinitrogen complexes have been synthesized from metals across the periodic table, with different modes of dinitrogen coordination (Figure 1.1).[4] There are both monometallic versus bimetallic, weakly activated versus strongly activated, and side-on versus end-on coordination. In group 4 transition metal chemistry, all six coordination modes have been identified.[4] Prior to this study, only one example of a side-on, end-on N_2 complex of a group 4 metal had been identified (Figure 1.5).[5]

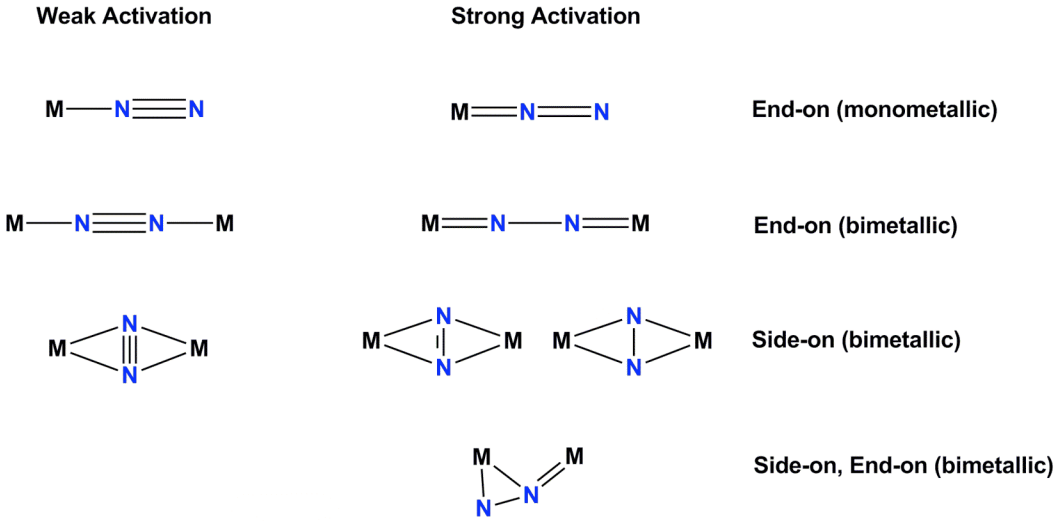

Figure 1.1. Modes of dinitrogen coordination.

The first zirconium dinitrogen complex was synthesized by Bercaw and coworkers from the alkali metal reduction of bis(pentamethylcyclopentadienyl) zirconium dichloride, $Cp^*_2ZrCl_2$. A dimeric complex with one bridging and two

terminal end-on bound N_2 ligands, $[Cp^*_2Zr(\eta^1\text{-}N_2)]_2(\mu_2, \eta^1,\eta^1\text{-}N_2)$ was isolated and structurally characterized.[6] Based on the X-ray metrical parameters, the N-N bond distance is indicative of a weakly activated dinitrogen ligand, which is further corroborated by its reactivity; attempts to hydrogenate resulted in loss of N_2 gas and formation of two equivalents of $Cp^*_2ZrH_2$.[7] Interestingly, protonation of this weakly activated dinitrogen complex with hydrochloric acid results in formation of hydrazinium chloride salt[8] while hydrolysis results in simply loss of N_2 and formation of a bridging oxo hydride, $[Cp^*_2ZrH]_2(\mu_2, \eta^1,\eta^1\text{-}O)$ (Figure 1.2).[9]

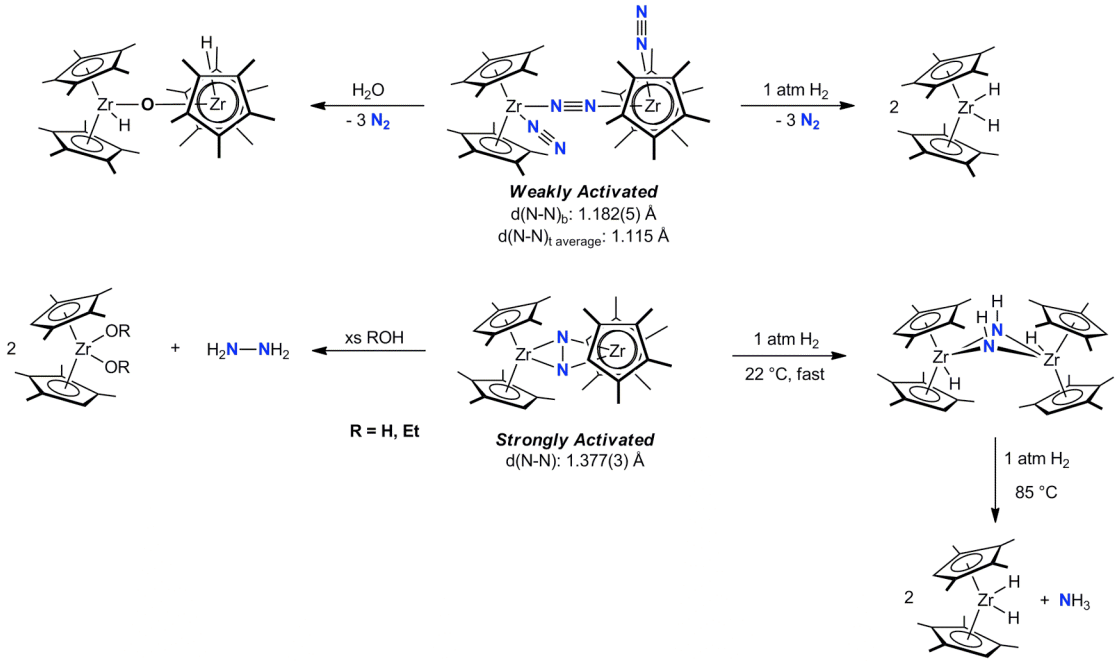

Figure 1.2. Reactivity similarity and differences between a weakly and a strongly activated zirconocene dinitrogen complexes.

Removal of one methyl group per cyclopentadienyl ring and subsequent alkali metal reduction of the corresponding zirconocene dichloride affords the first strongly activated zirconocene dinitrogen complex that hydrogenates without loss of N_2. The dinitrogen complex is dimeric with one strongly activated side-on bound N_2 ligand, $[(\eta^5\text{-}C_5Me_4H)_2Zr]_2(\mu_2, \eta^2,\eta^2\text{-}N_2)$, as established by X-ray crystallography and reactivity

studies.[10] Upon hydrogenation, two equivalents of H_2 are formally added across the Zr-N bonds, forming a dimeric zirconocene hydrazido hydride, $[(\eta^5\text{-}C_5Me_4H)_2ZrH]_2(\mu_2, \eta^2,\eta^2\text{-}N_2H_2)$ (Figure 1.2). Upon heating to 85 ºC, small quantities of ammonia are detectable. Interestingly, protonation of this strongly activated dinitrogen complex with either a strong acid like hydrochloric acid or a weak Brønsted acid such as water or ethanol result in hydrazinium chloride and $N_2H_4{\cdot}ROH$, respectively (Figure 1.2).[11] Clearly, formation of a hydrazine derivative upon protonolysis of a dinitrogen complex with a weak acid is an indication that the dinitrogen is four electron reduced by the metal center(s).

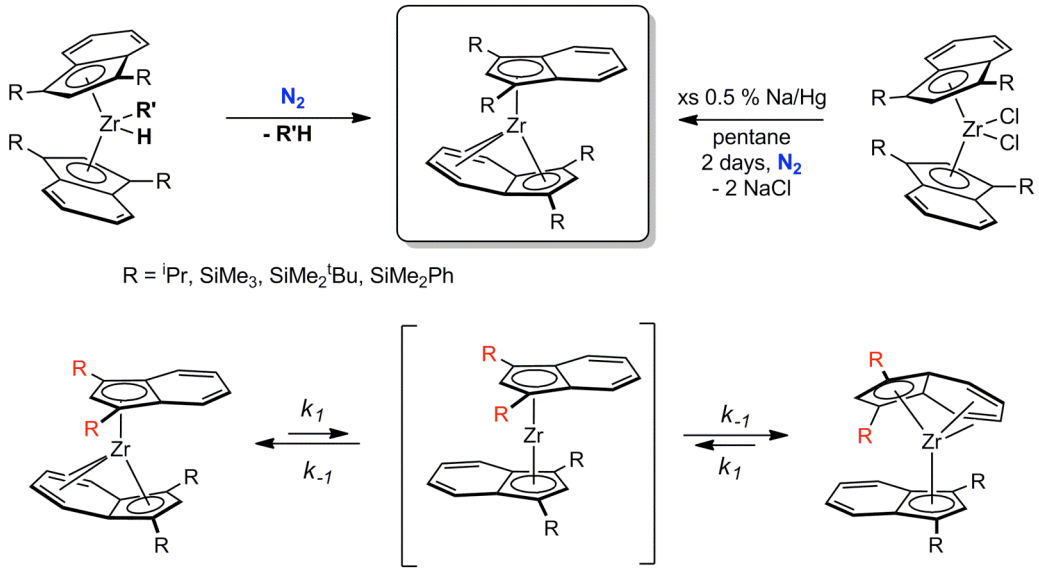

Figure 1.3. Preparation of η^9, η^5 bis(indenyl) zirconocene sandwich complexes via reductive elimination (top left) or alkali metal reduction (top right). η^9, η^5 to η^5, η^9 ring interconversion via an η^5, η^5 intermediate (bottom).

Also discovered in our laboratory was the formation of unique η^9, η^5 bis(1,3-disubstituted indenyl) zirconium sandwich complexes from either reductive elimination of the corresponding η^5, η^5 bis(indenyl) zirconocene alkyl hydrides or alkali metal reduction of the zirconocene dichlorides (Figure 1.3a).[12] The ^{1}H NMR spectra of all bis(indenyl) zirconocene sandwich compounds exhibit an overall

broadness of peaks that sharpens upon cooling. This is attributed to a rapid interconversion of the η^9 and η^5-bound indenyl rings, accessed through an η^5, η^5 bis(indenyl) zirconocene intermediate (Figure 1.3b). This formally Zr(II) intermediate has also been confirmed computationally[13] and inferred through reactivity studies, such as the oxidative addition of C-H and C-O bonds.[12,14] It should also be noted that these zirconocene sandwich complexes with bulky substituents on the 1 and 3 positions are unreactive with one atmosphere of dinitrogen at ambient temperature.

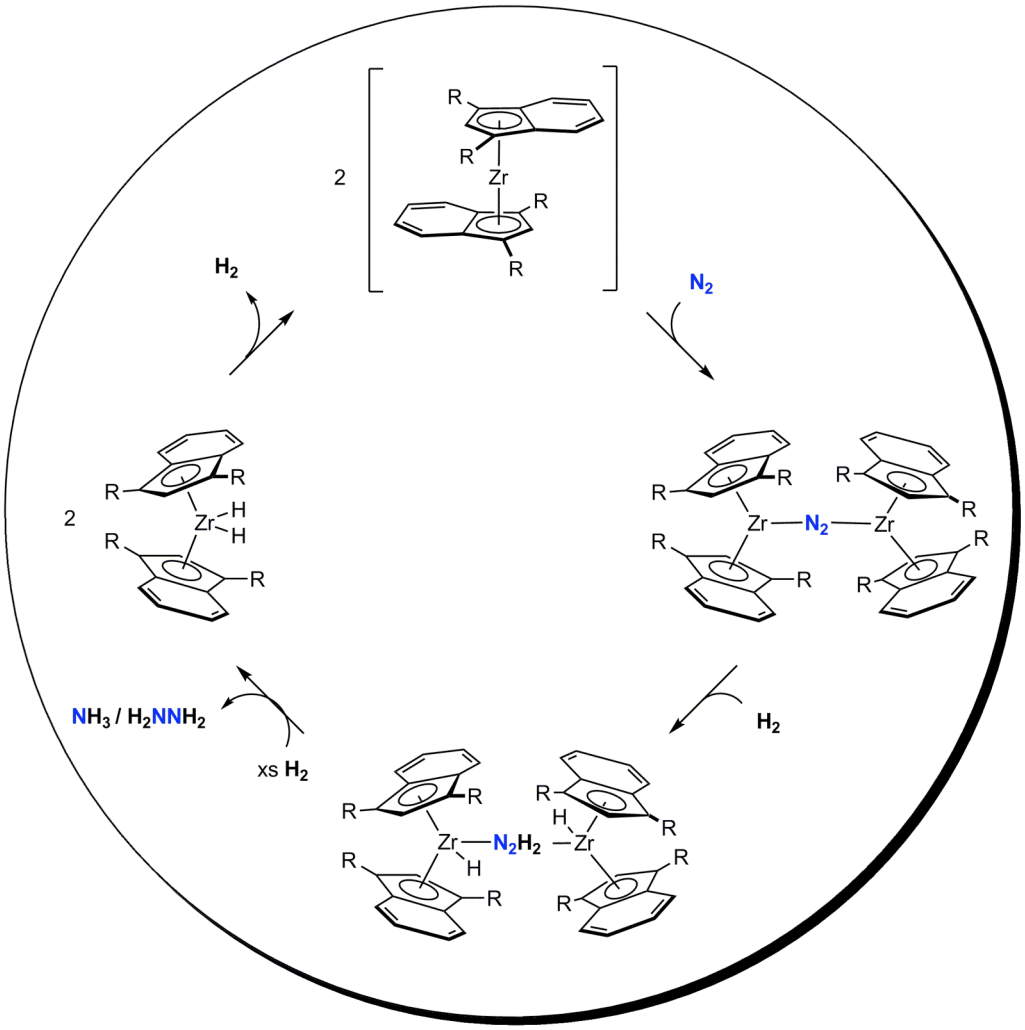

Figure 1.4. Proposed catalytic cycle for the hydrogenation of dinitrogen with bis(indenyl) zirconium compounds.

With these indenyl zirconocene alkyl hydrides that readily undergo reductive elimination to form sandwich complexes, it would be interesting to destabilize the η^9 interaction and allow for zirconium coordination to a dinitrogen ligand instead of an indenyl benzo ring. One could envision a catalytic cycle whereby dinitrogen binds to the bis(indenyl) zirconocene (II) intermediate, then hydrogenates to ultimately liberate ammonia or hydrazine and zirconocene dihydride, which will reductively eliminate dihydrogen and continue on the catalytic cycle (Figure 1.4).

In addition to its utility, this cycle is important because the propensity of these compounds to promote reductive elimination would obviate the need for harsh alkali metal reductions typically required for the preparation of early metal dinitrogen complexes. While commonly observed for titanium, from both isolable titanocene complexes[5,15,16] and upon reductive elimination of the titanocene monohydride,[17,18] the direct coordination of dinitrogen has only been observed in a few examples for zirconium via reductive elimination of a zirconocene dihydride[19] or two alkyl hydrides.[20,21] Shown in Figure 1.5 are other examples including Gambarotta's reduced bis(amidinate) vanadium complex that coordinates N_2 at elevated temperatures, forming a vanadium dimer[22] and Fryzuk's dincuclear tantalum[23] tetrahydride complex that readily reductively eliminates one equivalent of H_2 to form a unique side-on, end-on dinitrogen complex. More recently, the full cleavage of dinitrogen with Kawaguchi's dimeric tris(alkoxide) niobium tetrahydride was observed and crystallographically characterized.[24] Reported here are the attempts at dinitrogen activation with indenyl zirconocene complexes with the hopes of forming some of the complexes outlined in the catalytic cycle outlined in Figure 1.4. Particular emphasis was placed on indenyl rings with less sterically bulky substituents than those previously studied in the hopes of favoring dimeric dinitrogen complex formation.

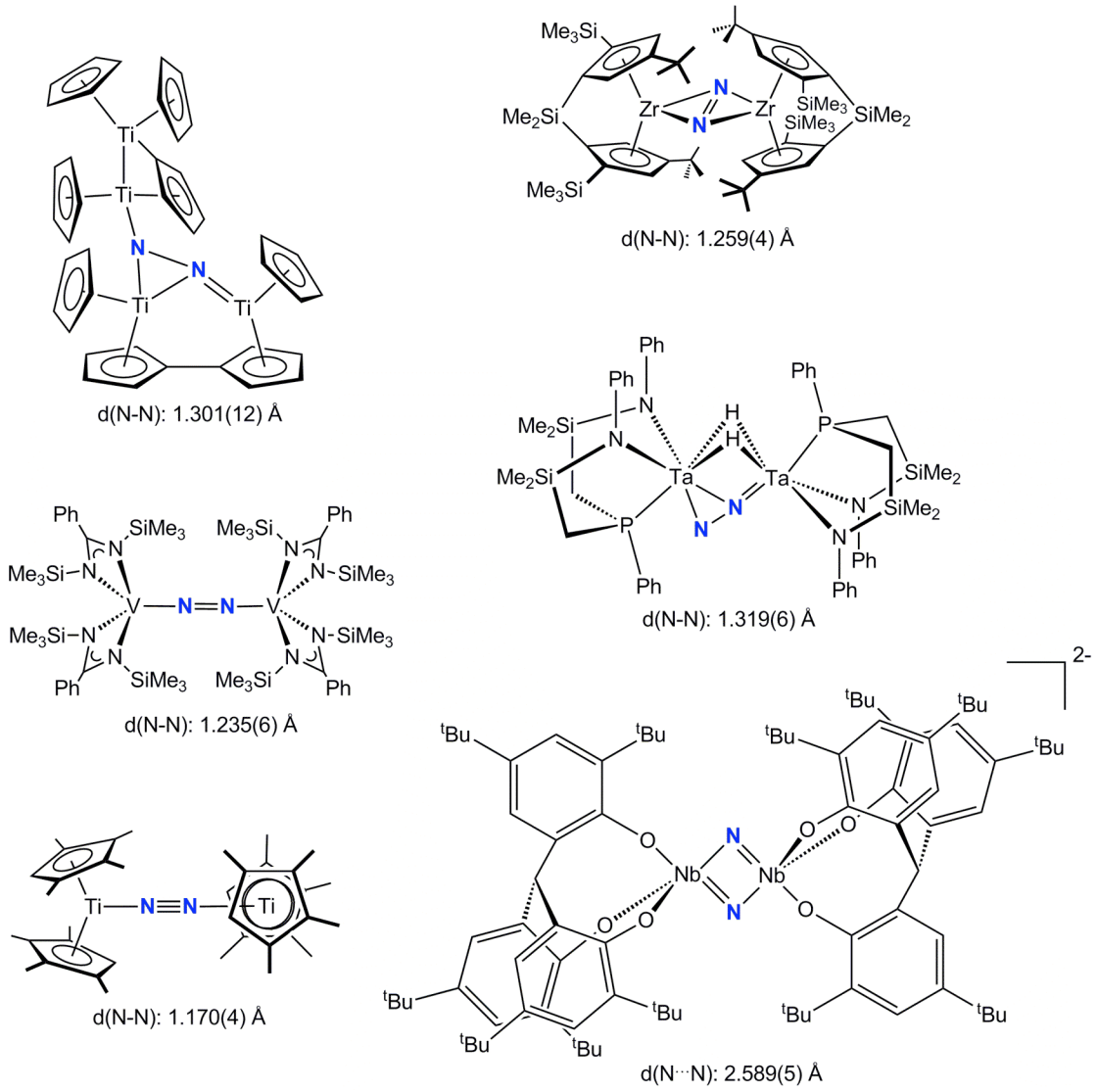

Figure 1.5. Examples of N_2 activation from (left) isolable reduced complexes and (right) the reductive elimination of metal hydride precursors.

Results and Discussion

Synthesis of Cyclopentadienyl Indenyl Zirconium Sandwich Complexes. Based on the previous studies with the bulkier bis-1,3-disubstituted indenyl zirconium compounds that form sandwich complexes that are inert toward N_2, one indenyl ligand was replaced by the less sterically hindered pentamethylcyclopentadienyl (Cp*) ring in order to explore the limits of the η^9 interaction. Bradley et al. previously reported

the formation of an η^9, η^5 zirconocene sandwich complex upon reduction of a mixed ring zirconocene dichloride, $(\eta^5\text{-}C_9H_5\text{-}1,3\text{-}(CHMe_2)_2)(\eta^5\text{-}C_5Me_5)ZrCl_2$, **8-Cl$_2$**.[25] In this study, a number of less sterically demanding indenyl ligands were also chosen. Depicted in Figure 1.6 are the series of mixed ring, Cp* indenyl zirconocene dihalide complexes explored for reduction.

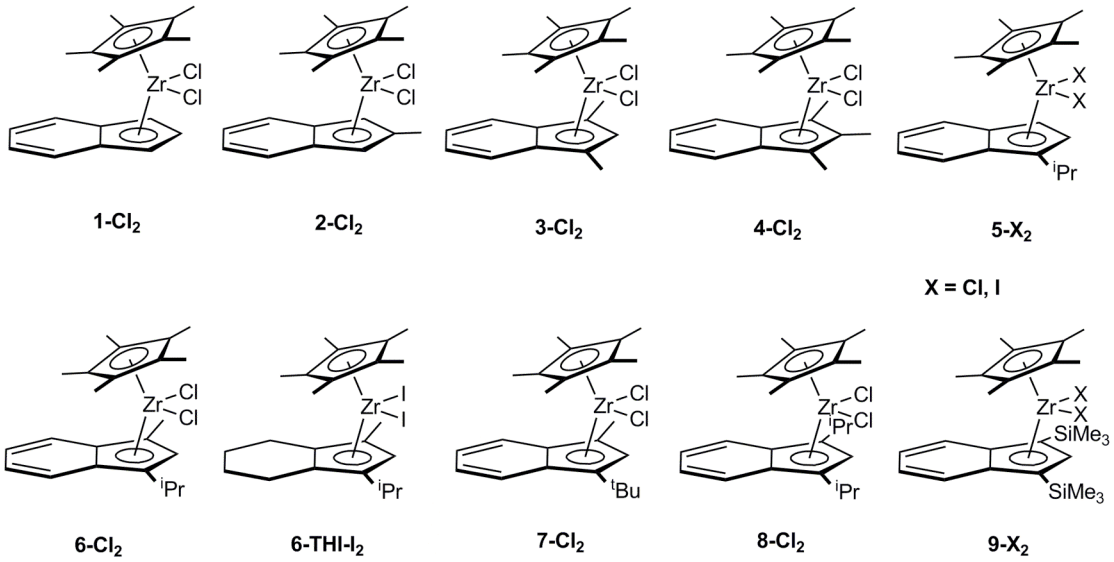

Figure 1.6. The Cp* indenyl zirconocene dihalides reduced in this study.

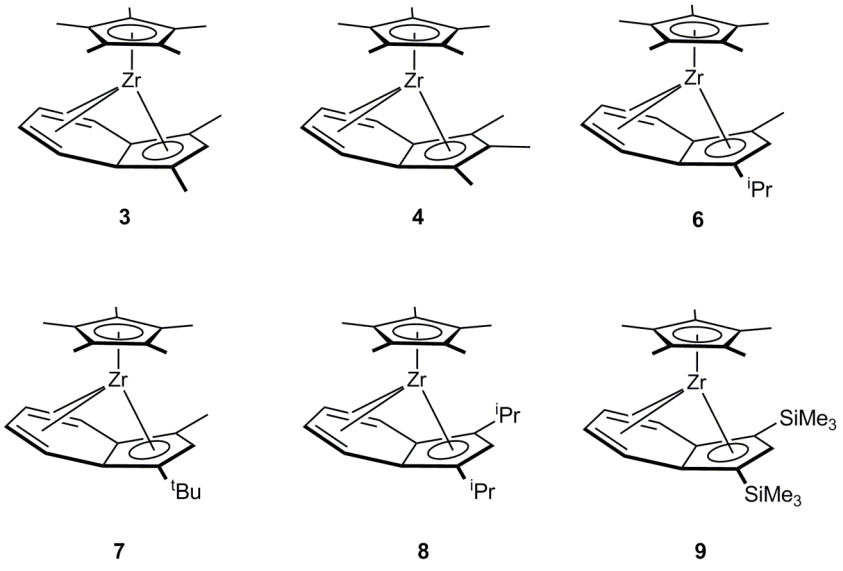

Figure 1.7. Isolable Cp* indenyl zirconocene sandwiches prepared.

Revisiting (η^9-C_9H_5-1,3-$(CHMe_2)_2$)(η^5-C_5Me_5)Zr, **8**, established that the sandwich compound is inert towards one atmosphere of N_2 for months in pentane solution. Similarly, the presence of methyl substituents on the one, two and three positions of the indenyl – as in (η^5-C_9H_4-1,2,3-Me_3)(η^5-C_5Me_5)$ZrCl_2$, **4-Cl$_2$**, also resulted in monomeric sandwich, (η^9-C_9H_4-1,2,3-Me_3)(η^5-C_5Me_5)Zr, **4**, which is also stable for months under N_2. In both cases, η^9 hapticity of the indenyl ring was observed based on ^{1}H and ^{13}C NMR spectroscopy. The number of and the upfield-shifting of resonances for the indenyl benzo are indicative of a C_s symmetric compound where the zirconium interacts with both the cyclopentadienyl and the benzo rings of the indenyl.[12] As an example, a benzene-d_6 solution of **4** exhibits a doublet of doublets centered at 3.83 and another at 5.04 ppm in the ^{1}H NMR spectrum as well as resonances centered at 66.2 and 94.9 ppm in the ^{13}C NMR spectrum.

The solid state structure of **8** was determined by X-ray diffraction (Figure 1.8) and confirms the η^9 hapticity of the indenyl ring. Selected metrical parameters and a comparison to the previously reported bis(indenyl) zirconocene sandwich complex are presented in Table 1.1.[12] Similar to the bis(indenyl) zirconium complex, the benzo carbons in **4** are elongated to 1.423(2) and 1.390(3) Å, indicative of ligand reduction by the formally zirconium (II) center. Also notable is the bending of the planar indenyl in order to accommodate this unique coordination mode: a deviation of 37 º from planarity between the Cp and the benzo rings was observed and is accompanied by an 8.2 º "buckle" within the benzo ring. Clearly, in the case of the 1,3-diisopropyl substituted indenyl, there is little difference when replacing an indenyl with a Cp* ring, which is reflected by its stability to dinitrogen.

Sodium amalgam reduction of (η^5-C_9H_5-1,3-$(SiMe_3)_2$)(η^5-C_5Me_5)$ZrCl_2$, **9-Cl$_2$**, under an argon atmosphere resulted in formation of the corresponding sandwich compound, **9**. Allowing **9** to stand in solution at -35 ºC or at higher temperatures

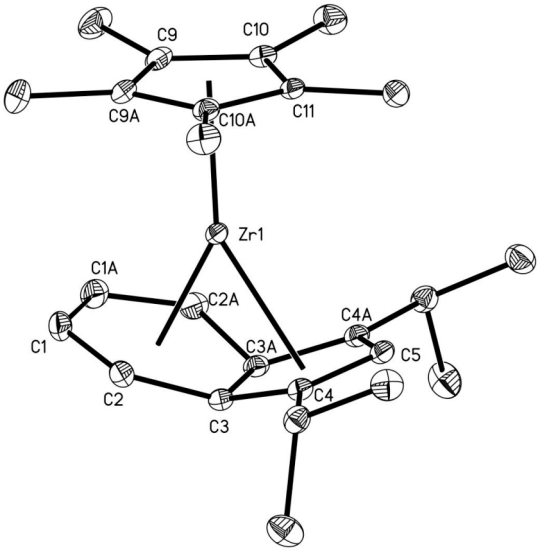

Figure 1.8. Molecular structure for **8** at 30 % probability elipsoids. Hydrogen atoms omitted for clarity.

Table 1.1. Comparison of selected crystallographic data for **8** and (η^9-C_9H_5-1,3-$(CHMe_2)_2$)(η^5-C_9H_5-1,3-$(CHMe_2)_2$)Zr.

Numbering Scheme for Indenyl[a]

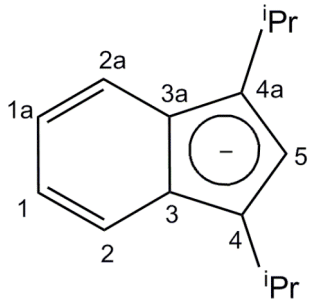

	8	(η^9-C_9H_5-1,3-$(CHMe_2)_2$)(η^5-C_9H_5-1,3-$(CHMe_2)_2$)Zr
C(1)-C(2) (Å)	1.423(2)	1.418(3)
C(1)-C(1a) (Å)	1.390(3)	1.395(3)
C(1a)-C(2a) (Å)	1.423(2)	1.426(3)
η^9 Fold Angle (°)[b]	37.0	37.6
Buckle (°)[c]	8.2	6.3

[a] Indenyl labeling scheme based on the structure in Figure 1.8. [b] Defined as the angle between the planes formed by the five-membered cyclopentadienyl and the six-membered benzo rings of the indenyl. [c] Defined as the deviation from planarity of the benzo ring, which is the angle between the planes formed by C(2)-C(3)-C(3a)-C(2a) and C(2)-C(1)-C(1a)-C(2a).

resulted in conversion to a zirconocene cyclometalated hydride, **9-CMH** (eq 1.1). Only one of the two possible diastereomers of **9-CMH** was detected by ^{1}H and ^{13}C NMR spectroscopy. The identity of the compound was determined by a NOESY NMR experiment as the isomer on the left in equation 1.1. Diagnostic crosspeaks between the zirconium hydride and the indenyl cyclopentadienyl proton were observed. Importantly, the alternative isomer was eliminated based on lack of correlation between the zirconium hydride and any benzo protons.

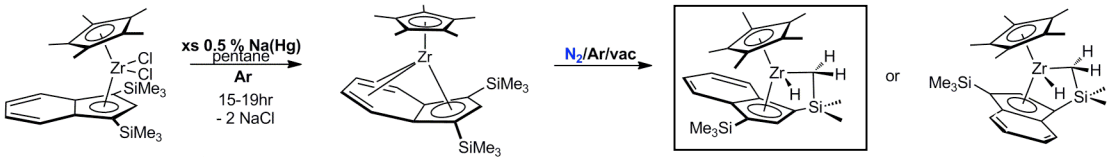

(eq. 1.1)

Decreasing the steric bulk around the zirconium, such as those complexes bearing 1-R, 3-Me substituted indenyl ligands, $(\eta^5\text{-}C_9H_5\text{-}1\text{-}R,3\text{-}Me)(\eta^5\text{-}C_5Me_5)ZrCl_2$, **3-Cl$_2$** (R = Me), **6-Cl$_2$** (R = $CHMe_2$) and **7-Cl$_2$** (R = CMe_3), also yielded sandwich complexes **3**, **6** and **7** when the reduction was performed under argon. However, the removal of all substituents as in the parent indenyl complex, $(\eta^5\text{-}C_9H_7)(\eta^5\text{-}C_5Me_5)ZrCl_2$, **1-Cl$_2$**, or leaving a methyl, $(\eta^5\text{-}C_9H_6\text{-}2\text{-}Me)(\eta^5\text{-}C_5Me_5)ZrCl_2$, **2-Cl$_2$**, or – surprisingly – a single isopropyl group, $(\eta^5\text{-}C_9H_6\text{-}3\text{-}CHMe_2)(\eta^5\text{-}C_5Me_5)ZrCl_2$, **5-Cl$_2$** resulted in drastically different reduction chemistry. All attempts to reduce the compounds under an argon or a dinitrogen atmosphere yielded intractable paramagnetic products, oftentimes with elimination of indenyl ligand. Performing the reduction in the presence of a strong field ligand such as carbon monoxide resulted in no reaction suggesting that the paramagnetic products are tightly bound dimers or clusters. The result from reduction of **5-Cl$_2$** was surprising so the corresponding diiodide complex, **5-I$_2$** was prepared. Unfortunately, the outcome was the same as from **5-Cl$_2$**. Therefore, it appears that disubstitution of the indenyl is necessary to

prevent protonation of the basic indenyl position and indene elimination from the metal.

Activation of Dinitrogen with Indenyl Zirconium Sandwich Complexes. While both **4** and **8** were inert to N_2, allowing pentane solutions of **3**, **6** or **7** to stand at -35 ºC under a dinitrogen atmosphere resulted in a color change from burgundy to purple. X-ray diffraction studies on the product of **6** established dinitrogen activation/coordination as $[(\eta^5\text{-}C_5Me_5)Zr]_2\,[\mu_2\text{-}\eta^2,\eta^2\text{-}\{4,5\text{-}(\eta^5\text{-}C_9H_5\text{-}1\text{-}CHMe_2\text{-}3\text{-}Me)\}_2]$ $(\mu_2\text{-}\eta^1,\eta^1\text{-}N_2)$, $\mathbf{6_2\text{-}N_2}$ (Figure 1.9). It is a C_2 symmetric dimeric end-on bound

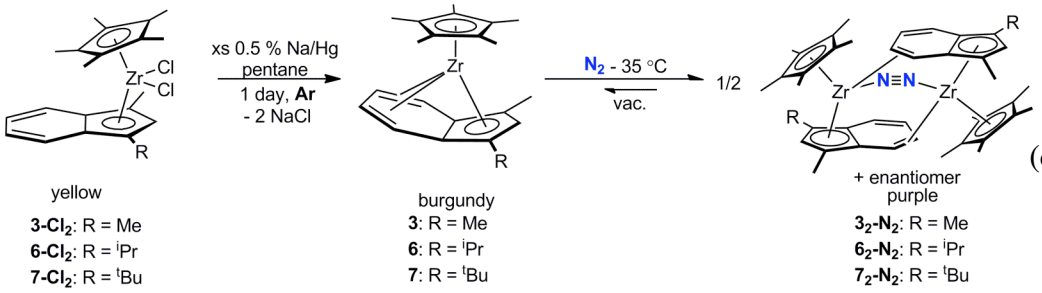

(eq. 1.2)

dinitrogen complex with an N-N bond distance of 1.197(3) Å, similar to that observed in $[Cp^*_2Zr(\eta^1\text{-}N_2)]_2(\mu_2, \eta^1,\eta^1\text{-}N_2)$ – without the terminal dinitrogen ligands – which has a bridging N_2 bond length of 1.182 Å.[26] Additionally, each indenyl is not only coordinated η^5 to a zirconium by the cyclopentadienyl ring but also η^2 from the adjacent benzo carbons (C7-C8) resulting in an encapsulation of the dinitrogen. This coordinative saturation is likely the reason why there are no terminal dinitrogen ligands in the solid state. As shown in Figure 1.9, the top view of the structure portrays the smaller methyl group and Cp* protecting the N_2 while the bulkier isopropyl group hangs in the periphery. It appears that replacing the methyl group with a larger substituent or having a substituent at the 2 position sterically hinders this dimerization that is essential for activation of dinitrogen. Examination of the bond distances of the η^2 carbons in Table 1.2 shows that this particular double bond (C5-

C6) is reduced from 1.350(3) to 1.429(3) Å suggesting dialkyl character. This suggests that in this diamagnetic compound, each monomeric fragment is an 18 electron complex with a zirconium (IV) center, an X_2-type η^2-alkene and an L-type dinitrogen ($[N_2]^0$) ligand as shown in the resonance on the left of Figure 1.10. An alternative resonance structure is depicted on the right of Figure 1.10 consisting of 18 electron zirconium (IV) centers with L-type Dewar-Chatt-Duncanson η^2-alkene and imido-like dinitrogen ($[N_2]^{4-}$)

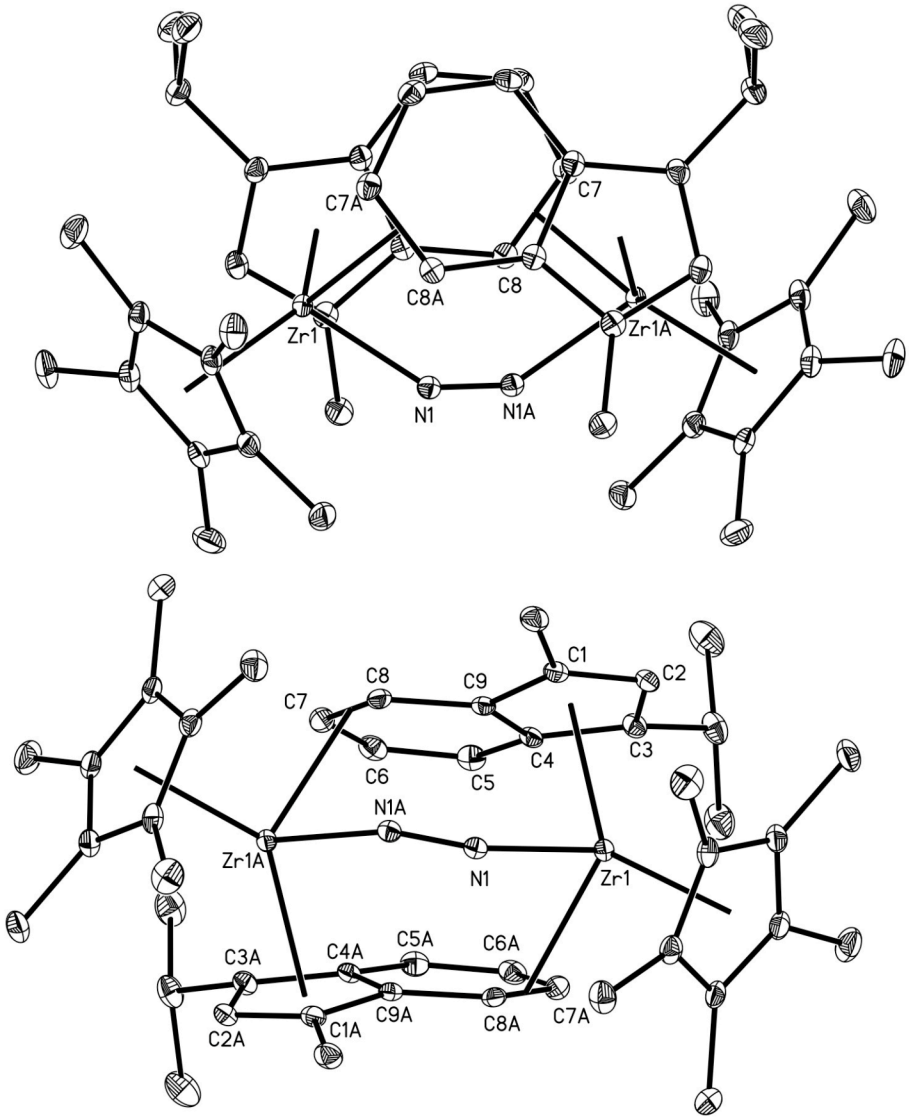

Figure 1.9. Molecular structure of $\mathbf{6_2N_2}$ at 30 % probability ellipsoids top view (top), side view (bottom).

Table 1.2. Comparison of selected crystallographic data for $\mathbf{6_2\text{-}N_2}$ and $\mathbf{16\text{-}N_2Cl}$.

Numbering Scheme for Indenyl[a]

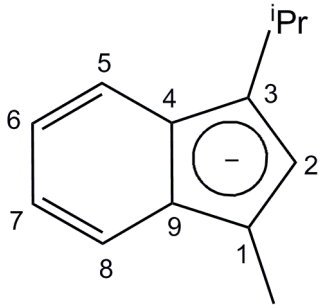

	$\mathbf{6_2\text{-}N_2}$	$\mathbf{16\text{-}N_2Cl}$
C(4)-C(5) (Å)	1.435(3)	1.445(3)
C(5)-C(6) (Å)	1.350(3)	1.418(3)
C(6)-C(7) (Å)	1.433(3)	1.390(3)
C(7)-C(8) (Å)	1.429(3)	1.402(4)
C(8)-C(9) (Å)	1.435(3)	1.458(3)
N(1)-N(1a)/N(2) (Å)	1.197(3)	1.196(4)
		1.220(10)
Zr(1)-N(1) (Å)	2.0610(15)	
η^9 Fold Angle (°)[b]	10.2	1.6
Buckle (°)[c]	1.0	23.2
Dihedral Angle (°)[d]	57.9	1.2

[a] Indenyl labeling scheme based on the structure in Figure 1.9. [b] Defined as the angle between the planes formed by the five-membered cyclopentadienyl and the six-membered benzo rings of the indenyl. [c] Defined as the deviation from planarity of the benzo ring, which is the angle between the planes formed by C(5)-C(4)-C(9)-C(8) and C(5)-C(6)-C(7)-C(8). [d] Defined as the angle between the planes of the zirconium and the cyclopentadienyl centroids.

ligands. However there is little contribution to this later resonance form based on the short N-N bond distance and long Zr-N bond distances of 2.0610(15) Å, consistent with a triple and a single bond, respectively.

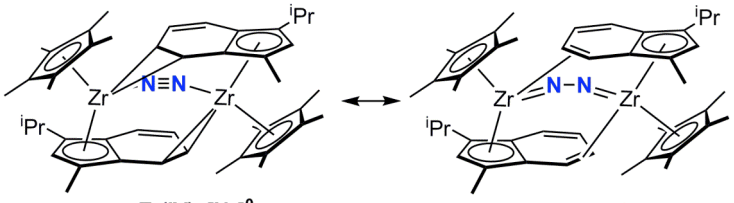

Figure 1.10. Possible resonance structures for $\mathbf{3_2\text{-}N_2}$, $\mathbf{6_2\text{-}N_2}$ or $\mathbf{7_2\text{-}N_2}$.

NMR spectroscopy confirms the connectivity in $\mathbf{6_2\text{-}N_2}$ with an NOESY experiment verifying that the isopropyl groups are *syn* to one another (Figure 1.11). First, the hydrogens in the benzo were assigned, using the same numbering scheme as that used in numbering the carbon atoms denoted in Table 1.2. These correlations are denoted by the crosspeaks in the boxes. Benzo 5 at 6.41 is adjacent to benzo 6 at 6.33, which also correlates to the upfield shifted benzo 7 at 3.30, which is adjacent to benzo 8 at 2.63 ppm. These assignment is further corroborated by the dashed boxes demonstrating that benzo 8 is near the methyl group at 2.25, while benzo 5 and 6 near the isopropyl methyl groups at 1.34 ppm. The circles highlight the interactions between the Cp* methyl groups at 1.80 ppm and the indenyl protons, particularly with benzo 7 and 8. The proximity specifies that the carbons attached to benzo 7 and 8, and not benzo 6 nor 5, are coordinated η^2 to the zirconium center. The η^5, η^2 coordination mode of the indenyl ligand is readily identified by ^{1}H NMR spectroscopy: the η^2 coordinated benzos of $\mathbf{6_2\text{-}N_2}$ appear at 2.63 and 3.30 ppm, upfield of even the η^9 resonances at 3.68, 3.84, 5.02 and 5.13 ppm in **6** in benzene-d_6. A singlet centered at 598.7 ppm in the ^{15}N NMR spectrum verifying equivalent nitrogen atoms was obtained by exchange of $^{15}N_2$ gas to a benzene-d_6 solution of $\mathbf{6_2\text{-}N_2}$. The pentane solution infrared spectrum exhibits a single stretch at 1563 cm^{-1} indicative of a bridging dinitrogen ligand. The corresponding signal for $[Cp^*_2Zr(\eta^1\text{-}N_2)]_2(\mu_2\text{-}\eta^1,\eta^1\text{-}N_2)$ appears at 1578 cm^{-1} as a medium intensity band.[6b]

The readiness of the formation of dinitrogen complexes from sandwich compounds was established by monitoring a benzene-d_6 solution of **6** at 22 ºC over several days. The half-life is approximately three days but unfortunately decomposition from $\mathbf{6_2\text{-}N_2}$ also occurred preventing a more definitive measurement. Partial conversion of **3** or **7** to $\mathbf{3_2\text{-}N_2}$ or $\mathbf{7_2\text{-}N_2}$, respectively, took one month. Exposure of $\mathbf{6_2\text{-}N_2}$ to vacuum or heating to 45 ºC resulted in dissociation of the

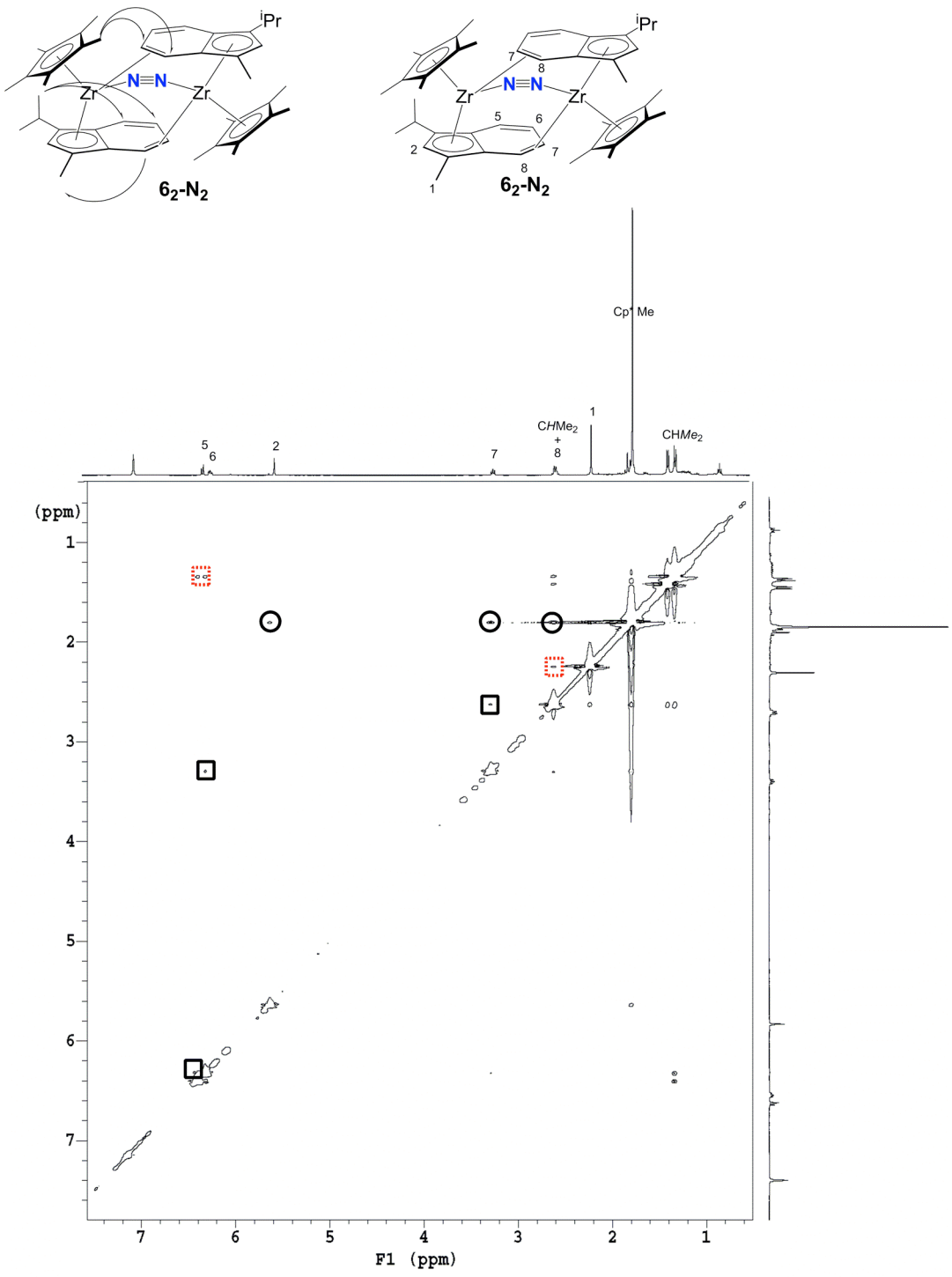

Figure 1.11. NOESY NMR spectrum of $\mathbf{6_2\text{-}N_2}$ in benzene-d_6.

dinitrogen ligand and regeneration of **6**. Again, decomposition to free indenyl ligand accompanied this reaction making it difficult to determine equilibrium constants. No reaction occurred when a benzene-d_6 solution of **6** was allowed to stand under vacuum.

Protonation studies of the new end-on dinitrogen complexes were conducted. Typical of all activated N_2 compounds, addition of hydrochloric acid resulted in liberation of 45 % hydrazinium chloride, while addition of a weak acid such as water or ethanol did not, consistent with the crystallographic data that these complexes have weakly bound $[N_2]^0$ ligands. Attempts to hydrogenate the compound only resulted in loss of dinitrogen and formation of zirconocene dihydrides,[7] which under prolonged hydrogenation, insert hydrogen atoms into the benzo ring in a *syn* manner with respect to the zirconium center, similar to hydrogenation of the bis(indenyl)zirconium dihydrides,[14] forming $(\eta^5\text{-}C_5Me_5)(\eta^5\text{-}C_9H_9\text{-}1\text{-}CHMe_2\text{-}3\text{-}Me)ZrH_2$, **6-THI-H$_2$**, (eq 1.3).

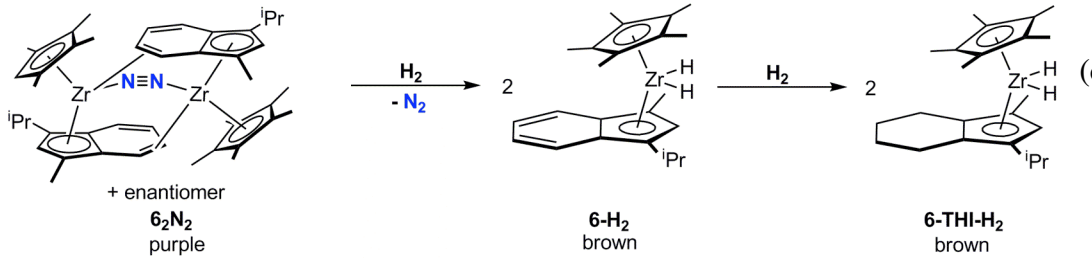

(eq. 1.3)

Formation of Side-on, End-on Dinitrogen Complexes. While sodium amalgam reduction of **6-Cl$_2$**, **7-Cl$_2$** and **9-Cl$_2$** under argon afforded the respective sandwich complexes, reduction under dinitrogen for two days produced a different outcome. All reduction products exhibit benzo resonances even more upfield than that of η^5, η^2 or η^9 hapticity, indicative of stronger backdonation from the metal center. As a representative example, the reduction product of **6-Cl$_2$** in a benzene-d_6 solution shows two isomers in a 3:1 ratio[27] with benzos at 2.23, 3.55, 3.83 and 4.74 ppm for the major isomer. Interestingly, there are two different Cp* ligands per indenyl ring. Free

indene was also detected by ^{1}H NMR spectroscopy in the crude reduction mixture. ^{15}N NMR labeling of the ^{15}N-isotopologue[28] established inequivalent nitrogen environments: a set of doublets centered at 490.0 and 599.9 ppm with a $^{1}J_{N\text{-}N}$ = 20 Hz for the major isomer and another set at 494.9 and 610.1 ppm with a $^{1}J_{N\text{-}N}$ = 21 Hz for the minor.

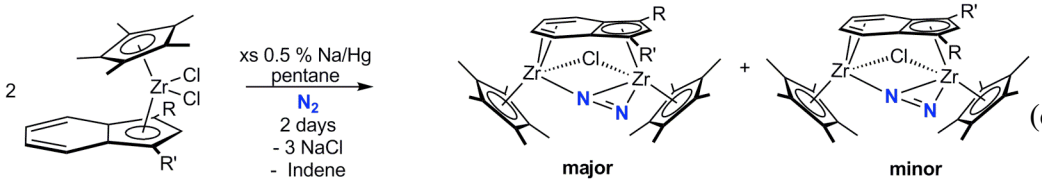

yellow

6-Cl$_2$: R = ^{i}Pr, R' = Me
7-Cl$_2$: R = ^{t}Bu, R' = Me
9-Cl$_2$: R = R' = SiMe$_3$

brown

16-N$_2$Cl: R = ^{i}Pr, R' = Me (3 : 1)
17-N$_2$Cl: R = ^{t}Bu, R' = Me (1.5 : 1)
18-N$_2$Cl: R = R' = SiMe$_3$ (only one isomer)

(eq. 1.4)

X-ray diffraction established the identity of complexes as bimetallic side-on, end-on bound N_2 compounds with a bridging η^5,η^4-indenyl ligand, $[(\eta^5\text{-}C_5Me_5)Zr]_2[\mu_2\text{-}\eta^5,\eta^4\text{-}(\eta^5\text{-}C_9H_5\text{-}1\text{-}R\text{-}3\text{-}R')]$ $(\mu_2\text{-}\eta^2,\eta^1\text{-}N_2)$ $(\mu_2\text{-}\eta^1,\eta^1\text{-}Cl)$: **16-N$_2$Cl** (R = $CHMe_2$, R' = Me), **17-N$_2$Cl** (R = CMe_3, R' = Me) and **18-N$_2$Cl** (R = R' = $SiMe_3$) (eq 1.4). While only one compound was observed in the NMR spectrum of **18-N$_2$Cl**, X-ray crystallography established that not only was this dinitrogen complex present but one with two bridging chlorine atoms, **18-Cl$_2$**, was also located in the unit cell (eq 1.5). This paramagnetic mixed valence impurity is likely an intermediate along the way to nitrogen activation. An EPR spectrum of a toluene solution of the reduction products exhibits one signal at g = 1.98 with hyperfine coupling to ^{91}Zr (I = 5/2), consistent with a zirconium (III) monohalide. Unfortunately, as judged by EPR spectroscopy, prolonged reduction with sodium amalgam did not result in complete conversion to the desired product. Hence, **9-I$_2$** was synthesized for reduction under dinitrogen in the hopes that the better leaving iodide group would facilitate formation of the dinitrogen complex. This procedure was effective in eliminating the paramagnetic impurity but yielded only 5 % of the desired **18-N$_2$I** product (eq 1.6).

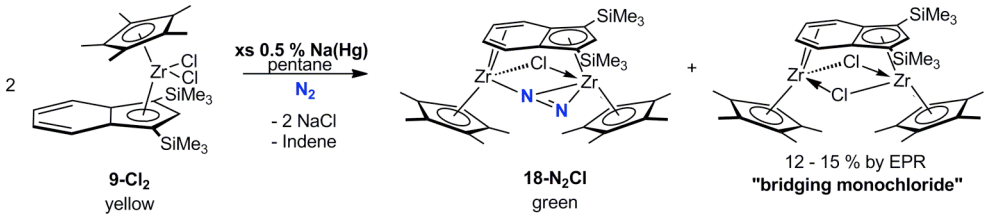

(eq. 1.5)

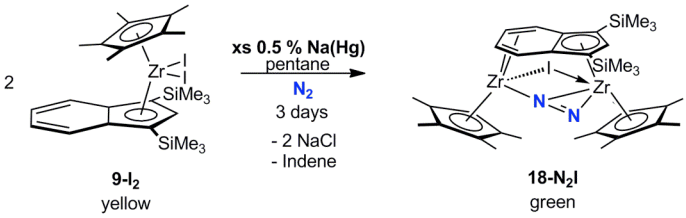

(eq. 1.6)

A crystal structure of **16-N_2Cl**, where this compound was synthesized in 72 % yield without any EPR active species, was also obtained. Recall that two possible diastereomers are possible and observable by NMR spectroscopy. One is where the isopropyl group is *syn* to the dinitrogen and the other where it is *anti*. The unit cell contained a 4:1 ratio of the *anti* : the *syn*. The N-N bond distances are 1.196(4) and 1.220(10) Å for the major and minor isomers, respectively, indicating weak to modest N_2 activation.

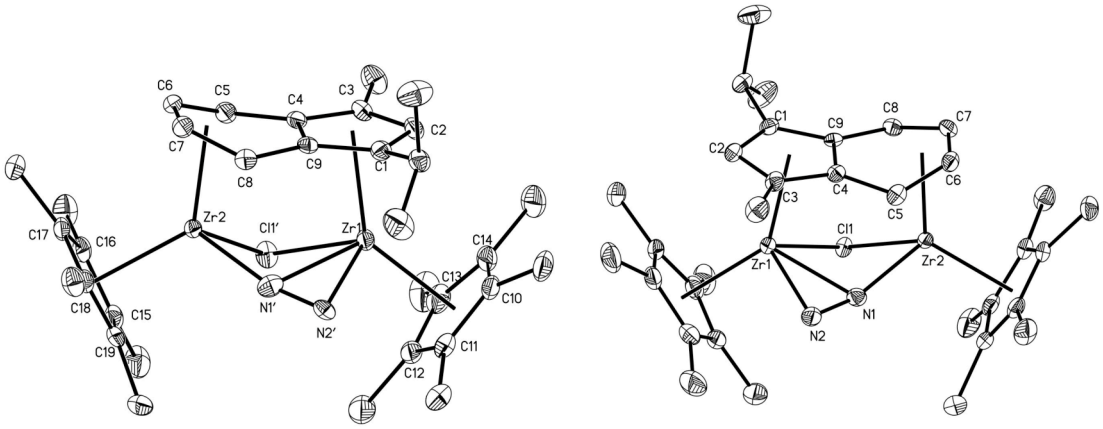

Figure 1.12. Molecular structures of the major (left) and minor (right) isomers of **16-N_2Cl** at 30 % probability ellipsoids.

For a comparison, Fryzuk's bimetallic tantalum side-on, end-on dinitrogen compound with a strongly activated $[N_2]^{4-}$ ligand depicted in Figure 1.5 has an N-N

bond distance of 1.319(4) Å.[29] A solid state N-N stretch for **16-N_2Cl** of 1583 cm^{-1} (which shifts appropriately to 1533 cm^{-1} for the ^{15}N isotopologue) in the infrared spectrum is at higher energy than the tantalum example (1165 cm^{-1}) and is another indication that **16-N_2Cl** has at most only a modestly reduced dinitrogen ligand.[29] The reduced degree of activation is attributed to the bridging chloride ligand and the 2 electron reduction of the indenyl benzo. As shown in Table 1.2, the elongated C(5)-C(6) and C(7)-C(8) distances of 1.418(3) and 1.402(4) Å and the 23.2 ° deviation from planarity of the benzo ring or "buckle" are consistent with zirconium coordination to the C(5) and C(8) atoms, suggesting a resonance structure like the one depicted on the right of Figure 1.13. Likely, this diamagnetic compound consists of an 18 and a 16 electron zirconium (IV) center, with a dialkyl-like benzo and an $[N_2]^{2-}$ ligand.

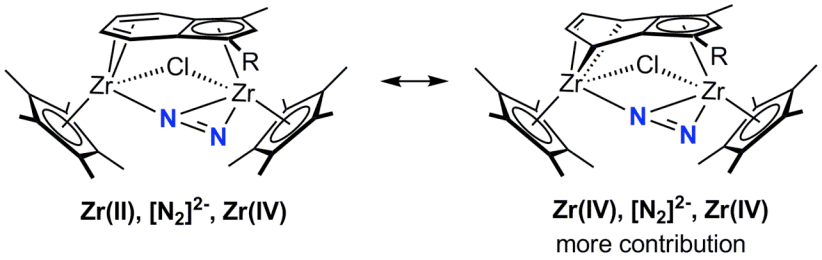

Figure 1.13. Possible resonance structures for **16-N_2Cl** and **17-N_2Cl**.

Protonation studies of the unique side-on, end-on dinitrogen complexes were also conducted. As with the weakly-bound, end-on N_2 compounds, protonation with hydrochloric acid resulted in liberation of hydrazinium chloride, but unlike the former, protonation with a weak acid such as water or ethanol also yielded 73 and 66 % N_2H_4, respectively, reiterating the crystallographic data that suggests that these complexes have at least modestly activated $[N_2]^{2-}$ ligands. Unfortunately, no reaction was observed upon hydrogenation of these complexes, even at elevated temperatures and pressures.

Because these reductions to form the side-on, end-on dinitrogen zirconium

compounds involve the loss of an indenyl ring, the reduction of an equimolar amount of zirconium dichloride and Cp^*ZrCl_3 should also theoretically form the N_2 complexes. Sodium amalgam reduction of **6-Cl$_2$** and Cp^*ZrCl_3 under dinitrogen for two days reduced only the trichloride leaving **6-Cl$_2$** intact. Further reduction of the mixture only resulted in a mixture of products and not the desired dinitrogen compound. It is important to stress the different relative rates of reduction for both zirconocene chloride complexes, but it likely appears that ring ejection is not the first step in the formation of these side-on, end-on compounds; displacement of an indenyl must occur after at least a one electron reduction of the zirconium centers and dimerization to form a precursor to the complex with two bridging chlorine atoms observed with **9-Cl$_2$**.

Reduction of a Tetrahydroindenyl Zirconium Diiodide Complex in the Presence of Dinitrogen. Because all of the newly formed indenyl zirconium dinitrogen compounds exhibit coordination of the indenyl benzo, the reduction chemistry of a cyclopentadienyl, tetrahydroindenyl zirconium dihalide was explored in the hopes that if there was no benzo to backdonate to the zirconium, more electron density would be available to activate the dinitrogen. Another possibility could be coordination of additional dinitrogen ligands, such as the case in $[Cp^*_2Zr(\eta^1\text{-}N_2)]_2(\mu_2\text{-}\eta^1,\eta^1\text{-}N_2)$.

Treatment of the final hydrogenation product of **6$_2$-N$_2$**, **6-THI-H$_2$**, with a five fold excess of iodotrimethylsilane, resulted in clean conversion to **6-THI-I$_2$** and trimethylsilane. Sodium amalgam reduction of **6-THI-I$_2$** however did not form any nitrogen containing species as judged by degradation studies with hydrochloric acid (analyzing for hydrazinium chloride or ammonium chloride). Instead, trace amounts of a cyclometalated zirconocene iodide were detected, which upon hydrogenation converts to a 5:1 mixture of the two isomers of the corresponding zirconium hydrido

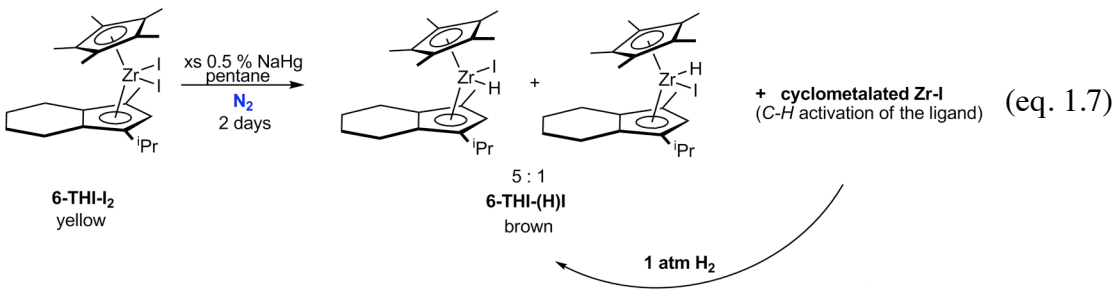

(eq. 1.7)

iodide, **6-THI-(H)I** (eq. 1.7). Both isomers have upfield shifted hydride peaks in the ^{1}H NMR spectrum at 7.96 and 8.08 ppm for the major and minor isomers, respectively, diagnostic of monomeric zirconium hydrides.[7,14,19] In addition, the structure was verified by independent synthesis: treating **6-THI-H$_2$** with only one equivalent of iodotrimethylsilane. While the source of the hydride is unknown, it is plausible that it arises from the mechanism depicted in Figure 1.14, where the reduction of the starting diiodide does initially form an η^5,η^5-

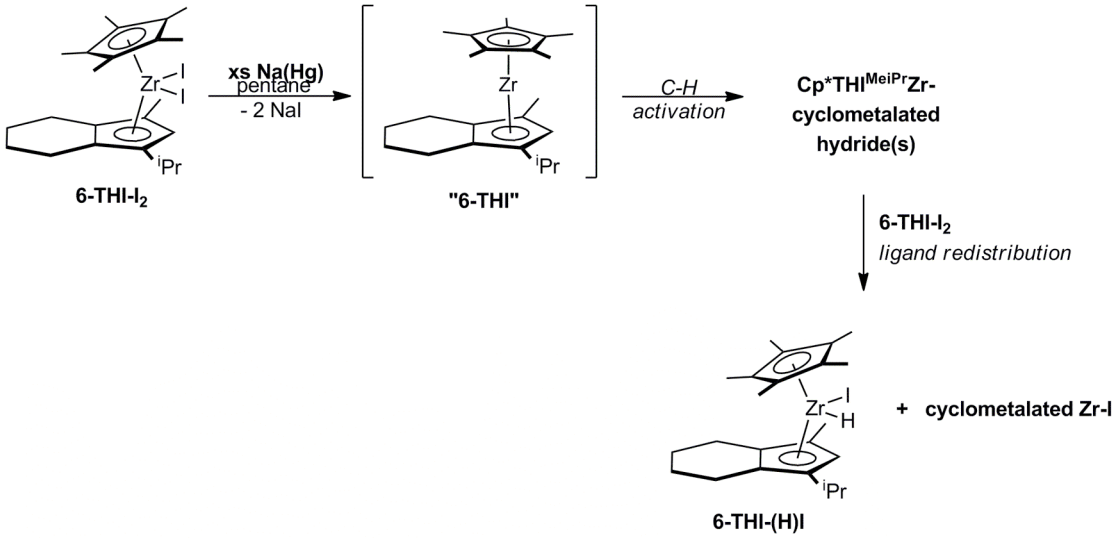

Figure 1.14. Possible mechanism for the formation of **6-THI-(H)I** from the reduction of **6-THI-I$_2$**.

Cp* indenyl zirconocene sandwich intermediate, which instead of coordinating dinitrogen does a C-H bond activation of the ligand forming a cyclometalated hydride(s). Then this latter compound and the starting **6-THI-I$_2$** undergo a ligand redistribution of the hydride and an iodide, resulting in formation of **6-THI-(H)I** and

the observed cyclometalated iodide, though the two were not observed in a 1:1 ratio. Another possibility is that the hydride comes from the solvent although C-H activation of pentane is unlikely. In any event, exchange of the indenyl for a tetrahydroindenyl, clearly, was a poor choice because of the change in both electronics and sterics. Additionally, it appears that the benzo portion of the indenyl ligand is necessary for stabilizing resulting N_2 complexes.

Sandwich Formation with Bis(indenyl) Zirconium Complexes.[30] Based on the success with the indenyl ligands with less sterically hindered substituents, the corresponding homoleptic bis(indenyl) zirconium dichlorides were also reduced. Shown in Figure 1.15 are the zirconocene dihalides explored. All reductions were performed under conditions identical to that of the mixed-ring zirconocenes. In cases where two 1-R, 3-Me (R = $CHMe_2$, CMe_3) substituted indenyl ligands are present, *rac* and *meso* diastereomers were present. Both **13-Cl$_2$** (R = $CHMe_2$) and **14-Cl$_2$** (R = CMe_3) were prepared as an equimolar mixture of *rac* and *meso* isomers and no attempts were made to separate the two prior to alkali metal reduction. Despite the lack of any tractable product when reducing **2-Cl$_2$**, **10-Cl$_2$** – with two of the 2-Me-indenyl ligands – was included to ensure that the balance of substituting the smaller cyclopentadienyl with an indenyl ligand with only one substituent did not yield a new result.

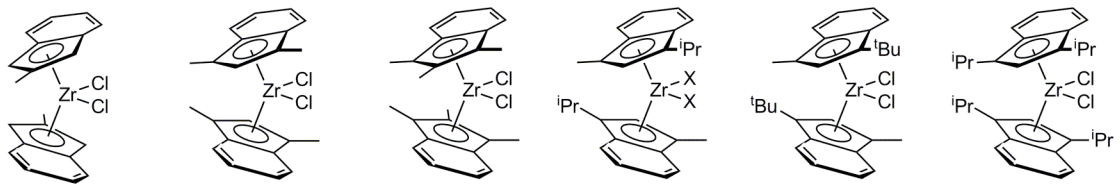

10-Cl$_2$ **11-Cl$_2$** **12-Cl$_2$** ***r/m*-13-X$_2$** **X = Cl, Br, I** ***r/m*-14-Cl$_2$**

Figure 1.15. Bis(indenyl) zirconocene dihalides reduced in this study.

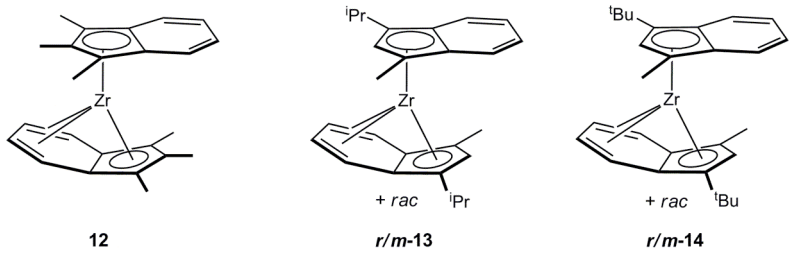

Figure 1.16. Isolable bis(indenyl) zirconocene sandwich complexes prepared.

All attempts to reduce **10-Cl$_2$** under argon or N_2 resulted in partial elimination of the indene and a small amount of C-H activation of the methyl group as evidenced by ^{1}H NMR spectroscopy. It appears that substitution on the 1 and 3 positions is necessary to ensure that ligand modification/loss does not occur upon reduction with harsh alkali metals.

Surprisingly, no tractable product formed when there are two dimethyl indenyl ligands as in **11-Cl$_2$** where the mixed ring zirconocene resulted in formation of a sandwich complex that weakly activated dinitrogen. Here, the reduction only formed unidentifiable paramagnetic complexes. In order to rule out formation of a zirconium (III) intermediate, the paramagnetic species was reduced further with sodium amalgam, but only resulted in loss of the indenyl ligand.

Meanwhile, reductions of the more hindered complexes, **12-Cl$_2$**, *r*/*m*-**13-Cl$_2$** and *r*/*m*-**14-Cl$_2$** under an atmosphere of argon resulted in isolation of zirconium sandwich complexes, (η^9-C_9H_4-1,2,3-Me_3)(η^5-C_9H_4-1,2,3-Me_3)Zr, **12**, *rac*/*meso*(η^9-C_9H_5-1-CHMe_2,3-Me)(η^5-C_9H_5-1-CHMe_2,3-Me)Zr, *r*/*m*-**13** and *rac*/*meso*(η^9-C_9H_5-1-CMe_3,3-Me)(η^5-C_9H_5-1-CMe_3,3-Me)Zr, *r*/*m*-**14**, respectively (Figure 1.16). It is interesting to note that while **13** is formed as an equimolar mixture of *rac* and *meso* diastereomers, recrystallization selectively crystallized *meso*-**13**. However, with *rac*/*meso*-**14**, the ratio of sandwich isomers did not appear to deviate from 1:1, despite attempts to separate by recrystallization. All three sets of zirconocene sandwich

complexes exhibit diagnostic upfield shifted benzo protons and carbons indicative of η^9 coordination of the indenyl ligand. Due to the interconversion between the η^9, η^5 and the η^5, η^9 bis(indenyl) zirconium sandwich forms depicted earlier in Figure 1.3b, the ^{1}H NMR spectra have broad benzo peaks, like all previously reported bis(indenyl) zirconium sandwich complexes.[12]

X-ray diffraction studies on *meso*-**13** were performed previously.[30] The crystal structure, as shown in Figure 1.17, verified the η^9, η^5 bis(indenyl) zirconocene sandwich structure. Similar to other zirconocene sandwich complexes, the η^9-coordinated indenyl ring exhibits a bending of 38.9 ° from planarity between the benzo and the cyclopentadienyl rings. Elongated C(5)-C(6) and C(7)-C(8) bond

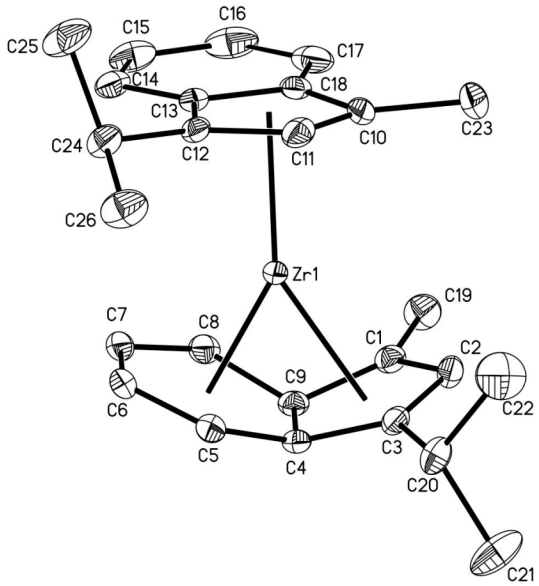

Figure 1.17. Molecular structure of ***meso*-13** with 30 % probability elipsoids.

distances of 1.417(2) and 1.417(2) Å and a slight benzo pucker of 5.9 ° are consistent with a two electron reduction of the indenyl.

With these isolable bis(indenyl) zirconocene sandwich complexes in hand, attempts were made to activate dinitrogen. ^{1}H NMR studies in benzene-d_6 established the ease of accessing the η^5, η^5 bis(indenyl) zirconium (II) intermediate of ring

interconversion, so coordination of dinitrogen is theoretically possible. However after months under an atmosphere of N_2, no change was observed by ^1H NMR spectroscopy. This is likely due to the presence of the additional bulky indenyl that prevents the dimerization that appears necessary for stabilizing a zirconocene dinitrogen complex.

Table 1.3. Comparison of selected crystallographic data for ***meso*-13**, **[13-NaCl]$_2$N$_2$**, **[13-NaI]$_2$N$_2$** and **[13-Cl]$_2$N$_2$(Na){Na(18-crown-6)$_{1.5}$}**.

Numbering Scheme for Indenyl[a]

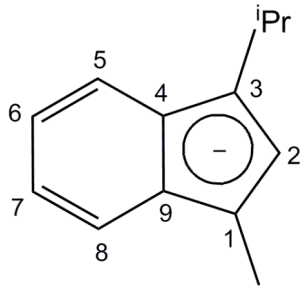

	***meso*-13**	**[13-NaCl]$_2$N$_2$**	**[13-NaI]$_2$N$_2$**	**[13-Cl]$_2$N$_2$(Na){Na(18-crown-6)$_{1.5}$}[d]**
C(4)-C(5) (Å)	1.4636(18)	1.399(8)	1.418(5)	1.434(6)
C(5)-C(6) (Å)	1.417(2)	1.369(9)	1.360(5)	1.366(6)
C(6)-C(7) (Å)	1.389(2)	1.437(10)	1.399(6)	1.415(7)
C(7)-C(8) (Å)	1.417(2)	1.322(9)	1.353(6)	1.371(6)
C(8)-C(9) (Å)	1.4606(19)	1.415(8)	1.420(5)	1.412(6)
N(1)-N(1a)/N(2) (Å)	N/A	1.347(7)	1.316(5)	1.315(4)
Zr(1)-N(1) (Å)	N/A	1.879(4)	1.901(2)	1.884(3) 1.891(3)
η^9 Fold Angle (°)[b]	38.9	N/A	N/A	N/A
η^5 Fold Angle (°)[b]	0.5	6.1 7.3 (with Na coord)	1.6 5.2 (with Na coord)	6.1/4.2 3.1/4.2 (with Na coord)
Dihedral Angle (°)[c]	N/A	61.6	63.1	74.5

[a] Indenyl labeling scheme based on the structure in Figure 1.17. [b] Defined as the angle between the planes formed by the five-membered cyclopentadienyl and the six-membered benzo rings of the indenyl. [c] Defined as the angle between the planes of the zirconium and the cyclopentadienyl centroids. [d] The numbering scheme for the crystal structure of **[13-Cl]$_2$N$_2$(Na){Na(18-crown-6)$_{1.5}$}** differs slightly from the others so the bond distances are shown based on the figure included with the table for comparison.

Strong Activation of Dinitrogen with Bis(indenyl) Zirconium Complexes.[30] While dinitrogen activation from isolable bis(indenyl) zirconium sandwich compounds was unsuccessful, the sodium amalgam reduction of **13-Cl$_2$** under an atmosphere of N_2 yielded an interesting result. (Reduction of **12-Cl$_2$** and *r*/*m*-**14-Cl$_2$** under dinitrogen still afforded the zirconocene sandwiches **12** and *r*/*m*-**14**, respectively.). Unfortunately, NMR spectroscopy was not helpful since all peaks were broad at 22 ºC in a benzene-d_6 solution. Protonation with HCl yielded 45 % of N_2H_4·HCl. Toepler pump analysis of the decomposed product and elemental analysis all tested positive for nitrogen (vide infra). Unfortunately, a clear N-N stretch was not detected by infrared spectroscopy.

As shown in Figure 1.18a, the structure of [(η^5-C_9H_5-1-$CHMe_2$-3-(Me))(η^5-C_9H_5-1-(^{i}Pr)-3-(Me))Zr(NaCl)]$_2$(μ_2-η^1,η^1-N_2), **[13-NaCl]$_2$N$_2$** was determined by X-ray diffraction and found to be a dimeric dinitrogen complex with inclusion of two equivalents of sodium chloride, where the sodium cations are bound η^2 to indenyl benzo rings. Like in the structure of **13**, the indenyl ligands about each zirconium center are ligated in a *meso* manner. As presented in Table 1.3, the N-N bond distance of 1.352(5) Å and short Zr=N bond lengths of 1.878(3) Å are indicative of a strongly activated $[N_2]^{4-}$ ligand such as in [(η^5-$C_5Me_4H)_2Zr]_2$(μ_2-η^2,η^2-N_2) (1.377(3) Å) and suggestive of zirconium imido character.[31] Also, it is important to note that the coordination of the benzo with a sodium atom instead of a zirconium does not appear to reduce the benzo ring. As a comparison to the η^9 indenyl ligand in **13**, the indenyl ligand that is coordinated η^2 to a Na on **[13-NaCl]$_2$N$_2$** has C(5)-C(6) and C(7) C(8) of 1.370(7) and 1.377(7) Å, is not as elongated as that in **13**: 1.417(2) and 1.417(2) Å. In addition, the indenyl in **13** is folded in such a way that the cyclopentadienyl and benzo rings deviate from planarity by 38.9 °, whereas they barely do so in **[13- NaCl]$_2$N$_2$** with an angle of 7.3 °. With all of these data, along with the presence of chloride

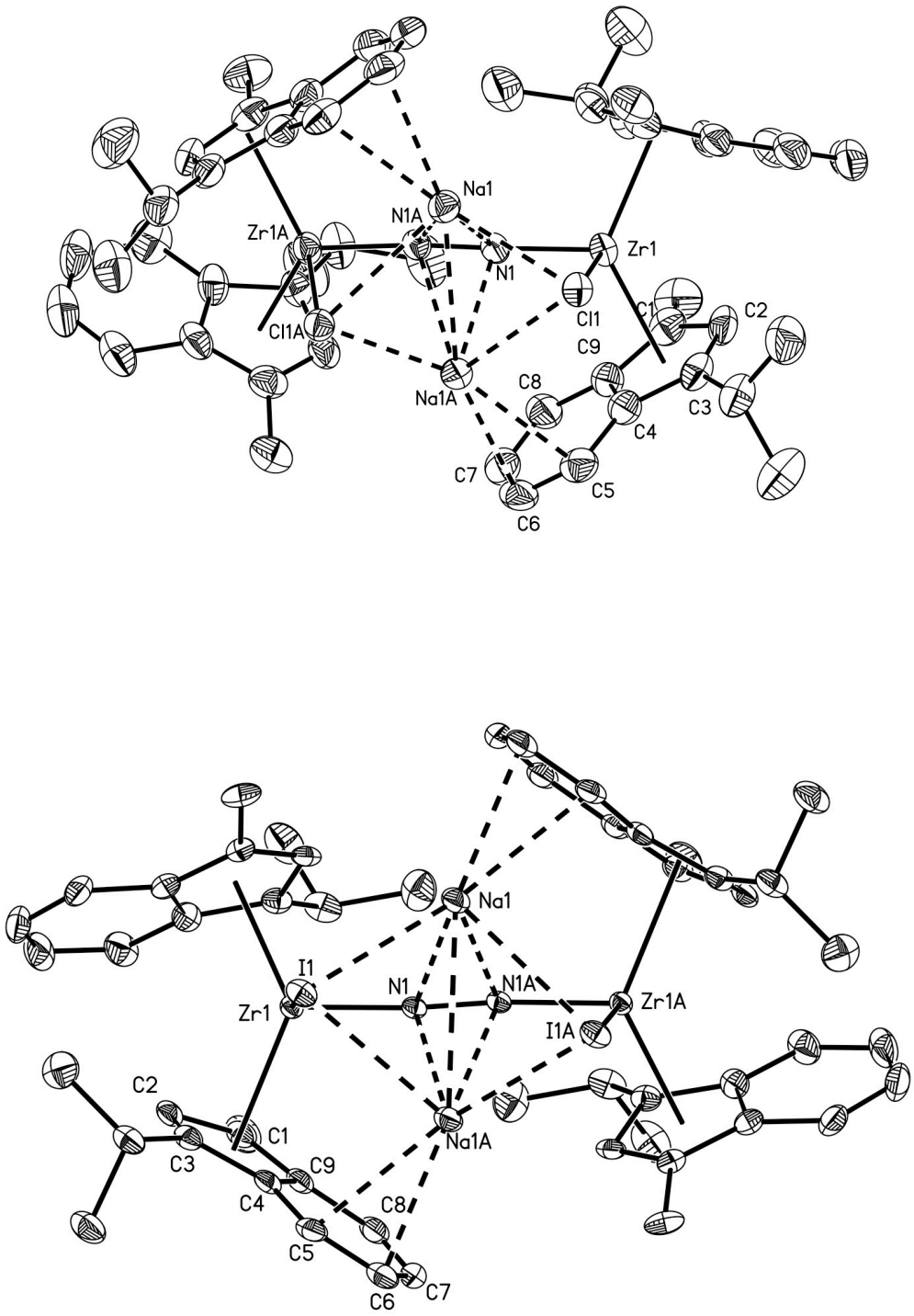

Figure 1.18. Molecular structures of **[13-NaCl]$_2$N$_2$** (top) and **[13-NaI]$_2$N$_2$** (bottom) at 30 % probability elipsoids. Hydrogen atoms removed for clarity.

ligands, each zirconium center can be assigned as an 18 electron Zr(IV) atom in this dianionic complex.

Recall that attempts were made to eliminate zirconium coordination of the benzo rings by replacement of an indenyl with a tetrahydroindenyl ligand; however dinitrogen activation was not observed. Clearly, the formation of **[13-NaCl]$_2$N$_2$** is a better indication of the role of the benzo ring in stabilizing zirconium dinitrogen compounds. With the sodium cations peeling the benzos away from the zirconium, it does, indeed, allow for more back-donation into the dinitrogen ligand, increasing the degree of activation.

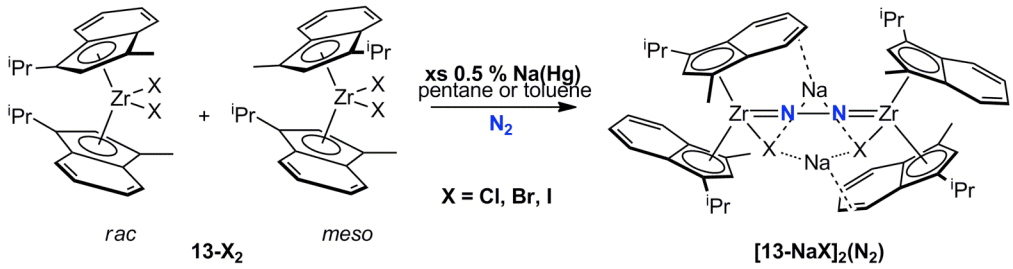

(eq.1.7)

In addition to **[13-NaCl]$_2$N$_2$**, the corresponding sodium bromide, **[13-NaBr]$_2$N$_2$**, and sodium iodide, **[13-NaI]$_2$N$_2$**, compounds were also synthesized from *rac*/*meso*-**13-Br$_2$** and *rac*/*meso*-**13-I$_2$** (eq 1.7). **[13-NaI]$_2$N$_2$** was also characterized by single crystal X-ray crystallography and depicts a structure similar to that of the sodium chloride compound as shown in Figure 1.18b. As shown in Table 1.3, the N-N bond distance of 1.316(5) and Zr-N length of 1.901(2) Å portray a slightly weaker activation of dinitrogen due to the attenuation of the zirconium to nitrogen backbonding. Just as with **[13-NaCl]$_2$N$_2$**, the sodium cations are bound η^2 to indenyl benzos and as judged by the metrical parameters of the benzo ring show little to no ligand reduction and only a slight 5.2 ° deviation from planarity between the cyclopentadienyl and the benzo rings.

Despite the fact that single crystal X-ray crystallography establish that these

dicationic complexes are diamagnetic with two Zr(IV) centers, the peaks in the ^{1}H NMR spectra are all broad but within a small 7 ppm shift range. Most bis(indenyl) zirconium (II) or (IV) complexes have resonances in this window. Magnetic susceptibility measurements verify the diamagnetism and EPR spectroscopy indicated < 5 % amount of EPR active material. Variable temperature ^{1}H NMR experiments of a toluene-d_8 solution of **[13-NaCl]$_2$N$_2$** ranging from -80 to 60 ºC established only a minimal sharpening of peaks at lower temperatures. Likely, the broadness is due to the salt inclusion or interaction with the trace quantity of paramagnetic material.

Like NMR spectroscopy, infrared spectroscopy was also inconclusive in confirming the identity of the bulk of the reduction product by sodium amalgam of **13-X$_2$** as no clear N_2 stretch was observed. Careful probing for a stretch around 1600 - 700 cm^{-1} that shifted appropriately with ^{15}N-labeled **[13-NaCl]$_2$^{15}N$_2$** (made by performing the reduction under an atmosphere of $^{15}N_2$ gas) was not informative. Raman spectroscopy would be ineffective as the isomer of the crystal structure is not centrosymmetric, though an attempt was made on **[13-NaCl]$_2$N$_2$** and nothing informative was obtained. As a calibration, Cummins and coworkers report a centrosymmetric bis{tri(amido)molybdenum}-end-on dinitrogen complex, $\{(N[^tBu]Ar)_3Mo[B(Ar^F)_4]\}_2(\mu_2\text{-}\eta^1,\eta^1\text{-}N_2)$ (Ar = 3,5-$C_6H_3Me_2$; Ar^F = 3,5-$C_6H_3(CF_3)_2$), where the dinitrogen is a "diimido-type", with an intense Raman N-N shift at 1503 which shifted appropriately to 1438 cm^{-1} for the ^{15}N isotopologue.[32] In Schrock and coworkers', "diimido-type" Ta=N-N=Ta complex, $[(CHCMe_3)Me(PMe_3)_2Ta]_2(\mu_2\text{-}\eta^1,\eta^1\text{-}N_2)$, the only infrared band that shifted in the ^{15}N-labeled complex was observed at 847 cm^{-1}, which is likely the Ta-N stretch.[33]

The identity of the bulk reduction products was confirmed as the structures determined by the two single-crystal X-ray structures by combustion analysis (2.44 of the expected 2.77 % N for **[13-NaCl]$_2$N$_2$**) and reactivity studies. Toepler pump

analysis of the degradation of **[13-NaCl]$_2$N$_2$** with either I_2 or $PbCl_2$ afforded 95 and 91 % of the expected dinitrogen gas, along with the appropriate **13-X$_2$** (X = I, Cl) compound. Importantly, protonation of each dinitrogen complex with either hydrochloric acid or water afforded 45 % N_2H_4·HCl or 96 % N_2H_4, respectively, which not only verifies the presence of a dinitrogen complex but also confirms that the N_2 is highly activated, consistent with the X-ray metrical parameters.

The hydrogenation of these strongly activated dinitrogen complexes afforded the same products – as judged by the identical complex mixture of sharp peaks in the ^{1}H NMR spectra despite the different starting material – along with free indene. It appears that the addition of hydrogen results in loss of two equivalents of NaX, which in some cases displaces a coordinated indene as well. Importantly, there is no zirconocene dihydride observed, indicating retention of the coordinated N_2. Infrared spectroscopy indicates the formation of an N-H bond by a stretch at 3238 which shifts appropriately to 2403 cm^{-1} upon addition of deuterium gas to either of the three **[13-NaX]$_2$N$_2$** complexes. Protonation of these hydrogenated products with either hydrochloric acid or water afford hydrazonium chloride, suggesting a hydrazido, [HN-NH], ligand (eq 1.9).

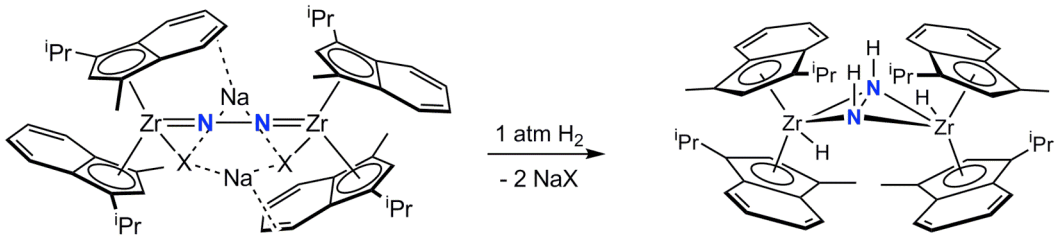

[13-NaX]$_2$(N$_2$) + 9 isomers **[13-H]$_2$(N$_2$H$_2$)** (eq. 1.9)

The remainder of the structure was confirmed by a combination of ^{1}H-^{15}N HSQC and ^{1}H-^{15}N HMBC NMR spectroscopy (Figure 1.20), which depicted the presence of at least ten different Zr-[HN-NH]-Zr cores and showed that there were $^2J_{N\text{-}H}$ couplings between the hydrazido *N*-Hs and another set of hydrides centered about

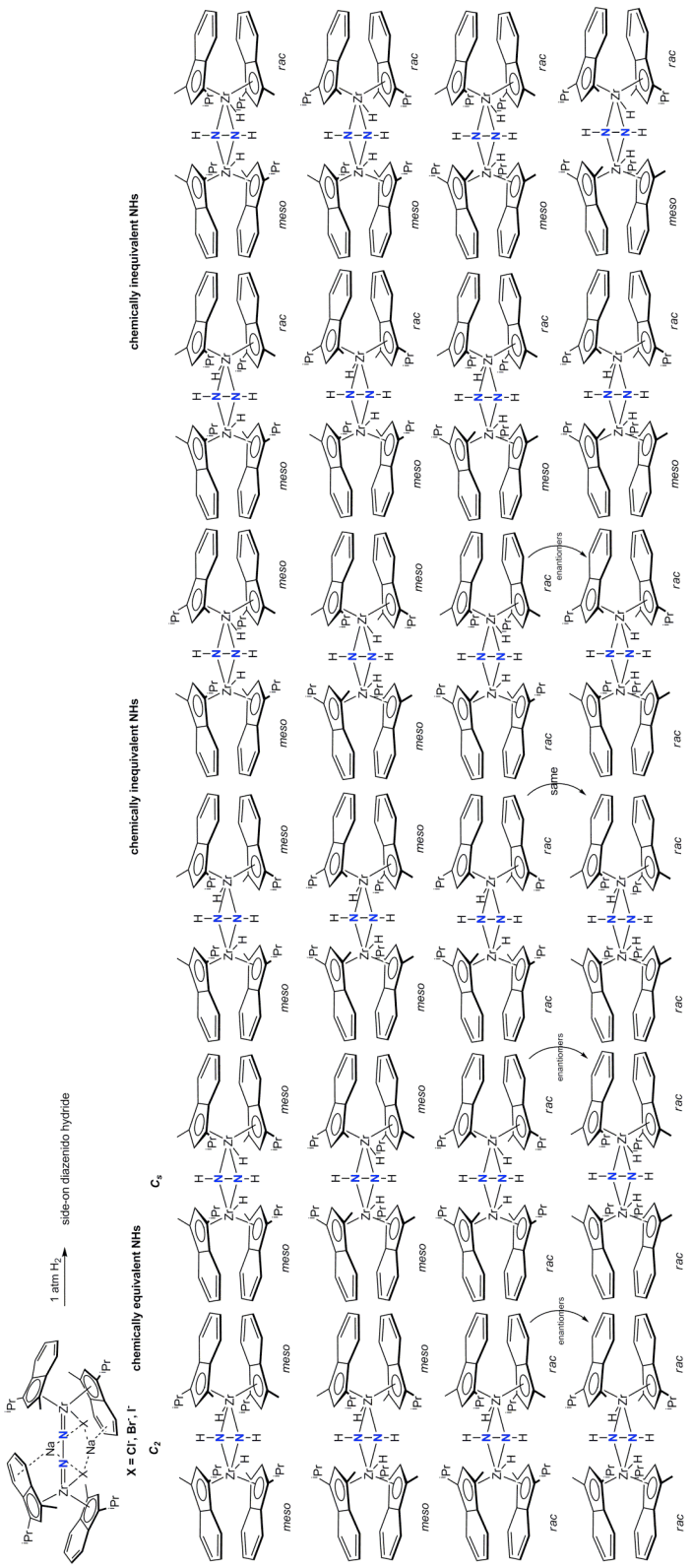

Figure 1.19. Different possible isomers of **[13-H]$_2$(N_2H_2)**.

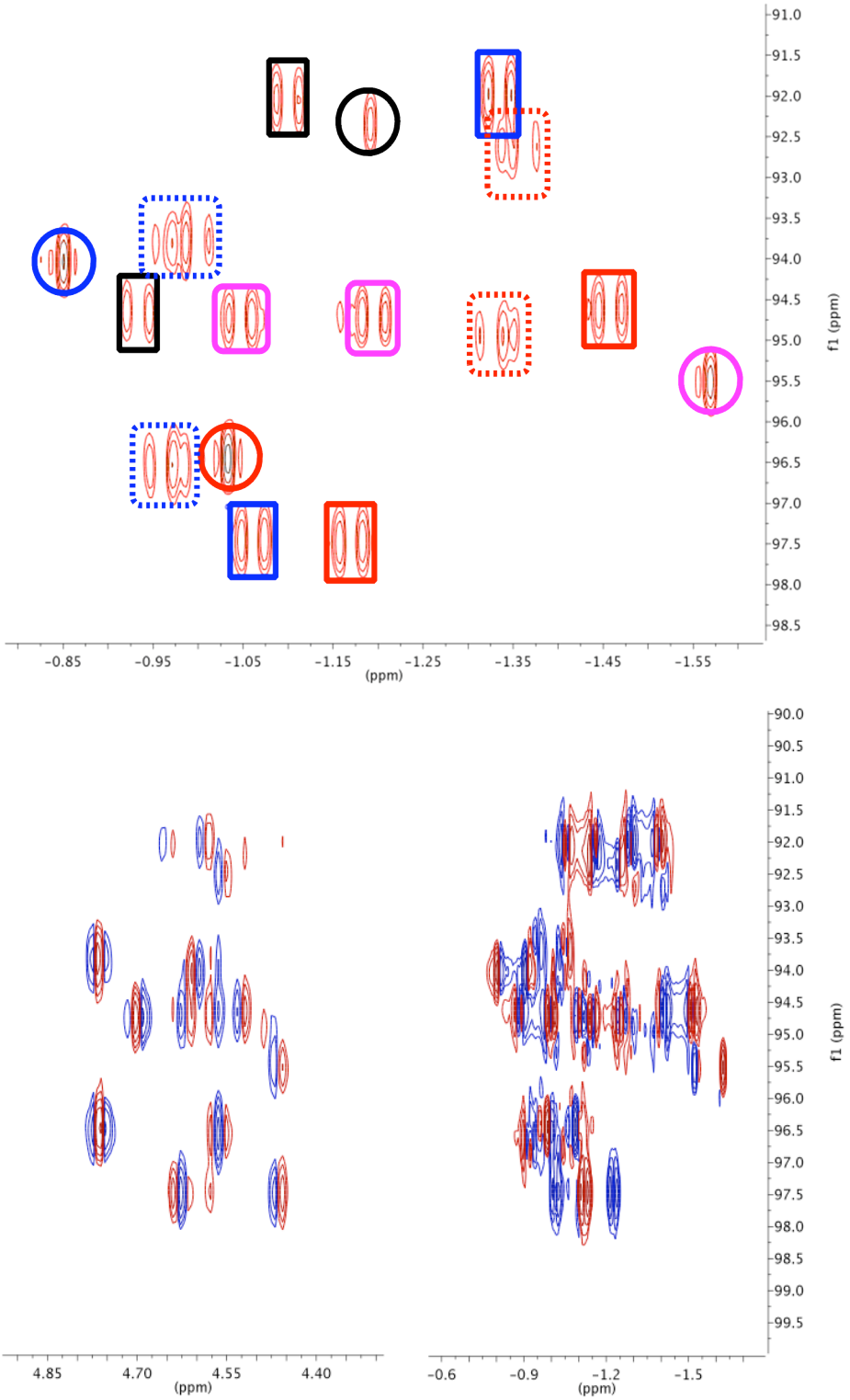

Figure 1.20. ^{1}H, ^{15}N HSQC (top) and ^{1}H, ^{15}N HMBC (bottom) NMR spectra of the hydrogenation products of **[13-NaX]$_2$N$_2$**. The top spectrum depicts ten different isomers.

4.5 ppm, suggesting a zirconium hydride bond. Importantly, the two-dimensional NMR experiments established that the ^{15}N NMR shifts appear between 92 and 98 ppm and the hydrazido N-*H*s between –0.81 and –1.44 ppm, indicative of side-on hydrazido coordination.[11] The ten different isomers arise from the presence of both *rac* or *meso* diastereomers in dimeric structures, along with various possible Zr-H and N-H bond stereochemistries that results in 20 different possible isomers which are distinguishable by NMR spectroscopy as depicted in Figure 1.19.

Computational studies have posited that "side-on, η^2 coordination of N_2 in transition-metal systems is required for its hydrogenation."[34] Therefore, the observation of these end-on dinitrogen complexes that hydrogenate to form a side-on bound hydrazido hydride complex, **[13-H_2](N_2H_2)** refutes this claim. Also interesting about these results are that side-on hydrazido hapticity is the same as that from the hydrogenation of zirconocene[9,35,36] and hafnocene[37] side-on bound dinitrogen complexes! This verifies the mechanism of hydrogenation originally proposed in the zirconocene side-on bound dinitrogen complexes,[35] where the first step is formation of a end-on bound dinitrogen complex where the zirconium-nitrogen bond is "imido-like" just like the structure of **[13-NaX]$_2$$N_2$** depicts. Then, the rate determining step is the formal 1,2 addition of hydrogen across the Zr=N bond to form an end-on hydrazido hydride, which quickly isomerizes to the observed side-on bound hydrogenated product. It appears that in the bis(indenyl)zirconium system the presence of the NaX prevents the side-on N_2 coordination and that upon hydrogenation, which results in loss of the salt, the hydrazido can finally coordinate side-on between the two zirconium centers.

With a bis(indenyl) zirconocene hydrazido hydride in hand, various electrophiles were added. Addition of iodomethane, methylene chloride or methyl triflate all resulted in the disappearance of the zirconium hydride, balanced by the

formation of methane or chloroform, as evidenced by ^{1}H NMR spectroscopy. In the benzene-d_6 ^{1}H NMR spectrum, the originally upfield shifted N-*H* resonances around 0 ppm have shifted downfield to 7 - 9 ppm, as verified by treatment of the electrophiles with the deuterated **[13-D$_2$]$_2$(N$_2$D$_2$)**. This downfield shift indicates end-on coordination of the hydrazido ligand, forming **[13-X]$_2$(N$_2$H$_2$)** (X = I, Cl, OTf) (eq 1.10).[11]

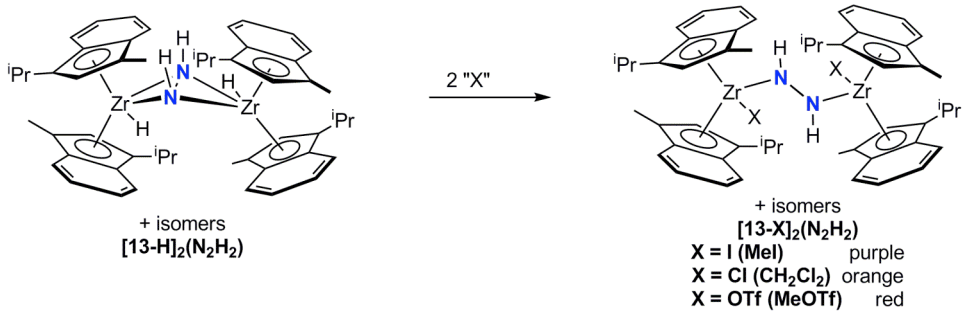

(eq. 1.10)

Addition of Crown Ethers to Dianionic Dinitrogen Complexes. Finally having achieved a set of strongly activated end-on dinitrogen complexes that hydrogenate to hydrazido hydride compounds, attempts were made to remove the sodium cations. Treatment of a benzene-d_6 solution of **[13-NaX]$_2$N$_2$** with two equivalents of either 18-crown-6 or the more appropriate 15-crown-5, resulted in rapid dark brown precipitate formation. Some of the product was still in solution and the ^{1}H NMR showed a sharpening of numerous peaks, indicative of several isomers. Interestingly, in both sets of cryptand additions, only one resonance was observed for the bound ethers. Protonolysis of the products of all three dinitrogen complexes and 15-crown-5 showed the same results: formation of 38 % hydrazinium chloride when protonated with hydrochloric acid and loss of dinitrogen gas when protonated with a weak Brønsted acid. These results highlight the importance of the sodium ions in blocking the indenyl benzos from coordinating to the zirconium center and limiting the degree of

backbonding ability to the dinitrogen, resulting in a less reduced N_2 ligand. Importantly, attempts to hydrogenate the sodium cation sequestered dinitrogen complexes, **[13-X]$_2$(N_2){Na(crown-ether)}$_2$**, resulted in no reaction after one week under the same conditions used to hydrogenate **[13-NaX]$_2$$N_2$**, likely due to the inability to remove the halide ion. All of the above results were the same when an excess of 20 equivalents of tetrahydrofuran were used in place of 15-crown-5, with the exception that no precipitate formed.

Protonolysis of the products of all three dinitrogen complexes with incorporated 18-crown-6, however, resulted in formation of 43 % of the expected hydrazium salt when treated with water, meaning not all of the products had weakly activated N_2 ligands. This inefficiency of 18-crown-6 to sequester both sodium ions in all of the dinitrogen complexes was clearly explained by obtaining a crystal structure of one of the products that had immediately precipitated upon addition of the cryptand. As shown in Figure 1.21, only one sodium cation had been removed from the coordination sphere of the zirconocene, resulting in a dinitrogen ligand that is still modestly activated. As shown in Table 1.3, the bond distances of **[13-Cl]$_2$(N_2)(Na){Na(crown-ether)}$_n$** (n = 1.5) only differ slightly from that of **[13-NaCl]$_2$$N_2$** but the N-N is still slightly contracted from 1.352(5) to 1.315(4), while the Zr-N distance does not appear to change: 1.878(3) to 1.884(3) Å. Likely, this n = 1.5 product is a result of its rapid precipitation upon the introduction of the crown ether, which also forms the other products where n = 1, 2. This fast precipitation of products with varying degree of N_2 activation is the reason for the low value obtained in the hydrazine test.

What Dictates N_2 Activation? As briefly mentioned previously, it appears that there is a small window for indenyl zirconocene complexes to coordinate dinitrogen. If the

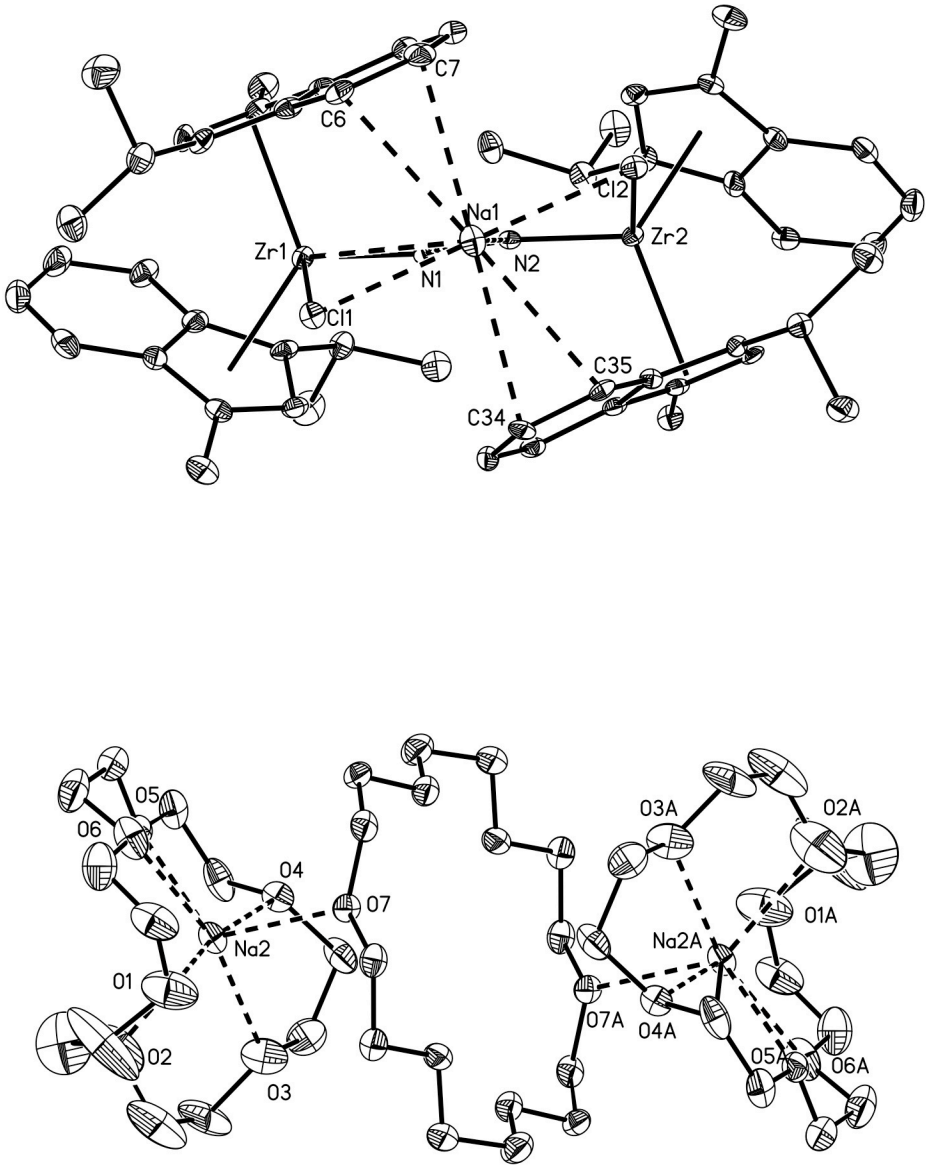

Figure 1.21. Molecular structures of dianion (top) and cation x 2 (bottom) for **[13-Cl]$_2$(N$_2$)(Na){Na(crown-ether)}$_{1.5}$.**

substituents on the indenyl ring are too bulky, stable η^9 indenyl zirconocene sandwich compounds are formed whether reduced under dinitrogen or not; if the substituents are too small, neither sandwich nor N_2 complexes are formed. As depicted in Figure 1.22, the intermediate where there is a methyl group on the 1 position and an isopropyl on the 3 position is sterically poised for a wealth of dinitrogen activation, varying depending on the conditions of reduction. However, there is no clear explanation as to why **9-X$_2$** (X = Cl, I), with one di(trimethylsilyl)indenyl ligand, would form a side-on, end-on N_2 compound upon reduction under an atmosphere of dinitrogen. The bis(indenyl)zirconcene conformer shows no affinity to bind N_2, only formation of the sandwich complex and cyclometalated hydride with a structure similar to **9-CMH**.

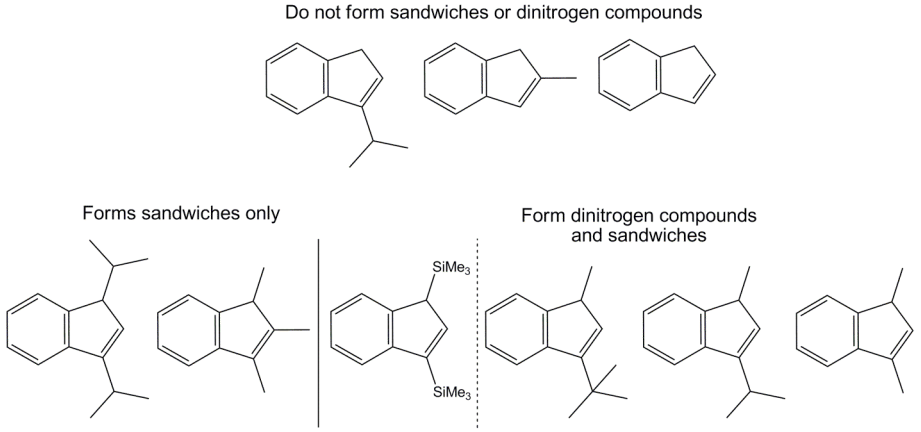

Figure 1.22. Categorizing of indenyl ligands that only formed stable sandwiches, activated N_2 or none of the above.

An evaluation of the electronics of these different zirconocene complexes was undertaken by preparing the corresponding dicarbonyl compounds. All were synthesized by reducing the dihalides with either magnesium or sodium amalgam under an atmosphere of CO. Presented in Table 1.4, are the carbonyl stretching frequencies of the zirconocene dicarbonyls, including that for N_2 activator $Cp^*_2Zr(CO)_2$[38] and sandwich forming bis(diisopropylindenyl)zirconium dicarbonyl.[39] Note that several dicarbonyl complexes have multiple symmetric and asymmetric

carbonyl stretching frequencies; this is due to different rotamers of the complexes that are distinguishable by the IR experiment and has been observed previously in other bis(indenyl) zirconocene dicarbonyl compounds.[39] It appears that there are no clear trends, especially since both **2-(CO)$_2$** – whose corresponding dichloride reduction did not produce any tractable products – and **3-(CO)$_2$** – whose dichloride formed an isolable sandwich complex which activates N_2 – have the same symmetric and asymmetric stretching frequencies. In fact, with the exception of **1-(CO)$_2$**, all of the mixed ring zirconocene dicarbonyls are very similar electronically. Therefore, it seems that N_2 activation within this series of sufficiently electron rich ligands is dictated primarily by steric effects.

Table 1.4. Comparison of carbonyl stretching frequencies for the corresponding dicarbonyl complexes of all zirconocene dihalides reduced.

Compound	$\nu(CO)_{sym}$ (cm^{-1})	$\nu(CO)_{asy}$ (cm^{-1})	$\nu(CO)_{ave}$ (cm^{-1})
Cp*$_2$Zr(CO)$_2$[38]	1946	1853	1899.5
1-(CO)$_2$	1961	1873	1917
2-(CO)$_2$	1952	1863	1907.5
3-(CO)$_2$	1952	1863	1907.5
4-(CO)$_2$	1950	1858	1904
5-(CO)$_2$	1954	1864	1909
6-(CO)$_2$	1950	1860	1905
7-(CO)$_2$	1948	1859	
	1954	1864	
	1960	1871	
8-(CO)$_2$	1949	1856	1902.5
9-(CO)$_2$	1951	1864	
	1964	1881	
10-(CO)$_2$	1956	1872	1914
11-(CO)$_2$	1956	1872	1914
12-(CO)$_2$	1953	1862	1907.5
***r*/*m*-13-(CO)$_2$**	1956, 1967	1866	
***r*/*m*-14-(CO)$_2$**	1971,1966	1885, 1881	
	1958, 1951	1873, 1865	
(C_9H_5-1,3-(iPr)$_2$)$_2$Zr(CO)$_2$[39]	1952	1859	1905.5

Conclusions

A series of indenyl zirconium dinitrogen complexes were synthesized with weakly activated end-on; modestly activated side-on, end-on; and highly activated end-on N_2 ligands. Importantly, while no catalytic cycle to activate and functionalize dinitrogen was found with these compounds, the activation was shown to occur readily from three isolable zirconocene sandwich complexes – without the direct use of harsh alkali metals. It also appears that the steric environment of the indenyl is the predominant factor to whether or not an indenyl zirconocene complex will coordinate dinitrogen. Interestingly, different modes of indenyl coordination were observed in each set of dinitrogen complexes: η^2 to Zr, η^4 to Zr, and η^2 to Na. Seemingly, removal of benzo coordination to the zirconium center allows for a greater degree of dinitrogen activation as the η^2 and η^4-benzo to zirconium are only weakly to modestly activated. Additionally, the removal of the sodium atoms from the coordination sphere in the strongly activated examples results in re-coordination to the zirconocene and an attenuation of dinitrogen reduction.

Also shown was the first example of hydrogenation from a set of strongly activated end-on dinitrogen complexes, where the hydrazido ligand is coordinated in a side-on fashion between the two zirconium centers. This observation refutes an earlier computational claim that only side-on bound dinitrogen complexes can undergo hydrogenation to form elaborated nitrogen centers and provides evidence for a hydrogenation mechanism that involves 1, 2 addition of dihydrogen across end-on Zr=N bonds.

Experimental

General Considerations. All air- and moisture-sensitive manipulations were carried out using standard vacuum line, Schlenk or cannula techniques or in an M. Braun inert atmosphere drybox containing an atmosphere of purified nitrogen. Solvents for air-

and moisture-sensitive manipulations were initially dried and deoxygenated using literature procedures.[40] Benzene-d_6 was distilled from sodium metal under an atmosphere of argon and stored over 4 Å molecular sieves or titanocene. Argon and hydrogen gas were purchased from Airgas Incorporated and passed through a column containing manganese oxide on vermiculite and 4 Å molecular sieves before admission to the high vacuum line. Carbon monoxide was passed through a liquid nitrogen cooled trap immediately before use. 18-crown-6 was dried overnight on a vacuum line and 15-crown-5 distilled from calcium hydride.

^{1}H NMR spectra were recorded on a Varian Inova 400 Spectrometer operating at 399.779 MHz (^{1}H), while ^{13}C spectra were collected on a Varian Inova 500 spectrometer operating at 125.704 MHz. All chemical shifts are reported relative to $SiMe_4$ using ^{1}H (residual) or ^{13}C NMR chemical shifts of the solvent as a secondary standard. ^{15}N NMR spectra were recorded on a Varian Inova 500 Spectrometer operating at 50.663 MHz and chemical shifts were externally referenced to liquid ammonia. NOESY experiments were recorded on a Varian 500 Inova spectrometer operating at 499.920 MHz for ^{1}H. HSQC and HMBC experiments were recorded on a Varian 600 Inova spectrometer operating at 599.773 MHz for ^{1}H and 60.779 MHz for ^{15}N. ^{2}H NMR spectra were recorded on a Varian Inova 500 spectrometer operating at 76.740 MHz and the spectra were referenced using an internal benzene-d_6 standard.

Single crystals suitable for X-ray diffraction were coated with polyisobutylene oil in a drybox and were quickly transferred to the goniometer head of a Siemens SMART CCD Area detector system equipped with a molybdenum X-ray tube (δ = 0.71073 A). Preliminary data revealed the crystal system. A hemisphere routine was used for data collection and determination of lattice constants. The space group was identified and the data were processed using the Bruker SAINT program and corrected for absorption using SADABS. The structures were solved using direct methods

(SHELXS) completed by subsequent Fourier synthesis and refined by full-matrix least-squares procedures. Infrared spectra were collected on a Thermo Nicolet spectrometer. Elemental analyses were performed at Robertson Microlit Laboratories, Inc., in Madison, NJ. The following compounds were prepared according to literature procedures: Cp^*ZrCl_3,[41] **1**,[42] **C_9H_6-1,3-$(Me)_2$**, [43] **C_9H_6-1,2,3-$(Me)_3$**,[3] **8-Cl_2**,[44] **8,**[4] **8-$(CO)_2$**[4] and **10-Cl_2**[45]

Preparation of C_9H_7-1-(Me). A 500 mL round bottom flask was charged with 6.30 g (51.21 mmol) of Li[C_9H_7] and THF was added. A 180° needle valve was attached and the assembly was removed from the drybox and evacuated on a vacuum line. Against an argon counterflow, 4.7 mL (51.68 mmol) of dimethyl sulphate was added at –78 °C. The solution was warmed to room temperature and stirred for twelve hours. To the reaction mixture, 5 mL of concentrated NH_4OH was added and stirred for half an hour, quenching the excess dimethyl sulphate. Approximately 100 mL of H_2O was then added, the product extracted with three portions of diethyl ether, and dried over $MgSO_4$. Filtration followed by solvent removal *in vacuo* afforded 5.3 g (80 %) of a yellow oil identified as **C_9H_7-1-(Me)** as reported.[46]

Preparation of C_9H_6-1-(^{i}Pr)-3-(Me). A 500 mL round bottom flask was charged with 7.05 g (43.00 mmol) of Li[C_9H_6-1-(^{i}Pr)] and dissolved in THF. An 180 ° needle valve was attached and the reaction was removed from the drybox and evacuated on a high vacuum line. Against an argon counterflow, 13.4 (215 mmol) of iodomethane was added via syringe to the solution at -78 °C. The reaction mixture was stirred overnight and the solvent removed *in vacuo*. The resulting yellow oil was extracted into pentane in a drybox and filtered through Celite. Subsequent solvent removal afforded 6.30 g (85 %) of a yellow oil identified as C_9H_6-1-(^{i}Pr)-3-(Me) as reported.[47] ^{1}H NMR

(benzene-d_6): δ = 1.12 (d, 8 Hz, 3H, *Me*), 1.19 (d, 4 Hz, 3H, CH*Me*$_2$), 1.21 (d, 4 Hz, 3H, CH*Me*$_2$), 2.76 (m, 1H, C*H*Me$_2$), 3.22 (q, 8 Hz, 1H, allyl C*H*), 5.94 (s, 1H, Cp*H*), 7.18 (br, 1H, benzo), 7.23 (br, 1H, benzo), 7.26 (br, 2H, benzo). ^{13}C {^{1}H} NMR (benzene-d_6): δ = 16.9, 22.4 (2), 27.4 (CHMe$_2$/*Me*), 44.1 (allyl *C*), 120.2, 123.4, 125.4, 126.9, 132.9, 144.8, 150.0, 151.0 (Cp/Benzo).

Preparation of C_9H_6-1-(^{t}Bu)-3-(Me). This molecule was prepared in an identical manner to C_9H_6-1-(^{i}Pr)-3-(Me) with 6.24 g (35.00 mmol) of Li[C_9H_6-1-(^{t}Bu) and 10.9 mL (175 mmol) of iodomethane. Subsequent workup afforded 5.67 g (87 %) of a yellow oil identified as C_9H_6-1-(^{t}Bu)-3-(Me) as reported.[7] ^{1}H NMR (benzene-d_6): δ = 1.11 (d, 7 Hz, 3H, *Me*), 1.31 (s, 9H, C*Me*$_3$), 3.17 (q, 7 Hz, 1H, allyl C*H*), 5.97 (s, 1H, Cp*H*), 7.13 (br, 1H, Benzo), 7.19 (m, 1H, Benzo), 7.27 (m, 7 Hz, 1H, Benzo), 7.52 (m, 7 Hz, 1H, Benzo). ^{13}C {^{1}H} NMR (benzene-d_6): δ = 16.57, 29.53, 33.00 (CMe$_3$/*Me*), 43.08 (allyl *C*), 122.56, 123.18, 124.62, 126.21, 133.29, 151.43, 151.84 (Cp/Benzo). One Cp/Benzo resonance not located.

Preparation of Li[C_9H_5-1-(^{i}Pr)-3-(Me)]. A 1000 mL round bottom flask was charged with 6.30 g (37.00 mmol) of [C_9H_6-1-(^{i}Pr)-3-(Me)], approximately 120 mL of pentane was added and the resulting solution was chilled in a liquid nitrogen cooled cold well for 20 minutes. To the light yellow solution, 25 mL (40.7 mmol) of 1.6 M ^{n}BuLi in hexanes was added and the reaction was stirred overnight depositing an off-white solid. The resulting lithium salt was collected by filtration on a medium porosity frit yielding 4.47 g (71 %) of Li[C_9H_5-1-(^{i}Pr)-3-(Me)].

Preparation of Li[C_9H_5-1-(^{t}Bu)-3-(Me)]. This molecule was prepared in an identical manner to Li[C_9H_5-1-(^{i}Pr)-3-(Me)] using 5.67 g (30.50 mmol) of C_9H_6-1-(^{t}Bu)-3-(Me)]

and 21 mL (34 mmol) of 1.6 M ^{n}BuLi yielding 3.63 g (62 %) of Li[C_9H_5-1-(^{t}Bu)-3-(Me)].

Preparation of (η^5-C_5Me_5)(η^5-C_9H_6-2-Me)$ZrCl_2$ (2-Cl_2). A 100 mL round bottom flask was charged with 500 mg (1.50 mmol) of Cp*$ZrCl_3$ and dissolved in approximately 70 mL of diethyl ether. The pale yellow solution was chilled in a liquid nitrogen cooled cold well for 20 minutes and 205 mg (1.51 mmol) of Li[C_9H_6-2-Me] was then added to the solution and the reaction stirred for two days. The solvent was removed *in vacuo* and the resulting yellow solid washed with pentane and subsequently extracted into toluene and filtered through Celite. Removal of the toluene *in vacuo* yielded 450 mg (70 %) of **2-Cl_2**. Anal. Calcd. for $C_{20}H_{24}ZrCl_2$: C, 56.32; H, 5.67. Found: C, 56.43; H, 5.58. ^{1}H NMR (benzene-d_6): δ = 1.74 (s, 15H, Cp* *Me*), 2.02 (s, 3H, Ind *Me*), 5.99 (s, 2H, Cp*H*), 6.94 (m, 2H, Benzo), 7.31 (m, 2H, Benzo). ^{13}C {^{1}H} NMR (benzene-d_6): δ = 12.40, 16.75 (C_5Me_5, Ind *Me*), 105.99, 123.93, 124.35, 125.05, 127.13, 133.81 (Cp/Benzo).

Preparation of (η^5-C_5Me_5)(η^5-C_9H_5-1,3-$(Me)_2$)$ZrCl_2$ (3-Cl_2). This molecule was prepared in a similar manner to **2-Cl_2** in a 250 mL round bottom flask with 783 mg (2.36 mmol) of Cp*$ZrCl_3$, 353 mg (2.35 mmol) of Li[C_9H_5-1,3-$(Me)_2$] and approximately 140 mL of diethyl ether. This yielded 1.00 g (97 %) of yellow **3-Cl_2**. Anal. Calcd. for $C_{21}H_{26}ZrCl_2$: C, 57.25; H, 5.95. Found: C, 57.01; H, 5.98. ^{1}H NMR (benzene-d_6): δ = 1.79 (s, 15H, Cp* *Me*), 2.07 (s, 6H, Ind *Me*), 5.99 (s, 1H, Cp*H*), 7.14 (m, 2H, Benzo), 7.60 (m, 2H, Benzo). ^{13}C {^{1}H} NMR (benzene-d_6): δ = 12.2, 12.5 (C_5Me_5, Ind *Me*), 109.7, 124.0, 124.6, 125.2, 128.5, 131.5 (Cp/Benzo).

Preparation of (η^5-C_5Me_5)(η^5-C_9H_4-1,2,3-$(Me)_3$)$ZrCl_2$ (4-Cl_2). This molecule was prepared in a similar manner to **2-Cl_2** in a 250 mL round bottom flask with 1100 mg (3.31 mmol) of Cp*$ZrCl_3$, 546 mg (3.31 mmol) of Li[C_9H_4-1,2,3-$(Me)_3$] and approximately 100 mL of diethyl ether. This yielded 1.15 g (76 %) of yellow **4-Cl_2**. Anal. Calcd. for $C_{22}H_{28}ZrCl_2$: C, 58.13; H, 6.21. Found: C, 58.01; H, 6.24. ^{1}H NMR (benzene-d_6): δ = 1.65 (s, 15H, Cp* *Me*), 2.03 (s, 3H, Ind 2-*Me*), 2.15 (s, 6H, Ind 1,3-*Me*), 6.83 (m, 2H, Benzo), 7.30 (m, 2H, Benzo). ^{13}C {^{1}H} NMR (benzene-d_6): δ = 10.7, 11.7, 14.0 (C_5Me_5, Ind *Me*), 110.47, 122.6, 123.5, 124.3, 124.6, 141.0 (Cp/Benzo).

Preparation of (η^5-C_5Me_5)(η^5-C_9H_6-1-(^{i}Pr))$ZrCl_2$ (5-Cl_2). This molecule was prepared in a similar manner to **2-Cl_2** in a 100 mL round bottom flask with 500 mg (1.50 mmol) of Cp*$ZrCl_3$, 247 mg (1.50 mmol) of Li[C_9H_6-1-^{i}Pr] and approximately 70 mL of diethyl ether. This yielded 530 mg (78 %) of yellow **5-Cl_2**. Anal. Calcd. for $C_{22}H_{28}ZrCl_2$: C, 58.13; H, 6.21. Found: C, 57.75; H, 6.25. ^{1}H NMR (benzene-d_6): δ = 1.12 (d, 8 Hz, 3H, CH(CH_3)$_2$), 1.15 (d, 8 Hz, 3H, CH(CH_3)$_2$), 1.80 (s, 15H, Cp* *Me*), 3.76 (m, 1H, C*H*(CH_3)$_2$), 5.57 (d, 2.8 Hz, 1H, Cp*H*), 5.66 (d, 2.8 Hz, 1H, Cp*H*), 7.08 (m, 1H, Benzo), (m, 1H, Benzo), 7.17 (m, 1H, Benzo), 7.62 (m, 1H, Benzo). One benzo resonance not located. ^{13}C {^{1}H} NMR (benzene-d_6): δ = 12.70 (C_5Me_5), 20.79, 24.57, 27.98 ($CHMe_2$), 96.14, 109.72, 123.88, 124.41, 125.69, 125.88, 133.06, 136.66 (Cp/Benzo).

Preparation of (η^5-C_5Me_5)(η^5-C_9H_6-1-(^{i}Pr)ZrI_2 (5-I_2). This molecule was prepared in a similar manner to **2-Cl_2** in a 20 mL scintillation vial with 160 mg (0.26 mmol) of Cp*ZrI_3, 48 mg (0.29 mmol) of Li[C_9H_6-1-^{i}Pr] and approximately 7 mL of diethyl ether. This yielded 68 mg (40 %) of yellow **5-I_2**. ^{1}H NMR (benzene-d_6): δ = 0.96 (d,

7 Hz, 3H, CH(CH_3)$_2$), 1,04 (d, 7 Hz, 3H, CH(CH_3)$_2$), 1.88 (s, 15H, Cp* *Me*), 4.16 (m, 1H, C*H*(CH$_3$)$_2$), 5.40 (d, 2.8 Hz, 1H, Cp*H*), 5.57 (d, 2.8 Hz, 1H, Cp*H*), 7.04 (m, 1H, Benzo), 7.12 (m, 2H, Benzo), (m, 1H, Benzo), 7.77 (m, 1H, Benzo).

Preparation of (η^5-C_5Me_5)(η^5-C_9H_5-1-(^{i}Pr)-3-(Me))$ZrCl_2$ (6-Cl_2). This molecule was prepared in a similar manner to **2-Cl_2** in a 500 mL round bottom flask with 2.21 g (6.64 mmol) of Cp*$ZrCl_3$, 1.18 g (6.64 mmol) of Li[C_9H_5-1-(^{i}Pr)-3-(Me)] and approximately 320 mL of diethyl ether. This yielded 2.56 g (82 %) of yellow **6-Cl_2**. Anal. Calcd. for $C_{23}H_{30}ZrCl_2$: C, 58.95; H, 6.45. Found: C, 57.93; H, 6.34. ^{1}H NMR (benzene-d_6): δ = 1.21 (d, 9.2 Hz, 3H, CH*Me*$_2$), 1.28 (d, 9.2 Hz, 3H, CH*Me*$_2$), 1.79 (s, 15H, Cp* *Me*), 2.12 (s, 3H, *Me*), 3.26 (m, 1H, C*H*Me$_2$), 5.77 (s, 1H, Cp*H*), 7.05 (m, 2H, Benzo), 7.49 (d, 8.4 Hz, 1H, Benzo), 7.67 (d, 8.4 Hz, 1H, Benzo). ^{13}C {^{1}H} NMR (benzene-d_6): δ = 12.42, 12.44 (Cp* *Me*/Ind *Me*), 23.47, 24.00, 28.69 (CHMe$_2$), 119.13, 124.40, 124.73, 125.00, 125.14, 125.35 (Cp/Benzo).

Preparation of (η^5-C_5Me_5)(η^5-C_9H_5-1-(^{t}Bu)-3-(Me))$ZrCl_2$ (7-Cl_2). This molecule was prepared in a similar manner to **2-Cl_2** in a 250 mL round bottom flask with 736 mg (2.21 mmol) of Cp*$ZrCl_3$, 425 mg (2.21 mmol) of Li[C_9H_5-1-(^{t}Bu)-3-(Me)] and approximately 140 mL of diethyl ether. This yielded 700 mg (66 %) of yellow **7-Cl_2**. Anal. Calcd. for $C_{24}H_{32}ZrCl_2$: C, 59.73; H, 6.68. Found: C, 59.50; H, 6.68. ^{1}H NMR (benzene-d_6): δ = 1.37 (s, 9H, C*Me*$_3$), 1.82 (s, 15H, Cp* *Me*), 2.08 (s, 3H, *Me*), 5.81 (s, 1H, Cp*H*), 7.04 (m, 2H, Benzo), 7.51 (m, 1H, Benzo), 7.93 (m, 1H, Benzo). ^{13}C {^{1}H} NMR (benzene-d_6): δ = 12.67, 13.01 (Cp* *Me*/Ind *Me*), 32.32, 35.3 (CMe$_3$), 95.08, 116.91, 124.54, 124.71, 124.79, 125.48, 126.89 (Cp/Benzo). Three Cp/Benzo resonances not located.

Preparation of (η^5-C_5Me_5)(η^5-C_9H_5-1,3-$(SiMe_3)_2$)$ZrCl_2$ (9-Cl_2). This molecule was prepared in a similar manner to **2-Cl_2** in a 250 mL round bottom flask with 476 mg (1.43 mmol) of Cp*$ZrCl_3$, 381 mg (1.43 mmol) of Li[C_9H_5-1,3-$(SiMe_3)_2$] and approximately 100 mL of diethyl ether. This yielded 441 mg (55 %) of yellow **9-Cl_2**. Anal. Calcd. for $C_{25}H_{38}SiZrCl_2$: C, 53.92; H, 6.88. Found: C, 53.66; H, 6.79. ^{1}H NMR (benzene-d_6): δ = 0.36 (s, 18H, Si*Me*$_3$), 1.91 (s, 15H, Cp* *Me*), 6.62 (s, 1H, Cp*H*), 7.12 (m, 2H, Benzo), 7.85 (m, 2H, Benzo). ^{13}C {^{1}H} NMR (benzene-d_6): δ = 1.41 ($SiMe_3$), 13.27 (Cp* *Me*), 118.13, 125.32, 125.37, 128.34, 134.53, 138.74 (Cp/Benzo).

Preparation of (η^5-C_5Me_5)(η^5-C_9H_5-1,3-$(SiMe_3)_2$)ZrI_2 (9-I_2). This molecule was prepared in a similar manner to **2-Cl_2** in a 20 mL scintillation vial with 305 mg (0.50 mmol) of Cp*ZrI_3, 150 mg (0.56 mmol) of Li[C_9H_5-1,3-$(SiMe_3)_2$] and approximately 15 mL of diethyl ether. This yielded 286 mg (77 %) of yellow **9-I_2**. Anal. Calcd. for $C_{25}H_{38}SiZrI_2$: C, 40.59; H, 5.18. Found: C, 40.61; H, 5.38. ^{1}H NMR (benzene-d_6): δ = 0.33 (s, 18H, Si*Me*$_3$), 2.02 (s, 15H, Cp* *Me*), 6.68 (s, 1H, Cp*H*), 7.07 (m, 2H, Benzo), 7.99 (m, 2H, Benzo). ^{13}C {^{1}H} NMR (benzene-d_6): δ = 2.22 ($SiMe_3$), 15.83 (Cp* *Me*), 120.77, 125.09, 126.48, 132.88, 134.35, 137.43 (Cp/Benzo).

Preparation of (η^5-C_9H_5-1,3-$(Me)_2$)$_2ZrCl_2$ (11-Cl_2). A 500 mL round-bottom flask was charged with 2.54 g (16.90 mmol) of Li[C_9H_5-1,3-$(Me)_2$] and dissolved in approximately 150 mL of diethyl ether. The pale yellow solution was chilled in a liquid nitrogen cooled cold well for 20 minutes and 1.97 g (8.45 mmol) of $ZrCl_4$ was then added to the solution and the reaction stirred for two days. The solvent was removed *in vacuo* and the resulting yellow solid washed with pentane and subsequently extracted into methylene chloride and filtered through Celite. Removal of the methylene chloride *in vacuo* yielded 0.70 g (9 %) of **11-Cl_2**. ^{1}H NMR (benzene-

d$_6$): δ = 2.07 (s, 12H, Ind 1,3-*Me*), 5.46 (s, 2H, Cp*H*), 6.97 (m, 3.2 Hz, 4H, Benzo), 7.32 (m, 3.2 Hz, 4H, Benzo).

Preparation of (η^5-C_9H_5-1,3-$(Me)_2)_2ZrCl_2$ (11-I_2). A 20 mL scintillation vial was charged with 0.31 g (0.69 mmol) of **11-Cl_2** and dissolved in approximately 7 mL of toluene. The yellow solution was chilled at -35 ºC for for 20 minutes and 0.69 g (3.45 mmol) of iodotrimethylsilane dissolved in one mL of methylene chloride was then added to the solution and the reaction stirred for five days. The solvent was removed *in vacuo* and the resulting red solid washed with pentane yielding 0.70 g (9 %) of **11-I_2**. ^{1}H NMR (benzene-*d*$_6$): δ = 2.03 (s, 12H, Ind 1,3-*Me*), 5.83 (s, 2H, Cp*H*), 6.92 (m, 3.2 Hz, 4H, Benzo), 7.42 (m, 3.2 Hz, 4H, Benzo).

Preparation of (η^5-C_9H_4-1,2,3-$(Me)_3)_2ZrCl_2$ (11-Cl_2). This molecule was prepared in a similar manner to **11-Cl_2** in a 500 mL round bottom flask with 2.07 g (12.54 mmol) of Li[C_9H_4-1,2,3-$(Me)_3$], 1.46 g (6.27 mmol) of $ZrCl_4$ and approximately 200 mL of diethyl ether. This yielded 1.46 g (49 %) of **12-Cl_2**. Anal. Calcd. for $C_{24}H_{26}ZrCl_2$: C, 60.48; H, 5.50. Found: C, 60.26; H, 5.80. ^{1}H NMR (benzene-*d*$_6$): δ = 1.77 (s, 12H, Ind 1,3-*Me*), 1.88 (s, 6H, Ind 2-*Me*), 6.85 (m, 3.2 Hz, 4H, Benzo), 7.11 (m, 3.2 Hz, 4H, Benzo). ^{13}C {^{1}H} NMR (benzene-*d*$_6$): δ = 9.8, 13.6 (Ind *Me*), 112.0, 123.8, 124.0, 124.5, 140.87 (Cp/Benzo).

Preparation of *rac*/*meso*-(η^5-C_9H_5-1-(^{i}Pr)-3-(Me))$_2ZrCl_2$ (*rac*/*meso*-13-Cl_2). This molecule was prepared in a similar manner to **11-Cl_2** in a 250 mL round bottom flask with 2.53 g (14.20 mmol) of Li[C_9H_5-1-^{i}Pr-3-Me], 1.65 g (7.10 mmol) of $ZrCl_4$ and approximately 200 mL of diethyl ether. This yielded 2.81 g (78 %) of yellow **13-**Cl_2 as a mixture of *racemo* and *meso* isomers. Anal. Calcd. for $C_{26}H_{30}ZrCl_2$: C, 61.88; H,

5.99. Found: C, 61.76; H, 5.89. ^{1}H NMR (benzene-d_6): δ = 0.98 (d, 7 Hz, 6H, CHMe_2), 1.02 (d, 7 Hz, 6H, CHMe_2), 1.14 (d, 7 Hz, 6H, CHMe_2), 1.17 (d, 7 Hz, 6H, CHMe_2), 2.07 (s, 6H, *Me*), 2.08 (s, 6H, *Me*), 3.22 (m, 2H, C*H*Me$_2$) 3.50 (m, 2H, C*H*Me$_2$), 5.71 (s, 2H, Cp*H*), 5.84 (s, 2H, Cp*H*), 6.91 (m, 6H, Benzo), 7.02 (m, 2H, Benzo), 7.17 (m, 2H, Benzo), 7.22 (m, 2H, Benzo), 7.40 (m, 2H, Benzo). ^{13}C {^{1}H} NMR (benzene-d_6): δ = 12.8, 12.9 (*Me*), 21.6, 22.2, 25.0, 25.1, 27.4, 28.2 (CHMe$_2$), 107.0, 112.8, 120.8, 123.6, 124.4, 124.5, 125.0, 125.2, 125.29, 125.32, 125.36, 125.41, 125.9, 126.8, 126.9, 129.8, 130.8 (Cp/Benzo). One Cp/benzo resonance not located.

Preparation of *rac*/*meso*-(η^5-C$_9$H$_5$-1-(^{i}Pr)-3-(Me))$_2$ZrBr$_2$ (*rac*/*meso*-13-Br$_2$). This molecule was prepared in a similar manner to **11-Cl$_2$** in a 100 mL round bottom flask with 300 mg (1.68 mmol) of Li[C$_9$H$_5$-1-^{i}Pr-3-Me], 346 mg (0.842 mmol) of ZrBr$_4$ and approximately 200 mL of diethyl ether. This yielded 200 mg (40 %) of yellow **13-Br$_2$** as a mixture of *racemo* and *meso* isomers. Anal. Calcd. for C$_{26}$H$_{30}$ZrBr$_2$: C, 52.61; H, 5.09. Found: C, 52.94; H, 4.75. ^{1}H NMR (benzene-d_6): δ = 0.97 (d, 7 Hz, 6H, CHMe_2), 0.99 (d, 7 Hz, 6H, CHMe_2), 1.13 (d, 7 Hz, 6H, CHMe_2), 1.19 (d, 7 Hz, 6H, CHMe_2), 1.98 (s, 6H, *Me*), 2.09 (s, 6H, *Me*), 3.21 (m, 2H, C*H*Me$_2$) 3.67 (m, 2H, C*H*Me$_2$), 5.89 (s, 2H, Cp*H*), 6.17 (s, 2H, Cp*H*), 6.90 (m, 6H, Benzo), 6.99 (m, 2H, Benzo), 7.17 (m, 2H, Benzo), 7.23 (m, 2H, Benzo), 7.35 (m, 2H, Benzo), 7.42 (m, 2H, Benzo). ^{13}C {^{1}H} NMR (benzene-d_6): δ = 12.35, 12.91 (*Me*), 21.16, 21.70, 24.88, 24.94, 27.13, 28.58 (CHMe$_2$), 109.24, 112.78, 121.80, 124.11, 124.48, 124.81, 124.98, 125.11, 125.43, 125.45, 125.60, 126.46, 126.81, 128.76, 130.70 (Cp/Benzo). Three Cp/Benzo resonances not located.

Preparation of *rac*/*meso*-(η^5-C$_9$H$_5$-1-(^{i}Pr)-3-(Me))$_2$ZrI$_2$ (*rac*/*meso*-13-I$_2$). A 20 mL scintillation vial was charged with 630 mg (1.25 mmol) of **13-Cl$_2$** and dissolved in 5

mL of toluene. To the yellow solution, 1.25 g (6.24 mmol) of iodotrimethylsilane was added dropwise and the reaction stirred for 3 days. The solvent was removed *in vacuo* and the resulting orange solid washed with cold pentane yielding 748 mg (87 %) **13-I_2** as a mixture of *racemo* and *meso* isomers. Anal. Calcd. for $C_{26}H_{30}ZrI_2$: C, 45.42; H, 4.40. Found: C, 45.25; H, 4.29. ^{1}H NMR (benzene-d_6): δ = 0.93 (d, 7 Hz, 6H, CH*Me*$_2$), 0.97 (d, 7 Hz, 6H, CH*Me*$_2$), 1.12 (d, 7 Hz, 6H, CH*Me*$_2$), 1.26 (d, 7 Hz, 6H, CH*Me*$_2$), 1.83 (s, 6H, *Me*), 2.12 (s, 6H, *Me*), 3.22 (m, 2H, C*H*Me$_2$) 3.95 (m, 2H, C*H*Me$_2$), 6.39 (s, 2H, Cp*H*), 6.77 (s, 2H, Cp*H*), 6.85 (m, 6H, Benzo), 6.91 (m, 2H, Benzo), 7.11 (m, 2H, Benzo), 7.25 (m, 4H, Benzo), 7.43 (m, 2H, Benzo). ^{13}C {^{1}H} NMR (benzene-d_6): δ = 14.08, 16.00 (*Me*), 21.13, 21.52, 25.34, 25.64, 27.37, 30.06 (CHMe$_2$), 113.07, 116.33, 117.89, 123.66, 123.97, 124.84, 125.14, 125.25, 125.73, 126.04, 126.29, 126.33, 126.77, 127.17, 130.76 (Cp/Benzo). Three Cp/Benzo resonances not located.

Preparation of *rac*/*meso*-(η^5-C_9H_5-1-(^{t}Bu)-3-(Me))$ZrCl_2$ (*rac*/*meso* 14-Cl_2). This molecule was prepared in a similar manner to **11-Cl_2** in a 250 mL round bottom flask with 4.32 g (22.50 mmol) of Li[C_9H_5-1-^{t}Bu-3-Me], 2.62 g (11.25 mmol) of $ZrCl_4$ and approximately 200 mL of diethyl ether. This yielded 3.30 g (55 %) of yellow **14-Cl_2** as a mixture of *racemo* and *meso* isomers. Anal. Calcd. for $C_{28}H_{34}ZrCl_2$: C, 63.13; H, 6.43. Found: C, 63.25; H, 6.58. ^{1}H NMR (benzene-d_6): δ = 1.33 (s, 18H, C*Me*$_3$), 1.41 (s, 18H, C*Me*$_3$), 2.14 (s, 6H, *Me*), 2.25 (s, 6H, *Me*), 5.62 (s, 2H, Cp*H*), 5.90 (s, 2H, Cp*H*), 6.96 (m, 10H, Benzo), 7.20 (m, 2H, Benzo), 7.41 (m, 1H, Benzo), 7.73 (m, 1H, Benzo), 7.80 (m, 2H, Benzo). ^{13}C {^{1}H} NMR (benzene-d_6): δ = 14.0, 14.4 (*Me*), 31.6, 31.9, 35.2, 35.6 (CMe$_3$), 111.2, 112.7, 118.0, 118.2, 124.8, 124.91, 124.93, 124.99, 125.02, 125.04, 126.77, 126.84, 129.5, 130.5, 130.6, 132.7, 133.3 (Cp/Benzo). One Cp/benzo resonance not located.

Preparation of (η^9-C_9H_5-1,2-$(Me)_2$)(η^5-C_5Me_5)Zr (3). A 100 mL round bottom flask was charged with 8.26 g (41.2 mmol) of mercury and approximately 3 mL of pentane in a nitrogen drybox. While stirring, 41 mg (1.78 mmol) of sodium metal was added and the resulting amalgam was stirred for 20 minutes. A pentane slurry containing 132 mg (0.30 mmol) of **3-Cl$_2$** was added. The resulting reaction mixture was stirred vigorously for twenty hours under argon and the burgundy solution was decanted from the amalgam and filtered through Celite. Removal of the pentane *in vacuo* afforded 52 mg (53 %) of **3** as a burgundy oil. ^{1}H NMR (benzene-d_6): δ = 1.77 (s, 15H, Cp* *Me*), 2.06 (s, 6H, Ind *Me*), 3.80 (dd, 8, 4 Hz, 2H, η^9-Benzo), 5.07 (dd, 8, 4 Hz, 2H, η^9-Benzo), 5.34 (s, 1H, Cp*H*). ^{13}C {^{1}H} NMR (benzene-d_6): δ = 11.35 (Cp* *Me*), 12.02 (Ind *Me*), 66.45, 94.62 (η^9-Benzo), 113.86 (Cp* Cp), 114.68, 119.74, 121.23 (Ind Cp).

Preparation of [(η^5-C_5Me_5)Zr]$_2$ [μ_2-η^2,η^2-{4,5-(η^5-C_9H_5-1,3-Me_2)}$_2$] (μ_2-η^1,η^1-N_2) ($\mathbf{3_2}$**-$\mathbf{N_2}$).** This compound was prepared in a similar manner to **$\mathbf{6_2}$-$\mathbf{N_2}$** (*vide infra*) by allowing 73 mg (0.19 mmol) **3** dissolved in pentane to chilled at -35 ºC for 20 days affording 5 mg (7 %) of a brown precipitate identified as **$\mathbf{3_2}$-$\mathbf{N_2}$**. ^{1}H NMR (benzene-d_6): δ = 1.76 (s, 6H, Ind *Me*), 1.81 (s, 30H, Cp* *Me*), 1.92 (s, 6H, Ind *Me*), 2.55 (d, 7.6 Hz, 2H, η^2-Benzo), 3.34 (m, 8, 6 Hz, 2H, η^2-Benzo), 5.71 (s, 2H, Cp*H*), 6.14 (m, 2H, Benzo), 6.24 (d, 8 Hz, 2H, Benzo). ^{13}C {^{1}H} NMR (benzene-d_6): δ = 12.01 (Cp* *Me*), 12.06 (Ind *Me*), 14.24 (Ind *Me*), 67.31 (η^2-Benzo), 75.93 (η^2-Benzo), 104.77, 109.74, 111.99, 112.38, 114.33, 114.98, 124.63 (Benzo/Cp). One Benzo/Cp resonance not located.

Preparation of (η^9-C_9H_4-1,2,3-$(Me)_3$)(η^5-C_5Me_5)Zr (4). A 100 mL round bottom flask was charged with 24.29 g (121.07 mmol) of mercury and approximately 10 mL of pentane in a nitrogen drybox. While stirring, 121 mg (5.26 mmol) of sodium metal

was added and the resulting amalgam was stirred for 20 minutes. A pentane slurry containing 400 mg (0.88 mmol) of **4-Cl$_2$** was added. The resulting reaction mixture was stirred vigorously for four days and the burgandy solution was decanted from the amalgam and filtered through Celite. Removal of the pentane *in vacuo* followed by recrystallization from pentane at -35 °C afforded **4** as a burgundy solid. Anal. Calcd. for $C_{22}H_{28}Zr$: C, 68.87; H, 7.36. Found: C, 68.68; H, 7.57. ^{1}H NMR (benzene-d_6): δ = 1.44 (s, 3H, Ind 2-*Me*), 1.74 (s, 15H, Cp* *Me*), 1.95 (s, 6H, Ind 1,3-*Me*), 3.83 (dd, 2.4, 1.6 Hz, 2H, η^9-Benzo), 5.04 (dd, 2.4, 1.6 Hz, 2H, η^9-Benzo). ^{13}C {^{1}H} NMR (benzene-d_6): δ = 10.2, 10.5, 11.0 (*Me*), 66.2, 94.9 (η^9-Benzo) , 113.0, 113.2, 120.0, 130.2 (Cp).

Preparation of (η^9-C$_9$H$_5$-1-(^{i}Pr)-3-(Me))(η^5-C$_5$Me$_5$)Zr (6). This compound was prepared in a similar manner to **4** using 8.84 g (44.05 mmol) of mercury, 44 mg (1.91 mmol) of sodium metal and 150 mg (0.32 mmol) of **6-Cl$_2$**. Stirring the reaction for 24 hours under argon and subsequent workup in a nitrogen drybox affords 126 mg (99 %) of **6** as a burgundy oil. ^{1}H NMR (benzene-d_6): δ = 1.10 (d, 6.8 Hz, 3H, CH*Me*$_2$), 1.12 (d, 6.8 Hz, 3H, CH*Me*$_2$), 1.78 (s, 15H, Cp* *Me*), 2.05 (s, 3H, Ind *Me*), 3.24 (m, 1H, C*H*Me$_2$), 3.68 (m, 1H, η^9-Benzo), 3.84 (m, 1H, η^9-Benzo), 5.02 (d, 6Hz, 1H, η^9-Benzo), 5.13 (d, 6Hz, 1H, η^9-Benzo), 5.56 (s, 1H, Cp*H*). ^{13}C {^{1}H} NMR (benzene-d_6): δ = 11.49, 12.06 (*Me*), 22.13, 27.05, 28.94 (CHMe), 65.47, 66.45, 94.03, 96.19 (η^9-Benzo), 112.08, 113.90, 118.51 (Cp). Three Cp resonances not located.

Preparation of [(η^5-C$_5$Me$_5$)Zr]$_2$ [μ$_2$-η^2,η^2-{4,5-(η^5-C$_9$H$_5$-1-(^{i}Pr)-3-(Me))}$_2$] (μ$_2$-η^1,η^1-N$_2$) (6$_2$-N$_2$). In a dinitrogen drybox, a 20 mL scintillation vial was charged with 116 mg of **6** and dissolved in approximately 3 mL pentane and chilled at -35 ºC for one week, resulting in a purple solution with precipitate. This brown precipitate was

isolated as as 20 mg of (17 %) **6_2-N_2**. Anal. Calcd. for $C_{46}H_{60}Zr_2N_2$: C, 67.10; H, 7.34; N, 3.40. Found: C, 67.25; H, 7.31; N, 3.03. ^{1}H NMR (benzene-d_6): δ = 1.34 (d, 6.5 Hz, 3H, CH*Me*$_2$), 1.42 (d, 6.5 Hz, 3H, CH*Me*$_2$), 1.80 (s, 15H, Cp* *Me*), 2.25 (s, 3H, Ind *Me*), 2.63 (m, 2H, C*H*Me$_2$, η^2-Benzo), 3.30 (m, 1H, η^2-Benzo), 5.64 (s, 1H, Cp*H*), 6.33 (m, 1H, Benzo), 6.41 (d, 8 Hz, 1H, Benzo). ^{13}C {^{1}H} NMR (benzene-d_6): δ = 12.06 (Cp* *Me*), 13.51 (Ind *Me*), 24.82, 25.45 (CH*Me*), 29.56 (*C*HMe), 66.03, 77.68 (η^2-Benzo), 103.97 (Cp), 109.63 (Ind *Cp*H), 112.09 (Cp), 112.54 (Benzo), 124.16 (Cp), 126.05 (Benzo). Two Cp/Benzo resonances not located. ^{15}N {^{1}H} NMR (benzene-d_6): δ = 598.69. IR (pentane): ν(NN) = 1563 cm^{-1}.

Preparation of [(η^5-C_5Me_5)Zr]$_2$ [μ$_2$-η^5,η^4-(η^5-C_9H_5-1-(^{i}Pr)-3-(Me))] (μ$_2$-η^2,η^1-N_2) (μ$_2$-η^1,η^1-Cl) (16-N_2Cl). This compound was prepared in a similar manner to **4** using 8.84 g (44.05 mmol) of mercury, 44 mg (1.91 mmol) of sodium metal and 150 mg (0.32 mmol) of **6-Cl_2**. Stirring the reaction for 2 days and subsequent workup in a nitrogen drybox affords a brown oil. Recrystallization from pentane affords 79 mg (72 %) of a brown solid identified as two isomers of **16-N_2Cl** in a 3 to 1 ratio. Anal. Calcd. for $C_{33}H_{45}Zr_2N_2Cl$: C, 57.64; H, 6.60; N, 4.07. Found: C, 57.61; H, 6.47; N, 3.87. ^{1}H NMR (benzene-d_6): δ = 0.58 (d, 8 Hz, 3H, minor CH*Me*$_2$), 0.63 (d, 8 Hz, 3H, major CH*Me*$_2$), 0.74 (s, 3H, major Ind *Me*), 0.91 (d, 8 Hz, 3H, minor CH*Me*$_2$), 1.04 (s, 3H, minor Ind *Me*), 1.11 (d, 8 Hz, 3H, major CH*Me*$_2$), 1.90 (s, 15H, major Cp* *Me*), 1.91 (s, 15H, minor Cp* *Me*), 1.94 (s, 15H, major Cp* *Me*), 1.95 (s, 15H, minor Cp* *Me*), 1.96 (m, 2H, major/minor C*H*Me$_2$), 2.22 (dd, 8 Hz, 4 Hz, 1H, major Benzo), 2.66 (dd, 8 Hz, 4 Hz, 1H, minor Benzo), 3.49 (m, 1H, minor Benzo), 3.83 (dd, 8 Hz, 4 Hz, 1H, major Benzo), 4.34 (s, 1H, major Cp*H*), 4.42 (s, 1H, minor Cp*H*), 4.73 (m, 1H, major Benzo), 4.85 (d, 8 Hz, 1H, minor Benzo). ^{13}C {^{1}H} NMR (benzene-d_6): δ = 9.15 (major Ind *Me*), 11.86, (major Cp* *Me*), 11.96 (minor Cp* *Me*), 11.98 (major

Cp* *Me*), 12.06 (minor Cp* *Me*), 22.56 (major $CHMe_2$), 22.90 (minor $CHMe_2$), 24.81 (major $CHMe_2$), 25.07, 27.14 (minor $CHMe_2$), 27.87 (major $CHMe_2$), 68.24, 68.45, 83.19, 84.08, 87.52, 93.11, 93.79, 94.39, 95.72, 95.88, 100.81, 106.36, 114.95, 115.25, 115.97, 116.02, 116.39, 118.29, 119.15, 119.90, 120.58, 121.87 (Cp/Benzo). Minor Ind *Me* resonance not located. ^{15}N {^{1}H} NMR (benzene-d_6): δ = 490.0 (d, 20 Hz, major), 494.9 (d, 21 Hz, minor), 599.9 (d, 20 Hz, major), 610.1 (d, 204 Hz, minor). IR (pentane): ν(NN) = 1584 cm^{-1}. IR (KBr): ν(NN) = 1583 cm^{-1}. IR (KBr): ν($^{15}N^{15}N$) = 1533 cm^{-1}.

Preparation of (η^5-C_5Me_5)(η^5-C_9H_5-1-(^{i}Pr)-3-(Me))ZrH_2 (6-H_2). A J. Young tube was charged with 11 mg (0.03 mmol) of either **6** or **6$_2$-N$_2$** and dissolved in approximately 0.5 mL of benzene-d_6. On the high vacuum line the tube was frozen in liquid nitrogen, degassed and an atmosphere of dihydrogen was admitted. Upon thawing, the tube was shaken for a few minutes during which time the solution turned brown. ^{1}H NMR (benzene-d_6): δ = 1.26 (d, 4 Hz, 3H, $CHMe_2$), 1.37 (d, 4 Hz, 3H, $CHMe_2$), 1.82 (s, 15H, Cp* *Me*), 2.15 (s, 3H, *Me*), 3.62 (m, 1H, $CHMe_2$), 6.80 (m, 4 Hz, 2H, Benzo), 7.13 (m, 1H, Benzo), 7.26 (s, 1H, Cp*H*), 7.32 (m, 1H, Benzo). ^{13}C {^{1}H} NMR (benzene-d_6): δ = 12.06 (Cp* *Me*), 22.01, 26.30, 28.20, 30.18 (Ind *Me*/$CHMe_2$), 105.48, 113.85, 119.37, 121.77, 122.20, 122.46, 123.00, 123.28, 123.42 (Cp/Benzo). One Cp/Benzo resonance not located.

Preparation of (η^5-C_5Me_5)(η^5-C_9H_9-1-(^{i}Pr)-3-(Me))ZrH_2 (6-THI-H_2). A thick walled glass vessel was charged with 263 mg (0.66 mmol) **6** and dissolved in approximately 4 mL of toluene. On the high vacuum line, the bomb was frozen in liquid nitrogen, degassed and an atmosphere of dihydrogen condensed. After allowing the solution to warm up to room temperature, the reaction vessel was heated in a 45 ºC

silicone oil bath for 36 hours resulting in a color change from red to brown. The toluene and excess dihydrogen was removed *in vacuo* affording 121 mg (49 %) **6-THI-H_2** as a brown oil. ^{1}H NMR (benzene-d_6): δ = 1.06 (d, 8 Hz, 3H, CH*Me*$_2$), 1.19 (d, 8 Hz, 3H, CH*Me*$_2$), 1.68 (s, 3H, *Me*), 2.05 (s, 15H, Cp* *Me*), 2.2 – 3.1 (m, 9H, THI/C*H*Me$_2$), 4.59 (s, 1H, Cp*H*), 7.37 (s, 1H, Zr-*H*), 7.45 (s, 1H, Zr-*H*). ^{13}C {^{1}H} NMR (benzene-d_6): δ = 12.85 (Cp* *Me*), 23.57, 23.88, 24.00, 24.71, 25.70, 26.08, 28.75 (THI/CHMe$_2$), 102.58, 113.52, 118.92, 119.61, 125.02, 132.20 (Cp). One Ind *Me* resonance not located.

Preparation of (η^5-C_5Me_5)(η^5-C_9H_9-1-(^{i}Pr)-3-(Me))ZrI_2 (6-THI-I_2). A 20 mL scintillation vial was charged with 41 mg of (0.10 mmol) 6-THI-H_2 and dissolved in approximately 1 mL of toluene. To this brown solution, 94 mg (0.47 mmol) of iodotrimethylsilane was added dropwise and then capped and stirred for five days. The volatiles were removed *in vacuo* affording a yellow oil which was then washed with cold pentane leaving behind 54 mg (81 %) of 6-THI-I_2 as a yellow powder, Anal. Calcd. for $C_{23}H_{34}ZrI_2$: C, 42.14; H, 5.23. Found: C, 42.57; H, 5.25. ^{1}H NMR (benzene-d_6): δ = 0.96 (d, 8 Hz, 3H, CH*Me*$_2$), 0.98 (d, 8 Hz, 3H, CH*Me*$_2$), 1.49 (s, 3H, *Me*), 1.59 (m, 4H, THI), 2.00 (s, 15H, Cp* *Me*), 2.53 (m, 1H, THI), 2.75 (m, 2H, THI, C*H*Me$_2$), 3.75 (m, 2H, THI), 5.13 (s, 1H, Cp*H*). ^{13}C {^{1}H} NMR (benzene-d_6): δ = 14.15 (Ind *Me*), 15.31 (Cp* *Me*), 22.35, 22.72, 23.45, 27.36, 27.69, 29.51 (THI/CHMe$_2$), 108.34, 119.19, 124.49, 132.63, 133.68, 135.18 (Cp).

Preparation of (η^5-C_5Me_5)(η^5-C_9H_9-1-(^{i}Pr)-3-(Me))Zr(H)(I) (4-THI-(H)(I)). This compound was prepared in a similar manner to **4** using 1.56 g (7.80 mmol) of mercury, 8 mg (0.35 mmol) of sodium metal and 37 mg (0.06 mmol) of **4-THI-I_2** (*vide infra*). Stirring the reaction for 2 days in a nitrogen drybox and subsequent

workup affords 16 mg (53 %) of a brown oil identified as two isomers **4-THI-(H)(I)** in a 5:1 ratio. ^{1}H NMR (benzene-d_6): δ =1.02 (d, 8 Hz, 3H, major CH*Me*$_2$), 1.03 (d, 8 Hz, 3H, major CH*Me*$_2$), 1.11 (d, 8 Hz, 3H, minor CH*Me*$_2$), 1.23 (d, 8 Hz, 3H, minor CH*Me*$_2$), 1.64 (s, 3H, major *Me*), 1.66 (s, 3H, minor *Me*), 1.97 (s, 15H, minor Cp* *Me*), 1.98 (s, 15H, major Cp* *Me*), 2.07 (m, 3H, minor THI), 2.19 (m, 3H, major THI), 2.47 (m, 2H, major THI), 2.66 (m, 2H, major C*H*Me$_2$, minor C*H*Me$_2$), 2.77 (m, 1H, major THI), 3.09 (m, 1H, major THI), 3.83 (m, 1H, major THI), 4.64 (s, 1H, minor Cp*H*), 4.70 (s, 1H, major Cp*H*), 7.96 (s, 1H, major Zr-*H*), 8.08 (s, 1H, minor Zr-*H*). Five minor THI resonances not located. ^{13}C {^{1}H} NMR (benzene-d_6): δ = 13.22 (major Ind *Me*), 13.82 (major Cp* *Me*), 22.75, 23.39, 23.59, 23.90, 26.04, 26.95, 28.40 (major THI/CHMe$_2$), 105.92, 115.50, 120.27, 127.02, 130.06, 131.61 (major Cp); 11.70 (minor Ind *Me*), 13.76 (minor Cp* *Me*), 22.79, 23.54, 24.06, 24.98, 25.67, 26.16, 29.26 (minor THI/CHMe$_2$), 107.51, 111.06, 120.18, 130.45, 131.83 (minor Cp). On minor Cp resonance not located.

Preparation of (η^5-C$_5$Me$_5$)(η^5-C$_9$H$_5$-1-(^{i}Pr)-3-(Me))ZrMe$_2$ (6-Me$_2$). A 20 mL scintillation vial was charged with 25 mg of (0.10 mmol) 6-Cl$_2$ and dissolved in approximately 1 mL of toluene. The resulting yellow solution was chilled in a drybox freezer at –35 ºC for 15 minutes and 0.074 mL (0.12 mmol) of 1.6 M MeLi in Et$_2$O was added to the solution dropwise. The resulting reaction mixture was then evacuated for briefly to remove residual diethyl ether introduced from the MeLi solution. The solution was then stirred for half an hour forming a clear solution, when the solvent was removed *in vacuo* and the white powder extracted into pentane and filtered through Celite. The pentane was removed *in vacuo* leaving 13 mg (57 %) of a white solid identified as **6-Me$_2$.** ^{1}H NMR (benzene-d_6): δ = -1.19 (s, 3H, Zr-*Me*), -0.47 (s, 3H, Zr-*Me*), 1.06 (d, 8 Hz, 3H, CH*Me*$_2$), 1.23 (d, 8 Hz, 3H, CH*Me*$_2$), 1.73 (s, 15H,

Cp* *Me*), 2.01 (s, 3H, *Me*), 3.21 (m, 1H, C*H*Me_2), 5.11 (s, 1H, Cp*H*), 7.05 (m, 1H, Benzo), 7.15 (m, 1H, Benzo), 7.26 (m, 1H, Benzo), 7.63 (m, 1H, Benzo).

Preparation of (η^9-C_9H_5-1-(^{t}Bu)-3-(Me))(η^5-C_5Me_5)Zr (7). This compound was prepared in a similar manner to **4** using 8.58 g (42.76 mmol) of mercury, 43 mg (1.87 mmol) of sodium metal and 150 mg (0.31 mmol) of **7-Cl$_2$**. Stirring the reaction for 24 hours under argon and subsequent workup in a nitrogen drybox affords 22 064mg (18 50 %) of **7** as a burgundy oil. ^{1}H NMR (benzene-d_6): δ = 1.35 (s, 9H, C*Me*$_3$), 1.79 (s, 15H, Cp* *Me*), 2.02 (s, 3H, Ind *Me*), 3.57 (m, 8Hz, 1H, η^9-Benzo), 3.86 (m, 8Hz, 1H, η^9-Benzo), 4.90 (d, 8Hz, 1H, η^9-Benzo), 5.29 (d, 6Hz, 1H, η^9-Benzo), 5.69 (s, 1H, Cp*H*). ^{13}C {^{1}H} NMR (benzene-d_6): δ = 11.69 (*Me*), 29.52, 30.18, 34.63 (CMe_3), 66.45, 69.44, 91.67, 97.15 (η^9-Benzo), 113.79, 120.58, 122.55, 123.17, 124.61, 126.20 (Cp).

Preparation of [(η^5-C_5Me_5)Zr]$_2$[μ_2-η^2,η^2-{4,5-(η^5-C_9H_5-1-(^{t}Bu)-3-(Me))}$_2$] (μ_2-η^1,η^1-N_2) (7$_2$-N$_2$). This compound was prepared in a similar manner to **6a-N$_2$** by allowing 54 mg (0.13 mmol) **7** dissolved in pentane to chilled at –35 ºC for one month affording 5 mg (9 %) of a brown precipitate identified as **7$_2$-N$_2$**. ^{1}H NMR (benzene-d_6): δ = 1.41 (s, 18H, C*Me*$_3$), 1.84 (s, 30H, Cp* *Me*), 2.31 (s, 6H, Ind *Me*), 2.74 (d, 7.6 Hz, 2H, η^2-Benzo), 3.33 (m, 8, 6 Hz, 2H, η^2-Benzo), 5.67 (s, 2H, Cp*H*), 6.38 (m, 2H, Benzo), 6.53 (d, 8 Hz, 2H, Benzo). ^{13}C {^{1}H} NMR (benzene-d_6): δ = 12.34 (Cp* *Me*), 28.59, 30.18, 34.63 (CMe_3/Ind *Me*), 66.08, 78.78 (η^2-Benzo), 108.85, 109.02, 109.77, 112.22, 113.63, 124.63, 124.96, 126.27 (Benzo/Cp). IR (pentane): ν(NN) = 1565 cm^{-1}.

Preparation of [(η^5-C_5Me_5)Zr]$_2$[μ_2- η^5,η^4-(η^5-C_9H_5-1-(^{t}Bu)-3-(Me))](μ_2-η^2,η^1-N$_2$) (μ_2-η^1,η^1-Cl) (17-N$_2$Cl). This compound was prepared in a similar manner to **4** using

8.58 g (42.76 mmol) of mercury, 0.043 g (1.87 mmol) of sodium metal and 0.150 g (0.31 mmol) of **17-Cl_2**. Stirring the reaction for 2 days and subsequent workup in a nitrogen drybox affords a brown oil. Recrystallization from pentane affords 0.004 g (4 %) of a brown solid identified as two isomers of **17-N_2Cl** a 1.5 to 1 ratio. ^{1}H NMR (benzene-d_6): □ = 0.77 (s, 3H, major *Me*), 0.90 (s, 9H, minor C*Me*$_3$), 0.96 (s, 9H, major C*Me*$_3$), 1.03 (s, 3H, major *Me*), 1.90, 1.91, 1.98 (s, 60H, major Cp* *Me*, major Cp* *Me*), 2.96 (m, 8 Hz, 1H, major Benzo), 3.25 (m, 8Hz, 1H, minor Benzo), 3.47 (m, 2H, minor Benzos), 3.60 (m, 8Hz, 1H, major Benzo), 3.79 (m, 1H, 8Hz, major Benzo), 4.48 (s, 1H, major CpH), 4.57 (s, 1H, minor CpH), 4.67 (m, 8Hz, 1H, major Benzo), 4.87 (m, 1H, 8Hz, minor Benzo).

Preparation of (η^9-C_9H_5-1,3-($SiMe_3$)$_2$)(η^5-C_5Me_5)Zr (9). This compound was prepared in a similar manner to **4** using 3.31 g (16.49 mmol) of mercury, 17 mg (0.74 mmol) of sodium metal and 60 mg (0.11 mmol) of **9-Cl_2**. Stirring the reaction for 20 hours under argon and subsequent workup in a nitrogen drybox affords 60 mg of a burgundy oil in which **9** is observed. ^{1}H NMR (benzene-d_6): δ = 0.39 (s, 18H, Si*Me*$_3$), 1.80 (s, 15H, Cp* *Me*), 3.70 (m, η^9-Benzo), 5.25 (m, η^9-Benzo), 6.30 (s, 1H, Cp*H*). ^{13}C {^{1}H} NMR (benzene-d_6): δ = 2.01 (Si*Me*$_3$), 12.10 (Cp* *Me*), 73.90, 96.22 (η^9-Benzo), 114.03, 133.03 (Cp). Two Cp resonances not located.

Preparation of (η^5-C_5Me_5) (η^5-C_9H_5-1,3-($SiMe_3$)$_2$)Zr(CMH) (9-CMH). This compound was prepared in a similar manner to **4** using 2.61 g (13.0 mmol) of mercury, 13 mg (0.57 mmol) of sodium metal and 70 mg (0.11 mmol) of **9-I_2**. Stirring the reaction for 2.5 days under argon and subsequent workup in a nitrogen drybox affords 40 mg of a yellow oil identified as **9-CMH**. ^{1}H NMR (benzene-d_6): δ = -2.11 (d, 12.8 Hz, 1H, $SiMe_2CH_2$), -1.76 (d, 12.8 Hz, 1H, $SiMe_2CH_2$), 0.32 (s, 9H, Si*Me*$_3$),

0.59 (s, 3H, SiMe_2CH_2), 0.64 (s, 3H, SiMe_2CH_2), 1.65 (s, 15H, Cp* *Me*), 6.30 (s, 1H, Cp*H*), 6.76 (m, 1H, Benzo), 6.88 (m, 1H, Benzo), 7.37 (m, 2H, Benzo), 7.97 (s, 1H, Zr-*H*). ^{13}C {^1H} NMR (benzene-d_6): δ = -0.82, -0.77, (SiMe_2CH_2), 0.93 (Cp* *Me*), 3.71 (SiMe$_2$*C*H$_2$), 102.45, 110.29, 119.28, 122.79, 123.86, 124.24, 125.15, 125.60, 125.95, 127.52 (Cp/Benzo).

Preparation of [(η^5-C_5Me_5)Zr]$_2$ [μ$_2$-η^5,η^4-(η^5-C_9H_5-1,3-($SiMe_3$)$_2$)] (μ$_2$-η^2,η^1-N_2) (18-N_2Cl). This compound was prepared in a similar manner to **4** using 8.27 g (41.22 mmol) of mercury, 41 mg (1.78 mmol) of sodium metal and 150 mg (0.30 mmol) of **9-Cl$_2$**. Stirring the reaction for 2 days and subsequent workup in a nitrogen drybox affords a brown oil. Recrystallization from pentane affords 13 mg (11 %) of a brown solid identified as **18-N_2Cl**. Anal. Calcd. for $C_{35}H_{53}Si_2N_2Zr_2Cl$: C, 54.18; H, 6.89; N, 3.61. Found: C, 54.18; H, 7.19; N, 3.54. ^1H NMR (benzene-d_6): δ = 0.01 (s, 9H, SiMe_3), 0.08 (s, 9H, SiMe_3), 1.87 (s, 15H, Cp* *Me*), 2.03 (s, 15H, Cp* *Me*), 2.25 (m, 8 Hz, 1H, Benzo), 3.48 (m, 8Hz, 1H, Benzo), 3.60 (m, 1H, Benzo), 4.73 (m, 1H, Benzo), 4.85 (s, 1H, CpH). ^{13}C {^1H} NMR (benzene-d_6): δ = 1.27, 1.66 (SiMe_3), 12.07, 12.91 (Cp* *Me*), 69.38, 82.87, 97.59, 104.79 (Benzo), 116.15, 118.01, 118.95, 119.18, 119.65, 119.91, 120.12 (Cp).

Preparation of [(η^5-C_5Me_5)Zr]$_2$ [μ$_2$-η^5,η^4-(η^5-C_9H_5-1,3-($SiMe_3$)$_2$)] (μ$_2$-η^2,η^1-N_2) (18-N_2I). This compound was prepared in a similar manner to **4** using 5.60 g (27.90 mmol) of mercury, 28 mg (1.21 mmol) of sodium metal and 150 mg (0.20 mmol) of **9-I$_2$**. Stirring the reaction for 3 days and subsequent workup in a nitrogen drybox affords a brown oil. Recrystallization from pentane affords 4 mg (5 %) of a brown solid identified as **9-N_2I**. ^1H NMR (benzene-d_6): δ = -0.09 (s, 9H, major SiMe_3), 0.15 (s, 9H, major SiMe_3), 1.93 (s, 15H, Cp* *Me*), 2.12 (s, 15H, Cp* *Me*), 2.26 (m, 8 Hz,

1H, Benzo), 3.76 (m, 8Hz, 1H, Benzo), 4.23 (m, 1H, Benzo), 4.83 (m, 2H, CpH/Benzo).

Preparation of (η^9-C_9H_4-1,2,3-$(Me)_3$)(η^5-C_9H_4-1,2,3-$(Me)_3$)Zr (12). This compound was prepared in a similar manner to **4** using 23.17 g (115.48 mmol) of mercury, 116 mg (5.04 mmol) of sodium metal and 400 mg (0.84 mmol) of **12-Cl_2**. Workup after reducing for five days and recrystallization from pentane at -35 °C afforded 32 mg (8 %) of **12** as a burgundy solid. Anal. Calcd. for $C_{24}H_{26}Zr$: C, 70.64; H, 6.42. Found: C, 70.32; H, 6.36. ^{1}H NMR (benzene-d_6): δ = 1.83 (s, 6H, Ind 1,3-*Me*), 1.96 (s, 6H, Ind 1,3-*Me*), 2.05 (s, 6H, Ind 2-Me), 3.83 (br s, 2H, η^9-Benzo), 4.83 (br s, 2H, η^9-Benzo), 6.85 (m, 2H, η^5-Benzo), 7.11 (m, 2H, η^5-Benzo). ^{13}C {^{1}H} NMR (benzene-d_6): δ = 9.96, 14.24, 22.69, 34.39 (*Me*), 68.59, 95.78 (η^9-Benzo), 119.95 (η^5-Benzo), 120.40 (Cp), 121.13 (η^5-Benzo), 122.48, 122.60, 122.87, 123.39, 124.15 (Cp).

Preparation of *rac*/*meso*-(η^9-C_9H_5-1-(^{i}Pr)-3-(Me))(η^5-C_9H_5-1-(^{i}Pr)-3-(Me))Zr (*rac*/*meso*-13). This compound was prepared in a similar manner to **4** using 17.67 g (88.07 mmol) of mercury, 88 mg (3.84 mmol) of sodium metal and 323 mg (0.64 mmol) of ***rac*/*meso*-13-Cl_2**. Stirring the reaction for 24 hours under argon and subsequent workup in a nitrogen drybox affords 69 mg (25 %) of ***meso*-13** as a burgundy solid. Aliquots of the reaction mixture indicate roughly equimolar amounts of ***rac*/*meso*-13** are present, suggesting enrichment of the one isomer due to fortuitous crystallization. ^{1}H NMR (benzene-d_6): δ = 1.04 (d, 8 Hz, 3H, CHMe_2), 1.07 (d, 8 Hz, 3H, CHMe_2), 1.13 (m, 6H, CHMe_2), 1.82 (s, 3H, *Me*), 1.94 (s, 3H, *Me*), 2.45 (m, 1H, C*H*Me_2), 2.94 (m, 1H, C*H*Me_2), 3.56 (m, 1H, η^9-Benzo, 3.84 (m, 1H, η^9-Benzo), 4.75 (m, 1H, η^9-Benzo), 4.91 (m, 1H, η^9-Benzo), 5.54 (s, 1H, Cp*H*), 6.60 (s, 1H, Cp*H*), 6.85 (m, 1H, Benzo), 6.90 (m, 1H, Benzo), 7.03 (m, 8 Hz, 1H, benzo), 7.22 (m, 8 Hz,

1H, Benzo). ^{13}C {^{1}H} NMR (benzene-d_6): δ = 13.2 (2) (*Me*), 22.0, 23.2, 26.3, 26.9, 27.1, 28.9 (CHMe), 68.1, 71.1, 96.1, 96.9 (η^9-Benzo), 102.6, 106.3, 114.4, 116.9, 119.1, 119.9, 120.9, 121.2, 122.7, 122.8, 122.9, 123.7, 129.4 (Cp/Benzo).

Preparation of [(η^5-C_9H_5-1-(^{i}Pr)-3-(Me))(η^5-C_9H_5-1-(^{i}Pr)-3-(Me))Zr(NaCl)]$_2$(μ_2-η^1,η^1-N_2) ([13-NaCl]$_2$-N_2). This compound was prepared in a similar manner to 4 using 23.19 g (115.69 mmol) of mercury, 116 mg (5.04 mmol) of sodium metal and 424 mg (0.84 mmol) of ***rac*/*meso*-13-Cl$_2$**. Stirring the reaction for 2 days in a dinitrogen filled drybox and subsequent workup affords 152 mg (36 %) of **[13-NaCl]$_2$-N$_2$** as a burgundy solid. Anal. Calcd. for $C_{52}H_{60}Zr_2N_2Na_2Cl_2$: C, 61.69; H, 5.97; N, 2.77. Found: C, 61.29; H, 6.16; N, 2.44. ^{1}H NMR (benzene-d_6): δ = 1.05 – 1.86 (br m, 24H, CH*Me*$_2$), 2.43 – 2.66 (br m, 12H, *Me*), 2.90 – 3.87 (br m, 6H, benzo/C*H*Me$_2$), 4.28 – 4.98 (br m, 2H, Benzo), 6.35 – 6.89 (br m, 2H, benzo/Cp*H*), 7.19 - 8.19 (br m, 14H, Benzo/Cp*H*).

Preparation of [(η^5-C_9H_5-1-(^{i}Pr)-3-(Me))(η^5-C_9H_5-1-(^{i}Pr)-3-(Me))Zr(NaBr)]$_2$(μ_2-η^1,η^1-N_2) ([13-NaBr]$_2$N$_2$). This compound was prepared in a similar manner to [**1-NaCl]$_2$N$_2$** using 6.98 g (34.80 mmol) of mercury, 35 mg (1.52 mmol) of sodium metal and 150 mg (0.25 mmol) of ***rac*/*meso*-13-Br$_2$**. Stirring the reaction for 2 days affords 30 mg (22 %) of **[13-NaBr]$_2$N$_2$** as a red solid. Anal. Calcd. for $C_{52}H_{60}Zr_2N_2Na_2Br_2$: C, 56.71; H, 5.49; N, 2.54. Found: C, 56.83; H, 5.32; N, 2.46. ^{1}H NMR (benzene-d_6): δ = 1.05 – 1.91 (br m, 24H, CH*Me*$_2$), 2.45 – 2.59 (br m, 12H, *Me*), 3.36 – 3.55 (br m, 4H, C*H*Me$_2$), 6.72 – 7.10 (br m, 10H, benzo/Cp*H*), 7.32 – 7.80 (br m, 10H, Benzo/Cp*H*).

Preparation of [(η^5-C_9H_5-1-(^{i}Pr)-3-(Me))(η^5-C_9H_5-1-(^{i}Pr)-3-(Me))Zr(NaI)]$_2$(μ_2-η^1,η^1-N_2) [13-NaI]$_2$N$_2$). This compound was prepared in a similar manner to [**13-**

NaCl]$_2$N$_2$ using 6.02 g (30.01 mmol) of mercury, 30 mg (1.30 mmol) of sodium metal and 150 mg (0.22 mmol) of ***rac*/*meso*-13-I$_2$**. Stirring the reaction for 2 days affords 42 mg (32 %) of **[13-NaI]$_2$N$_2$** as a red solid. Anal. Calcd. for $C_{52}H_{60}Zr_2N_2Na_2I_2$: C, 52.33; H, 5.07; N, 2.35. Found: C, 52.42; H, 5.41; N, 1.97. ^{1}H NMR (benzene-d_6): δ = 1.05 – 1.80 (br m, 24H, CH*Me*$_2$), 2.49 – 2.64 (br m, 12H, *Me*), 3.43 – 3.62 (br m, 4H, C*H*Me$_2$), 6.40 – 7.04 (br m, 10H, benzo/Cp*H*), 7.19 - 7.78 (br m, 10H, Benzo/Cp*H*).

Preparation of ([(η^5-C$_9$H$_5$-1-(^{i}Pr)-3-(Me))$_2$]Zr(H))$_2$(μ$_2$-η^2,η^2-N$_2$H$_2$) ([13-H]$_2$(N$_2$H$_2$)). A thick walled glass vessel was charged with 135 mg (0.11 mmol) of **[13-NaI]$_2$N$_2$**[*] and dissolved in approximately 6 mL of toluene. On the high vacuum line, the vessel was frozen in liquid nitrogen and evacuated. 1 atm of of hydrogen was added at -196 ˚C. The contents of the vessel were thawed and stirred at room temperature for two days producing a color change from red to brown. The solvent was removed *in vacuo* and extracted through Celite with pentane. After solvent removal *in vacuo*, the brown solid was washed multiple times with cold pentane until the filtrate was no longer brown. This yielded 31 mg (30 %) of a tan solid identified as **[13-H]$_2$(N$_2$H$_2$)**. Anal. Calcd. for $C_{52}H_{64}Zr_2N_2$: C, 69.43; H, 7.17; N, 3.11. Found: C, 69.07; H, 6.81; N, 2.94. ^{1}H NMR (benzene-d_6): δ = -1.44 – -0.81 (s, 2H, N*H*), 0.87 – 1.93 (d, 24H, CH*Me*$_2$), 2.23 – 2.87 (s, 12H, *Me*), 2.99 – 3.47 (m, 4H, C*H*Me$_2$), 4.52 – 4.81 (s, 2H, Zr*H*), 5.31 – 5.66 (s, 4H, Cp*H*), 6.77 – 7.95 (m, 16H, benzo). ^{15}N {^{1}H} NMR (benzene-d_6): δ = 91.9 – 97.5. IR (KBr) ν(NH) = 3238 cm^{-1}. IR (KBr): ν(ND) = 2403 cm^{-1}.

Preparation of ([(η^5-C$_9$H$_5$-1-(^{i}Pr)-3-(Me))$_2$]Zr(I))$_2$(μ$_2$-η^2,η^2-N$_2$H$_2$) ([13-I]$_2$(N$_2$H$_2$)). A J. Young NMR tube was charged with 5 mg (0.005 mmol) of **[13-NaBr]$_2$N$_2$**[*] and

[*] **[13-NaI]$_2$N$_2$** can be substituted with either **[13-NaCl]$_2$N$_2$** or **[13-NaBr]$_2$N$_2$**.
[*] **13-(NaBr)$_2$N$_2$** can be substituted with either **13-(NaCl)$_2$N$_2$** or **13-(NaI)$_2$N$_2$**.

dissolved in approximately 0.5 mL of benzene-d_6. On the high vacuum line, the vessel was frozen in liquid nitrogen and evacuated. 1 atm of hydrogen was added at -196 ˚C. The contents of the tube were thawed and shaken at room temperature for two days producing a color change from red to brown. The tube was, then, degassed at -196 ºC and two equivalents (6 torr in a 31.6 mL bulb) of iodomethane were added. After two days at room temperature, the solution had turned purple forming methane gas, **[13-I]$_2$(N_2H_2)** and free ligand, which could not be further removed to purify the compound. Clearly observable ^{1}H NMR (benzene-d_6): δ = 6.10, 6.16, 6.36, 6.42, 6.53 (s, N*H*). IR (KBr) ν(NH) = 3238 cm^{-1}. IR (KBr): ν(NH) = 3200 - 3210 cm^{-1}. IR (KBr): ν(ND) = 2399 - 2405 cm^{-1}.

Addition of 18-crown-6 to 13-(NaCl)$_2$$N_2$. To a J. Young NMR tube charged with 9 mg (0.01 mmol) of **13-(NaCl)$_2$$N_2$** dissolved in approximately 0.5 mL of benzene-d_6, 5 mg (0.02 mmol) of 18-crown-6 was added, resulting in an immediately color change from red to black with dark precipitate. After allowing the mixture to stand overnight, protonolysis with either excess HCl via calibrated gas bulb addition or excess H_2O via syringe, was performed. Quantification of the hydrazine librerated showed 33 and 43 % of the expected hydrazine with HCl and H_2O, respectively.

Addition of 15-crown-5 to 13-(NaCl)$_2$$N_2$. This addition was performed in a similar manner to the 18-crown-6 addition with 9 mg (0.01 mmol) of **13-(NaCl)$_2$$N_2$** and 3.5 μL (0.02 mmol) of 15-crown-5, resulting in an immediately color change from red to black with dark precipitate. Quantification of the hydrazine librerated with HCl and H_2O showed 38 and 0 % of the expected hydrazine, respectively.

Preparation of *rac*/*meso*-(η^9-C_9H_5-1-(^{t}Bu)-3-(Me))(η^5-C_9H_5-1-(^{t}Bu)-3-(Me))Zr (*rac*/*meso*-14). This compound was prepared in a similar manner to **4** using 12.50 g (62.30 mmol) of mercury, 62 mg (2.72 mmol) of sodium metal and 241 mg (0.452 mmol) of *rac-meso*-**14-Cl$_2$**. Workup and recrystallization from pentane at -35 °C afforded 71 mg (34 %) of *rac*/*meso*-**14** as a burgundy solid. Anal. Calcd. for $C_{28}H_{34}Zr$: C, 72.3; H, 7.42. Found: C, 72.64; H, 7.34. ^{1}H NMR (benzene-d_6): δ = 1.23 (s, 9H, C*Me*$_3$), 1.27 (s, 18H, C*Me*$_3$), 1.31 (s, 9H, C*Me*$_3$), 1.82 (s, 3H, *Me*), 1.92 (s, 3H, *Me*), 2.00 (s, 3H, *Me*), 2.06 (s, 3H, *Me*), 3.54 (m, 1H, η^9-Benzo), 3.61 (m, 1H, η^9-Benzo), 3.95 (m, 1H, η^9-Benzo), 4.02 (m, 1H, η^9-Benzo), 4.65 (m, 1H, η^9-Benzo), 5.03 (m, 1H, η^9-Benzo), 5.10 (m, 1H, η^9-Benzo), 5.33 (m, 1H, η^9-Benzo), 5.45 (s, 1H, Cp*H*), 5.64 (s, 1H, Cp*H*), 5.75 (s, 1H, Cp*H*), 6.21 (s, 1H, Cp*H*), 6.69 (m, 2H, Benzo), 6.79 (m, 2H, Benzo), 7.11 (m, 1H, Benzo), 7.27 (m, 1H, Benzo), 7.45 (m, 1H, Benzo), 7.63 (m, 1H, Benzo). ^{13}C {^{1}H} NMR (benzene-d_6): δ = 12.9, 13.2, 14.2, 22.7, 32.5, 32.8, 34.2, 34.4 (CMe_3/Me), 94.6, 95.2 (η^9-Benzo), 120.0, 121.7, 122.3, 123.8, 124.1 (Cp/Benzo). Six η^9-Benzo and twenty Cp/Benzo resonances not located.

Preparation of (η^5-C_5Me_5)(η^5-C_9H_7)Zr(CO)$_2$ (1-(CO)$_2$). To a flame dried thick-walled glass bomb charged with 47 mg (0.19 mmol) of activated magnesium turnings, 80 mg (0.19 mmol) of **1-Cl$_2$** dissolved in approximately 4 mL of THF was added. The reaction vessel was attached to the vacuum line and one atmosphere of CO was condensed at -196 ºC. The vessel was warmed to room temperature and stirred for a day. The excess CO and solvent were removed *in vacuo* leaving a green residue. The bomb was taken into the drybox and the residue extracted into pentane. Filtration through Celite followed by solvent removal afforded 77 mg (100 %) green **1-(CO)$_2$**. ^{1}H NMR (benzene-d_6): δ = 1.61 (s, 15H, Cp* *Me*), 4.97 (d, 3.2 Hz, 2H, Ind 1,3-Cp*H*),

5.69 (t, 3.2 Hz, 1H, Ind 2-Cp*H*), 6.81 (m, 2.8 Hz, 2H, Benzo), 7.09 (m, 2.8 Hz, 2H, Benzo). ^{13}C {^{1}H} NMR (benzene-d_6): δ = 11.19 (C_5Me_5), 86.57, 97.54, 107.01, 117.28, 122.65, 124.34 (Cp/Benzo), 269.69 (Zr-*C*O). IR (pentane): ν(CO) = 1961, 1873 cm^{-1}.

Preparation of (η^5-C_5Me_5)(η^5-C_9H_6-2-Me)Zr(CO)$_2$ (2-(CO)$_2$). This molecule was prepared in a similar manner to **1-(CO)$_2$** with 80 mg (0.19 mmol) of **2-Cl$_2$** and 45 mg (1.85 mmol) of activated magnesium turnings. This yielded 47 mg (61 %) of green **2-(CO)$_2$**. ^{1}H NMR (benzene-d_6): δ = 1.61 (s, 15H, Cp* *Me*), 2.09 (s, 3H, Ind *Me*), 4.88 (s, 2H, Cp*H*), 6.81 (m, 2H, Benzo), 7.05 (m, 2H, Benzo). ^{13}C {^{1}H} NMR (benzene-d_6): δ = 11.13 (C_5Me_5/Ind *Me*), 88.70, 106.92, 115.61, 117.05, 122.17, 123.93 (Cp/Benzo), 272.06 (Zr-*C*O). One C_5Me_5/Ind *Me*) resonance not located.). IR (pentane): ν(CO) = 1952, 1863 cm^{-1}.

Preparation of (η^5-C_5Me_5)(η^5-C_9H_5-1,3-(Me)$_2$)Zr(CO)$_2$ (3-(CO)$_2$). This molecule was prepared in a similar manner to **1-(CO)$_2$** with 100 mg (0.23 mmol) of **3-Cl$_2$** and 74 mg (3.04 mmol) of activated magnesium turnings. This yielded 62 mg (64 %) of forest green **3-(CO)$_2$**. ^{1}H NMR (benzene-d_6): δ = 1.55 (s, 15H, Cp* *Me*), 2.03 (s, 6H, Ind *Me*), 5.29 (s, H, Cp*H*), 6.81 (m, 2H, Benzo), 7.09 (m, 2H, Benzo). ^{13}C {^{1}H} NMR (benzene-d_6): δ = 10.70, 12.13 (C_5Me_5/Ind *Me*), 95.94, 103.95, 106.34, 116.33, 121.49, 122.08 (Cp/Benzo), 272.31 (Zr-*C*O). IR (pentane): ν(CO) = 1952, 1863 cm^{-1}.

Preparation of (η^5-C_5Me_5)(η^5-C_9H_4-1,2,3-(Me)$_3$)Zr(CO)$_2$ (4-(CO)$_2$). A J. Young NMR tube was charged with 10 mg (0.03 mmol) of **4** and approximately 0.5 mL of benzene-d_6 was added. The tube was cooled in liquid nitrogen and one atmosphere of CO was admitted forming a forest green product identified as **4-(CO)$_2$**. ^{1}H NMR

(benzene-d_6): δ = 1.53 (s, 15H, Cp* *Me*), 1.91 (s, 3H, Ind 2-Cp*H*), 1.98 (s, 6H, Ind 1,3-Cp*H*), 6.81 (m, 3.2 Hz, 2H, Benzo), 7.08 (m, 3.2 Hz, 2H, Benzo). ^{13}C {^{1}H} NMR (benzene-d_6): δ = 10.30 (Ind *Me*), 10.63 (Cp* *Me*), 11.95 (Ind *Me*), 96.38, 106.11, 115.35, 117.44, 120.87, 121.50 (Cp/Benzo), 274.47 (Zr-*C*O). IR (pentane): ν(CO) = 1950, 1858 cm^{-1}.

Preparation of (η^5-C_5Me_5)(η^5-C_9H_6-1-(^{i}Pr))Zr(CO)$_2$ (5-(CO)$_2$). A flame dried thick-walled glass bomb was charged with 4.86 g (24.21 mmol) of mercury and approximately 3 mL of toluene in a nitrogen drybox. While stirring, 24 mg (1.04 mmol) of sodium metal was added and the resulting amalgam was stirred for 20 minutes. A toluene solution of 80 mg (0.176 mmol) of **5-Cl$_2$** was added. The reaction vessel was attached to the vacuum line and one atmosphere of CO was condensed at -196 ºC. The vessel was warmed to room temperature and stirred for 15 hours. The excess CO and solvent were then removed *in vacuo* leaving a green residue. The bomb was taken into the drybox and the residue extracted into pentane. Filtration through Celite followed by solvent removal afforded forest green **5-(CO)$_2$**. ^{1}H NMR (benzene-d_6): δ = 1.19 (d, 7.2 Hz, 3H, CH*Me*$_2$), 1.22 (d, 7.2 Hz, 3H, CH*Me*$_2$), 1.6 (s, 15H, Cp* *Me*), 2.82 (m, 1H, C*H*Me$_2$), 4.87 (m, 3.6 Hz, 1H, Cp*H*), 5.56 (m, 1H, Cp*H*), 6.78 (m, 4H, Benzo), 7.22 (m, 4H, Benzo). ^{13}C {^{1}H} NMR (benzene-d_6): δ = 11.01 (C$_5$*Me*$_5$), 22.88, 25.55, 30.18 (CHMe$_2$), 85.21, 99.22, 106.25, 112.88, 115.75, 117.12, 121.85, 121.96, 122.93, 123.67 (Cp/Benzo), 272.45 (Zr-*C*O). One Zr-*C*O resonance not found. IR (pentane): ν(CO) = 1954, 1864 cm^{-1}.

Preparation of (η^5-C_5Me_5)(η^5-C_9H_5-1-(^{i}Pr)-3-(Me))Zr(CO)$_2$ (6-(CO)$_2$). This compound was prepared in a similar manner to **4-(CO)$_2$,** using 10 mg (0.03 mmol) of **6** forming a forest green product identified as **6-(CO)$_2$**. ^{1}H NMR (benzene-d_6): δ =

1.13 (d, 6.8 Hz, 3H, CH*Me*$_2$), 1.20 (d, 6.8 Hz, 3H, CH*Me*$_2$), 1.54 (s, 15H, Cp* *Me*), 2.05 (s, 3H, *Me*), 2.80 (m, 1H, C*H*Me$_2$), 5.38 (s, 1H, Cp*H*), 6.76 (m, 2H, Benzo), 7.07 (m, 1H, Benzo), 7.12 (m, 1H, Benzo). ^{13}C {^{1}H} NMR (benzene-d_6): δ = 10.67, 12.35 (Cp* *Me*/Ind *Me*), 22.34, 25.90, 26.71 (CHMe$_2$), 95.82, 101.94, 105.84, 110.55, 114.76, 116.66, 121.26, 121.40, 122.41 (Cp/Benzo), 273.66, 273.77 (Zr-*C*O). One Cp/Benzo resonance not located. IR (pentane): ν(CO) = 1950, 1860 cm^{-1}.

Preparation of (η^5-C$_5$Me$_5$)(η^5-C$_9$H$_5$-1-(^{t}Bu)-3-(Me))Zr(CO)$_2$ (7-(CO)$_2$). This molecule was prepared in a similar manner to **1-(CO)$_2$** with 0.090 g (0.19 mmol) of **7-Cl$_2$** and 0.045 g (1.85 mmol) of activated magnesium turnings. This yielded 52 mg (60 %) of forest green **7-(CO)$_2$**. ^{1}H NMR (benzene-d_6): δ = 1.35 (s, 9H, C*Me*$_3$), 1.51 (s, 15H, Cp* *Me*), 2.13 (s, 3H, *Me*), 5.12 (s, 1H, Cp*H*), 6.71 (m, 8Hz, 1H, Benzo), 6.80 (m, 8Hz, 1H, Benzo), 6.92 (m, 8Hz, 1H, Benzo), 7.24 (m, 8Hz, 1H, Benzo). ^{13}C{^{1}H} NMR (benzene-d_6): δ = 10.70, 13.23, 32.52, 32.99 (Cp* *Me*/Ind *Me*/CMe$_3$), 98.16, 100.65, 100.72, 105.47, 114.63, 115.67, 116.82, 120.88, 121.16, 121.71 (Cp/Benzo), 269.76, 271.45 (Zr-*C*O). One Cp/Benzo resonance not located. IR (pentane): *ν*(CO) = 1960, 1954, 1948, 1871, 1864, 1859 cm^{-1}.

Preparation of (η^5-C$_5$Me$_5$)(η^5-C$_9$H$_5$-1,3-(SiMe$_3$))Zr(CO)$_2$ (9-(CO)$_2$). This compound was prepared in a similar manner to **1-(CO)$_2$** using 0.100 g (0.18 mmol) of **9-Cl$_2$** and 0.049 g (2.02 mmol) of activated magnesium turnings yielding 19 mg (20 %) of a forest green product identified as **9-(CO)$_2$**. ^{1}H NMR (benzene-d_6): δ = 0.38 (s, 18H, Si*Me*$_3$), 1.48 (s, 15H, Cp* *Me*), 5.11 (s, 1H, Cp*H*), 6.83 (m, 2H, Benzo), 7.19 (m, 2H, Benzo). ^{13}C{^{1}H} NMR (benzene-d_6): δ = 0.58 (Si*Me*$_3$), 10.76 (Cp* *Me*), 96.15, 105.74, 106.20, 123.36, 124.80, 126.49 (Cp/Benzo), 265.31 (Zr-*C*O). IR (pentane): *ν* (CO) = 1964, 1951, 1880, 1864 cm^{-1}.

Preparation of (η^5-C_9H_4-1,2,3-$(Me)_3)_2Zr(CO)_2$ (12-$(CO)_2$). This compound was prepared in a similar manner to **4-$(CO)_2$**, using 7 mg (0.02 mmol) of **12** forming a forest green product identified as **10-$(CO)_2$**. ^{1}H NMR (benzene-d_6): δ = 1.65 (s, 6H, Ind 2-*Me*), 1.75 (s, 12H, Ind 1,3-*Me*), 6.78 (m, 3.2 Hz, 4H, Benzo), 6.95 (m, 3.2 Hz, 4H, Benzo). ^{13}C {^{1}H} NMR (benzene-d_6): δ = 9.96, 11.47 (*Me*), 96.44, 114.98, 116.20, 121.18, 121.92 (Cp/Benzo), 275.68 (Zr-*C*O). IR (pentane): ν(CO) = 1954, 1861 cm^{-1}.

Preparation of *rac*/*meso*-(η^5-C_9H_5-1-(^{i}Pr)-3-(Me))$_2ZrCl_2$ (*rac*/*meso*-13-$(CO)_2$). This molecule was prepared in a similar manner to **1-$(CO)_2$** with 214 mg (0.42 mmol) of **13-Cl_2** and 103 mg (4.24 mmol) of activated magnesium turnings. Subsequent workup and recrystallization in pentane at -35 °C afforded 97 mg (47 %) **13-$(CO)_2$** as a forest green solid. ^{1}H NMR (benzene-d_6): δ = 0.90 (d, 7 Hz, 6H, CH*Me*$_2$), 1.01 (d, 7 Hz, 6H, CH*Me*$_2$), 1.03 (d, 7 Hz, 6H, CH*Me*$_2$), 1.05 (d, 7 Hz, 6H, CH*Me*$_2$), 1.78 (s, 6H, *Me*), 1.88 (s, 6H, *Me*), 2.37 (m, 2H, C*H*Me$_2$), 2.57 (m, 2H, C*H*Me$_2$), 4.97 (s, 2H, Cp*H*), 5.06 (s, 2H, Cp*H*), 6.74 (m, 6H, Benzo), 6.89 (m, 4H, Benzo), 6.91 (m, 1H, Benzo), 6.94 (m, 1H, Benzo), 7.03 (m, 4H, Benzo). ^{13}C {^{1}H} NMR (benzene-d_6): δ = 12.3, 12.6 (*Me*), 22.4, 22.5, 25.8, 26.1, 26.6, 27.0 (CHMe$_2$), 95.9, 96.3, 101.0, 101.4, 111.2, 111.3, 114.6, 114.9, 116.7, 122.05, 122.07, 122.3, 122.4, 122.8, 122.9, 123.5 (Cp/Benzo), 274.0, 274.1, 275.2 (Zr-*C*O). One Cp/Benzo resonance not located. IR (pentane): ν(CO) = 1956, 1866 cm^{-1}.

Preparation of *rac*/*meso*-(η^5-C_9H_5-1-(^{t}Bu)-3-(Me))Zr$(CO)_2$ (*rac*/*meso* 14-$(CO)_2$). This compound was prepared in a similar manner to **4-$(CO)_2$,** using 30 mg (0.06 mmol) of **14** forming a forest green product identified as **14-$(CO)_2$**. ^{1}H NMR

(benzene-d_6): δ = 1.21 (s, 18H, CMe_3), 1.25 (s, 18H, CMe_3), 1.92 (s, 6H, *Me*), 2.08 (s, 6H, *Me*), 4.74 (s, 2H, Cp*H*), 4.92 (s, 2H, Cp*H*), 6.71 (m, 4H, Benzo), 6.77 (m, 2H, Benzo), 6.85 (m, 2H, Benzo), 6.94 (m, 2H, Benzo), 6.99 (m, 2H, Benzo), 7.36 (m, 2H, Benzo). IR (pentane): ν(CO) = 1865, 1873, 1881, 1885, 1951, 1958, 1966, 1971 cm^{-1}.

Preparation of *rac*/*meso*-(η^5-C_9H_5-1-(^{i}Pr)-3-(Me))$_2$Zr(PhCCPh)$_2$ (*rac*/*meso*-13-(PhCCPh)$_2$). A J. Young NMR tube was charged with 10 mg (0.011 mmol) of **13-N$_2$** and 15 mg (0.084 mmol) of diphenylacetylene and dissolved in approximately 0.5 mL of benzene-d_6. This reaction tube was then placed in a 45 °C oil bath for 2.5 days forming a brown solution identified as ***rac*/*meso*-11-(PhCCPh)$_2$**. ^{1}H NMR (benzene-d_6): δ = 0.65 (d, 6.8 Hz, 6H, CHMe_2), 0.66 (d, 6.8 Hz, 6H, CHMe_2), 0.98 (d, 6.8 Hz, 6H, CHMe_2), 0.99 (d, 6.8 Hz, 6H, CHMe_2), 2.24 (s, 6H, *Me*), 2.29 (s, 6H, *Me*), 2.70 (m, 2H, C*H*Me$_2$), 3.15 (m, 2H, C*H*Me$_2$), 5.77 (s, 2H, Cp*H*), 6.27 (s, 2H, Cp*H*), 6.75 (m, 2H, Benzo/PhCCPh phenyl), 6.82 (m, 12H, Benzo/PhCCPh phenyl), 6.92 (m, 6H, Benzo/PhCCPh phenyl), 7.10 (m, 8H, Benzo/PhCCPh phenyl), 7.18 (m, 2H, Benzo/PhCCPh phenyl), 7.23 (m, 2H, Benzo/PhCCPh phenyl), 7.30 (m, 2H, Benzo/PhCCPh phenyl), 7.46 (m, 2H, Benzo/PhCCPh phenyl).

REFERENCES

[1] Allen, A. D.; Senoff, C. V. *J. Chem. Soc. Chem. Commun.* **1965**, 621.

[2] Smil, V. *Enriching the Earth: Fritz Haber, Carl Bosch and the Transformation of World Food Production*; MIT Press: Cambridge, MA, 2001.

[3] MacLachlan, E. A.; Fryzuk, M. D. *Organometallics* **2006**, *25*, 1530.

[4] Fryzuk, M. D.; Johnson, S. A. *Coord. Chem. Rev.* **2000**, *200-202*, 379.

[5] Pez, G. P.; Apgar, P.; Crissey, R. K. *J. Am. Chem. Soc.* **1982**, *104*, 482.

[6] (a) Manriquez, J. M.; Bercaw, J. E. *J. Am. Chem. Soc.* **1974**, *96*, 6229. (b) Sanner, R. D.; Manriquez, J. M.; Marsh, R. E.; Bercaw, J. E. *J. Am. Chem. Soc.* **1976**, *98*, 8351.

[7] Manriquez, J. M.; McAlister, D. R.; Sanner, R. D.; Bercaw, J. E. *J. Am. Chem. Soc.* **1976**, *98*, 6733.

[8] Manriquez, J. M.; Sanner, R. D.; Marsh, R. E.; Bercaw, J. E. *J. Am. Chem. Soc.* **1976**, *98*, 3043.

[9] Hillhouse, G. L.; Bercaw, J. E. *J. Am. Chem. Soc.* **1994**, *106*, 5472.

[10] Pool, J. A.; Lobkovsky, E.; Chirik, P. J. *Nature*. **2004**, *427*, 527.

[11] Bernskoetter, W. H.; Pool, J. A.; Lobkovsky, E.; Chirik, P. J. *J. Am. Chem. Soc.* **2005**, *127*, 7901.

[12] Bradley, C. A.; Keresztes, I.; Lobkovsky, E.; Young, V. G.; Chirik, P. J. *J. Am. Chem. Soc.* **2004**, *126*, 16937.

[13] Veiros, L. F. *Chem. Eur. J.* **2005**, *11*, 2505.

[14] Bradley, C. A.; Lobkovsky, E.; Keresztes, I.; Chirik, P. J. *J. Am. Chem. Soc.* **2006**, *128*, 6455.

[15] (a) Bercaw, J. E.; Brintzinger, H. H. *J. Am. Chem. Soc.* **1971**, *93*, 2045. (b) Bercaw, J. *J. Am. Chem. Soc.* **1974**, *96,* 5087.

[16] (a) Hanna, T. E.; Lobkovsky, E.; Chirik, P. J. *J. Am. Chem. Soc.* **2004**, *126*, 14688. (b) Hanna, T. E.; Lobkovsky, E.; Chirik, P. J. *J. Am. Chem. Soc.* **2006**, *128*, 6018. (c) Hanna, T. E.; Lobkovsky, E.; Chirik, P. J. *Organometallics* **2009**, *28*, 4079.

[17] de Wolf, J. M.; Blaauw, R.; Meetsma, A.; Teuben, J. H.; Gyepes, R.; Varga, V.; Mach, K.; Veldman, N.; Spek, A. L. *Organometallics* **1996**, *15*, 4977.

[18] Hanna, T. E.; Bernskoetter, W. H.; Bouwkamp, M. W.; Lobkovsky, E.; Chirik, P. J. *Organometallics* **2007**, *26*, 2431.

[19] Chirik, P. J.; Henling, L. M.; Bercaw, J. E.; *Organometallics* **2001**, *20*, 534.

[20] Pool, J. A.; Lobkovsky, E.; Chirik, P. J. *J. Am. Chem. Soc.* **2003**, *125*, 2241.

[21] Pool, J. A.; Lobkovsky, E.; Chirik, P. J. *Organometallics* **2003**, *22*, 2797.

[22] Hao, S.; Berno, P.; Minhas, R. K.; Gambarotta, S. *Inorg. Chim. Acta.* **1996**, *244*, 37.

[23] Fryzuk, M. D. *Acc. Chem. Res.* **2008**,

[24] Akagi, F.; Matsu, T.;Kawaguchi, H. *Angew. Chem., Int. Ed.* **2007**, *46*, 8778.

[25] Bradley, C. A.; Keresztes, I.; Lobkovsky, E.; Chirik, P. J. *Organometallics* **2006**, *25*, 2080.

[26] Sanner, R. D.; Manriquez, J. M.; Marsh, R. E.; Bercaw, J. E. *J. Am. Chem. Soc.* **1976**, *98*, 8351.

[27] The reduction of **7-Cl$_2$** also results in two products, but the reduction of **9-Cl$_2$** where the positions on the 1 and 3 positions are both trimethylsilyl groups, only one product is observed by NMR spectroscopy. This fact along with the similar NMR shifts for the different products leads one to conclude that they are isomers.

[28] ^{15}N labeling into the compound could only be achieved by performing the reduction of **6-Cl$_2$** under an atmosphere of $^{15}N_2$ gas. No incorporation was observed by exchange of the reduction product with $^{15}N_2$ gas.

[29] Fryzuk, M. D.; Johnson, S. A.; Patrick, B. O.; Albinati, A.; Mason, S. A.; Koetzle, T. F. *J. Am. Chem. Soc.* **2001**, *123*, 3960.

[30] Bradley, C. A. Thesis. Cornell University, 2006.

[31] Walsh, P. J.; Hollander, F. J.; Bergmann, R. G. *Organometallics* **1993**, *12*, 3705.

[32] Curley, J. J.; Cook, T. R.; Reece, S. Y.; Müller, P.; Cummins, C. C. *J. Am. Chem. Soc.* **2008**,

[33] Turner, H. W.; Fellmann, J. D.; Rocklage, S. M.; Schrock, R. R. *J. Am. Chem. Soc.* **1980**, *102*, 7811.

[34] Bobadova-Parvanova, P.; Wang, Q.; Morokuma, K.; Musaev, D. G. *ACIE.* **2005**, *44*, 7101.

[35] Bernskoetter, W. H.; Lobkovsky, E.; Chirik, P. J. *J. Am. Chem. Soc.* **2005**, *127*, 14051.

[36] Hanna, T. E.; Kerestzes, I.; Lobkovsky, E.; Chirik, P. J. *Inorg. Chem.* **2007**, *46*, 1675.

[37] Bernskoetter, W. H.; Olmos, A. V.; Lobkovsky, E.; Chirik, P. J. *Organometallics* **2006**, *25*, 1021.

[38] Zachmanoglou, C. E.; Docrat, A.; Bridgewater, B. M.; Parkin, G.; Brandow, C. G.; Bercaw, J. E.; Jardine, C. N.; Lyall, M.; Green, J. C.; Keister, J. B. *J. Am. Chem. Soc.* **2002**, *124*, 9525.

[39] Bradley, C. A.; Flores-Torres, S.; Lobkovsky, E.; Abruña, H. D.; Chirik, P. J. *Organometallics* **2004**, *23*, 5332.

[40] Pangborn, A. B.; Giardello, M. A.; Grubbs, R. H.; Rosen, R. K.; Timmers, F. J. *Organometallics* **1996**, *15*, 1518.

[41] Wolczanski, P. T.; Bercaw, J. E. *Organometallics* **1982**, *1*, 793.

[42] Chirik, P. J.; Day, M. W.; Bercaw, J. E. *Organometallics* **1999**, *18*, 1873.

[43] Ready, T. E.; Chien, J. C. W.; Rausch, M. D. *J. Organomet. Chem.* **1999**, *583*, 11.

[44] Bradley, C. A.; Keresztes, I.; Lobkovsky, E.; Chirk, P. J. *Organometallics* **2006**, *25*, 2080.

[45] Lee, G. Y.; Xue, M.; Kang, M. S.; Lee, Y.-S.; Kim, H. S.; Lee, H.; Lee, I.-M. *J. Organomet. Chem.* **1998**, *558*, 11.

[46] Grimmer, N. E.; Coville, N. J.; de Koning, C. B.; Smith, J. M.; Cook, L. M. *J. Organomet. Chem.* **2000**, *616*, 112.

[47] Kawamura, S.; Takeuchi, R.; Masuyama, A.: Nojima, M.; McCullough, K. J. *J. Org. Chem.* **1998**, *63*, 5617.

Chapter 2

Synthesis and Reactivity of Reduced Bis(Indenyl) Hafnium Compounds *

Abstract

The reduction of indenyl hafnium dihalide complexes was studied. While little success was achieved with cyclopentadienyl indenyl hafnocene dihalides, (η^5-C_5Me_5)(η^5-C_9H_5-1-R,3-R')HfX_2, (R = $CHMe_2$, R' = Me; R = R' = $CHMe_2$), sodium amalgam reduction of a bis(indenyl) hafnium dichloride, (η^5-C_9H_5-1-3-$(SiMe_3)_2)_2HfCl_2$, furnished different reduction products depending on the solvent. Reduction in the presence of good donor solvents such as tetrahydrofuran (THF) or 1,2-dimethoxyethane (DME), induced haptotropic rearrangement of one of the indenyl ligands and yielded the hafnium (II) species, (η^6-C_9H_5-1-3-$(SiMe_3)_2$)(η^5-C_9H_5-1-3-$(SiMe_3)_2$)Hf-L (L = THF, DME). Reduction of the bis(indenyl) hafnocene dichloride in the presence of less coordinating solvents such as diethyl ether, 2-methyltetrahydrofuran or 2,5-dimethyltetrahydrofuran afforded a rare example of a monomeric hafnocene (III) monochloride complex, (η^5-C_9H_5-1-3-$(SiMe_3)_2)_2HfCl$. The reduction in pentane or toluene, however, resulted in decomposition. A byproduct of the η^6,η^5 bis(indenyl) hafnium DME reduction was also characterized and identified as an unusual sodium chloride complex, [(η^6-C_9H_5-1-3-$(SiMe_3)_2$)(η^5-C_9H_5-1-3-$(SiMe_3)_2$)$HfCl]_2Na[Na(DME)_3]$, where the hafnium is, again, in the 2+ oxidation state. The reactivity of all reduced bis(indenyl) hafnium complexes was explored.

Introduction

Since Wilkinson's initial characterization of ferrocene, (η^5-$C_5H_5)_2Fe$, in 1952[1], other metal sandwich complexes across the transition series have been synthesized.[2]

---

* Reproduced in part with permission from Pun, D.; Leopold, S. M.; Bradley, C. A.; Lobkovsky, E.; Chirik, P. J. *Organometallics.* **2009**, *28*, 2471. Copyright 2009 American Chemical Society.

While examples from Groups 4 – 10 were prepared successfully, the earlier transition metal sandwich complexes have proven elusive due to tendencies to cyclometalate or coordinate dinitrogen.[3] Group 3 and 4 metallocenes are particularly sought after due to successes in Zieglar-Natta olefin polymerizations[3,4] and application as reductants for organic synthesis.[5] It was not until 1998 that the first isolable titanocene that did not coordinate N_2 was crystallographically characterized; it involved utilizing bulky substituents on the cyclopentadienyl ligand, $(\eta^5\text{-}C_5Me_4SiMe_2{}^tBu)_2Ti$.[6] However, the synthesis and characterization of bis(cyclopentadienyl) zirconium or hafnium sandwich complexes has proven even more challenging.

Substituting the cyclopentadienyl with a 1,3-disubstituted indenyl ring has allowed the synthesis of unique η^9, η^5-bis(indenyl) zirconocene sandwich complexes, $(\eta^9\text{-}C_9H_5\text{-}1\text{-}R',3\text{-}R)(\eta^5\text{-}C_9H_5\text{-}1\text{-}R',3\text{-}R)Zr$ (Figure 2.1).[7] These complexes with η^9 hapticity can be prepared either from the reductive elimination of the zirconocene alkyl hydride or sodium amalgam reduction of the corresponding zirconocene dichloride. With bulky substituents such as R = R' = $CHMe_2$ (**1**), R = R' = $SiMe_3$ (**2**), R = R' = $SiMe_2{}^tBu$ or R = R' = $SiMe_2Ph$, the sandwich complexes have been readily isolated and characterized. Both NMR spectroscopy[7] and computational studies[8] have established a facile interconversion of the η^9 and η^5 rings via an η^5, η^5-bis(indenyl) zirconium intermediate, or the long sought after zirconocene. Interestingly, when the substituents on the indenyl ring are silyl groups, addition of tetrahydrofuran (THF), induces an η^9 to η^6 haptotropic shift, forming $(\eta^6\text{-}C_9H_5\text{-}1\text{-}R',3\text{-}R)(\eta^5\text{-}C_9H_5\text{-}1\text{-}R',3\text{-}R)$Zr-THF complexes, such as R = R' = $SiMe_3$ (**2-THF**) (Figure 2.1).[9,10] Aside from THF, such unique η^6, η^5 hapticity has also been observed with other strong σ-donor ligands, such as other ethers,[10,11] thioethers[12] and phosphines.[10] No such examples of η^6, η^5 hapticity have been observed when the substituents on the indenyl rings are alkyl groups. Computationally, it has been shown that the electron-rich alkyl groups

disfavor the coordination of THF because of its σ-donating ability[13] and that when this L-type ligand is substituted with a π-accepting L-type ligand, the preferred hapticity is η^5, η^5,[14] as experimentally observed.[10,11] All examples involving X-type ligands have also been observed as the η^5, η^5 haptomer.[7,10,11,12,15]

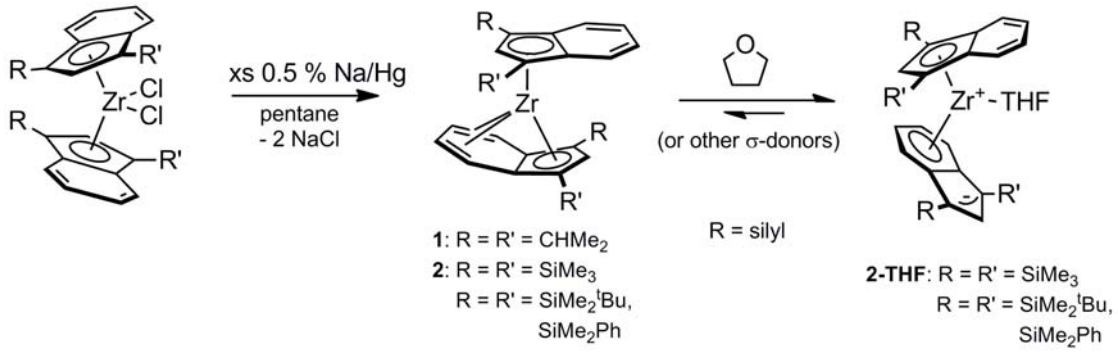

Figure 2.1. Formation of unique η^9, η^5 (center) and η^6, η^5 bis(indenyl) zirconocene sandwich complexes.

When the substituents on the indenyl are R = $CHMe_2$ and R' = Me, sodium amalgam reduction of the zirconium dihalide precursor under an atmosphere of dinitrogen results in activation of N_2 forming a highly activated dimeric dinitrogen complex, with inclusion of two equivalents of NaX (X = Cl, Br, I).[16] Replacement of an indenyl with a pentamethylcyclopentadienyl (Cp*) ligand, allows for a range of dinitrogen activation, including formation of isolable η^9, η^5 sandwich complexes that readily coordinate dinitrogen.[17]

Recently, hafnium has stepped "into the limelight,"[18] with the syntheses of hafnium compounds that compete with or surpass their zirconium congeners in dinitrogen[19] and C-H activation.[20] These observations provided motivation to prepare a bis(indenyl) hafnocene sandwich analogue. Here, we describe attempts at alkali metal reduction of bis(indenyl) and mixed ring Cp* indenyl hafnocene dihalides with the goal of either isolating a sandwich complex or a dinitrogen compound. Also reported is the reactivity of the reduced hafnium complexes.

Results and Discussion

Reduction of Indenyl Hafnocene Dihalide Complexes. With the triumph of forming both interesting indenyl zirconocene dinitrogen and unique η^9, η^5 indenyl zirconocene sandwich complexes, a similar strategy was employed with the hafnium congeners using the most versatile indenyl ligands. Therefore, 1-R',3-R-disubstituted indenyl ligands were ligated to hafnium, where R = R' = $SiMe_3$ or $CHMe_2$ with the goal of isolating a bis(indenyl) hafnocene sandwich, or where R' = Me, R = $CHMe_2$ in the hopes of dinitrogen activation. Listed in Figure 2.2 are the Cp* indenyl and the bis(indenyl) hafnocene dihalides explored in this study. All were reduced with six equivalents of 0.5 % sodium amalgam in toluene or pentane – conditions identical to that of the analogous zirconium chemistry.[16,17]

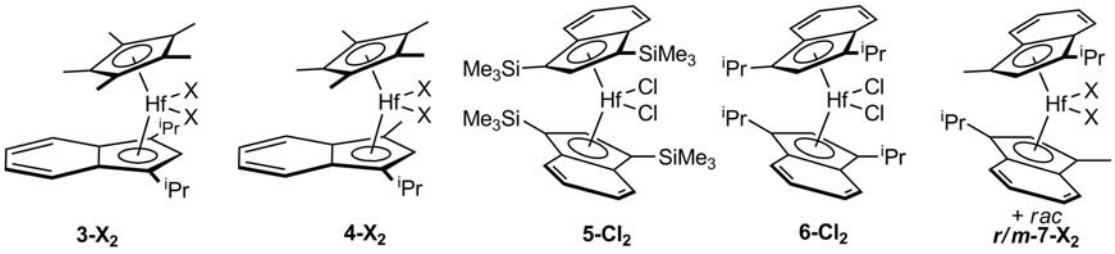

Figure 2.2. The indenyl hafnocene dihalides reduced in this study (X = Cl, I).

In all cases, reduction of the hafnium dichlorides produced intractable mixtures likely due to the propensity of hafnium to attain its highest oxidation state. Nitrogen activation was observed when **4-Cl_2** was reduced under an N_2 atmosphere. This product – not observed when the reduction was performed under an argon atmosphere – was only detectable by inference from a positive hydrazine test as other byproducts and the starting material were also present in the reduction mixture. Attempts to isolate or identify the dinitogen-containing species were unsuccessful.

The difficulty in reducing hafnocene dichlorides was also observed in the reduction of bis(cyclopentadienyl) hafnium dichlorides; reduction of (η^5-

$C_5Me_4H)_2HfCl_2$[19] or Me_2Si-(η^5-C_5Me_4)(η^5-C_5H_3-3-CMe_3)$HfCl_2$ also yielded intractable products. However, the sodium amalgam reduction of the corresponding diiodides afforded a strongly activated dinitrogen complex with a wealth of reactivity to form elaborated nitrogen-containing small molecules.[19,21,22,23] The Cp* indenyl hafnium diiodide compound, (η^5-C_5Me_5)(η^5-C_9H_5-1,3-$(CHMe_2)_2$)HfI_2, **3-I$_2$**, was synthesized by treating Cp*HfI_3 with the appropriate lithium indenide (*vide infra*). Unfortunately, the same intractable products were obtained from alkali metal reduction of **3-I$_2$** whether performed under an atmosphere of dinitrogen or argon.

The iodination of *rac*/*meso*-(η^5-C_9H_5-1-$CHMe_2$,3-Me)$_2HfCl_2$, *r/m*-**7-Cl$_2$** was attempted by treating *r/m*-**7-Cl$_2$** with boron triiodide. However, at short reaction times, a mixture of the two desired diiodide isomers, the hafnocene piano stool compound, (η^5-C_9H_5-1-$CHMe_2$,3-Me)HfI_3, **8-I$_3$**, and the starting **7-Cl$_2$** were observed. Treatment of *r/m*-**7-Cl$_2$** with iodotrimethylsilane only resulted in slow, partial conversion to the mixture of products. No free indene ligand was observed, but fulvene and other organic materials were, accounting for the displaced ligand. Longer reaction times only increased **8-I$_3$**, so rather than a lengthy purification process or fine-tuning the ratios of the iodinating agents, all hafnium compounds were converted to **8-I$_3$**, which was simply washed with pentane to remove all byproducts. **8-I$_3$** was, then, treated with lithium indenide to finally afford ***r/m*-7-I$_2$**. As an alternative, more atom-efficient method, **8-I$_3$** can be prepared from iodination of the corresponding trichloride. ***r/m*-7-I$_2$** were prepared as an equimolar mixture of *rac* and *meso* isomers and no attempts were made to separate the two diastereomers prior to alkali metal reduction. The iodination of the other two bis(indenyl) hafnium complexes, however, was met with limited success, as no clean product was achieved from a similar method. Treating two equivalents of lithium indenide with HfI_4 or adding excess methyl iodide to the bis(indenyl)hafnium dihydride (*vide infra)* produced different

products, so further attempts to synthesize these two diiodides were abandoned.

Unfortunately all attempts to reduce ***r/m*-7-I_2** – under N_2 or argon atmospheres, with excess sodium amalgam or potassium graphite – resulted in formation of a mixture of products. Included in the product mixture were three NMR distinctive isomers of *rac/meso*-(η^5-C_9H_5-1-$CHMe_2$,3-Me)$_2$Hf(H)I (two *meso* and one *rac* isomer), ***r/m*-7-(H)I**, and two isomers of *rac/meso*-(η^5-C_9H_5-1-$CHMe_2$,3-Me)$_2$$HfH_2$ (one *meso* and one *rac*), ***r/m*-7-H_2**, as judged by five downfield Hf-H resonances between 12 and 15 ppm (eq 1).[24] As further proof for these complexes, upon treatment with excess iodomethane, methane and ***r/m*-7-I_2** were generated. Importantly, neither hydrazine nor ammonia were detected upon protonalysis to indicate dinitrogen activation. Additionally, no upfield shifted benzo resonances were observed in the benzene-d_6 ^{1}H NMR spectrum to indicate η^9-indenyl coordination.

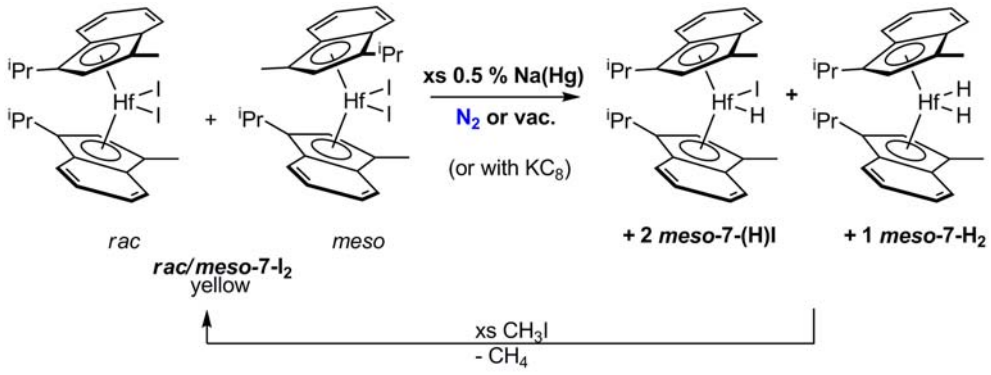

(eq. 2.1)

Electronics of Hafnocene Complexes: An Examination of Indenyl Hafnocene Dicarbonyl Compounds. Owing to the difficulty in reducing the hafnium congeners of zirconocene complexes that exhibit rich sandwich and dinitrogen chemistry, the indenyl hafnocene dicarbonyl compounds shown in Figure 2.3 were synthesized in order to evaluate the electronics of the third versus the second row transition metal. All of the desired compounds were synthesized by reducing the hafnium dichlorides with either magnesium or sodium amalgam under an atmosphere of CO. Presented in

Table 2.1 are the carbonyl stretching frequencies of the hafnocene dicarbonyl compounds. The zirconium congeners are also included for comparison.[15] Note that several dicarbonyl complexes have multiple symmetric and asymmetric carbonyl stretching frequencies; a consequence of the presence of different rotamers with distinct and detectable electronic differences.[15] For both zirconium and hafnium complexes, silyl substituted indenyls are more electron withdrawing than the alkyls. Also, as expected, the hafnium complexes are more reducing than their zirconium congeners, which should render them excellent candidates for dinitrogen activation and η^9-sandwich formation. Likely, the problem with the reduction chemistry of the dihalides is overcoming the barrier required to reduce the metal center so that it can in turn impart some of its electron density onto these N_2 or benzo ligands. It may also be that the desired hafnium (II) species is very reactive and converts back to the hafnocene (IV) dihalide complexes or decomposes.

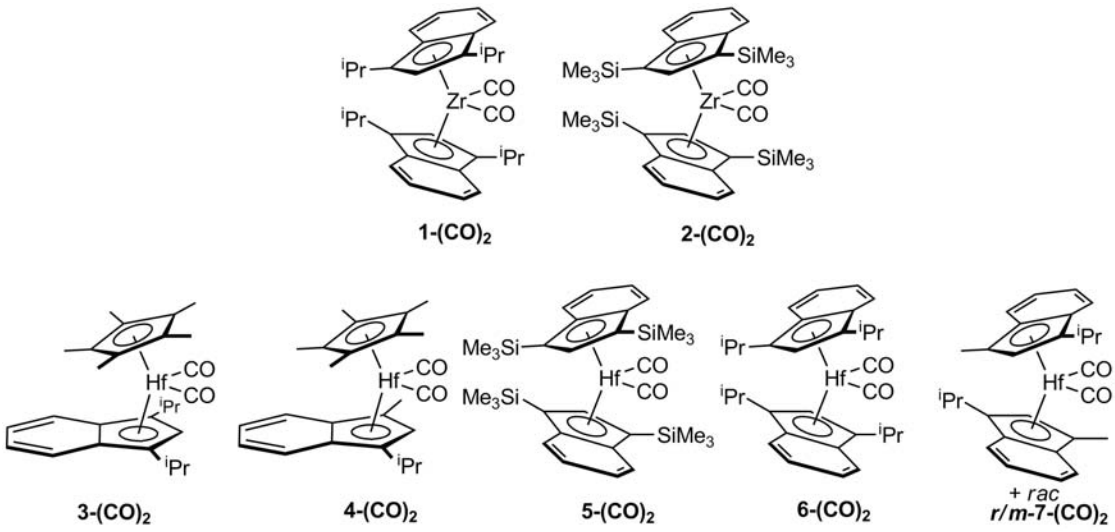

Figure 2.3. The bottom row consists of the hafnocene dicarbonyls prepared for this study. (The top row is included to designate some Zr shorthand naming.)

Table 2.1. Comparison of carbonyl stretching frequencies for the corresponding dicarbonyl complexes of all hafnocene dihalides reduced, along with their zirconium congeners.

Compound	$\nu(CO)_{sym}$ (cm^{-1})	$\nu(CO)_{asy}$ (cm^{-1})	$\nu(CO)_{ave}$ (cm^{-1})
Zirconium:			
Cp*(C_9H_5-1,3-(^{i}Pr)$_2$)$_2$Zr(CO)$_2$[14]	1956	1872	1914
Cp*(C_9H_5-1-^{i}Pr,3-Me)Zr(CO)$_2$[16]	1950	1860	1905
1-(CO)$_2$[15]	1952	1859	1905.5
2-(CO)$_2$[15]	1980, 1964 1956	1901, 1882 1874	
***r/m*-(C_9H_5-1-^{i}Pr,3-Me)$_2$Zr(CO)$_2$**[17]	1967, 1956	1866	
Hafnium:			
3-(CO)$_2$	1954, 1942	1863, 1847	
4-(CO)$_2$	1954, 1944	1862, 1850	
6-(CO)$_2$	1944	1849	1896.5
5-(CO)$_2$	1971, 1956 1948	1888, 1871 1863	
***r/m*-7-(CO)$_2$**	1961, 1948	1871, 1864	

Synthesis of η^6, η^5-Bis(indenyl) Hafnium THF and DME Complexes. With no success in activating dinitrogen (at least with no evidence for it) or in forming isolable hafnocene sandwich complexes, attention was focused on synthesizing other stabilized forms of reduced hafnium. Recalling the success with isolating η^6, η^5-bis(indenyl) zirconium-L compounds (L = good σ donors such as coordinating ethers,[9,10,11] thioethers[12] and phosphines[10]), where the zirconium is formally in the 2+ oxidation state, sodium amalgam reduction of (η^5-C_9H_5-1,3-$SiMe_3$)$_2$$HfCl_2$, **5-Cl$_2$**, in diethyl ether with 22 equivalents of THF present was attempted, yielding the desired (η^6-C_9H_5-1,3-($SiMe_3$)$_2$)(η^5-C_9H_5-1,3-($SiMe_3$)$_2$)Hf(THF), **5-THF**. THF adduct formation was not attempted on the other hafnocene complexes as no observable zirconocene-THF compounds could be synthesized when the substituents on the indenyl are not silyl groups. Analogous to the zirconocene congener, **2-THF**,[9] the ^{1}H NMR spectrum of a

benzene-d_6 solution of C_s symmetric **5-THF** exhibits one upfield shifted benzo resonance at 3.62 ppm for the η^6-bound indenyl. The other is located at 6.75 ppm. Additionally, the cyclopentadienyl hydrogen of the η^5-bound indenyl appears at 3.69 ppm. This diagnostic upfield shifting of protons on different indenyl ligands is suggestive of transannular ring currents rather than due to unusual hapticity.[10]

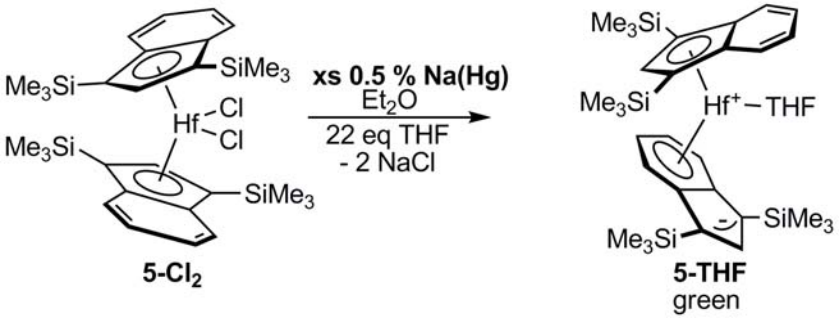

(eq. 2.2)

X-ray crystallographic studies on **5-THF** established two independent molecules in the asymmetric unit with strikingly similar metrical parameters to its zirconium congener (Figure 2.4). Selected bond distances and angles for both molecules of **5-THF** and **2-THF** are presented in Table 2.2 for comparison. Verifying the η^6, η^5 bis(indenyl) hapticity that was assigned based on NMR spectroscopy, the crystal structures also establish that the two indenyl ligands are oriented *anti* to one another, with a rotational angle of 178.5(3)/170.6(1) º. Also similar to the zirconium compound, the carbons on the η^6-benzo of **5-THF** are elongated to 1.427(3)/1.443(3) and 1.433(4)/1.419(3) Å for C(1)-C(2) and C(3)-C(4), respectively, while contracted to 1.378(4)/1.385(3) Å for C(2)-C(3), indicative of ligand reduction by the formally hafnium (II) center, suggesting considerable hafnium(IV) character. In particular, the relatively short Hf-C(1) and Hf-C(4) distances of 2.284(2)/2.299(2) and 2.294(2)/2.283(2) Å denote dialkyl character of the ligand. Also notable is the bending of the benzo ring or the "buckle" angle, deviating 22.95(11)/22.44(18) º from

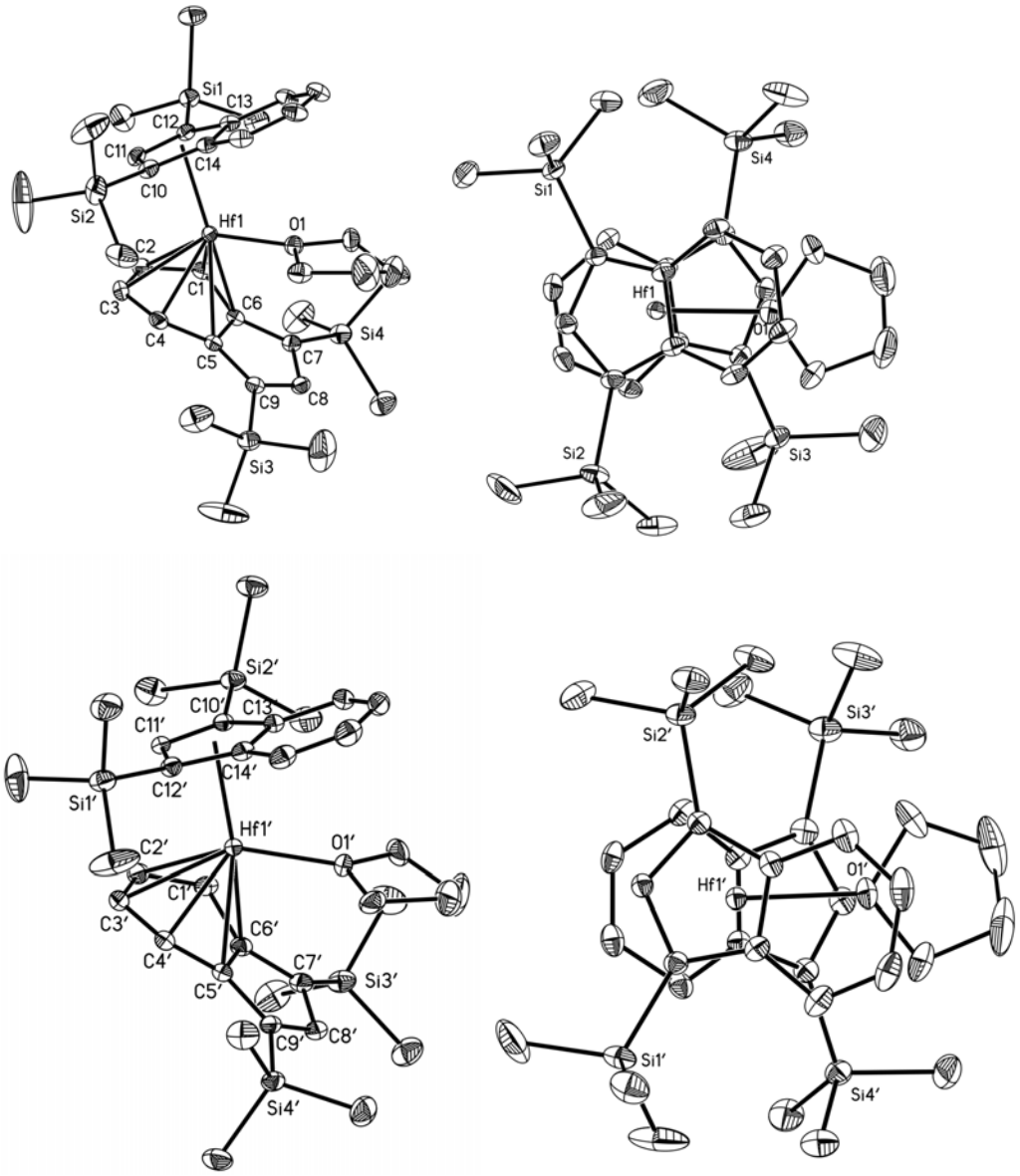

Figure 2.4. Respresentation of the two molecules of **5-THF** with the side views on the left and the top views on the right at 30 % probability elipsoids.

planarity. These metrical parameters suggest that the indenyl benzo is best described as an L_2X_2 ligand as depicted in Figure 2.5. Comparing all of these values to that in the **2-THF** show that these distortions are slightly more pronounced for the hafnium congener, likely due to the fact that hafnium is more reducing than zirconium. This is also reiterated in the M-O(1) bond lengths, shorter in the hafnium compound due to its

greater oxophilicity.

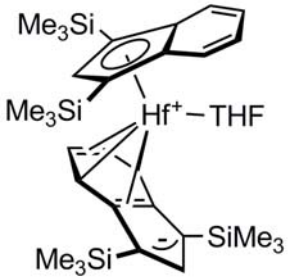

Figure 2.5. Depiction of **5-THF** with an L_2X_2 type benzo ligand and a Hf(IV) center.

Table 2.2. Comparision of select metrical parameters of the two molecules of **5-THF** and the zirconium congener, **2-THF**.

	5-THF	**5-THF**	**2-THF**[9]
M(1)-O(1) (Å)	2.1977(16)	2.1888(15)	2.254(2)
M(1)-C(1) (Å)	2.284(2)	2.299(2)	2.340(2)
M(1)-C(2) (Å)	2.459(2)	2.462(2)	2.472(3)
M(1)-C(3) (Å)	2.455(2)	2.460(2)	2.493(2)
M(1)-C(4) (Å)	2.294(2)	2.283(2)	2.355(3)
M(1)-C(5) (Å)	2.475(2)	2.441(2)	2.468(3)
M(1)-C(6) (Å)	2.448(2)	2.469(2)	2.487(3)
M(1)-C(10) (Å)	2.470(2)	2.473(2)	2.623(3)
M(1)-C(11) (Å)	2.410(2)	2.434(2)	2.501(3)
M(1)-C(12) (Å)	2.445(2)	2.483(2)	2.454(3)
M(1)-C(13) (Å)	2.575(2)	2.600(2)	2.494(2)
M(1)-C(14) (Å)	2.602(2)	2.590(2)	2.608(3)
C(1)-C(2) (Å)	1.427(3)	1.443(3)	1.425(4)
C(1)-C(6) (Å)	1.463(3)	1.464(3)	1.458(4)
C(2)-C(3) (Å)	1.378(4)	1.385(3)	1.394(4)
C(3)-C(4) (Å)	1.433(4)	1.419(3)	1.414(4)
C(4)-C(5) (Å)	1.464(3)	1.469(3)	1.466(3)
C(5)-C(6) (Å)	1.432(3)	1.434(3)	1.444(3)
Dihedral Angle (°)[a]	22.95(11)	22.44(18)	19.0(1)
Rotational Angle (°)[b]	178.5(3)	170.6(1)	177.8(1)

[a] Defined as the deviation from planarity of the benzo ring, which is the angle between the planes formed by C(1)-C(2)-C(3)-C(4) and C(4)-C(5)-C(6)-C(1). [b] Defined as the angle formed between the plane defined by Hf(1), C(8) and the centroid between C(5)-C(6) and the plane defined by Hf(1), C(11) and the centroid between C(13)-C(14) in molecule 1.

Interestingly, while **2-THF** is in equilibrium with **2** and free THF in solution on the NMR timescale, this is not the case with the hafnium counterpart. In fact, unlike the zirconium congener where the ether is labile enough to be removed by vacuum, **5-THF** does not display any signs of decomposition even after several cycles of trituration with pentane, likely due to the greater metal-oxygen bond strength with the third row metal. However, this tightly coordinated ligand is rapidly exchanged by 1,2-dimethoxyethane (DME), forming a formally 18 electron η^6, η^5 bis(indenyl) hafnium complex, (η^6-C_9H_5-1,3-$SiMe_3$)(η^5-C_9H_5-1,3-$SiMe_3$)Hf(DME), **5-DME**. This compound was also prepared by sodium amalgam reduction of **5-Cl$_2$** in the presence of DME (eq. 2.3). Similar to **5-THF**, **5-DME** is C_s symmetric in solution as evidenced by its ^{1}H NMR spectrum and has one upfield shifted benzo and one cyclopentadienyl hydrogen at 3.91 and 4.30 ppm, respectively, diagnostic of η^6, η^5 hapticity.

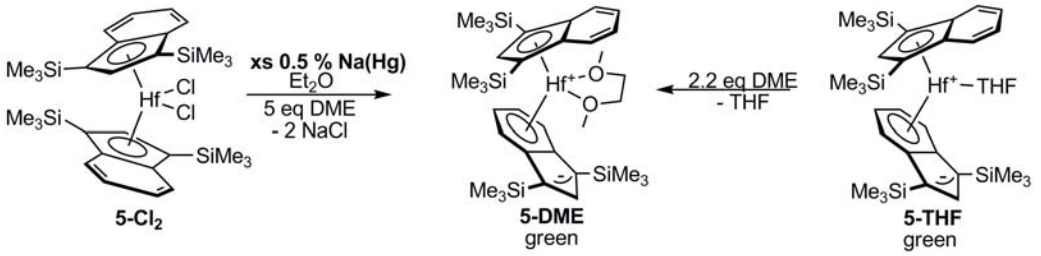

(eq. 2.3)

Characterization of an Unusual Hafnocene Sodium Chloride Compound. Attempting to grow X-ray quality crystals of green **5-DME** resulted in isolation of pale yellow crystals. Instead of **5-DME**, the crystal structure established the molecular structure of an unusual dimeric hafnocene sodium chloride compound, [(η^6-C_9H_5-1,3-$SiMe_3$)(η^5-C_9H_5-1,3-$SiMe_3$)HfCl]$_2$Na{Na(DME)$_3$}, **[5-Cl]$_2$Na{Na(DME)$_3$}**. Benzene-d_6 solution NMR spectra of the crystals and the mother liquor verify that a new C_s symmetric compound had crystallized leaving **5-DME** in solution. Based on

the ^{1}H NMR spectrum and X-ray structure, this new complex also exhibits η^6, η^5 bis(indenyl) hapticity with a diagnostic benzo resonance centered at 3.64 ppm. This is the first example of η^6, η^5 hapticity involving an X-type ligand; all previous contain neutral ligands such as ethers,[9,10,11] thioethers[12] or phosphines.[10]

Presented in Figure 2.6 is the X-ray crystal structure of the anion. There was disorder in the $Na(DME)_3$ cation and the SQUEEZE program utilized to remove it from the final solution of the structure. This anionic hafnocene dimer is comprised of two η^6, η^5 bis(indenyl) hafnium monochloride monomers bridged by a sodium atom via the chlorides and the unsubstituted cyclopentadienyl carbon. The four coordinate sodium atom has a square planar geometry as the sum of the angles is 360.00(16) º. Similar to **5-THF**, the two indenyl rings on the hafnium center are oriented *anti* to one another, with a rotational angle of 174.1(1) º. Also characteristic of η^6, η^5-indenyl coordination, the C(1)-C(2) and C(3)-C(4) bonds are elongated to 1.4580(5) and 1.455(5), while the C(2)-C(3) bond contracted to 1.370(6) Å. There is a buckle angle which deviates 25.37(28) º from planarity (Table 2.3). Again, this η^6-bound benzo shows a two electron reduction, suggesting an L_2X_2 ligand. All metrical parameters appear to show that in bis(indenyl) hafnium chemistry, there is little difference when replacing a coordinating ether with essentially a NaCl molecule.

Addition of 1 atmosphere of carbon monoxide to **[5-Cl]$_2$Na{Na(DME)$_3$}** resulted in formation of the hafnocene dicarbonyl, **5-(CO)$_2$**, and precipitation of sodium chloride. Unlike typical zirconocene (III) and hafnocene (III) monochlorides, where a mixture of hafnocene dicarbonyl and dichloride complexes are formed,[25] no **5-Cl$_2$** was detected. This suggests that **[5-Cl]$_2$Na{Na(DME)$_3$}** behaves more like a sodium chloride adduct of hafnium (II) than a hafnium (III) monochloride (*vide infra*), reinforcing the crystallographic similarities between this complex and that of the THF adduct, **5-THF**.

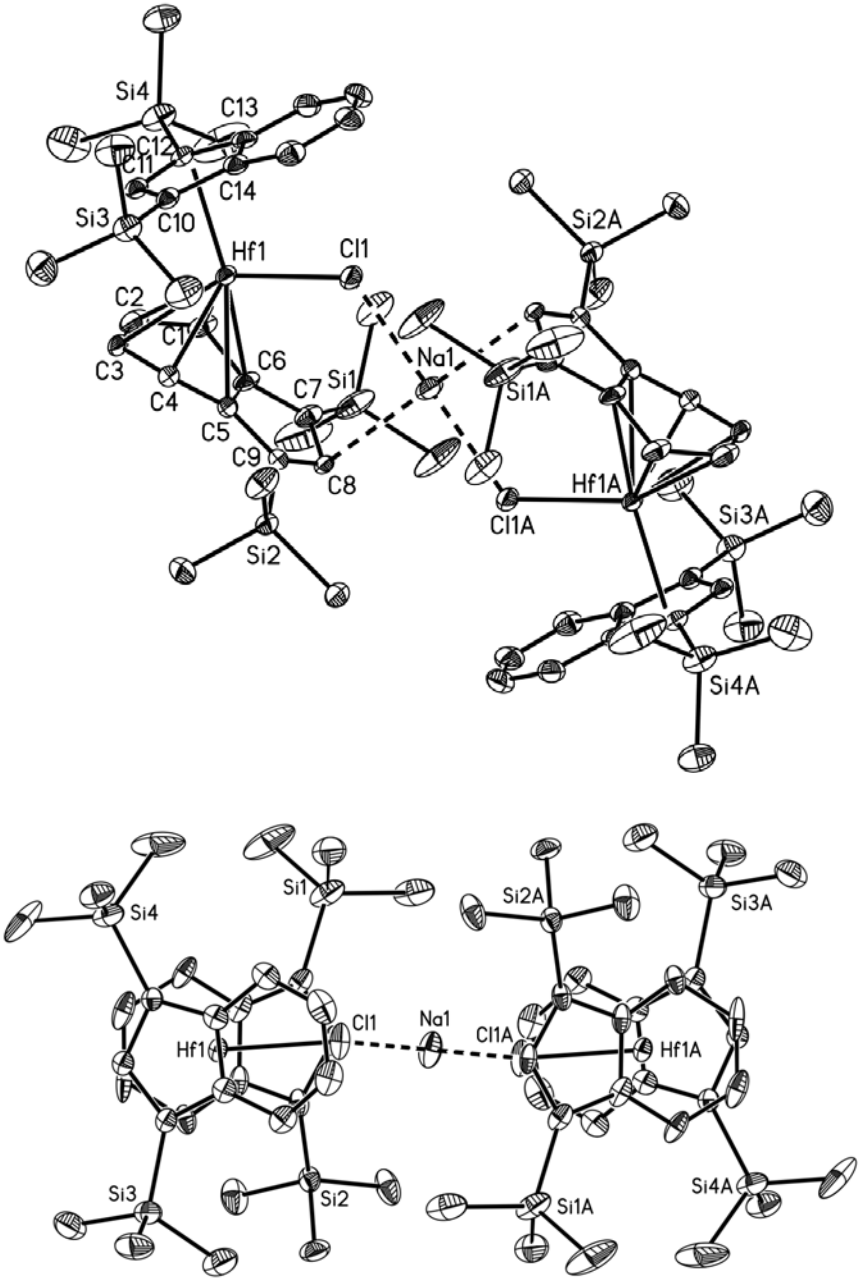

Figure 2.6. Side (top) and top (bottom) views of **[5-Cl]$_2$Na{Na(DME)$_3$}** at 30 % probability elipsoids.

Table 2.3. Comparision of select metrical parameters of **[5-Cl]$_2$Na{Na(DME)$_3$}**.

	{[5-Cl]$_2$Na}$^-$
Hf(1)-Cl(1) (Å)	2.4235(9)
Hf(1)-C(1) (Å)	2.284(3)
Hf(1)-C(2) (Å)	2.479(4)
Hf(1)-C(3) (Å)	2.473(4)
Hf(1)-C(4) (Å)	2.291(3)
Hf(1)-C(5) (Å)	2.499(4)
Hf(1)-C(6) (Å)	2.478(3)
Hf(1)-C(10) (Å)	2.477(3)
Hf(1)-C(11) (Å)	2.413(3)
Hf(1)-C(12) (Å)	2.484(3)
Hf(1)-C(13) (Å)	2.612(3)
Hf(1)-C(14) (Å)	2.617(3)
C(1)-C(2) (Å)	1.408(5)
C(1)-C(6) (Å)	1.4580(5)
C(2)-C(3) (Å)	1.370(6)
C(3)-C(4) (Å)	1.437(5)
C(4)-C(5) (Å)	1.455(5)
C(5)-C(6) (Å)	1.436(5)
Na(1)-C(8) (Å)	2.722(3)
Dihedral Angle (°)[a]	25.37(28)
Rotational Angle (°)[b]	174.1(1)

[a] Defined as the deviation from planarity of the benzo ring, which is the angle between the planes formed by C(1)-C(2)-C(3)-C(4) and C(4)-C(5)-C(6)-C(1). [b] Defined as the angle formed between the plane defined by Hf(1), C(8) and the centroid between C(5)-C(6) and the plane defined by Hf(1), C(11) and the centroid between C(13)-C(14) in molecule 1.

Synthesis of a Monomeric Hafnocene (III) Monochloride Compound. With the success of reducing **5-Cl$_2$** in the presence of good coordinating solvents such as THF and DME as opposed to non-coordinating pentane, solvents in between these extremes were attempted. Ideally, a hafnocene solvent adduct can be formed where the solvent could be easily replaced with a cyclopentadienyl ring on the η^6-indenyl ligand,

forming an isolable η^9, η^5 bis(indenyl) hafnocene sandwich. Sodium amalgam reduction of a diethyl ether solution of **5-Cl$_2$** in the presence of excess 2-methyltetrahydrofuran or 2,5-dimethyltetrahydrofuran afforded a green paramagnetic compound identified as the hafnocene (III) monochloride, (η^5-C_9H_5-1-3-$(SiMe_3)_2)_2HfCl$, **5-Cl**. **5-Cl** was also readily prepared in pure diethyl ether (eq. 2.4).

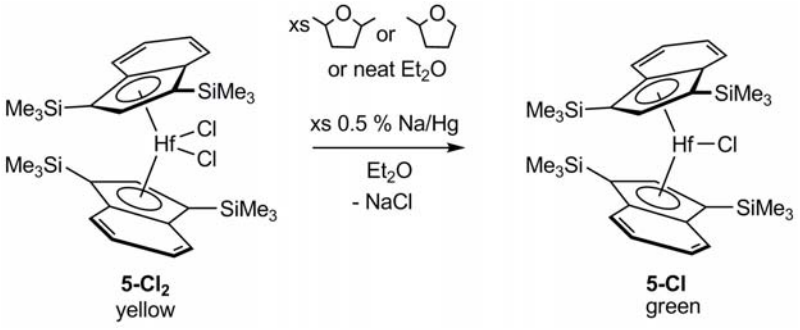

(eq. 2.4)

The solid state structure of **5-Cl** was confirmed by X-ray diffraction and established a monomeric compound (Figure 2.7). Two independent molecules were located in the asymmetric unit. Both indenyl ligands have η^5 hapticity, with only a minimal deviation from planarity by approximately 10 º. As shown in the top views of Figure 2.7, the two indenyl rings are oriented in a nearly eclipsed manner with rotational angles of 31.8(1) and 27.2(1) º. The single chlorine atom is located at the center of the metallocene wedge.

To our knowledge, this is the first example of a crystallographically characterized monomeric hafnium (III) species. While several dimeric zirconocene (III) examples both paramagnetic[25] and diamagnetic[25,26] exist, only one monomeric case has been structurally characterized, with bulky substituents on the cyclopentadienyl ligand, $(\eta^5$-C_5H_3-1-3-$(CMe_3)_2)_2ZrCl$.[27] For hafnium, compounds of this type are very rare. Janus and coworkers report the reduction of HfI_4 with aluminum metal to produce HfI_3, characterizing it via powder diffraction and magnetic susceptibility measurements.[28] In 1990, both Cotton[29] and Girolami[30] have independently obtained crystallographic evidence of the first hafnium (III) species; all

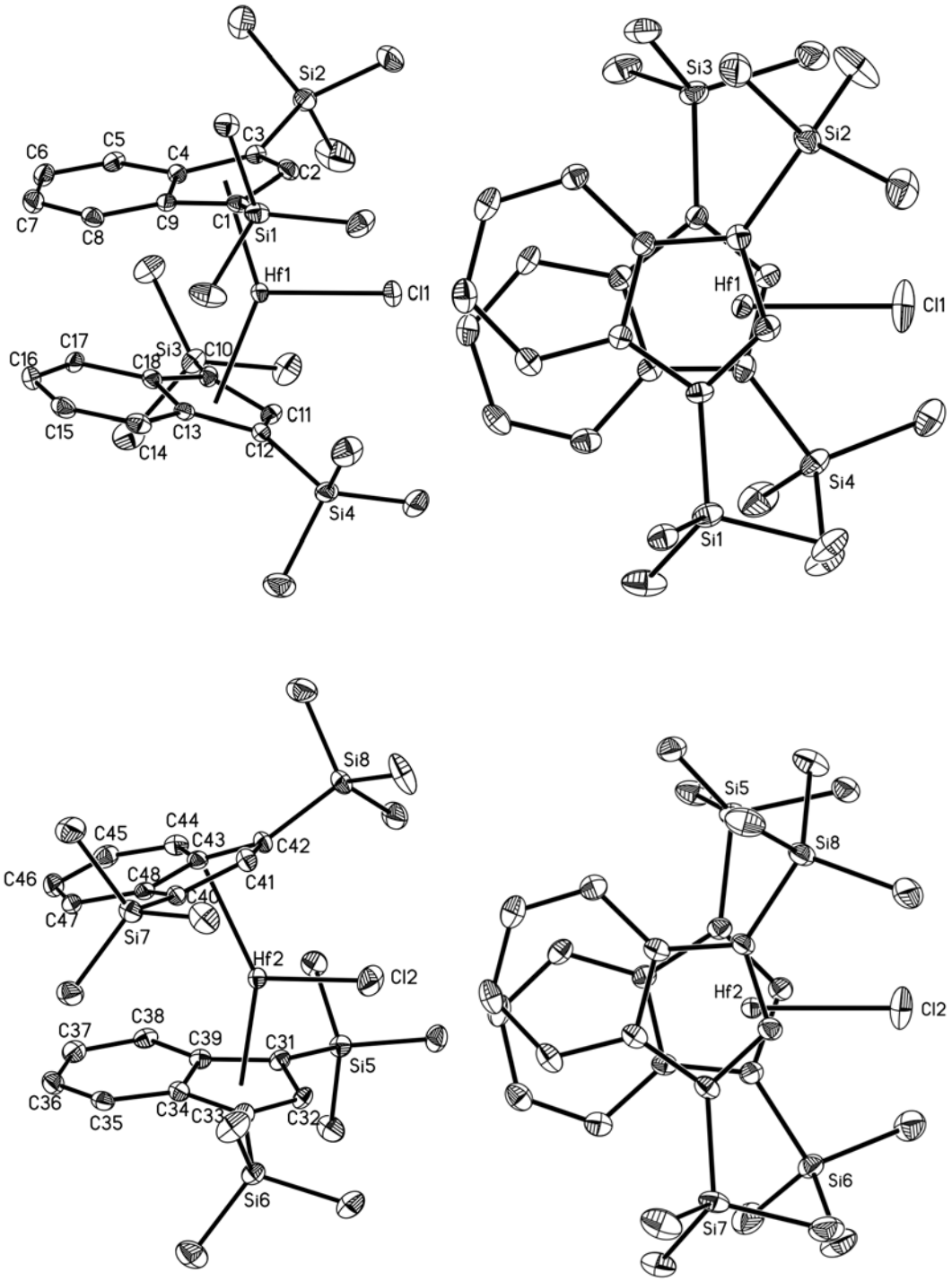

Figure 2.7. Views of the two molecules of **5-Cl** with the side views on the left and the top views on the right.

Table 2.4. Select metrical parameters of the two molecules of **5-Cl**.

	1-Cl		**1-Cl**
Hf(1)-Cl(1) (Å)	2.3807(7)	Hf(2)-Cl(2)	2.3855(8)
Hf(1)-C(1) (Å)	2.451(2)	Hf(2)-C(31)	2.436(3)
Hf(1)-C(2) (Å)	2.417(2)	Hf(2)-C(32)	2.433(3)
Hf(1)-C(3) (Å)	2.481(3)	Hf(2)-C(33)	2.489(3)
Hf(1)-C(4) (Å)	2.580(3)	Hf(2)-C(34)	2.556(3)
Hf(1)-C(9) (Å)	2.574(2)	Hf(2)-C(39)	2.539(3)
Hf(1)-C(10) (Å)	2.436(2)	Hf(2)-C(40)	2.447(3)
Hf(1)-C(11) (Å)	2.438(2)	Hf(2)-C(41)	2.423(3)
Hf(1)-C(12) (Å)	2.492(3)	Hf(2)-C(42)	2.481(3)
Hf(1)-C(13) (Å)	2.556(2)	Hf(2)-C(43)	2.592(3)
Hf(1)-C(18) (Å)	2.543(2)	Hf(2)-C(48)	2.592(3)
C(5)-C(6) (Å)	1.359(4)	C(35)-C(36)	1.350(4)
C(6)-C(7) (Å)	1.401(4)	C(36)-C(37)	1.420(4)
C(7)-C(8) (Å)	1.360(4)	C(37)-C(38)	1.353(4)
C(14)-C(15) (Å)	1.368(4)	C(44)-C(45)	1.353(4)
C(15)-C(16) (Å)	1.400(4)	C(45)-C(46)	1.404(4)
C(16)-C(17) (Å)	1.367(4)	C(46)-C(47)	1.350(4)
Indenyl Fold Angles (°)[a]	8.79(9)/8.21(15)	Indenyl Fold Angles[a]	7.96(16)/9.63(8)
Dihedral Angle (°)[b]	2.63(13)/2.59(28)	Dihedral Angles[b]	3.02(25)/2.64(19)
Rotational Angle (°)[c]	31.8(1)	Rotational Angle[c]	27.2(1)

[a] Defined as the angle between the planes formed by the five-membered cyclopentadienyl and the six-membered benzo rings of the indenyl. [b] Defined as the deviation from planarity of the benzo ring, which is the angle between the planes formed by C(5)-C(4)-C(9)-C(8) and C(5)-C(6)-C(7)-C(8) in molecule 1. [c] Defined as the angle formed between the plane defined by Hf(1), C(2) and the centroid between C(4)-C(9) and the plane defined by Hf(1), C(11) and the centroid between C(13)-C(18) in molecule 1.

diamagnetic, dimeric hafnium (III) complexes with phosphine ligands. Sodium amalgam reduction of $(\eta^5\text{-}C_5H_5)_2HfCl_2$ resulted in formation of dimeric $[(\eta^5\text{-}C_5H_5)_2HfCl]_2$,[31] while electrochemical reduction of the former produced the hafnocene (III) anion, $[(\eta^5\text{-}C_5H_5)_2HfCl_2]^-$, which was characterized by EPR spectroscopy and has a g value centered at 1.9839.[32] Lappert has also synthesized and

characterized a hafnocene dialkyl anion[33] and a monoalkyl[34] via EPR spectroscopy, reporting g values of 1.943 and 1.987, respectively. However, (η^5-C_5H_3-1-3-$(CMe_3)_2)_2HfCl$, the hafnium congener of the monomeric zirconocene monochloride, is the only authentic example of a monomeric hafnium (III) species, but has not been characterized crystallographically.[27]

5-Cl was also characterized by EPR spectroscopy at several temperatures between 5 and 293 K. The spectra exhibit a rhombic signal with $g_x = 1.98$, $g_y = 1.96$ and $g_z = 1.70$, along with hyperfine coupling to both ^{179}Hf (I = 9/2, 13.8 % abundance) and ^{177}Hf (I = 7/2, 18.5 % abundance) at 77 K (Figure 2.8). Attempts were made to fit the data in order to obtain the coupling constants, but with the complex splitting and multitude of hafnium isotopes, a good approximation was difficult to achieve.

Addition of one atmosphere of carbon monoxide to **5-Cl** resulted in formation of an equimolar mixture of **5-(CO)$_2$** and **5-Cl$_2$**, behaving like a typical zirconocene (III) or hafnocene (III) monochloride,[25,26] and offering reactivity distinct from **[5-Cl]$_2$Na{Na(DME)$_3$}**. Oxidation of **5-Cl** with lead dichloride resulted in clean conversion back to **5-Cl$_2$**.

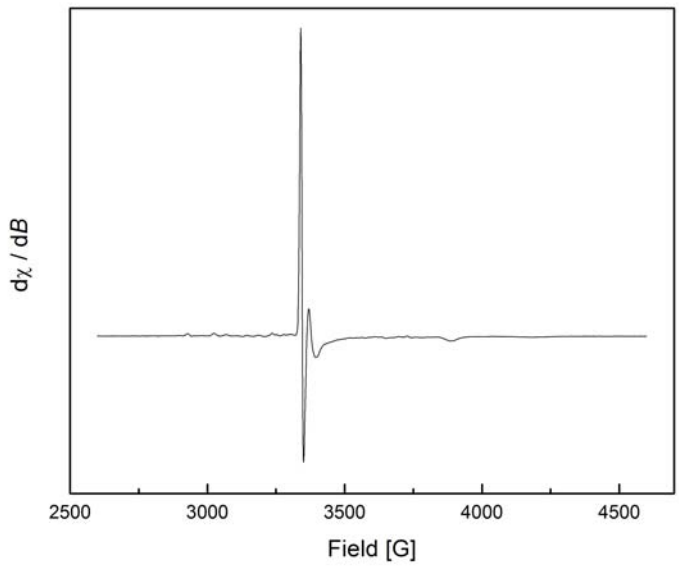

Figure 2.8. Toluene glass EPR spectrum of **5-Cl** collected at 77 K. $g_x = 1.98$, $g_y = 1.96$ and $g_z = 1.70$.

C-O Bond Cleavage with 5-THF and 5-DME. With several isolable formally hafnocene (II) complexes in hand, their reactivity was explored. Unfortunately, given the difficulty in reliably synthesizing the sodium chloride complex – preparation of a crown-ether derivative was attempted but without success – focus was maintained on only **5-THF** and **5-DME**.

Allowing a benzene-d_6 solution of **5-THF** to stand under vacuum for one month at ambient temperature resulted in formation of two new products in a 2.7:1 ratio, along with free tetrahydrofuran. The major product was identified as arising from C-O bond cleavage of the THF, forming a C_s symmetric hafnocene alkyl alkoxide, (η^5-C_9H_5-1-3-$(SiMe_3)_2)_2$Hf-*cyclo*-$O(CH_2)_3CH_2$, **5-*cyclo*-$O(CH_2)_3CH_2$**. The minor product was the result of C-H bond activation of one of the $SiMe_3$ substituents, forming a C_1 symmetric hafnocene cyclometalated hydride, (η^5-C_9H_5-1,3-$(SiMe_3)_2$)(η^5-C_9H_5-η^1-1-$SiMe_3$-3-$SiMe_2CH_2$)]HfH, **5-CMH**. The C-O cleavage product has also been observed in analogous bis(indenyl) zirconocene chemistry from thermolysis of **2-THF** at 85 ºC[11] and in bis(pentamethylcyclopentadienyl) zirconocene chemistry via Mg reduction of the zirconocene dichloride in the presence of THF.[35] Heating a benzene-d_6 solution of **5-THF** to 85 ºC for three days resulted in faster conversion, favoring the C-O cleavage product in a 4:1 ratio (eq. 2.5). The best yields of **5-*cyclo*-$O(CH_2)_3CH_2$**, a 10:1 ratio, were obtained from heating **5-THF** in the presence of five equivalents of THF.

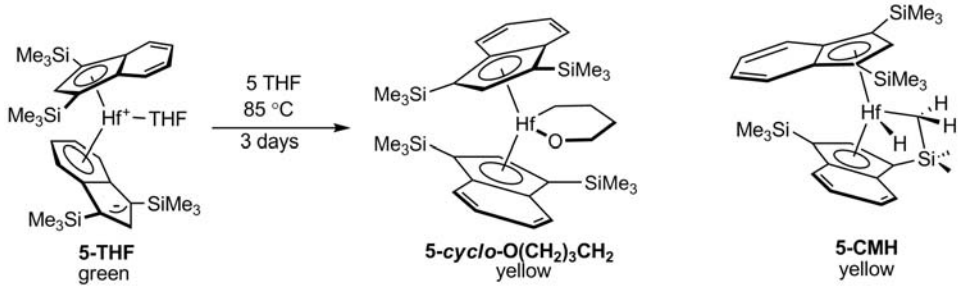

5-THF green **5-*cyclo*-$O(CH_2)_3CH_2$** yellow **5-CMH** yellow (eq. 2.5)

C-O bond cleavage with **5-DME** occurred over two days at ambient temperature, forming a 2:1 mixture of a hafnocene dimethoxy, (η^5-C_9H_5-1-3-$(SiMe_3)_2)_2Hf(OMe)_2$, **5-(OMe)$_2$** and a hafnacyclopentane, (η^5-C_9H_5-1-3-$(SiMe_3)_2)_2$Hf-*cyclo*-$(CH_2)_4$, **5-*cyclo*-C_4H_8** (eq. 2.6). The latter compound has been independently synthesized from treatment of **5-THF** with ethylene gas; two equivalents are coupled and exhibit diagnostic upfield shifted benzene-d_6 ^{1}H NMR resonances at 0.39 and 1.63 ppm for the hydrogens on the hafnacycle. This differs from the zirconium counterpart where a formally zirconocene (II) η^2-ethylene adduct is isolated and crystallographically characterized,[11] again reiterating hafnium's propensity to stay in the hafnium (IV) oxidation state.

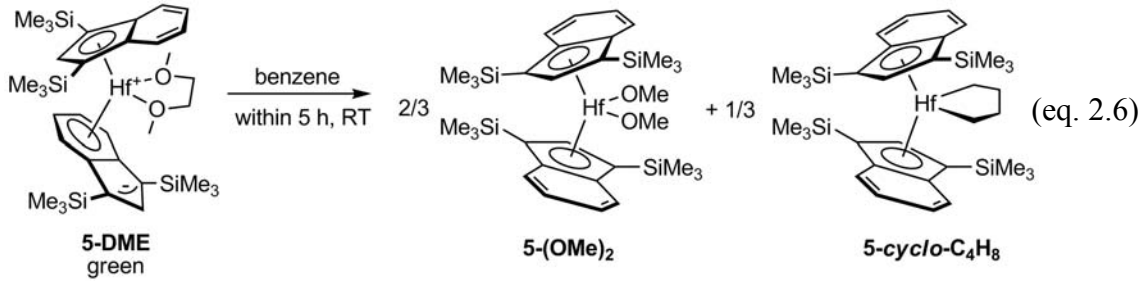

5-DME green — **5-(OMe)$_2$** — **5-*cyclo*-C_4H_8** (eq. 2.6)

Hydrogenation of Bis(indenyl) Hafnium (II) Compounds. In a final attempt to synthesize an η^9, η^5 bis(indenyl) hafnocene sandwich complex, the preparation of a bis(indenyl) hafnocene dihydride was targeted, with the goal that H_2 reductive elimination would be facile. Hydrogenation of hafnium (II) complexes were initially explored. Exposure of a pentane or benzene solution of **5-THF** to one atmosphere of H_2 resulted in a color change from green to yellow. Monitoring the reaction by ^{1}H NMR spectroscopy revealed that instead of the desired hafnocene dihydride, insertion of a hydrogen into an indenyl benzo ring had occurred, concomitant with an η^6 to η^5, η^3 hapticity change, forming (η^5-C_9H_5-1,3$(SiMe_3)_2$)(η^5, η^3- C_9H_6-1,3$(SiMe_3)_2$)HfH, **5-DHID-H** (eq. 2.7). In benzene-d_6, the ^{1}H NMR spectrum exhibits the number of resonances expected for a C_1 symmetric compound, with a hafnium hydride centered

at 3.03 and the methylene resonances at 2.32 and 2.51 ppm. The former upfield shifted resonance is indicative of a hafnium hydride on a saturated, 18 electron metallocene. Deuterium labeling of **5-DHID-H** by addition of D_2 gas to **5-THF** shows that the latter peak is that of the inserted hydrogen.

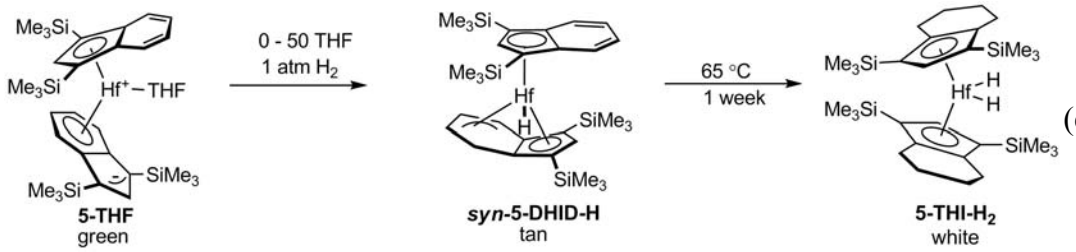

(eq. 2.7)

There are two possible diastereomers of **5-DHID-H**: one where the hafnium hydride is *syn* to the methylene carbon and one where it is *anti*. Both isomers have been observed in bis(indenyl) zirconium chemistry; the *syn* diastereomer is the predominant product from hydrogenation of the zirconocene dihydride, while *anti* from hydrogenation of the zirconocene THF complex, **2-THF**. Interestingly, the *anti* isomer isomerizes to the *syn* isomer over time, which is inhibited by the presence of excess tetrahydrofuran. Therefore, it is interesting that for hafnium, only one isomer was observed and does not seem to convert to another isomer over time. The stereochemistry of this isomer was assigned based on a NOESY NMR experiment (Figure 2.9). As depicted in the circles and ovals in the two-dimensional NMR spectrum, the protons of the six-membered ring of the dihydroindenediyl ligand were first assigned, which resulted in the assignment of the two methylene hydrogens. Crosspeaks between the inserted hydrogen on the methylene carbon and the hafnium hydride shown in the bold squares demonstrate that the *syn* isomer was prepared. An NOE between the proton on the adjacent allylic carbon and the hafnium hydride was also observed. As further definitive proof, no correlation was observed between the hafnium hydride and the other allylic protons, ruling out the *anti* isomer. Attempts were made to try to synthesize the *anti* isomer, but the hydrogenation of **5-THF** in the

presence of 50 equivalents of THF only resulted in the observation of ***syn*-5-DHID-H** by NMR spectroscopy within the first five minutes of reaction. It is likely that like the zirconium case, the *anti* isomer is formed but immediately isomerizes to the *syn* isomer. It is also possible that for hafnium, the *syn* is thermodynamically favored.

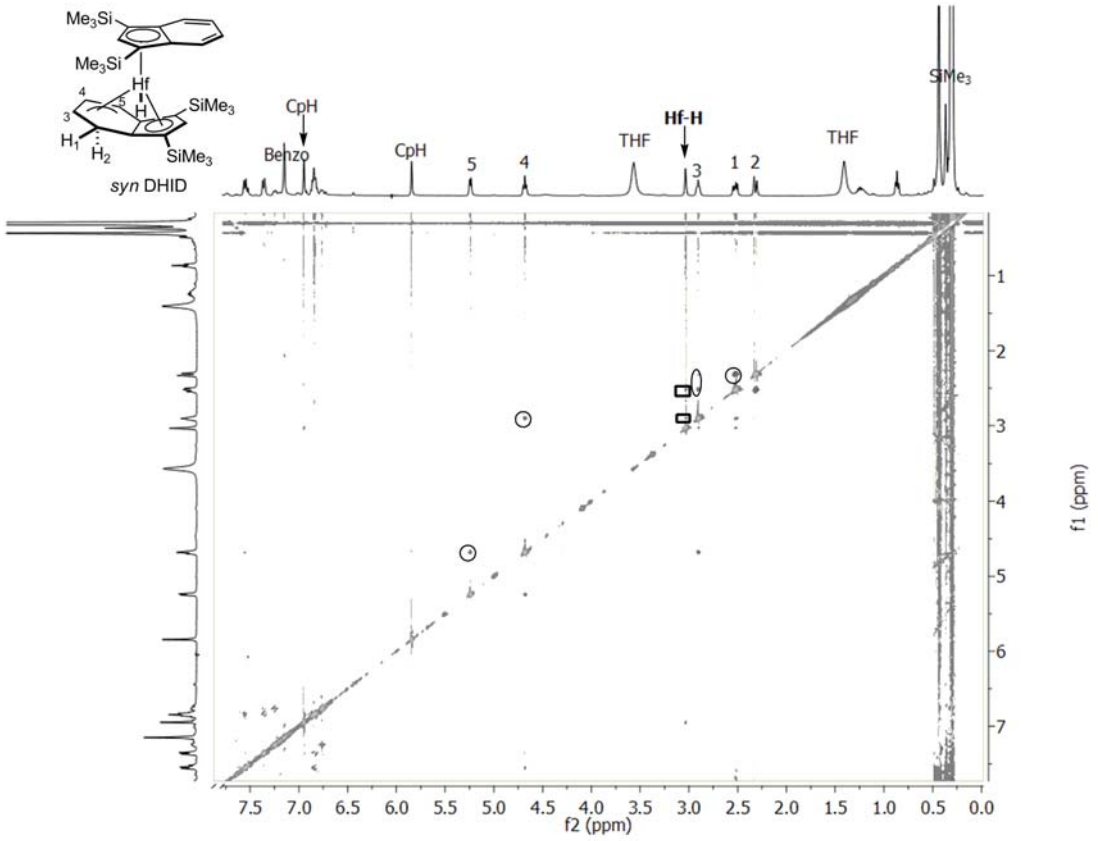

Figure 2.9. NOESY NMR spectrum of **5-DHID-H** which depicts a *syn* isomer. Circles and ovals denote assignment of the dihydroindenediyl ring, while bold squares the orientation of the Hf-*H* over H_1 and H_3.

Analogous to the corresponding zirconium chemistry, heating **5-DHID-H** in the presence of excess dihydrogen at 65 ºC for one week resulted in hydrogen insertion into the benzo ring of both indenyl ligands, forming C_{2v} symmetric (η^5-C_9H_9-1-3-$(SiMe_3)_2)_2HfH_2$, **5-THI-H$_2$** (eq. 2.7), with diagnostic upfield shifted tetrahydroindenyl (THI) resonances around 2 ppm in benzene-d_6. A downfield resonance at 14.95 ppm for the hafnium hydride is an indication that the previously

saturated **5-DHID-H** with its hydride resonance at 3.03 has now formed an unsaturated 16 electron complex. These **5-THI-H_2** ^{1}H NMR peaks have been verified by heating a solution of **5-THF** in the presence of excess D_2 gas, establishing exclusive deuterium incorporation into the *endo* positions of the THI ligand, as expected for an intramolecular insertion mechanism.

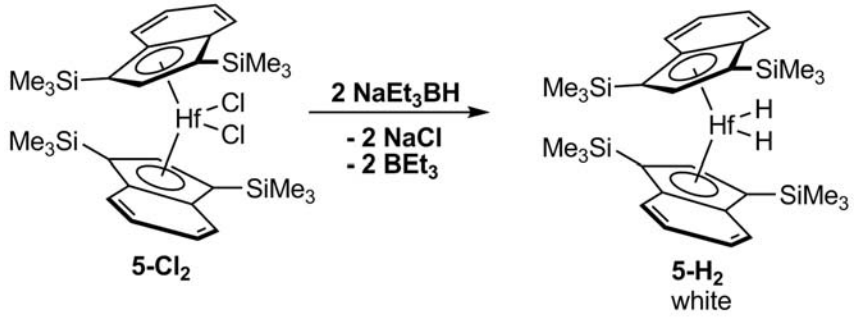

5-Cl_2 **5-H_2** white (eq. 2.8)

Alternative methods to synthesize hafnocene dihydride complexes were also explored. Addition of 2 equivalents of $NaEt_3BH$ to a toluene solution of **5-Cl_2**, yielded the desired (η^5-C_9H_5-1-3-$(SiMe_3)_2)_2HfH_2$, **5-H_2** as a white crystalline solid (eq. 2.8). Consistent with a monomeric 16 electron species, the hafnium hydride appears at 14.85 ppm.[24] Upon addition of either H_2 or D_2 gas at ambient temperature, the hydride quickly exchanges as evidenced by either a broadening of the hafnium hydride resonance or a disappearance of the peak altogether in the ^{1}H NMR spectrum, forming **5-D_2** without detectable deuterium scrambling into the ligand in the later case, analogous to permethylzirconocene chemistry.[24]

To probe the intermediacy of **5-H_2** to **5-DHID-H**, a benzene-d_6 solution of **5-H_2** was allowed to stand at room temperature. However, only minimal conversion to **5-DHID-H** was observed. Heating the solution at 65 ºC did not increase the amount of conversion. However, the addition of one equivalent of THF to a solution of **5-H_2** at 23 ºC did result in 66 % conversion, while ten and fifty equivalents of THF, gave 84 and 94 % conversion, respectively. These conversions do not increase with time. Similar results were observed when treating **5-D_2** with THF; appearance of the *endo*

methylene and the hafnium deuteride for **5-DHID-D** was observed but with the 14.85 ppm **5-D_2** hafnium deuteride resonance remaining in the ^{2}H NMR spectrum. These incomplete conversions appear to show that the insertion of hydrogen to form **5-DHID-H** does not occur from an η^5, η^5 bis(indenyl) hafnocene dihydride (**5-H_2**), but rather an η^5, η^5 bis(indenyl) hafnocene THF complex as there is a THF concentration dependence.

Complete conversion of **5-H_2** to **5-DHID-H** was only observed when treating a solution of **5-H_2** with both excess THF and H_2 gas. Heating this solution at 65 ºC does result in formation of the fully hydrogenated product, **5-THI-H_2**. As a control, heating a solution of **5-H_2** under an atmosphere of H_2 in the absence of THF did not furnish any **5-THI-H_2**.

Reactivity with Diphenyldiazomethane. Synthesis of a bis(indenyl) hafnium alkylidene was also explored. While a few examples of hafnium alkylidenes are known, they were prepared by laser ablation[36] or α abstraction of a hafnium dialkyl,[37] so it would be interesting to try utilizing dinitrogen elimination from diazoalkanes using a discrete hafnium (II) source. Upon addition of one equivalent of diphenyldiazomethane to a solution of **5-THF**, C_s symmetric (η^5-C_9H_5-1-3-$(SiMe_3)_2)_2$Hf-N_2CPh_2(THF), **5-N_2CPh_2(THF)**, was produced, without loss of the THF ligand (eq. 2.9). Similar η^1-coordination of the diazoalkane was observed on a titanocene complex, (η^5-C_5H_2-1-3-$(SiMe_3)_2)_2$Ti-N_2CPh_2 which readily underwent η^1 to η^2-diazoalkane hapticity changes upon warming.[38] Addition of dihydrogen resulted in facile 1,2 addition across the Ti=N bond. For hafnium, addition of H_2 to **5-N_2CPh_2(THF)** resulted in loss of THF and formal 1,2 addition of dihydrogen across the Hf=N bond, forming (η^5-C_9H_5-1-3-$(SiMe_3)_2)_2$Hf-NHNCPh_2(H), **5-(NHNCPh_2)H** (eq. 2.9). By infrared spectroscopy, the N-H stretch appears at 3320, which shifts

appropriately to 2467 cm^{-1} upon deuterium labeling, and by ^1H NMR spectroscopy, the Hf-*H* and N-*H* appear at 9.31 and 6.22 ppm, which was also corroborated by deuterium labeling. In an attempt to induce N_2 loss from **5-N_2CPh_2(THF)**, a benzene-d_6 solution of the diazoalkane complex was heated at 65 ºC for one day, resulting in formation of orange C_1 symmetric hafnocene cyclometalated hydrazenido, (η^5-C_9H_5-1,3-($SiMe_3$)$_2$)(η^5-C_9H_5-η^1-1-$SiMe_3$-3-$SiMe_2CH_2$)]Hf(NHN=CPh_2), **5-CM(NHN=CPh_2)** (eq. 2.10). This complex arises from a 1,2 addition of a $SiMe_3$ C-H bond across the Hf=N bond. It appears that with this indenyl ligand and metal set, a greater propensity for inducing cyclometalation of the ligand exists over N_2 loss.

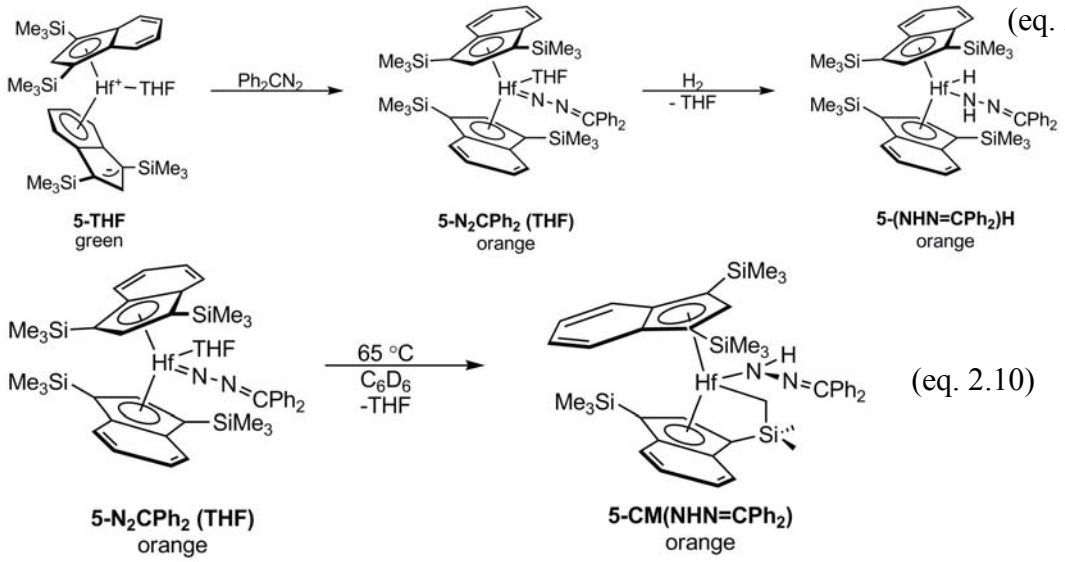

With the difficulty in inducing loss of dinitrogen from **5-N_2CPh_2(THF)**, the chemistry of the analogous bis(indenyl) zirconocene complexes were explored. Addition of diphenyldiazomethane to **2-THF** also produced similar reactivity; formation of **2-N_2CPh_2(THF)** was observed which yielded **2-(NHN=CPh_2)H** upon hydrogenation (eq. 2.11). Unlike **5-N_2CPh_2(THF)**, **2-N_2CPh_2(THF)** is particularly unstable and readily decomposes. It is possible that it decomposes via a transient zirconocene alkylidene, though there is no evidence as the decomposition products include free indenyl ligand and other unknown organic compounds. Switching to an

alkyl substituted indenyl for a more electron rich zirconium center, **1**'s reactivity with Ph_2CN_2 was investigated. Recall that there is no alkyl substituted indenyl zirconium THF complex, so a bis(indenyl) zirconium sandwich was utilized instead, as it, too, is formally Zr(II). Because **1** does not have an additional THF ligand, the diazoalkane coordinates η^2 to the zirconium, forming $(\eta^5\text{-}C_9H_5\text{-}1\text{-}3\text{-}(CHMe_2)_2)_2Zr\text{-}(\eta^2\text{-}N_2CPh_2)$, **1-$N_2CPh_2$** (eq. 2.12). Upon hydrogenation, it, similarly, forms **1-(NHN=CPh_2)H**. Heating a benzene-d_6 solution of **1-N_2CPh_2** to 65 ºC for two days produced no change, but heating to 95 ºC resulted in decomposition. Amongst the identifiable products was free fulvene, an indication of β-H elimination of the indenyl ring, leaving a mono(indenyl) zirconium hydride complex that is capable of causing other decomposition pathways at elevated temperatures.

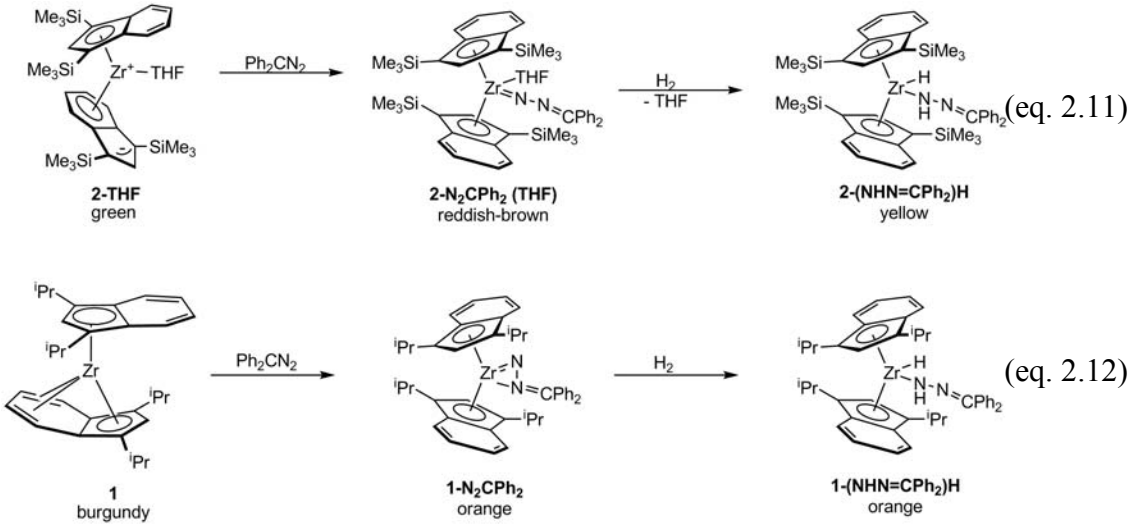

Conclusions

The reduction chemistry of a series of indenyl hafnocene compounds was explored. While neither an isolable η^9, η^5 indenyl hafnocene sandwich nor a dinitrogen complex was synthesized, different examples of formally bis(indenyl) hafnium (II) and one hafnium (III) species were prepared. The hafnocene (II)

complexes exhibit η^6, η^5 indenyl hapticity with THF, DME and NaCl, which was never observed with zirconium. The reactivity of these reduced hafnium compounds, while in many ways similar to that of the zirconium counterparts, demonstrate the more reducing nature of the third row transition metal. This was inferred by crystallographic data of **5-THF** versus **2-THF**, carbonyl stretching frequencies of the dicarbonyl compounds, the faster rates of C-O cleavage and the synthesis of **5-*cyclo*-C_4H_8** over an η^2 ethylene complex from the C-O bond cleavage of **5-DME**.

Also demonstrated was the ability of **5-THF** to serve as an isolable hafnium (II) source by readily undergoing oxidative addition of dihydrogen. Addition of a diazoalkane results in an η^1 diazo compound which readily undergoes 1,2 addition of H-H or C-H bonds.

Experimental

General Considerations. All air- and moisture-sensitive manipulations were carried out using standard vacuum line, Schlenk or cannula techniques or in an M. Braun inert atmosphere drybox containing an atmosphere of purified nitrogen. Solvents for air- and moisture-sensitive manipulations were initially dried and deoxygenated using literature procedures.[39] Benzene-d_6 was distilled from sodium metal under an atmosphere of argon and stored over 4 Å molecular sieves or titanocene. Argon and hydrogen gas were purchased from Airgas Incorporated and passed through a column containing manganese oxide on vermiculite and 4 Å molecular sieves before admission to the high vacuum line. Chlorotrimethylsilane was purchased from Acros Organics and dried over CaH_2 before use. Carbon monoxide was passed through a liquid nitrogen cooled trap immediately before use. C_9H_6-1,3-$(SiMe_3)_2$,[40,41] Li[C_9H_5-1,3-$(SiMe_3)_2$],[41] Cp*$HfCl_3$,[24] **1**[10] and **2-THF**[9] were prepared according to literature procedures.

^{1}H NMR spectra were recorded on a Varian Inova 400 Spectrometer operating at 399.779 MHz (^{1}H), while ^{13}C spectra were collected on a Varian Inova 500 spectrometer operating at 125.704 MHz. All chemical shifts are reported relative to $SiMe_4$ using ^{1}H (residual) or ^{13}C NMR chemical shifts of the solvent as a secondary standard. NOESY experiments were recorded on a Varian 500 Inova spectrometer operating at 499.920 MHz for ^{1}H. ^{2}H NMR spectra were recorded on a Varian Inova 500 spectrometer operating at 76.740 MHz and the spectra were referenced using an internal benzene-d_6 standard. X-Band ESR spectra were recorded on a Bruker EMX spectrometer at a frequency of 9.55 GHz under standard conditions in 4 mm i.d. quartz tubes. The tubes were sealed under vacuum at 77 K. Spectra at temperatures 4.2-77 K were recorded using a liquid helium cryostat, ESR-10 (Oxford Instruments Ltd., England).

Single crystals suitable for X-ray diffraction were coated with polyisobutylene oil in a drybox and were quickly transferred to the goniometer head of a Siemens SMART CCD Area detector system equipped with a molybdenum X-ray tube (δ = 0.71073 A). Preliminary data revealed the crystal system. A hemisphere routine was used for data collection and determination of lattice constants. The space group was identified and the data were processed using the Bruker SAINT program and corrected for absorption using SADABS. The structures were solved using direct methods (SHELXS) completed by subsequent Fourier synthesis and refined by full-matrix least-squares procedures. Infrared spectra were collected on a Thermo Nicolet spectrometer. Elemental analyses were performed at Robertson Microlit Laboratories, Inc., in Madison, NJ.

Preparation of (η^5-C_5Me_5)(η^5-C_9H_5-1,3-$(CHMe_2)_2$)$HfCl_2$ (3-Cl_2). This molecule was prepared in a similar manner to **5-Cl_2** (*vide infra*) with 0.27 g (1.29 mmol) of

Li[C_9H_5-1,3-($CHMe_2$)$_2$] and 0.54 g (1.29 mmol) of Cp*$HfCl_3$ yielding 0.47 g (62%) of **3-Cl_2**. ^{1}H NMR (benzene-d_6): δ = 1.09 (d, 8 Hz, 6H, CH*Me_2*), 1.43 (d, 8 Hz, 6H, CH*Me_2*), 1.76 (s, 15H, Cp* *Me*), 3.55 (m, 2H, C*H*Me_2), 6.72 (s, 1H, Cp*H*), 6.84 (m, 2H, Benzo), 7.40 (m, 2H, Benzo). ^{13}C NMR (benzene-d_6): δ = 11.70 (Cp* *Me*), 21.19, 25.32, 27.09 ($CHMe_2$), 122.86, 124.13, 124.20, 124.68 (Benzo/Cp). Two Cp/Benzo resonances not located.

Preparation of (η^5-C_5Me_5)(η^5-C_9H_5-1,3-($CHMe_2$)$_2$)HfI_2 (3-I_2). This molecule was prepared in a similar manner to **5-Cl_2** (*vide infra*) with 0.15 g (0.73 mmol) of Li[C_9H_5-1,3-($CHMe_2$)$_2$] and 0.51 g (0.73 mmol) of Cp*HfI_3 yielding 0.15 g (27%) of **3-Cl_2**. ^{1}H NMR (benzene-d_6): δ = 1.08 (d, 8 Hz, 6H, CH*Me_2*), 1.46 (d, 8 Hz, 6H, CH*Me_2*), 1.90 (s, 15H, Cp* *Me*), 3.77 (m, 2H, C*H*Me_2), 6.78 (m, 2H, Benzo), 7.37 (m, 4H, Benzo). One Cp*H* resonance not located.

Preparation of (η^5-C_5Me_5)(η^5-C_9H_5-1-($CHMe_2$)-3-Me)$HfCl_2$ (4-Cl_2). This molecule was prepared in a similar manner to **5-Cl_2** (*vide infra*) with 0.24 g (1.33 mmol) of Li[C_9H_5-1-$CHMe_2$-3-Me] and 0.56 g (1.33 mmol) of Cp*$HfCl_3$ yielding 0.40 g (54%) of **4-Cl_2**. ^{1}H NMR (benzene-d_6): δ = 1.18 (d, 8 Hz, 3H, CH*Me_2*), 1.34 (d, 8 Hz, 3H, CH*Me_2*), 1.89 (s, 15H, Cp* *Me*), 2.15 (s, 3H, *Me*), 3.19 (m, 1H, C*H*Me_2), 5.68 (s, 1H, Cp*H*), 7.06 (m, 2H, Benzo), 7.51 (m, 1H, Benzo), 7.69 (m, 1H, Benzo). ^{13}C NMR (benzene-d_6): δ = 12.32 (Cp* *Me*), 23.83, 24.21, 28.81 ($CHMe_2$/Me), 101.52, 106.21, 118.09, 121.14, 122.44, 125.00, 125.11, 125.36 (Benzo/Cp). One $CHMe_2$/Me resonance not located. Two Benzo/Cp resonances not located.

Preparation of (η^5-C_9H_5-1,3-($SiMe_3$)$_2$)$_2HfCl_2$ (5-Cl_2). A 500 mL round-bottomed

flask was charged with 3.65 g (13.7 mmol) of Li[C_9H_5-1,3($SiMe_3$)$_2$] and approximately 150 mL of diethyl ether. The resulting yellow solution was chilled in a cold well cooled to liquid nitrogen temperature and 2.19 g (6.85 mmol) of $HfCl_4$ was added. The reaction mixture was stirred for one day and the solvent was removed *in vacuo*. The resulting solid was dissolved in dichloromethane and filtered through a pad of Celite. Removal of dichloromethane *in vacuo* yielded a brown oil that was recrystallized from diethyl ether at –35 ºC to afford 2.21 g (42%) of **5-Cl$_2$** as a yellow solid. Anal. Calcd. for $C_{30}H_{46}Si_4HfCl_2$: C, 46.89; H, 6.03. Found: C, 46.75; H, 6.23. ^{1}H NMR (benzene-d_6): δ = 0.37 (s, 36H, $SiMe_3$), 6.93 (s, 2H, Cp*H*), 7.00 (m, 4H, Benzo), 7.74 (m, 4H, Benzo). ^{13}C NMR (benzene-d_6): δ = 1.73 (Si*Me*$_3$), 119.31, 126.49, 133.18, 138.29 (Cp/Benzo). One Cp/Benzo resonance not located.

Preparation of (η^5-C_9H_5-1,3-($CHMe_2$)$_2$)$_2$$HfCl_2$ (6-Cl$_2$). This molecule was prepared in a similar manner to **5-Cl$_2$** with 2.05 g (9.94 mmol) of Li[C_9H_5-1,3-($CHMe_2$)$_2$] and 1.60 g (5.00 mmol) of $HfCl_4$ yielding 2.16 g (67%) of **6-Cl$_2$**. Anal. Calcd. for $C_{30}H_{38}HfCl_2$: C, 55.60; H, 5.91. Found: C, 56.56; H, 3.78. ^{1}H NMR (benzene-d_6): δ = 0.94 (d, 8 Hz, 12H, CH*Me*$_2$), 1.24 (d, 8 Hz, 12H, CH*Me*$_2$), 2.98 (m, 4H, C*H*Me_2), 6.76 (s, 2H, Cp*H*), 6.91 (m, 4H, Benzo), 7.24 (m, 4H, Benzo). ^{13}C NMR (benzene-d_6): δ = 20.74, 25.42, 25.62 ($CHMe_2$), 123.69, 125.04, 125.85, 125.95 (Cp/Benzo). One Cp/Benzo resonance not located.

Preparation of *rac/meso*-(η^5-C_9H_5-1-(^{i}Pr)-3-(Me))$_2$$HfCl_2$ (*rac/meso*-7-Cl$_2$). This molecule was prepared in a similar manner to **5-Cl$_2$** in a 100 mL round bottom flask with 2.00 g (11.22 mmol) of Li[C_9H_5-1-^{i}Pr-3-Me], 1.80 g (5.61 mmol) of $HfCl_4$ and approximately 160 mL of diethyl ether. This yielded 2.34 g (72 %) of yellow **7-Cl$_2$** as a mixture of *racemo* and *meso* isomers. Anal. Calcd. for $C_{26}H_{30}HfCl_2$: C, 52.76; H,

5.11. Found: C, 52.80; H, 4.77. ^{1}H NMR (benzene-d_6): δ = 0.99 (d, 7 Hz, 6H, CH*Me*$_2$), 1.06 (d, 7 Hz, 6H, CH*Me*$_2$), 1.14 (d, 7 Hz, 12H, CH*Me*$_2$), 2.20 (s, 6H, *Me*), 2.21 (s, 6H, *Me*), 3.31 (m, 2H, C*H*Me$_2$) 3.52 (m, 2H, C*H*Me$_2$), 5.59 (s, 2H, Cp*H*), 5.67 (s, 2H, Cp*H*), 6.92 (m, 6H, Benzo), 7.01 (m, 2H, Benzo), 7.17 (m, 2H, Benzo), 7.23 (m, 2H, Benzo), 7.37 (m, 2H, Benzo), 7.44 (m, 2H, Benzo). ^{13}C {^{1}H} NMR (benzene-d_6): δ = 12.47, 12.75 (*Me*), 21.26, 22.21, 24.91, 24.93, 27.25, 27.84 (CHMe$_2$), 100.22, 105.31, 109.49, 113.21, 117.95, 119.34, 121.11, 122.99, 123.60, 124.55, 124.77, 124.87, 124.99, 125.59, 126.75, 129.98 (Cp/Benzo). Two Cp/Benzo resonances not located.

Preparation of (η^5-C$_9$H$_5$-1-(^{i}Pr)-3-(Me))HfI$_3$ (8-I$_3$). A 100 mL round-bottom flask was charged with 1.70 g (2.87 mmol) of *r/m*-**7-Cl$_2$** and approximately 60 mL of toluene was added. 1.41 g (3.59 mmol) of BI_3 was added slowly to the yellow solution and the resulting mixture stirred for two days. The solvent was removed *in vacuo* and the resulting brown solid washed with cold pentane yielding 1.32 g (63 %) **8-I$_3$** instead of the desired diiodide species (**7-I$_2$**).. ^{1}H NMR (benzene-d_6): δ = 0.93 (d, 7 Hz, 3H, CH*Me*$_2$), 1.29 (d, 7 Hz, 3H, CH*Me*$_2$), 2.30 (s, 3H, *Me*), 3.70 (m, 1H, C*H*Me$_2$), 6.48 (s, 1H, Cp*H*), 6.75 (m, 2H, Benzo), 7.34 (m, 2H, Benzo).

Preparation of *rac/meso*-(η^5-C$_9$H$_5$-1-(^{i}Pr)-3-(Me))$_2$HfI$_2$ (*rac/meso*-7-I$_2$). A 100 mL round-bottom flask was charge with 0.921 g (1.26 mmol) of **8-I$_3$** and approximately 30 mL of diethyl ether was added. The pale yellow solution was chilled in a liquid nitrogen cooled cold well for 20 min and 0.225 g (1.26 mmol) of Li[C$_9$H$_5$-1-(^{i}Pr)-3-(Me)] was added to the solution and the resulting mixture stirred for two days. The solvent was removed *in vacuo* and the orange solid washed with pentane and subsequently extracted into toluene and filtered through Celite. Removal of the

toluene *in vacuo* yielded 0.888 g (91 %) of **7-I_2** as a yellow powder. Anal. Calcd. for $C_{26}H_{30}HfI_2$: C, 40.30; H, 3.90. Found: C, 39.63; H, 3.40. ^{1}H NMR (benzene-d_6): δ = 0.97 (d, 7 Hz, 6H, CH*Me*$_2$), 0.98 (d, 7 Hz, 6H, CH*Me*$_2$), 1.12 (d, 7 Hz, 6H, CH*Me*$_2$), 1.19 (d, 7 Hz, 6H, CH*Me*$_2$), 2.08 (s, 6H, *Me*), 2.28 (s, 6H, *Me*), 3.32 (m, 2H, C*H*Me$_2$) 3.95 (m, 2H, C*H*Me$_2$), 6.01 (s, 2H, Cp*H*), 6.42 (s, 2H, Cp*H*), 6.86 (m, 4H, Benzo), 6.92 (m, 4H, Benzo), 7.17 (m, 2H, Benzo), 7.28 (m, 2H, Benzo), 7.33 (m, 2H, Benzo), 7.43 (m, 2H, Benzo). ^{13}C {^{1}H} NMR (benzene-d_6): δ = 12.73, 14.21 (*Me*), 21.28, 22.05, 25.53, 25.84, 27.73, 30.16 (CHMe$_2$), 106.85, 110.17, 122.91, 123.83, 124.15, 124.25, 124.99, 125.20, 125.50, 125.79, 126.48, 126.64, 126.92, 127.04, 127.29, 128.59 (Cp/Benzo). Two Cp/Benzo resonances not located.

Preparation of (η^5-C_5Me_5)(η^5-C_9H_5-1,3-(CHMe$_2$)$_2$)Hf(CO)$_2$ (3-(CO)$_2$). This molecule was prepared in a similar manner to **7-(CO)$_2$** (*vide infra*) with 0.036 g (1.57 mmol) of Na metal, 7.3 g (36.39 mmol) of Hg and 0.10 g (0.17 mmol) of **3-Cl_2** yielding **3-(CO)$_2$**. ^{1}H NMR (benzene-d_6): δ = 1.08 (d, 8 Hz, 6H, CH*Me*$_2$), 1.30 (d, 8 Hz, 6H, CH*Me*$_2$), 1.56 (s, 15H, Cp* *Me*), 2.83 (m, 2H, C*H*Me$_2$), 5.47 (s, 1H, Cp*H*), 6.68 (m, 2H, Benzo), 7.10 (m, 2H, Benzo). One Cp*H* resonance not located. ^{13}C NMR (benzene-d_6): δ = 10.53 (Cp* *Me*), 21.90, 26.11, 26.55 (CHMe$_2$), 97.86, 103.03, 107.81, 113.18, 121.61, 121.92 (Cp/Benzo), 275.59 (Hf-*C*O). ν(CO) (pentane) = 1847, 1863, 1942, 1954 cm^{-1}.

Preparation of (η^5-C_5Me_5)(η^5-C_9H_5-1-(CHMe$_2$)-3-Me)Hf(CO)$_2$ (4-(CO)$_2$). This molecule was prepared in a similar manner to **7-(CO)$_2$** (*vide infra*) with 0.038 g (1.65 mmol) of Na metal, 7.5 g (37.39 mmol) of Hg and 0.10 g (0.17 mmol) of **4-Cl_2** yielding **4-(CO)$_2$**. ^{1}H NMR (benzene-d_6): δ = 1.18 (d, 8 Hz, 3H, CH*Me*$_2$), 1.22 (d, 8 Hz, 3H, CH*Me*$_2$), 1.61 (s, 15H, Cp* *Me*), 1.76 (s, 3H, *Me*), 2.81 (m, 1H, C*H*Me$_2$), 5.07

(s, 1H, Cp*H*), 6.72 (m, 2H, Benzo), 7.10 (m, 2H, Benzo). ^{13}C NMR (benzene-d_6): δ = 10.70 (Cp* *Me*), 12.29 (*Me*), 22.75, 25.97, 27.12 ($CHMe_2$), 93.30, 100.64, 103.77, 108.03, 112.76, 115.42, 121.65, 122.01, 122.42, 122.57 (Cp/Benzo), 273.22, 273.90 (Hf-*C*O). ν(CO) (pentane) = 1850, 1862, 1944, 1954 cm^{-1}.

Preparation of (η^5-C_9H_5-1,3-($SiMe_3$)$_2$)$_2$Hf(CO)$_2$ (5-(CO)$_2$). A small thick walled glass vessel was charged with 0.080 g of **5-THF** and approximately 10 mL of pentane. The contents of the vessel were cooled to –196 ºC and evacuated. At this temperature, 1 atm of CO was admitted. The resulting reaction mixture was warmed to ambient temperature and stirred for two days during which time the dark-green solution turned black. The contents of the vessel were cooled again and the excess CO and solvent was removed in vacuo yielding a dark foam. Recrystallization from pentane at -35 °C yields 0.070 g (89%) of **5-(CO)$_2$** as a forest green solid. Anal. Calcd. for $C_{32}H_{46}Si_4O_2Hf$: C, 51.00; H, 6.15. Found: C, 50.69; H, 5.87. ^{1}H NMR (benzene-d_6): δ = 0.31 (s, 36 H, Si*Me*$_3$), 5.69 (s, 2H, Cp), 6.79 (m, 3.2 Hz, 4H, Benzo), 7.24 (m, 3.2 Hz, 4H, Benzo). ^{13}C NMR (benzene-d_6): δ = 1.16 ($SiMe_3$), 94.24, 103.93, 124.73, 125.61, 126.94 (Cp/benzo), 258.65 (Hf-CO). ν(CO) (pentane) = 1863, 1871, 1888, 1948, 1956, 1971 cm^{-1}.

Preparation of (η^5-C_9H_5-1,3-($CHMe_2$)$_2$Hf(CO)$_2$ (6-(CO)$_2$). A thick walled glass vessel was charged with 0.264 g (0.407 mmol) of **2-Cl$_2$** and 0.115g (4.07 mmol) of activated Mg powder. On the high vacuum line, approximately 15 mL of THF was vacuum transferred onto the solids and the resulting slurry frozen in liquid nitrogen. One atmosphere of carbon monoxide was added to the vessel at -196 ºC. The vessel was thawed and then placed in a 45 °C oil bath for one day. The CO atmosphere and the solvent were then removed *in vacuo* leaving a green residue. The vessel was taken

into the dry box and the residue extracted into pentane. Filtration through Celite followed by solvent removal and recrystallization from pentane at -35 ° affords **6-(CO)$_2$** along with **6-Cl$_2$**. ^{1}H NMR (benzene-d_6): δ = 0.95 (d, 7 Hz, 12H, CHMe_2), 1.03 (d, 7 Hz, 12H, CHMe_2), 2.32 (m, 4H, CHMe$_2$), 5.18 (s, 2H, CpH), 6.73 (m, 4H, Benzo), 7.00 (m, 4H, Benzo). ^{13}C NMR (benzene-d_6): δ = 21.22, 25.73, 25.94 (CHMe$_2$), 96.92, 107.82, 112.46, 122.33, 122.96 (Cp/benzo), 281.95 (Hf-CO). ν(CO) (pentane) = 1849, 1944 cm^{-1}.

Preparation of *rac/meso*(η^5-C$_9$H$_5$-1-Me-3-CHMe$_2$Hf(CO)$_2$ (*rac/meso*-7-(CO)$_2$). A thick walled glass bomb was charged with 2.85 g (14.21 mmol) of mercury and approximately 3 mL of toluene in a nitrogen drybox. While stirring, 14 mg (0.61 mmol) of sodium metal was added and the resulting amalgam was stirred for 20 minutes. A toluene solution of 80 mg (0.103 mmol) of **7-Cl$_2$** was added. The reaction vessel was attached to the vacuum line and one atmosphere of CO was added at -196 ºC. The vessel was warmed to room temperature and stirred for 15 hours. The excess CO was removed *in vacuo* and brought into the dry box. Filtration through Celite followed by solvent removal and recrystallization from pentane at -35 ºC yields 0.045 g (75%) of ***rac/meso*-7-(CO)$_2$** as a forest green solid in a two to one ratio. Anal. Calcd. for $C_{28}H_{30}O_2Hf$: C, 58.28; H, 5.24. Found: C, 57.99; H, 5.46. ^{1}H NMR (benzene-d_6): δ = 1.05 (d, 8 Hz, 3H, minor CHMe_2), 1.08 (d, 8 Hz, 3H, major CHMe_2), 1.12 (d, 8 Hz, 3H, minor CHMe_2), 1.13 (d, 8 Hz, 3H, major CHMe_2), 1.90 (s, 3H, major Me), 1.98 (s, 3H, minor Me), 2.48 (m, 1H, minor CHMe$_2$), 2.63 (m, 1H, major CHMe$_2$), 4.55 (s, 2H, major CpH), 4.79 (s, 2H, minor CpH), 6.71 (m, 8H, major/minor Benzo), 6.94 (m, 2H, major Benzo), 7.01 (m, 2H, minor Benzo), 7.09 (m, 2H, major Benzo), 7.17 (m, 2H, minor Benzo) ^{13}C NMR (benzene-d_6): δ = 12.14, 12.17 (Me), 22.41, 22.98, 25.47, 25.74, 26.74, 27.38 (CHMe$_2$), 93.81, 99.27, 99.59, 108.24, 112.26, 115.21, 122.06,

122.23, 122.34, 122.64, 122.67, 122.75, 123.16, 123.57, 125.64, 128.51, 129.28 (Cp/Benzo), 271.71, 274.12 (Hf-CO). One Cp/Benzo and one Hf-CO resonance not located. ν(CO) (pentane) = 1871, 1864, 1961, 1948 cm^{-1}.

Preparation of (η^6-C_9H_5-1,3-$(SiMe_3)_2$)(η^5-C_9H_5-1,3$(SiMe_3)_2$)Hf(C_4H_8O) (5-THF). A 20 mL scintillation vial was charged with 3.56 g of mercury and approximately 3 mL of diethyl ether. To the stirring mixture, 0.020 g (0.875 mmol) of sodium was added and the slurry was stirred for 10 minutes to ensure amalgamation. A diethyl ether slurry (~8 mL containing 0.100 g (0.130 mmol) of **5-Cl_2** was then added followed by 0.250 g of THF. The resulting reaction mixture was stirred vigorously for 1 hour. Filtration of the green solution through Celite followed by solvent removal in vacuo yielded a green foam. Recrystallization from pentane at -35 °C yielded 0.070 g (70%) of a green solid identified as **5-THF**. Anal. Calcd. for $C_{34}H_{54}Si_4OHf$: C, 53.06; H, 7.07. Found: C, 53.12; H, 6.73. ^{1}H NMR (benzene-d_6): δ = 0.27 (s, 18H, SiMe_3), 0.30 (s, 18H, SiMe_3), 0.74 (br, 4H, THF), 2.48 (br, 4H, THF), 3.62 (m, 2H, Benzo), 3.69 (s, 1H, Cp), 5.98 (s, 1H, Cp), 6.75 (m, 2H, Benzo), 6.86 (m, 2H, Benzo), 7.75 (m, 2H, Benzo). ^{13}C NMR (benzene-d_6): δ = 1.38, 1.77 (SiMe_3), 24.08, 74.83 (THF), 83.70, 90.28, 103.86, 114.47, 118.44, 122.89, 125.11, 126.19, 135.91, 142.43 (Cp/Benzo).

Preparation of (η^6-C_9H_5-1,3$(SiMe_3)_2$)(η^5-C_9H_5-1,3$(SiMe_3)_2$)Hf($C_4H_{10}O_2$) (5-DME). To a 20 mL scintillation vial with 0.119 g (0.155 mmol) of **5-THF** dissolved in approximately 6 mL of benzene, 35 mL (0.031 mg, 0.34 mmol) of dimethoxyethane was added dropwise. The green solution was stirred for 90 minutes. Solvent removal *in vacuo* followed by recrystallization from diethyl ether at -35 °C yielded 0.50 g (48 %) of **5-DME** as a green solid. Anal. Calcd. for $C_{34}H_{56}Si_4O_2Hf$: C, 51.84; H, 7.17.

Found: C, 51.39; H, 6.58. ^{1}H NMR (benzene-d_6): δ = 0.23 (s, 18H, $SiMe_3$), 0.44 (s, 18H, $SiMe_3$), 1.49 (br s, 4H, OCH_2s), 3.53 (s, 6H, OCH_3), 3.91 (m, 2H, benzo), 4.30 (s, 1H, Cp), 6.20 (m, 2H, benzo), 6.72 (s, 1H, Cp), 6.79 (m, 2H, benzo), 7.16 (s, 1H, Cp), 7.53 (m, 2H, benzo). ^{13}C NMR (benzene-d_6): δ = 1.92, 3.11 ($SiMe_3$), 68.19 (OCH_2), 69.12 (OCH_3), 118.46, 141.38 (Cp), 79.22, 105.02, 123.81, 125.54 (benzo), 83.86, 107.86, 120.40, 137.28 (benzo).

Characterization of [(η^6-C_9H_5-1-3-$(SiMe_3)_2$)(η^5-C_9H_5-1-3-$(SiMe_3)_2$)HfCl]$_2$Na[Na(DME)$_3$] ([5-Cl]$_2$Na[Na(DME)$_3$]). ^{1}H NMR (benzene-d_6): δ = 0.36 (s, 36H, Si*Me*$_3$), 0.46 (s, 36H, Si*Me*$_3$), 1.27 (br s, 18H, DME *Me*), 1.61 (br s, 12H, DME C*H*$_2$), 3.64 (s, 4H, Benzo), 6.10 (s, 2H, Cp*H*), 6.61 (m, 4H, Benzo), 7.02 (m, 4H, Benzo), 7.73 (m, 4H, Benzo). One Cp*H* resonance not located.

Preparation of [(η^5-C_9H_5-1,3-$(SiMe_3)_2$)$_2$HfCl] (5-Cl). A 50 mL round bottom flask was charged with 14.37 g (0.072 mol) of mercury and approximately 10 mL of diethyl ether was added. To the stirring solution, 0.072 g (3.13 mmol) of sodium was added and the slurry was stirred for 20 minutes to ensure amalgamation. A diethyl ether slurry (~30 mL containing 0.400 g (0.521 mmol) of **5-Cl$_2$** was then added. The resulting reaction mixture was stirred vigorously for 1.25 hours. Filtration of the green solution through Celite followed by solvent removal in vacuo yielded a brown-green foam. Recrystallization from pentane at -35 °C yielded 70 mg (18 %) of green crystals identified as **5-Cl**. Anal. Calcd. for $C_{30}H_{46}Si_4HfCl$: C, 49.16; H, 6.33. Found: C, 48.88; H, 6.35. ^{1}H NMR (benzene-d_6): δ = 5.72 ($\Delta\nu_{1/2}$ = 287 Hz). EPR (toluene): g_x = 1.98, g_y = 1.96, g_z = 1.70.

Preparation of (η^5-C_9H_5-1,3$(SiMe_3)_2$Hf-*cyclo*-O$(CH_2)_3CH_2$ (5-*cyclo*-O$(CH_2)_3CH_2$).

A flame dried thick-walled glass vessel was charged with 0.078 g (0.10 mmol) of **5-THF** and dissolved in approximately 5 mL of benzene. On the vacuum line, the reaction vessel was degassed and 91 torr (0.49 mmol) of THF was admitted via a 100.1 mL calibrated gas bulb. The green solution was then heated in an oil bath for 3 days at 85 ºC. Solvent was removed *in vacuo* and the resulting yellow oil was identified as **5-*cyclo*-O(CH$_2$)$_3$CH$_2$**. Attempts to recrystallize the compound as a solid have been unsuccessful for elemental analysis. ^{1}H NMR (benzene-d_6); δ = 0.35 (s, 18H, Si*Me*$_3$), 0.41 (s, 18H, Si*Me*$_3$), 0.74 (m, 2H, OCH$_2$CH$_2$CH$_2$C*H*$_2$), 0.80 (m, 2H, OCH$_2$C*H*$_2$CH$_2$CH$_2$), 1.52 (m, 2H, OCH$_2$CH$_2$C*H*$_2$CH$_2$), 3.87 (t, 5 Hz, 2H, OC*H*$_2$CH$_2$CH$_2$CH$_2$), 6.01 (s, 2H, Cp*H*), 6.96 (m, 2H, Benzo), 7.12 (m, 2H, Benzo), 7.60 (m, 2H, Benzo), 7.81 (m, 2H, Benzo). ^{13}C {^{1}H} NMR (benzene-d_6): δ = 1.36, 1.58 (Si*Me*$_3$), 27.49 (OCH$_2$CH$_2$*C*H$_2$CH$_2$), 32.61 (OCH$_2$*C*H$_2$CH$_2$CH$_2$), 46.31 (OCH$_2$CH$_2$CH$_2$*C*H$_2$), 73.63 (O*C*H$_2$CH$_2$CH$_2$CH$_2$), 83.41, 103.52, 123.81, 124.67, 126.28, 126.82, 132.71, 137.24, 138.31 (Cp/Benzo).

Characterization of (η^5-C$_9$H$_5$-1,3-(SiMe$_3$)$_2$)(η^5-C$_9$H$_5$-η^1-1-SiMe$_3$-3-SiMe$_2$CH$_2$)]HfH (5-CMH). ^{1}H NMR (benzene-d_6): -2.23 (d, 12 Hz, 1H, Zr-C*H*$_2$), -1.98 (d, 12 Hz, 1H, Zr-C*H*$_2$), 0.20 (s, 9H, Si*Me*$_3$), 0.23 (s, 9H, Si*Me*$_3$), 0.39 (s, 9H, Si*Me*$_3$), 0.45 (s, 3H, Si*Me*$_2$CH$_2$), 0.62 (s, 3H, Si*Me*$_2$CH$_2$), 6.76 (s, 1H, Cp*H*), 6.79 (m, 2H, Benzo), 6.84 (m, 2H, Benzo), 7.39 (m, 1H, Benzo), 7.41 (m, 1H, Benzo), 7.71 (m, 2H, Benzo), 7.84 (s, 1H, Cp*H*), 13.26 (s, 1H, Zr-*H*). ^{13}C {^{1}H} NMR (benzene-d_6): δ = -2.66, -1.03, -0.79, 1.23, 1.83 (Si*Me*$_3$/Si*Me*$_2$), 34.38 (Zr-*C*H$_2$), 91.22, 113.73, 114.88, 118.07, 121.65, 122.47, 123.04, 123.27, 124.05, 125.04, 125.15, 125.81, 126.48. Five Cp/Benzo resonances not located.

Dimethoxyethane Cleavage from 5-DME. A J. Young NMR tube was charged with

0.010 g (0.013 mmol) of **5-DME** dissolved in approximately 0.5 mL of benzene-d_6 was allowed to sit at room temperature and the reaction monitored over two days via NMR spectroscopy. Reaction results in cleavage of the dimethoxyethane to give a yellow solution of **5-OMe$_2$** and **5-C$_4$H$_8$**.

Characterization of (η^5-C$_9$H$_9$-1,3-(SiMe$_3$)$_2$)$_2$Hf(OMe)$_2$ (5-OMe$_2$). ^{1}H NMR (benzene-d_6): δ = 0.25 (s, 36H, Si*Me*$_3$), 3.64 (s, 6H, O*Me*), 6.71 (s, 2H, Cp), 7.17 (m, 4H, Benzo), 7.72 (m, 4H, Benzo). ^{13}C NMR (benzene-d_6): δ = -0.03 (Si*Me*$_3$), 78.85 (O*Me*), 114.00, 123.20, 124.64, 141.29, 141.68 (Cp/Benzo).

Preparation of (η^5-C$_9$H$_9$-1,3-(SiMe$_3$)$_2$)$_2$Hf(C$_4$H$_8$) (5-*cyclo*-C$_4$H$_8$). A J. Young NMR tube was charged with 0.020 g (0.026 mmol) of **5-THF** and approximately 0.5 mL of benzene-d_6 was added. The tube was submerged in a -196 ºC bath and excess (approximately 250 torr) of ethylene was admitted. A rapid color change from green to yellow was observed upon thawing. Removal of the excess ethylene *in vacuo* and recrystallization in pentane afforded 10 mg of a yellow solid identified as **5-*cyclo*-C$_4$H$_8$**. Anal. Calcd. for $C_{34}H_{54}Si_4Hf$: C, 54.19; H, 7.22. Found: C, 53.91; H, 7.20. ^{1}H NMR (benzene-d_6): δ = 0.33 (s, 36H, Si*Me*$_3$), 0.39 (m, 4H, Hf-C*H*$_2$), 1.63 (m, 4H, Hf-CH$_2$C*H*$_2$), 6.32 (s, 2H, Cp), 7.17 (m, 4H, Benzo), 7.77 (m, 4H, Benzo). ^{13}C NMR (benzene-d_6): δ = 1.58 (Si*Me*$_3$), 28.91 (Hf-CH$_2$*C*H$_2$), 57.62 (Hf-*C*H$_2$CH$_2$) 115.80, 122.90, 125.31, 130.64, 136.97 (Cp/Benzo).

Preparation of (η^5-C$_9$H$_5$-1,3(SiMe$_3$)$_2$)(η^5, η^3- C$_9$H$_6$-1,3(SiMe$_3$)$_2$)HfH. (5-DHID-H). A thick walled glass vessel was charged with 0.055 g (0.072 mmol) of **5-THF** and approximately 10 mL of pentane. The contents of the vessel were frozen in liquid nitrogen, the vessel evacuated and one atmosphere of dihydrogen added. After

thawing, the solution immediately changed color from a dark forest green to light yellow. The volatiles were removed in vacuo and the residue was recrystallized from pentane to yield 0.042 g (83 %) of a flaky tan solid identified as **5-DHID-H**. Anal. Calcd. for $C_{30}H_{48}Si_4Hf$: C, 51.51; H, 6.92. Found: C, 51.12; H, 6.51. ^{1}H NMR (benzene-d_6): δ = 0.29 (s, 9H, $SiMe_3$), 0.31 (s, 9H, $SiMe_3$), 0.32 (s, 9H, $SiMe_3$), 0.44 (s, 9H, $SiMe_3$), 2.32 (d, 12Hz, 1H, CH_2), 2.51 (m, 1H, CH_2), 2.91 (br, 1H, allyl CH), 3.03 (s, 1H, Hf-H), 4.68 (m, 1H, allyl CH), 5.24 (d, 1H, 6.4 Hz, allyl CH), 5.84 (s, 1H, Cp), 6.85 (m, 2H, benzo), 6.95 (s, 1H, Cp), 7.25 (m, 1H, benzo), 7.56 (m, 1H, benzo). ^{13}C {^{1}H} NMR (benzene-d_6): δ = 1.20, 1.42, 2.14, 2.67 (Si*Me*$_3$), 22.49 (*C*H_2), 37.61 (allyl *C*H), 95.44, 99.70, 102.82, 103.46, 105.86, 109.39, 109.45, 116.98, 123.58, 123.74, 124.68, 125.36, 125.97, 126.51, 126.92, 126.98 (Cp/Benzo).

Preparation of (η^5- C_9H_9-1,3-$(SiMe_3)_2)_2HfH_2$ (5-THI). A J. Young NMR tube was charged with 0.015 g (0.021 mmol) of **5-DHID-H** and approximately 0.5 mL of benzene-d_6. The contents of the tube were heated at 65 °C for 1 week. No significant color change was observed. ^{1}H NMR (benzene-d_6): 0.28 (s, 36H, Si*Me*$_3$), 1.73 (m, 4H, anti to Hf THI), 2.10 (m, 4H, syn THI), 2.75 (m, 4H, anti THI), 2.84 (m, 4H, syn THI), 5.82 (s, 2H, Cp*H*), 14.95 (s, 2H, Hf-*H*). ^{13}C {^{1}H} NMR (benzene-d_6): δ = 1.36 (Si*Me*$_3$), 23.95, 27.86 (THI), 111.87, 117.55, 137.10 (Cp).

Preparation of (η^5-C_9H_5-1,3$(SiMe_3)_2)_2HfH_2$. (5-H_2). A 20 mL scintillation vial was charged with 0.240 g (0.312 mmol) of **5-Cl_2** and dissolved in approximately 5 mL of toluene. The yellow solution was chilled at -35 °C for 20 minutes and 0.656 mL (0.656 mmol) of a 1.0 molar solution of sodium triethylborylhydride in toluene was syringed in. The resultant amber solution was stirred for three hours and the solvent removed *in vacuo*. The residue was taken into pentane and extracted through Celite

and the solvent removed *in vacuo*. Recrystallization from pentane at -35 °C affords 0.081 g (37 %) of a white crystalline solid identified as **5-H_2.** Anal. Calcd. for $C_{30}H_{48}Si_4Hf$: C, 51.51; H, 6.92. Found: C, 51.23; H, 6.96. ^{1}H NMR (benzene-d_6): δ = 0.31 (s, 18H, $SiMe_3$), 6.78 (m, 4H, Benzo), 7.25 (m, 4H, Benzo), 7.53 (s, 2H, Cp*H*), 14.85 (s, 1H, Zr-*H*). ^{13}C {^{1}H} NMR (benzene-d_6): δ = 1.31 ($SiMe_3$), 110.36, 124.31, 126.21, 127.52, 131.56 (Cp/Benzo).

Preparation of ($(\eta^5$-C_9H_5-1,3-$(SiMe_3)_2)_2$Hf(N_2CPh_2)(THF) (5-N_2CPh_2(THF)). A 20 mL scintillation vial was charged with 0.040 g (0.059 mmol) of **5-THF** and 0.012 g (0.062 mmol) of diphenyldiazomethane and approximately 5 mL of pentane was added. The reddish-brown solution was stirred for 3 hours after which the solvent was removed *in vacuo*. Recrystallization in pentane afforded 0.010 g (19 %) of an orange solid identified as **5-N_2CPh_2(THF)**. In benzene-d_6 solution, the compound is reddish-orange. Anal. Calcd. for $C_{47}H_{64}Si_4HfN_2O$: C, 58.57; H, 6.69; N, 2.91. Found: C, 58.22; H, 6.35; N, 2.83. ^{1}H NMR (benzene-d_6): 0.42 (s, 18H, $SiMe_3$), 0.53 (s, 18H, $SiMe_3$), 1.10 (m, 2H, THF), 1.94 (m, 4H, THF), 2.99 (m, 2H, THF), 6.85 (m, 4H, Benzo/Ph), 6.99 (m, 2H, Benzo/Ph), 7.11 (m, 2H, Benzo/Ph), 7.27 (m, 4H, Benzo/Ph), 7.31 (s, 2H, Cp*H*), 7.36 (m, 2H, Benzo/Ph), 7.95 (m, 2H, Benzo/Ph), 8.12 (m, 2H, Benzo/Ph). ^{13}C {^{1}H} NMR (benzene-d_6): δ = 0.61, 1.29 ($SiMe_3$), 25.72, 77.71 (Hf-THF), 107.87, 121.13, 121.20, 121.96, 122.72, 126.41, 126.47, 127.02, 127.48, 130.58, 139.59, 140.15, 140.85, 141.47, 142.58, 150.97 (Cp/Benzo). Two Cp/Benzo resonances not located.

Preparation of ($(\eta^5$-C_9H_5-1,3-$(SiMe_3)_2)_2$Hf(NHN=CPh_2)H (5-(NHN=CPh_2)H). A flame dried thick walled glass reaction vessel was charged with 0.037 g (0.038 mmol) of **5-N_2CPh_2(THF)** and approximately 3 mL of pentane was added. While attached to

the high vacuum line, the contents of the vessel were frozen at -196 ºC and evacuated. At this temperature, 1 atm of dihydrogen was admitted. After thawing, the resulting orange solution was stirred vigorously for 2 hours after which time the solvent was removed *in vacuo* resulting in an orange solid. Recrystallization from pentane at -35 ºC yielded 33 mg (94 %) of an orange solid identified as **5-(NHN=CPh$_2$)H**. Anal. Calcd. for $C_{43}H_{58}Si_4HfN_2$: C, 57.78; H, 6.54; N, 3.13. Found: C, 57.53; H, 6.43; N, 2.84. ^{1}H NMR (benzene-d_6): 0.42 (s, 18H, Si*Me*$_3$), 0.45 (s, 18H, Si*Me*$_3$), 6.22 (br s, 1H, N*H*), 6.53 (m, 4H, Benzo/Ph), 6.89 (m, 2H, Benzo/Ph), 7.08 (m, 2H, Benzo/Ph), 7.12 (s, 2H, Cp*H*), 7.18 (m, 2H, Benzo/Ph), 7.26 (m, 4H, Benzo/Ph), 7.52 (m, 2H, Benzo/Ph), 7.68 (m, 2H, Benzo/Ph), 9.31 (s, 1H, Hf-*H*). ^{13}C {^{1}H} NMR (benzene-d_6): δ = 1.95, 1.98 (Si*Me*$_3$), 93.99, 122.47, 123.77, 123.86, 124.13, 125.15, 125.88, 126.29, 126.72, 126.97, 127.22, 129.11, 130.47, 131.52, 135.71, 139.40, 145.38 (Cp/Benzo). One Cp/Benzo resonance not located. IR (KBr): ν(*NH*) = 3320 cm^{-1}; ν(*ND*) = 2467 cm^{-1}.

Preparation of (η^5-C$_9$H$_5$-1,3-(SiMe$_3$)$_2$)(η^5-C$_9$H$_5$-η^1-1-SiMe$_3$-3-SiMe$_2$CH$_2$)]Hf(NHN=CPh$_2$) (5-CM(NHN=CPh$_2$)). A J. Young NMR tube charged with 0.008 g (0.01 mmol) of **5-THF** and 0.002 g (0.01 mmol) of diphenyldiazomethane dissolved in approximately 0.5 mL of benzene-d_6 was heated at 65 ºC for one day resulting in a color change from red-orange to orange and was identified as **5-CM(NHN=CPh$_2$)**. Attempts to recrystallize as a solid have been unsuccessful for elemental analysis. ^{1}H NMR (benzene-d_6): -1.86 (d, 12 Hz, 1H, Zr-C*H*$_2$), -0.67 (d, 12 Hz, 1H, Zr-C*H*$_2$), 0.23 (s, 9H, Si*Me*$_3$), 0.36 (s, 9H, Si*Me*$_3$), 0.51 (s, 9H, Si*Me*$_3$), 0.72 (s, 3H, Si*Me*$_2$), 0.77 (s, 3H, Si*Me*$_2$), 4.65 (s, 1H, N-*H*), 6.46 (m, 1H, Benzo/Ph), 6.78 (m, 2H, Benzo/Ph), 6.89 (m, 4H, Benzo/Ph), 7.02 (m, 3H, Benzo/Ph), 7.13 (m, 3H, Benzo/Ph), 7.39 (s, 1H, Cp*H*), 7.70 (m, 3H, Benzo/Ph), 7.77 (s, 1H,

Cp*H*), 7.78 (m, 1H, Benzo/Ph), 7.95 (m, 1H, Benzo/Ph). ^{13}C {^{1}H} NMR (benzene-d_6): δ = 1.50, 1.61, 1.83, 1.92, 2.05 (Si*Me*$_3$/Si*Me*$_2$), 33.00 (Zr-*C*H$_2$), 104.63, 105.56, 110.47, 111.81, 117.42, 123.65, 123.69, 124.77, 125.78, 126.46, 128.94, 129.42, 129.44, 129.46, 129.49, 130.56, 130.58, 130.60, 135.57, 136.44, 137.26, 139.72, 144.24 (Benzo/Cp/Ph). Four Benzo/Cp/Ph resonances not located. IR (KBr): ν(*NH*) = 3290 cm^{-1};

Preparation of ((η^5-C$_9$H$_5$-1,3-(SiMe$_3$)$_2$)$_2$Zr(N$_2$CPh$_2$)(THF) (2-N$_2$CPh$_2$(THF)). This compound was prepared in a similar manner to **5-N$_2$CPh$_2$(THF)** in a J. Young NMR tube with 0.020 g (0.030 mmol) of **2-THF** and 0.006 g (0.031 mmol) of diphenyldiazomethane and approximately 0.5 mL of benzene-d_6. The resulting reddish-brown solution was identified as **2-N$_2$CPh$_2$(THF)**. This particular compound is unstable to vacuum so no elemental analysis was obtained. ^{1}H NMR (benzene-d_6): 0.42 (s, 18H, Si*Me*$_3$), 0.49 (s, 18H, Si*Me*$_3$), 0.86 (m, 4H, THF), 2.14 (m, 4H, THF), 6.85 (m, 4H, Benzo/Ph), 6.94 (m, 2H, Benzo/Ph), 7.07 (m, 2H, Benzo/Ph), 7.21 (m, 4H, Benzo/Ph), 7.41 (s, 2H, Cp*H*), 7.51 (m, 2H, Benzo/Ph), 7.57 (m, 2H, Benzo/Ph), 7.83 (m, 2H, Benzo/Ph). ^{13}C {^{1}H} NMR (benzene-d_6): δ = 1.22, 1.71 (Si*Me*$_3$), 26.03, 76.66 (Hf-THF), 111.15, 121.92, 122.95, 123.86, 124.04, 124.20, 125.70, 126.06, 126.67, 126.72, 129.41, 130.95, 133.89, 134.61, 136.63, 138.45 (Cp/Benzo/Ph). Two Cp/Benzo/Phenyl resonances not located.

Preparation of ((η^5-C$_9$H$_5$-1,3-(SiMe$_3$)$_2$)$_2$Zr(N$_2$CPh$_2$)H) (2-(NHNCPh$_2$)H). A thick walled glass vessel was flame dried bomb and charged with 0.156 g (0.230 mmol) of **2-THF** and approximately 10 mL of pentane was added. Also to the vessel, 0.045 g (0.232 mmol) of diphenyldiazomethane dissolved in 1 mL of pentane was added. The resulting reddish brown solution of **2-N$_2$CPh$_2$(THF)** was stirred for three hours. On

the high vacuum line, the contents of the vessel were frozen at -196 ºC and then evacuated. At this temperature, 1 atm of dihydrogen was added. After thawing, the resulting yellow solution was stirred vigorously for 2 hours after which time the solvent was removed *in vacuo* resulting in an yellow solid. Recrystallization from pentane at -35 ºC yielded 65 mg (32 %) of an yellow solid identified as **2-(NHN=CPh$_2$)H**. Anal. Calcd. for $C_{43}H_{58}Si_4ZrN_2$: C, 57.78; H, 6.54; N, 3.13. Found: C, 57.30; H, 7.00; N, 3.34. ^{1}H NMR (benzene-d_6): 0.39 (s, 18H, Si*Me*$_3$), 0.50 (s, 18H, Si*Me*$_3$), 4.61 (s, 2H, Cp*H*), 5.35 (br s, 1H, N*H*), 5.57 (s, 1H, Zr-*H*), 6.61 (m, 2H, Benzo/Ph), 6.69 (m, 2H, Benzo/Ph), 7.01 (m, 2H, Benzo/Ph), 7.13 (m, 2H, Benzo/Ph), 7.19 (m, 2H, Benzo/Ph), 7.33 (m, 4H, Benzo/Ph), 7.64 (m, 2H, Benzo/Ph), 7.86 (m, 2H, Benzo/Ph). ^{13}C {^{1}H} NMR (benzene-d_6): δ = 1.80, 1.92 (Si*Me*$_3$), 123.51, 123.55, 123.86, 124.94, 125.66, 126.06, 126.74, 127.22, 127.41, 129.20, 129.33, 129.59, 129.75, 129.91, 131.79, 138.08, 146.70, 147.76 (Cp/Benzo/Ph). IR (pentane): ν(*NH*) = 3303 cm^{-1}; ν(*ND*) = 2455 cm^{-1}.

Preparation of ((η^5-C$_9$H$_5$-1,3-(CHMe$_2$)$_2$Zr(η^2-N$_2$CPh$_2$)) (1-N$_2$CPh$_2$). This compound was prepared in a similar manner to **1-N$_2$CPh$_2$(THF)** in with 0.084 g (0.171 mmol) of **1** and 0.033 g (0.170 mmol) of diphenyldiazomethane and approximately 8 mL of pentane. Recrystallization from pentane at -35 °C yielded 28 mg (24 %) identified as **1-N$_2$CPh$_2$**. Anal. Calcd. for $C_{43}H_{48}N_2Zr$: C, 75.50; H, 7.07; N, 4.09. Found: C, 75.27; H, 6.84; N, 3.58. ^{1}H NMR (benzene-d_6): 0.93 (d, 8Hz, 6H, CH*Me*$_2$), 0.98 (d, 8Hz, 6H, CH*Me*$_2$), 1.05 (d, 8Hz, 12H, CH*Me*$_2$), 2.66 (m, 2H, CH*Me*$_2$), 2.75 (m, 2H, CH*Me*$_2$), 6.64 (s, 2H, Cp*H*), 6.83 (m, 2H, Benzo/Ph), 6.92 (m, 2H, Benzo/Ph), 7.12 (m, 6H, Benzo/Ph), 7.23 (m, 6H, Benzo/Ph), 7.34 (m, 2H, Benzo/Ph), 8.31. ^{13}C {^{1}H} NMR (benzene-d_6): δ = 20.93, 21.51, 24.57, 24.89, 25.34, 25.43 (CHMe$_2$), 115.70, 122.70, 122.76, 123.28, 124.07, 124.44, 124.65, 124.76,

125.11, 125.37, 125.88, 126.20, 128.45, 128.48, 128.66, 137.86, 141.01 (Cp/Benzo/Ph). One Cp/Benzo/Ph resonance not located.

Preparation of (η^5-C_9H_5-1,3-$(CHMe_2)_2$Zr(N_2CPh_2)H) (1-($NHNCPh_2$)H). This compound was prepared in a similar manner to **5-($NHN=CPh_2$)H** using 0.053 g (0.077 mmol) of **1-N_2CPh_2**. Recrystallization from pentane at -35 °C yielded 33 mg (62 %) identified as **1-($NHN=CPh_2$)H**. Anal. Calcd. for $C_{43}H_{50}N_2Zr$: C, 75.28; H, 7.35; N, 4.08. Found: C, 75.03; H, 7.61; N, 4.98. ^{1}H NMR (benzene-d_6): 1.25 (d, 8Hz, 6H, CHMe_2), 1.28 (d, 8Hz, 6H, CHMe_2), 1.32 (d, 8Hz, 6H, CHMe_2), 1.34 (d, 8Hz, 6H, CHMe_2), 3.45 (m, 4H, CHMe_2), 4.82 (s, 2H, Cp*H*), 5.58 (br s, 1H, N*H*/Zr-*H*), 5.79 (s, 1H, N*H*/Zr-*H*), 6.64 (m, 2H, Benzo/Ph), 6.73 (m, 2H, Benzo/Ph), 7.11 (m, 4H, Benzo/Ph), 7.26 (m, 4H, Benzo/Ph), 7.32 (m, 2H, Benzo/Ph), 7.38 (m, 2H, Benzo/Ph), 7.40 (m, 2H, Benzo/Ph), 8.05 (m, 2H, Benzo/Ph). ^{13}C {^{1}H} NMR (benzene-d_6): δ = 22.78, 23.95, 24.80, 25.72, 27.97, 28.33 ($CHMe_2$), 110.24, 117.35, 118.90, 121.94, 122.31, 122.64, 123.07, 123.98, 126.52, 126.65, 127.83, 129.29, 129.91, 132.50, 138.50 (Cp/Benzo/Ph). One Cp/Benzo/Ph resonance not located. IR (pentane): ν(*NH*) = 3298 cm^{-1}. ν(*ND*) = 2448 cm^{-1}.

REFERENCES

[1] Wilkinson, G.; Rosenblum, M.; Whiting, M. C.; Woodward, R. B. *J. Am. Chem. Soc.* **1952**, *74*, 2125.

[2] Crabtree, R. H.; *The Organometallic Chemistry of the Transition Metals,* 4th ed.; Wiley-Interscience: New Haven, Connecticut, 2005.

[3] *Comprehensive Organometallic Chemistry III*. Mingos, D. M. P.; Crabtree, R. H.; Bochmann, M., Eds.; Elsevier: Amsterdam, Netherlands, 2007; Vol. 4.

[4] Coates, G. W.; *Chem. Rev.* **2000**, *100*, 1223.

[5] (a) *Titanium and Zirconium in Organic Synthesis.* Marek, I., Ed.; Wiley-VCH, Weinheim, Germany, 2002. (b) Negishi, E.I.; Takahashi, T. *Acc. Chem. Res.* **1994**, *27*, 124.

[6] Hitchcock, P. B.; Kerton, F.; Lawless, G. A. *J. Am. Chem. Soc.* **1998**, *120*, 10264.

[7] Bradley, C. A.; Keresztes, I.; Lobkovsky, E.; Young, V. G.; Chirik, P. J. *J. Am. Chem. Soc*. **2004**, *126*, 16937.

[8] Veiros, L. F. *Chem. Eur. J.* **2005**, *11*, 2505.

[9] Bradley, C. A.; Lobkovsky, E.; Chirik, P. J. *J. Am. Chem. Soc.* **2003**, *125*, 8110.

[10] Bradley, C. A.; Lobkovsky, E.; Keresztes, I.; Chirik, P. J. *J. Am. Chem. Soc.* **2005**, *127*, 10291.

[11] Bradley, C. A.; Veiros, L. F.; Pun, D.; Lobkovsky, E.; Keresztes, I.; Chirik, P. J. *J. Am. Chem. Soc.* **2006**, *128*, 16600.

[12] Bradley, C. A.; Veiros, L. F.; Chirik, P. J. *Organometallics* **2007**, *26*, 3191.

[13] Veiros, L. F. *Organometallics* **2006**, *25*, 2266.

[14] Veiros, L. F. *Organometallics* **2006**, *25*, 4698.

[15] Bradley, C. A.; Flores-Torres, S.; Lobkovsky, E.; Abruña, H. D.; Chirik, P. J. *Organometallics* **2004**, *23*, 5332.

[16] Pun, D.; Bradley, C. A.; Lobkovsky, E.; Keresztes, I.; Chirik, P. J. *J. Am. Chem. Soc*. **2008**, *130*, 14046.

[17] Pun, D.; Lobkovsky, E.; Chirik, P. J. *J. Am. Chem. Soc.* **2008**, *130*, 6047.

[18] Marschner, C. *Angew. Chem., Int. Ed.* **2007**, *46*, 6770.

[19] Bernskoetter, W. H.; Olmos, A. V.; Lobkovsky, E.; Chirik, P. J. *Organometallics.* **2006**, *25*, 1021.

[20] Beweries, T.; Burlakov, V. V.; Bach, M. A.; Peitz, S.; Arndt, P.; Baumann, W.; Spannenberg, A.; Rosenthal, U.; Pathak, B.; Jemmis, E. D.; *Angew. Chem., Int. Ed.* **2007**, *46*, 6907.

[21] Bernskoetter, W. H.; Lobkovsky, E.; Chirik, P. J. *Angew. Chem., Int. Ed.* **2007**, *46*, 2858.

[22] Bernskoetter, W. H.; Olmos, A. V.; Pool, J. A.; Lobkovsky, E.; Chirik, P. J. *J. Am. Chem. Soc.* **2006**, *128*, 10696.

[23] Knobloch, D. J.; Lobkovsky, E.; Chirik, P. J. *Nature Chem. Accepted.*

[24] Roddick, D. M.; Fryzuk, M. D.; Seidler, P. F.; Hillhouse, G. L.; Bercaw, J. E. *Organometallics* **1985**, *4*, 97.

[25] Pool, J. A.; Chirik, P. J. *Can. J. Chem.* **2005**, *83*, 286.

[26] Wielstra, Y.; Gambarotta, S.; Meetsma, A.; De Boer, J. L. *Organometallics* **1989**, *8*, 250.

[27] Urazowski, I. F.; Ponomaryev, V. I.; Nifant'ev, I. E.; Lemenovskii, D. A. *J. Organomet. Chem.* **1989**, *368*, 287.

[28] Baker, W. A.; Janus, A. R. *J. Inorg. Nucl. Chem.* **1964**, *26*, 2087.

[29] Cotton, F. A.; Kibla, P. A.; Wojtczak, W. A.; *Inorg. Chim. Acta.* **1990**, *177*, 1.

[30] (a) Morse, P. M.; Wilson, S. R.; Girolami, G. S. *Inorg. Chem.* **1990**, *29*, 3200. (b) Riehl, M. E.; Wilson, S. R.; Girolami, G. S. *Inorg. Chem.* **1993,** *32*, 218.

[31] Chenca, T.; Royo, P. *J. Organomet. Chem.* **1985**, *293*, 61.

[32] Fakhr, A.; Mugnier, Y.; Gautheron, B.; Laviron, E. *J. Organometal. Chem.* **198**6 *302*, C7.

[33] Lappert, M. F.; Raston, C. L. *Chem. Commun.* **1980**, 1284.

[34] Lappert, M. F.; Pickett, C. J.; Riley, P. I.; Yarrow, P. I. W. *J. Chem. Soc. Dalton* **1981**, 805.

[35] Beweries, T.; Jäger-Fiedler, U.; Bach, M. A.; Burlakov, V. V.; Arndt, P.; Baumann, W.; Spannenberg, A.; Rosenthal, U. *Organometallics* **2007**, *26*, 3000.

[36] (a) Cho, H. G.; Andrews, L. *Organometallics* **2004**, *23*, 4357. (b) Cho, H. G.; Wang, X. F.; Andrews, L. *Organometallics* **2005**, *24*, 2854.

[37] Fryzuk, M. D.; Duval, P. B.; Patrick, B. O.; Rettig, S. J. *Organometallics* **2001**, *20*, 1608.

[38] Hanna, T. E.; Lobkovsky, E.; Chirik, P. J. *J. Am. Chem. Soc.* **2004**, *126*, 14688.

[39] Pangborn, A. B.; Giardello, M. A.; Grubbs, R. H.; Rosen, R. K.; Timmers, F. J. *Organometallics* **1996**, *15*, 1518.

[40] Davison, A.; Rakita, P. E. *J. Organomet. Chem.* **1970**, *23*, 407.

[41] Brady, E. D.; Overby, J. S.; Meredith, M. B.; Mussman, A. B.; Cohn, M. A.; Hanusa, T. P.; Yee, G. T.; Pink, M. *J. Am. Chem. Soc.* **2002**, *124*, 9556.

Chapter 3

C-C Bond Formation with η^9 Indenyl Zirconium Sandwiches: Cycloaddition of Dienes and Insertion of Ketones[*]

Abstract

Addition of 1,6-dienes to isolable indenyl zirconocene sandwich complexes resulted in formation of metallocyclopentane complexes, which upon addition of water or dihydrogen released cyclopentane and pyrrolidine derivatives. Unfortunately, attempts to form tetrahydrofuran derivatives resulted in C-O bond cleavage of the starting diene. Addition of carbon monoxide to one zirconacyclopentane resulted in *in situ* formation of the desired Pauson-Khand ketone, followed by rapid oxidative addition of the enol tautomer, forming a zirconocene enolate hydride. However, treatment of the indenyl zirconocene sandwich complexes with excess ketones typically resulted in insertion of the carbonyl compound into the indenyl ligand. Probing this divergent product formation with different ketones demonstrated that pK_a, steric bulk and concentration of the ketone reagent were important to the outcome of the reaction. Further mechanistic studies showed that for the insertion pathway, there are multiple products observed, whereby double insertion into the indenyl benzo appears to be the thermodynamic pathway, while insertion into both the indenyl cyclopentadiene and benzo the kinetic pathway. Addition of cyclopentanone into the smaller Cp* indenyl zirconocene sandwich complex resulted in a mixture of products including observation of a single insertion intermediate, where the new C-C bond formed at the indenyl cyclopentadiene. Experimental data reaffirm that the rate determining step is the first insertion of the ketone into the cyclopentadienyl ring.

[*] Reproduced in part with permission from Pun, D.; Lobkovsky, E.; Keresztes, I.; Chirik, P. J. *Angew. Chemie., Int. Ed.* **2010** – submitted. Unpublished work copyright 2010 Wiley-VCH.

Introduction

Reduced organozirconium compounds are synthetically valuable as stoichiometric C-C bond forming reagents as evident by the formation of zirconacycles upon addition of olefins or alkynes, which has demonstrated utility in natural product syntheses.[1] The Negishi method of generating low-valent zirconocene, or "$(\eta^5\text{-}C_5H_5)_2Zr$," is the most common: treatment of a tetrahydrofuran solution of zirconocene dichloride with two equivalents of butyllithium or butylmagnesium halide at -78 ºC and using the reagent *in situ*.[2] Of particular interest is the formation of cyclic compounds by the facile bicyclization of diene, diyne and enyne substrates upon addition to Negishi's reagent. These five and six-membered rings can be further elaborated off of the zirconium metal with proton sources, CO, dihalides, etc. to furnish organic compounds useful in natural product syntheses.[1a,3,4,5,6,7] Outlined in Figure 3.1 are a representative sampling of the dienes and functionalization reagents that have been previously published.[1a,3,4,5,6,7]

The exact composition of Negishi's reagent, however, is very complex. Instead of the expected "$(\eta^5\text{-}C_5H_5)_2Zr$," it has been well established that the dialkylzirconocene, $(\eta^5\text{-}C_5H_5)_2Zr(^nBu)_2$, is initially formed upon treatment of $(\eta^5\text{-}C_5H_5)_2ZrCl_2$ with butyllithium. Then, it was initially believed to undergo β-H abstraction releasing butane and generating a butene complex, $(\eta^5\text{-}C_5H_5)_2Zr(\eta^2\text{-}CH_2{=}CHCH_2CH_3)$, commonly referred to as Negishi's reagent.[1] However, Harrod has demonstrated that the zirconium dialkyl in the absence of exogenous substrates readily converts to a mixture of products upon slow warming to temperatures above the *in situ* preparation temperature. These products include Zr(II), Zr(III) and Zr(IV) species, in both monomeric and dimeric form.[8] An equilibrium was also established between the zirconocene butene and a crotyl hydride complex (eq. 3.1), which under Negishi

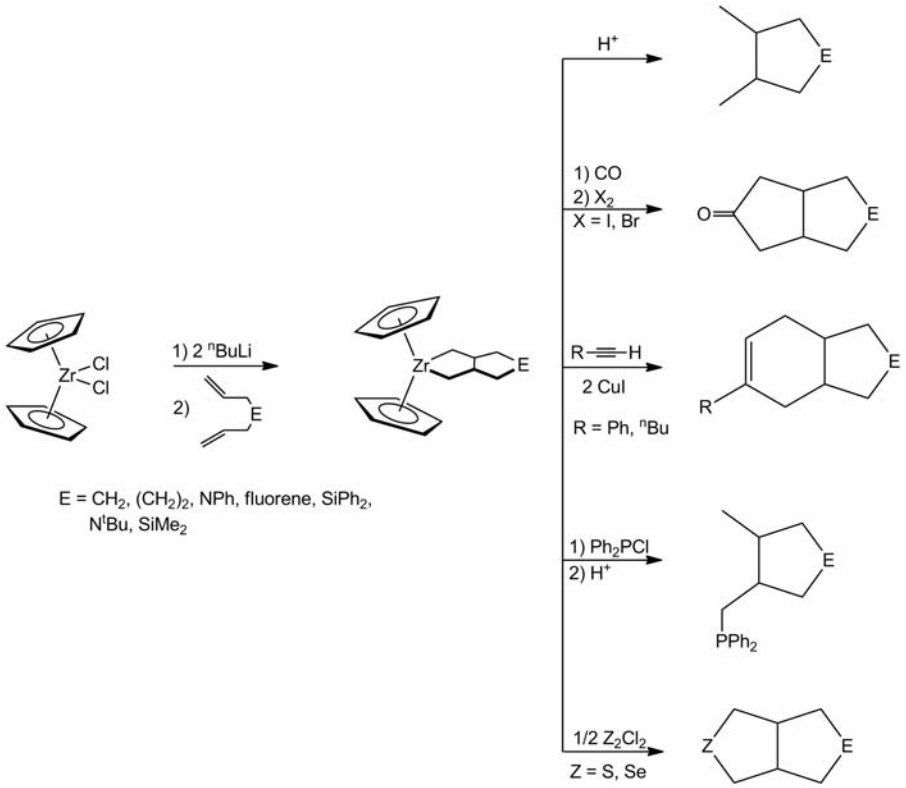

Figure 3.1. Formation of zirconacyclopentane derivatives and subsequent functionalization to afford cyclic compounds.

conditions is implied based on reactivity.[9] This clearly demonstrated the complexity of the reduced zirconium source prepared *in situ* for C-C bond formation.

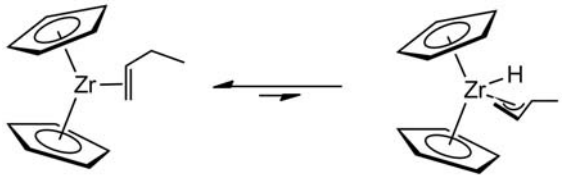

(eq. 3.1)

Waymouth and coworkers have established that that the cyclization of dienes can be performed in the presence of stoichiometric Grignard reagent with catalytic amounts of zirconocene dichloride (1 – 10 mol %).[3] Subsequent aqueous workup affords the desired cyclopentane/cyclohexane. Importantly, it was also shown that isolable zirconacyclopentane complexes are catalytically competent, although the stoichiometric reducing agent is still required.

Our laboratory has recently demonstrated that isolable η^9, η^5 bis(indenyl)

zirconocene (II) sandwich complexes exhibit reactivity similar to Negishi's reagent, forming η^5, η^5 bis(indenyl) zirconacycles upon addition of olefins and internal alkynes.[10] In this study, we expand upon the reactivity of our isolable Zr(II) source through the addition of dienes and subsequent functionalization.

Results and Discussion

Cycloaddition of Dienes to Isolable Zirconocene Sandwich Complexes. With only one reported example of an isolable reduced zirconocene that cyclized 1,6-dienes,[3] studies with an isolable, formally zirconium (II) source, (η^9-C_9H_5-1,3-$(CHMe_2)_2$)(η^5-C_9H_5-1,3-$(CHMe_2)_2$)Zr, **1**, commenced with the addition of hydrocarbons: 1,6-heptadiene, 1,7-octadiene and 9,9-diallylfluorene. In all cases, the dienes readily formed the expected zirconacyclopentane/cyclohexane derivatives, (η^5-C_9H_5-1,3-$(CHMe_2)_2$)$_2$Zr$(CH_2CHCH_2)_2$E, **1-$(CH_2CHCH_2)_2$E** (E = CH_2, CH_2CH_2, fluorene) at 22 ºC. In the former two cases, two isomers assigned as the *cis* – with an overall C_s symmetry possessing two chemically inequivalent cyclopentadienyl protons – or the *trans* – with overall C_2 symmetry possessing only one chemically equivalent cyclopentadienyl proton – were, initially, observed in a 1:1 ratio. However, allowing the mixture of **1-$(CH_2CHCH_2)_2(CH_2)$** to stand at 22 ºC in benzene-d_6 for one week or heating **1-$(CH_2CHCH_2)_2(CH_2)_2$** to 105 ºC for 24 hours resulted in > 98 % conversion to the corresponding *trans* isomer, consistent with the well established reversibility of alkene cyclozirconation.[11,12] These thermodynamic ratios are similar to that observed for the addition of these dienes to Negishi's reagent,[3,13,14,15] where the *trans* isomer is the thermodynamic product.[3,13,16] With the bulky fluorenyl substituent, only the *trans* diastereomer was observed at 22 ºC, the expected thermodynamic product, similar to what was reported in bis(cyclopentadienyl) zirconocene.[3]

With similar results observed for hydrocarbon diene addition to **1** and *in situ*

prepared zirconocene (II) sources, other dienes were explored: both previously utilized in the literature ($R^1 = R^1 = H$, E = $SiMe_2$, N^tBu, O) and others ($R^1 = R^2 = H$, E = NCH_2Ph, N-tosyl; $R^1 = R^2 = Me$, E = N^rBu; $R^1 = Me$, $R^2 = H$, E = N^tBu) (eq. 3.2). The diastereoselectivity at 22 ºC for each is summarized in Table 3.1. Replacement of the methylene with an amine resulted in a 4:1 or 5:1 ratio of *cis*:*trans* isomers at 22 ºC,

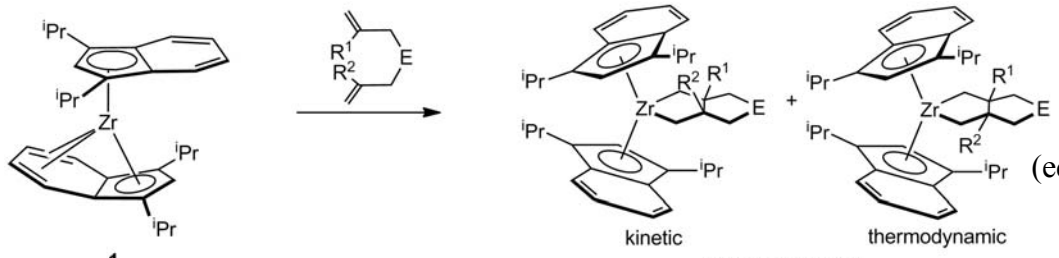

(eq. 3.2)

Table 3.1. Diastereoselectivity as a function of substituent.

E	R^1	R^2	T (ºC)	***cis* : *trans***
CH_2	H	H	22	1 : 50
$(CH_2)_2$	H	H	22	1 : 1
$(CH_2)_2$	H	H	105	1 : 50
fluorene	H	H	22	0 : 1
$SiMe_2$	H	H	23	0 : 1
N^tBu	H	H	23	5 : 1
N^tBu	H	H	105	1 : 25
N^tBu	Me	H	22	1 : 0
N^tBu	Me	Me	22	1 : 0
NCH_2Ph	H	H	22	5 : 1
N-tosyl	H	H	22	4 : 1

with > 96 % conversion to *trans*-**1-(CH_2CHCH_2)N^tBu** upon heating to 105 ºC, for two days, demonstrating that there is only a small energy difference between the two diastereomers, as previously shown with bis(cyclopentadienyl) zirconium.[16] Use of the bulkier 2-methylallyl, allyl tertbutylamine and bis(2-methylallyl) tertbutylamine resulted in solely *syn* addition such that the resulting metallocycle has *cis* bridgehead protons, with full conversion after 2 and 48 hours, respectively, in benzene-d_6 at

ambient temperature. With diallyl dimethylsilane as a substrate, only the *trans* isomer was observed.

The molecular structure of one newly formed zirconacyclopentane derivative was characterized by X-ray diffraction: *cis*-**1-(CH_2CHCH_2)N^{t}Bu** which readily crystallizes, leaving the *trans* isomer in solution. As shown in Figure 3.2, the structure is of a typical metallocyclopentane,[16] with a newly formed single bond (C(32)-C(35)) of 1.525(2) Å, along with elongated C(31)-C(32) and C(35)-C(36) bond lengths of 1.542(2) and 1.525(2) Å, respectively.

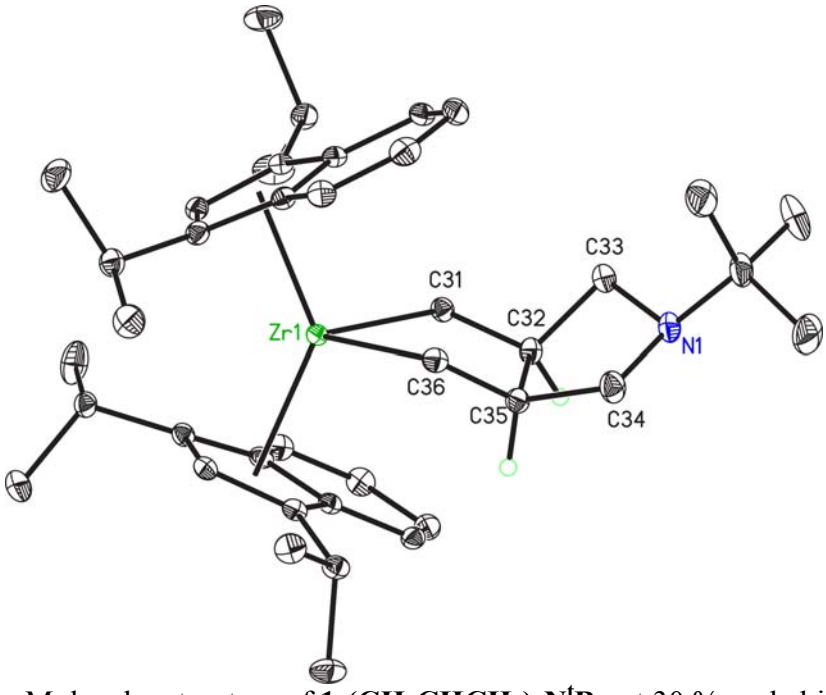

Figure 3.2. Molecular structure of **1-(CH_2CHCH_2)$_2$N^{t}Bu** at 30 % probability ellipsoids.

While cycloaddition resulted when the heteroatom was a nitrogen or a silicon, bond cleavage occurred when it was an oxygen. Treatment of **1** with diallylether resulted in rapid C-O bond cleavage and formation of a zirconocene alkyl alkoxide, (η^5-C_9H_5-1,3-$(CHMe_2)_2)_2$Zr(OCH_2CHCH_2)($CH_2CHCH_2)_2$, **1-(OCH_2CHCH_2)(CH_2CHCH_2)** (eq. 3.3). In the analogous reaction with bis(cyclopentadienyl) zirconocene, the zirconocene alkyl alkoxide is only one of three

products observed, along with those from ligand exchange, $(\eta^5\text{-}C_5H_5)_2Zr(CH_2CHCH_2)_2$ and $(\eta^5\text{-}C_5H_5)_2Zr(OCH_2CHCH_2)_2$.[13] Interestingly, in the benzene-d_6 ^{1}H NMR spectrum of **1-$(OCH_2CHCH_2)(CH_2CHCH_2)$**, the resonances associated with the allyl protons broaden due to a rapid η^1 to η^3 interconversion of the allyl group at 22 ºC. However, cooling a toluene-d_8 solution of the sample to -80 ºC allows for observation of these peaks as shown in Figure 3.3.

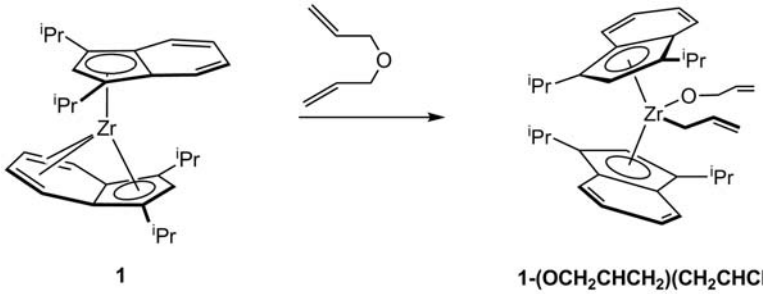

(eq. 3.3)

1 **1-$(OCH_2CHCH_2)(CH_2CHCH_2)$**

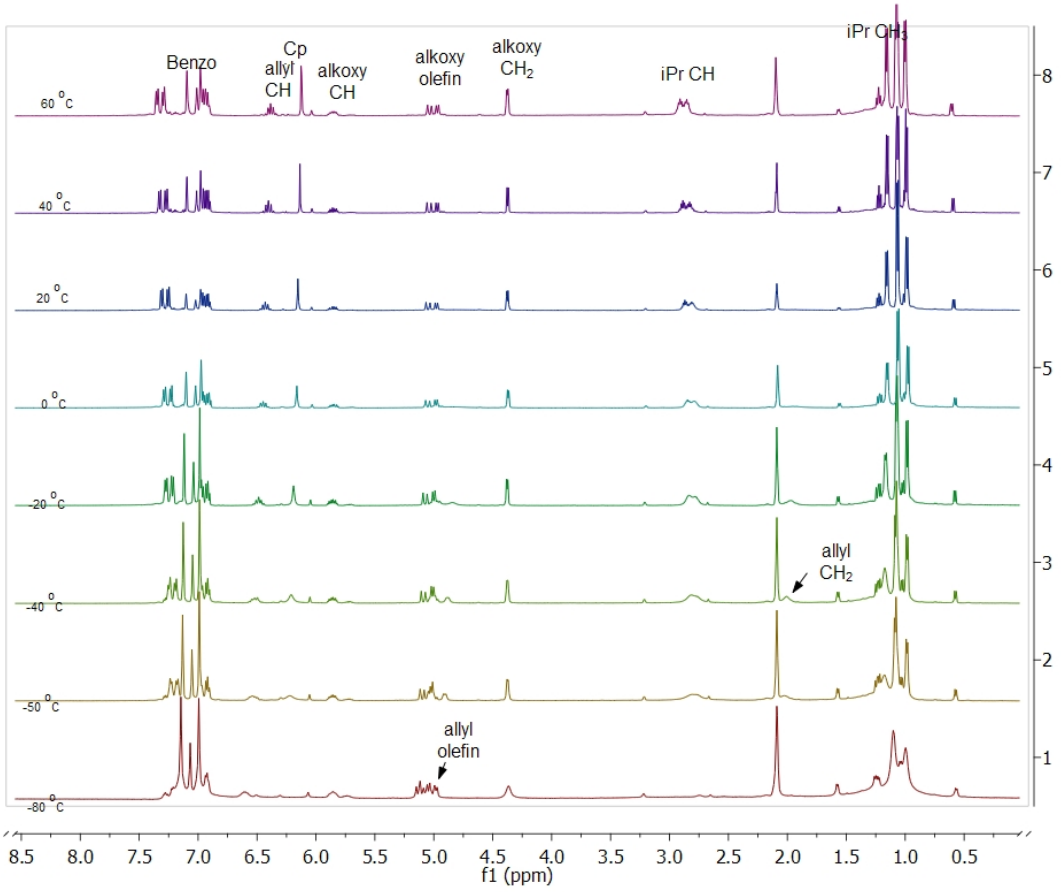

Figure 3.3. Stack plot of the ^{1}H NMR spectra of a toluene-d_8 solution of **1-$(OCH_2CHCH_2)(CH_2CHCH_2)$** at variable temperatures.

Functionalization of Zirconacycles. Attempts to functionalize the cyclic species and their subsequent removal from zirconium was explored. Treatment of each metallocene with H_2O resulted in protonation of the pentacycle/hexacycle, forming the appropriate dimethyl cyclopentane, cyclohexane, pyrrolidine or silacycle derivative with the same diastereoselectivity as the zirconacyles (eq. 3.4). Further functionalization attempts were aimed at elaborating **1-(CH_2CHCH_2)N^{t}Bu** as only one other zirconacycle with this tertbutyl amine derivative has been reported.[4] Addition of either one atmosphere of dihydrogen or two equivalents of phenylsilane resulted in release of *cis*/*trans* 3,4-dimethyltertbutylpyrrolidine along with zirconocene dihydride or zirconocene silane products (eq. 3.5). Attempts to form a bicyclic heptane derivative were unsuccessful as the reductive elimination did not occur at elevated temperatures, only isomerization to the *trans* metallocycle. Changing the substituents of the indenyl ring by replacement of the isopropyl with trimethylsilyl groups, such to encourage reductive elimination, afforded (η^5-C_9H_5-1,3-($SiMe_3$)$_2$)$_2$Zr(CH_2CHCH_2)$_2$N^{t}Bu, **2-(CH_2CHCH_2)$_2$N^{t}Bu**. Unfortunately, similar to that of **1-(CH_2CHCH_2)$_2$N^{t}Bu**, reductive elimination did not occur even at temperatures as high as 105 ºC.

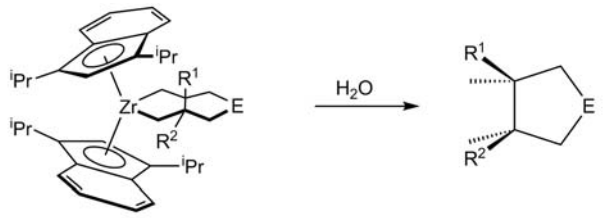

(eq. 3.4)

1-(CH_2CRCH_2)$_2$E

$R^1 = R^2 = H$, E = CH_2, $(CH_2)_2$, fluorene, N^{t}Bu, NCH_2Ph, N-tosyl, $SiMe_2$
$R^1 = R^2 = Me$, E = N^{t}Bu
$R^1 = Me$, $R^2 = H$, E = N^{t}Bu

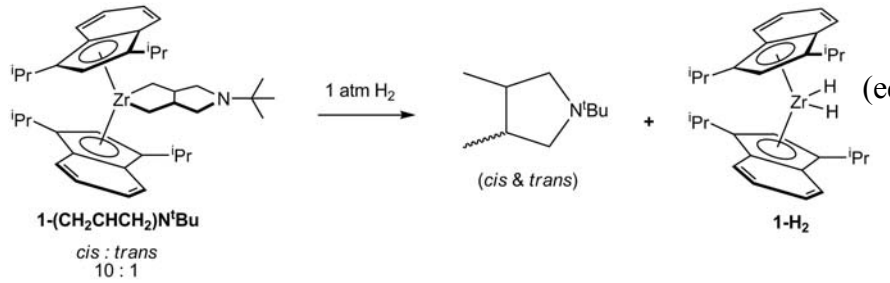

(eq. 3.5)

Pauson-Khand reactions were also explored. Interestingly, addition of an excess of carbon monoxide did not furnish the expected CO insertion or reductive elimination products, cyclic ketone and zirconocene dicarbonyl; the was determined by the lack of a carbonyl stretch in the infrared spectrum. Instead, a single organometallic species was observed arising from ketone addition to the zirconium center, yielding the zirconocene enolate hydride, (η^5-C_9H_5-1,3-$(CHMe_2)_2)_2ZrOC(CH)CH_2(CHCH_2)_2N^tBu$, **1-OC(CH)CH$_2$(CHCH$_2$)$_2$N^{t}Bu** (eq. 3.6). The ^{1}H NMR spectrum of this compound in a benzene-d_6 solution exhibits an olefinic C*H* resonance at 4.45 and a Zr-*H* at 6.16 ppm. Based on the ^{13}C NMR resonances of the C-O at 161.64 and the adjacent olefinic carbon at 103.86 ppm ($^1J_{CH}$ = 161 Hz), the structure can be assigned as coordinated η^1 through the oxygen[17] as opposed to an η^3 oxaallyl.[18] Its formation is quite intriguing as no intermediates were observed during the reaction, so different commercially available ketones were added to a possible intermediate, **1**, as one can envision a possible mechanism whereby reductive elimination of the CO insertion product forms the ketone and **1**, which then readily reacts with the ketone – or the enol tautomer – forming the observed product.

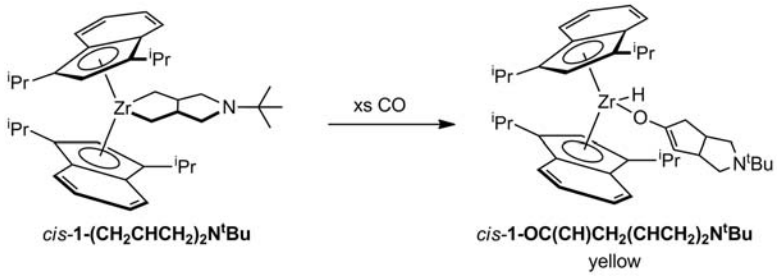

(eq. 3.6)

Addition of Cyclopentanone to Isolable Zirconium (II) Species. To probe the mechanism, cyclopentanone was added to **1**. Instead of the expected C_s symmetric product with an olefinic C*H* resonance, a C_1 symmetric compound with diagnostic upfield shifted indenyl benzo resonances was observed by ^{1}H NMR spectroscopy, along with **1**. As shown in Figure 3.4a, single crystal X-ray diffraction demonstrates insertion of two equivalents of ketone into one of the indenyl ligands, one at the 1 position on the cyclopentyl and one at the 4 position on the benzo ring, forming a zirconocene bis(alkoxide), (η^5-C_9H_5-1,3-$(CHMe_2)_2$)(η^1-C_9H_5-1,3-$(CHMe_2)_2$-1-C(κ^1-O)$(CH_2)_4$-4-C(κ^1-O)$(CH_2)_4$)Zr, **1-(O^cPent)$_2$-1,4** (eq. 3.7), giving rise to the upfield shifted benzo resonances of only one of the indenyl rings, such that the proton on the sp^3 hybridized carbon appears at 3.70, with the other resonances appearing at 4.78, 5.23 and 3.97 ppm. As shown in Table 3.2, these newly formed C-C bonds are 1.589(3) and 1.567(3) Å long, which are slightly long for C-C single bonds. Further examination of the modified indenyl ring revealed that it is coordinated to the zirconium center in an η^1 fashion, via position 7, with only a zirconium-carbon bond distance of 2.323(2), much shorter than the average 2.5 – 2.6 Å bond found in zirconocenes.[19] While the adjacent carbon atoms are close to the zirconium center with bond distances of 2.609(2) and 2.5762(19) Å, η^3 hapticity has been ruled out as a suitable bonding scheme for the indenyl ligand involves three double bonds and two sp^3 hybridized carbons, leaving one carbon for coordination to the zirconium as depicted in Table 3.2.

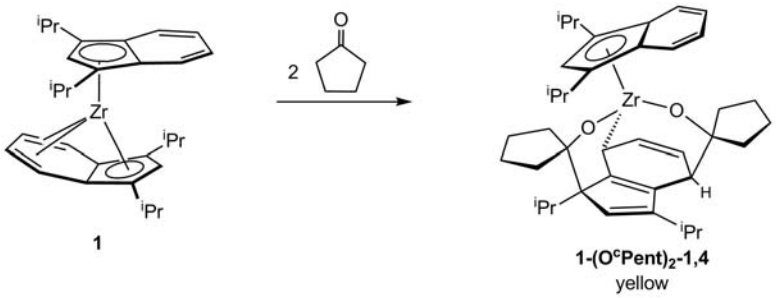

(eq. 3.7)

Table 3.2. Comparison of metrical parameters of **1-(O^{c}Pent)$_2$-1,4**, **3-(O^{c}Pent)$_2$-1,4** and **1-(OMe$_2$)$_2$-4,7**.

Numbering Scheme for Indenyl Ring in these Crystal Structures

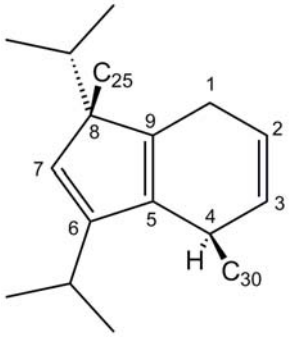

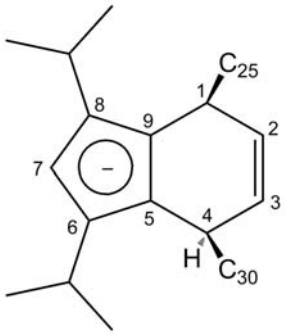

	1-(O^{c}Pent)$_2$-1,4	3-(O^{c}Pent)$_2$-1,4	1-(OMe$_2$)$_2$-4,7
Zr(1)-O(1) (Å)	1.9655(13)	1.989(3)	1.964(2)
Zr(1)-O(2) (Å)	1.9688(13)	1.980(3)	1.968(3)
O(1)-C(25) (Å)	1.433(2)	1.417(6)	1.408(4)
O(2)-C(30) (Å)	1.419(2)	1.426(6)	1.409(4)
C(8)/C(1)-C(25) (Å)	1.589(3)	1.603(8)	1.592(4)
C(4)-C(30) (Å)	1.567(3)	1.570(7)	1.597(5)
Zr(1)-C(1) (Å)	2.323(2)	2.341(5)	N/A
Zr(1)-C(2) (Å)	2.609(2)	2.574(5)	N/A
Zr(1)-C(3) (Å)	2.864(2)	2.739(5)	N/A
Zr(1)-C(4) (Å)	3.089(2)	3.004(5)	N/A
Zr(1)-C(5) (Å)	2.936(2)	2.861(5)	2.461(3)
Zr(1)-C(9) (Å)	2.5762(19)	2.556(5)	2.482(3)
C(1)-C(2) (Å)	1.431(3)	1.426(7)	1.495(5)
C(2)-C(3) (Å)	1.346(3)	1.351(7)	1.313(6)
C(3)-C(4) (Å)	1.516(3)	1.529(7)	1.491(5)
C(4)-C(5) (Å)	1.516(3)	1.502(7)	1.508(5)
C(5)-C(6) (Å)	1.490(3)	1.493(7)	1.422(4)
C(6)-C(7) (Å)	1.341(3)	1.317(7)	1.415(4)
C(7)-C(8) (Å)	1.505(3)	1.508(6)	1.395(4)
C(8)-C(9) (Å)	1.526(3)	1.524(8)	1.425(4)
C(1)-C(9) (Å)	1.445(3)	1.429(7)	1.507(4)
C(5)-C(9) (Å)	1.365(3)	1.372(7)	1.423(4)

This transformation whereby two equivalents of ketone are inserted into a single indenyl ring is unique. Rosenthal and Takahashi have both reported the coupling of cyclopentadienyl or indenyl ligands with the diene moiety of

titanacyclopentadienes and zirconacyclopentadienes to form indene or fluorene derivatives via an intramolecular mechanism.[20,21] Recently, Boag demonstrated that ethyl vinyl ketone can be added in a Diels-Alder fashion to the exo-face of a platinum η^5 bound cyclopentadienyl.[22]

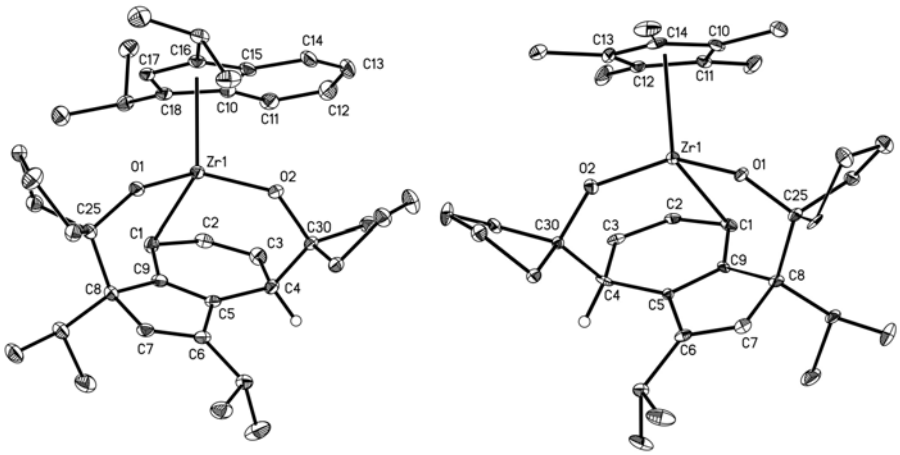

Figure 3.4. Molecular structures of **1-(O^{c}Pent)$_2$-1,4** (left) and **3-(O^{c}Pent)$_2$-1,4** (right) at 30 % probability elipsoids.

Zirconocene ketone complexes are typically coordinated η^2, such as Erker's $(\eta^5\text{-}C_5H_5)_2Zr(\eta^2\text{-}O{=}CPh_2)$[23] which readily insert olefins and terminal alkynes to form zirconadihydrofurans and zirconatetrahydrofurans.[24] Only two examples of isolable zirconocene η^1 ketone complexes have been reported, $(\eta^5\text{-}C_5Me_5)[\eta^5\text{-}C_5Me_4CH_2B(C_6F_5)_3]Zr(Ph)(\eta^1\text{-}O{=}C(Me)R)$ (R = Me, Ph),[25] although many examples are known for first row and late transition metal complexes.[26] More common is the insertion of ketones into zirconacyclopropene complexes to afford zirconatetrahydrofurans.[27] Erker found that treatment of two equivalents of ketone to zirconocene alkyl ylides afforded a zirconocene alkyl enolate along with the Wittig olefination product and phosphine oxide.[28] A similar acyclic alkyl enolate product was observed by Bergman upon addition of acetone to a zirconacyclobutene

derivative.[29] There is one example of ketone addition to a Negishi-type *in situ* prepared zirconocene complex from two equivalents of varying RMgBr (R = ^{n}Pr, ^{n}Bu, ^{n}Hex) reagents to zirconocene dichloride. Due to the equilibrium between the zirconocene olefin and zirconocene allyl hydride shown in eq. 3.1, the ketone underwent a 1,2 addition across the zirconium-hydride bond to form a zirconium

Table 3.3. Comparison of ^{1}H NMR resonances (ppm) of 1,4 cyclopentanone insertion products in benzene-d_6.

IUPAC Numbering Scheme for Indenyl Ring

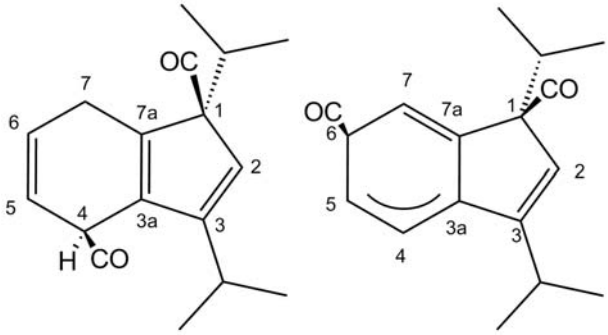

	1-(O^{c}Pent)$_2$-1,4	2-(O^{c}Pent)$_2$-1,4	3-(O^{c}Pent)$_2$-1,4	3-(O^{c}Pent)$_2$-1,6
C2	5.91	6.54	6.02	5.10
C4	3.70	3.93	3.85	5.53
C5	4.78	4.52	5.04	3.90
C6	5.23	5.32	5.24	3.81
C7	3.97	5.15	3.98	5.38

Table 3.4. Comparison of ^{13}C NMR resonances (ppm) of 1,4 cyclopentanone insertion products in benzene-d_6.

	1-(O^{c}Pent)$_2$-1,4	2-(O^{c}Pent)$_2$-1,4	3-(O^{c}Pent)$_2$-1,4	3-(O^{c}Pent)$_2$-1,6
C1	67.27	67.58	67.82	66.10
C2	130.78	153.64	131.39	114.74
C3	153.93	143.92	153.74	149.16
C3a	137.50	145.01	137.18	97.95
C4	49.17	50.11	49.59	119.16
C5	120.86	120.85	118.29	95.36
C6	119.67	118.09	119.86	51.46
C7	73.87	72.58	72.65	112.26
C7a	152.30	146.34	152.52	155.02
C-O	97.71	97.09	97.08	
	133.12	133.45	131.62	120.60

alkenyl alkoxide complex.[30] Addition of acetophenone to an isolable ylide-like silylene – which is isolobal to Cp_2Zr – allowed for sole isolation of an silyl enolate hydride.[31]

A series of 2-dimensional NMR spectroscopic experiments (COSY, ^{1}H-^{13}C HSQC and ^{1}H-^{13}C HMBC), were used to assign the ^{1}H and ^{13}C NMR spectra of **1-(O^cPent)$_2$-1,4**. Presented in Tables 3.3 and 3.4 are the assignments for the functionalized indenyl ligand. The ^{13}C NMR resonances were particularly informative with respect to bond order assignment as the two sp^3 carbons appeared at 67.27 and 49.17 ppm for the C1 and C4 resonances, respectively. The carbon directly bound to the zirconium, C7, appeared at 73.87 ppm, demonstrating sp^3 character. The remaining of the carbon atoms on the indenyl ring are downfield of 119 ppm, consistent with double bond character. The *C*-O carbons are significantly upfield shifted from that of the free ketone at 216.99 to 97.71 and 133.12 ppm, consistent with carbonyl reduction.

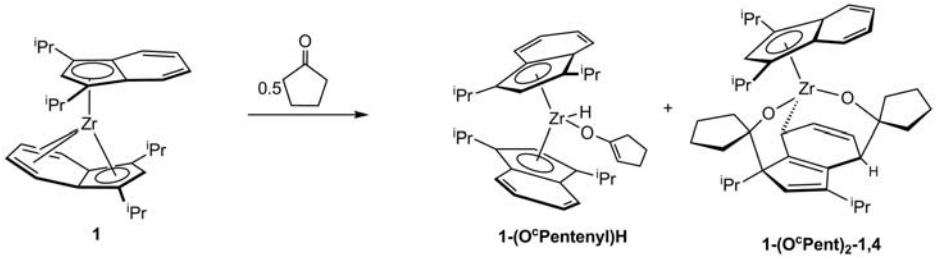

(eq. 3.8)

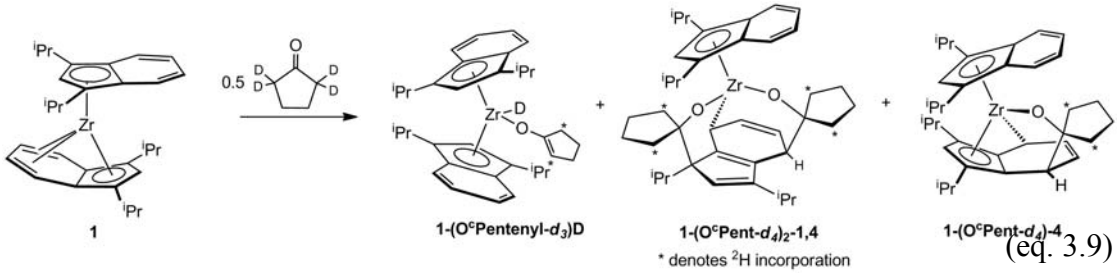

(eq. 3.9)

When only 0.5 equivalents of cyclopentanone is added to **1**, initial 25 % conversion to **1-(O^cPent)$_2$-1,4** was observed, but after 24 hours at 22 ºC, the originally expected product, the zirconocene enolate hydride, **1-(O^cPentenyl)H**, was

observed with **1-(O^{c}Pent)$_2$-1,4** in a 1.0 : 0.9 ratio (eq. 3.8) (35 % conversion, 65 % remaining **1**). Repeating the experiment with 0.5 equivalents of 2,2,5,5-cyclopentanone-d_4 also immediately resulted in a 25 % conversion to **1-(O^{c}Pent-d_4)$_2$-1,4**. After 48 hours at 22 ºC, 27 % of **1-(O^{c}Pentenyl-d_3)D** and 27 % of a new C_1 symmetric product identified as **1-(O^{c}Pent-d_4)-4** were observed (eq. 3.9). This later product is derived from formal selective cyclopentanone deinsertion from the 1-position of the modified indenyl. Subsequent addition of excess ketone to these mixtures did not appear to change the quantity of the enolate hydride compound, suggesting that its formation is not reversible. Therefore it is plausible that in the formation of **1-OC(CH)CH$_2$(CHCH$_2$)$_2$N^{t}Bu** from **1- (CH$_2$CHCH$_2$)$_2$N^{t}Bu** and CO that reductive elimination to form the ketone is rate determining and ketone addition to the zirconium is fast such that no double insertion product is observed. Addition of excess isolated ketone to a benzene-d_6 solution of **1** afforded two new C_1 symmetric products which shifts similar to insertion products. A total of four isomers are possible with this ketone.

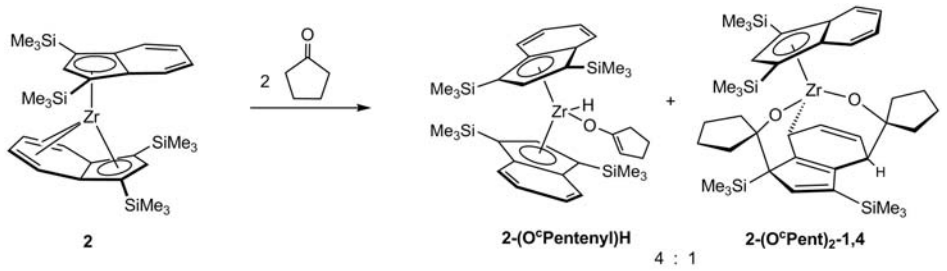

(eq. 3.10)

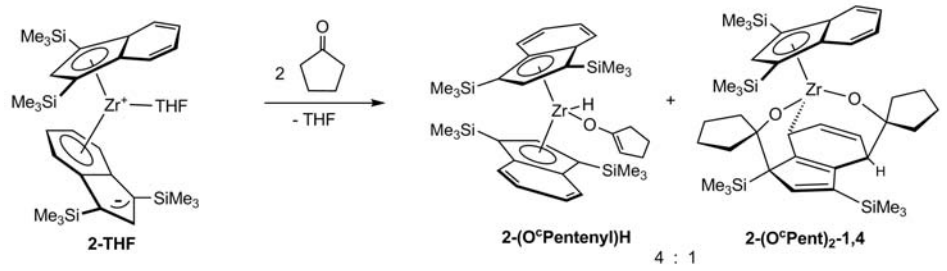

(eq. 3.11)

With this unique C-C bond forming reaction in hand, two equivalents of

cyclopentanone were also added to different zirconium (II) species: (η^9-C_9H_5-1,3-$(SiMe_3)_2$)(η^5-C_9H_5-1,3-$(SiMe_3)_2$)Zr, **2**, (η^6-C_9H_5-1,3-$(SiMe_3)_2$)(η^5-C_9H_5-1,3-$(SiMe_3)_2$)Zr-THF, **2-THF**, and (η^9-C_9H_5-1,3-$(CHMe_2)_2$)(η^5-C_5Me_5)Zr, **3**. Whether starting from the sandwich, **2**, or the tetrahydrofuran adduct, **2-THF**, a 4:1 ratio of the enolate hydride, **2-(O^{c}Pentenyl)H**, to the double insertion product, **2-(O^{c}Pent)$_2$-1,4** were observed (eq. 3.10 & 3.11). By the ^{13}C NMR shifts and a combination of ^{1}H-^{13}C HSQC and ^{1}H-^{13}C HMBC NMR experiments, the ketone additions on the latter compound were confirmed as one at the 1 position on the cyclopentyl and one at the 4 position on the benzo ring. These assignments are shown in Table 3.3 and 3.4 and are comparable to those found in **1-(O^{c}Pent)$_2$-1,4**. When cyclopentanone is added at -130 ºC to a thawing pentane solution of **2-THF**, the ratio was 1.5:1 still favoring the enolate hydride product. In an attempt to slow the C-H activation necessary for formation of **2-(O^{c}Pentenyl)H**, cyclopentanone-*d*$_4$ (deuteration in the alpha positions to the carbonyl) was added to **2-THF** at both 22 and -130 ºC, resulting in a 1.7:1 and a 0.5:1 ratio, respectively. Therefore, C-H/C-D activation is or precedes the rate-determining step in formation of the enolate hydride. Determination of other kinetic isotope effects will be discussed later in this chapter.

2-(O^{c}Pentenyl)H was also independently prepared free of insertion product by addition of the *in situ* prepared lithium enolate to a THF solution of (η^5-C_9H_5-1,3-$(SiMe_3)_2$)$_2$Zr-(H)Cl, **2-(H)Cl**, and demonstrated no formation of **2-(O^{c}Pent)$_2$-1,4** upon addition of excess cyclopentanone, establishing the irreversibility of enolate hydride formation (*vide infra*). Attempts to probe the reversibility of insertion to form enolate hydride, however, were unsuccessful as decomposition of **2-(O^{c}Pent)$_2$-1,4** occurred simultaneously.

Given the outcome of the previous experiments, increasing the stoichiometry of the ketone should increase the amount of insertion product; addition of five

equivalents of cyclopentanone to **2-THF** at 22 ºC slightly changed the product ratio such that instead of a 4:1 of **2-(O^{c}Pentenyl)H** : **2-(O^{c}Pent)$_2$-1,4**, a 3:1 ratio was observed. Addition of excess ketone at -130 ºC further improved the yield to 1.4:1. A negligible difference in product ratio was observed when either 2 or 5 equivalents of cyclopentanone-d_4 was added to the zirconocene complex at this lower temperature.

Treatment of **3** with two equivalents of cyclopentanone afforded a 1:0.7 ratio of two distinct double insertion products: one with the expected insertion into the 1 and 4 positions, (η^5-C_5Me_5)(η^1-C_9H_5-1,3-$(CHMe_2)_2$-1-C(κ^1-O)$(CH_2)_4$-4-C(κ^1-O) $(CH_2)_4$)Zr, **3-(O^{c}Pent)$_2$-1,4** and the other arising from insertion into the 1 and 6 positions, (η^5-C_5Me_5)(η^1-C_9H_5-1,3-$(CHMe_2)_2$-1-C(κ^1-O)$(CH_2)_4$-6-C(κ^1-O) $(CH_2)_4$)Zr, **3-(O^{c}Pent)$_2$-1,6** (eq. 3.12). In the later compound, based on ^{13}C NMR assignments of the elaborated indenyl, the zirconium is coordinated η^3 to the carbons at positions C3a, C4 and C5, instead of η^1 like in the former complex. Reported in Table 3.3 and 3.4 are the ^{1}H and ^{13}C NMR resonances for the functionalized indenyl ligands on both compounds.

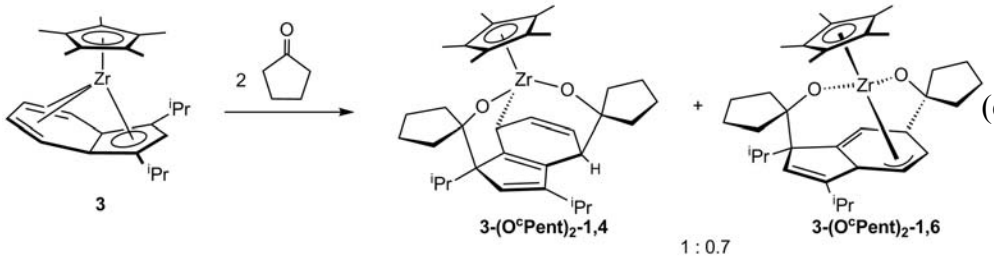

(eq. 3.12)

As shown in Figure 3.4b, the solid state structure of **3-(O^{c}Pent)$_2$-1,4** by X-ray diffraction confirms its connectivity. With similar bond lengths to that found in **1-(O^{c}Pent)$_2$-1,4**, the newly formed C-C bonds are 1.570(7) and 1.603(8) Å long. The carbon bound η^1 to the zirconium center is only 2.341(5) Å away from the Zr atom.

Treatment of **3** with only 0.5 equivalents of cyclopentanone, initially, afforded the two double insertion products in the same ratio along with unreacted **3** and a *C$_1$*

symmetric intermediate identified by ^{13}C NMR spectroscopy as the mono insertion at the 1 position on the indenyl product, (η^5-C_5Me_5)(η^4-C_9H_5-1,3-$(CHMe_2)_2$-1-C(κ^1-O)$(CH_2)_4$)Zr, **3-(O^{c}Pent)-1**. Allowing this mixture of complexes to stand at ambient temperature with an internal $(SiMe_3)_2O$ standard allowed for a slow disappearance of both **3-(O^{c}Pent)-1** and **3-(O^{c}Pent)$_2$-1,4** and an appearance of the mono insertion product at the 4 position, (η^5-C_5Me_5)(η^5-C_9H_5-1,3-$(CHMe_2)_2$-4-C(κ^1-O)$(CH_2)_4$)Zr, **3-(O^{c}Pent)-4**, along with the enolate hydride, **3-(O^{c}Pentenyl)H** (eq. 3.13). Shown in Table 3.5 are the ratios over the course of 24 hours. Importantly, the 1,6 insertion product, **3-(O^{c}Pent)$_2$-1,6** does not decrease nor is a mono insertion product at the 6 position observed, implying a different pathway of formation from **3-(O^{c}Pent)$_2$-1,4**. Addition of more cyclopentanone depleted **3-(O^{c}Pent)-4** while the amount of **3-(O^{c}Pent)$_2$-1,4** increased. While it is important to note that formation of this double insertion product occurred because **3** was present, the ratio of newly formed **3-(O^{c}Pent)$_2$-1,4** to **3-(O^{c}Pent)$_2$-1,6** was greater than the consistent 1:0.7 ratio observed upon initial addition of the ketone to **3**, implying a second equivalent of cyclopentanone adding from **3-(O^{c}Pent)$_2$-1** to form **3-(O^{c}Pent)$_2$-1,4**.

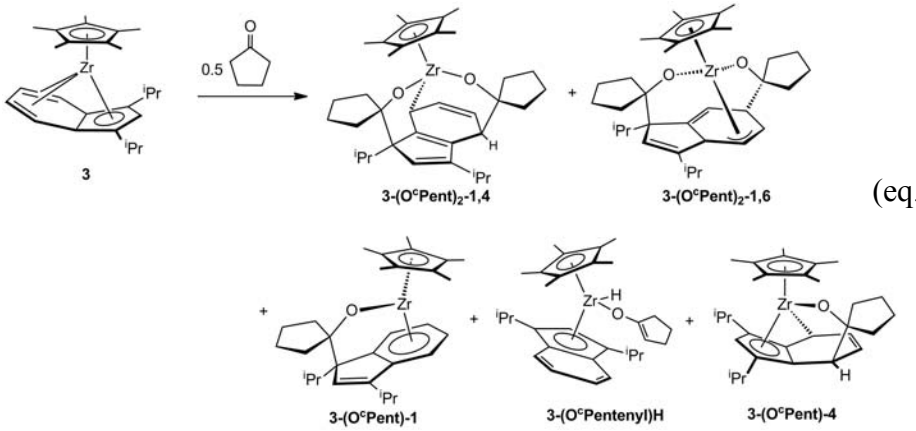

(eq. 3.13)

Interestingly, allowing solutions of **1-(O^{c}Pent)$_2$-1,4** to stand at ambient temperature resulted in trace quantities of a new C_s and a new C_1 symmetric products. Heating a benzene-d_6 solution of **1-(O^{c}Pent)$_2$-1,4** at 90 ºC for one week resulted in full

Table 3.5. Quantity of each compound with time (or upon addition of excess ketone) when **3** is treated with 0.5 equivalents of cyclopentanone.

Time (h)	**3**	**Free ligand**[a]	**3-(O^cPent)$_2$-1,4**	**3-(O^cPent)$_2$-1,6**	**3-(O^cPent)$_2$-1**	**3-(O^cPent)$_2$-4**	**3-($O^cPentenyl$)H**
0.08	0.58	-	0.12	0.09	0.09	-	-
2	0.55	0.05	0.10	0.09	0.05	-	0.05
4	0.52	0.05	0.07	0.09	0.03	0.03	0.08
8	0.50	0.05	0.06	0.09	0.01	0.06	0.10
12	0.49	0.05	0.05	0.09	0.01	0.07	0.13
24	0.47	0.06	0.03	0.09	-	0.09	0.15
	-	0.06	0.30	0.32	-	-	0.21

[a] Protonated diisopropylindene.

conversion to equimolar quantities of the thermodynamic C_s symmetric product where the insertion is at the 4 and 7 positions, **1-(O^cPent)$_2$-4,7**, along with an unidentified C_1 symmetric compound, which exhibits ^{1}H and ^{13}C resonances very similar to that of the C_s symmetric product, suggesting an asymmetric diastereomer (eq. 3.14). A COSY NMR experiment of the C_1 symmetric compound demonstrated that bothcyclopentanone insertions occurred at the 4 and 7 positions of the same indenyl ring, similar to that of the C_s symmetric compound, implying a different conformer. Takahashi did report that the coupling of cyclopentadienyl or indenyl ligands with diene moieties was reversible via ^{13}C labeling of the cyclopentadienyl ring and observation of scrambling of the label in the intermediate and final products.[21b]

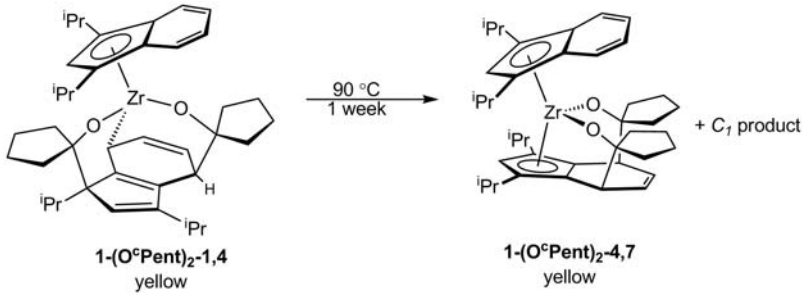

(eq. 3.14)

Both **2-(O^cPent)$_2$-1,4** and **3-(O^cPent)$_2$-1,4** readily decompose in solution at ambient temperature over the course of days, while heating a benzene-d_6 solution of **3-**

(O^{c}Pent)$_2$-1,6 to 105 ºC for three days resulted in no reaction, demonstrating the thermal stability of the 18 electron complex such that ketone deinsertion was not observed in the earlier substoichiometric addition of cyclopentanone to **3** experiment.

Addition of Other Ketones to Isolable Zirconium (II) Species. With the observation of interesting reactivity between cyclopentanone and isolable bis(indenyl) zirconium sandwich complexes, other ketones were explored, including acetophenones, dicyclic ketones and substituted cyclopentanones. As a general procedure, two equivalents of the ketone were added to a benzene-d_6 or pentane solution of **1** at ambient temperature. Summarized in Figure 3.5 are the results, where either the zirconocene enolate hydride, (η^5-C_9H_5-1,3-$(CHMe_2)_2$)$_2$Zr(OC(CH)R)H, **1-(OR')H**, or exclusive double insertion into the 1 and 4 positions of one of the indenyl rings, (η^5-C_9H_5-1,3-$(CHMe_2)_2$)(η^1-C_9H_5-1,3-$(CHMe_2)_2$-1-C(κ^1-O)(R^1R^2)-4-C(κ^1-O)(R^1R^2))Zr, **1-(OCR^{1}R^2)$_2$-1,4** was observed.

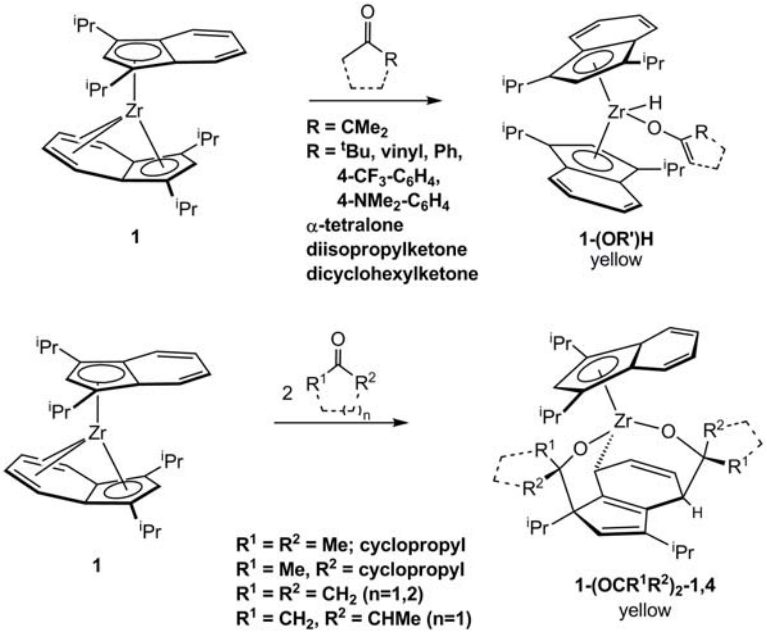

Figure 3.5. Divergent product formation upon two equivalents of various ketones to a pentane or benzene solution of **1** at 22 °C.

Cyclohexanone, acetone and 2-methylcyclopentanone react like cyclopentanone doubly inserting into the indenyl ligand. For the last substrate, 2-methylcyclopentanone, at least four isomers were observed due to the two stereocenters per reduced ketone. The addition of a second methyl group on the cyclopentanone in 2,2-dimethylcyclopentanone resulted in formation of the enolate hydride; a similar observation was made for the related acyclic pinacolone (methyl tert-butyl ketone) and dicyclohexyl ketone, suggesting a steric disposition of the ketone influences the outcome of the reaction.

Similar to the thermodynamic product of cyclopentanone insertion to **1**, **1-(O^cPent)$_2$-4,7**, addition of an excess of three equivalents of acetone to a benzene-d_6 or pentane solution of **1** resulted in immediate formation of **1-(OMe_2)$_2$-1,4**, but allowing it to stir for 1.5 hours at 22 ºC produced C_s symmetric **1-(OMe_2)$_2$-4,7**. Single crystal X-ray diffraction further confirmed the structure of **1-(OMe_2)$_2$-4,7**. As shown in Figure 3.6, the hapticities of both indenyl rings are η^5 and are oriented in a nearly anti configuration with a rotational angle of 143.8 º. Selected bond distances are shown in Table 3.2, comparing this 4,7 ketone insertion with the 1,4 insertion products. The newly formed C(1)-C(25) and C(4)-C(30) bonds are 1.592(4) and 1.597(5) Å, respectively. The benzo ring has been dearomatized such that C(1)-C(2), C(3)-C(4), C(4)-C(5) and C(1)-C(9) have been elongated to between 1.491(5) and 1.508(5) Å, while C(2)-C(3) contracted to 1.313(6) Å.

Both cyclopropyl methyl ketone and dicyclopropyl ketone formed insertion products exclusively, without any detectable opening of the cyclopropyl ring, a likely indication that this reaction does not involve radical intermediates. Gently warming a benzene-d_6 solution of the C_1 symmetric insertion product of two equivalents of dicyclopropyl ketone, **1-(O^cPr)$_2$-1,4**, to 45 ºC afforded the thermodynamically favored

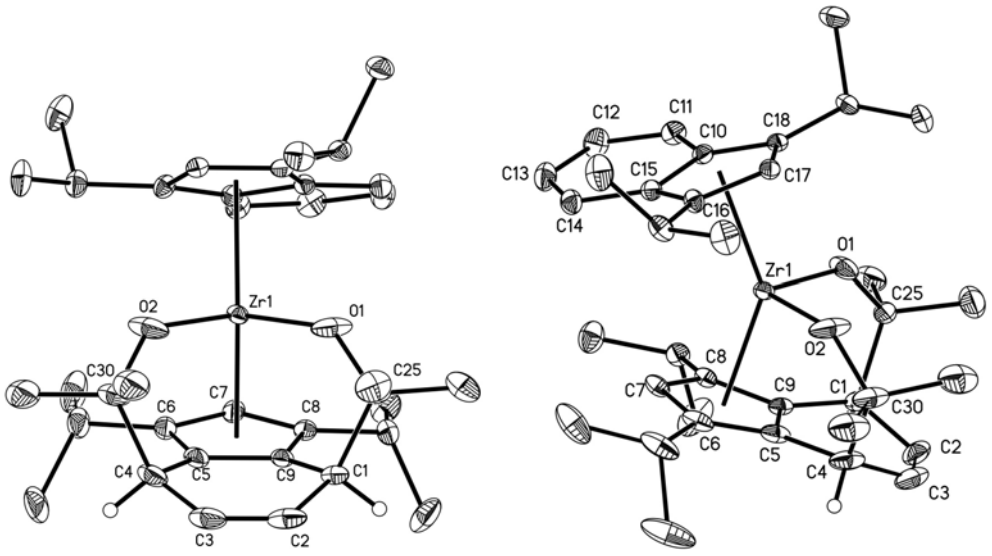

Figure 3.6. Molecular structure of **1-(OMe$_2$)$_2$-4,7** at 30 % probability ellipsoids.

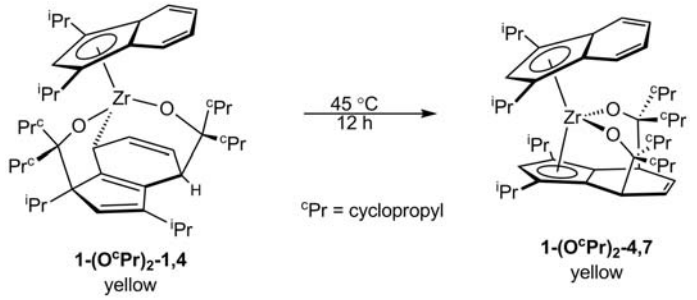

(eq. 3.15)

double insertion into the benzo positions 4 and 7, **1-(O^{c}Pr)$_2$-4,7** (eq. 3.15). Addition of only 0.5 equivalents of dicyclopropyl ketone, initially formed **1-(O^{c}Pr)$_2$-1,4** along with the ring-opened and cyclometalated product of a single cyclopropyl ring, **1-*c*-OC(**^{c}**Pr)CHCH$_2$CH$_2$**, without any detectable enolate hydride formation (eq. 3.16). Over the course of 24 hours at ambient temperature, the double insertion product reversibly deinserted a ketone, allowing for addition to another equivalent of **1**, resulting in a benzene-d_6 solution mixture consisted of only **1-*c*-OC(**^{c}**Pr)CHCH$_2$CH$_2$** and the mono insertion product at the benzo 4 position, **1-(O^{c}Pr)-4**, in a 1:1 ratio. Addition of an additional 1.5 equivalents of dicyclopropyl ketone did reconvert **1-(O^{c}Pr)-4** to **1-(O^{c}Pr)$_2$-1,4**, further suggesting the intermediacy of a mono insertion at the benzo ring before the second insertion occurs. Interestingly, addition of 2 – 10

equivalents of the acyclic diisopropyl ketone at either 22 or -130 ºC formed only the zirconocene enolate hydride. The disparity between dicyclopropyl ketone and diisopropyl ketone is likely due to the difficulty in deprotonating the position alpha to the carbonyl. Deuteration of the alpha carbon for diisopropyl ketone required stirring the ketone-d_0 in 1M NaOD for two days, then another day with fresh NaOD/D_2O.[32] Meanwhile, harsher conditions were required for dicyclopropylketone: refluxing the ketone-d_0 in D_2O with catalytic KOD for a week, then another week with fresh KOD/D_2O.

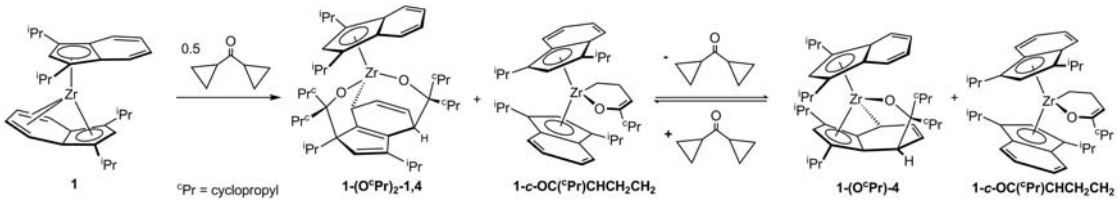

(eq. 3.16)

Addition of two equivalents of acetophenone to **1** yielded only the zirconocene enolate hydride. Altering the ketone electronically with either an electron-donating dimethylamino or an electron-withdrawing trifluoromethyl group at the para position did not result in observation of any insertion product. Addition of the deuterated p-dimethylaminoacetophenone-d_3 to a pentane solution of **1** at -130 ºC in an attempt to suppress C-H activation still afforded the zirconocene enolate deuteride. A competition experiment using 10 equivalents each of the p-NMe_2 and the p-CF_3 substituted acetophenones appear to show the expected faster relative rate for the electron-withdrawing ketone. However, upon further investigation, the ratio of enolate hydrides did change over time in the presence of the excess acetophenones, implying exchange of enolates. Interestingly, addition of the less sterically bulky alkenyl ketone, methyl vinyl ketone, to **1** also resulted in enolate hydride formation, which over the course of 24 hours cleanly converted to the cyclometalated **1-*c*-OCH(Me)CHCH$_2$** (eq. 3.17), as evidenced by the singlet methyl resonance appearing

at 1.72 ppm in benzene-d_6. This result demonstrates that in this case the acidity of the proton on the carbon alpha to the carbonyl plays a larger factor than the sterics.

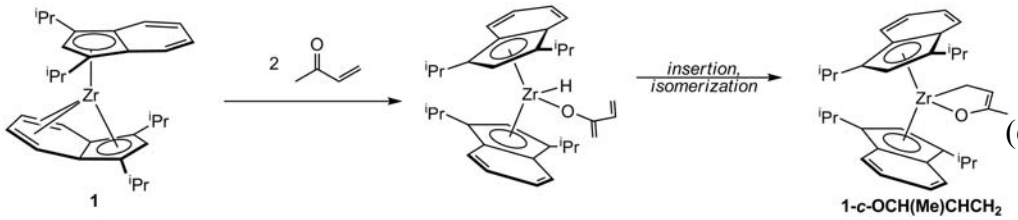

(eq. 3.17)

Shown in Figure 3.7 are the pK_as of some of the ketones catergorized based on product formation. Clearly, while there are some trends since the more enolizable ketones afford enolate hydride as a product, ketones with the higher pK_as, where there is a large steric bulk on at least one side of the carbonyl do as well. Product formation

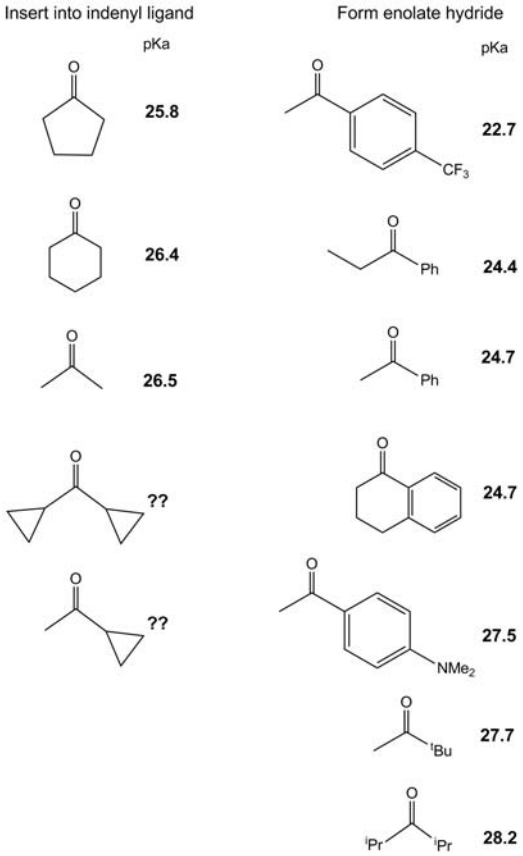

Figure 3.7. pK_as of the ketones in this study. The ones on the left column form a 1,4 double insertion product, while the ones on the right produce the zirconocene enolate hydride compound upon addition of excess ketone to a solution of **1**.[33]

is relatively slow for the latter ketones, without observable intermediates at ambient temperature. Further confirmation is demonstrated by the no reaction when the sufficiently bulky non-enolizable ditert-butylketone is added to **1**.

Addition of Non-Enolizable Ketones to Isolable Zirconium (II) Complexes. The use of non-enolizable ketones should prohibit the formation of zirconium enolate hydride products. Addition of 1 – 4 equivalents of benzophenone to a pentane or benzene solution of **1** inserted only one equivalent of ketone into one indenyl ligand at the benzo 4 position forming, resulting in isolation of orange **1-(OPh$_2$)-4** (eq. 3.18). Further attempts to insert an additional equivalent of benzophenone only produced an orange insoluble solid and a clear oil identified as two indenyl ligands coupled together (eq. 3.19). Insertion of

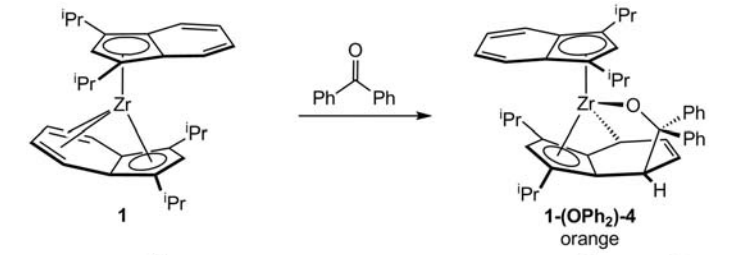

(eq. 3.18)

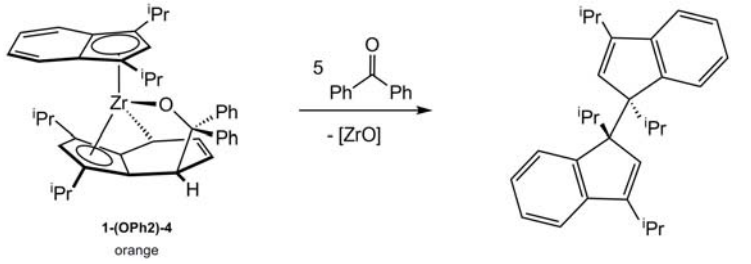

(eq. 3.19)

the smaller cyclopentanone to **1-(OPh$_2$)-4** furnished products whereby the benzophenone has deinserted and the ortho position of one of the phenyl rings has attacked the cyclopentanone carbonyl carbon, forming a zirconocene bisalkoxide complex (eq. 3.20). Addition of benzophenone to an isolable ylide-like silylene yielded a similar dearomatized benzophenone structure.[31] Based on a series of ^{1}H-^{13}C HSQC and ^{1}H-^{13}C HMBC NMR experiments on the coupled ketone compound, one of

the indenyl rings has ^{13}C NMR resonances indicative of η^1 hapticity, while the other remains coordinated η^5. As the zirconium is coordinatively unsaturated, the coupled ketone complex decomposed within a few hours at ambient temperature, releasing free indene, benzophenone and cyclopentanone. Direct protonation of the compound prior to decomposition also afforded the uncoupled ketones, implying that formation of the C-C bonds ire also reversible.

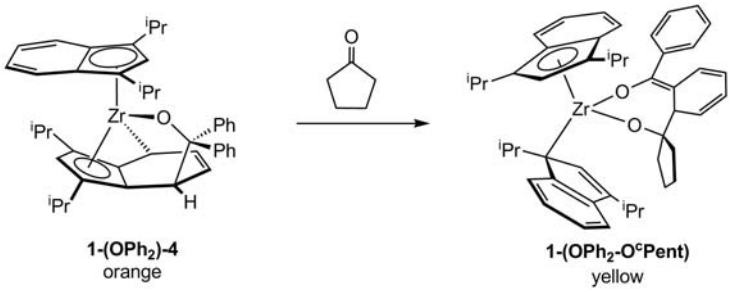

1-(OPh$_2$)-4
orange

1-(OPh$_2$-O^{c}Pent)
yellow

(eq. 3.20)

Interestingly, addition of 2 equivalents of benzophenone to the less sterically congested Cp* indenyl zirconium sandwich, **3**, afforded the C_s symmetric double insertion into the 4 and 7 positions of the indenyl ring – the thermodynamic insertion product of less sterically hindered ketones – **3-(OPh$_2$)$_2$-4,7**. Slow titration of benzophenone to a benzene-d_6 solution of **3** generated the mono insertion product observed in the bis(indenyl) zirconium case, **3-(OPh$_2$)-4**, along with **3-(OPh$_2$)$_2$-4,7**, (eq. 3.21) implying the stepwise addition of ketone.

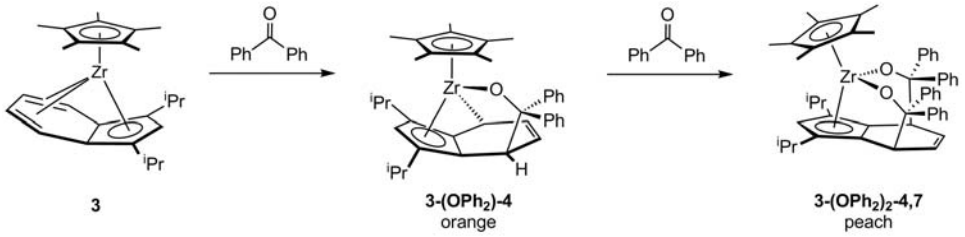

3

3-(OPh$_2$)-4
orange

3-(OPh$_2$)$_2$-4,7
peach

(eq. 3.21)

The constrained 9-fluorenone was another ketone with non-enolizable protons that was studied. Titration experiments indicated that the red product has two equivalents of the ketone incorporated as substoichiometric amounts of 9-fluorenone resulted in partial conversion to the product. The benzene-d_6 ^1H NMR spectrum exhibits the number of resonances expected for a C_1 symmetric compound with one

substituted indenyl ligand as judged by the 4 upfield shifted benzo resonances. However, further analyses of NMR data by a combination of two-dimensional techniques showed that these upfield shifted "benzo" ^{1}H shifts are actually attributed to a phenyl ring on one of the fluorenone molecules. The carbon on the fluorenone 1 position attacked the other fluorenone carbonyl carbon making it an sp^3 hybridized carbon center resulting in dearomatization of the phenyl ring. The overall compound is an η^5, η^5 bis(indenyl) zirconocene bisalkoxide complex, **1-(Ofluorenyl)$_2$** (eq. 3.22), which explains the absence of upfield shifted indenyl benzo resonances between 3 – 6.5 ppm.

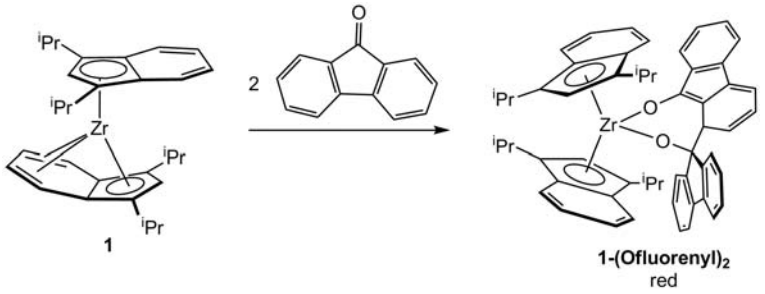

(eq. 3.22)

Single crystal X-ray diffraction confirmed the structure of **1-(Ofluorenyl)$_2$** determined by NMR spectroscopy. As shown in Figure 3.8, the hapticities of both indenyl rings are η^5 and are oriented in a nearly anti configuration with a rotational angle of 172.5 º. Reported in Table 3.6 are some selected bond lengths; the newly formed C(30)-C(45) bond is 1.575(5) Å and one of the phenyl rings has clearly been dearomaticized with two adjacent bonds (C(26)-C(45) and C(45)-C(46)) of 1.501(5) Å each.

Unlike the benzophenone-cyclopentanone coupled product, **1-(Ofluorenyl)$_2$** was stable in benzene-d_6 solution for months due to its η^5, η^5 hapticity. Similar to **1-(OPh$_2$-O^{c}Pent)**, protonation of **1-(Ofluorenyl)$_2$** with either HCl or H_2O resulted in liberation of the free 9-fluorenone, further establishing the reversibility of the C-C bond formation. Addition of a one-electron oxidant such as iodine also produced free

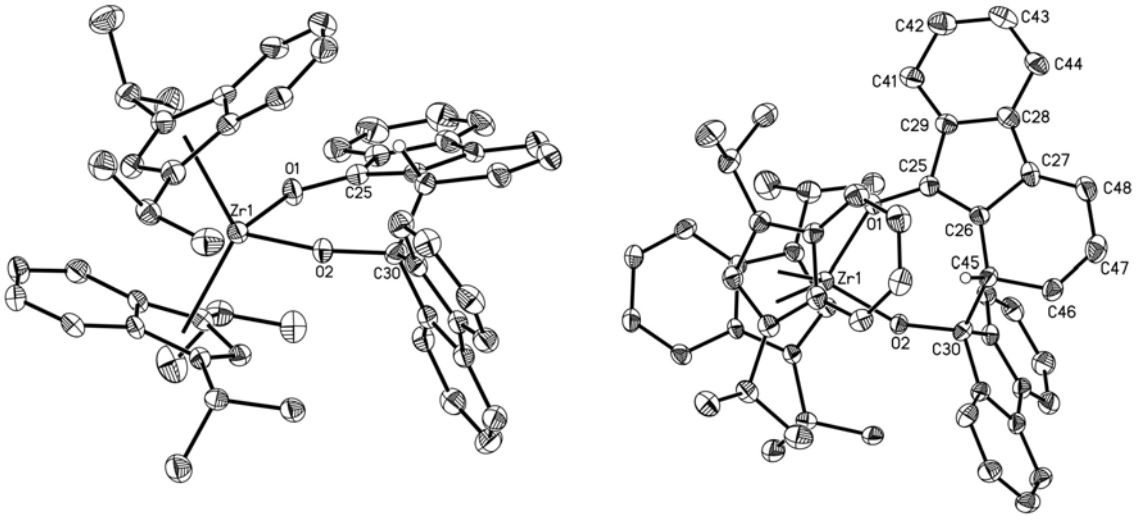

Figure 3.8. Side (left) and top (right) views of **1-(Ofluorenyl)$_2$** at 30 % probability elipsoids.

Table 3.6. Selected metrical parameters of **1-(Ofluorenyl)$_2$**.

	1-(Ofluorenyl)$_2$
Zr(1)-O(1) (Å)	2.014(2)
Zr(1)-O(2) (Å)	1.920(2)
O(1)-C(25) (Å)	1.332(4)
O(2)-C(30) (Å)	1.432(4)
C(25)-C(26) (Å)	1.376(5)
C(26)-C(27) (Å)	1.463(5)
C(27)-C(48) (Å)	1.339(5)
C(47)-C(48) (Å)	1.458(5)
C(46)-C(47) (Å)	1.328(5)
C(45)-C(46) (Å)	1.501(5)
C(26)-C(45) (Å)	1.501(5)
C(30)-C(45) (Å)	1.575(5)

9-fluorenone. Heating a benzene-d_6 solution of **1-(Ofluorenyl)$_2$** also afforded the free starting ketone, along with indene and fulvene, indications of β-H elimination of the indenyl ring and reductive elimination of the other indenyl.

In an attempt to investigate the mechanism of the 9-fluorenyl coupling, a slow titration of 9-fluorenone to a benzene-d_6 solution of **3** was performed in the hopes of stabilizing an indenyl elaborated intermediate. Unfortunately, only one new complex

was observed but readily decomposed at ambient temperature.

Mechanistic Studies for Enolate Hydride Versus Insertion Product Formation. Based on the studies on cyclopentanone addition to isolable sandwich complexes where addition of excess ketone at lower temperatures favored the insertion product over enolate hydride formation, it appears that excess ketone favors the insertion pathway. Additionally, knowing that at least some of the insertion steps are reversible while enolate hydride formation is irreversible, it seems likely that the barrier for insertion is lower than enolate hydride formation, with enolate hydride being the thermodynamic product.

As mentioned previously, optimizing the conditions for ketone insertion with the ketones on the right column of Figure 3.6, those that only formed enolate hydride products upon addition to a solution of **1** at ambient temperature, mainly resulted in observable zirconocene enolate hydride product. The one exception is pinacolone, which is sufficiently bulky on one side of the carbonyl but has a high pKa. Addition of two equivalents of pinacolone to a pentane solution of **1** at -130 ºC resulted in a 1:1 ratio of **1-(OC(CH$_2$)C^{t}Bu)H** : a new *C$_1$* symmetric product identified as (η^5-C$_9$H$_5$-1,3-(CHMe$_2$)$_2$)(η^1-C$_9$H$_5$-1,3-(CHMe$_2$)$_2$-1-H-4-C(κ^1-O)(C(Me)^{t}Bu)Zr(OC(CH$_2$)C^{t}Bu), **1-(OC(CH$_2$)C^{t}Bu)-(OC(Me)^{t}Bu)-4**, where insertion of one ketone has occurred at the 4 position of the indenyl ring along with enolization, protonating the indenyl at the 1 position (eq. 3.23). The ^{1}H NMR spectrum of a benzene-*d$_6$* solution of this mixed insertion/enolate product exhibits both upfield shifted benzos at 3.87, 4.36 and 5.12 (2 concident peaks) ppm, two olefinic resonances for the enolate at 4.01 and 4.24 ppm, and the new proton on the indenyl at 3.11 ppm. The latter set of resonances were confirmed by addition of pinacolone-*d$_3$*, where the product ratio was 1:3, favoring the mixed product (eq. 3.23). The formation of this new compound as opposed to a

double insertion product reiterates the influences of steric bulk of the ketone which appears to disfavor insertion thermodynamically. Likely, insertion occurred first, whether a single or double is unclear. The double insertion is too thermodynamically disfavored – if even kinetically viable – so the second ketone underwent deinsertion, allowing for enolization and protonation of the indenyl ring, resulting in the observed product. Further deinsertion of the first ketone resulted in formation of the irreversible enolate hydride product.

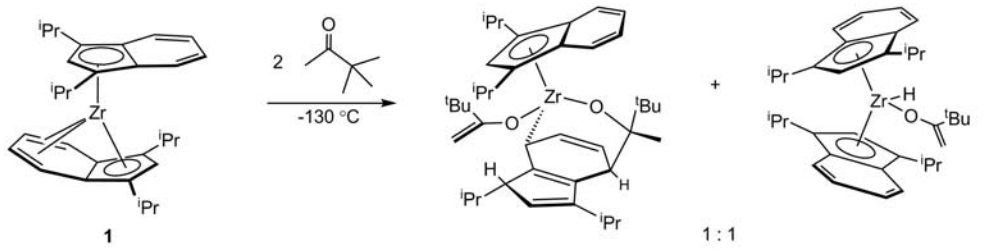

(3.23)

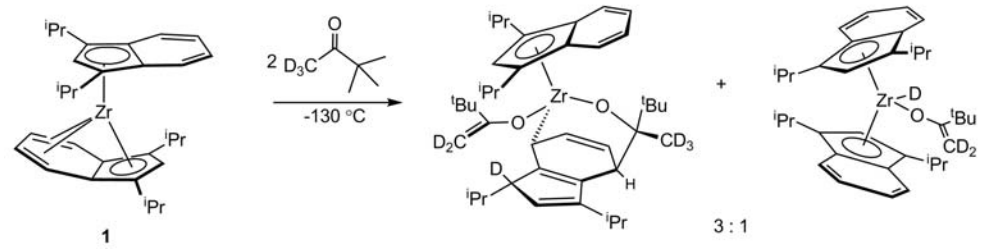

(3.24)

Determination of rate constants for formation of both types of products were attempted by *in situ* infrared spectroscopy. For enolate hydride formation, the addition of varying equivalents of diisopropyl ketone to a toluene solution of **1** at -40 °C resulted in a sigmoidal order in ketone, suggestive of competing pathways. For ketone insertion to a toluene solution of **1**, dicyclopropylketone was used at -78 °C. Kinetic data was initially attempted with cyclopentanone but was > 100 faster than with dicyclopropyl ketone at this temperature, completing within two minutes. No definitive order could be obtained due to the rapid reaction.

Kinetic isotope effects were measured for zirconocene enolate hydride formation by competition experiments with pinacolone and pinacolone-d_3. Addition of a 20 fold excess of an equimolar mixture of the two isotopologues to a benzene-d_6

solution of **1** at 22 ºC and measurement by ^{1}H NMR spectroscopy yielded a value of k_H/k_D of 1.2(1) as the average of three independent trials (eq. 3.25), consistent with a normal secondary kinetic isotope effect. A control experiment, where the enolate deuteride, **1-(O(CD$_2$)^{t}Bu)D**, was treated with excess pinacolone-d_0 produced no reaction, demonstrating the irreversibility of enolate hydride/deuteride formation.

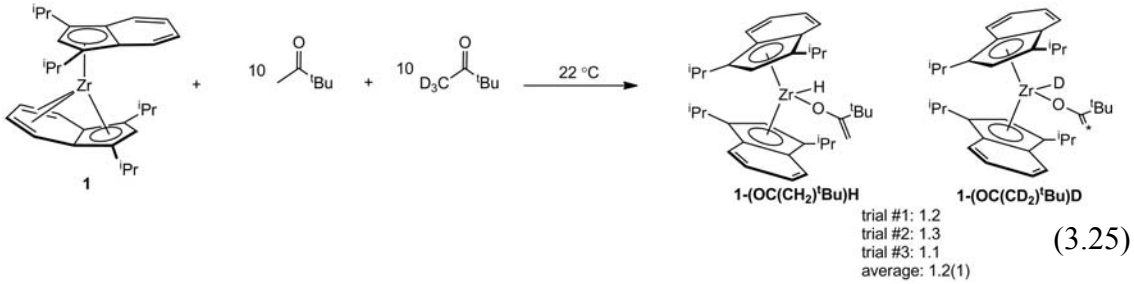

(3.25)

As it has been previously established that at least the first ketone insertion is reversible, measurement of an equilibrium isotope effect was attempted by ^{1}H NMR spectroscopy. However due to peak overlap, the only appropriate ketone was acetone as the acetone methyl resonances are clearly separated from those of the indenyl isopropyl methyl groups. Unfortunately, addition of excess protio acetone to a benzene-d_6 solution of the deuterated insertion product, **1-(O(CD$_3$)$_2$)$_2$-1,4**, initially, exchanged some of the acetone-d_6 in the C1 position, affording approximately 25 % of **1-(O(CH$_3$)$_2$)-1-(O(CD$_3$)$_2$)-4** (eq. 3.26).[34] Over the course of an hour, the mixture of products underwent isomerization to the thermodynamic insertion product, where both ketones are inserted into the benzo positions (eq. 3.26). Interestingly, the major product is the one where acetone-d_0 has inserted into both positions, with a ratio of 11:1 for CH_3:CD_3 groups. The major product of **1-(OMe$_2$)$_2$-4,7-*d$_0$*** implies that the second ketone insertion from the 1,4 double insertion product is also reversible. The reversibility of the formation of the 4,7 double insertion product was also probed by monitoring a benzene-d_6 solution of **1-(OMe$_2$)$_2$-4,7-*d$_{12}$*** with excess acetone-d_0 by ^{1}H NMR spectroscopy. No reaction occurred. Addition of a 10 – 20 fold excess of equimolar mixtures of the two isotopologues to a benzene-d_6 solution of **1** and

allowing the mixture to stand at ambient temperature for 1 hour yielded the expected k_H/k_D of 1.0(1) as the average of four independent trials, consistent with no C-H/D activation occurring prior to the rate determining step in the isomerization from the C_1 to the C_s symmetric product.

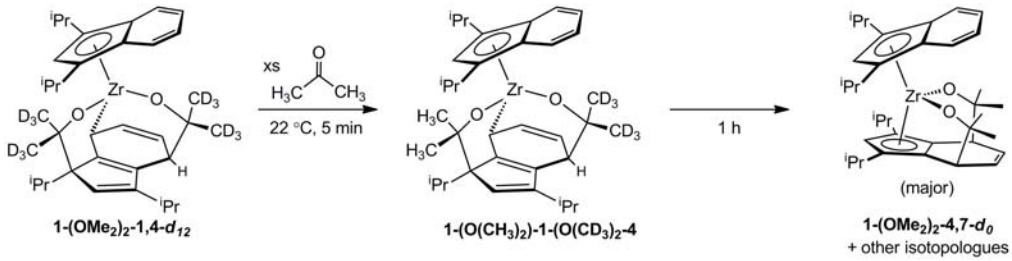

(3.26)

As another competition experiment, addition of an excess of an equimolar mixture of two different ketones with different rates of insertion to **1** was performed, utilizing cyclopentanone and the slower dicyclopropylketone. A 1:1.4 ratio of two C_1 symmetric products was observed, **1-(O^{c}Pent)$_2$-1,4** to the new mixed ketone product, **1-(O^{c}Pent)-1-(O^{c}Pr$_2$)-4**, where the dicyclopropylketone inserted in the benzo and the cyclopentanone in the cyclopentadienyl positions (eq. 3.27). None of the double insertion of dicyclopropylketone product was observed unless a larger ratio of this ketone was employed.

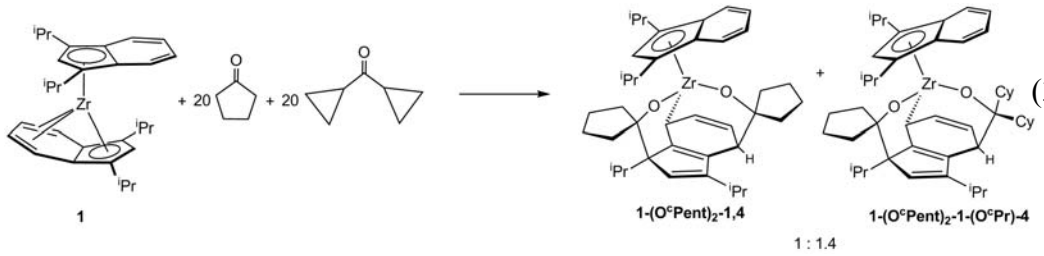

(3.27)

As a crossover experiment a benzene-d_6 solution consisting of a mixture of the **3-(O^{c}Pent)$_2$-1,4** and **3-(O^{c}Pent)$_2$-1,6** was allowed to stand at 22 ºC in the presence of 2 equivalents of **1**. After 24 hours, **3-(O^{c}Pent)$_2$-1,4** was completely consumed and both **3-(O^{c}Pent)-4** and **1-(O^{c}Pentenyl)H** observed (eq. 3.28), while the concentration of **3-(O^{-c}Pent)$_2$-1,6** remained constant. A control experiment showed that treating a benzene-d_6 solution of **1-(O^{c}Pent)$_2$-1,6** with **1** showed no reaction at ambient

temperature. The conversion of **3-(O^{c}Pent)$_2$-1,4** to **3-(O^{c}Pent)-4** reinterates the reversibility of the C-C bond formation to form the thermodynamically preferred product with η^5 indenyl hapticity.

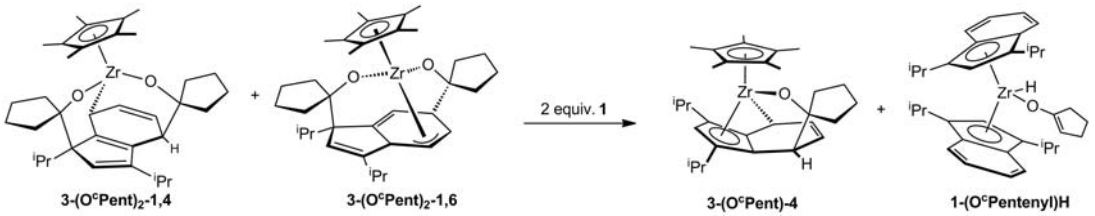

(3.28)

Based on these experimental data, a mechanism for both reactions is proposed in Figure 3.8. It was previously measured for η^9, η^5 bis(indenyl) zirconocene sandwich complexes, experimentally[10] and computationally,[35] that the η^9, η^5 to η^5, η^9 interconversion accessing an η^5, η^5 bis(indenyl) zirconium intermediate (Figure 3.9) is faster for silyl substituted indenyl ligands than for alkyl substituted. The barrier for interconversion of **2** is roughly 3 kcal/mol lower than for **1**.[10] Based on the observation of **2-(O^{c}Pentenyl)H** and **2-(O^{c}Pent)$_2$-1,4** upon addition of 2 equivalents of cyclopentanone to **2** while only **1-(O^{c}Pent)$_2$-1,4** under the same conditions for **1**,this implies that enolate hydride formation occurs through the η^5, η^5 bis(indenyl) zirconium intermediate. For ketone insertion, the first equivalent of ketone likely inserts from the η^9, η^5 bis(indenyl) zirconium complex – although insertion from the η^6, η^5 bis(indenyl) zirconium zwitterion cannot be ruled out – with the C1 carbon undergoing a nucleophilic attack at the carbonyl. Recall that this compound was observed upon addition of cyclopentanone to **3**, **3-(O^{c}Pent)-1**. Based on the competition experiment between large excesses of equimolar quantities of cyclopentanone and dicyclopropyl ketone to a solution of **1**, the first insertion is rate determining while the second ketone insertion to the C4 position is faster. In the absence of excess ketone, the first inserted ketone isomerizes to the C4 position,

resulting in the **3-(O^{c}Pent)-4** intermediate observed at low quantities of cyclopentanone. Then the second equivalent of ketone inserts into the C1 position, affording the double insertion product. Importantly, k_{-6} is larger than k_{-5} (or the

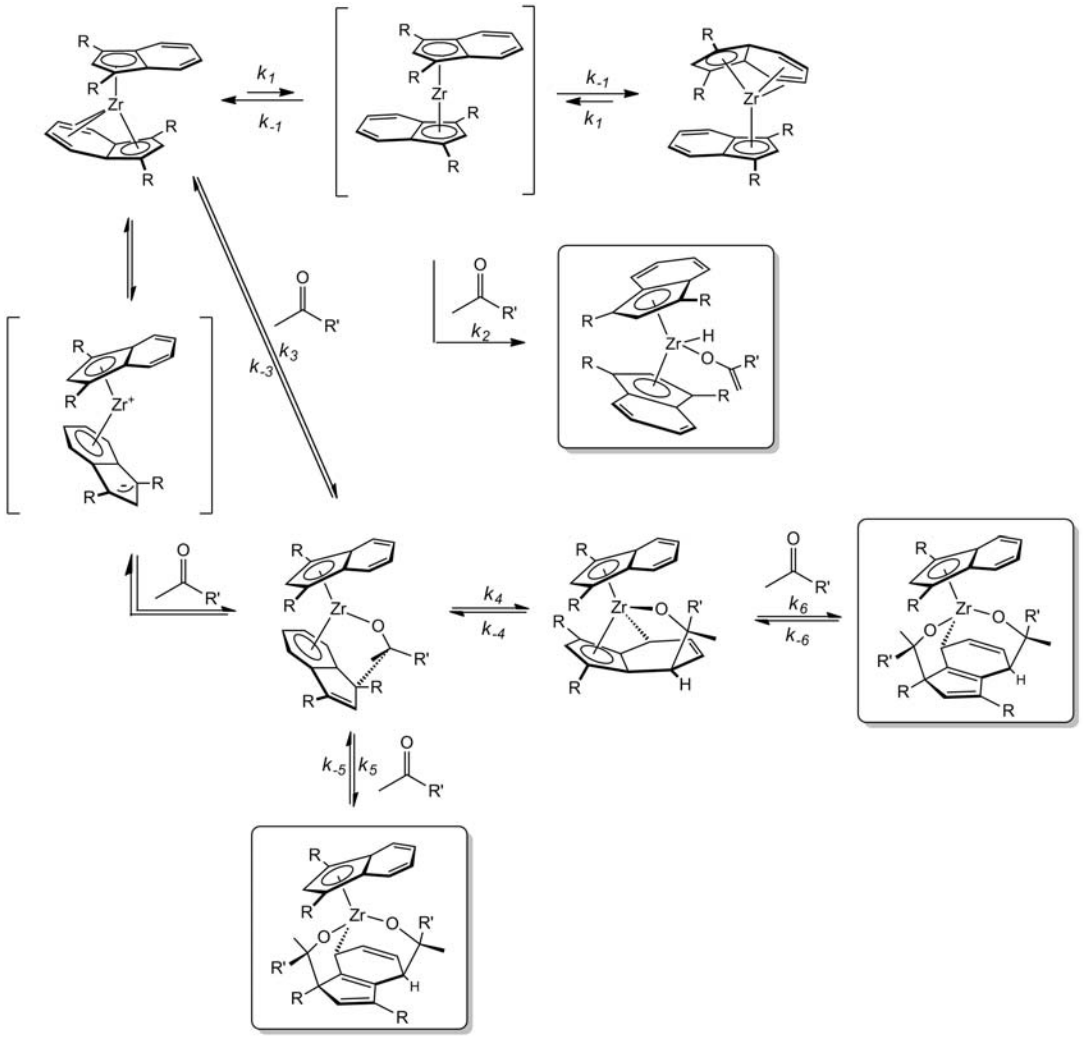

Figure 3.9. Proposed mechanisms for both enolate hydride formation and ketone insertion.

reverse reaction to form the Zr(IV) mono insertion into C4 position is faster than the reverse reaction to form the Zr(II) mono insertion into the C1 position) which explains the initial product from addition of excess acetone-d_0 to **1-(OMe$_2$)$_2$-1,4-d_{12}** experiment; the monoinsertion product at C4 is formed but quickly trapped by an equivalent of acetone-d_0.

Conclusions

The reactivity of η^9, η^5 indenyl zirconocene sandwich complexes as isolable versions of Negishi's reagent was explored. Addition of dienes afforded the expected zirconacyclopentane/hexane derivatives with similar stereochemistries to the bis(cyclopentadienyl) zirconocene complexes. Functionalization with H_2O and H_2 afforded the expected cyclopentane/hexane derivatives. Addition of CO resulted in rapid insertion, reductive elimination of the ketone and subsequent enolization and addition to the reduced zirconium center to form the observed zirconocene enolate hydride. The addition of other ketones demonstrated the divergent reactivity with isolable reduced η^9, η^5 indenyl zirconocene sandwich complexes, forming either the enolate hydride and/or the double ketone insertion product into the indenyl C1 and C4 positions. Exploring the reaction conditions showed that both excess ketone and addition at lower temperatures inhibits the formation of enolate hydride. This trend does not hold for ketones with low pKas or large steric bulk on at least one side of the carbonyl, which form solely enolate hydride complexes.

Mechansitic studies show that for formation of the C1, C4 double insertion product, all the steps are reversible with addition of the first equivalent to the indenyl C1 position as rate limiting. It is however not reversible upon double insertion into the indenyl C4 and C7 positions, which is occurred upon heating or in the presence of excess ketone. This reversibility of the 1,4 insertion products allows for the observation of the thermodynamically favored and irreversible zirconocene enolate hydride products. Kinetic studies show that formation of the enolate hydride arises from the η^5, η^5 indenyl zirconocene sandwich complex, with C-H activation occurring just after the rate determining step.

Non-enolizable aromatic ketones were shown to undergo other C-C bond formation via nucleophilic attack of a carbonyl by the carbon at the ortho position,

forming zirconocene coupled bis(alkoxide) complexes.

Experimental

General Considerations. All air- and moisture-sensitive manipulations were carried out using standard vacuum line, Schlenk or cannula techniques or in an M. Braun inert atmosphere drybox containing an atmosphere of purified nitrogen. Solvents for air- and moisture-sensitive manipulations were initially dried and deoxygenated using literature procedures.[36] Benzene-d_6 was distilled from sodium metal under an atmosphere of argon and stored over 4 Å molecular sieves or titanocene. Argon and hydrogen gas were purchased from Airgas Incorporated and passed through a column containing manganese oxide on vermiculite and 4 Å molecular sieves before admission to the high vacuum line. Carbon monoxide was passed through a liquid nitrogen cooled trap immediately before use.

^{1}H NMR spectra were recorded on a Varian Inova 400 Spectrometer operating at 399.779 MHz (^{1}H), while ^{13}C spectra were collected on a Varian Inova 500 spectrometer operating at 125.704 MHz. All chemical shifts are reported relative to $SiMe_4$ using ^{1}H (residual) or ^{13}C NMR chemical shifts of the solvent as a secondary standard. ^{19}F NMR spectra were recorded on a Varian Inova 400 Spectrometer operating at 376.12 MHz and chemical shifts were externally referenced to trifluoroacetic acid. NOESY experiments were recorded on a Varian 500 Inova spectrometer operating at 499.920 MHz for ^{1}H. HSQC and HMBC experiments were recorded on a Varian 600 Inova spectrometer operating at 599.773 MHz for ^{1}H and 150.811 MHz for ^{13}C. ^{2}H NMR spectra were recorded on a Varian Inova 500 spectrometer operating at 76.740 MHz and the spectra were referenced using an internal benzene-d_6 standard. Single crystals suitable for X-ray diffraction were coated with polyisobutylene oil in a drybox and were quickly transferred to the

goniometer head of a Siemens SMART CCD Area detector system equipped with a molybdenum X-ray tube (δ = 0.71073 A). Preliminary data revealed the crystal system. A hemisphere routine was used for data collection and determination of lattice constants. The space group was identified and the data were processed using the Bruker SAINT program and corrected for absorption using SADABS. The structures were solved using direct methods (SHELXS) completed by subsequent Fourier synthesis and refined by full-matrix least-squares procedures. Infrared spectra were collected on a Thermo Nicolet spectrometer. Elemental analyses were performed at Robertson Microlit Laboratories, Inc., in Madison, NJ. The following compounds were prepared according to literature procedures: **1**,[10] **2**[37], **3**[38], diallyl dimethylsilane,[39] 9,9-diallylfluorene,[3] diallyl tertbutylamine (methyl substituted derivatives were also prepared in a similar manner),[40] diallyl benzylamine,[40] and diallyl tosylamine.[41] All deuterated ketones were prepared in the same manner as literature procedures for 3,3-dimethyl-1,1,1-trideuterio-2-butanone, [42] with the exception of dicyclopropylketone-d_2 which required prolonged heating in the presence of KOD instead of K_2CO_3.

Preparation of ($(\eta^5$-C_9H_5-1,3-$(CHMe_2)_2)_2Zr(CH_2CHCH_2)_2CH_2$) (1-$(CH_2CHCH_2)_2CH_2$). This molecule was prepared in a similar manner to **1-$(CH_2CHCH_2)_2N^tBu$)** (*vide infra*) with 0.009 g (0.02 mmol) of **1** and 0.002 g (0.02 mmol) of 1,6-heptadiene immediately affords yellow ***cis*** and ***trans*-1-$(CH_2CHCH_2)_2CH_2$** in a 1 : 1 ratio. Allowing the mixture to sit over the course of a week results in > 98 % conversion to the ***trans*** product. ^{1}H NMR of ***trans*-1-$(CH_2CHCH_2)_2CH_2$** (benzene-d_6): δ = -0.49 (m, 2H, Zr-CH_2), -0.20 (m, 2H, C*H*), 0.48 (dd, 16 Hz, 8 Hz, 2H, Zr-CH_2), 0.79 (m, 2H, CH_2), 1.21 (d, 8 Hz, 6H, CHMe_2), 1.24 (d, 8 Hz, 12H, CHMe_2), 1.27 (d, 8 Hz, 6H, CHMe_2), 1.74 (m, 4H, CH_2), 1.75 (m, 4H,

C*H*Me$_2$), 5.65 (s, 2H, Cp*H*), 6.98 (m, 4H, Benzo), 7.42 (m, 2H, Benzo), 7.47 (m, 2H, Benzo). ^{1}H NMR of ***cis*-1-(CH$_2$CHCH$_2$)$_2$CH$_2$** (benzene-d_6): δ = -0.79 (dd, 16 Hz, 8 Hz, 2H, Zr-C*H*$_2$), 0.93 (m, 2H, C*H*$_2$), 1.03 (d, 8 Hz, 6H, CH*Me*$_2$), 1.23 (d, 8 Hz, 12H, CH*Me*$_2$), 1.31 (d, 8 Hz, 6H, CH*Me*$_2$), 1.51 (m, 4H, C*H*$_2$), 2.18 (m, 2H, C*H*), 3.09 (m, 2H, C*H*Me$_2$), 3.42 (m, 2H, C*H*Me$_2$), 5.27 (s, 1H, Cp*H*), 6.09 (s, 1H, Cp*H*), 6.91 (m, 4H, Benzo), 7.52 (m, 4H, Benzo). One Zr-C*H*$_2$ resonance not located. ^{13}C NMR of ***trans*-1-(CH$_2$CHCH$_2$)$_2$CH$_2$** (benzene-d_6): δ = 18.46, 23.10, 23.75, 24.72, 24.87, 28.18 (CHMe$_2$/CH$_2$), 38.36, 41.72, 59.64 (CH$_2$), 108.00, 119.81, 120.98, 123.23, 123.61, 125.19, 125.38, 125.60 (Cp/Benzo). One Cp/Benzo resonance not located.

Preparation of ((η^5-C$_9$H$_5$-1,3-(CHMe$_2$)$_2$)$_2$Zr(CH$_2$CHCH$_2$)$_2$(CH$_2$)$_2$) (1-(CH$_2$CHCH$_2$)$_2$(CH$_2$)$_2$). This molecule was prepared in a similar manner to **1-(CH$_2$CHCH$_2$)$_2$N^{t}Bu)** (*vide infra*) with 0.006 g (0.01 mmol) of **1** and 0.001 g (0.01 mmol) of 1,7-octadiene immediately affords yellow ***cis*** and ***trans*-1-(CH$_2$CHCH$_2$)$_2$(CH$_2$)$_2$** in a 1 : 1 ratio. Heating the mixture to 105 ºC for 24 hours results in > 97 % conversion to the ***trans*** product. ^{1}H NMR of ***trans*-1-(CH$_2$CHCH$_2$)$_2$(CH$_2$)$_2$** (benzene-d_6): δ = -0.77 (m, 2H, Zr-C*H*$_2$), -0.16 (m, 2H, Zr-C*H*$_2$), 0.59 (m, 2H, C*H*$_2$), 0.66 (m, 2H, C*H*), 1.08 (d, 8 Hz, 6H, CH*Me*$_2$), 1.19 (d, 8 Hz, 6H, CH*Me*$_2$), 1.22 (d, 8 Hz, 6H, CH*Me*$_2$), 1.24 (d, 8 Hz, 6H, CH*Me*$_2$), 1.38 (m, 4H, C*H*$_2$), 1.69 (m, 2H, C*H*$_2$), 3.16 (m, 4H, C*H*Me$_2$), 3.27 (m, 4H, C*H*Me$_2$), 5.70 (s, 2H, Cp*H*), 7.05 (m, 4H, Benzo), 7.44 (m, 2H, Benzo), 7.64 (m, 2H, Benzo). ^{1}H NMR of ***cis*-1-(CH$_2$CHCH$_2$)$_2$(CH$_2$)$_2$** (benzene-d_6): δ = -0.91 (m, 2H, Zr-C*H*$_2$), -0.02 (dd, 16 Hz, 8 Hz, 2H, Zr-C*H*$_2$), 1.06 (d, 8 Hz, 8H, CH*Me*$_2$/C*H*$_2$), 1.19 – 1.25 (d, 8 Hz, 12H, CH*Me*$_2$), 1.29 (d, 8 Hz, 6H, CH*Me*$_2$), 1.52 (m, 2H, C*H*$_2$), 2.11 (m, 2H, C*H*), 3.16 (m, 4H, C*H*Me$_2$), 3.27 (m, 4H, C*H*Me$_2$), 5.59 (s, 1H, Cp*H*), 5.78 (s, 1H, Cp*H*), 7.00 (m, 4H, Benzo), 7.12 (m, 2H, Benzo), 7.58 (m, 2H, Benzo). Four C*H*$_2$ resonances not

located. ^{13}C NMR of ***trans*-1-$(CH_2CHCH_2)_2(CH_2)_2$** (benzene-d_6): δ = 22.71, 24.15, 24.43, 25.07, 27.41, 27.92, 28.76, 41.53, 46.16 ($CHMe_2$/*C*H/*C*H_2), 65.45 (Zr-*C*H_2), 109.18, 120.32, 122.08, 123.77, 124.07, 125.68, 125.95, 126.02 (Cp/Benzo). One Cp/Benzo resonance not located. ^{13}C NMR of ***cis*-1-$(CH_2CHCH_2)_2(CH_2)_2$** (benzene-d_6): δ = 23.64, 24.21, 24.30, 24.74, 28.48, 34.70 ($CHMe_2$), 61.29 (Zr-*C*H_2), 109.89, 111.05, 120.96, 121.70, 123.62, 124.10, 125.59, 125.99, 126.50 (Cp/Benzo). Three *C*H/*C*H_2 resonances not located.

Preparation of $((\eta^5\text{-}C_9H_5\text{-}1,3\text{-}(CHMe_2)_2)_2Zr(CH_2CHCH_2)_2$fluorene) (1-$(CH_2CHCH_2)_2$fluorene). This molecule was prepared in a similar manner to **1-$(CH_2CHCH_2)_2N^tBu$)** (*vide infra*) with 0.006 g (0.01 mmol) of **1** and 0.003 g (0.01 mmol) of diallyl fluorene affords yellow ***trans*-1-$(CH_2CHCH_2)_2$fluorene)**. ^{1}H NMR (benzene-d_6): δ = -0.53 (m, 2H, Zr-CH_2), 0.50 (m, 2H, Zr-CH_2), 0.61 (m, 2H, C*H*), 1.06 (m, 2H, CCH_2), 1.18 (d, 6H, CH*Me*$_2$), 1.24 (d, 18H, CH*Me*$_2$), 1.50 (m, 2H, CCH_2), 2.09 (m, 2H, C*H*), 3.20 (m, 4H, C*H*Me_2), 5.72 (s, 2H, Cp*H*), 6.95 – 7.68 (m, 16H, Benzo/fluorene). ^{13}C NMR (benzene-d_6): δ = 22.94, 23.75, 24.76, 24.97, 28.14, 28.60 ($CHMe_2$), 40.65 (CH_2CHCH_2), 51.36 (spiro C), 56.08, 58.81 (CH_2CHCH_2), 107.67, 119.96, 120.12, 121.71, 123.02, 124.00, 125.35, 125.70, 125.89, 125.91, 126.54, 127.68, 133.97, 140.05, 157.31 (Cp/Benzo/fluorene).

Preparation of $((\eta^5\text{-}C_9H_5\text{-}1,3\text{-}(CHMe_2)_2)_2Zr(CH_2CHCH_2)_2SiMe_2$) (1-$(CH_2CHCH_2)_2SiMe_2$). This molecule was prepared in a similar manner to **1-$(CH_2CHCH_2)_2N^tBu$)** (*vide infra*) with 0.009 g (0.02 mmol) of **5** and 0.004 g (0.02 mmol) of diallyl dimethylsilane affords yellow *trans*-**1-$(CH_2CHCH_2)_2SiMe_2$)**. ^{1}H NMR (benzene-d_6): δ = -0.50 (m, 2H, CH_2), -0.06 (m, 2H, CH_2), 0.16 (s, 6H, Si*Me*$_2$), 0.38 (dd, 12 Hz, 4 Hz, 2H, CH_2), 0.61 (m, 2H, C*H*), 0.88 (dd, 12 Hz, 4 Hz, 2H, CH_2),

1.12 (d, 8 Hz, 6H, CH*Me*$_2$), 1.20 (d, 8 Hz, 6H, CH*Me*$_2$), 1.23 (d, 8 Hz, 12H, CH*Me*$_2$), 3.15 (m, 2H, C*H*Me$_2$), 3.26 (m, 2H, C*H*Me$_2$), 5.69 (s, 2H, Cp*H*), 7.05 (m, 4H, Benzo), 7.43 (m, 2H, Benzo), 7.57 (m, 2H, Benzo). ^{13}C NMR (benzene-d_6, 23 °C): δ = -0.97 (Si*Me*$_2$), 22.82, 24.03, 24.56, 25.06, 28.02, 28.70, 31.28 (CHMe$_2$/SiCH$_2$), 46.21 (*C*H), 68.36 (Zr-*C*H$_2$), 108.76, 120.17, 121.68, 123.68, 123.96, 125.49, 125.66, 125.73, 125.91 (Cp/Benzo).

Preparation of ((η^5-C$_9$H$_5$-1,3-(CHMe$_2$)$_2$)$_2$Zr(CH$_2$CHCH$_2$)$_2$N^{t}Bu) (1-(CH$_2$CHCH$_2$)$_2$N^{t}Bu). A 20 mL scintillation vial was charged with 0.107 g (0.22 mmol) of **1** and approximately 8 mL of pentane was added. To this stirring burgundy solution, 0.033 g (0.22 mmol) of diallyl tert-butylamine diluted in 2 mL of pentane was syringed. The solution was stirred for two hours and the solvent removed *in vacuo*. Recrystallization from pentane affords 0.062 g (44 %) of ***cis*-1-(CH$_2$CHCH$_2$)$_2$N^{t}Bu)** as yellow crystals. Aliquots of the reaction mixture indicate a five to one ratio of the *cis* to *trans* product. Anal. Calcd. for C$_{40}$H$_{57}$NZr: C, 74.70; H, 8.93; N, 2.18. Found: C, 74.35; H, 9.30; N, 1.96. ^{1}H NMR of ***cis*-1-(CH$_2$CHCH$_2$)$_2$N^{t}Bu** (benzene-d_6): δ = -0.89 (dd, 20 Hz, 8 Hz, 2H, Zr-C*H*$_2$), -0.28 (dd, 16 Hz, 8Hz, 2H, Zr-C*H*$_2$), 1.03 (d, 8 Hz, 6H, CH*Me*$_2$), 1.14 (s, 9H, NC*Me*$_3$), 1.21 (d, 8 Hz, 6H, CH*Me*$_2$), 1.25 (d, 8 Hz, 6H, CH*Me*$_2$), 1.29 (d, 8 Hz, 6H, CH*Me*$_2$), 1.72 (m, 2H, NC*H*$_2$), 2.33 (m, 2H, C*H*), 2.89 (m, 2H, NC*H*$_2$), 3.09 (m, 2H, C*H*Me$_2$), 3.39 (m, 2H, C*H*Me$_2$), 5.31 (s, 1H, Cp*H*), 6.05 (s, 1H, Cp*H*), 6.88 (dd, 2H, Benzo), 7.18 (m, 2H, Benzo), 7.50 (m, 4H, Benzo). ^{1}H NMR of ***trans*-1-(CH$_2$CHCH$_2$)$_2$N^{t}Bu** (benzene-d_6): δ = -0.41 (m, 2H, Zr-C*H*$_2$), -0.06 (m, 2H, C*H*), 0.25 (dd, 12 Hz, 4Hz, 2H, Zr-C*H*$_2$), 1.03 (d, 8 Hz, 6H, CH*Me*$_2$), 1.07 (s, 9H, NC*Me*$_3$), 1.22 (d, 8 Hz, 12H, CH*Me*$_2$), 1.25 (d, 8 Hz, 6H, CH*Me*$_2$), 1.87 (m, 2H, NC*H*$_2$), 2.78 (m, 2H, NC*H*$_2$), 3.18 (m, 4H, C*H*Me$_2$), 5.65 (s, 2H, Cp*H*), 6.98 (m, 4H, Benzo), 7.41 (m, 2H, Benzo), 7.46

(m, 2H, Benzo). ^{13}C NMR of ***cis*-1-$(CH_2CHCH_2)_2N^tBu$** (benzene-d_6): δ = 22.52, 23.41, 24.31, 24.37, 24.89, 26.56, 28.17, 28.75 ($CHMe_2$/$CHCH_2NCMe_3$), 39.63, 59.31 ($CHCH_2NCMe_3$), 59.72 (Zr-*C*H_2), 110.07, 111.92, 121.72, 121.90, 123.23, 124.37, 125.46, 125.51, 125.56, 126.61 (Cp/Benzo). ^{13}C NMR of ***trans*-1-$(CH_2CHCH_2)_2N^tBu$** (benzene-d_6): δ = 23.48, 24.67, 24.74, 28.48, 28.63, 34.39, 36.28, 51.42, 52.34, 55.44, 61.33 ($CHMe_2$/$CH_2CHCH_2NCMe_3$), 109.11, 120.98, 121.30, 123.64, 123.69, 125.63, 125.77, 125.81 (Cp/Benzo). One Cp/Benzo resonance not located.

Preparation of $((\eta^5\text{-}C_9H_5\text{-}1,3\text{-}(CHMe_2)_2)_2Zr(CH_2CHCH_2)_2NCH_2Ph)$ (1-$(CH_2CHCH_2)_2NCH_2Ph$). This molecule was prepared in a similar manner to **1-$(CH_2CHCH_2)_2N^tBu$)** with 0.011 g (0.02 mmol) of **1** and 0.004 g (0.02 mmol) of diallyl benzylamine affords yellow **1-$(CH_2CHCH_2)_2NCH_2Ph$)** with a 5:1 ratio of the *cis* to *trans* product. ^{1}H NMR of ***cis*-1-$(CH_2CHCH_2)_2NCH_2Ph$** (benzene-d_6): δ = -0.76 (dd, 20 Hz, 8 Hz, 2H, Zr-CH_2), -0.28 (dd, 12 Hz, 8 Hz, 2H, Zr-CH_2), 1.02 (d, 8 Hz, 6H, CHMe_2), 1.21 (d, 8 Hz, 12H, CHMe_2), 1.27 (d, 8 Hz, 6H, CHMe_2), 1.52 (m, 2H, NCH_2), 2.37 (m, 2H, C*H*), 2.96 (m, 2H, NCH_2), 3.06 (m, 2H, C*H*Me_2), 3.34 (m, 2H, C*H*Me_2), 3.55 (s, 2H, NCH_2Ph), 5.18 (s, 1H, Cp*H*), 6.09 (s, 1H, Cp*H*), 6.87 (m, 4H, Benzo), 7.17 – 7.53 (m, 9H, Benzo/Ph). ^{1}H NMR of ***trans*-1-$(CH_2CHCH_2)_2NCH_2Ph$** (benzene-d_6): δ = -0.40 (m, 2H, Zr-CH_2), 0.08 (m, 2H, C*H*), 0.19 (m, 2H, Zr-CH_2), 0.75 (d, 8 Hz, 6H, CHMe_2), 1.25 (d, 8 Hz, 12H, CHMe_2), 1.31 (d, 8 Hz, 6H, CHMe_2), 2.01 (m, 2H, NCH_2), 2.73 (m, 2H, NCH_2), 3.15 (m, 2H, C*H*Me_2), 3.66 (m, 2H, C*H*Me_2), 5.82 (s, 2H, Cp*H*), 7.17 – 7.53 (m, 13H, Benzo/Ph). One NCH_2Ph resonance not located.

Preparation of $((\eta^5\text{-}C_9H_5\text{-}1,3\text{-}(CHMe_2)_2)_2Zr(CH_2CHCH_2)_2NSO_2tolyl)$ (1-$(CH_2CHCH_2)_2N$tosyl). This molecule was prepared in a similar manner to **1-**

$(CH_2CHCH_2)_2N^tBu$) with 0.009 g (0.02 mmol) of **1** and 0.005 g (0.02 mmol) of diallyl tosylamine affords yellow **1-$(CH_2CHCH_2)_2$Ntosyl)** with a five to one ratio of the *cis* to *trans* product. ^{1}H NMR of ***cis*-1-$(CH_2CHCH_2)_2$Ntosyl** (benzene-d_6): δ = -1.28 (dd, 14 Hz, 7 Hz, 2H, Zr-CH_2), -0.61 (dd, 14 Hz, 7 Hz, 2H, Zr-CH_2), 1.12 (d, 8 Hz, 6H, CHMe_2), 1.14 (d, 8 Hz, 6H, CHMe_2), 1.22 (d, 8 Hz, 6H, CHMe_2), 1.24 (d, 8 Hz, 6H, CHMe_2), 1.98 (s, 3H, tosyl *Me*), 2.42 (m, 2H, C*H*), 2.80 (m, 2H, NCH_2), 2.97 (m, 2H, C*H*Me$_2$), 3.25 (m, 2H, C*H*Me$_2$), 5.54 (s, 1H, Cp*H*), 5.82 (s, 1H, Cp*H*), 6.89 (m, 2H, Benzo/Ph), 6.95 (m, 2H, Benzo/Ph), 7.24 (m, 2H, Benzo/Ph), 7.31 (m, 4H, Benzo/Ph), 7.87 (m, 2H, Benzo/Ph). One NCH_2 resonance not located. ^{1}H NMR of ***trans*-1-$(CH_2CHCH_2)_2$Ntosyl** (benzene-d_6): δ = -1.03 (m, 2H, Zr-CH_2), -0.31 (m, 2H, C*H*), -0.14 (m, 2H, Zr-CH_2), 0.46 (d, 8 Hz, 6H, CHMe_2), 0.50 (d, 8 Hz, 6H, CHMe_2), 0.60 (d, 8 Hz, 6H, CHMe_2), 0.75 (d, 8 Hz, 6H, CHMe_2), 2.21 (m, 2H, NCH_2), 2.51 (m, 2H, C*H*Me$_2$), 2.65 (m, 2H, C*H*Me$_2$), 3.33 (m, 2H, NCH_2), 5.63 (s, 2H, Cp*H*), 6.91 – 7.82 (m, 12H, Benzo/Ph).

Preparation of $((\eta^5\text{-}C_9H_5\text{-}1,3\text{-}(CHMe_2)_2)_2Zr(CH_2CMeCH_2N^tBuCH_2CHCH_2)$ (1-$(CH_2CMeCH_2N^tBuCH_2CHCH_2)$). This molecule was prepared in a similar manner to **1-$(CH_2CHCH_2)_2N^tBu$)** with 0.009 g (0.02 mmol) of **1** and 0.003 g (0.02 mmol) of 2-methylallyl, allyl tert-butylamine affords yellow **1-$(CH_2CMeCH_2N^tBuCH_2CHCH_2)$**. ^{1}H NMR (benzene-$d_6$): δ = -0.72 (d, 16 Hz, 1H, Zr-CH_2CMe), -0.20 (m, 1H, Zr-CH_2CH), 0.09 (d, 16 Hz, 1H, Zr-CH_2CMe), 0.48 (m, 1H, Zr-CH_2CH), 1.09 (d, 8 Hz, 3H, CHMe_2), 1.10 (d, 8 Hz, 3H, CHMe_2), 1.17 (s, 9H, CMe_3), 1.23 (m, 12H, CHMe_2), 1.26 (d, 8 Hz, 3H, CHMe_2), 1.31 (d, 8 Hz, 3H, CHMe_2), 2.03 (d, 8 Hz, 1H, NCH_2CMe), 2.09 (d, 8 Hz, 1H, NCH_2CH), 2.45 (d, 8 Hz, 1H, NCH_2CMe), 3.08 (d, 8 Hz, 1H, NCH_2CH), 3.11 (m, 1H, C*H*Me$_2$), 3.16 (m, 1H, C*H*Me$_2$), 3.25 (m, 1H, C*H*Me$_2$), 3.33 (m, 1H, C*H*Me$_2$), 5.26 (s, 1H, Cp*H*), 6.00 (s, 1H, Cp*H*), 6.82 (m, 1H,

Benzo), 7.05 (m, 1H, Benzo), 7.12 (m, 1H, Benzo), 7.14 (m, 1H, Benzo), 7.17 (m, 2H, Benzo), 7.51 (m, 2H, Benzo), 7.64 (m, 1H, Benzo), 7.70 (m, 1H, Benzo). ^{13}C NMR (benzene-d_6): δ = 23.66, 23.84, 24.07, 24.37, 24.40, 24.53, 24.60, 27.22, 28.04, 28.38, 28.67, 29.13, 33.81, 45.24, 47.63, 51.75, 58.24, 59.68, 61.15, 63.58 ($CH_2MeCH_2N^tBuCH_2CHCH_2/CHMe_2$), 111.26, 112.40, 121.58, 121.61, 121.82, 122.10, 123.35, 123.84, 124.24, 124.36, 125.34, 125.63, 125.90, 126.27, 126.39, 126.44, 126.59 (Cp/Benzo). One Cp/Benzo resonance not located.

Preparation of ($(\eta^5$-C_9H_5-1,3-$(SiMe_3)_2)_2Zr(CH_2CHCH_2)_2N^tBu$) (2-$(CH_2CHCH_2)_2N^tBu$). This molecule was prepared in a similar manner to **1-$(CH_2CHCH_2)_2N^tBu$)** with 0.007 g (0.01 mmol) of **2** and 0.003 g (0.02 mmol) of diallyl tert-butylamine affords yellow *cis* and *trans*-**2-$(CH_2CHCH_2)_2N^tBu$** in a 1.7 to 1 ratio. ^{1}H NMR of *cis*-**2-$(CH_2CHCH_2)_2N^tBu$** (benzene-d_6): δ = 0.14 (m, 2H, Zr-CH_2), 0.22 (m, 2H, Zr-CH_2), 0.33 (s, 18H, SiMe_3), 0.34 (s, 18H, SiMe_3), 1.10 (s, 9H, NCMe_3), 1.75 (m, 2H, CH_2), 2.75 (m, 2H, C*H*), 2.90 (m, 2H, CH_2), 5.32 (s, 2H, Cp*H*), 6.95 (m, 2H, Benzo), 7.24 (m, 2H, Benzo), 7.62 (m, 4H, Benzo), 7.48 (s, 1H, Cp*H*). ^{1}H NMR of *trans*-**2-$(CH_2CHCH_2)_2N^tBu$** (benzene-d_6): δ = -0.17 (m, 2H, C*H*), 0.26 (s, 18H, SiMe_3), 0.34 (s, 18H, SiMe_3), 0.53 (m, 4H, Zr-CH_2), 1.04 (s, 9H, NCMe_3), 1.95 (m, 2H, CH_2), 2.75 (m, 2H, CH_2), 6.19 (s, 2H, Cp*H*), 7.05 (m, 4H, Benzo), 7.66 (m, 4H, Benzo).

Characterization of 1-tertbutyl-3,3,4-trimethylpyrrolidine. ^{1}H NMR (benzene-d_6): δ = 0.77 (d, 4 Hz, 3H, CH*Me*), 0.88 (s, 3H, CMe_2), 0.96 (s, 3H, CMe_2), 1.02 (s, 9H, CMe_3), 1.21 (m, 1H, C*H*Me), 2.34 (m, 1H, CHCH_2), 2.44 (d, 4 Hz, 1H, CMe_2CH_2), 2.51 (d, 4 Hz, 1H, CMe_2CH_2), 2.86 (d, 4 Hz, 1H, CHCH_2). ^{13}C NMR (benzene-d_6): δ = 12.88, 22.16 (*Me*), 26.04 (CMe_3), 27.34 (*Me*), 27.54 (*C*Me$_2$), 39.28 (N*C*Me$_3$), 42.77,

53.69, 61.24 (CH_2). EI MS (*m/z*) 169.

Preparation of ($(\eta^5$-C_9H_5-1,3-$(CHMe_2)_2)_2Zr(CH_2CMeCH_2)_2N^tBu$) (1-$(CH_2CMeCH_2)_2N^tBu$). This molecule was prepared in a similar manner to **1-$(CH_2CHCH_2)_2N^tBu$)** with 0.010 g (0.02 mmol) of **1** and 0.004 g (0.02 mmol) of bis(2-methylallyl) tert-butylamine affords yellow **1-$(CH_2CMeCH_2)_2N^tBu$)**. ^{1}H NMR (benzene-d_6): δ = 0.48 (d, 16 Hz, 2H, Zr-CH_2), 0.82 (d, 16 Hz, 2H, Zr-CH_2), 1.02 (s, 6H, *Me*), 1.08 (d, 8 Hz, 6H, CH*Me*$_2$), 1.20 (s, 9H, C*Me*$_3$), 1.21 (d, 8 Hz, 6H, CH*Me*$_2$), 1.28 (d, 8 Hz, 6H, CH*Me*$_2$), 1.34 (d, 8 Hz, 6H, CH*Me*$_2$), 2.43 (d, 8 Hz, 2H, NCH_2), 2.88 (d, 8 Hz, NCH_2), 3.04 (m, 2H, C*H*Me$_2$), 3.48 (m, 2H, C*H*Me$_2$), 4.44 (s, 1H, Cp*H*), 6.93 (s, 1H, Cp*H*), 7.01 (m, 2H, Benzo), 7.13 (m, 2H, Benzo), 7.60 (m, 2H, Benzo), 7.72 (m, 2H, Benzo). ^{13}C NMR (benzene-d_6): δ = 23.45, 25.10, 25.26, 26.33, 26.96, 28.71, 29.77, 31.36 (CHMe$_2$/C*Me*/C*Me*$_3$), 51.91, 52.67, 65.86, 69.53 (CH_2CCH_2/*C*Me$_3$), 116.30, 122.96, 123.09, 123.46, 124.03, 125.11, 125.78, 127.44, 128.91 (Cp/Benzo).

Characterization of N-tert-butyl-3,3,4,4-tetramethylpyrrolidine. ^{1}H NMR (benzene-d_6): δ = 0.88 (s, 12H, *Me*), 1.02 (s, 9H, C*Me*$_3$), 2.61 (s, 4H, CH_2). ^{13}C NMR (benzene-d_6): δ = 26.22 (C*Me*$_3$), 27.01 (*Me*), 41.62 (*C*Me$_3$), 60.00 (*C*H_2). One *C*H_2 resonance not located. EI MS (*m/z*) 183.

Preparation of ($(\eta^5$-C_9H_5-1,3-$(CHMe_2)_2)_2Zr(OCH_2CHCH_2)(CH_2CHCH_2)$) (1-$(OCH_2CHCH_2)(CH_2CHCH_2)$). This molecule was prepared in a similar manner to **1-$(CH_2CHCH_2)_2N^tBu$)** with 0.030 g (0.06 mmol) of **5** and 0.006 g (0.06 mmol) of diallyl ether immediately affords yellow **1-$(OCH_2CHCH_2)(CH_2CHCH_2)$)**. Anal. Calcd. for $C_{36}H_{48}OZr$: C, 73.45; H, 8.23. Found: C, 73.45; H, 8.60. ^{1}H NMR

(benzene-d_6, 23 °C): δ = 1.00 (d, 8 Hz, 6H, CHMe_2), 1.07 (d, 8 Hz, 6H, CHMe_2), 1.09 (d, 8 Hz, 6H, CHMe_2), 1.17 (d, 8 Hz, 6H, CHMe_2), 2.86 (m, 4H, CHMe$_2$), 4.38 (d, 8 Hz, 2H, OCH_2), 5.01 (m, 2H, OCH$_2$CHCH_2), 5.86 (m, 1H, OCH$_2$CHCH$_2$), 6.18 (s, 2H, CpH), 6.50 (pseudo q, 1H, Zr-CH$_2$CHCH$_2$), 6.95 (m, 4H, Benzo), 7.30 (m, 2H, Benzo), 7.33 (m, 2H, Benzo). ^{1}H NMR (toluene-d_8, -50 °C): 1.04 (m, 12H, CHMe_2), 1.22 (m, 12H, CHMe_2), 2.03 (br m, 2H, Zr-CH$_2$CHCH_2), 2.78 (br, 4H, CHMe$_2$), 4.37 (br pseudo s, 2H, OCH_2), 5.03 (m, 2H, Zr-CH$_2$CHCH_2), 5.07 (m, 2H, OCH$_2$CHCH_2), 5.86 (m, 1H, OCH$_2$CHCH$_2$), 6.21 (br s, 2H, CpH), 6.54 (m, 1H, Zr-CH$_2$CHCH$_2$), 6.95 (m, 4H, Benzo), 7.18 (m, 2H, Benzo), 7.23 (m, 2H, Benzo). ^{13}C NMR (benzene-d_6, 23 °C): δ = 21.67, 22.43, 25.20, 25.26, 25.53, 25.90 (CHMe$_2$), 74.30 (OCH$_2$), 114.58, 117.35, 120.95, 122.55, 122.84, 123.89, 124.11, 124.41 (Cp/Benzo), 138.78, 148.32 (OCH$_2$$CHCH_2$). Zr-$CH_2$$CHCH_2$ resonances not located.

Preparation of ((η^5-C$_9$H$_5$-1,3-(CHMe$_2$)$_2$)$_2$Zr(OC(CH)CH$_2$(CHCH$_2$)$_2$NtBu)H (*cis*-1-(OC(CH)CH$_2$(CHCH$_2$)$_2$NtBu)H. A flame-dried thick walled glass vessel was charged with 0.49 g (0.08 mmol) of ***cis*-1-(CH$_2$CHCH$_2$)$_2$N^{t}Bu)** and approximately 3 mL of benzene was added. On the vacuum line, the reaction vessel was submerged in liquid nitrogen and degassed. While at -196 °C, approximately 50 equivalents (700 torr in a 100.1 mL bulb) of CO was added to the yellow solution. The solution was stirred for ten minutes and the solvent removed *in vacuo*. Recrystallization from pentane affords 0.031 g (61 %) of yellow ***cis*-1-(OC(CH)CH$_2$(CHCH$_2$)$_2$NtBu)H**. Anal. Calcd. for $C_{41}H_{57}NOZr$: C, 73.38; H, 8.56; N, 2.09. Found: C, 73.27; H, 8.53; N, 1.98. ^{1}H NMR (benzene-d_6): δ = 1.11 (s, 9H, CMe_3), 1.14 (d, 8 Hz, 6H, CHMe_2), 1.15 (d, 8 Hz, 6H, CHMe_2), 1.27 (d, 8 Hz, 6H, CHMe_2), 1.29 (d, 8 Hz, 6H, CHMe_2), 2.00 (m, 1H, CH_2), 2.35 (m, 1H, CH_2), 2.39 (m, 1H, CH_2), 2.47 (m, 1H, CH_2), 2.64 (m, 1H, bridgehead CH), 2.78 (m, 2H, CH_2), 2.88 (m, 1H, CHMe$_2$), 3.01 (m, 1H, CHMe$_2$),

3.06 (m, 1H, C*H*Me$_2$), 3.14 (m, 1H, C*H*Me$_2$), 3.19 (m, 1H, bridgehead C*H*), 4.45 (pseudo s, 1H, olefinic C*H*), 6.11 (s, 1H, Cp*H*), 6.12 (s, 1H, Cp*H*), 6.16 (s, 1H, Zr-*H*), 6.94 (m, 4H, Benzo), 7.30 (m, 2H, Benzo), 7.36 (m, 1H, Benzo), 7.40 (m, 1H, Benzo). ^{13}C NMR (benzene-d_6): δ = 21.60, 21.97, 22.18, 22.47, 22.94, 23.0625.35, 25.40 (CH*Me$_2$*), 25.44, 25.50 (C*H*Me$_2$), 26.30 (C*Me$_3$*), 26.63, 27.00 (C*H*Me$_2$), 38.21 (bridgehead *C*H), 41.27 (*C*H$_2$), 45.52 (bridgehead *C*H), 51.45 (*C*Me$_3$), 53.78, 54.53 (*C*H$_2$), 103.86 ($^1J_{CH}$ = 161 Hz, olefinic *C*H), 112.44, 112.79 (*Cp*H), 119.35, 119.63, 120.02, 120.65, 122.11, 122.22, 122.58, 122.66, 123.32, 123.52, 123.59, 124.88, 125.03, 126.52, 128.28 (Cp/Benzo), 161.64 (C-O). One Cp/Benzo resonance not located. IR (pentane): ν_{CO} = 1637 cm^{-1}.

Preparation of Pauson Khand ketone formed in previous reaction (*cis*-OC(CH$_2$CHCH$_2$)$_2$N^{t}Bu). A 20 mL scintillation vial charged with 95 mg (0.14 mmol) of ***cis*-1-(OC(CH)CH$_2$(CHCH$_2$)$_2$N^{t}Bu)H** was dissolved in 5 mL of hexanes on the bench. While stirring 1μL of H_2O was added and the yellow solution stirred vigorously for 4 hours. The clear reaction mixture was purified by passing through silica gel with hexanes and ethyl acetate to remove the indene and finally methanol. The volatiles of the methanol solution were removed *in vacuo* to afford XX (XX %) of ***cis*-OC(CH$_2$CHCH$_2$)$_2$N^{t}Bu**. ^{1}H NMR (benzene-d_6): δ = 0.88 (s, 9H, *Me*), 1.86 (m, 2H, C*H$_2$*), 2.05 (m, 2H, C*H*$_2$), 2.10 (m, 2H, NC*H*$_2$), 2.21 (m, 2H, C*H*), 2.41 (m, 2H, NC*H*$_2$). ^{13}C NMR (benzene-d_6): δ = 25.94 (C*Me$_3$*), 37.46 (*C*H), 44.08 (*C*H$_2$), 53.57 (N*C*H$_2$), 217.01 (*C*O). *C*Me$_3$ resonance not located. EI MS (*m/z*) 166[43]. IR (pentane): ν_{CO} = 1751 cm^{-1}.

Characterization Data for (1-(O^{c}Pent)$_2$-1,4). Anal. Calcd. for $C_{40}H_{54}O_2Zr$: C, 73.01; H, 8.27. Found: C, 72.64; H, 8.34. ^{1}H NMR (benzene-d_6): δ = 0.78 (d, 8 Hz, 3H,

CH*Me*$_2$), 0.86 (d, 8 Hz, 3H, CH*Me*$_2$), 0.88 (d, 8 Hz, 3H, CH*Me*$_2$), 0.91 (d, 8 Hz, 3H, CH*Me*$_2$), 0.92 (d, 8 Hz, 3H, CH*Me*$_2$), 1.15 (m, 4H, CH*Me*$_2$), 1.18 (d, 8 Hz, 3H, CH*Me*$_2$), 1.20 (m, 1H, cyclopentanone C*H*$_2$), 1.23 (d, 8 Hz, 3H, CH*Me*$_2$), 1.33 (m, 1H, cyclopentanone C*H*$_2$), 1.37 (m, 4H, CH*Me*$_2$/ cyclopentanone C*H*$_2$), 1.53 (d, 8 Hz, 3H, CH*Me*$_2$), 1.57 (m, 6H, CH*Me*$_2$/three cyclopentanone C*H*$_2$), 1.61 (d, 8 Hz, 3H, CH*Me*$_2$), 1.74 (m, 1H, cyclopentanone C*H*$_2$), 1.81 (m, 6H, cyclopentanone C*H*$_2$), 2.03 (m, 1H, C*H*Me$_2$), 2.08 (m, 1H, cyclopentanone C*H*$_2$), 2.71 (m, 1H, C*H*Me$_2$), 3.19 (m, 1H, C*H*Me$_2$), 3.33 (m, 1H, C*H*Me$_2$), 3.70 (dd, 4 Hz, 1 Hz, 1H, C4-*H*), 3.97 (d, 6 Hz, 1H, C7-*H*), 4.78 (dd, 9 Hz, 4 Hz, 1H, C5-*H*), 5.23 (dd, 9 Hz, 6 Hz, 1H, C6-*H*), 5.91 (s, 1H, C2-*H*), 6.43 (s, 1H, Cp*H*), 6.90 (m, 1H, η^5 Benzo), 6.98 (m, 1H, η^5 Benzo), 7.26 (m, 1H, η^5 Benzo), 7.56 (m, 1H, η^5 Benzo). ^{2}H NMR of **(1-(O^{c}Pent)$_2$-1,4)-*d*$_4$** (benzene-d_0): 1.20, 1.34, 1.43 (cyclopentanone α C*H*$_2$ on C4), 1.56, 1.60, 1.78 (cyclopentanone α C*H*$_2$ on C1), 1.79 (cyclopentanone α C*H*$_2$ on C4), 1.80 (cyclopentanone α C*H*$_2$ on C1). ^{13}C NMR (benzene-d_6): δ = 18.63, 20.28, 20.98, 21.90 (CH*Me*$_2$), 21.93, 22.40 (cyclopentanone *C*H$_2$), 22.67 (CH*Me*$_2$), 23.17, 24.13 (cyclopentanone *C*H$_2$), 24.90, 25.62, 26.09 (CH*Me*$_2$), 27.52 (*C*HMe$_2$ on η^5 Ind), 27.61 (*C*HMe$_2$ on η^1 Ind), 27.90 (*C*HMe$_2$ on η^5 Ind), 31.22 (*C*HMe$_2$ on η^1 Ind), 37.06 (cyclopentanone α *C*H$_2$ on C4), 37.82 (cyclopentanone α *C*H$_2$ on C1), 40.60 (cyclopentanone α *C*H$_2$ on C4), 42.52 (cyclopentanone α *C*H$_2$ on C1), 49.17 (*C4*), 67.27 (*C1*), 73.87 (*C7*), 97.71 (*C*-O insert at C1), 112.18 (CpH), 118.53, 119.02 (Cp), 119.67 (*C6*), 120.86 (*C5*), 121.83, 122.33, 123.68, 124.18, 124.60, 126.49 (Benzo), 130.78 (*C2*), 133.12 (*C*-O insert at C4), 137.50 (*C3a*), 152.30 (*C7a*), 153.93 (*C3*).

Preparation of (η^5-C$_9$H$_5$-1,3-(CHMe$_2$)$_2$)(η^1-C$_9$H$_5$-1,3-(CHMe$_2$)$_2$-4-C(κ^1-O)(CH$_2$)$_4$-7-C(κ^1-O)(CH$_2$)$_4$)Zr (1-(O^{c}Pent)$_2$-4,7). A J. Young NMR tube charged with 0.010 g (0.02 mmol) of **1-(O^{c}Pent)$_2$-1,4** dissolved in 0.5 mL of benzene-d_6 was heated to 65

°C for 8 days, resulting in two isomers of **1-(O^cPent)$_2$-4,7** in a 1 : 1 ratio. ***C_s* symmetric isomer**: ^{1}H NMR (benzene-d_6): δ = 1.02 (d, 8 Hz, 6H, CH*Me*$_2$), 1.16 (d, 8 Hz, 6H, CH*Me*$_2$), 1.18 (d, 8 Hz, 6H, CH*Me*$_2$), 1.56 (d, 8 Hz, 6H, CH*Me*$_2$), 1.55 (m, 2H, cyclopentanone C*H*$_2$), 1.65 (m, 2H, cyclopentanone C*H*$_2$), 1.77 (m, 2H, cyclopentanone C*H*$_2$), 2.00 (m, 2H, cyclopentanone C*H*$_2$), 2.75 (m, 2H, C*H*Me$_2$), 3.46 (m, 2H, C*H*Me$_2$), 3.63 (m, 2H, C4-*H*/C7-*H*), 5.53 (s, 1H, C2-*H*), 5.83 (m, 2H, C5-*H*/C6-*H*), 6.54 (s, 1H, Cp*H*), 6.93 (m, 2H, η^5 Benzo), 7.42 (m, 2H, η^5 Benzo). Eight cyclopentanone C*H*$_2$ resonances not located. ^{13}C NMR of (benzene-d_6): δ = 20.64 (CH*Me*$_2$), 21.93, 22.40 (cyclopentanone *C*H$_2$), 22.93, 24.04, 25.00 (CH*Me*$_2$), 26.60, 26.70 (*C*HMe$_2$), 39.72, 44.11 (cyclopentanone *C*H$_2$), 44.94 (*C4*/*C7*), 104.76 (*C2*), 112.35 (*C*-O insert at C4/C7), 116.53 (CpH), 119.59 (Cp), 121.81 (Benzo), 122.29 (Cp), 124.13 (*C1*/*C3*), 124.62 (Benzo), 126.77 (*C5*/*C6*), 135.29 (*C3a*/*C7a*). Two cyclopentanone *C*H$_2$ resonances not located. ***C_1* symmetric isomer**: ^{1}H NMR (benzene-d_6): δ = 0.97 (d, 8 Hz, 3H, CH*Me*$_2$), 1.06 (d, 8 Hz, 3H, CH*Me*$_2$), 1.17 (d, 8 Hz, 3H, CH*Me*$_2$), 1.25 (d, 8 Hz, 6H, CH*Me*$_2$), 1.40 (d, 8 Hz, 3H, CH*Me*$_2$), 1.46 (d, 8 Hz, 3H, CH*Me*$_2$), 1.61 (d, 8 Hz, 3H, CH*Me*$_2$), 1.40 – 2.39 (m, 16H, cyclopentanone C*H*$_2$), 2.97 (m, 1H, C*H*Me$_2$), 3.16 (m, 1H, C*H*Me$_2$), 3.41 (m, 1H, C7-*H*),3.48 (m, 1H, C*H*Me$_2$), 3.49 (m, 1H, C*H*Me$_2$), 3.76 (m, 1H, C4-*H*), 5.66 (s, 1H, C2-*H*), 5.77 (m, C5-*H*), 5.78 (m, 2H, C6-*H*), 6.40 (s, 1H, Cp*H*), 6.89 (m, 1H, η^5 Benzo), 6.93 (m, 1H, η^5 Benzo), 7.48 (m, 1H, η^5 Benzo), 7.54 (m, 1H, η^5 Benzo). ^{13}C NMR (benzene-d_6): δ = 21.11, 21.14, 22.00, 22.80, 22.99, 24.27, 25.16, 25.62 (CH*Me*$_2$), 27.21, 27.24, 27.95 (*C*HMe$_2$), 42.01 (cyclopentanone *C*H$_2$), 44.76 (*C7*), 45.78 (*C4*), 106.86 (*C2*), 110.82 (CpH), 113.81 (*C*-O insert at C7), 117.82 (Cp), 121.78 (2) (Benzo), 122.58, 122.94 (Cp), 123.10, 123.46 (Benzo), 124.50 (Cp), 124.86 (*C3*), 125.82 (*C6*), 126.15 (*C1*), 126.96 (*C5*), 131.90 (*C3a*), 135.74 (*C7a*). One *C*HMe$_2$, eight cyclopentanone *C*H$_2$ and one *C*-O resonance not located.

Addition of 0.5 equivalents of cyclopentanone to 1. A J. Young NMR tube charged with 0.008 g (0.02 mmol) of **1** and approximately 0.5 mL of benzene-d_6. Using a 10 μL syringe, 0.7 μL (0.01 mmol) of cyclopentanone was added. After one day at 22 ºC, both **1-(O^{c}Pent)$_2$-1,4** and **1-(O^{c}Pentenyl)H**, as well as starting **1** were observed in a 0.9 : 1.0 : 3.5 ratio by ^{1}H NMR spectroscopy.

Addition of 0.5 equivalents of cyclopentanone-*d*$_4$ to 1. A J. Young NMR tube charged with 0.008 g (0.02 mmol) of **1** and approximately 0.5 mL of benzene-d_6. Using a 10 μL syringe, 0.8 μL (0.01 mmol) of cyclopentanone-d_4 was added. After one day at 22 ºC, both **1-(O^{c}Pent)$_2$-1,4-*d*$_8$**, **1-(O^{c}Pentenyl-*d*$_3$)D** and **1-(O^{c}Pent)-4-*d*$_4$**, as well as starting **1** were observed in a 1.1 : 1.0 : 0.7 : 1.3 ratio by ^{1}H NMR spectroscopy.

Characterization of (η^5-C$_9$H$_5$-1,3-(CHMe$_2$)$_2$)$_2$Zr(OCCHCH$_2$CH$_2$CH$_2$)H (1-(O^{c}Pentenyl)H). ^{1}H NMR (benzene-d_6): δ = 1.11 (d, 8 Hz, 3H, CH*Me*$_2$), 1.15 (d, 8 Hz, 3H, CH*Me*$_2$), 1.24 (d, 8 Hz, 3H, CH*Me*$_2$), 1.26 (d, 8 Hz, 3H, CH*Me*$_2$), 1.81 (m, 2H, cyclopentanone C*H*$_2$), 2.16 (m, 2H, cyclopentanone C*H*$_2$), 2.35 (m, 2H, cyclopentanone C*H*$_2$), 2.98 (m, 1H, C*H*Me$_2$), 3.06 (m, 1H, C*H*Me$_2$), 4.52 (pseudo s, 1H, C*H*), 5.95 (s, 2H, Cp*H*), 6.09 (s, 1H, Zr-*H*), 6.91 (m, 2H, Benzo), 6.94 (m, 2H, Benzo), 7.28 (m, 2H, Benzo), 7.34 (m, 2H, Benzo). ^{13}C NMR (benzene-d_6): δ = 22.68, 24.93, 24.99, 25.28 (CH*Me*$_2$), 25.43, 26.67 (*C*HMe$_2$), 28.68, 34.72 (cyclopentanone *C*H$_2$), 98.95 (olefinic *C*H), 112.22 (CpH), 119.67, 121.93 (Cp), 122.42, 123.02 (Benzo), 123.35 (Cp), 124.61 (Benzo), 162.93 (*C*-O). One cyclopentanone CH$_2$, one Cp and one Benzo resonance not located.

Characterization of (η^5-C_9H_5-1,3-($CHMe_2$)$_2$)(η^5-C_9H_5-1,3-($CHMe_2$)$_2$-4-C(κ^1-O)(CH_2)$_4$)Zr (1-(O^cPent)-4-*d*$_4$). ^{1}H NMR (benzene-d_6): δ = 0.74 (d, 8 Hz, 3H, CH*Me*$_2$), 1.02 (d, 8 Hz, 3H, CH*Me*$_2$), 1.06 (d, 8 Hz, 3H, CH*Me*$_2$), 1.17 (d, 8 Hz, 3H, CH*Me*$_2$), 1.18 (d, 8 Hz, 3H, CH*Me*$_2$), 1.24 (d, 8 Hz, 3H, CH*Me*$_2$), 1.46 (d, 8 Hz, 3H, CH*Me*$_2$), 1.47 (d, 8 Hz, 3H, CH*Me*$_2$), 1.49 (m, 1H, cyclopentanone C*H*$_2$), 1.64 (m, 1H, cyclopentanone C*H*$_2$), 1.85 (m, 1H, cyclopentanone C*H*$_2$), 2.07 (m, 1H, cyclopentanone C*H*$_2$), 3.00 (m, 1H, C*H*Me$_2$), 3.29 (m, 1H, C*H*Me$_2$), 3.34 (m, 1H, C*H*Me$_2$), 3.35 (dd, 9 Hz, 6 Hz, 1Hz, 1H, C4-*H*), 3.52 (dd, 9 Hz, 6 Hz, 1H, C7-*H*), 5.17 (dd, 9 Hz, 6 Hz, 1H, C5-*H*), 5.62 (s, 1H, C2-*H*), 6.51 (dd, 9 Hz, 6 Hz, 1H, C6-*H*), 6.82 (m, 1H, Benzo), 6.89 (m, 1H, Benzo), 7.36 (m, 2H, Benzo). One C*H*Me$_2$ resonance not located. ^{13}C NMR (benzene-d_6): δ = 20.86, 21.91, 21.99 (CH*Me*$_2$), 22.36 (cyclopentanone *C*H$_2$), 23.13 (2) (*C*HMe$_2$), 24.01 (cyclopentanone *C*H$_2$), 24.88, 25.31, 26.54 (CH*Me*$_2$), 26.62, 27.32, 27.49 (*C*HMe$_2$), 46.56 (*C*-4), 73.45 (*C*-7), 108.06 (Cp), 108.38 (*C*-2), 114.40 (Cp-H), 116.83 (Cp), 117.21 (*C*-5), 121.79, 122.38, 122.84 (2) (Benzo), 123.92 (Cp), 123.99 (*C*-1), 123.92 (Cp), 126.53 (*C*-7a), 126.78 (Cp), 129.77 (*C*-3a), 129.18 (*C*-6), 134.96 (*C*-3). One *C*HMe$_2$, two cyclopentanone *C*D$_2$ and one *C*-O resonances not located.

Addition of cyclopentanone to 2-THF. A 20 mL scintillation vial charged with 0.61 g (90 mmol) of **2-THF**[*] was dissolved in approximately 5 mL of pentane. Using a microsyringe, 16 μL (18 mmol) of cyclopentanone was added resulting in a color change from burgundy to yellow. After stirring for 2 minutes at ambient temperature, the volatiles were removed *in vacuo*. The products of the reaction were identified as **2-(O^cPentenyl)H** and **2-(O^cPent)$_2$-1,4**, formed in a 4:1 ratio, as determined by ^{1}H NMR spectroscopy.

The same ratio of products can be achieved substituting **2-THF** with **2.**

Characterization of (η^5-C_9H_5-1,3-($SiMe_3$)$_2$)$_2$Zr(OCCHCH_2CH_2CH_2)H (2-(O^cPentenyl)H). ^{1}H NMR (benzene-d_6): δ = 0.43 (s, 18H, Si*Me*$_3$), 0.46 (s, 18H, Si*Me*$_3$), 1.75 (m, 2H, C*H*$_2$), 2.06 (m, 2H, C*H*$_2$), 2.26 (m, 2H, C*H*$_2$), 4.46 (pseudo s, 1H, C*H*), 5.71 (s, 2H, Cp*H*), 5.72 (s, 1H, Zr-*H*), 6.66 (m, 2H, Benzo), 6.74 (m, 2H, Benzo), 7.05 (m, 2H, Benzo), 7.27 (m, 2H, Benzo). ^{13}C NMR (benzene-d_6): δ = -0.04, 1.05 (Si*Me*$_3$), 22.24, 28.78, 35.20 (*C*H$_2$), 99.75 (olefinic *C*H), 106.42, 110.54 (Cp), 123.45, 123.79, 123.97, 124.12 (Benzo), 130.09 (CpH), 131.15, 133.26 (Cp), 163.22 (*C*-O).

Characterization of (η^5-C_9H_5-1,3-($SiMe_3$)$_2$)(η^1-C_9H_5-1,3-($SiMe_3$)$_2$-1-C(κ^1-O)(CH_2)$_4$-4-C(κ^1-O)(CH_2)$_4$)Zr (2-(O^cPent)$_2$-1,4). ^{1}H NMR (benzene-d_6): δ = 0.06 (s, 9H, Si*Me*$_3$), 0.19 (s, 9H, Si*Me*$_3$), 0.45 (s, 9H, Si*Me*$_3$), 0.52 (s, 9H, Si*Me*$_3$), 1.19 (m, 1H, C*H*$_2$), 1.38 (m, 2H, C*H*$_2$), 1.52 (m, 1H, C*H*$_2$), 1.67 (m, 1H, C*H*$_2$), 1.70 (m, 1H, C*H*$_2$), 1.73 (m, 2H, C*H*$_2$), 1.80 (m, 2H, C*H*$_2$), 1.99 (m, 1H, C*H*$_2$), 2.15 (m, 1H, C*H*$_2$), 3.93 (dd, 4 Hz, 2 Hz, 1H, C4-*H*), 4.52 (dd, 9 Hz, 4 Hz, 1H, C5-*H*), 5.15 (dd, 5 Hz, 1 Hz, 1H, C7-*H*), 5.32 (ddd, 9Hz, 5 Hz, 1 Hz, 1H, C6-*H*), 6.54 (s, 1H, C2-*H*), 6.97 (s, 1H, Cp*H*), 6.93 (m, 1H, Benzo), 7.01 (m, 1H, Benzo), 7.44 (m, 1H, Benzo), 7.87 (m, 1H, Benzo). Four C*H*$_2$ resonances not located.^{13}C NMR (benzene-d_6): δ = -0.81, -0.20, -0.04, 1.73 (Si*Me*$_3$), 23.48, 23.67, 37.15, 40.59, 42.01, 43.39 (*C*H$_2$), 50.11 (*C*4), 67.58 (*C*1), 72.58 (*C*7), 107.91, 111.74 (Cp), 118.09 (*C*6), 120.85 (*C*5), 123.00, 123.02, 124.24, 126.62 (Benzo), 132.43 (CpH), 134.42, 136.20 (Cp), 143.92 (*C*3), 146.34 (*C*7a), 145.01 (*C*3a), 153.64 (*C*2). Two *C*H$_2$ resonances not located.

Preparation of (η^5-C_9H_5-1,3-($SiMe_3$)$_2$)$_2$Zr(H)Cl (2-(H)Cl). A 20 mL scintillation vial in a dry box was charged with 278 mg (0.408 mmol) of **2-Cl$_2$** and dissolved in 5 mL of toluene. After chilling the solution in the dry box freezer for 20 minutes, a 1.0

M solution of $NaEt_3BH$ is then added dropwise over the course of 5 minutes. After stirring for 3 hours, the solution is filtered through a Celite filled pipette and solvent is removed *in vacuo* to afford 240 mg (91%) of a yellow-green oil identified as **2-(H)Cl**. Anal. Calcd. for $C_{30}H_{47}Si_4ZrCl$. 55.71 C; 7.33 H. Found 55.41 C; 6.98 H. ^{1}H NMR (benzene-d_6): δ = 0.40 (s, H, Si*Me*$_3$), 0.42 (s, H, Si*Me*$_3$), 5.93 (s, 1H, Cp), 6.65 (t, 1H, Benzo), 6.69 (t, 1H, Benzo), 6.76 (s, 1H, Zr-*H*), 6.98 (d, 1H, Benzo), 7.23 (d, 1H, Benzo). ^{13}C NMR (benzene-d_6):δ = 1.47 (Si*Me*$_3$), 1.58 (Si*Me*$_3$), 110.31 (Cp), 112.29 (Cp), 124.58 (Cp), 125.16, 125.38, 125.50, 131.27, 132.06, 132.97 (Benzo).

Preparation of (η^5-C_5Me_5)(η^1-C_9H_5-1,3-$(CHMe_2)_2$-1-C(κ^1-O)$(CH_2)_4$-4-C(κ^1-O)$(CH_2)_4$)Zr (3-(O^cPent)$_2$-1,4). This compound was prepared in a similar manner to **1-(O^cPent)$_2$-1,4** using 0.109 g (0.26 mmol) of **3** dissolved in approximately 10 mL of pentane and 43 mg (0.51 mmol) of cyclopentanone affording a yellow solution. Recrystallization from pentane at -35 °C affords 52 mg (34 %) of **3-(O^cPent)$_2$-X,Y** as a yellow solid without cocrystallization of the other products. Anal. Calcd. for $C_{35}H_{50}O_2Zr$: C, 70.77; H, 8.48. Found: C, 70.49; H, 8.76. ^{1}H NMR (benzene-d_6): δ = 0.83 (d, 8 Hz, 3H, CH*Me*$_2$), 0.95 (d, 8 Hz, 3H, CH*Me*$_2$), 1.00 (d, 8 Hz, 3H, CH*Me*$_2$), 1.22 (d, 8 Hz, 3H, CH*Me*$_2$), 1.56 (m, 8 H, cyclopentanone C*H*$_2$), 1.84 (m, 2H, cyclopentanone C*H*$_2$), 1.94 (s, 15H, Cp* *Me*), 2.06 (m, 7H, C*H*Me$_2$/cyclopentanone C*H*$_2$), 2.83 (m, 1H, C*H*Me$_2$), 3.85 (dd, 4 Hz, 1H, C4-*H*), 3.98 (dd, 6 Hz, 1H, C7-*H*), 5.04 (ddd, 9 Hz, 4 Hz, 1H, C5-*H*), 5.24 (ddd, 9 Hz, 6 Hz, 1H, C6-*H*), 6.02 (s, 1H, C2-*H*). ^{13}C NMR (benzene-d_6): δ = 11.35 (Cp* *Me*), 18.66, 20.34, 21.23, 21.95, 23.38, 23.82, 24.54, 26.31, 27.65, 31.71, 37.17, 37.66, 40.74, 43.63 (CHMe$_2$/cyclopentanone *C*H$_2$), 49.59 (*C4*), 67.82 (*C1*), 72.65 (*C7*), 97.08 (*C*-O), 118.29 (*C5*), 118.59 (Cp), 119.86 (*C6*), 131.39 (*C2*), 131.62 (*C*-O), 137.18 (*C3a*), 152.52 (*C-7a*), 153.74 (*C3*).

Addition of 0.5 equivalents of cyclopentanone to 3. A J. Young NMR tube charged with 0.008 g (0.02 mmol) of **3** and approximately 0.5 mL of benzene-d_6. Using a 10 μL syringe, 0.8 μL (0.01 mmol) of cyclopentanone was added. Monitoring the reaction by ^{1}H NMR spectroscopy revealed an initial ratio of remaining **3** and the bis(insertion) products, **3-(O^{c}Pent)$_2$-1, 4** and **3-(O^{c}Pent)$_2$-1,6**, as well as the mono(insertion) product, **3-(O^{c}Pent)-1** were observed in a 1.0 : 0.21 : 0.16 : 0.16 ratio. Over the course of one day at 22 ºC, **3-(O^{c}Pent)-1** was consumed and **3-(O^{c}Pent)H** and **3-(O^{c}Pent)-4** formed in the ratio of 1 : 0.06 : 0.19 : 0.32 : 0.19 for **3** : **3-(O^{c}Pent)$_2$-1, 4**: **3-(O^{c}Pent)$_2$-1,6** : **3-(O^{c}Pentenyl)H**: **3-(O^{c}Pent)-4**.

Characterization of (η^5-C$_5$Me$_5$)(η^1-C$_9$H$_5$-1,3-(CHMe$_2$)$_2$-1-C(κ^1-O)(CH$_2$)$_4$-6-C(κ^1-O) (CH$_2$)$_4$)Zr (3-(O^{c}Pent)$_2$-1,6). ^{1}H NMR (benzene-d_6): δ = 0.81 (d, 8 Hz, 3H, CH*Me*$_2$), 0.93 (d, 8 Hz, 3H, CH*Me*$_2$), 1.23 (d, 8 Hz, 3H, CH*Me*$_2$), 1.27 (d, 8 Hz, 3H, CH*Me*$_2$), 1.94 (s, 15H, Cp* *Me*), 1.40 – 2.10 (m, 16H, cyclopentanone C*H*$_2$), 1.98 (m, 1H, C*H*Me$_2$), 2.60 (m, 1H, C*H*Me$_2$), 3.81 (dd, 5 Hz, 4Hz, 1 H, C6-*H*), 3.90 (ddd, 9 Hz, 4 Hz, 2Hz, 1 H, C5-*H*), 5.10 (s, 1H, C2-*H*), 5.38 (d, 5 Hz, 1 H, C7-*H*), 5.53 (d, 9 Hz, 1 H, C4-*H*). ^{13}C NMR (benzene-d_6): δ = 11.43 (Cp* *Me*), 19.41, 20.24, 20.85, 21.72, 22.82, 22.92, 23.18, 23.22, 23.62, 24.07, 24.23, 24.32, 27.37, 31.26 (CHMe$_2$/cyclopentanone *C*H$_2$), 51.46 (*C*-6), 66.10 (*C*-1), 95.36 (*C*-5), 97.95 (*C*-3a), 112.26 (*C*-7), 114.74 (*C*-2), 118.56 (Cp*), 119.44 (*C*-4), 120.61 (*C*-O), 149.16 (*C*-3), 155.02 (*C*-7a). One *C*-O resonance not located.

Characterization of (η^5-C$_5$Me$_5$)(η^5-C$_9$H$_5$-1,3-(CHMe$_2$)$_2$)Zr(OCCHCH$_2$CH$_2$CH$_2$)H (3-(O^{c}Pentenyl)H). ^{1}H NMR (benzene-d_6): δ = 1.20 (d, 8 Hz, 3H, CH*Me*$_2$), 1.23 (d, 8 Hz, 3H, CH*Me*$_2$), 1.42 (d, 8 Hz, 3H, CH*Me*$_2$), 1.45 (d, 8 Hz, 3H, CH*Me*$_2$), 1.77 (s, 15H, Cp* *Me*), 1.40 – 2.10 (m, 6H, cyclopentanone C*H*$_2$), 3.29 (m, 1H, C*H*Me$_2$), 3.60

(m, 1H, C*H*Me$_2$), 4.52 (pseudo s, 1H, C*H*), 6.05 (s, 1H, Zr-*H*), 6.35 (s, 1H, Cp*H*), 6.87 (m, 2H, Benzo), 7.36 (m, 1H, Benzo), 7.42 (m, 1H, Benzo). ^{13}C NMR (benzene-d_6): δ = 11.46 (Cp* *Me*), 22.15, 22.17, 25.40, 25.44 (CH*Me*$_2$), 26.08 (*C*HMe$_2$), 28.91, 36.26 (cyclopentanone *C*H$_2$), 97.64 (olefinic *C*H), 107.04, 108.70 (Cp), 113.69 (CpH), 118.51, 118.73 (Cp), 121.58, 122.42, 122.84 (Benzo), 163.26 (*C*-O). One *C*HMe$_2$, one cyclopentanone CH$_2$, one Cp and one Benzo resonance not located.

Characterization of (η^5-C_5Me_5)(η^4-C_9H_5-1,3-(CHMe$_2$)$_2$-1-C(κ^1-O)(CH$_2$)$_4$)Zr (3-(O^{c}Pent)-1). ^{1}H NMR (benzene-d_6): δ = 0.72 (d, 8 Hz, 3H, CH*Me*$_2$), 0.75 (d, 8 Hz, 3H, CH*Me*$_2$), 1.05 (d, 8 Hz, 3H, CH*Me*$_2$), 1.06 (d, 8 Hz, 3H, CH*Me*$_2$), 1.40 – 2.10 (m, 8H, cyclopentanone C*H*$_2$), 1.79 (m, 1H, C*H*Me$_2$), 2.18 (m, 1H, C*H*Me$_2$), 2.89 (ddd, 9 Hz, 6Hz, 1Hz, 1H, C5-*H*), 3.37 (ddd, 9 Hz, 6Hz, 1Hz, 1H, C6-*H*), 4.46 (dd, 6Hz, 1 Hz, 1H, C7-*H*), 4.74 (dd, 6Hz, 1Hz, 1H, C4-*H*), 5.32 (s, 1H, C2-*H*). One Cp* *Me* resonance not located. ^{13}C NMR (benzene-d_6): δ = 11.67 (Cp* *Me*), 16.42, 18.95, 20.08, 22.11 (CH*Me*$_2$), 26.21, 27.06 (*C*HMe$_2$), 70.91 (*C*-1), 75.32 (*C*-4), 78.76 (*C*-7), 113.81 (*C*-5), 115.74 (*C*-6), 131.63 (*C*-2), 139.64 (*C*-3a), 143.50 (*C*-7a), 148.72 (*C*-3). Four cyclopentanone *C*H$_2$, one Cp and one *C*-O resonance not located.

Characterization of (η^5-C_5Me_5)(η^5-C_9H_5-1,3-(CHMe$_2$)$_2$-4-C(κ^1-O)(CH$_2$)$_4$)Zr (3-(O^{c}Pent)-4). ^{1}H NMR (benzene-d_6): δ = 0.89 (d, 8 Hz, 3H, CH*Me*$_2$), 1.16 (d, 8 Hz, 3H, CH*Me*$_2$), 1.20 (d, 8 Hz, 3H, CH*Me*$_2$), 1.22 (d, 8 Hz, 3H, CH*Me*$_2$), 1.17 – 2.10 (m, 8H, cyclopentanone C*H*$_2$), 1.71 (m, 1H, C*H*Me$_2$), 1.94 (s, 1H, Cp* *Me*), 3.06 (m, 1H, C*H*Me$_2$), 3.47 (dd, 9 Hz, 6 Hz, 1Hz, 1H, C4-*H*), 3.69 (dd, 9 Hz, 6 Hz, 1H, C7-*H*), 5.21 (dd, 9 Hz, 6 Hz, 1H, C5-*H*), 5.70 (s, 1H, C2-*H*), 6.53 (dd, 9 Hz, 6 Hz, 1H, C6-*H*). ^{13}C NMR (benzene-d_6): δ = 11.56 (Cp* *Me*), 21.73, 23.56 (CH*Me*$_2$), 24.91 (*C*HMe$_2$), 25.95, 26.48 (CH*Me*$_2$), 26.58 (*C*HMe$_2$), 38.14, 40.27, 44.09 (cyclopentanone *C*H$_2$),

46.79 (*C*-4), 72.31 (*C*-7), 106.91 (C-*O*), 108.43 (*C*-2), 116.75 (*C*-5), 117.05 (Cp*), 123.37 (*C*-1), 126.97 (*C*-7a), 128.95 (*C*-3a), 129.13 (*C*-6), 134.89 (*C*-3). One cyclopentanone *C*H_2 resonance not located.

Preparation of (η^5-C_9H_5-1,3-($CHMe_2$)$_2$)$_2$Zr(OCCHCH_2CH_2CMe_2)H (1-(dimethylcyclopentenoxy)H). This compound was prepared in a similar manner to **1-(O^cPent)$_2$-1,4** using 0.010 g (0.02 mmol) of **1** dissolved in 0.5 mL of benzene-d_6 and 2.6 μL (0.02 mmol) of 2,2-dimethylcyclopentanone affording yellow **1-(dimethylcyclopentenoxy)H**. ^{1}H NMR (benzene-d_6): δ = 0.95 (s, 6H, *Me*), 1.25 (d, 8 Hz, 6H, CH*Me*$_2$), 1.27 (d, 8 Hz, 6H, CH*Me*$_2$), 1.39 (d, 8 Hz, 6H, CH*Me*$_2$), 1.41 (d, 8 Hz, 6H, CH*Me*$_2$), 1.67 (m, 2H, C*H*$_2$), 2.20 (m, 2H, C*H*$_2$), 3.24 (m, 2H, C*H*Me$_2$), 3.34 (m, 2H, C*H*Me$_2$), 4.25 (m, 1H, olefinic C*H*), 4.93 (s, 2H, Cp*H*), 5.82 (s, 1H, Zr-*H*), 6.81 (m, 2H, Benzo), 6.87 (m, 2H, Benzo), 7.38 (pseudo d, 8 Hz, 2H, Benzo), 7.53 (pseudo d, 8 Hz, 2H, Benzo). ^{13}C NMR (benzene-d_6): δ = 23.28, 24.45 (CHMe$_2$), 24.74 (cyclopentanone *C*H_2), 25.24, 25.51 (CHMe$_2$), 26.35 (cyclopentanone C*Me*$_2$), 27.51, 28.39 (CHMe$_2$), 39.32 (cyclopentanone *C*H_2), 43.04 (cyclopentanone *C*Me$_2$), 98.67 (cyclopentanone *C*H), 113.68 (CpH), 119.85, 120.85, 122.91, 123.15, 123.44, 123.91, 124.27, 124.43 (Benzo/Cp), 166.88 (*C*-O).

Preparation of (η^5-C_9H_5-1,3-($CHMe_2$)$_2$)$_2$Zr(OC(CH_2)CMe_3)H (1-(OC(CH_2)CMe_3)H). This compound was prepared in a similar manner to **1-(O^cPent)$_2$-1,4** using 0.007 g (0.02 mmol) of **1** dissolved in 0.5 mL of benzene-d_6 and 1.8 μL (0.02 mmol) of pinacolone affording yellow **1-(OC(CH_2)CMe_3)H)**. ^{1}H NMR (benzene-d_6): δ = 0.94 (s, 9H, *Me*), 1.29 (d, 8 Hz, 12H, CH*Me*$_2$), 1.45 (d, 8 Hz, 6H, CH*Me*$_2$), 1.47 (d, 8 Hz, 6H, CH*Me*$_2$), 3.31 (m, 2H, C*H*Me$_2$), 3.46 (m, 2H, C*H*Me$_2$), 3.76 (m, 1H, olefinic C*H*), 3.94 (m, 1H, olefinic C*H*), 4.60 (s, 2H, Cp*H*), 5.75 (s, 1H,

Zr-*H*), 6.80 (m, 2H, Benzo), 6.88 (m, 2H, Benzo), 7.43 (pseudo d, 8 Hz, 2H, Benzo), 7.58 (pseudo d, 8 Hz, 2H, Benzo). ^{13}C NMR (benzene-d_6): δ = 23.50, 24.65, 25.37, 25.54, 28.15, 28.74, 28.77 (CHMe$_2$/C*Me*$_3$), 36.15 (*C*Me$_3$), 86.71, 113.94, 120.05, 120.71, 123.00, 123.35, 123.44, 123.95, 124.27, 124.99 (Cp/Benzo/olefinic *C*H$_2$), 171.45 (*C*-O).

Addition of pinacolone to a thawing solution of 1. A 20 mL scintillation vial charged with 0.008 g (0.02 mmol) of **1** was dissolved in 0.5 mL of pentane. The resulting burgundy solution was frozen in a liquid nitrogen chilled coldwell for 20 minutes. Upon, thawing 4.1 μL (0.03 mmol) of pinacolone was added, resulting in a gradual color change to yellow upon warming. The volatiles were removed *in vacuo* and the product mixture dissolved in 0.5 mL of benzene-d_6. The solution consisted of a 1 : 1 ratio of **1-(OC(CH$_2$)C^{t}Bu)H** : **1-(OC(CH$_2$)C^{t}Bu)-(OC(Me)^{t}Bu)-4** by ^{1}H NMR spectroscopy.

Characterization of (η^5-C$_9$H$_5$-1,3-(CHMe$_2$)$_2$)(η^1-C$_9$H$_5$-1,3-(CHMe$_2$)$_2$-1-H-4-C(κ^1-O)(C(Me)^{t}Bu)Zr(OC(CH$_2$)C^{t}Bu) (1-(OC(CH$_2$)C^{t}Bu)-(OC(Me)^{t}Bu)-4). ^{1}H NMR (benzene-d_6): δ = 0.66 (d, 8 Hz, 3H, CH*Me*$_2$), 1.04 (s, 9H, C*Me*$_3$ on inserted ketone), 1.05 (d, 8 Hz, 3H, CH*Me*$_2$), 1.06 (s, 9H, C*Me*$_3$ on enolate), 1.17 (s, 3H, *Me* on inserted ketone), 1.18 (d, 8 Hz, 3H, CH*Me*$_2$), 1.19 (d, 8 Hz, 3H, CH*Me*$_2$), 1.26 (d, 8 Hz, 3H, CH*Me*$_2$), 1.37 (d, 8 Hz, 3H, CH*Me*$_2$), 1.46 (d, 8 Hz, 3H, CH*Me*$_2$), 1.51 (d, 8 Hz, 3H, CH*Me*$_2$), 2.05 (m, 1H, C*H*Me$_2$), 2.58 (m, 1H, C*H*Me$_2$), 3.11 (m, 1H, allyl Cp*H*), 3.31 (m, 1H, C*H*Me$_2$), 3.35 (m, 1H, C*H*Me$_2$), 3.87 (m, 1H, C7-*H*), 4.01 (m, 1H, olefinic C*H*), 4.24 (m, 1H, olefinic C*H*), 4.36 (d, 1H, C4-*H*), 5.12 (m, 2H, C5-*H* and C6-*H*), 5.95 (s, 1H, Cp*H*), 6.47 (s, 1H, Cp*H*), 6.91 (m, 1H, Benzo), 6.97 (m, 1H, Benzo), 7.49 (m, 1H, Benzo), 7.56 (m, 1H, Benzo). ^{13}C NMR (benzene-d_6): δ = 16.40, 21.98, 22.30,

23.07, 24.09 (CH*Me*$_2$), 24.09 (*Me*), 24.32, 24.57, 25.64 (CH*Me*$_2$), 27.11, 27.57, 27.85 (*C*HMe$_2$), 28.71 (C*Me*$_3$ on inserted ketone), 29.14 (*C*HMe$_2$), 29.18 (C*Me*$_3$ on enolate), 37.00 (*C*Me$_3$ on enolate), 39.97 (*C*Me$_3$ on inserted ketone), 46.04 (*C*-4), 55.35 (*C*-1), 73.93 (*C*-7), 87.81 (olefinic *C*H$_2$), 112.70 (CpH), 120.59 (Cp), 120.98 (*C*-O on inserted ketone), 120.99 (Cp), 122.69, 122.70, 123.33, 123.46 (Benzo), 123.48 (*C*-2), 123.66 (*C*-3a), 123.87 (*C*-6), 123.91 (Cp), 125.77 (*C*-5), 125.88 (Cp), 155.43 (*C*-3), 173.76 (*C*-O on enolate). *C*-7a resonance not located.

Preparation of (η^5-C$_9$H$_5$-1,3-(CHMe$_2$)$_2$)$_2$Zr(*c*-OCH(Me)CHCH$_2$) (1-*c*-OCH(Me)CHCH$_2$). This compound was prepared in a similar manner to **1-(OMe$_2$)$_2$-1,4** using 0.007 g (0.01 mmol) of **1** dissolved in approximately 0.5 mL of benzene-d_6 and two equivalents (17 torr in a 31.6 mL bulb) of methylvinylketone affording a yellow solution identified as **1-*c*-OCH(Me)CHCH$_2$**. ^{1}H NMR (benzene-d_6): δ = 1.15 (d, 8 Hz, 12H, CH*Me*$_2$), 1.30 (d, 8 Hz, 6H, CH*Me*$_2$), 1.33 (m, 2H, Zr-C*H*$_2$), 1.52 (d, 8 Hz, 6H, CH*Me*$_2$), 1.72 (s, 3H, OCH*Me*), 3.00 (m, 2H, C*H*Me$_2$), 3.10 (m, 2H, C*H*Me$_2$), 4.47 (m, 1H, olefinic C*H*), 4.62 (s, 2H, Cp*H*), 6.14 (s, 1H, Zr-*H*), 6.90 (m, 4H, Benzo), 7.54 (m, 4H, Benzo). ^{13}C NMR (benzene-d_6): δ = 22.63, 24.10, 24.12, 24.66, 25.40, 28.03, 28.93 (CHMe$_2$/OCHMe), 53.62 (Zr-*C*H$_2$), 102.24, 114.17, 122.60, 122.80, 122.83, 124.72, 126.45, 127.39 (Cp/Benzo/olefinic *C*H), 148.58 (*C*-O). Two Cp/Benzo/olefinic CH resonances not located.

Preparation of (η^5-C$_9$H$_5$-1,3-(CHMe$_2$)$_2$)$_2$Zr(OC(CH$_2$)Ph)H (1-(OC(CH$_2$)C$_6$H$_5$)H). This compound was prepared in a similar manner to **1-(O^{c}Pent)$_2$-1,4** using 0.012 g (0.02 mmol) of **1** dissolved in 0.5 mL of benzene-d_6 and 2.85 μL (0.02 mmol) of acetophenone affording yellow **1-(OC(CH$_2$)C$_6$H$_5$)H)**. ^{1}H NMR (benzene-d_6): δ = 1.14 (d, 8 Hz, 6H, CH*Me*$_2$), 1.23 (d, 8 Hz, 6H, CH*Me*$_2$), 1.24 (d, 8 Hz, 6H, CH*Me*$_2$),

1.31 (d, 8 Hz, 6H, CH*Me*$_2$), 3.17 (m, 2H, C*H*Me$_2$), 3.24 (m, 2H, C*H*Me$_2$), 4.21 (m, 1H, olefinic C*H*), 4.66 (m, 1H, olefinic C*H*), 5.49 (s, 2H, Cp*H*), 6.22 (s, 1H, Zr-*H*), 6.81 (m, 3H, Benzo/Ph), 7.10 (m, 2H, Benzo/Ph), 7.19 (m, 2H, Benzo/Ph), 7.38 (m, 2H, Benzo/Ph), 7.44 (m, 2H, Benzo/Ph), 7.57 (m, 2H, Benzo/Ph). ^{13}C NMR (benzene-d_6): δ = 22.99, 23.64, 25.12, 25.39 (CH*Me*$_2$), 26.84, 27.87 (*C*HMe$_2$), 88.56 ($^1J_{CH}$ = 160 Hz, olefinic *C*H$_2$), 112.87 (*Cp*H), 120.56, 120.86, 123.02, 123.16, 123.53, 123.63, 123.70, 124.78 (Cp/Benzo), 126.10, 137.63 (Ph), 162.30 (*C*-O). One phenyl resonance not located.

Preparation of (η^5-C$_9$H$_5$-1,3-(CHMe$_2$)$_2$)$_2$Zr(OC(CH$_2$)(4-CF$_3$-C$_6$H$_4$))H (1-(OC(CH$_2$)(4-CF$_3$-C$_6$H$_4$))H). This compound was prepared in a similar manner to **1-(O^{c}Pent)$_2$-1,4** using 0.006 g (0.01 mmol) of **1** dissolved in 0.5 mL of benzene-d_6 and 5 mg (0.03 mmol) of 4-trifluoromethylacetophenone affording yellow **1-(OC(CH$_2$) (4-CF$_3$-C$_6$H$_4$))H)**. ^{1}H NMR (benzene-d_6): δ = 1.15 (d, 8 Hz, 6H, CH*Me*$_2$), 1.20 (d, 8 Hz, 6H, CH*Me*$_2$), 1.22 (d, 8 Hz, 6H, CH*Me*$_2$), 1.31 (d, 8 Hz, 6H, CH*Me*$_2$), 3.23 (m, 2H, C*H*Me$_2$), 3.25 (m, 2H, C*H*Me$_2$), 4.19 (m, 1H, olefinic C*H*), 4.54 (m, 1H, olefinic C*H*), 5.26 (s, 2H, Cp*H*), 6.09 (s, 1H, Zr-*H*), 6.75 (m, 4H, Benzo/Ph), 6.90 (m, 2H, Benzo/Ph), 7.36 (m, 2H, Benzo/Ph), 7.41 (m, 4H, Benzo/Ph). ^{13}C NMR (benzene-d_6): δ = 23.10, 23.77, 25.07, 25.44, 27.13, 28.10 (CHMe$_2$), 90.11, 112.81, 114.89, 120.64, 121.12, 123.22, 123.39, 123.55, 123.70, 123.77, 124.63, 126.28, 128.62, 129.81 (Benzo/Cp/Ph/olefin), 160.58 (*C*-O). ^{19}F NMR (benzene-d_6): δ = -61.9.

Preparation of (η^5-C$_9$H$_5$-1,3-(CHMe$_2$)$_2$)$_2$Zr(OC(CH$_2$)(4-NMe$_2$-C$_6$H$_4$))H (1-(OC(CH$_2$)(4-NMe$_2$-C$_6$H$_4$))H). This compound was prepared in a similar manner to **1-(O^{c}Pent)$_2$-1,4** using 0.008 g (0.02 mmol) of **1** dissolved in 0.5 mL of benzene-d_6 and 5 mg (0.03 mmol) of 4-dimethylaminoacetophenone affording yellow **1-**

(OC(CH_2) (4-NMe_2-C_6H_4))H). ^{1}H NMR (benzene-d_6): δ = 1.15 (d, 8 Hz, 6H, CHMe_2), 1.27 (d, 8 Hz, 6H, CHMe_2), 1.30 (d, 8 Hz, 6H, CHMe_2), 1.32 (d, 8 Hz, 6H, CHMe_2), 3.17 (m, 2H, C*H*Me_2), 3.26 (m, 2H, C*H*Me_2), 4.20 (m, 1H, olefinic C*H*), 4.71 (m, 1H, olefinic C*H*), 5.70 (s, 2H, Cp*H*), 6.30 (s, 1H, Zr-*H*), 6.61 (m, 2H, Benzo/Ph), 6.87 (m, 4H, Benzo/Ph), 7.42 (m, 2H, Benzo/Ph), 7.49 (m, 2H, Benzo/Ph). ^{13}C NMR (benzene-d_6): δ = 22.99, 23.51, 25.18, 25.38, 26.59, 27.72 ($CHMe_2$), 40.09 (NMe_2), 111.68, 112.87, 120.41, 120.74, 122.88, 123.00, 123.41, 123.67, 123.71, 124.91, 127.10 (Benzo/Cp/Ph/olefin), 162.87 (*C*-O). Two Cp/Benzo/Ph resonances not located.

Preparation of (η^5-C_9H_5-1,3-($CHMe_2$)$_2$)$_2$Zr(α-tetralenoxy)H (1-(α-tetralenoxy)H). This compound was prepared in a similar manner to **1-(O^cPent)$_2$-1,4** using 0.008 g (0.02 mmol) of **1** dissolved in 0.5 mL of benzene-d_6 and 4.4 μL (0.03 mmol) of α-tetralone affording yellow **1-(α-tetralenoxy)H)**. ^{1}H NMR (benzene-d_6): δ = 1.16 (d, 8 Hz, 6H, CHMe_2), 1.28 (d, 8 Hz, 6H, CHMe_2), 1.29 (d, 8 Hz, 6H, CHMe_2), 1.35 (d, 8 Hz, 6H, CHMe_2), 2.27 (m, 2H, CH_2), 2.62 (m, 2H, CH_2), 3.30 (m, 4H, C*H*Me_2), 4.87 (m, 1H, olefinic C*H*), 5.37 (s, 2H, Cp*H*), 6.14 (s, 1H, Zr-*H*), 6.79 (m, 4H, Benzo/Ph), 7.23 (m, 2H, Benzo/Ph), 7.39 (m, 2H, Benzo/Ph), 7.45 (m, 2H, Benzo/Ph), 7.55 (m, 2H, Benzo/Ph). ^{13}C NMR (benzene-d_6): δ = 22.75, 23.15, 23.83, 25.15, 25.47, 27.03, 28.07, 29.10 ($CHMe_2$/CH_2), 102.07, 112.92, 120.38, 120.63, 122.94, 122.96, 123.37, 123.55, 123.68, 123.70, 124.62, 125.76, 127.07, 127.10, 128.29, 137.00 (Cp/Benzo/Ph/olefinic *C*H), 154.98 (*C*-O).

Preparation of (η^5-C_9H_5-1,3-($CHMe_2$)$_2$)$_2$Zr(2,4-Me_2-pent-2-en-3-oxy)H (1-(2,4-Me_2-pent-2-en-3-oxy)H). This compound was prepared in a similar manner to **1-(O^cPent)$_2$-1,4** using 0.006 g (0.01 mmol) of **1** dissolved in 0.5 mL of benzene-d_6 and

3.5 μL (0.02 mmol) of diisopropylketone affording yellow **1-(2,4-Me$_2$-pent-2-en-3-oxy)H)**. ^{1}H NMR (benzene-d_6): δ = 0.91 (d, 8 Hz, 6H, enol CH*Me*$_2$), 1.21 (d, 8 Hz, 6H, CH*Me*$_2$), 1.23 (d, 8 Hz, 6H, CH*Me*$_2$), 1.46 (d, 8 Hz, 6H, CH*Me*$_2$), 1.49 (d, 8 Hz, 6H, CH*Me*$_2$), 1.54 (s, 3H, enol C*Me*$_2$), 1.58 (s, 3H, enol C*Me*$_2$), 2.53 (m, 1H, enol C*H*Me$_2$), 3.46 (m, 2H, C*H*Me$_2$), 3.58 (m, 2H, C*H*Me$_2$), 4.52 (s, 2H, Cp*H*), 5.65 (s, 1H, Zr-*H*), 6.76 (m, 2H, Benzo), 6.86 (m, 2H, Benzo), 7.40 (m, 2H, Benzo), 7.61 (m, 2H, Benzo). ^{13}C NMR (benzene-d_6): δ = 18.20, 19.64, 20.88, 22.60, 24.47, 25.47, 25.49, 28.56, 29.39 (CHMe$_2$/C*Me*$_2$), 100.00, 112.51, 122.34, 123.08, 123.75, 123.84, 123.97 (Benzo/Cp/olefinic), 155.17 (*C*-O). One CHMe$_2$/C*Me*$_2$ and two Cp/Benzo/olefinic resonances not located.

Preparation of (η^5-C$_9$H$_5$-1,3-CHMe$_2$)$_2$)$_2$Zr(cyclohexyl(cyclohexylidene)methoxy)H (1-(cyclohexyl(cyclohexylidene)methoxy)H). This compound was prepared in a similar manner to **1-(O^{c}Pent)$_2$-1,4** using 0.008 g (0.02 mmol) of **1** dissolved in 0.5 mL of benzene-d_6 and 3.8 μL (0.02 mmol) of dicyclohexylketone affording yellow **1-(cyclohexyl(cyclohexylidene)methoxy)H)**. ^{1}H NMR (benzene-d_6): δ = 0.74 (m, 1H, cyclohexyl C*H*$_2$), 0.99 (m, 1H, cyclohexyl C*H*$_2$), 1.23 (d, 8 Hz, 6H, enol CH*Me*$_2$), 1.25 (d, 8 Hz, 6H, CH*Me*$_2$), 1.34 (m, 2H, cyclohexyl C*H*$_2$), 1.51 (d, 8 Hz, 12H, CH*Me*$_2$), 1.85 (m, 2H, cyclohexyl C*H*$_2$), 2.20 (m, 2H, cyclohexyl C*H*$_2$), 3.34 (m, 2H, C*H*Me$_2$), 3.56 (m, 2H, C*H*Me$_2$), 4.50 (s, 2H, Cp*H*), 5.65 (s, 1H, Zr-*H*), 6.78 (m, 2H, Benzo), 6.88 (m, 2H, Benzo), 7.41 (m, 2H, Benzo), 7.65 (m, 2H, Benzo). Thirteen cyclohexyl C*H*$_2$/C*H* resonances not located. ^{13}C NMR (benzene-d_6): δ = 22.97, 24.51, 25.36, 27.05, 27.30, 27.61, 27.93, 28.48, 29.03, 31.00, 40.01 (CHMe$_2$/cyclohexyl *C*H$_2$), 108.62, 112.63, 120.05, 122.43, 123.10, 123.60, 123.87, 124.08, 125.23 (Benzo/Cp/olefinic), 153.54 (*C*-O). Two CHMe$_2$/cyclohexyl *C*H$_2$ and one Cp/Benzo/olefinic resonances not located.

Preparation of (η^5-C_9H_5-1,3-$(CHMe_2)_2$)(η^1-C_9H_5-1,3-$(CHMe_2)_2$-1-C(κ^1-O)$(CH_2)_5$-4-C(κ^1-O)$(CH_2)_5$)Zr (1-(O^cHex)$_2$-1,4). This compound was prepared in a similar manner to **1-(O^cPent)$_2$-1,4** using 0.008 g (0.02 mmol) of **1** dissolved in 0.5 mL of benzene-d_6 and 3.4 μL (0.03 mmol) of cyclohexanone affording yellow **1-(O^cHex)$_2$-1,4**. Anal. Calcd. for $C_{42}H_{58}O_2Zr$: C,; H,. Found: C,; H,. ^{1}H NMR (benzene-d_6): δ = 0.78 (d, 8 Hz, 3H, CH*Me*$_2$), 0.92 (d, 8 Hz, 3H, CH*Me*$_2$), 1.04 (d, 8 Hz, 3H, CH*Me*$_2$), 1.17 (d, 8 Hz, 3H, CH*Me*$_2$), 1.21 (d, 8 Hz, 3H, CH*Me*$_2$), 1.31 (m, 6H, cyclohexanone C*H*$_2$), 1.48 (m, 3H, CH*Me*$_2$), 1.53 (d, 8 Hz, 3H, CH*Me*$_2$), 1.67 (d, 8 Hz, 3H, CH*Me*$_2$), 1.73 (m, 4H, cyclohexanone C*H*$_2$), 2.14 (m, 1H, C*H*Me$_2$), 2.64 (m, 1H, C*H*Me$_2$), 3.26 (m, 1H, C*H*Me$_2$), 3.42 (m, 1H, C*H*Me$_2$), 3.53 (dd, 4 Hz, 2 Hz, 1H, C4-*H*), 4.08 (d, 6 Hz, 1H, C7-*H*), 4.85 (dd, 9 Hz, 4 Hz, 1H, C5-*H*), 5.26 (dd, 9 Hz, 6 Hz, 1H, C6-*H*), 5.85 (s, 1H, C2-*H*), 6.51 (s, 1H, Cp*H*), 6.85 (m, 1H, η^5 Benzo), 6.94 (m, 1H, η^5 Benzo), 7.24 (m, 1H, η^5 Benzo), 7.66 (m, 1H, η^5 Benzo). ^{13}C NMR (benzene-d_6): δ = 18.63, 20.90, 21.26, 21.60, 23.23 (CH*Me*$_2$), 23.72, 23.82 (cyclohexanone *C*H$_2$), 24.05 (CH*Me*$_2$), 24.91 (*C*H$_2$), 25.66, 25.96 (CH*Me*$_2$), 27.04 (*C*H$_2$), 27.61, 28.10, 28.21, 29.79 (*C*HMe$_2$), 34.24, 37.61, 38.88, 41.77 (*C*H$_2$), 50.29 (*C4*), 70.26 (*C1*), 74.55 (*C7*), 89.00 (*C-O*), 112.43 (CpH), 118.30, 118.78 (Cp), 119.38 (*C5*), 119.92 (*C6*), 121.72, 122.59, 122.72, 123.82 (Benzo), 124.54 (Cp), 125.47 (*C-O*), 126.89 (Cp), 129.68 (*C2*), 136.50 (*C3a*), 152.35 (*C7a*), 154.72 (*C3*). Two cyclohexyl *C*H$_2$ resonances not located.

Preparation of (η^5-C_9H_5-1,3-$(CHMe_2)_2$)(η^1-C_9H_5-1,3-$(CHMe_2)_2$-1-C(κ^1-O)$(CH(CH_2)_2)_2$-4-C(κ^1-O)$(CH(CH_2)_2)_2$)Zr (1-(O^cPr)$_2$)$_2$-1,4). This compound was prepared in a similar manner to **1-(O^cPent)$_2$-1,4** using 0.007 g (0.02 mmol) of **1** dissolved in 0.5 mL of benzene-d_6 and 3.2 μL (0.03 mmol) of dicyclopropylketone

affording yellow **1-(O(^{c}Pr)$_2$-1,4)$_2$**. Anal. Calcd. for $C_{44}H_{58}O_2Zr$: C, 74.42; H, 8.23. Found: C, 74.02; H, 7.80. ^{1}H NMR (benzene-d_6): δ = 0.01 (m, 2H, cyclopropyl C*H*$_2$), 0.14 (m, 2H, cyclopropyl C*H*$_2$), 0.20 (m, 1H, cyclopropyl C*H*), 0.33 (m, 4H, cyclopropyl C*H*$_2$), 0.42 (m, 3H, cyclopropyl C*H*/C*H*$_2$), 0.51 (m, 1H, cyclopropyl C*H*), 0.53 (m, 2H, cyclopropyl C*H*$_2$), 0.66 (m, 2H, cyclopropyl C*H*$_2$), 0.75 (m, 2H, cyclopropyl C*H*$_2$), 0.84 (d, 8 Hz, 3H, CH*Me*$_2$), 0.93 (d, 8 Hz, 3H, CH*Me*$_2$), 1.16 (d, 8 Hz, 3H, CH*Me*$_2$), 1.19 (d, 8 Hz, 6H, CH*Me*$_2$), 1.41 (d, 8 Hz, 3H, CH*Me*$_2$), 1.43 (d, 8 Hz, 3H, CH*Me*$_2$), 1.45 (m, 1H, cyclopropyl C*H*), 1.49 (m, 3H, CH*Me*$_2$), 2.54 (m, 1H, C*H*Me$_2$), 2.75 (m, 1H, C*H*Me$_2$), 3.18 (m, 1H, C*H*Me$_2$), 3.34 (m, 1H, C*H*Me$_2$), 3.91 (dd, 4 Hz, 2 Hz, 1H, C4-*H*), 4.12 (d, 5 Hz, 1H, C7-*H*), 5.35 (dd, 9 Hz, 4 Hz, 1H, C5-*H*), 5.38 (dd, 9 Hz, 5 Hz, 1H, C6-*H*), 5.99 (s, 1H, C2-*H*), 6.50 (s, 1H, Cp*H*), 6.83 (m, 1H, η^5 Benzo), 6.98 (m, 1H, η^5 Benzo), 7.26 (m, 1H, η^5 Benzo), 7.50 (m, 1H, η^5 Benzo). ^{13}C NMR (benzene-d_6): δ = 0.73, 2.29, 2.40, 3.26, 3.38, 3.59, 4.17, 6.76 (cyclopropyl *C*H$_2$), 16.04, 17.11 (cyclopropyl *C*H), 18.85 (CH*Me*$_2$), 20.55 (cyclopropyl *C*H), 20.77, 21.24, 21.80, 22.72, 23.02 (CH*Me*$_2$), 24.67 (cyclopropyl *C*H), 25.07, 25.46 (CH*Me*$_2$), 27.70, 27.87, 28.34, 31.48 (C*H*Me$_2$), 50.91 (*C4*), 71.81 (*C1*), 76.18 (*C7*), 86.98 (*C*-O insert at C1), 100.08 (*C7a*), 113.56 (*Cp*H), 118.98, 119.08 (Cp), 119.26 (*C6*), 121.49 (*C5*), 121.96, 122.80, 122.83, 123.93 (Benzo), 124.49, 127.28 (Cp), 130.90 (*C2*), 138.61 (*C*-O insert at C4), 151.22 (*C3a*), 152.31 (*C3*).

Preparation of (η^5-C$_9$H$_5$-1,3-(CHMe$_2$)$_2$)(η^5-C$_5$Me$_5$)(η^5-C$_9$H$_5$-1,3-(CHMe$_2$)$_2$-4-C(κ^1-O)(CH(CH$_2$)$_2$)$_2$-7-C(κ^1-O)(CH(CH$_2$)$_2$)$_2$)Zr (1-(O(^{c}Pr)$_2$)$_2$-4,7). A J. Young NMR tube charged with 0.01 g (0.01 mmol) of **1-(O(^{c}Pr)$_2$)$_2$-1,4** dissolved in approximately 0.5 mL of benzene-d_6 was heated at 45 °C for 12 hours, resulting in formation of **1-(O(^{c}Pr)$_2$)$_2$-4,7**. ^{1}H NMR (benzene-d_6): δ = 0.23 (m, 2H, cyclopropyl C*H*/C*H*$_2$), 0.34

(m, 2H, cyclopropyl C*H*/CH_2), 0.39 (m, 2H, cyclopropyl C*H*/CH_2), 0.39 (m, 2H, cyclopropyl C*H*/CH_2), 0.45 (m, 2H, cyclopropyl C*H*/CH_2), 0.49 (m, 2H, cyclopropyl C*H*/CH_2), 0.81 (m, 2H, cyclopropyl C*H*/CH_2), 0.97 (m, 2H, cyclopropyl C*H*/CH_2), 0.98 (d, 8 Hz, 6H, CH*Me*$_2$), 1.03 (m, 2H, cyclopropyl C*H*/CH_2), 1.19 (d, 8 Hz, 6H, CH*Me*$_2$), 1.20 (d, 6H, CH*Me*$_2$), 1.56 (d, 8 Hz, 6H, CH*Me*$_2$), 3.36 (m, 2H, C*H*Me$_2$), 3.38 (m, 2H, C*H*Me$_2$), 3.87 (d, 3 Hz, 2H, C4-*H* & C7-*H*), 6.13 (d, 3 Hz, 2H, C5-*H* & C6-*H*), 5.58 (s, 1H, C2-*H*), 6.47 (s, 1H, Cp*H*), 6.91 (m, 2H, Benzo), 7.57 (m, 2H, Benzo). ^{13}C NMR (benzene-d_6): δ = 2.59, 2.72, 2.79, 2.89, 3.72, 9.77, (cyclopropyl *C*H/*C*H$_2$), 20.71, 21.67, 24.60, 26.05 (CH*Me*$_2$), 26.69, 27.99 (*C*HMe$_2$), 49.44 (*C4 & C7*), 107.01 (*C2*), 103.93 (*C*-O), 115.14 (CpH), 120.16 (Cp), 121.95 (Benzo), 123.01 (Cp), 123.32 (Benzo), 127.16 (*C1 & C3*), 127.61 (*C5 & C6*), 127.15, 134.58 (*C3a & C7a*).

Preparation of (η^5-C_9H_5-1,3-(CHMe$_2$)$_2$)(η^1-C_9H_5-1,3-(CHMe$_2$)$_2$-1-C(κ^1-O)Me$_2$-4-C(κ^1-O)Me$_2$)Zr (1-(OMe$_2$)$_2$-1,4). A J. Young NMR tube was charged with 0.007 g (0.01 mmol) of **1** and dissolved in approximately 0.5 mL of benzene-d_6. On the vacuum line, the tube was frozen in liquid nitrogen and degassed. While at -196 °C, two equivalents (31 torr in a 17.2 mL bulb) of acetone were added. Upon thawing, the solution turned yellow and was identified as **1-(OMe$_2$)$_2$-1,4**. ^{1}H NMR (benzene-d_6): δ = 0.68 (d, 8 Hz, 3H, CH*Me*$_2$), 0.89 (d, 8 Hz, 3H, CH*Me*$_2$), 0.93 (d, 8 Hz, 3H, CH*Me*$_2$), 1.15 (d, 8 Hz, 3H, CH*Me*$_2$), 1.18 (s, 3H, OC*Me*), 1.21 (d, 8 Hz, 3H, CH*Me*$_2$), 1.23 (d, 3H, CH*Me*$_2$), 1.28 (s, 3H, OC*Me*), 1.35 (s, 3H, OC*Me*), 1.39 (s, 3H, OC*Me*), 1.51 (d, 8 Hz, 3H, CH*Me*$_2$), 1.61 (d, 8 Hz, 3H, CH*Me*$_2$), 1.92 (m, 1H, C*H*Me$_2$), 2.57 (m, 1H, C*H*Me$_2$), 3.14 (m, 1H, C*H*Me$_2$), 3.26 (dd, 5 Hz, 1 Hz, 1H, C7-*H*), 3.36 (m, 1H, C*H*Me$_2$), 3.64 (dd, 4 Hz, 2 Hz,1H, C4-*H*), 5.08 (dd, 9 Hz, 4 Hz, 1H, C6-*H*), 5.14 (ddd, 9 Hz, 4 Hz, 1 Hz, 1H, C5-*H*), 5.88 (s, 1H, C2-*H*), 6.71 (s, 1H, Cp*H*), 6.96 (m, 1H,

Benzo), 7.02 (m, 1H, Benzo), 7.39 (m, 1H, Benzo), 7.42 (m, 1H, Benzo). ^{13}C NMR (benzene-d_6): δ = 18.53, 20.65, 20.75, 21.63, 21.71, 24.84, 25.52, 26.07 (CH*Me*$_2$), 27.37, 27.40 (*C*HMe$_2$), 27.43 (OC*Me*$_2$), 27.99 (*C*HMe$_2$), 30.81 (2, *C*HMe$_2$ & OC*Me*$_2$), 32.38, 34.70 (OC*Me*$_2$), 49.09 (*C4*), 69.41 (*C1*), 78.08 (*C7*), 86.33 (*C*-*O*), 111.80 (CpH), 119.02 (*C5*), 119.70, 120.50 (Cp), 120.98 (*C6*), 121.23, 121.96 (Benzo), 123.41 (Cp), 123.81 (Benzo), 124.19 (Cp), 124.28 (Benzo), 130.90 (*C2*), 135.90 (*C3a*), 152.79 (*C7a*), 154.44 (*C3*).

Preparation of (η^5-C$_9$H$_5$-1,3-(CHMe$_2$)$_2$)(η^1-C$_9$H$_5$-1,3-(CHMe$_2$)$_2$-4-C(κ^1-O)Me$_2$-7-C(κ^1-O)Me$_2$)Zr (1-(OMe$_2$)$_2$-4,7). A thick walled glass vessel charged with 0.054 g (0.11 mmol) of **1** was dissolved in 3mL of pentane. On the vacuum line, the reaction vessel was frozen in liquid nitrogen and degassed. While at –196 °C, an excess of 3 equivalents (60 torr in a 100.1 mL bulb) of acetone were added. Upon thawing, the solution turned yellow, was allowed to stir for 1.5 hours and the volatiles removed *in vacuo*. Recrystallization from pentane afforded 30 mg (45 %) of yellow crystals identified as **1-(OMe$_2$)$_2$-4,7**. Anal. Calcd. for C$_{36}$H$_{50}$O$_2$Zr: C, 71.35; H, 8.32. Found: 71.54; H, 8.57. ^{1}H NMR (benzene-d_6): δ = 0.98 (d, 8 Hz, 6H, CH*Me*$_2$), 1.18 (d, 8 Hz, 6H, CH*Me*$_2$), 1.21 (d, 8 Hz, 6H, CH*Me*$_2$), 1.34 (s, 6H, OC*Me*), 1.47 (s, 6H, OC*Me*), 1.59 (d, 8 Hz, 6H, CH*Me*$_2$), 2.76 (m, 2H, C*H*Me$_2$), 3.44 (m, 2H, C*H*Me$_2$), 3.55 (d, 4 Hz, 2H, C4-*H* and C7-*H*), 5.40 (s, 1H, C2-*H*), 5.77 (d, 4 Hz, 2H, C5-*H* and C6-*H*), 6.63 (s, 1H, Cp*H*), 6.94 (m, 2H, Benzo), 7.44 (m, 2H, Benzo). ^{13}C NMR (benzene-d_6): δ = 20.46, 23.17, 23.58, 24.65 (CH*Me*$_2$), 26.67, 27.13 (*C*HMe$_2$), 29.91, 34.96 (OC*Me*$_2$), 46.84 (*C*-4 & *C*-7), 105.96 (*C*-2), 115.61 (Cp*H*), 120.10 (Cp), 121.44 (Benzo), 121.90 (Cp), 122.25 (Benzo), 124.48 (*C*-1 & *C*-3), 127.40 (*C*-5 & *C*-6), 134.88 (*C*-3a & *C*-7a).

Preparation of (η^5-C_9H_5-1,3-($CHMe_2$)$_2$)(η^1-C_9H_5-1,3-($CHMe_2$)$_2$-4-C(κ^1-O)Ph_2)Zr (1-(OPh_2)-4). This compound was prepared in a similar manner to **1-(O^cPent)$_2$-1,4** using 0.17 g (0.35 mmol) of **1** dissolved in approximately 10 mL of pentane and 65 mg (0.36 mmol) of benzophenone affording an orange solution. Recrystallization from pentane at -35 °C affords 129 mg (55 %) of **1-(OPh_2)-4** as an orange solid. Anal. Calcd. for $C_{56}H_{58}O_2Zr$: C, 76.88; H, 7.20. Found: C, 76.64; H, 7.03. ^{1}H NMR (benzene-d_6): δ = 0.81 (d, 8 Hz, 3H, CHMe_2), 0.84 (d, 8 Hz, 3H, CHMe_2), 0.87 (d, 8 Hz, 3H, CHMe_2), 1.06 (d, 8 Hz, 3H, CHMe_2), 1.21 (m, 1H, C*H*Me$_2$), 1.30 (m, 1H, C*H*Me$_2$), 1.39 (d, 8 Hz, 3H, CHMe_2), 1.41 (m, 3H, C*H*Me$_2$), 1.44 (m, 3H, CHMe_2), 1.46 (d, 8 Hz, 3H, CHMe_2), 3.37 (m, 1H, C*H*Me$_2$), 3.42 (m, 1H, C*H*Me$_2$), 3.86 (d, 6 Hz, 1H, C7-*H*), 4.66 (d, 6Hz, 1H, C4-*H*), 4.84 (dd, 12 Hz, 6 Hz, 1H, C5-*H*), 5.85 (s, 1H, Cp*H*), 5.98 (s, 1H, C2-*H*), 6.30 (dd, 12 Hz, 6 Hz, 1H, C6-*H*), 6.96 (m, 2H, Ph), 6.99 (m, 1H, η^5 Benzo), 7.03 (m, 2H, Ph), 7.06 (m, 1H, η^5 Benzo), 7.19 (m, 2H, Ph), 7.30 (m, 2H, Ph), 7.47 (m, 2H, Ph), 7.72 (m, 2H, η^5 Benzo). ^{13}C NMR (benzene-d_6): δ = 21.27, 22.74 (CHMe_2 on η^5, η^1 Ind), 23.99 24.06, 25.13 (CHMe_2 on η^5 Ind), 25.18 (*C*HMe$_2$ on η^5, η^1 Ind), 25.41 (CHMe_2 on η^5 Ind), 26.19 (*C*HMe$_2$ on η^5, η^1 Ind), 26.40, 26.51 (CHMe_2 on η^5, η^1 Ind), 28.94, 29.23 (*C*HMe$_2$ on η^5 Ind), 49.01 (*C4*), 74.44 (*C7*), 102.91 (*C*-O insert at C4), 109.54 (*C2*), 114.86 (*Cp*H on η^5 Ind), 118.41 (*C5*), 119.72, 120.15 (Cp on η^5 Ind), 123.51, 123.54, 123.66, 123.74 (Benzo on η^5 Ind), 124.19 (*C1*), 124.87 (Ph), 125.34, 125.75 (Cp on η^5 Ind), 125.88, 126.47, 127.06 (Ph), 128.28 (*C7a*), 128.56 (Ph), 129.39 (*C6*), 129.75 (*C3a*), 135.93 (*C3*), 151.82 (Ph).

Preparation of 1,1'-(1,3-diisopropylindene)$_2$. To a 20 mL scintillation vial charged with 0.057 g (0.12 mmol) of **1** dissolved in 5 mL of pentane was added 0.10 g (0.55 mmol) of benzophenone, resulting in a color change from burgundy to orange to red with precipitate within minutes. The solution was extracted through Celite, leaving 39

mg (84 %) of the coupled indene, **1,1'-(1,3diisopropylindene)$_2$**. ^{1}H NMR (benzene-d_6): δ = 0.43 (d, 8 Hz, 6H, CH*Me*$_2$), 0.45 (d, 8 Hz, 6H, CH*Me*$_2$), 1.19 (d, 8 Hz, 6H, CH*Me*$_2$), 1.20 (d, 8 Hz, 6H, CH*Me*$_2$), 2.35 (m, 2H, C*H*Me$_2$), 2.75 (m, 2H, C*H*Me$_2$), 6.50 (s, 2H, Cp*H*), 6.97 (m, 2H, Benzo), 7.09 (m, 4H, Benzo), 7.43 (m, 2H, Benzo), 7.65 (m, 2H, Benzo). ^{13}C NMR (benzene-d_6): δ = 19.67, 20.79, 21.84, 21.96, 27.03, 34.18 (CHMe$_2$), 64.20 (Cp), 119.84, 124.70, 124.99, 126.70, 133.74, 145.80, 149.64, 151.26 (Ind). EI MS (*m/z*) 199.3 (for half the molecule).

Preparation of (η^5-C$_9$H$_5$-1,3-(CHMe$_2$)$_2$)$_2$Zr(OC(Ph)CCH(O^{c}Pent)CHCHCHCH) (1-(OPh$_2$-O^{c}Pent). To a J. Young NMR tube charged with 0.006 g (0.01 mmol) of 1-(OPh$_2$)-4 dissolved in approximately 0.5 mL of benzene-d_6, 0.8 μL (0.01 mmol) of cyclopentanone was added resulting in a color change from orange to yellow. The compound was identified as **1-(OPh$_2$-O^{c}Pent)** by NMR spectroscopy. This complex decomposes over the course of hours at ambient temperature. ^{1}H NMR (benzene-d_6): δ = 0.64 (d, 8 Hz, 3H, CH*Me*$_2$), 1.02 (d, 8 Hz, 3H, CH*Me*$_2$), 1.19 (d, 8 Hz, 3H, CH*Me*$_2$), 1.21 (d, 8 Hz, 3H, CH*Me*$_2$), 1.24 (d, 8 Hz, 3H, CH*Me*$_2$), 1.44 (d, 8 Hz, 3H, CH*Me*$_2$), 1.48 (d, 8 Hz, 3H, CH*Me*$_2$), 1.50 (d, 8 Hz, 3H, CH*Me*$_2$), 1.54 (m, 1H, cyclopentanone C*H*$_2$), 1.67 (m, 1H, cyclopentanone C*H*$_2$), 1.80 (m, 1H, cyclopentanone C*H*$_2$), 1.89 (m, 1H, cyclopentanone C*H*$_2$), 2.39 (d, 6 Hz, 1H, ortho Ph), 2.74 (m, 1H, C*H*Me$_2$), 2.82 (m, 1H, C*H*Me$_2$), 3.41 (m, 1H, C*H*Me$_2$), 3.44 (m, 1H, C*H*Me$_2$), 5.57 (dd, 9 Hz, 5 Hz, 1H, meta Ph), 5.81 (dd, 9 Hz, 6 Hz, 1H, meta Ph), 6.03 (s, 1H, Cp*H*), 6.12 (dd, 9 Hz, 5 Hz, 1H, para Ph), 6.79 (s, 1H, Cp*H*), 6.83 (d, 9 Hz, 1H, ortho Ph), 6.93 (m, 2H, Benzo), 7.04 (m, 2H, Benzo), 7.12 (m, 4H, Benzo/Ph), 7.30 (m, 1H, Benzo/Ph), 7.59 (m, 1H, Benzo/Ph), 7.64 (m, 2H, Benzo/Ph), 7.68 (m, 1H, Benzo/Ph). ^{13}C NMR (benzene-d_6): δ = 19.61, 21.55, 21.96, 22.09, 22.17, 22.69, 23.89, 24.04 (CH*Me*$_2$), 27.12, 27.20, 28.89, 30.39 (*C*HMe$_2$), 35.32, 37.80, 37.84, 41.44 (cyclopentanone

C*H*$_2$), 46.15 (ortho Ph), 66.82 (*C*-3), 98.62 (cyclopentanone *C*-*O*), 112.45 (ipso Ph), 114.49 (CpH), 117.54 (Ph), 119.30 (*C*-7), 121.48 (Cp), 122.26 (Cp), 124.38 (*C*-2), 124.43 (*C*-4), 124.88 (Ph), 125.14 (*C*-5), 125.63 (Cp), 126.44 (*C*-6), 126.55 (Ph), 127.18 (Ph), 127.36 (Ph), 128.91 (Cp), 129.26 (Ph), 129.77 (Ph), 139.07 (Ph), 145.11 (*C*-7a), 150.66 (*C*-3a), 151.38 (*C*-1), 158.04 (benzophenone *C*-O). Four Benzo and two Ph resonances not located.

Preparation of (η^5-C_5Me_5)(η^5-C_9H_5-1,3-$(CHMe_2)_2$-4-C(κ^1-O)Ph_2-7-C(κ^1-O)Ph_2)Zr (3-$(OPh_2)_2$-4,7). This compound was prepared in a similar manner to **1-$(O^cPent)_2$-1,4** using 0.056 g (0.13 mmol) of **3** dissolved in approximately 6 mL of pentane and 63 mg (0.35 mmol) of benzophenone affording a red solution. Recrystallization from pentane at -35 °C affords 21 mg (20 %) of **3-$(OPh_2)_2$-4,7** as an orange solid. Anal. Calcd. for $C_{51}H_{54}O_2Zr$: C, 77.52; H, 6.89. Found: C, 77.78; H, 7.01. ^{1}H NMR (benzene-d_6): δ = 0.86 (d, 8 Hz, 6H, CH*Me*$_2$), 0.95 (d, 8 Hz, 6H, CH*Me*$_2$), 1.72 (m, 3H, C*H*Me$_2$), 2.20 (s, 15H, Cp* *Me*), 4.83 (d, 3 Hz, 2H, C4-*H* & C7-*H*), 5.54 (d, 3 Hz, 2H, C5-*H* & C6-*H*), 5.71 (s, 1H, C2-*H*), 6.89 (m, 2H, Ph), 7.03 (m, 2H, Ph), 7.10 (m, 6H, Ph), 7.19 (m, 2H, Ph), 7.46 (m, 2H, Ph), 7.50 (m, 4H, Ph), 7.98 (m, 2H, Ph). ^{13}C NMR (benzene-d_6): δ = 12.23 (Cp* *Me*), 21.72 (CH*Me*$_2$), 25.80 (*C*HMe$_2$), 26.12 (CH*Me*$_2$), 45.72 (*C4* & *C7*), 107.78 (*C2*), 108.65 (*C*-O), 120.18 (Cp*), 124.89, 125.38 (Ph), 125.65 (*C1* & *C3*), 126.33, 126.76, 127.01 (Ph), 127.25 (*C5* & *C6*), 127.15, 127.44, 127.56 (Ph), 134.94 (*C3a* & *C7a*), 149.16, 152.97 (Ph).

Characterization of (η^5-C_5Me_5)(η^5-C_9H_5-1,3-$(CHMe_2)_2$-4-C(κ^1-O)Ph_2)Zr (3-(OPh_2)-4). ^{1}H NMR (benzene-d_6): δ = 0.74 (d, 8 Hz, 3H, CH*Me*$_2$), 0.89 (d, 8 Hz, 3H, CH*Me*$_2$), 0.91 (d, 8 Hz, 3H, CH*Me*$_2$), 1.18 (d, 8 Hz, 3H, CH*Me*$_2$), 1.51 (m, 1H,

C*H*Me$_2$), 1.83 (m, 1H, C*H*Me$_2$), 2.07 (s, 15H, Cp* *Me*), 3.76 (d, 6 Hz, 1H, C7-*H*), 4.74 (m, 8 Hz, 5 Hz, 1H, C5-*H*), 4.76 (m, 5 Hz, 1H, C4-*H*), 5.69 (s, 1H, C2-*H*), 6.29 (dd, 8 Hz, 6 Hz, 1H, C6-*H*), 6.95 (m, 2H, Ph), 7.00 (m, 2H, Ph), 7.20 (m, 2H, Ph), 7.42 (m, 2H, Ph), 7.79 (m, 2H, Ph). ^{13}C NMR (benzene-d_6): δ = 11.59 (Cp* *Me*), 21.82, 22.94 (CH*Me*$_2$), 24.81 (*C*HMe$_2$), 25.75 (CH*Me*$_2$), 25.78 (*C*HMe$_2$), 26.10 (CH*Me*$_2$), 48.94 (*C4*), 73.93 (*C7*), 101.64 (*C*-O), 109.63 (*C2*), 117.61 (*C5*), 123.31 (*C1*), 124.61, 125.02, 125.13, 125.48, 125.74, 125.90 (Ph), 128.41 (*C7a*), 128.54 (*C3a*), 128.68 (Ph), 129.33 (*C6*), 135.22 (*C3*).

Preparation of (η^5-C$_9$H$_5$-1,3-(CHMe$_2$)$_2$)$_2$Zr(Ofluorenyl)$_2$ (1-(Ofluorenyl)$_2$). This compound was prepared in a similar manner to **1-(cyclopentanone)$_2$** using 0.054 g (0.11 mmol) of **1** dissolved in approximately 3 mL of pentane and 50 mg (0.28 mmol) of 9-fluorenone in 5 mL of pentane affording an red solution. Recrystallization from pentane at -35 °C affords 37 mg (39 %) of **1-(Ofluorenyl)$_2$** as an orange solid. Anal. Calcd. for C$_{56}$H$_{54}$O$_2$Zr: C, 79.11; H, 6.40. Found: C, 79.37; H, 6.19. ^{1}H NMR (benzene-d_6): δ = 0.51 (d, 8 Hz, 3H, CH*Me*$_2$), 0.73 (d, 8 Hz, 3H, CH*Me*$_2$), 1.10 (d, 8 Hz, 3H, CH*Me*$_2$), 1.19 (d, 8 Hz, 3H, CH*Me*$_2$), 1.21 (d, 8 Hz, 3H, CH*Me*$_2$), 1.37 (d, 8 Hz, 3H, CH*Me*$_2$), 1.38 (d, 8 Hz, 3H, CH*Me*$_2$), 1.70 (d, 8 Hz, 3H, CH*Me*$_2$), 2.72 (m, 1H, C*H*Me$_2$), 3.12 (m, 2H, C*H*Me$_2$), 3.69 (m, 1H, C*H*Me$_2$), 3.82 (d, 4 Hz, 1H, fluorenyl C1-*H*), 4.21 (s, 1H, Cp*H*), 5.17 (dd, 10 Hz, 4 Hz, 1H, fluorenyl C2-*H*), 5.64 (dd, 10 Hz, 6 Hz, 1H, fluorenyl C3-*H*), 6.13 (m, 6 Hz, 1H, fluorenyl C4-*H*), 6.27 (s, 1H, Cp*H*), 6.73 (m, 1H, Benzo), 6.83 (m, 4H, Benzo/Ph), 7.04 (m, 1H, Ph), 7.11 (m, 1H, Benzo), 7.20 (m, 1H, Ph), 7.27 (m, 1H, Ph), 7.36 (m, 1H, Ph), 7.41 (m, 1H, Ph), 7.46 (m, 1H, Benzo), 7.50 (m, 2H, Benzo/Ph), 7.80 (m, 1H, Benzo), 7.84 (m, 1H, Ph), 7.86 (m, 1H, Ph), 7.89 (m, 1H, Benzo), 8.10 (m, 1H, Ph). ^{13}C NMR (benzene-d_6): δ = 20.01, 20.31, 22.67, 22.73, 23.35, 25.11, 25.34, 25.77, 27.57, 28.38, 28.72, 29.84

($CHMe_2$), 49.86 (fluorenyl *C1*), 94.57 (*C*-*O*), 109.01 (Ph), 113.44 (fluorenyl *C*-4), 115.30 (CpH), 117.88 (Cp), 118.15 (fluorenyl *C*-8), 119.34 (Ph), 119.57 (Benzo), 119.58, 122.53 (Ph), 123.27 (Cp), 123.41, 123.50, 124.08 (Benzo), 124.42 (Cp), 124.67 (fluorenyl *C*-5), 124.71 (fluorenyl *C*-6), 124.86 (Benzo), 125.14 (fluorenyl *C*-3), 125.51 (Ph), 125.73 (Benzo), 125.85 (Ph), 126.01 (Cp), 126.02 (Benzo), 126.98 (Ph) 127.22 (fluorenyl *C*-7), 127.34, 127.42 (Ph), 127.54 (Benzo), 128.57 (Cp), 128.73 (Ph), 128.93 (fluorenyl *C*-2), 130.02, 132.92 , 134.05 (Cp), 134.07, 138.97, 140.62, 141.04, 148.06, 148.71 (Ph), 160.71 (fluorenyl *C*9-O).

Characterization of (η^5-C_9H_5-1,3-$(CHMe_2)_2$)(η^1-C_9H_5-1,3-$(CHMe_2)_2$-1-C(κ^1-O)$(CH_2)_4$-6-C(κ^1-O)$(CH(CH_2)_2)_2$Zr (1-(O^cPent)-1,(O^c(Prop)$_2$)-4). ^{1}H NMR (benzene-d_6): δ = 0.22 (m, 3H, cyclopropyl C*H*), 0.36 (m, 3H, cyclopropyl C*H*/CH_2), 0.72 (d, 8 Hz, 3H, CHMe_2), 0.89 (d, 8 Hz, 3H, CHMe_2), 1.29 (d, 8 Hz, 3H, CHMe_2), 1.34 (d, 8 Hz, 3H, CHMe_2), 1.48 (d, 8 Hz, 3H, CHMe_2), 1.49 (d, 8 Hz, 3H, CHMe_2), 1.40 – 2.10 (m, 8H, cyclopentanone CH_2), 2.01 (m, 1H, C*H*Me_2), 3.14 (m, 1H, C*H*Me_2), 3.30 (m, 1H, C*H*Me_2), 3.68 (m, Hz, 1H, C7-*H*), 4.02 (m, Hz, Hz, 1H, C4-*H*), 5.26 (m, 1H, C6-*H*), 5.39 (d, 5 Hz, 1H, C5-*H*), 5.89 (s, 1H, Cp*H*), 6.41 (s, 1H, Cp*H*), 6.92 (m, 2H, Benzo), 7.36 (m, 1H, Benzo), 7.47 (m, 1H, Benzo). Two CHMe_2, one C*H*Me_2 and four cyclopropyl CH_2/C*H* resonances not located.

Preparation of (η^5-C_5Me_5)(η^1-C_9H_5-1,3-$(CHMe_2)_2$-1-C(κ^1-O)Me_2-4-C(κ^1-O)Me_2)Zr (3-$(OMe_2)_2$-1,4). This compound was prepared in a similar manner to **1-$(OMe_2)_2$-1,4** using 0.007 g (0.02 mmol) of **3** dissolved in approximately 0.5 mL of benzene-d_6 and two equivalents (19 torr in a 31.6 mL bulb) of acetone affording yellow **3-$(OMe_2)_2$-1,4**. ^{1}H NMR (benzene-d_6): δ = 0.79 (d, 8 Hz, 3H, CHMe_2), 0.96 (d, 8 Hz, 3H, CHMe_2), 1.01 (d, 8 Hz, 3H, CHMe_2), 1.19 (d, 8 Hz, 3H, CHMe_2), 1.27 (s,

3H, OC*Me*), 1.31 (s, 3H, OC*Me*), 1.35 (s, 3H, OC*Me*), 1.38 (s, 3H, OC*Me*), 1.54 (s, 15H, Cp* *Me*), 2.05 (m, 1H, C*H*Me_2), 2.69 (m, 1H, C*H*Me_2), 3.71 (d, 4 Hz,1H, C4-*H*), 4.01 (d, 6 Hz, 1 Hz, C7-*H*), 5.18 (dd, 10 Hz, 4 Hz, 1H, C5-*H*), 5.26 (dd, 10 Hz, 6 Hz, 1 Hz, 1H, C6-*H*), 5.97 (s, 1H, C2-*H*). ^{13}C NMR (benzene-d_6): δ = 11.64 (Cp* *Me*), 18.68, 20.71, 20.96, 26.34, 27.83, 28.12 ($CHMe_2$), 31.09, 31.41, 31.63, 35.02 (OCMe_2), 49.38 (*C4*), 69.78 (*C1*), 73.78 (*C7*), 85.72 (*C3*), 117.48, 118.45, 120.34, 128.29, 130.61, 135.83 (Cp/Benzo), 152.97, 154.76 (*C*-O).

Preparation of (η^5-C_5Me_5)(η^5-C_9H_5-1,3-($CHMe_2$)$_2$)Zr(OC(CH_2)CMe_3)H (3-(OC(CH_2)CMe_3)H). This compound was prepared in a similar manner to **1-(O^{c}Pent)$_2$-1,4** using 0.008 g (0.02 mmol) of **3** dissolved in 0.5 mL of benzene-d_6 and 3.5 μL (0.03 mmol) of pinacolone affording yellow **3-(OC(CH_2)CMe_3)H)**. ^{1}H NMR (benzene-d_6): δ = 1.11 (s, 9H, *Me*), 1.30 (d, 8 Hz, 3H, CHMe_2), 1.39 (d, 8 Hz, 3H, CHMe_2), 1.42 (d, 8 Hz, 3H, CHMe_2), 1.44 (d, 8 Hz, 3H, CHMe_2), 1.82 (s, 15H, Cp* *Me*), 3.28 (m, 1H, C*H*Me_2), 3.56 (m, 1H, C*H*Me_2), 3.95 (m, 1H, olefinic C*H*), 4.04 (m, 1H, olefinic C*H*), 6.01 (s, 1H, Cp*H*), 6.05 (s, 1H, Zr-*H*), 6.85 (m, 2H, Benzo), 7.46 (pseudo d, 8 Hz, 1H, Benzo), 7.54 (pseudo d, 8 Hz, 1H, Benzo). ^{13}C NMR (benzene-d_6): δ = 11.89 (Cp* *Me*), 23.68, 23.98, 25.32, 27.40, 29.29, 29.62, 36.28 ($CHMe_2$/CH_2), 86.42, 115.49, 119.10, 122.70, 122.88, 122.97, 123.86, 124.69, 128.29 (Cp/Benzo/olefinic *C*H), 172.70 (*C*-O). One $CHMe_2$/CH_2 and two Cp/Benzo/olefinic CH resonances not located.

REFERENCES

[1] (a) Negishi, E.; Takahashi, T. *Acc. Chem. Res.* **1994**, *27*, 124. (b) Negishi, E.; Takahashi, T. *Bull. Chem. Soc. Jpn.* **1998**, *71*, 755. (c) Takahashi, T.; Kotora, M.; Hara, R.; Xi, Z. *Bull. Chem. Soc. Jpn.* **1999**, *72*, 2591. (d) *Comprehensive Organometallic Chemistry III*. Mingos, D. M. P.; Crabtree, R. H.; Bochmann, M., Eds.; Elsevier: Amsterdam, Netherlands, 2007; Vol. 4.

[2] Negishi, E.; Cederbaum, F. E.; Takahashi, T. *Tetrahedron Lett.* **1966**, *27*, 2829.

[3] Knight, K. S.; Wang, D.; Waymouth, R. M.; Ziller, J. *J. Am. Chem. Soc.* **1994**, *116*, 1845.

[4] Martin, S.; Brintzinger, H. *Inorganica Chimica Acta*. **1998**, *280*, 189.

[5] Liu, Y.; Shen, B.; Kotora, M.; Takahashi, T. *Angew. Chem., Int. Ed.* **1999**, *38*, 7.

[6] Nishihara, Y.; Aoyagi, K.; Hara, R.; Suzuki, N.; Takahashi, T. *Inorg. Chim. Acta.* **1996**, *252*, 91.

[7] Fagan, P. J.; Nugent, W. A.; Calabrese, J. C. *J. Am. Chem. Soc.* **1994**, *116*, 1880.

[8] Dioumaev, V. K.; Harrod, J. F. *Organometallics* **1997**, *16*, 1452.

[9] Fujita, K.; Yorimitsu, H.; Oshima, K. *Chem. Rec.* **2004**, *4*, 110.

[10] Bradley, C. A.; Keresztes, I.; Lobkovsky, E.; Chirik, P. J. *J. Am. Chem. Soc.* **2004**, *126*, 16937.

[11] Taber, D. F.; Louey, J. P.; Lim, J. A. *Tetrahedron Lett.* **1993**, *34*, 1993.

[12] Takahashi, T.; Fujimori, T.; Takashi, S.; Saburi, M.; Uchida, Y.; Rousset, C. J.; Negishi, E. *J. Chem. Soc., Chem. Commun.* **1990**, 182.

[13] Rousset, C. J.; Swanson, D. R.; Lamaty, F.; Negishi, E. *Tetrahedron Lett.* **1989**, *30*, 5105.

[14] Nugent, W. A.; Taber, D. F. *J. Am. Chem. Soc.* **1989**, *111*, 6435.

[15] Taber, D. F.; Louey, J. P.; Wang, Y.; Nugent, W. A.; Dixon, D. A.; Harlow, R. L. *J. Am. Chem. Soc.* **1994**, *116*, 9457.

[16] Taber, D. F.; Louey, J. P.; Wang, Y.; Nugent, W. A.; Dixon, D. A.; Harlow, R. L. *J. Am. Chem. Soc.* **1994**, *116*, 9457.

[17] Hansen, M. M.; Bartlett, P. A.; Heathcock, C. H. *Organometallics* **1987**, *6*, 2069.

[18] (a) Slough, G. A.; Hayashi, R.; Ashbaugh, J. R.; Shamblin, S. L.; Aukamp, A. M. *Organometallics* **1994**, *13*, 890. (b) Werner, H.; Mahr, N.; Frenking, G.; Jonas, V. *Organometallics* **1995**, *14*, 619. (c) Panichakul, D.; Su, Y.; Li, Y.; Deng, W.; Zhao, J.; Li, X. *Organometallics* **2008**, *27*, 6390.

[19] Erker, G.; Dorf, U.; Czisch, P.; Petersen, J. L. *Organometallics* **1986**, *5*, 668.

[20] Tillack, A.; Baumann, W.; Ohff, A.; Lefeber, C.; Spannenberg, A.; Kempe, R.; Rosenthal, U. *J. Organomet. Chem.* **1996**, *520*, 187.

[21] (a) Takahashi, T.; Kuzuba, Y.; Kong, F.; Nakajima, K.; Xi, Z. *J. Am. Chem. Soc.* **2005**, *127*, 17188. (b) Takahashi, T.; Song, Z.; Hsieh, Y.; Nakajima, K.; Kanno, K. *J. Am. Chem. Soc.* **2008**, *130*, 15236. (c) Ren, S.; Igarashi, E.; Nakajima, K.; Kanno, K.; Takahashi, T. *J. Am. Chem. Soc.* **2009**, *131*, 7492.

[22] Boag, N. M.; Rao, K. M. *Chem. Commun.* **2009**, 1499.

[23] (a) Rosenfeldt, F.; Erker, G. *Tetrahedron Lett.* **1980**, *21*, 1637. (b) Erker, G.; Dorf, U.; Czisch, P.; Petersen, J. L. *Organometallics* **1986**, *5*, 668.

[24] Erker, G.; Rosenfeldt, F. *J. Organomet. Chem.* **1982**, *224*, 29.

[25] Sun, Y.; Piers, W. E.; Yap, G. P. A. *Organometallics* **1997**, *16*, 2509.

[26] Shambatati, V. S.; Crowe, W. E.; Schreiber, S. L. *Angew. Chem., Int. Ed.* **1990**, *29*, 256.

[27] Peulecke, N.; Ohff, A.; Tillack, A.; Baumann, W.; Kempe, R.; Burlakov, V. V.; Rosenthal, U. *Organometallics* **1996**, *15*, 1340.

[28] Erker, G.; Czisch, P.; Mynott, R. *J. Organomet. Chem.* **1987**, *334*, 91.

[29] Hanna, T. A.; Baranger, A. M.; Bergman, R. G. *J. Org. Chem.* **1996**, *61*, 4532.

[30] Fujita, K.; Yorimitsu, H.; Shinokubo, H.; Oshima, K. *J. Org. Chem.* **2004**, *69*, 3302.

[31] Xiong, Y.; Yao, S.; Driess, M. *Chem. Eur. J.* **2009**, *15*, 5545.

[32] Lynch, R. A.; Vincenti, S. P.; Lin, Y. T.; Smucker, L. D.; Subba Rao, S. C. *J. Am. Chem. Soc.* **1972**, *94*, 8351.

[33] Bordwell pK_a tables. Reich, H. J. **2008**. Hhttp://www.chem.wisc.edu/areas/reich/pkatable/

[34] A similar experiment was performed by treating a benzene-d_6 solution of the cyclopentanone compound, **1-(O^{c}Pent-d_4)$_2$-1,4**, with 2.4 equivalents of natural abundance cyclopentanone. As measured by ^{1}H, ^{13}C HSQC NMR spectroscopy, conversion to the mixed isotopologue, **1-(O^{c}Pent)-1-(O^{c}Pent-d_4)-4** where the protio ketone had exchanged solely into the 1-position of the indenyl occurred after 24 hours at 22 ºC. After 50 hours, isomerization occurred to form **1-(O^{c}Pent)$_2$-4,7**.

[35] Veiros, L. F. *Organometallics* **2006**, *25*, 2266.

[36] Pangborn, A. B.; Giardello, M. A.; Grubbs, R. H.; Rosen, R. K.; Timmers, F. J. *Organometallics* **1996**, *15*, 1518.

[37] Bradley, C. A.; Lobkovsky, E.; Chirik, P. J. *J. Am. Chem. Soc.* **2003**, *125*, 8110.

[38] Bradley, C. A.; Keresztes, I.; Lobkovsky, E.; Chirik, P. J. *Organometallics* **2006**, *25*, 2080.

[39] Osadchev, A. Y.; Pushkarev, A. R.; Nikitina, Y. Y.; Shamanin, V.; Skorokhodov, S. S. *Russian J. of Gen. Chem.* **2000**, *70*, 1378.

[40] Hennion, G.F.; Odes, R. H. *J. Org. Chem.* **1966**, *31*, 1975.

[41] Varray, S.; Lazaro, R.; Martinez, J.; Lamaty, F. *Organometallics* **2003**, *22*, 2426.

[42] Wanat, R. A.; Collum, D. B. *Organometallics* **1986**, *5*, 120.

[43] The parent ion was not observed. 166 m/z was observed corresponding to the fragment consistent to loss of a methyl on the tertbutyl substituent.

Chapter 4

Fundamental Studies of Dinitrogen Activation and Reduction with *ansa*-Zirconocene Complexes

Abstract

The reduction of a series of *ansa*-zirconocene complexes was studied with the goal of promoting the activation and functionalization of dinitrogen. While alkali metal reduction of ethylene linked bis(indenyl) zirconocene dihalide complexes yielded the corresponding dimeric zirconocene (III) mono(halide) complexes, success was achieved with the reduction of the analogous [Me_2C]- and [Me_2Si]-linked *ansa* bis(cyclopentadienyl) zirconocene diiodide compounds. The stereochemistry of the zirconocene starting material influences the outcome of the reduction products. Sodium amalgam reduction of an equimolar *rac*/*meso* mixture of $Me_2Si(\eta^5\text{-}C_5H_3\text{-}3\text{-}CMe_3)_2ZrI_2$ furnished two new dimeric zirconocene dinitrogen complexes: one with *rac*, *rac* stereochemistry and the other with *rac, meso*. While reduction of pure *rac*-$Me_2Si(\eta^5\text{-}C_5H_3\text{-}3\text{-}CMe_3)_2ZrI_2$ furnished the dimeric *rac, rac* zirconocene dinitrogen complex, reduction of pure *meso*-$Me_2Si(\eta^5\text{-}C_5H_3\text{-}3\text{-}CMe_3)_2ZrI_2$ afforded both the expected dimeric *meso*, *meso* zirconocene dinitrogen compound along with a dimeric *meso*, *meso* zirconocene hydrido iodide complex. Interestingly, with *rac/meso*-$Me_2C(\eta^5\text{-}C_5H_3\text{-}3\text{-}R)_2ZrI_2$ (R = $SiMe_3$, CMe_3), only the *rac* isomer of the dimeric zirconocene dinitrogen complex was isolated, while the *meso* isomer only formed a dimeric zirconium mono iodide complex. Little success was achieved with the alkali metal reduction of the bulky *rac*-$Me_2Si(\eta^5\text{-}C_5H_2\text{-}1,3\text{-}(CMe_3)_2)_2ZrI_2$, and the corresponding zirconocene dihydride does not appear to undergo reductive elimination of dihydrogen under 4 atmospheres of dinitrogen to afford a dinitrogen complex. The hydrogenation of all zirconocene N_2 complexes was also explored.

Introduction

The functionalization of dinitrogen promoted by transition metal compounds has been widely explored,[1] with particular emphasis around studying and mimicking the Haber-Bosch cycle or nitrogenase enzymes, both of which functionalize N_2 to NH_3.[2,3] Recent advances in ammonia formation include homogeneous molybdenum catalysts that fix dinitrogen to ammonia by the "Chatt-cycle"[4] which involves a series of successive proton and electron transfer reactions.[5] Additionally, tantalum supported on a silica surface has demonstrated heterogeneous catalytic activity in the presence of dihydrogen to cleave N_2 and form N-H bond containing species.[6]

The use of low valent group 4 transition metals to activate and functionalize dinitrogen is of particular interest due to the ability of these compounds to impart electron density onto the coordinated N_2 ligand,[7] resulting in many examples of compounds with cyclopentadienyl,[8] guandinate, amidinate[8i,9] and multidentate ligands[10] with strongly activated side-on bound dinitrogen ligands. Many of these dinitrogen compounds have been shown to undergo addition of dihydrogen to afford at least one new N-H bond. While the majority of these complexes were prepared by alkali metal reductions and are likely incompatible with a catalytic cycle, dinitrogen activation has also been observed with isolable group 4 compounds (Figure 4.1) by mild alternatives. Pez and coworkers demonstrated the reactivity of a reduced titanocene dimer with dinitrogen to form a unique side-on, end-on dinitrogen complex (Figure 4.1a).[8a] Other isolable titanocene monohydrides have been shown to undergo reductive elimination to form dimeric dinitrogen complexes (Figure 4.1b & 4.1c).[8b,11] Similarly, one side-on bound dinitrogen complex supported by a sterically demanding *ansa*-ligand, *rac*-$[Me_2Si(\eta^5\text{-}C_5H_2\text{-}2\text{-}SiMe_3\text{-}4\text{-}CMe_3)_2Zr]_2(\mu_2,\eta^2,\eta^2\text{-}N_2)$, [*rac*-$BpZr]_2(\mu_2, \eta^2, \eta^2\text{-}N_2)$, was prepared in this manner from the corresponding monomeric zirconocene dihydride (Figure 4.1d),[8c] which is of utility for catalytic N_2

functionalization cycles that involve hydrogenation (Chapter 1, Figure 1.4). Unfortunately, the N-N bond length is only modestly elongated to 1.241(3) Å, suggestive of an $[N_2]^{2-}$ ligand rather than the desired $[N_2]^{4-}$ oxidation state. Upon hydrogenation, this compound readily reforms the zirconocene dihydride with loss of dinitrogen. Other zirconium dinitrogen complexes have also been synthesized by the reductive elimination of alkanes of the corresponding zirconocene alkyl hydrides (Figure 4.1e & 4.1f).[8d,12]

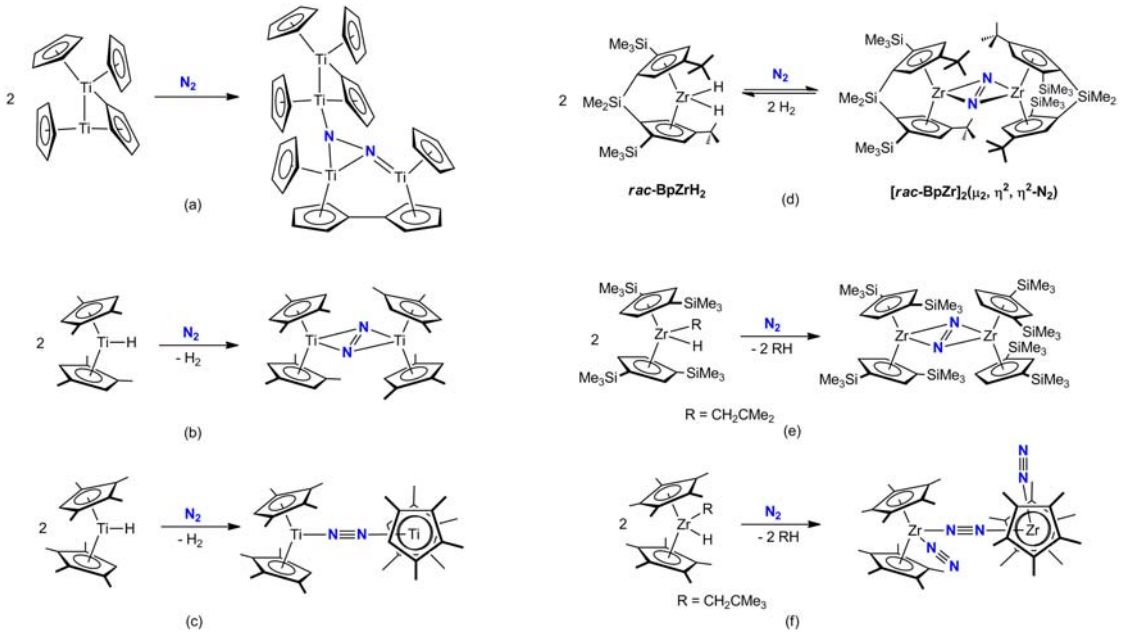

Figure 4.1. Activation of dinitrogen with isolable group 4 complexes.

Ansa-zirconocene complexes are attractive for dinitrogen activation due to their enhanced reactivity compared to their untethered counterparts,[13] and have found widespread application for olefin polymerization catalysis.[14] The configurational stability of the ancillary ligand framework allows for the rational synthesis of side-on bound dinitrogen complexes with zirconocene fragments twisted with respect to one another to impart additional zirconium-N_2 backbonding.[15] Ligands were chosen such that on the metal, the zirconium center would be slightly more reducing than with the

Bp ligand but ideally such that reductive elimination could still occur. Previously work in our laboratory focused on the preparation of $[Me_2Si(\eta^5\text{-}C_5Me_4)(\eta^5\text{-}C_5H_3\text{-}3\text{-}R)Zr]_2(\mu_2,\eta^2,\eta^2\text{-}N_2)$ (R = CMe_3, $CHMe_2$) by sodium amalgam reduction of the corresponding zirconocene dihalide. The resulting N_2 complexes are strongly activated with an N-N bond length of 1.406(4) Å for the R = CMe_3 derivative and as a result undergo hydrogenation to form two new N-H bonds.[8f,16] However, as demonstrated by the carbonyl stretching frequencies of the corresponding zirconocene dicarbonyl (Table 4.1), the metal center is likely too reducing for facile alkane or dihydrogen reductive elimination from the appropriate Zr(IV) alkyl hydride or dihydride compound.[8f] Therefore, both [Me_2Si] and [Me_2C] *ansa*-linked monosubstituted cyclopentadienyls with moderate electronic influences[17] were chosen as ligands for this study (Table 4.1). The well-known ethylene-1,2-bis(1-indenyl) ("EBI") ligand for olefin polymerization,[14] although likely too electron withdrawing,[17] along with a methylated version, were also explored.

Table 4.1. Infrared carbonyl stretching frequencies for zirconocene dicarbonyl complexes.

Compound	$\nu(CO)_{sym}$ (cm^{-1})	$\nu(CO)_{asy}$ (cm^{-1})	$\nu(CO)_{ave}$ (cm^{-1})
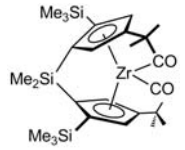 ***rac*-BpZr(CO)$_2$**	1967	1888	1927[17]
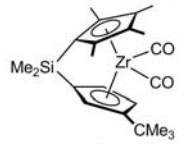 $Me_2Si(\eta^5\text{-}C_5Me_4)(\eta^5\text{-}C_5H_3\text{-}3\text{-}CMe_3)Zr(CO)_2$	1960	1873	1916.5[8f]
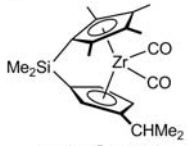 $Me_2Si(\eta^5\text{-}C_5Me_4)(\eta^5\text{-}C_5H_3\text{-}3\text{-}CHMe_2)Zr(CO)_2$	1962	1875	1918.5[8f]

Table 4.1. (continued)

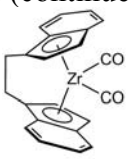 ***rac*-EBI-(CO)$_2$**	1977	1896	1936.5[17]
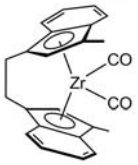 + meso ***rac/meso*-2-(CO)$_2$**	1975 1971	1888	
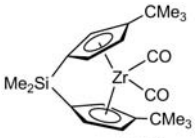 ***meso*-3-(CO)$_2$**	1969	1881	1925.0[17]
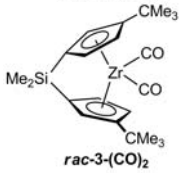 ***rac*-3-(CO)$_2$**	1968	1882	1925.0
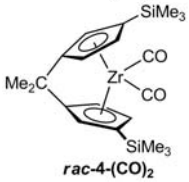 ***rac*-4-(CO)$_2$**	1972	1885	1928.5[16]
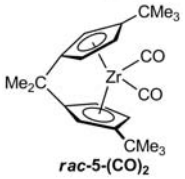 ***rac*-5-(CO)$_2$**	1967	1878	1922.5[16]
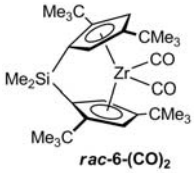 ***rac*-6-(CO)$_2$**	1962	1878	1920.0[17]

Results and Discussion

Reduction of Ethylene Bridged Bis(indenyl) Zirconocene Dihalide Complexes.

The reduction of commercially available EBI-zirconocene dichloride, *rac*-$CH_2CH_2(\eta^5\text{-}C_9H_6)_2ZrCl_2$, the corresponding zirconocene diiodide, ***rac*-1-I$_2$**, and methyl substituted EBI-zirconocene dihalide compounds, $CH_2CH_2(\eta^5\text{-}C_9H_5\text{-}3\text{-}Me)_2ZrX_2$ (X = Cl, I), **2-X$_2$**

was initially explored. The latter was synthesized with the goal that the electron donating methyl group would produce a more electron rich zirconium center and result in four electron dinitrogen activation. While pure *rac*-(EBI)$ZrCl_2$ was readily prepared by amine elimination by treating $Zr(NMe_2)_4$ with the protio ligand followed by subsequent treatment with excess chlorotrimethylsilane,[18] the stereoselectivity in preparing **2-Cl$_2$** was not conserved, furnishing an equimolar mixture of both the *rac* and *meso* isomers when following a similar method (eq. 4.1). Both sets of complexes were reduced with either excess 0.5 % sodium amalgam or KC_8 in a toluene solution under one atmosphere of dinitrogen.

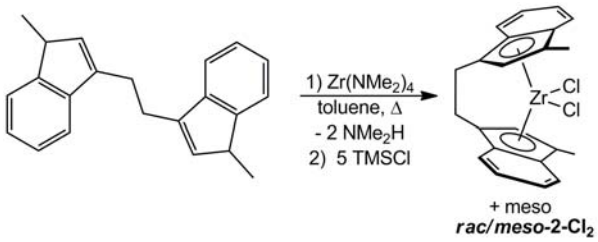

(eq. 4.1)

Intractable products along with the starting zirconocene were observed upon treatment of *rac*-(EBI)-$ZrCl_2$ with either reductant. However, both reaction conditions readily reduced ***rac*-1-I$_2$** to afford purple dimeric zirconocene bridging mono(iodide), [*rac*-(EBI)Zr]$_2$(μ_2-η^1,η^1-I)$_2$, **[*rac*-1-I]$_2$** (eq. 4.2), demonstrating the relative ease of reduction when employing metallocene diiodide precursors.[19] A similar green bridging chloride complex was observed when reducing the ethylene bridged bis(tetrahydroindenyl) titanium complex, $CH_2CH_2(\eta^5\text{-}C_9H_9)_2TiCl_2$ with magnesium turnings at 60 ºC.[20] Addition of one atmosphere of carbon monoxide to idealized D_2 symmetric **[*rac*-1-I]$_2$** resulted in formation of an equimolar mixture of ***rac*-ebi-Zr(CO)$_2$** and ***rac*-1-I$_2$**, behaving like a typical zirconocene (III) monohalide.[21] Longer reduction times did not afford any new tractable zirconium complexes.

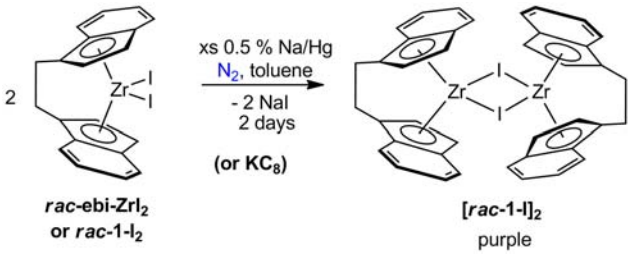

(eq. 4.2)

Unfortunately, reduction of ***rac/meso*-2-X_2** with either reducing agents also did not furnish any new tractable complexes. Examination of the carbonyl stretching frequencies of the corresponding zirconocene dicarbonyl compounds established insufficient electron density at the metal center for dinitrogen activation (Table 4.1).

Influence of the Stereochemistry on the Outcome of the Reduction of $Me_2Si(\eta^5\text{-}C_5H_3\text{-}3\text{-}CMe_3)_2ZrI_2$. Alkali metal reduction of zirconocene complexes containing modified "Bp" ligands was also studied. *Racemic* and *meso* diastereomers of $Me_2Si(\eta^5\text{-}C_5H_3\text{-}3\text{-}CMe_3)_2ZrX_2$ (X = Cl, I), ***rac/meso*-3-X_2**, were prepared according to literature procedures by addition of either excess chlorotrimethylsilane or excess pyridinium iodide to a toluene or THF solution of *r/m*-$Me_2Si(\eta^5\text{-}C_5H_3\text{-}3\text{-}CMe_3)_2Zr(NMe_2)_2$, ***r/m*-3-$(NMe_2)_2$** (eq. 4.3).[22] Pure ***meso*-3-X_2** and pure ***rac*-3-X_2** were also prepared in this manner starting from pure ***meso*-3-$(NMe_2)_2$** and pure ***rac*-3-{$Me_3SiN(CH_2)_3NSiMe_3$}**, respectively, and occurred without epimerization of the cyclopentadienyl ligand.[23] As removal of the bulky chelating $Me_3SiN(CH_2)_3NSiMe_3$ ligand was only achieved with HX sources, lutidinium chloride or pyridinium iodide was employed to afford ***rac*-3-Cl_2** or ***rac*-3-I_2**, respectively.

(eq. 4.3)

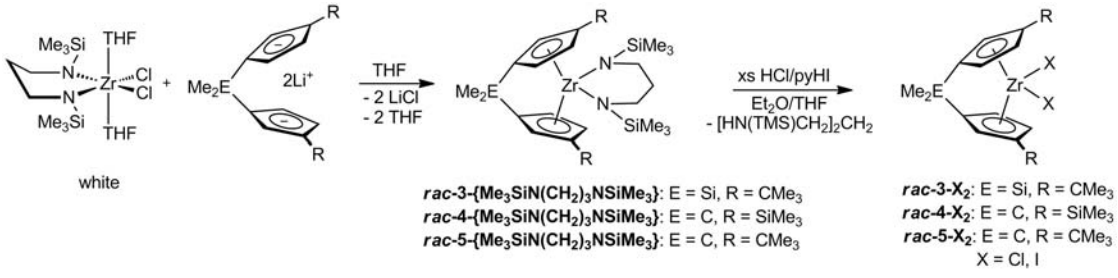

Sodium amalgam reduction of ***meso*-3-Cl$_2$** under an atmosphere of N_2 for one week only afforded purple [*meso*-$Me_2Si(\eta^5\text{-}C_5H_3\text{-}3\text{-}CMe_3)_2Zr]_2(\mu_2\text{-}\eta^1,\eta^1\text{-}Cl)_2$, **[*meso*-3-Cl]$_2$**, while the reduction of ***rac*-3-Cl$_2$** afforded **[*rac*-3-Cl]$_2$**, along with another unidentified complex. The reduction of an equimolar mixture of *rac/meso*-**3-Cl$_2$** furnished **[*meso*-3-Cl]$_2$**, **[*rac*-3-Cl]$_2$** and what is tentatively assigned as the C_1 symmetric mixed *rac, meso* stereoisomer.

(eq. 4.4)

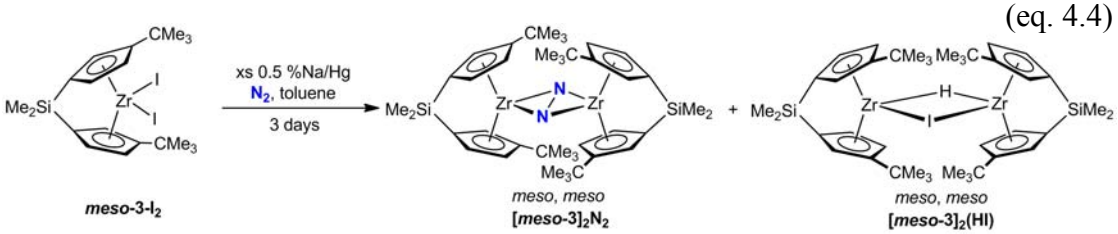

Reduction of a toluene solution of ***meso*-3-I$_2$** for three days with excess sodium amalgam under a dinitrogen atmosphere afforded two new products as judged by ^{1}H NMR spectroscopy, each with only one *meso* ligand environment (eq. 4.4). These two products with an overall teal color were difficult to separate from each another as successive crystallizations and extractions in different solvents only slightly changed the ratio of the compounds. Protonation of a 1:5 reduction mixture with HCl established that at least one contained a dinitrogen ligand as evidenced by the detection of 38 % of expected hydrazinium salt.[24] Fortuitous crystallization and single-crystal X-ray diffraction on the resulting complexes further established the activation of N_2 between two identical *meso* cyclopentadienyl bridged zirconocenes in a side-on manner forming, [*meso*-$Me_2Si(\eta^5\text{-}C_5H_3\text{-}3\text{-}CMe_3)_2Zr]_2(\mu_2\text{-}\eta^2,\eta^2\text{-}N_2)$, **[*meso*-3]$_2N_2$**. As shown in Figure 4.2, the dihedral angle defined as the angle formed by the planes of the zirconocene and the two cyclopentadienyl centroids is 46.5 º, similar to other dimeric side-on N_2 bound zirconocene complexes to allow for an appropriate twist for Zr_2N_2 backbonding.[15,8f,8i] An N(1)-N(2) bond length of 1.390(5) Å, is indicative of an $[N_2]^{4-}$ ligand, consistent with other twisted dimeric structures. The

Zr_2N_2 core of the molecule deviates from planarity by 17.0 º, similar to that found in a previously reported strongly activated side-on bound N_2 *ansa*-zirconocene[8f] and a series of mixed cyclopentadienyl guanidinate/amidinate zirconocene and hafnocene complexes.[8i] This puckering of the Zr_2N_2 core has been demonstrated experimentally[8i] and computationally[25] to correlate strongly with the N-N bond length; the greater the deviation the longer the d(N-N). There is no deviation from planarity in modestly activated [*rac*-BpZr]$_2$(μ_2, η^2, η^2-N_2).[8c] However, it is important to note that in the computational study, the correlation between the nonplanar geometry and the larger d(N-N) value was due to a mixing of the now properly oriented lone pairs on the ancillary amide ligand with the Zr_2N_2 core, allowing for a "more pronounced delocalization of the electron density of the N_2 ligand" and therefore longer d(N-N).[25] This correlation, however, is observed in another series of complexes that lack these ancillary ligand lone pairs.[8i]

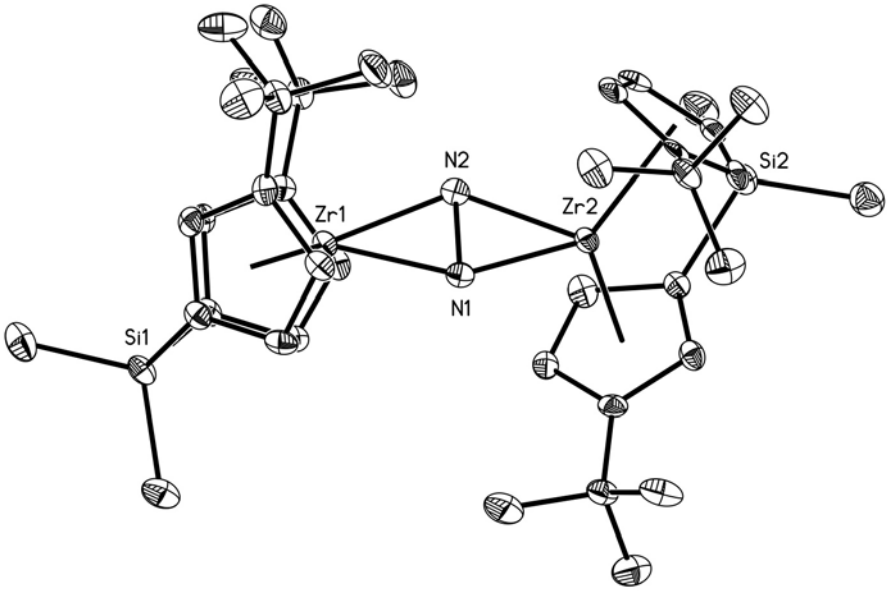

Figure 4.2. Molecular structure of **[*meso*-3]$_2$N$_2$** at 30 % probability ellipsoids. Hydrogen atoms omitted for clarity.

Addition of one atmosphere of carbon monoxide to a benzene-d_6 solution containing the reduction mixture formed neither the expected zirconocene dicarbonyl,

meso-$Me_2Si(\eta^5\text{-}C_5H_3\text{-}3\text{-}CMe_3)_2Zr(CO)_2$, ***meso*-3-(CO)$_2$**, nor ***meso*-3-I$_2$**. This observation appears to eliminate the possibility of a zirconocene (III) monoiodide complex as the second product, as only broad peaks were observed in the ^{1}H NMR spectrum of a benzene-d_6 solution. The unidentified reduction product was independently prepared by sodium amalgam reduction of ***meso*-3-I$_2$** under an argon atmosphere, further establishing the lack of an N_2 ligand, allowing for determination of the solid-state structure by X-ray diffraction. Due to residual co-crystallization with other crystals, the refinement was low but it does establish the connectivity of the molecule with only one iodide atom bridged between two zirconium centers (Figure 4.3). Interestingly, all of the bulky *tert*-butyl substituents lie on the same side of the iodide atom, likely to reduce the repulsion caused by the twisting of the metallocenes such that the Me_2Si linkers are oriented 58.6 º from one another. As the overall complex is diamagnetic, a hydride must also bridge the two zirconocenes, to allow for two Zr(III) centers that antiferromagnetically couple to one another to form [*meso*-$Me_2Si(\eta^5\text{-}C_5H_3\text{-}3\text{-}CMe_3)_2Zr](\mu_2\text{-}\eta^1,\eta^1\text{-}H, \mu_2\text{-}\eta^1,\eta^1\text{-}I)$, **[*meso*-3]$_2$(HI)**. While no obvious Zr-H stretch or resonance were observed in the infrared or ^{1}H NMR spectra, respectively, addition of excess iodomethane to a benzene-d_6 solution of **[*meso*-3]$_2$(HI)** furnished methane along with an equimolar mixture of both ***meso*-3-I$_2$** and *meso*-$Me_2Si(\eta^5\text{-}C_5H_3\text{-}3\text{-}CMe_3)_2Zr(Me)I$, ***meso*-3-(Me)I** (eq. 4.5).

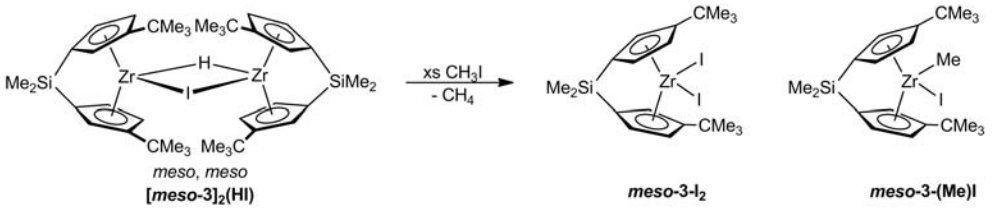

(eq. 4.5)

As further evidence, **[*meso*-3]$_2$(HI)** was prepared in the greatest yield by a sodium amalgam reduction of a toluene solution of ***meso*-3-I$_2$** in the presence of pyridinium iodide. While it is possible that the solvent is the source of the proton,

performing the reduction in benzene did not increase the ratio of **[*meso*-3]$_2$N$_2$** : **[*meso*-3]$_2$(HI)**, suggesting C-H activation of the ligand and intermolecular hydride migration. Reduction of ***meso*-3-I$_2$** for longer reaction times with excess sodium amalgam also did not change the product ratios.

While the observation of both zirconocene bridging monohalide and zirconocene bridging hydride dimers are common, mixed bridging hydride halide complexes of zirconium are rare. Royo reported a zirconocene dimer with a bridging hydride, a bridging chloride and a bridging fulvene; a solid-state Zr-H_b infrared stretch was reported at 1150 cm^{-1} and ^{1}H resonance in CH_2Cl_2 at -4.67 ppm.[26]

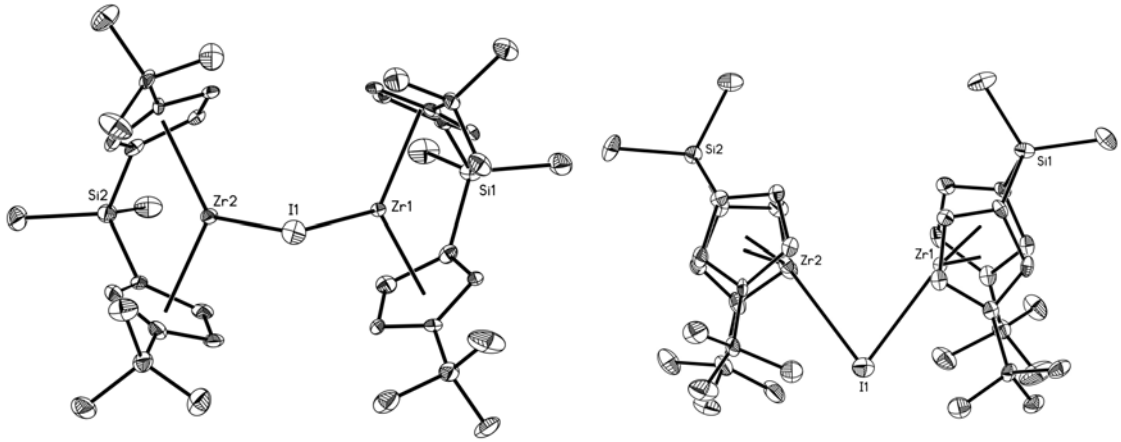

Figure 4.3. Molecular structure of **[*meso*-3]$_2$(H)I** at 30 % probability ellipsoids.

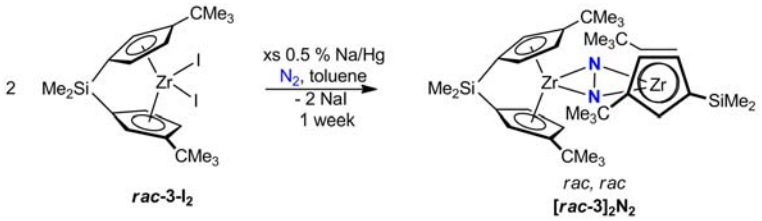

(eq. 4.6)

While reduction of the meso isomer of **3-I$_2$** afforded two products, only one product was observed for ***rac*-3-I$_2$**, requiring one week for its full conversion. Protonation of the reduction product with either HCl or H_2O yielded 75 and 63 % of the expected hydrazinium salt, respectively, suggesting a strongly activated dimeric side-on bound dinitrogen complex, [rac-$Me_2Si(\eta^5$-C_5H_3-3-$CMe_3)_2Zr]_2(\mu_2$-η^2,η^2-$N_2)$,

[*rac*-3]$_2$N$_2$ (eq. 4.6). Interestingly, sodium amalgam reduction of an equimolar mixture of *rac* and *meso*-**3-I$_2$** for three days under dinitrogen only afforded **[*rac*-3]$_2$N$_2$** along with a new C_1 symmetric product with 4 *tert*-butyl and 4 silyl methyl groups in a 1:4 ratio (eq. 4.7). None of **[*meso*-3]$_2$N$_2$** was observed, suggesting epimerization of

(eq. 4.7)

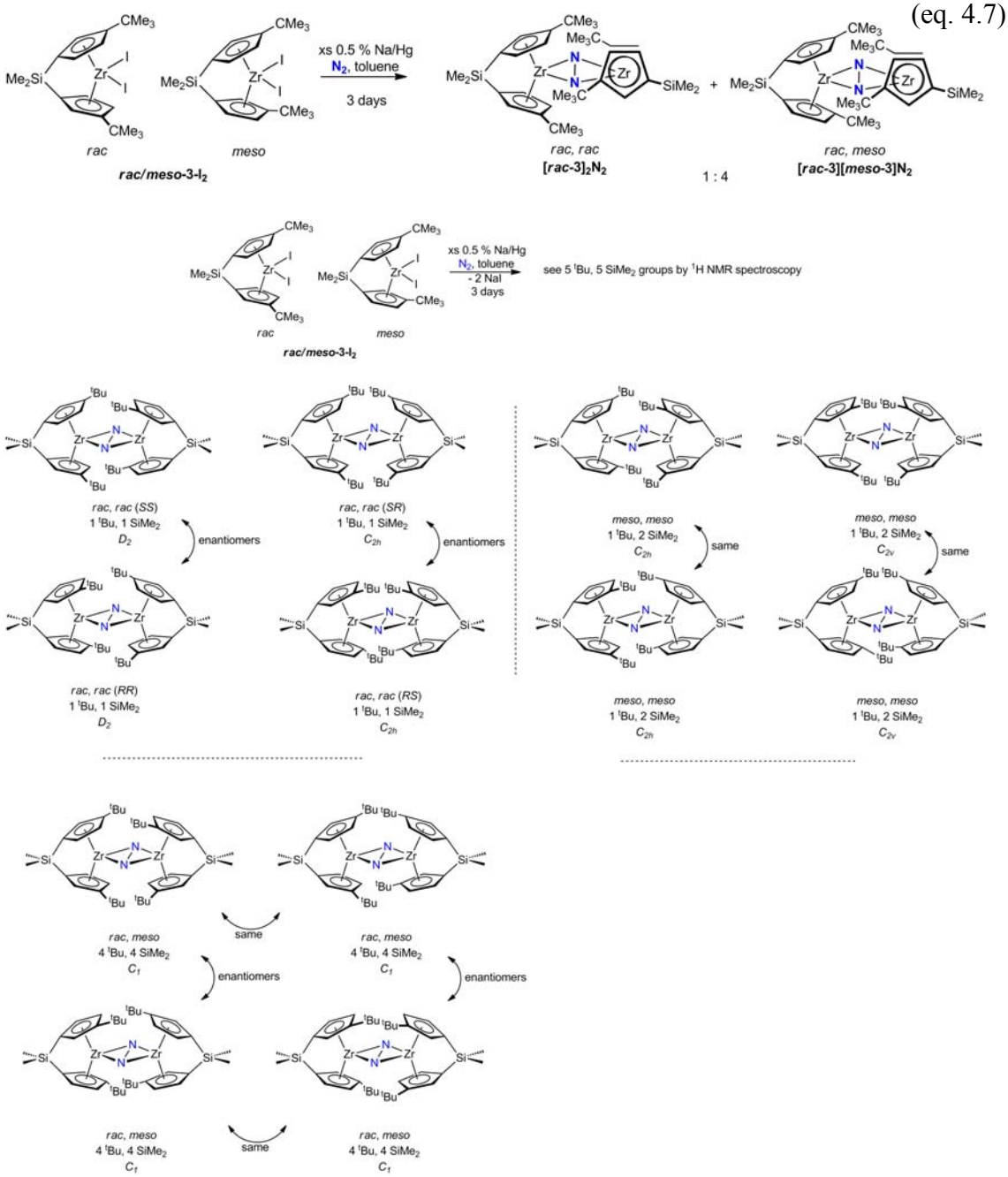

Figure 4.4. Different possible isomers of **3$_2$-N$_2$**, which demonstrate only 5 will be observable by ^{1}H NMR spectroscopy

the *meso* isomer observed only under these reduction conditions. Based on the different dimeric zirconocene dinitrogen complexes possible with this ligand set, this new complex is likely a heterochiral dimer with both a *rac* and a *meso ansa* linked cyclopentadienyl ligand (Figure 4.4). As further proof, addition of excess ditolylacetylene to the product mixture afforded both *rac* and *meso* zirconocene metallacyclopentadienes *rac/meso*-$Me_2Si(\eta^5\text{-}C_5H_3\text{-}3\text{-}CMe_3)_2Zr(cyclo\text{-}(Ctolyl)_4)$, ***rac/meso*-3-(*cyclo*-(Ctolyl)$_4$)** in a 1.2:1 ratio (eq. 4.8).[27]

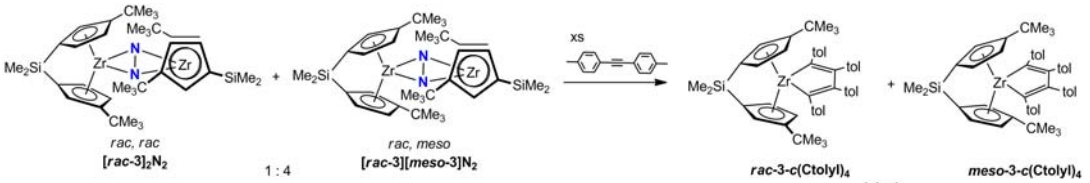

(eq. 4.8)

Similar to *rac*-$BpZrX_2$, addition of another *tert*-butyl substituent on each cyclopentadienyl ring yielded only the *racemic* isomer, *rac*-$Me_2Si(\eta^5\text{-}C_5H_2\text{-}1,3\text{-}(CMe_3)_2)_2ZrX_2$, ***rac*-6-X$_2$**, upon metalation of the dilithio salt, $Me_2Si(C_5H_3\text{-}1,3\text{-}(CMe_3)_2)_2$ with $ZrCl_4$.[28] Sodium amalgam reduction of ***rac*-6-I$_2$** in the presence of dinitrogen did not afford any tractable products that contained dinitrogen as evidenced by the lack of hydrazinium salt upon protonation with excess HCl.

Formation of Dinitrogen Complexes from only *Rac* Isomers of $Me_2C(\eta^5\text{-}C_5H_3\text{-}3\text{-}R)_2ZrI_2$ (R = $SiMe_3$, CMe_3). The sodium amalgam reduction of a series of equimolar *rac* and *meso* [Me_2C] *ansa* linked zirconocene dihalides was recently explored.[16] For example, when *rac/meso*-$Me_2C(\eta^5\text{-}C_5H_3\text{-}3\text{-}R)_2ZrI_2$ (R = $SiMe_3$, **4-I$_2$**; R = CMe_3, **5-I$_2$**) were reduced with excess sodium amalgam under an atmosphere of dinitrogen, dinitrogen complexes were only isolated with the *rac* zirconocenes, producing *rac*, *rac* dimeric side-on bound N_2 complexes, [*rac*-$Me_2C(\eta^5\text{-}C_5H_3\text{-}3\text{-}R)_2Zr]_2(\mu_2\text{-}\eta^2,\eta^2\text{-}N_2)$ (R = $SiMe_3$, **[*rac*-4]$_2$N$_2$**; R = CMe_3, **[*rac*-5]$_2$N$_2$**) in 5 - 10 % yield. In contrast, the *meso*

stereoisomer furnished *meso*, *meso* dimeric zirconocene bridging iodide complexes, [*meso*-$Me_2C(\eta^5\text{-}C_5H_3\text{-}3\text{-}R)_2Zr]_2(\mu_2\text{-}\eta^1\text{-}I)_2$ (R = $SiMe_3$, **[*meso*-4-I]$_2$**; R = CMe_3, **[*meso*-5-I]$_2$**), upon reduction. It is assumed that the steric nature of the *meso* isomer prevents complete reduction to the dinitrogen complex, as the sterically demanding $SiMe_3$ substituents cannot pack tightly enough to allow a side-on or end-on N_2 molecule access to the zirconocene core. Reduction of the mixture for longer periods of time had little impact on the yield of the dinitrogen complexes. As expected, reduction of the corresponding zirconocene dichlorides only afforded dimeric zirconocene bridging chloride complexes without dinitrogen activation. Reported here is the reduction chemistry of the pure *racemic* zirconocene diiodides.

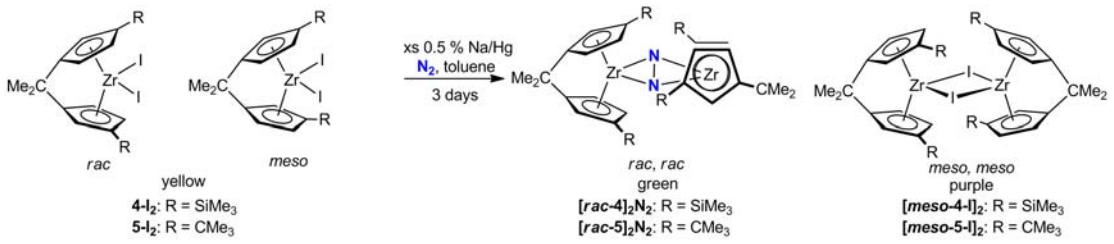

(eq. 4.9)

Both ***rac*-4-I$_2$** and ***rac*-5-I$_2$** were prepared in a similar manner ***rac*-3-I$_2$**, starting from ***rac*-4-{Me$_3$SiN(CH$_2$)$_3$NSiMe$_3$}** and ***rac*-5-{Me$_3$SiN(CH$_2$)$_3$NSiMe$_3$}**, respectively. Interestingly, the ligation of $Me_2C(\eta^5\text{-}C_5H_4\text{-}3\text{-}SiMe_3)_2$ to $Zr(NMe_2)_4$ in toluene formed solely the *rac* isomer of $Me_2C(\eta^5\text{-}C_5H_3\text{-}3\text{-}SiMe_3)_2Zr(NMe_2)_2$, ***rac*-4-(NMe$_2$)$_2$**, without formation of the *meso* isomer. Hence, as a potentially more expedient and higher yielding route to ***rac*-4-I$_2$**, iodination of ***rac*-4-(NMe$_2$)$_2$** with pyridinium iodide was employed (eq. 4.10). Reduction of either *rac* zirconocene diiodide, ***rac*-4-I$_2$** or ***meso*-5-I$_2$**, under dinitrogen afforded the desired dinitrogen complex in 55 % yield, without epimerization of the ligand to form any of the undesired *meso*, *meso* zirconocene monoiodide dimer.

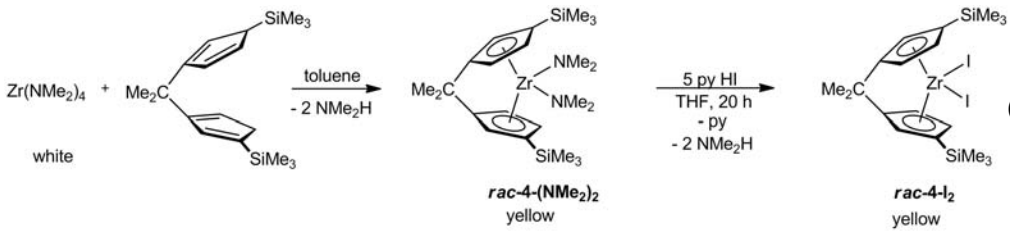

(eq. 4.10)

X-ray crystallographic studies on **[*rac*-4]$_2$N$_2$** established two independent side-on bound dinitrogen containing homochiral dimers each with two *rac* zirconocenes in the asymmetric unit (Figure 4.5). The stereochemistries of both molecules were assigned based on the Cahn-Ingold-Prelog configuration[29] as the (*SS*) enantiomers. Selected bond distances and angles for both molecules of **[*rac*-4]$_2$N$_2$** are presented in Table 4.2. Similar to **[*meso*-3]$_2$N$_2$**, the strongly activated $[N_2]^{4-}$ ligand has bond distances of 1.423(5) and 1.421(5) Å for the two molecules. Both monomers are twisted with respect to one another with a dihedral angle of 49.9 and 49.2 º and the Zr_2N_2 core of the molecule is puckered by 13.5 and 11.3°.

As shown in Table 4.2, it appears that in dimeric dinitrogen complexes, side-on coordination of N_2 such that the dihedral angle allows for zirconium N_2 backbonding is not the only prerequisite for strongly activated dinitrogen ligands. Based on Tables 4.1 and 4.2, the electron donating ability of the zirconium center and the steric bulk about the Zr_2N_2 core to allow for close dimerization as measured by the Zr-Zr distance are also factors that likely attribute to the modest N_2 activation found in [*rac*-Bp-Zr]$_2$(μ_2, η^2, η^2-N_2).[8c]

Similar to zirconocene dichlorides[17] and other zirconium dinitrogen complexes,[8c,8f] the introduction of either a [Me_2Si] or a [Me_2C] *ansa* linker results in an expansion of the inter-ring angle, α, and a modest contraction of the Cp_{cent}-M-Cp_{cent}, γ, angle from the unconstrained compounds, with a more pronounced effect in

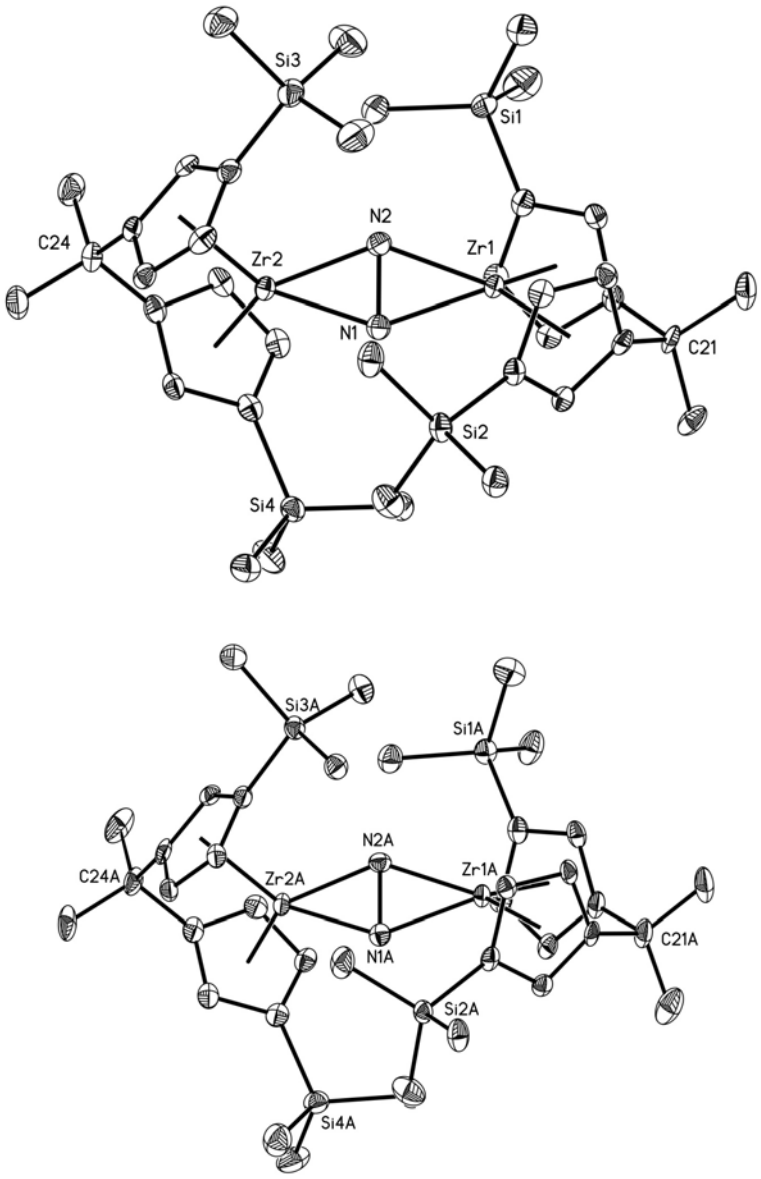

Figure 4.5. Views of both molecules of **(*SS*)-[*rac*-4]$_2$N$_2$** at 30 % probability ellipsoids. Hydrogen atoms omitted for clarity.

the carbon bridge (Table 4.2). Interestingly, this does not appear to explain the ability of ***meso*-3** to form a dimeric dinitrogen complex while ***meso*-5** only formed a dimeric bridging iodide complex, when both have one *tert*-butyl substituent on each cyclopentadienyl ring; the [Me_2C] *ansa* zirconocene complexes are more open and

Table 4.2. Comparison of selected metrical parameters for *ansa*-zirconocene dinitrogen complexes.

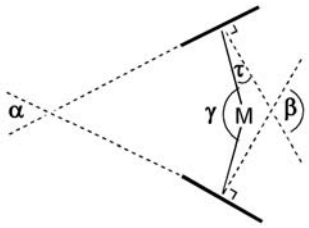

	[*rac*-BpZr]$_2$(μ_2, η^2, η^2-N_2)[8c]	[Me_2Si(η^5-C_5Me_4)(η^5-C_5H_3-3-CMe_3)Zr]$_2$(μ_2, η^2, η^2-N_2)[8f]	***meso*-3]$_2N_2$**	**[*rac*-4]$_2N_2$**	**[*rac*-4]$_2N_2$**[a]
N(1)-N(2) (Å)	1.241(3)	1.406(4)	1.390(5)	1.423(5)	1.421(5)
Zr-N (Å)	2.227(2)	2.090(3)	2.095(3)	2.101(4)	2.103(4)
	2.335(2)	2.087(3)	2.095(3)	2.092(4)	2.095(4)
	2.331(2)	2.079(3)	2.094(4)	2.085(4)	2.102(4)
	2.217(2)	2.102(3)	2.083(3)	2.100(4)	2.094(4)
Zr(1)-Zr(2) (Å)	4.373(3)	3.911(4)	3.903(5)	3.913(5)	3.929(5)
	4.383(3)				
Dihedral angle (º)	46.4	54.1	46.5	49.9	49.2
Zr_2N_2 deviation (º)	0.0	12.8	17.0	13.5	11.3
α (º)[b]	61.7	60.2	59.5	71.0	70.9
β (º)[b]	118.3	119.8	124.1	114.3	114.4
γ (º)	125.1	125.5	120.5	109.0	109.1
τ (º)	3.4	2.9	1.8	2.7	2.7

[a] Two molecules of **[*rac*-4]$_2N_2$** were located in the asymmetric unit. [b] Values taken as the average of both zirconocene monomers. [c] Figure to define metallocene geometries reprinted from reference 17. Copyright 2002 American Chemical Society.

should allow for close dimerization and activation of dinitrogen. It clearly is not an electronic effect as both **[*rac*-3]$_2N_2$** and **[*rac*-5]$_2N_2$** were formed readily. It should be noted however that α and γ do not appear to correlate to the Zr(1)-Zr(2) bond distance, as there is no difference between [Me_2Si] and [Me_2C] *ansa*-zirconocene complexes with strongly activated dinitrogen ligands.

Attempts of N_2 Activation via Reductive Elimination of *Ansa*-Zirconocene Dihydrides and Alkyl Hydrides. Based on the successful formation of [*rac*-Bp-Zr]$_2$(μ_2, η^2, η^2-N_2) from *rac*-BpZrH_2 and N_2, the reductive elimination of dihydrogen from the zirconocene dihydride, *rac*-$Me_2Si(\eta^5$-C_5H_2-1,3-$(CMe_3)_2)_2ZrH_2$, ***rac*-6-H_2** was targeted. ***Rac*-6-H_2** was readily prepared by heating a toluene solution of the zirconocene dimethyl, *rac*-$Me_2Si(\eta^5$-C_5H_2-1,3-$(CMe_3)_2)_2ZrMe_2$, ***rac*-6-Me_2**, at 45 ºC for 24 hours under an atmosphere of dihydrogen. Consistent with a monomeric 16 electron species,[30] the zirconium hydride appears at 7.29 ppm in the benzene-d_6 ^{1}H NMR spectrum, similar to *rac*-BpZrH_2.[8c] Also similar to *rac*-BpZrH_2, in the presence of excess H_2, this NMR resonance is not observed, suggesting rapid exchange between dihydrogen and the zirconium hydrides on the ^{1}H NMR time scale.[8c] Upon exposure to an atmosphere of N_2, the pale yellow solution immediately turned green, but did not appear to activate dinitrogen, even under 4 atmospheres of N_2. Attempts to prepare the corresponding zirconocene chloro hydride as a precursor for synthesis of a zirconocene alkyl hydride were unsuccessful; treatment of ***rac*-6-H_2** with Ph_3CCl or ***rac*-6-Cl_2** with one equivalent of $NaEt_3BH$ only furnished intractable products.

The hydrogenation of a benzene solution of *rac*-$Me_2C(\eta^5$-C_5H_3-3-$SiMe_3)_2ZrMe_2$, ***rac*-4-Me_2**, at 50 ºC for 48 hours afforded four dimeric zirconocene dihydride complexes, [*rac*-$Me_2C(\eta^5$-C_5H_3-3-$SiMe_3)_2ZrH]_2(\mu_2,\eta^1,\eta^1$-$H)_2$, **[*rac*-4-$H_2$]$_2$**, that are distinguishable by NMR spectroscopy (eq. 4.11). These four consist of one pair of homochiral dimers and one pair of heterochiral dimers. Each pair consists of one compound with *cis* terminal zirconium hydrides and one compound with *trans* hydrides. The homochiral dimers are consistent with having C_2 symmetry. The complex with *cisoid* terminal hydrides possesses a principal axis bisecting the bridging hydrides, exhibiting three zirconium hydride peaks located at -2.37 and 1.70 ppm for the bridging hydrides and one located at 3.94 for the terminal hydride. The

other homochiral dimer, with *transoid* terminal hydrides, possesses a principal axis perpendicular to the metallocene wedge, exhibiting one terminal zirconium hydride at 3.75 ppm and one bridging hydride at –0.01 ppm. The *cis* and *trans* heterochiral dimers exhibited C_1 (Zr-H_t: 3.76, 0.87; Zr-H_b: 1.21, 0.17 ppm) and C_i (Zr-H_t: 1.02; Zr-H_b: - 0.31 ppm) symmetry, respectively, which can be explained by the twisting of the metallocene equatorial planes commonly observed in other dimeric zirconocene dihydride complexes.[8c,13a]

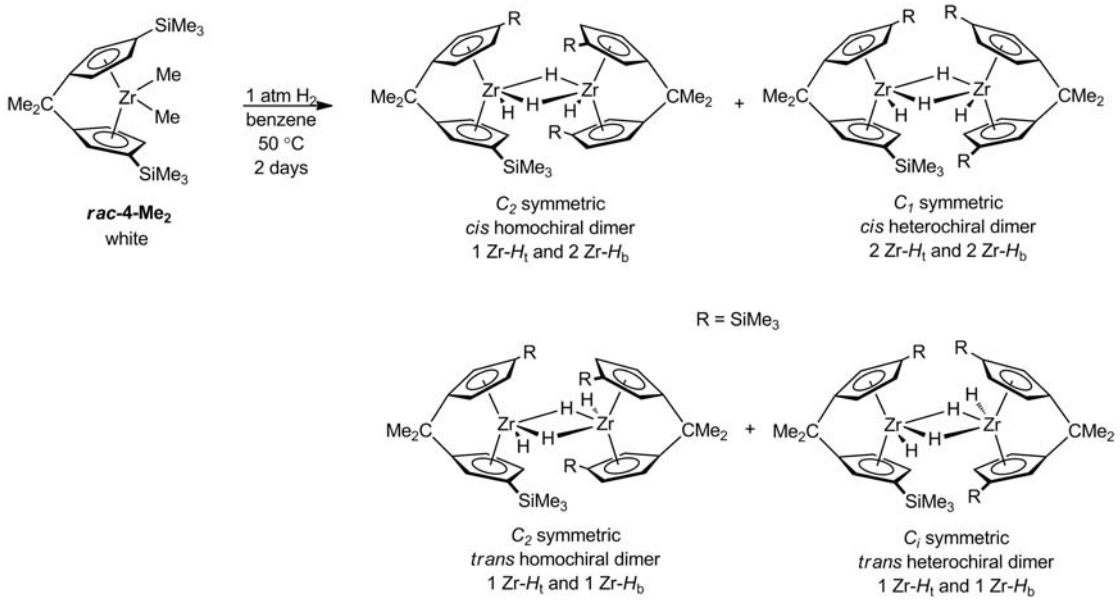

(eq. 4.11)

A ROESY NMR experiment on a benzene-d_6 solution of the **[*rac*-4-H_2]$_2$** diastereomers at 22 ºC demonstrated that on the NMR timescale, the two homochiral dimers were undergoing exchange with one another. As shown in Figure 4.6, the squares denote exchange occurring between the *cis* terminal hydride and both the *trans* terminal and bridging hydrides. The *cis* bridging hydride at 1.70 ppm was exchanging with the *trans* terminal hydride, while the *cis* bridging hydride at -2.37 ppm was exchanging with the *trans* bridging hydride. The same was occurring between the two heterochiral dimers; hydride exchange was denoted as ovals in Figure 4.6.

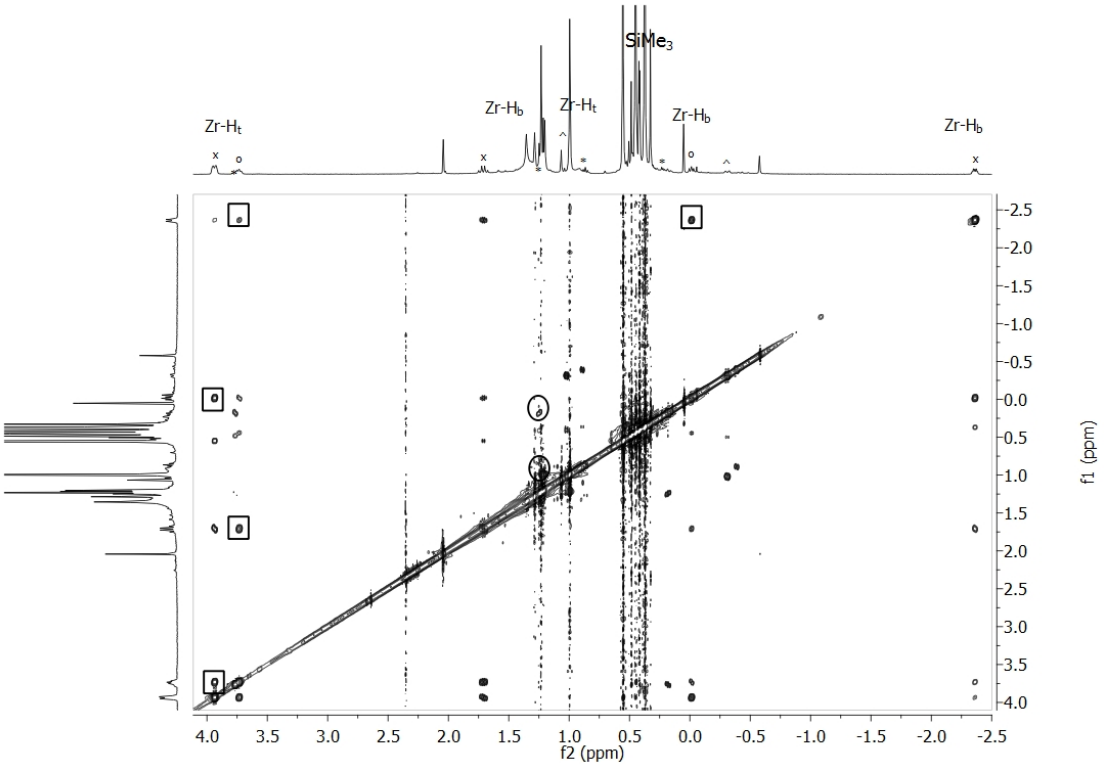

Figure 4.6. NOESY NMR spectrum of a benzene-d_6 solution of the four diastereomers of **[*rac*-4-H$_2$]$_2$**. The squares denote exchange between the hydrides of two homochiral dimers, while the ovals the hydrides of the two heterochiral dimers.

Attempts were also tried to prepare **[*rac*-4]$_2$N$_2$** via reductive elimination of the corresponding zirconocene dihydride, [*rac*-Me$_2$C(η^5-C$_5$H$_3$-3-SiMe$_3$)$_2$ZrH]$_2$(μ_2,η^1,η^1-H)$_2$, **[*rac*-4-H$_2$]$_2$**, or the zirconocene alkyl hydride. The latter was unsuccessfully prepared from alkyllithium addition to either of the zirconocene hydrido halide complexes, *rac*-Me$_2$C(η^5-C$_5$H$_3$-3-SiMe$_3$)$_2$Zr(H)X, ***rac*-4-(H)X** (X = Cl, I). Treating a benzene-d_6 solution of **[*rac*-4-H$_2$]$_2$** with Ph$_3$CCl only furnished ***rac*-4-Cl$_2$**, even with substoichiometric quantities of the Ph$_3$CCl reagent. Attempts to induce reductive elimination of dihydrogen from **[*rac*-4-H$_2$]$_2$** at 23 ºC have been unsuccessful.

Hydrogenation of Side-on Bound *Ansa*-Zirconocene Dinitrogen Complexes. The hydrogenation of both previously reported [Me$_2$Si(η^5-C$_5$Me$_4$)(η^5-C$_5$H$_3$-3-

R)Zr]$_2$(μ_2,η^2,η^2-N_2) (R = CMe_3, $CHMe_2$) demonstrated that while zirconocene hydrazido hydride complexes form readily under 1 atmosphere of dihydrogen at ambient temperature, upon heating at 55 ºC under vacuum, the hydrazide undergoes dehydrogenation to afford hydrido zirconocene dinitrogen complexes, [Me_2Si(η^5-C_5Me_4)(η^5-C_5H_3-3-R)ZrH]$_2$(μ_2,η^2,η^2-N_2) (eq. 4.12). The reactivity of these new side-on bound zirconocene dinitrogen complexes with dihydrogen was also explored.

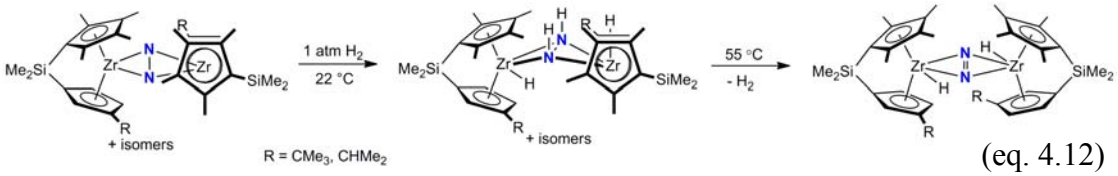

(eq. 4.12)

Exposure of benzene-d_6 solutions of either **[*meso*-3]$_2$N$_2$** or **[*rac*-3]$_2$N$_2$** to one atmosphere of dihydrogen at ambient temperature immediately afforded both the zirconocene hydrazido hydride, [Me_2Si(η^5-C_5H_3-3-CMe_3)$_2$ZrH]$_2$(μ_2,η^2,η^2-N_2H_2), **3$_2$-N$_2$H$_4$**, along with the hydrido zirconocene dinitrogen complexes, [Me_2Si(η^5-C_5H_3-3-CMe_3)$_2$ZrH]$_2$(μ_2,η^2,η^2-N_2), **3$_2$-H$_2$N$_2$**,[31] in a 2:1 and a 1:4 ratio for the *meso* and *rac* isomers, respectively (eq. 4.13 & 4.14). Over hours under an atmosphere of dihydrogen in benzene-d_6 solution, the dehydrogenated complex is enriched, with complete conversion to **3$_2$-H$_2$N$_2$** occurring under vacuum. Similar reactivity was observed with the reduction products from the equimolar mixture of both *rac* and *meso*-**3-I$_2$**, although the mixtures of products made the assignment of the mixed *rac*, *meso* zirconocene dimer products difficult.

Treatment of a benzene-d_6 solution of **[*rac*-4]$_2$N$_2$** with an atmosphere of dihydrogen furnished a minimum of two new zirconocene hydrazido hydride complexes, [Me_2C(η^5-C_5H_3-3-$SiMe_3$)$_2$ZrH]$_2$(μ_2,η^2,η^2-N_2H_2), **[*rac*-4]$_2$-N$_2$H$_4$**, along

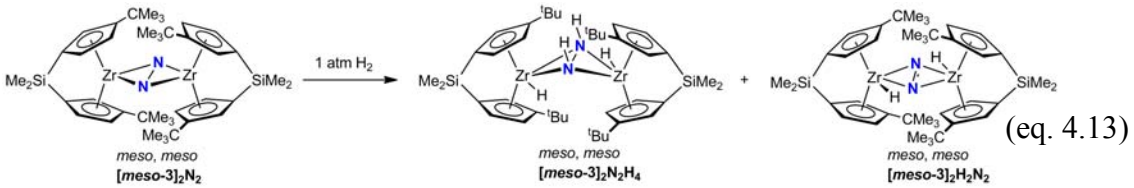

(eq. 4.13)

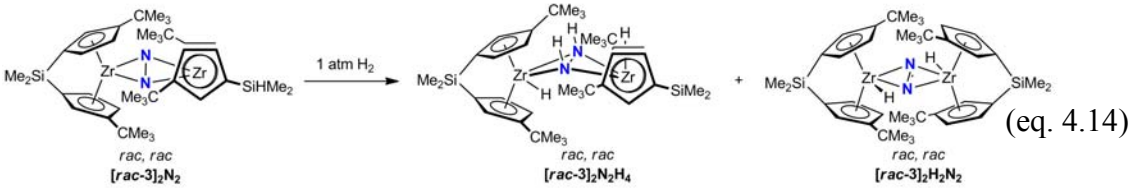

(eq. 4.14)

with one C_2 symmetric hydrido zirconocene dinitrogen complex, $[Me_2C(\eta^5\text{-}C_5H_3\text{-}3\text{-}SiMe_3)_2ZrH]_2(\mu_2,\eta^2,\eta^2\text{-}N_2)$, **[*rac*-4]$_2$-H$_2N_2$** (eq. 4.15). The ratio of the major **[*rac*-4]$_2$-N$_2$H$_4$** isomer to the single **[*rac*-4]$_2$-H$_2$N$_2$** isomer is approximately 4:1 immediately after H_2 addition, which remains constant in the presence of dihydrogen. In the absence of H_2, only **[*rac*-4]$_2$-H$_2$N$_2$** is observed. The decreased initial yield of dehydrogenated product is likely a consequence of the degree of dinitrogen reduction in the initial dinitrogen complex. As shown in Table 4.2, the dinitrogen complexes with shorter N-N bond distances form zirconocene hydrido hydrazido complexes that are more likely to undergo dehydrogenation. However, this is a comparison of very few data points.

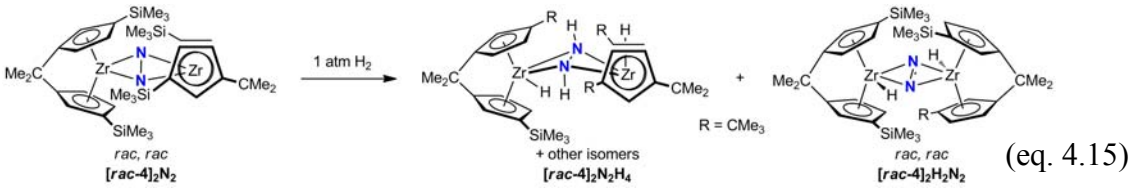

(eq. 4.15)

Heating benzene-d_6 solutions of either **[*rac*-4]$_2$-N$_2$H$_4$** or **[*rac*-4]$_2$-H$_2$N$_2$** to 65 ºC for 14 hours afforded a new C_2 symmetric product, commitant with loss of dihydrogen. The ^{1}H and ^{13}C NMR spectra are consistent with cyclometalation of one $SiMe_3$ substituent per zirconium center from sigma bond metathesis of a $SiMe_3$ C-H bond with the zirconium hydride. Likely structures of newly formed product, **[*rac*-4-**

CMH]$_2$N$_2$ are depicted in Figure 4.7 where the modified cyclopentadienyl rings are anti (left) or syn (right) to one another. Since there is a likely twisting of the metallocene equatorial planes, the anti diastereomer is likely the preferred and less sterically demanding isomer observed. Heating benzene-d_6 solutions of either **[*meso*-3]$_2$H$_2$N$_2$** or **[*rac*-3]$_2$H$_2$N$_2$** to 65 ºC for 24 hours resulted in no reaction, demonstrating the relative ease of activation of the C-H bond in a $SiMe_3$ versus a CMe_3 substituent.

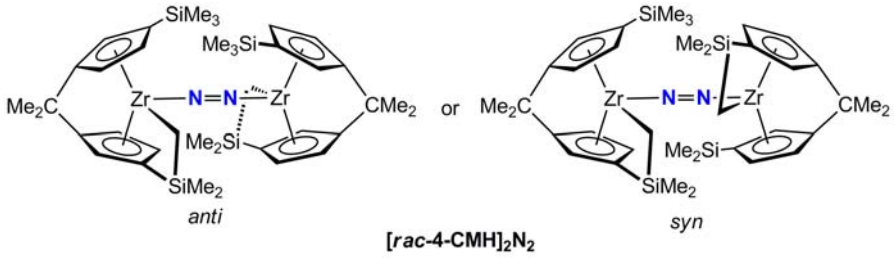

Figure 4.7. Possible C_2 symmetric products arising from the heating of either **[*rac*-4]$_2$-N$_2$H$_4$** or **[*rac*-4]$_2$-H$_2$N$_2$** to 65 ºC.

Conclusions

The reduction of a series of *ansa*-zirconocene complexes with [CH_2CH_2], [Me_2Si] and [Me_2C] bridges was explored. Interestingly, three different stereoisomers of side-on bound dinitrogen complexes were synthesized with *rac/meso*-$Me_2Si(\eta^5$-C_5H_3-3-$CMe_3)_2ZrI_2$ in the presence of dinitrogen: *meso*, *meso*; *rac*, *rac*; and *meso*, *rac* zirconocene dimers. Meanwhile, only *rac*, *rac* zirconocene dinitrogen dimers were synthesized when reducing $Me_2C(\eta^5$-C_5H_3-3-$R)_2ZrI_2$ (R = $SiMe_3$, CMe_3); better yields were achieved when starting with the pure *rac* isomers. All new dinitrogen compounds are reactive towards dihydrogen, furnishing zirconocene hydrazido hydride complexes. However, one equivalent of dihydrogen is readily lost, particularly in the absence of H_2, affording hydrido zirconocene dinitrogen complexes.

Experimental

General Considerations. All air- and moisture-sensitive manipulations were carried out using standard vacuum line, Schlenk or cannula techniques or in an M. Braun inert atmosphere drybox containing an atmosphere of purified nitrogen. Solvents for air- and moisture-sensitive manipulations were initially dried and deoxygenated using literature procedures.[32] Benzene-d_6 was distilled from sodium metal and stored over 4 Å molecular sieves or titanocene. Argon and hydrogen gas were purchased from Airgas Incorporated and passed through a column containing manganese oxide on vermiculite and 4 Å molecular sieves before admission to the high vacuum line. Carbon monoxide was passed through a column containing 4 Å molecular sieves before admission to the high vacuum line.

^{1}H NMR spectra were recorded on a Varian Inova 400 Spectrometer operating at 399.779 MHz (^{1}H), while ^{13}C spectra were collected on a Varian Inova 500 spectrometer operating at 125.704 MHz. All chemical shifts are reported relative to $SiMe_4$ using ^{1}H (residual) or ^{13}C NMR chemical shifts of the solvent as a secondary standard. ^{2}H NMR spectra were recorded on a Varian Inova 500 spectrometer operating at 76.740 MHz and the spectra were referenced using an internal benzene-d_6 standard. Single crystals suitable for X-ray diffraction were coated with polyisobutylene oil in a drybox and were quickly transferred to the goniometer head of a Siemens SMART CCD Area detector system equipped with a molybdenum X-ray tube (δ = 0.71073 A). Preliminary data revealed the crystal system. A hemisphere routine was used for data collection and determination of lattice constants. The space group was identified and the data were processed using the Bruker SAINT program and corrected for absorption using SADABS. The structures were solved using direct methods (SHELXS) completed by subsequent Fourier synthesis and refined by full-matrix least-squares procedures. Infrared spectra were collected on a Thermo Nicolet

spectrometer. Elemental analyses were performed at Robertson Microlit Laboratories, Inc., in Madison, NJ. *Rac*-ebi-$ZrCl_2$ was purchased from Strem and used without further purification. The following compounds were prepared according to literature procedures: $Zr(NMe_2)_4$,[18] $Li_2[CH_2CH_2(C_9H_6)_2]$,[14] $Li_2[Me_2C(C_5H_3\text{-}3\text{-}SiMe_3)_2]$,[16] $Li_2[Me_2C(C_5H_3\text{-}3\text{-}CMe_3)_2]$,[33] ***rac/meso*-3-$(NMe_2)_2$**,[22] ***meso*-3-$(NMe_2)_2$**,[22] ***rac*-3-{$Me_3SiN(CH_2)_3NSiMe_3$}**,[23b] ***rac/meso*-3-Cl_2**,[22] ***rac*-6-$ZrCl_2$**,[28] ***rac*-6-Me_2**.[28]

Preparation of $CH_2CH_2(C_9H_6\text{-}3\text{-}Me)_2$. A 250 mL round bottom flask was charged with 7.05 g (43.00 mmol) of $Li_2[CH_2CH_2(C_9H_6)_2]$ and dissolved in THF. An 180 ° needle valve was attached and the reaction was removed from the drybox and evacuated on a Schlenk line. Against an argon counterflow, 10.2 mL (164 mmol) of iodomethane was added via syringe to the solution at -78 °C. The reaction mixture was stirred for two days and the solvent removed *in vacuo*. The resulting yellow oil was extracted into toluene in a drybox and filtered through Celite. Subsequent solvent removal afforded 3.321 g (43 %) of a yellow oil identified as **$CH_2CH_2(C_9H_6\text{-}3\text{-}Me)_2$** as reported.[34] ^{1}H NMR (benzene-d_6): δ = 1.16 (d, 5 Hz, 6H, *Me*), 2.85 (s, 4H, CH_2 linker), 3.28 (q, 8 Hz, 2H, allyl C*H*), 6.00 (s, 2H, Cp*H*), 7.03 (m, 2H, benzo), 7.19 (m, 4H, benzo), 7.26 (br, 2H, benzo). ^{13}C {^{1}H} NMR (benzene-d_6): δ = 16.52 (*Me*), 26.26 (CH_2 linker), 43.90 (allyl CH), 119.13, 122.84, 124.97, 126.42, 135.53, 142.41, 144.73, 150.14 (Cp/Benzo).

Preparation of *rac*-$CH_2CH_2(\eta^5\text{-}C_9H_6)_2ZrI_2$ (*rac*-1-I_2 or *rac*-(EBI)-ZrI_2). A 20 mL scintillation vial was charged with 517 mg (1.24 mmol) of ***rac*-1-Cl_2** and dissolved in 5 mL of toluene. To the yellow solution, 1.32 g (6.60 mmol) of iodotrimethylsilane was added dropwise and the reaction stirred for 3 days. The solvent was removed *in vacuo* and the resulting orange solid washed with cold pentane yielding 400 mg (54

%) *rac*-**1-I$_2$**. ^{1}H NMR (benzene-d_6): δ = 2.76 (m, 4H, CH_2), 5.67 (d, 3Hz, 2H, Cp*H*), 6.81 (d, 3Hz, 2H, Cp*H*), 7.00 (m, 4H, Benzo), 7.48 (m, 4H, Benzo). ^{13}C {^{1}H} NMR (benzene-d_6): δ = 28.59 (CH_2 linker), 110.89, 113.57, 120.90, 122.56, 124.58, 126.82, 126.90 (Cp/Benzo). Two Cp/Benzo resonances not located.

Preparation of *rac/meso*-CH$_2$CH$_2$(η^5-C$_9$H$_5$-3-Me)$_2$ZrCl$_2$ (*rac/meso*-2-Cl$_2$). A 500 mL three-neck flask was charged with 4.104 g (8.52 mol) of **CH$_2$CH$_2$(η^5-C$_9$H$_6$-3-Me)$_2$** and 2.08 g (7.76 mol) of Zr(NMe$_2$)$_4$ and approximately 70 mL of toluene. The reaction mixture was stirred and heated to 100 ˚C for 17 hours and the NMe$_2$H was allowed to escape via a mineral oil bubbler. The red solution was cooled to room temperature and filtered. To the red filtrate, 5 mL (53.77 mol) of chlorotrimethylsilane was added dropwise and stirred for an additional hour and filtered. The orange solid was washed with hexanes and dried *in vacuo* yielding 450 mg (13 %) of ***rac/meso*-2-Cl$_2$** as reported.[34] ^{1}H NMR (benzene-d_6): δ = 2.22 (s, 6H, *Me*), 2.38 (s, 6H, *Me*), 2.89 (m, 4Hz, 2H, CH_2), 3.07 (m, 4Hz, 4H, CH_2), 3.42 (m, 4Hz, 2H, CH_2), 5.44 (s, 2H, Cp*H*), 5.48 (s, 2H, Cp*H*), 6.79 (m, 2H, Benzo), 6.92 (m, 4H, Benzo), 7.08 (m, 4H, Benzo), 7.21 (m, 6H, Benzo). ^{13}C {^{1}H} NMR (benzene-d_6): δ = 13.10, 13.40 (*Me*), 29.17, 29.38 (CH_2 linker), 113.16, 113.25, 115.24, 115.91, 118.75, 119.07, 119.55, 120.29, 121.75, 122.73, 123.57, 123.98, 124.19, 125.64, 125.96, 126.07, 126.15 (Cp/Benzo). One Cp/Benzo resonance not located.

Preparation of *rac/meso*-CH$_2$CH$_2$(η^5-C$_9$H$_5$-3-Me)$_2$ZrI$_2$ (*rac/meso*-2-I$_2$). This molecule was prepared in a similar manner to **1-I$_2$** using 200 mg (0.45 mmol) of ***rac/meso*-2-Cl$_2$** and 500 mg (2.50 mmol) of iodotrimethylsilane yielding 282 mg (93 %) of an red solid identified as ***rac*/meso-2-I$_2$**. ^{1}H NMR (benzene-d_6): δ = 2.52 (s, 6H, *Me*), 2.69 (s, 6H, *Me*), 2.76 (m, 7Hz, 2H, CH_2), 2.97 (m, 7Hz, 4H, CH_2), 3.26 (m, 7Hz,

2H, C*H*$_2$), 5.46 (s, 2H, Cp*H*), 5.54 (s, 2H, Cp*H*), 6.73 (m, 2H, Benzo), 6.86 (m, 4H, Benzo), 7.02 (m, 2H, Benzo), 7.10 (m, 4H, Benzo), 7.40 (m, 2H, Benzo), 7.46 (m, 2H, Benzo). ^{13}C {^{1}H} NMR (benzene-d_6): δ = 16.90, 17.41 (*Me*), 29.73, 29.83 (CH_2 linker), 117.53, 117.80, 118.53, 119.21, 119.34, 119.35, 119.62, 123.51, 124.51, 124.88, 125.45, 125.73, 125.85, 126.08, 126.20, 129.61, 130.16 (Cp/Benzo). One Cp/Benzo resonance not located.

Preparation of *rac/meso*-SiMe$_2$(η^5-C$_5$H$_3$-3-CMe$_3$)$_2$ZrI$_2$ (*rac/meso*-3-I$_2$). A 20 mL scintillation vial was charged with 2.130 g (4.46 mmol) of ***rac/meso*-3-(NMe$_2$)$_2$** and 2.15 g (11.14 mmol) of pyridinium iodide and approximately 18 mL of THF. The reaction mixture was stirred for 24 hours. The volatiles were removed *in vacuo* and the mixture extracted through Celite with pentane. The yellow solid was washed with pentane and dried *in vacuo* yielding 1.785 g (77.5 %) of yellow ***rac/meso*-3-I$_2$**. To enrich the *meso* isomer, pure ***meso*-3-(NMe$_2$)$_2$** was used as the starting material. ^{1}H NMR of ***meso*-3-I$_2$** (benzene-d_6): δ = 0.04 (s, 6H, Si*Me*$_2$), 0.18 (s, 6H, Si*Me*$_2$), 1.58 (s, 18H, CMe$_3$), 5.32 (m, 2H, Cp*H*), 6.23 (m, 2H, Cp*H*), 7.33 (m, 2H, Cp*H*). ^{13}C {^{1}H} NMR of ***meso*-3-I$_2$** (benzene-d_6): δ = -7.33, -2.71 (Si*Me*$_3$), 31.85 (C*Me*$_3$), 34.06, (*C*Me$_3$), 99.57, 110.95, 120.13, 132.47, 147.00, (Cp).

Preparation of *rac*-Me$_2$Si(η^5-C$_5$H$_3$-3-CMe$_3$)$_2$ZrI$_2$ (*rac*-3-I$_2$). This molecule was prepared in a similar manner to ***rac/meso*-3-I$_2$** but starting with 592 mg (0.98 mmol) of ***rac*-3-{Me$_3$SiN(CH$_2$)$_3$NSiMe$_3$}** and 2.15 g (11.14 mmol) of pyridinium iodide and stirred for 2 days with a benzene extraction, yielding 152 mg (18 %) of yellow ***rac*-3-I$_2$**. ^{1}H NMR (benzene-d_6): δ = 0.05 (s, 12H, Si*Me*$_2$), 1.50 (s, 18H, CMe$_3$), 5.70 (m, 2H, Cp*H*), 5.73 (m, 2H, Cp*H*), 7.17 (m, 2H, Cp*H*). ^{13}C {^{1}H} NMR (benzene-d_6): δ = -5.45, (Si*Me*$_3$), 31.25 (C*Me*$_3$), 34.45 (*C*Me$_3$), 102.38, 111.48, 116.43, 126.76, 153.95

(Cp).

Preparation of *rac*-$Me_2C(\eta^5\text{-}C_5H_3\text{-}3\text{-}SiMe_3)_2Zr\text{-}\{Me_3SiN(CH_2)_3NSiMe_3\}$ (*rac*-4-$\{Me_3SiN(CH_2)_3NSiMe_3\}$). A 100 mL round bottom flask was charged with 2.505 g (4.79 mmol) of $Zr\{Me_3SiN(CH_2)_3NSiMe_3\}Cl_2(THF)$ and 1.929 g $Li_2[Me_2C(C_5H_3\text{-}3\text{-}SiMe_3)_2]\cdot Et_2O$ and a 180 º needle valve attached. On the Schlenk line, the reaction vessel was degassed and approximately 70 mL of THF added at -196 ºC. The mixture was warmed to 0 ºC and stirred for 3 hours, then stirred at ambient temperature for an additional 15 hours. The volatiles of the resulting red solution were removed *in vacuo* and extracted through Celite with pentane. The tan solid was washed with cold pentane and the volatiles removed *in vacuo*, yielding 1.860 g (59 %) of a tan solid identified as ***rac*-4-$\{Me_3SiN(CH_2)_3NSiMe_3\}$**. ^{1}H NMR (benzene-$d_6$): δ = 0.22 (s, 18H, Si$Me_3$), 0.28 (s, 18H, Si$Me_3$), 1.06 (m, 2H, NCH_2CH_2), 1.53 (s, 6H, CMe_2), 3.06 (m, 2H, NCH_2CH_2), 3.40 (m, 2H, NCH_2), 5.70 (m, 2H, Cp*H*), 5.87 (m, 2H, Cp*H*), 6.93 (m, 2H, Cp*H*). ^{13}C {^{1}H} NMR (benzene-d_6): δ = -0.06, 3.53 (SiMe_3), 24.82, 27.90 (CMe_2), 36.05 (NCH_2CH_2), 45.98 (NCH_2), 105.08, 109.09, 120.84, 123.99 (Cp). One Cp resonance not located.

Preparation of *rac*-$Me_2C(\eta^5\text{-}C_5H_3\text{-}3\text{-}SiMe_3)_2Zr(NMe_2)_2$ (*rac*-4-$(NMe_2)_2$). A 250 mL round bottom flask was charged with 4.414 g (13.94 mmol) of **$Me_2C(\eta^5\text{-}C_5H_4\text{-}3\text{-}SiMe_3)_2$** and 3.80 g (14.20 mmol) of $Zr(NMe_2)_4$ and approximately 40 mL of toluene. A 180 º needle valve was attached and the reaction mixture degassed and stirred at ambient temperature for 20 hours, with the occasional degassing to remove some

NMe_2H. The volatiles of the yellow solution were removed *in vacuo*, yielding 6.30 g (91 %) of ***rac*-4-$(NMe_2)_2$** without any of the *meso* isomer. ^{1}H NMR (benzene-d_6): δ = 0.28 (s, 18H, Si*Me*$_3$), 1.53 (s, 6H, C*Me*$_2$), 2.74 (s, 12H, N*Me*$_2$), 5.57 (m, 2H, Cp*H*), 5.68 (m, 2H, Cp*H*), 6.45 (m, 2H, Cp*H*). ^{13}C {^{1}H} NMR (benzene-d_6): δ = 0.28 (Si*Me*$_3$), 24.95 (C*Me*$_2$), 36.37 (*C*Me$_2$), 48.01 (N*Me*$_2$), 106.88, 108.02, 119.23, 123.29, 130.37 (Cp).

Preparation of *rac*-$Me_2C(\eta^5$-C_5H_3-3-$SiMe_3)_2ZrI_2$ (*rac*-4-I_2). This molecule was prepared in a similar manner to ***rac*-3-I_2** with 1.860 (2.99 mmol) of ***rac*-4-{$Me_3SiN(CH_2)_3NSiMe_3$}** and 2.00 g (10.36 mmol) of pyridinium iodide and stirred for 2 days, yielding 300 mg (16 %) of yellow ***rac*-4-I_2**. Anal. Calcd for $C_{19}H_{30}Si_2I_2Zr$: C, 34.59; H, 4.58. Found: C, 34.90; H, 4.34. ^{1}H NMR (benzene-d_6): δ = 0.48 (s, 18H, Si*Me*$_3$), 0.99 (s, 6H, C*Me*$_2$), 5.29 (m, 2H, Cp*H*), 5.31 (m, 2H, Cp*H*), 7.17 (m, 2H, Cp*H*). ^{13}C {^{1}H} NMR (benzene-d_6): δ = 0.05 (Si*Me*$_3$), 23.48 (C*Me*$_2$), 36.63 (*C*Me$_2$), 109.86, 112.13, 120.03, 130.69, 132.40 (Cp).

Preparation of *rac*-$Me_2C(\eta^5$-C_5H_3-3-$SiMe_3)_2ZrMe_2$ (*rac*-4-Me_2). To a 50 mL round bottom flask charged with 418 mg (0.84 mmol) of ***rac*-4-$(NMe_2)_2$** dissolved in approximately and 8 mL of toluene, 790 mg (10.96 mmol) of $AlMe_3$ was slowly added and stirred for three days. The volatiles of the red solution mixture were carefully removed *in vacuo* and extracted through Celite with pentane. Recrystallization with pentane afforded 24 mg (7 %) of ***rac*-4-Me_2**. ^{1}H NMR (benzene-d_6): δ = 0.05 (s, 6H, Zr-*Me*), 0.33 (s, 18H, Si*Me*$_3$), 1.21 (s, 6H, C*Me*$_2$), 5.31 (m, 2H, Cp*H*), 5.35 (m, 2H,

Cp*H*), 6.53 (m, 2H, Cp*H*). ^{13}C {^{1}H} NMR (benzene-d_6): δ = -0.33 (Si*Me*$_3$), 24.14, 30.18, 30.52 (C*Me*$_2$/Zr-Me), 108.56, 110.25, 118.32, 121.87, 123.15 (Cp).

Preparation of [*rac*-Me$_2$C(η^5-C$_5$H$_3$-3-SiMe$_3$)$_2$ZrH$_2$]$_2$ ([*rac*-4-H$_2$]$_2$). A flame dried thick-walled glass bomb was charged with 90 mg (0.21 mmol) of ***rac*-4-Me$_2$** and dissolved in approximately 3 mL of benzene. The contents of the reaction vessel were frozen at -196 ºC and 1 atmosphere of H_2 added. The clear solution was heated to 50 ºC for 2 days and the volatiles removed *in vacuo*. Recrystallization from pentane under a dinitrogen atmosphere afforded 19 mg (11 %) of four isomers of **[*rac*-4-H$_2$]$_2$** as white crystals in a 1:1:0.6:0.2. Anal. Calcd for $C_{38}H_{64}Si_4Zr_2$: C, 55.95; H, 7.91. Found: C, 55.69; H, 8.22. ^{1}H NMR of major #1 isomer (benzene-d_6): δ = -2.37 (m, 1H, Zr-H_b), 0.37 (s, 18H, Si*Me*$_3$), 0.55 (s, 18H, Si*Me*$_3$), 0.99 (s, 6H, C*Me*$_2$), 1.23 (s, 6H, C*Me*$_2$), 1.70 (m, 1H, Zr-H_b), 3.94 (m, 2H, Zr-H_t), 5.41 (m, 2H, Cp*H*), 5.48 (m, 2H, Cp*H*), 5.54 (m, 2H, Cp*H*), 5.79 (m, 2H, Cp*H*), 6.13 (m, 2H, Cp*H*), 6.35 (m, 2H, Cp*H*). ^{1}H NMR of major #2 isomer (benzene-d_6): δ = -0.01 (m, 2H, Zr-H_b), 0.44 (s, 18H, Si*Me*$_3$), 0.45 (s, 18H, Si*Me*$_3$), 1.20 (s, 6H, C*Me*$_2$), 1.21 (s, 6H, C*Me*$_2$), 3.74 (m, 2H, Zr-H_t), 5.40 (m, 2H, Cp*H*), 5.57 (m, 2H, Cp*H*), 5.62 (m, 2H, Cp*H*), 5.81 (m, 2H, Cp*H*), 6.04 (m, 2H, Cp*H*), 6.42 (m, 2H, Cp*H*). ^{1}H NMR of minor isomer (benzene-d_6): δ = -0.31 (m, 2H, Zr-H_b), 0.42 (s, 18H, Si*Me*$_3$), 0.48 (s, 18H, Si*Me*$_3$), 1.02 (m, 2H, Zr-H_t), 1.24 (s, 6H, C*Me*$_2$), 1.28 (s, 6H, C*Me*$_2$), 5.46 (m, 2H, Cp*H*), 5.50 (m, 2H, Cp*H*), 5.55 (m, 2H, Cp*H*), 5.62 (m, 2H, Cp*H*), 6.18 (m, 2H, Cp*H*), 6.84 (m, 2H, Cp*H*). ^{1}H NMR of minor #2 isomer (benzene-d_6): δ = 0.17 (m, 1H, Zr-H_b), 0.36 (s, 9H, Si*Me*$_3$), 0.42 (s, 9H, Si*Me*$_3$), 0.48 (s, 9H, Si*Me*$_3$), 0.49 (s, 9H, Si*Me*$_3$), 0.87 (m, 1H, Zr-

H_t), 1.18 (s, 3H, CMe_2), 1.21 (m, 1H, Zr-H_b), 1.48 (s, 3H, CMe_2), 3.76 (m, 1H, Zr-H_t), 5.32 (m, 1H, Cp*H*), 5.36 (m, 2H, Cp*H*), 5.41 (m, 1H, Cp*H*), 5.46 (m, 1H, Cp*H*), 5.57 (m, 1H, Cp*H*), 5.60 (m, 1H, Cp*H*), 5.72 (m, 1H, Cp*H*), 6.18 (m, 1H, Cp*H*), 6.30 (m, 1H, Cp*H*), 6.52 (m, 1H, Cp*H*), 6.54 (m, 1H, Cp*H*). Two CMe_2 resonances not located. ^{13}C {^{1}H} NMR of major # 1 isomer (benzene-d_6): δ = 0.65, 1.02 (SiMe_3), 22.76, 24.13 (CMe_2), 34.83 (*C*Me$_2$), 96.48, 97.43, 97.82, 106.80, 111.36, 112.82, 113.10, 118.41, 122.63, 122.75 (Cp). ^{13}C {^{1}H} NMR of major # 2 isomer (benzene-d_6): δ = 0.69 (2) (SiMe_3), 23.87, 24.19 (CMe_2), 34.76 (*C*Me$_2$), 96.37, 97.82, 98.18, 109.88, 110.87, 114.20 (2), 116.45, 119.61, 125.52 (Cp). ^{13}C {^{1}H} NMR of minor isomer (benzene-d_6): δ = 0.15, 0.61 (SiMe_3), 23.96, 24.28 (CMe_2), 34.83 (*C*Me$_2$), 97.70, 100.59, 104.11, 112.72, 113.03, 114.20, 119.34, 120.54, 122.18, 123.48 (Cp). ^{13}C {^{1}H} NMR of minor #2 isomer (benzene-d_6): δ = 0.11, 0.63, 0.78 (SiMe_3), 98.08, 99.19, 100.59, 101.87, 106.29, 106.44, 108.28, 109.11, 109.96, 112.89 (2) , 113.97, 116.57, 118.20, 118.32, 121.86, 122.83, 123.56, 126.60, 128.98 (Cp). One SiMe_3, 6 CMe$_2$ and one Cp resonances not located.

Preparation of *rac*-Me$_2$C(η^5-C$_5$H$_3$-3-CMe$_3$)$_2$Zr-{Me$_3$SiN(CH$_2$)$_3$NSiMe$_3$} (*rac*-5-{Me$_3$SiN(CH$_2$)$_3$NSiMe$_3$}). This molecule was prepared in a similar manner to ***rac*-4-{Me$_3$SiN(CH$_2$)$_3$NSiMe$_3$}** with 1.512 g (2.89 mmol) of Zr{Me$_3$SiN(CH$_2$)$_3$NSiMe$_3$}Cl$_2$(THF) and 1.00 g Li$_2$[Me$_2$C(C$_5$H$_3$-3-CMe$_3$)$_2$] · 2/3 Et$_2$O yielding 891 mg (50 %) of ***rac*-5-{Me$_3$SiN(CH$_2$)$_3$NSiMe$_3$}** as a yellow solid. ^{1}H NMR (benzene-d_6): δ = 0.24 (s, 18H, SiMe_3), 1.07 (m, 2H, NCH_2), 1.20 (s, 18H, CMe_3), 1.52 (s, 6H, CMe_2), 3.14 (m, 2H, NCH$_2$CH_2), 3.37 (m, 2H, NCH_2), 5.58 (m,

4H, Cp*H*), 6.54 (m, 2H, Cp*H*). ^{13}C {^{1}H} NMR (benzene-d_6): δ = 3.11 (Si*Me*$_3$), 24.90, 28.16, 30.97, 33.18 (CMe_3/CMe_2), 35.62 (NCH_2CH_2), 45.41 (NCH_2), 100.20, 102.15, 109.99, 122.98, 141.33 (Cp).

Preparation of *rac*-$Me_2C(\eta^5\text{-}C_5H_3\text{-}3\text{-}CMe_3)_2ZrI_2$ (*rac*-5-I_2). This molecule was prepared in a similar manner to ***rac*-3-I_2** with 891 mg (1.43 mmol) of ***rac*-5-{$Me_3SiN(CH_2)_3NSiMe_3$}** and 829 mg (4.30 mmol) of pyridinium iodide and stirred for 3 days, yielding 585 mg (65 %) of yellow ***rac*-5-I_2**. ^{1}H NMR (benzene-d_6): δ = 0.97 (s, 6H, C*Me*$_2$), 1.46 (s, 18H, C*Me*$_3$), 5.19 (m, 4H, Cp*H*), 6.95 (m, 2H, Cp*H*).

Preparation of *rac*-$Me_2Si(\eta^5\text{-}C_5H_2\text{-}1,3\text{-}(CMe_3)_2)_2ZrI_2$ (*rac*-6-I_2). A 25 mL round bottom flask charged with 144 mg (0.25 mmol) of ***rac*-6-I_2** and 148 mg (0.38 mmol) of BI_3 and dissolved in approximately 10 mL of toluene. A 180 º needle valve was attached and the reaction mixture was stirred at ambient temperature for 2 days. The volatiles of the red solution were removed *in vacuo* and the resulting solid washed with pentane, affording 100 mg (53 %) of ***rac*-6-I_2** as an orange solid. ^{1}H NMR (benzene-d_6): δ = 0.60 (s, 6H, Si*Me*$_2$), 1.28 (s, 18H, C*Me*$_3$), 1.51 (s, 18H, C*Me*$_3$), 5.74 (m, 2H, Cp*H*), 7.53 (m, 2H, Cp*H*). ^{13}C {^{1}H} NMR (benzene-d_6): δ = 3.30 (Si*Me*$_2$), 30.65, 33.14, 34.85, 35.73 (CMe_3), 101.05, 112.22, 129.64, 149.59, 153.19 (Cp).

Preparation of *rac*-$Me_2Si(\eta^5\text{-}C_5H_2\text{-}1,3\text{-}(CMe_3)_2)_2ZrH_2$ (*rac*-6-H_2). A flame dried thick-walled glass bomb was charged with 147 mg (0.28 mmol) of ***rac*-6-Me_2** and dissolved in approximately 5 mL of toluene. The contents of the reaction vessel were

frozen at -196 ºC and 1 atmosphere of H_2 added. The clear solution was heated to 45 ºC for 2 days and the volatiles removed *in vacuo*. Recrystallization from pentane under a dinitrogen atmosphere afforded 72 mg (52 %) of ***rac*-6-H_2** as white crystals surrounded by a green solution. ^{1}H NMR (benzene-d_6): δ = 0.55 (s, 6H, Si*Me*$_2$), 1.24 (s, 18H, C*Me*$_3$), 1.44 (s, 18H, C*Me*$_3$), 5.63 (m, 2H, Cp*H*), 7.29 (s, 2H, Zr-*H*), 7.55 (m, 2H, Cp*H*). ^{13}C {^{1}H} NMR (benzene-d_6): δ = 3.78 (Si*Me*$_2$), 32.13, 32.77, 33.24, 34.60 (CMe_3), 112.73, 113.54, 147.88, 147.92 (Cp). One Cp resonance not located.

Preparation of [*rac*-$CH_2CH_2(\eta^5$-$C_9H_6)_2Zr]_2(\mu_2$-η^1,η^1-$I)_2$ ([*rac*-1-I]$_2$). A 100 mL round bottom flask was charged with 6.88 g (34.32 mmol) of mercury and approximately 10 mL of toluene in a nitrogen drybox. While stirring, 34 mg (1.48 mmol) of sodium metal was added and the resulting amalgam was stirred for 20 minutes. A toluene slurry containing 150 mg (0.25 mmol) of ***rac*-1-I_2** was added. The resulting reaction mixture was stirred vigorously for 2 days and the red solution was decanted from the amalgam and filtered through Celite. Removal of the pentane *in vacuo* followed by cold pentane washes affords 26 mg (22 %) of **[*rac*-1-I]$_2$** as a purple oil. ^{1}H NMR (benzene-d_6): δ = 2.95 (d, 4H, CH_2), 3.26 (d, 4H, CH_2), 4.50 (d, 3Hz, 4H, Cp*H*), 5.94 (d, 3Hz, 4H, Cp*H*), 6.59 (m, 4H, Benzo), 6.80 (m, 4H, Benzo), 6.87 (m, 4H, Benzo), 7.60 (m, 4H, Benzo).

Preparation of [*meso*-$Me_2Si(\eta^5$-C_5H_3-3-$CMe_3)_2Zr]_2(\mu_2$-η^1,η^1-$Cl)_2$ ([*meso*-3-Cl]$_2$). This molecule was prepared in a similar manner to **[*rac*-1-I]$_2$** using 90 mg (0.18 mmol) of ***meso*-3-Cl_2**, 6.75 g (0.03 mol) of mercury and 34 mg (1.48 mmol) of sodium

metal and stirring for 8 days, yielding 6 mg (7 %) of **[*meso*-3-Cl]$_2$** as a purple oil. ^{1}H NMR (benzene-d_6): δ = 0.42 (s, 6H, Si*Me*$_2$), 0.53 (s, 6H, Si*Me*$_2$), 1.49 (s, 36H, C*Me*$_3$), 5.58 (m, 4H, Cp*H*), 6.23 (m, 4H, Cp*H*), 6.61 (m, 4H, Cp*H*). ^{13}C {^{1}H} NMR (benzene-d_6): δ = -5.84, -3.84 (Si*Me*$_3$), 30.62 (C*Me*$_3$), 34.17 (*C*Me$_3$), 106.25, 107.72, 115.03, 117.81, 156.79 (Cp).

Reduction of *meso*-Me$_2$Si(η^5-C$_5$H$_3$-3-CMe$_3$)$_2$ZrI$_2$ with excess sodium amalgam. This reduction was set up in a similar manner to the preparation of ***rac*-1-I** with 300 mg (0.58 mmol) of ***meso*-3-I$_2$**, 16.027 g (0.08 mol) of mercury and 80 mg (3.48 mmol) of sodium metal and stirring for 3 days, yielding a 3 : 1 ratio of **[*meso*-3]$_2$N$_2$** : **[*meso*-3]$_2$(HI)**.

Characterization of [*meso*-Me$_2$Si(η^5-C$_5$H$_3$-3-CMe$_3$)$_2$Zr]$_2$(μ$_2$-η^2,η^2-N$_2$) ([*meso*-3]$_2$N$_2$). ^{1}H NMR (benzene-d_6): δ = 0.32 (s, 6H, Si*Me*$_2$), 0.56 (s, 6H, Si*Me*$_2$), 1.30 (s, 36H, C*Me*$_3$), 5.65 (m, 4H, Cp*H*), 5.96 (m, 4H, Cp*H*), 6.13 (m, 4H, Cp*H*). ^{13}C {^{1}H} NMR (benzene-d_6): δ = -7.33, -5.45, -2.71 (Si*Me*$_3$), 31.25, 31.85 (C*Me*$_3$), 34.06, 34.45 (*C*Me$_3$), 99.57, 102.38, 110.95, 111.48, 116.43, 120.13, 126.76, 132.47, 147.00, 153.95 (Cp).

Characterization of [*meso*-Me$_2$Si(η^5-C$_5$H$_3$-3-CMe$_3$)$_2$Zr]$_2$(μ$_2$-η^1,η^1-H, μ$_2$-η^1,η^1-I) ([*meso*-3]$_2$(HI)). ^{1}H NMR (benzene-d_6): δ = 0.03 (s, 6H, Si*Me*$_2$), 0.10 (s, 6H, Si*Me*$_2$), 2.00 (s, 36H, C*Me*$_3$), 3.35 (pseudo s, 4H, Cp*H*), 9.46 (pseudo s, 4H, Cp*H*), 14.96 (br pseudo s, 4H, Cp*H*).

Preparation of [*rac*-Me$_2$Si(η^5-C$_5$H$_3$-3-CMe$_3$)$_2$Zr]$_2$(μ_2-η^2,η^2-N$_2$) ([*rac*-3]$_2$N$_2$). This molecule was prepared in a similar manner to **[*rac*-1-I]$_2$** using 152 mg (0.23 mmol) of ***rac*-3-I$_2$**, 6.00 g (0.03 mol) of mercury and 30 mg (1.30 mmol) of sodium metal and stirring for 6 days, yielding 7 mg (6 %) of **[*rac*-3]$_2$N$_2$** as a green solid. Anal. Calcd for $C_{40}H_{60}N_2Si_2Zr_2$: C, 59.49; H, 7.49; N, 3.47. Found: C, 59.72; H, 7.79; N, 3.24. ^{1}H NMR (benzene-d_6): δ = 0.39 (s, 12H, Si*Me*$_2$), 1.40 (s, 36H, C*Me*$_3$), 5.80 (m, 8H, Cp*H*), 6.11 (m, 4H, Cp*H*). ^{13}C {^{1}H} NMR (benzene-d_6): δ = -5.02 (Si*Me*$_3$), 31.99 (C*Me*$_3$), 33.60 (*C*Me$_3$), 106.26, 108.27, 109.55, 148.83, 150.36 (Cp).

Preparation of *rac/meso*-Me$_2$Si(η^5-C$_5$H$_3$-3-CMe$_3$)$_2$Zr(*c*-(Ctolyl)$_4$) (*rac/meso*-3-*c*(Ctolyl)$_4$). A J. Young NMR tube was charged with 15 mg (0.03 mmol) of a 1:4 mixture of **[*rac*-3]$_2$N$_2$** : **[*rac*-3][*meso*-3]N$_2$** and 8 mg (0.04 mmol) of ditolylacetylene and dissolved in approximately 0.5 mL of benzene-d_6. The solution mixture was allowed to sit at room temperature for approximately 24 hours, resulting in a red solution of a 1.1 : 1 mixture of ***rac*-3-*c*(Ctolyl)$_4$** : ***meso*-3-*c*(Ctolyl)$_4$**. ^{1}H NMR (benzene-d_6): δ = 0.34 (s, 9H, *rac* & *meso* Si*Me*$_2$), 0.41 (s, 3H, *meso* Si*Me*$_2$), 1.44 (s, 18H, *meso* C*Me*$_3$), 1.59 (s, 18H, *rac* C*Me*$_3$), 1.88 (s, 3H, *meso* tolyl *Me*), 1.93 (s, 6H, tolyl *Me*), 2.00 (s, 6H, tolyl *Me*), 2.06 (s, 3H, *meso* tolyl *Me*), 2.08 (s, 6H, tolyl *Me*), 5.31 (m, 2H, Cp*H*), 5.38 (m, 2H, Cp*H*), 5.64 (m, 2H, Cp*H*), 5.93 (m, 2H, Cp*H*), 6.22 (m, 2H, Ph), 6.57 (m, 4H, Ph), 6.75 (m, 3H, Ph), 6.83 (m, 6H, Ph), 6.89 (m, 8H, Ph), 6.95 (m, 2H, Ph), 7.02 (m, 2H, Ph), 7.06 (m, 3H, Ph), 7.36 (m, 2H, Cp*H*), 7.50 (m, 2H, Ph). One Cp*H* resonance not located.

Preparation of [*rac*-$Me_2C(\eta^5\text{-}C_5H_3\text{-}3\text{-}SiMe_3)_2Zr]_2(\mu_2\text{-}\eta^2,\eta^2\text{-}N_2)$ ([*rac*-4]$_2N_2$). This molecule was prepared in a similar manner to **[*rac*-1-I]$_2$** using 263 mg (0.40 mmol) of ***rac*-4-I$_2$**, 11.0 g (0.05 mol) of mercury and 55 mg (2.39 mmol) of sodium metal and stirring for 3 days, yielding 92 mg (55 %) of **[*rac*-4]$_2$N$_2$** as a green solid. Anal. Calcd for $C_{38}H_{60}N_2Si_4Zr_2$: C, 54.36; H, 7.20; N, 3.37. Found: C, 54.31; H, 7.55; N, 3.40. ^{1}H NMR (benzene-d_6): δ = 0.36 (s, 36H, Si*Me*$_3$), 1.48 (s, 12H, C*Me*$_2$), 5.66 (m, 4H, Cp*H*), 5.69 (s, 4H, Cp*H*), 6.04 (m, 4H, Cp*H*). ^{13}C {^{1}H} NMR (benzene-d_6): δ = 0.55 (Si*Me*$_3$), 24.50 (C*Me*$_2$), 37.00 (*C*Me$_2$), 95.08, 105.67, 107.61, 112.97, 126.65 (Cp). ^{15}N NMR (benzene-d_6): δ = 604.1.

Preparation of [*rac*-$Me_2C(\eta^5\text{-}C_5H_3\text{-}3\text{-}CMe_3)_2Zr]_2(\mu_2\text{-}\eta^2,\eta^2\text{-}N_2)$ ([*rac*-5]$_2N_2$). This molecule was prepared in a similar manner to **[*rac*-1-I]$_2$** using 300 mg (0.48 mmol) of ***rac*-5-I$_2$**, 13.2 g (0.07 mol) of mercury and 66 mg (2.87 mmol) of sodium metal and stirring for 3 days, yielding 37 mg (15 %) of **[*rac*-5]$_2$N$_2$** as a green solid. ^{1}H NMR (benzene-d_6): δ = 1.40 (s, 36H, C*Me*$_3$), 1.43 (s, 6H, C*Me*$_2$), 5.36 (m, 4H, Cp*H*), 5.47 (m, 4H, Cp*H*), 5.82 (m, 4H, Cp*H*). ^{13}C {^{1}H} NMR (benzene-d_6): δ = 24.08, 31.30, 33.05, 36.59 (CMe$_2$/CMe$_3$), 97.12, 102.82, 102.95, 128.30, 144.55 (Cp).

Characterization of [*meso*-$Me_2Si(\eta^5\text{-}C_5H_3\text{-}3\text{-}CMe_3)_2ZrH]_2(\mu_2\text{-}\eta^2,\eta^2\text{-}N_2H_2)$ ([*meso*-3]$_2$N$_2$H$_4$). ^{1}H NMR (benzene-d_6): δ = 0.29 (s, 3H, Si*Me*$_2$), 0.41 (s, 3H, Si*Me*$_2$), 0.55 (s, 6H, Si*Me*$_2$), 1.29 (s, 18H, C*Me*$_3$), 1.33 (s, 18H, C*Me*$_3$), 5.92 (m, 2H, Cp*H*), 6.16 (m, 2H, Cp*H*), 6.51 (m, 2H, Cp*H*), 6.55 (m, 2H, Cp*H*), 6.63 (m, 2H, Cp*H*), 6.82 (m, 2H,

Cp*H*), 6.91 (m, 1H, Zr-*H*). One Zr-*H* and one N-*H* resonance not located. ^{13}C {^{1}H} NMR (benzene-d_6): δ = -6.92, -6.70, -2.62, -1.30 (Si*Me*$_2$), 31.84, 32.71 (C*Me*$_3$), 32.80, 33.12 (*C*Me$_3$), 101.85, 106.92, 108.64, 108.97, 110.17, 113.74, 114.61, 122.14, 147.58, 149.77 (Cp).

Preparation of [*meso*-Me$_2$Si(η^5-C$_5$H$_3$-3-CMe$_3$)$_2$ZrH]$_2$(μ$_2$-η^2,η^2-N$_2$) ([*meso*-3]$_2$H$_2$N$_2$). A J. Young NMR tube charged with 5 mg (0.01 mmol) of **[*meso*-3]$_2$N$_2$**, and dissolved in approximately 0.5 mL of benzene-d_6. On the high vacuum line, the tube was frozen in liquid nitrogen and evacuated. One atmosphere of hydrogen was added at -196 ºC. The tube was thawed, resulting in a color change from green to yellow and identified as **[*meso*-3]$_2$N$_2$H$_4$** and **[*meso*-3]$_2$H$_2$N$_2$** in a 1:2 ratio. Over hours, the ratio of **[*meso*-3]$_2$H$_2$N$_2$** increased with full conversion under vacuum. ^{1}H NMR (benzene-d_6): δ = 0.36 (s, 6H, Si*Me*$_2$), 0.39 (s, 6H, Si*Me*$_2$), 1.51 (s, 36H, C*Me*$_3$), 4.29 (m, 2H, Zr-*H*), 5.11 (m, 4H, Cp*H*), 5.19 (m, 4H, Cp*H*), 6.14 (m, 4H, Cp*H*). ^{13}C {^{1}H} NMR (benzene-d_6): δ = -6.77 (Si*Me*$_2$), 32.34 (C*Me*$_3$), 32.65 (*C*Me$_3$), 99.73, 101.23, 107.32, 111.79, 119.04 (Cp). One Si*Me*$_2$ resonance not located.

Preparation of [*rac*-Me$_2$Si(η^5-C$_5$H$_3$-3-CMe$_3$)$_2$ZrH]$_2$(μ$_2$-η^2,η^2-N$_2$) ([*rac*-3]$_2$H$_2$N$_2$). This molecule was prepared in a similar to **[*meso*-3]$_2$H$_2$N$_2$** using 8 mg (0.01 mmol) of **[*rac*-3]$_2$N$_2$** dissolved in approximately 0.5 mL of benzene-d_6. Upon addition of H_2, the solution turned red, yielding **[*rac*-3]$_2$H$_2$N$_2$**. ^{1}H NMR (benzene-d_6): δ = 0.12 (s, 6H, Si*Me*$_2$), 0.31 (s, 6H, Si*Me*$_2$), 1.39 (s, 18H, C*Me*$_3$), 1.56 (s, 18H, C*Me*$_3$), 4.34 (m, 2H, Zr-*H*), 4.86 (m, 2H, Cp*H*), 5.21 (m, 2H, Cp*H*), 5.92 (m, 2H, Cp*H*), 6.19 (m, 2H,

Cp*H*), 6.28 (m, 4H, Cp*H*). ^{13}C {^{1}H} NMR (benzene-d_6): δ = -6.57, -4.63 (Si*Me*$_2$), 31.58, 31.94 (C*Me*$_3$), 33.02, 33.64 (*C*Me$_3$), 96.93, 97.06, 100.66, 103.75, 104.87, 105.01, 107.80, 112.13, 144.31, 150.19 (Cp).

Preparation of [*rac*-Me$_2$C(η^5-C$_5$H$_3$-3-SiMe$_3$)$_2$ZrH]$_2$(μ$_2$-η^2,η^2-N$_2$) ([*rac*-4]$_2$H$_2$N$_2$). This molecule was prepared in a similar to **[*meso*-3]$_2$H$_2$N$_2$** using 9 mg (0.01 mmol) of **[*rac*-4]$_2$N$_2$** dissolved in approximately 0.5 mL of benzene-d_6. Upon addition of H_2, the solution turned red, yielding **[*rac*-4]$_2$H$_2$N$_2$**. ^{1}H NMR (benzene-d_6): δ = 0.34 (s, 18H, Si*Me*$_3$), 0.58 (s, 18H, Si*Me*$_3$), 1.08 (s, 6H, C*Me*$_2$), 1.42 (s, 6H, C*Me*$_2$), 4.10 (s, 2H, Zr-*H*), 4.55 (m, 2H, Cp*H*), 5.72 (m, 2H, Cp*H*), 5.78 (m, 2H, Cp*H*), 5.86 (m, 2H, Cp*H*), 6.15 (m, 2H, Cp*H*), 6.40 (m, 2H, Cp*H*). ^{13}C {^{1}H} NMR (benzene-d_6): δ = 0.08, 0.28 (Si*Me*$_3$), 22.48, 24.19 (C*Me*$_2$), 35.82 (*C*Me$_2$), 99.58, 100.53, 102.08, 107.94, 111.20, 114.11, 116.47, 118.56, 123.96 (Cp). One Cp resonance not located.

Preparation of [*rac*-Me$_2$C(η^5-C$_5$H$_3$-3-SiMe$_3$)(η^5-C$_5$H$_3$-3-SiMe$_2$CH$_2$)Zr-CMH]$_2$(μ$_2$-η^1,η^1-N$_2$) ([*rac*-4-CMH]$_2$N$_2$). A J. Young NMR tube was charged with 31 mg (0.04 mmol) of **[*rac*-4]$_2$N$_2$** dissolved in approximately 0.5 mL of benzene-d_6. On the high vacuum line, the tube was frozen in liquid nitrogen and evacuated. One atmosphere of hydrogen was added at -196 ºC. The tube was thawed, resulting in a color change from green to red. After half an hour, the tube was again frozen in liquid nitrogen and evacuated. After thawing, the tube was heated to 65 ºC for 14 hours yielding **[*rac*-4-CMH]$_2$N$_2$**. ^{1}H NMR (benzene-d_6): δ = -0.61 (d, 2H, Zr-C*H*$_2$), 0.32 (s, 18H, Si*Me*$_3$), 0.48 (s, 6H, Si*Me*$_2$), 0.50 (s, 6H, Si*Me*$_2$), 0.52 (d, 2H, Zr-C*H*$_2$), 1.31 (s, 6H, C*Me*$_2$),

1.47 (s, 6H, C*Me*$_2$), 5.24 (m, 2H, Cp*H*), 5.44 (m, 2H, Cp*H*), 5.48 (m, 2H, Cp*H*), 5.73 (m, 2H, Cp*H*), 5.79 (m, 2H, Cp*H*), 6.41 (m, 2H, Cp*H*). ^{13}C {^{1}H} NMR (benzene-d_6): δ = -1.94 (Si*Me*$_2$), 0.13 (Si*Me*$_3$), 3.08, 5.44 (Si*Me*$_2$), 23.46, 25.49 (C*Me*$_2$), 36.26 (*C*Me$_2$), 101.87, 104.13, 105.53, 109.10, 116.37, 119.14, 120.87, 122.74, 125.62, 129.26 (Cp).

Preparation of *rac*-CH$_2$CH$_2$(η^5-C$_9$H$_6$)$_2$Zr(CO)$_2$ (*rac*-1-(CO)$_2$ or *rac*-ebi-Zr(CO)$_2$). A flame dried thick-walled glass bomb was charged with 5.21 g (26.47 mmol) of mercury and approximately 3 mL of toluene in a nitrogen drybox. While stirring, 26 mg (1.13 mmol) of sodium metal was added and the resulting amalgam was stirred for 20 minutes. A toluene solution of 79 mg (0.189 mmol) of ***rac*-1-ZrCl$_2$** was added. The reaction vessel was attached to the vacuum line and one atmosphere of CO was condensed at -196 ºC. The vessel was warmed to room temperature and stirred for 17 hours. The excess CO and solvent were then removed *in vacuo* leaving a brown residue. The bomb was taken into the drybox and the residue extracted into pentane. Filtration through Celite followed by solvent removal afforded brown ***rac*-1-(CO)$_2$**. ^{1}H NMR (benzene-d_6): δ = 2.84 (d, 2H, C*H*$_2$), 3.07 (d, 2H, C*H*$_2$), 4.61 (d, 3Hz, 2H, Cp*H*), 5.55 (d, 3Hz, 2H, Cp*H*), 6.84 (m, 4H, Benzo), 7.49 (m, 4H, Benzo). IR (pentane): ν(CO) = 1977, 1896 cm^{-1}.

Preparation of *rac/meso*-CH$_2$CH$_2$(η^5-C$_9$H$_5$-3-(Me))$_2$Zr(CO)$_2$ (*rac/meso*-2-(CO)$_2$). This molecule was prepared in a similar manner to ***rac*-1-(CO)$_2$** using 3.77 g (18.76 mmol) of mercury, 19 mg (0.83 mmol) of sodium metal and 103 mg (0.16 mmol) of

***rac/meso*-3-I_2** to afford green ***rac/meso*-2-$(CO)_2$**. ^{1}H NMR (benzene-d_6): δ = 1.64 (s, 6H, *Me*), 1.91 (s, 6H, *Me*), 2.49 (m, 2H, CH_2), 2.90 (m, 2H, CH_2), 3.11 (d, 2H, CH_2), 3.16 (d, 2H, CH_2), 5.58 (s, 2H, Cp*H*), 5.91 (s, 2H, Cp*H*), 6.62 (m, 2H, Benzo), 6.72 (m, 2H, Benzo), 6.79 (m, 2H, Benzo), 6.88 (m, 4H, Benzo), 7.36 (m, 2H, Benzo), 7.57 (m, 2H, Benzo). ^{13}C {^{1}H} NMR (benzene-d_6): δ = 11.98, 12.53 (*Me*), 30.09, 31.41 (CH_2 linker), 95.42, 96.99, 100.62, 102.98, 111.03, 113.70, 113.82, 116.70, 118.16, 118.67, 121.07, 121.14, 122.58, 122.92, 123.58, 124.71, 125.26 (Cp/Benzo), 269.63, 275.27 (Zr-*C*O). One Cp/Benzo and one Zr-*C*O resonance not located. IR (pentane): ν(CO) = 1975, 1971 (shoulder), 1888 cm^{-1}.

REFERENCES

[1] Fryzuk, M. D.; Johnson, S. A. *Coord. Chem. Rev.* **2000**, *200-202*, 379.

[2] Smil, V. *Enriching the Earth: Fritz Haber, Carl Bosch and the Transformation of World Food Production*; MIT Press: Cambridge, MA, 2001.

[3] MacLachlan, E. A.; Fryzuk, M. D. *Organometallics* **2006**, *25*, 1530.

[4] Chatt, J.; Dilworth, J. R.; Richards, R. L. *Chem. Rev.* **1978**, *78*, 589.

[5] Yandulov, D. V.; Schrock, R. R. *Science* **2003**, *76*, 301.

[6] Avenier, P.; Taoufik, M.; Lesage, A.; Solans-Monfort, X.; Baudouin, A.; de Mallmann, A.; Veyre, L.; Basset, J.-M.; Eisenstein, O.; Emsley, L.; Quadrelli, E. A. *Science* **2007**, *317*, 1056.

[7] Ohki, Y.; Fryzuk, M. D. *Angew. Chem. Int. Ed.* **2007**, *46*, 2858.

[8] With titanium: (a) Pez, G. P.; Apgar, P.; Crissey, R. K. *J. Am. Chem. Soc.* **1982**, *104*, 482. (b) Hanna, T. E.; Bernskoetter, W. H.; Bouwkamp, M. W.; Lobkovsky, E.; Chirik, P. J. *Organometallics* **2007**, *26*, 2431. With zirconium: (c) Chirik, P. J.; Henling, L. M.; Bercaw, J. E. *Organometallics* **2001**, *20*, 534. (d) Pool, J. A.; Lobkovsky, E.; Chirik, P. J. *J. Am. Chem. Soc.* **2003**, *125*, 2241. (e) Pool, J. A.; Lobkovsky, E.; Chirik, P. J. *Nature*. **2004**, *427*, 527. (f) Hanna, T. E.; Keresztes, I.; Lobkovsky, E.; Chirik, P. J. *Inorg. Chem.* **2007**, *46*, 1675. (g) Pun, D.; Lobkovsky, E.; Chirik, P. J. *J. Am. Chem. Soc.* **2008**, *130*, 6047. (h) Pun, D.; Bradley, C. A.; Lobkovsky, E.; Keresztes, I.; Chirik, P. J. *J. Am. Chem. Soc.* **2008**, *130*, 14046. With both zirconium and hafnium: (i) Hirotsu, M.; Fontaine, P. P.; Zavalij, P. Y.; Sita, L. R. *J. Am. Chem. Soc.* **2007**, *129*, 12690. With hafnium: (j) Bernskoetter,

W. H.; Olmos, A. V.; Lobkovsky, E.; Chirik, P. J. *Organometallics* **2006**, *25*, 1021. (k) Knobloch, D. J.; Lobkovsky, E.; Chirik, P. J. *Nature Chem. Accepted.*

[9] Chomitz, W. A.; Arnold, J. *Chem. Commun.* **2007**, *4797*.

[10] (a) Fryzuk, M. D.; Haddad, T. S.; Rettig, S. J. *J. Am. Chem. Soc.* **1990**, *112*, 8185. (b) Cohen, J. D.; Fryzuk, M. D.; Loehr, T. M.; Mylvaganam, M.; Rettig, S. J. *Inorg. Chem.* **1998**, *37*, 112. (c) Fryzuk, M. D.; Love, J. B.; Rettig, S. J.; Young, V. G. *Science* **1997**, *275*, 1445. (d) Morello, L.; Yu, P.; Carmichael, C. D.; Patrick, B. O.; Fryzuk, M. D. *J. Am. Chem. Soc*. **2005**, *127*, 12796. (e) Chomitz, W. A.; Sutton, A. D.; Krinsky, J. L.; Arnold, J. *Organometallics* **2009**, *28*, 3338.

[11] de Wolf, J. M.; Blaauw, R.; Meetsma, A.; Teuben, J. H.; Gyepes, R.; Varga, V.; Mach, K.; Veldman, N.; Spek, A. L. *Organometallics* **1996**, *15*, 4977.

[12] Pool, J. A.; Lobkovsky, E.; Chirik, P. J. *Organometallics* **2003**, *22*, 2797.

[13] (a) Lee, H.; Desrosiers, P. J.; Guzei, I.; Rheingold, A. L.; Parkin, G. *J. Am. Chem. Soc.* **1998**, *120*, 3255. (b) Lee, H.; Bridgewater, B. M.; Parkin, G. *J. Chem. Soc., Dalton Trans.* **2000**, 4490.

[14] (a) Ewen, J. A. *J. Am. Chem. Soc.* **1984**, *106*, 6355. (b) Kaminsky, W.; Kulper, K.; Brintzinger, H. H.; Wild, F. R. W. P. *Angew. Chem. , Int. Ed.* **1985**, *24*, 507. (c) Mise, T.; Miya, S.; Yamazaki, H. *Chem. Lett.* **1989**, 1853.

[15] Pool, J. A.; Bernskoetter, W. H.; Chirik, P. J. *J. Am. Chem. Soc.* **2004**, *126*, 14326.

[16] Hanna, T. E. Thesis. Cornell University, 2007.

[17] Zachmanoglou, C. E.; Docrat, A.; Bridgewater, B. M.; Parkin, G.; Brandow, C. G.; Bercaw, J. E.; Jardine, C. N.; Lyall, M.; Green, J. C.; Keister, J. B. *J. Am. Chem. Soc.* **2002**, *124*, 9525.

[18] Diamond, G. M.; Jordan, R. F.; Petersen, J. L. *J. Am. Chem. Soc.* **1996**, *118*, 8024.

[19] Bernskoetter, W. H.; Olmos, A. V.; Lobkovsky, E.; Chirik, P. J. *Organometallics* **2006**, *25*, 1021.

[20] Beweries, T.; Jger-Fiedler, U.; Bach, M. A.; Burlakov, V. V.; Ardnt, P.; Baumann, W.; Spannenberg, A.; Rosenthal, U. *Organometallics* **2007**, *26*, 3000.

[21] Pool, J. A.; Chirik, P. J. *Can. J. Chem.* **2005**, *83*, 286.

[22] Diamond, G. M.; Jordan, R. F.; Petersen, J. L. *Organometallics* **1996**, *15*, 4045.

[23] (a) LoCoco, M. D.; Jordan, R. F. *Organometallics* **2003**, *22*, 5498. (b) Buck, R. M.; Vinayavekhin, N.; Jordan, R. F. *J. Am. Chem. Soc.* **2007**, *129*, 3468.

[24] Test for hydrazine performed according to: Manriquez, J. M.; Bercaw, J. E. *J. Am. Chem. Soc.* **1974**, *96*, 6229.

[25] Studt, F.; Morello, L.; Lehnert, N.; Fryzuk, M. D.; Tuczek, F. *Chem. Eur. J.* **2003**, *9*, 520.

[26] Royo, E.; Royo, P.; Cuenca, T.; Galaklov, M. *Organometallics* **2000**, *19*, 5559.

[27] The deviation from the expected 1.5 : 1 ratio of ***rac*-3-*c*(Ctolyl)$_4$** : ***meso*-3-*c*(Ctolyl)$_4$** is unknown.

[28] Zachmanoglou, C. E.; Melnick, J. G.; Bridgewater, B. M.; Churchill, D. G.; Parkin, G. *Organometallics* **2005**, *24*, 603.

[29] Halterman, R. L. in *The Metallocenes* vol. 1; Togni, A.; Halterman, R. L., Eds.; Wiley-VCH: New York, 1998, p. 461-468.

[30] Chirik, P. J.; Day, M. D.; Bercaw, J. E. *Organometallics* **1999**, *18*, 1873.

[31] The trace quantity of **[*meso*-3]$_2$(HI)** initially present also reacted with H_2 but formed an NMR silent product.

[32] Pangborn, A. B.; Giardello, M. A.; Grubbs, R. H.; Rosen, R. K.; Timmers, F. J. *Organometallics* **1996**, *15*, 1518.

[33] Urazowski, I. F.; Atovmyan, L. O.; Mkoyan, S. G.; Broussier, R.; Perron, P.; Gautheron, B.; Robert, F. *J. Organomet. Chem.* **1997**, *536-537*, 531.

[34] Ewen, J. A.; Elder, M. J.; Jones, R. L.; Haspeslagh, L.; Atwood, J. L.; Bott, S. G.; Robinson, K. *Makromol.Chem., Macromol. Symp.* **1991**, 48/49, 253.

Chapter 5

Catalytic Dehydrogenation of Substituted Amine-Boranes with Isolable Titanocene and Zirconocene Sandwich and Titanocene Dinitrogen Complexes*

Abstract

A series of isolable titanocene and zirconocene sandwich and titanium dinitrogen complexes was explored as potential catalysts for the dehydrogenation of R_2NHBH_3 (R = Me, H). Fundamental mechanistic studies were performed to understand the catalytic reaction cycle and to better design a more efficient dehydrogenation catalyst. During the course of catalysis with zirconocene compounds, a new series of products identified as the zirconium tetraborohydride hydride complexes was isolated and characterized by X-ray crystallography, infrared and NMR spectrocopy. While this new complex is still active for catalytic dehydrogenation, it does exhibit slower rates and can be considered a catalyst deactivation pathway.

Introduction

Research in hydrogen storage materials is a rapidly developing field as environmental concerns over the dependence and availability of petroleum-derived fuel intensifies.[1] In particular, ammonia-borane, H_3NBH_3, and other substituted amine-boranes are attracting interest since they possess a high percentage by weight of available hydrogen,[2] which can be released catalytically under mild conditions.[1] Several recent examples include Manners' heterogeneous catalysis with 0.5 mol % of $[M(1,5\text{-COD})(\mu_2\text{-Cl})]_2$ (M = Rh, Ir; COD = cyclooctadiene) which quantitatively releases dihydrogen gas over hours at 45 ºC,[3] and Goldberg's iridium pincer catalyst,

* Reproduced in part with permission from Pun, D.; Lobkovsky, E.; Chirik, P. J. *Chem Commun.* **2007**, *28*, 2471. Copyright 2007 Royal Society of Chemistry (RSC).

(κ^3-2,6-(OP^tBu_2)$_2C_6H_3$)IrH_2, which at a 0.25 mol % catalyst loading, catalysis is done within minutes at ambient temperature.[4] Using more abundant, first row metal catalysts, Baker has demonstrated that 10 mol % of bis(N-heterocyclic carbene) nickel complexes can competently dehydrogenate ammonia-borane at 65 ºC after a few hours,[5] although it has been demonstrated, computationally, that the free carbene[6] and the mono(NHC) nickel complex[7] are also catalytically active. A series of kinetic isotope effect studies involving partially and fully deuterated isotopologues of H_3NBH_3 indicate that both N-H and B-H bond cleavage are occurring during the rate-determining step, consistent with several competing active dehydrogenation catalysts.[5,7] Promise has been shown in using ammonia triborane, $NH_3B_3H_7$, as a hydrogen storage material as well, which can release up to 7 – 8 equivalents of H_2 within minutes upon addition of either excess HCl or catalytic amounts of [Rh(1,5-COD)(μ_2-Cl)]$_2$ or $RhCl_3$ at ambient temperature.[8]

Recently, Manners and coworkers have reported the catalytic dehydrogenation of Me_2NHBH_3 with 2 mol % of (η^5-C_5H_5)$_2TiCl_2$ activated with two equivalents of ^nBuLi; full conversion to a dimeric dehydrogenated amine-borane derivative is observed after 4 hours at 23 ºC (eq. 5.1).[9] Unfortunately, due to the unknown active species from the in situ preparation, which could be Ti(III),[10] Ti(II)[11] or a complex mixture,[12] mechanistic studies proved to be difficult.

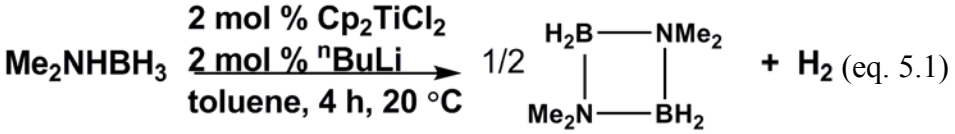

(eq. 5.1)

Motivated by these titanocene results, we decided to explore isolable well-defined titanocene (II) sandwich complexes as catalyst precursors. Knowing that many titanocene dinitrogen complexes readily lose N_2 in solution, examples of these compounds were also explored. With numerous well-defined, isolable titanocene dinitrogen[13] and sandwich[14] complexes in the literature, systematic studies of the

catalytic activity of Me_2NHBH_3 dehydrogenation as a function of cyclopentadienyl substituent could be readily explored. Extending our analysis to zirconium, isolable bis(indenyl) zirconium (II) sandwich complexes were also utilized.[15] After establishing the catalytic competency with dehydrogenating Me_2NHBH_3, we extended catalysis to the amine borane with the higher hydrogen weight percent, H_3NBH_3. Studies to elucidate the mechanism of this catalysis were also conducted.

Results and Discussion

Screening of Isolable Group IV Metallocene (II) Sources for Catalytic Dehydrogenation of Amine-Borane. Encouraged by the results from the generation of a titanocene derivative that was catalytically competent for the dehydrogenation of Me_2NHBH_3,[9] a family of isolable titanocene sandwich and dinitrogen compounds were assayed for dehydrogenation catalysis. Also screened were bis(indenyl) zirconium sandwich compounds and other zirconocene dihydrides. Depicted in Figure 5.1 are the catalyst precursors explored in this study. Each catalytic reaction was performed using a 0.61 M solution of Me_2NHBH_3 in benzene-d_6 with a 2 mol % catalyst loading[16] and the progress of the reaction was determined by both ^1H and ^{11}B NMR spectroscopy. In particular, ^{11}B NMR spectroscopy proved to be very useful as the borane containing starting material appears as a quartet at -13.4 ppm, distinct from the products, a dimer, $[Me_2NBH_2]_2$, at 5.0 ppm and a trimer, $[Me_2NBH_2]_3$, at 1.5 ppm, both of which appear as triplets (eq. 5.2). Dihydrogen gas was detected by ^1H NMR

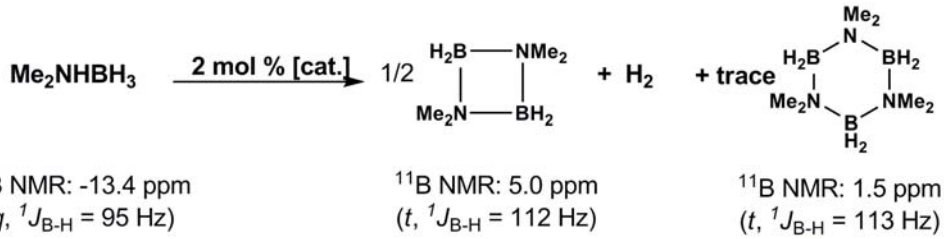

(eq. 5.2)

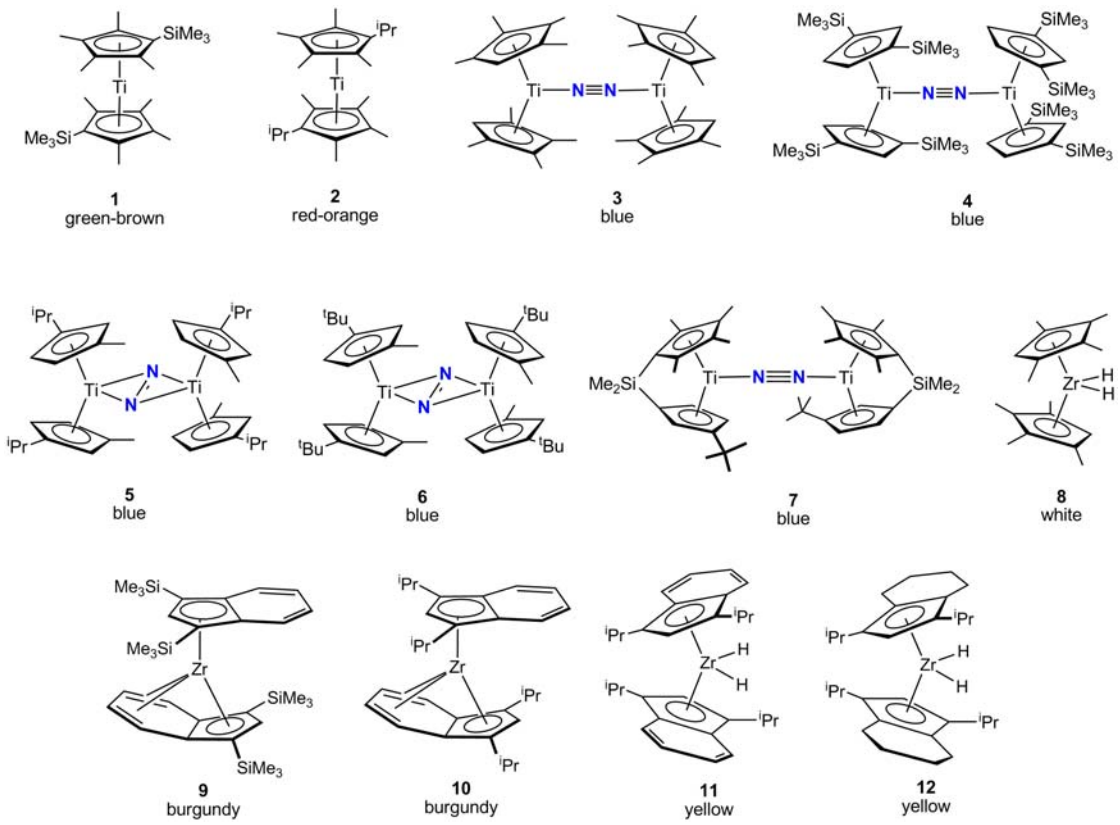

Figure 5.1. The titanocene and zirconocene compounds explored in this study for competency as amine-borane dehydrogenation catalysts.

Table 5.1. Results of catalytic metallocene catalyzed dehydrogenation.

Compound	Substrate	Solvent	T (ºC)	TOF (hr^{-1})
"(η^5-C_5H_5)$_2$Ti"	Me_2NHBH_3	benzene	23	1.4
1	Me_2NHBH_3	benzene	65	0.05
2	Me_2NHBH_3	benzene	65	100
3	Me_2NHBH_3	benzene	23	35
4	Me_2NHBH_3	benzene	23	> 420
5	Me_2NHBH_3	benzene	23	92
6	Me_2NHBH_3	benzene	23	14
7	Me_2NHBH_3	benzene	65	0.20
8	Me_2NHBH_3	benzene	65	0.04
9	Me_2NHBH_3	benzene	65	0.34
10	Me_2NHBH_3	benzene	65	0.08
11	Me_2NHBH_3	benzene	65	0.17
12	Me_2NHBH_3	benzene	65	0.02
4	Me_2NHBH_3	THF	23	0.29
4	NH_3BH_3	THF	65	0.31

spectroscopy and quantified by Toepler pump analysis (with catalyst **3**), providing 87 and 80 % of the expected combustible gas.

As shown in Table 5.1, all compounds catalytically turnover the amine-borane adduct. The first entry actually utilizes parent titanocene, $[(\eta^5\text{-}C_5H_5)Ti]_2(\mu_2,\eta^5\text{-}C_{10}H_8)(\mu_2\text{-}H)_2$, the product isolated from reduction of the titanocene dichloride.[9] Unlike Manners' in situ generated "titanocene," this isolated titanium (III) complex was six times slower in dehydrogenating the amine-borane, implying another active species is formed and is more active.

It appears that for titanocene catalyst precursors, highly substituted cyclopentadienyl rings such as in $(\eta^5\text{-}C_5Me_4R)_2Ti$ where R = $SiMe_3$ (**1**) or $CHMe_2$ (**2**), or even the more open *ansa* metallocene $[Me_2Si(\eta^5\text{-}C_5Me_4)_2Ti]_2(\mu_2\text{-}\eta^1,\eta^1\text{-}N_2)$, **7**, are poor catalyst precursors, requiring heating to 65 ºC in order to obtain reasonable turnover numbers. A control experiment was performed where a 0.61 M benzene-d_6 solution of Me_2NHBH_3 was heated at 65 ºC in the absence of any catalyst precursors; no reaction was observed after five days of heating. For compounds that do not have substitution on all five positions of the cyclopentadienyl, $[(\eta^5\text{-}C_5H_3\text{-}1,3\text{-}(SiMe_3)_2)_2Ti]_2(\mu_2\text{-}\eta^1,\eta^1\text{-}N_2)$, **4**, with withdrawing silyl groups exhibited the best turnover numbers, with > 99 % conversion within minutes at 23 ºC, proving to be the most active catalyst for Me_2NHBH_3 dehydrogenation to date.[1] Alkyl substitution in $[(\eta^5\text{-}C_5Me_4H)_2Ti]_2(\mu_2\text{-}\eta^1,\eta^1\text{-}N_2)$, **3**, and $[(\eta^5\text{-}C_5H_3\text{-}1\text{-}Me\text{-}3\text{-}R)_2Ti]_2(\mu_2\text{-}\eta^2,\eta^2\text{-}N_2)$, where R = $CHMe_2$ (**5**) and CMe_3 (**6**), show modest turnover frequencies. Following the steric trend established earlier, **5** is a better precatalyst than **6**. However, the dimethylsilyl linked ansa, **7**, is a poor catalyst precursor, but this is likely due to more of a steric contribution than an electronic one. The reversed trend exhibited between **1** and **2**, however, while reproducible, is difficult to explain.

Several zirconocene compounds were also explored as catalysts for

Me_2NHBH_3 dehydrogenation. While there are no bis(cyclopentadienyl) metallocene sandwich complexes known for zirconium, bis(indenyl) zirconium sandwich compounds, $(\eta^9\text{-}C_9H_5\text{-}1,3\text{-}R_2)(\eta^5\text{-}C_9H_5\text{-}1,3\text{-}R_2)Zr$, where R = $SiMe_3$ (**9**) and $CHMe_2$ (**10**), have been isolated and structurally characterized[15] and were explored as dehydrogenation catalysts. In attempts to probe the mechanism of the catalytic dehydrogenation reaction (*vide infra*), several zirconocene dihydrides were also evaluated. As shown in Table 5.1, each zirconium complex exhibits poor turnover frequencies compared to the titanium compound and all required heating to 65 ºC. As expected, the compound with the more electron deficient zirconium center, **9**, is a better precatalyst than **10**, which is better than the electron rich bis(tetrahydroindenyl) zirconium dihydride, $(\eta^5\text{-}C_9H_9\text{-}1,3\text{-}(CHMe_2)_2)_2ZrH_2$, **12**. Notably, the zirconium dihydride of **10**, $(\eta^5\text{-}C_9H_5\text{-}1,3\text{-}(CHMe_2)_2)ZrH_2$, **11**, exhibits slightly higher turnover frequencies than **10**. One bis(cyclopentadienyl) zirconium compound was evaluated in order to compare to a titanocene, $(\eta^5\text{-}C_5Me_4H)_2ZrH_2$, **8**. Compared to **3**, **8** clearly is not as catalytically efficient, requiring heating to 65 ºC to achieve a turnover frequency of 0.04 hr^{-1}, while for **3**, the catalysis is > 95 % complete after 2 hours at 23 ºC. Additionally, **8** is slower than the bis(indenyl) zirconium dihydride; this is likely due to the electron withdrawing ability of an indenyl compared to a cyclopentadienyl ligand.

The most active catalyst precursor, **4**, was also examined for the dehydrogenation of H_3NBH_3. However, due to the limited solubility of ammonia borane in benzene, the catalytic reactions were run in tetrahydrofuran. At 65 ºC, a modest turnover frequency of 0.31 hr^{-1} was observed, and yielded dihydrogen and $[H_2NBH_2]_3$ as the initial products. With time, the trimer underwent further dehydrogenation to form borazine, $[HNBH]_3$ (eq. 5.3). To determine if there was a solvent effect on the catalytic reaction, the dehydrogenation of Me_2NHBH_3 with **4** was

carried out in THF, resulting in a drastically diminished turnover frequency of 0.29 hr^{-1} at 23 ºC, meaning the switch in substrate is also a factor in the poor catalytic activity.

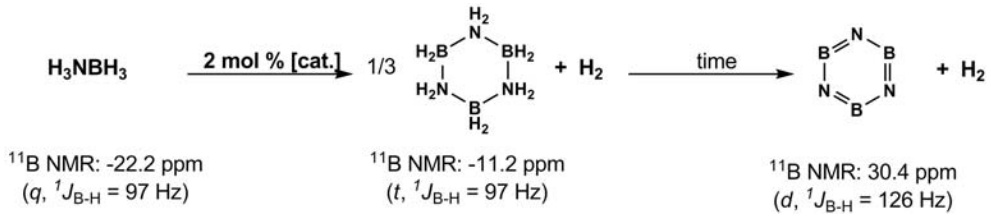

(eq. 5.3)

Mechanistic Studies on the Metallocene Catalyzed Dehydrogenation of Amine-Borane. With the catalytic competency of the metallocene complexes established, the mechanism of the catalytic dehydrogenation reaction was examined. With the titanocene sandwich complexes, **1** and **2**, only the starting compounds were observed during and after the course of the catalysis as judged by ^{1}H NMR spectroscopy. With the dinitrogen containing catalyst precursors, new paramagnetic species, likely titanocene sandwich derivatives,[13c] were observed during the course of reaction. Exposure of these new titanocene species to an atmosphere of dinitrogen regenerated the dinitrogen compounds. The regenerated precatalyst **3** was shown to be competent for the dehydrogenation reaction with comparable turnover frequencies to a fresh catalytic solution of **3**. Dimethylamine was detected as a byproduct by treating the volatiles of the catalysis with benzoylchloride, yielding N,N-dimethyl benzamide (eq. 5.4). Monitoring the rate of conversion of Me_2NHBH_3 to dihydrogen in the presence of 1 mol % of **3** (2 mol % of titanium) showed clean first order kinetics with an observed rate constant of 2.9(1) x 10^{-4} s^{-1} at 23 ºC.

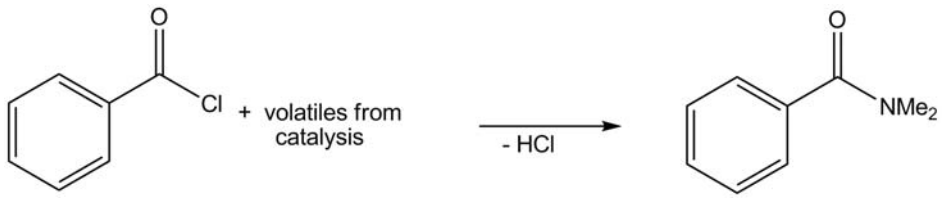

(eq. 5.4)

The reversibility of the catalytic reaction was also investigated. Performing the catalysis with **3** and Me_2NHBH_3 under an atmosphere of D_2 gas resulted in deuterium incorporation into the B-H positions of both the amine-borane starting material and the products. Deuterium incorporation into the N-H positions was also possible, but due to overlap with the starting protio isotopologue in the $^1H/^2H$ NMR and IR spectra, difficult to detect. Both H_2 and H-D gas were also detected in an approximately 1.3 : 1 ratio by ^1H NMR spectroscopy.

Based on these observations, a mechanism for the catalytic dehydrogenation of amine-borane with these metallocene precatalysts is shown in Figure 5.2. Similar to that previously proposed in Baker's nickel catalysis[5] and that computationally calculated for parent titanocene,[17] the first step is reversible oxidative addition of a B-H bond with the metallocene sandwich (the dinitrogen ligands are labile in all of the dinitrogen precursors). β-H elimination releases free $Me_2N{=}BH_2$, which has been detected in trace quantities during the course of the catalysis, appearing at 37.7 ppm (*t*, $^1J_{B\text{-}H}$ = 128 Hz) in the benzene-d_6 ^{11}B NMR spectrum.[9] Presumably, this olefinic analogue undergoes dimerization/trimerization in the presence of the metallocene, forming the observed cyclic products. Reductive elimination of dihydrogen from the remaining metallocene dihydride then regenerates the sandwich complex. Because the presence of D_2 gas can scramble deuterium into both the starting amine-borane and products, the reductive elimination and β-H elimination steps must be reversible. Based on the trends observed in Table 5.1 where the best catalyst precursors has a titanium metal center with electron-withdrawing substituents on the cyclopentadienyl ring, this reductive elimination step is likely rate determining. Assuming the same mechanism for the zirconocene compounds, this accounts for the diminished catalytic activity as compared to the titanocene complexes; zirconium does not reduce as easily as titanium.

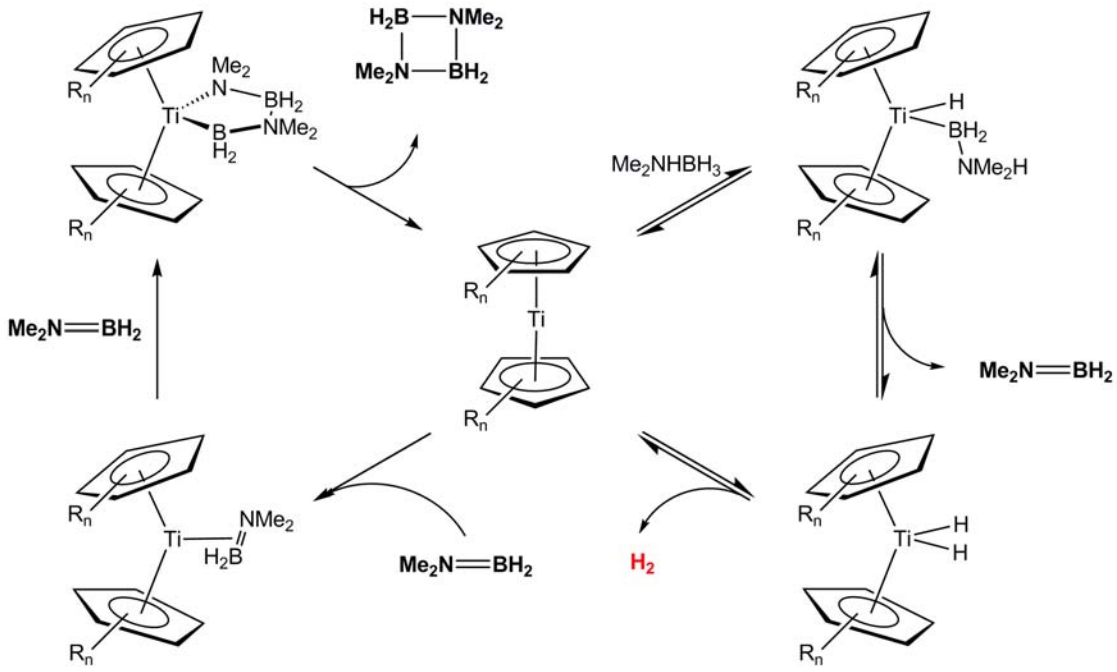

Figure 5.2. Proposed mechanism for the dehydrogenation of Me_2NHBH_2 with titanocene sandwich and dinitrogen complexes.

With the zirconocene catalyst precursors, new diamagnetic zirconocene complexes were isolated at the end of the catalytic reaction. Interestingly, the new compound derived from catalysis with **10** or **11**, is a C_1 symmetric zirconocene borohydride hydride complex where one of the indenyl rings has been hydrogenated to a tetrahydroindenyl ligand, (η^5-C_9H_5-1,3-$^i Pr_2$)(η^5-C_9H_9-1,3-$^i Pr_2$)Zr(BH_4)H, **14** (eq. 5.5). There is precedent for the hydrogenation of indenyl benzo rings on zirconium metal centers,[18,19,20] although it is rare to isolate a zirconocene complex where only one of the identical indenyl rings has undergone complete benzo hydrogenation, but likely this is simply a consequence of slow diffusion of H_2 gas. By ^{1}H NMR spectroscopy, there is one set of upfield shifted tetrahydroindenyl protons between 1.37 – 3.02 ppm, along with downfield shifted benzo protons at 6.70 – 7.25 ppm. Additionally, there is a broad BH_4 resonance at 0.03 and a Zr-*H* peak at 2.72 ppm,

indicative of a coordinatively saturated zirconium metal center.[20,21] The BH_4 resonance splits to the expected broad pseudo quartet at 90 ºC due to coupling to ^{11}B (I = 3/2, 81.2 % abundant) and ^{10}B (I = 3, 18.8 % abundant). The terminal and bridging hydrides of the BH_4 ligand undergo rapid exchange at 23 ºC, as judged by EXSY NMR spectroscopy, while no exchange was detected between the Zr-*H* and the borohydride up to 90 ºC with a mixing time of 500 ms. In the ^{11}B NMR spectrum, there is one broad resonance at 6.0 ppm, attributed to the borohydride. Both the ^{1}H and ^{11}B NMR resonances are similar to that of the bis(cyclopentadienyl) zirconocene borohydride hydride complexes.[22,23] The infrared spectrum of **15** also exhibits a Zr-*H* and $[BH_4]^-$ stretches, similar to that of $(\eta^5\text{-}C_5H_5)_2Zr(BH_4)H$.[24]

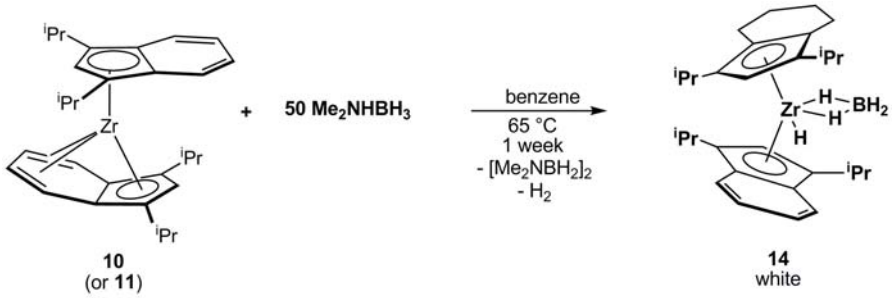

(eq. 5.5)

The molecular structure of **14** was also confirmed by a single crystal X-ray diffraction experiment. As shown in Figure 5.3, only one benzo ring has been hydrogenated, forming tetrahydroindenyl ligand. The two rings are *anti* to one another with a rotational angle of 169.1º. The hydrogen atoms were calculated but do fit well for a κ^2 tetrahydroborane ligand as shown in Table 5.2.[23]

Table 5.2. Comparison of selected metrical parameters for **14** and $(\eta^5\text{-}C_5H_5)_2Zr(BH_4)H$.

	14	$(\eta^5\text{-}C_5H_5)_2Zr(BH_4)H$[23]
Zr(1)-H(M) (Å)[a]	1.84(4)	1.70(7)
Zr(1)-H(1B) (Å)[b]	1.97(4)	2.07(7)
Zr(1)-H(2B) (Å)[b]	2.08(4)	2.09(7)
Zr(1)-B(1) (Å)	2.491(8)	2.538(11)
Rotational angle (°)	169.1	N/A

[a] Denotes zirconium metal hydride bond. [b] Denotes bridging hydride bond.

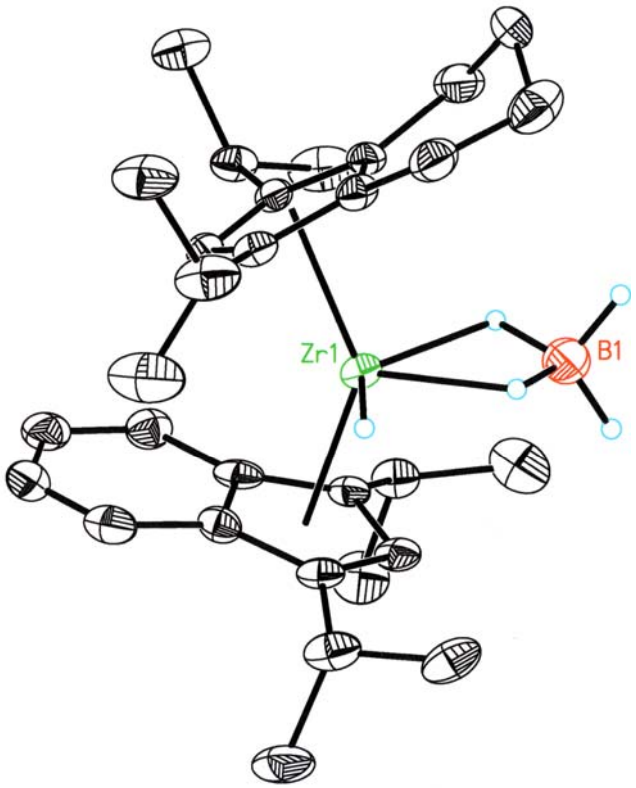

Figure 5.3. Molecular structure of **14** at 30 % probability ellipsoids.

After successfully characterizing **14**, the new zirconium complexes arising from the catalytic dehydrogenation of Me_2NHBH_3 with **8** and **12** were assigned as zirconocene borohydride hydrides, **13** and **16**, respectively, based on multinuclear NMR and IR spectroscopy (eq. 5.6 – 5.7). At least one new C_s symmetric organometallic compound was observed when **9** was used as the pre-catalyst. Unfortunately it was difficult to determine the saturation of the indenyl rings as other compounds obscured the pertinent regions of the ^{1}H NMR spectrum. Based on previous studies that established that benzo hydrogenation occurs faster for **9** than **10** under an atmosphere of dihydrogen[20] and **9** generates H_2 at a faster rate when catalytically dehydrogenating Me_2NHBH_3, the new zirconium complex should have two tetrahydroindenyl rings. These new zirconocenes are all, likely, the product of a competing "catalyst deactivation" pathway, where N-B bond cleavage occurs,

accounting for the observed dimethylamine. The BH_3 is then captured by a zirconocene dihydride, resulting in formation of the new zirconocene compounds. Similar N-B bond cleavage was observed in amine-borane dehydrogenation with iridium pincer catalysts, forming analogous iridium borohydride hydride complexes.[4] However, unlike the iridium model where this new species is catalytically inactive, **13** – **15** are still active for the dehydrogenation of Me_2NHBH_3 at 65 ºC, though with diminished turnover frequencies, implying that the coordination of BH_3 is reversible.

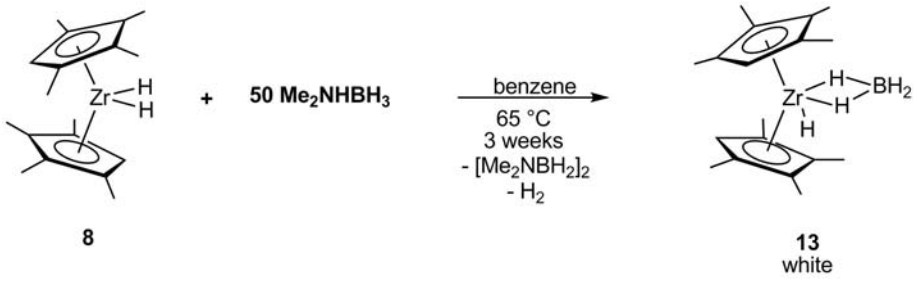

(eq. 5.6)

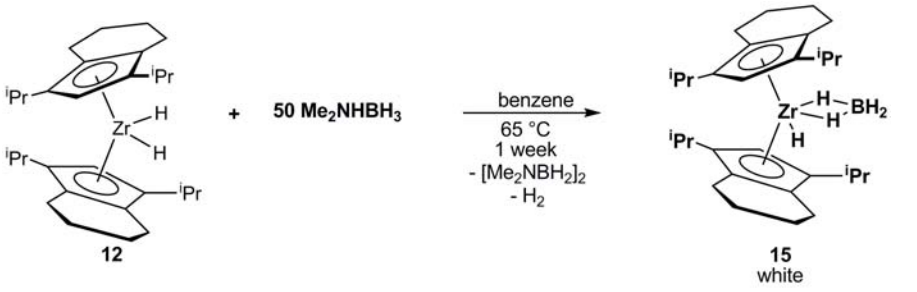

(eq. 5.7)

Conclusions

A series of isolable titanium and zirconium compounds have been evaluated for the catatytic dehydrogenation of Me_2NHBH_3. The titanocene complexes exhibit higher turnover frequencies than the zirconium compounds. Additionally, the presence electron withdrawing substituents favors the catalytic reaction, such that **4** is the best catalyst precursor explored in this study. The catalytic dehydrogenation of NH_3BH_3 with this titanium compound was also examined, though solubility issues lowered its catalytic activity. Through a series of experiments designed to probe the mechanism of the catalysis, it was shown that the activity trends observed are due to

the rate determining reductive elimination step; compounds that more readily undergo reductive elimination are the best catalysts. Also identified was a "catalyst deactivation" pathway as borohydride hydride compounds have been isolated that exhibit diminished catalytic activity from the starting metallocene complex.

Experimental

General Considerations. All air- and moisture-sensitive manipulations were carried out using standard vacuum line, Schlenk or cannula techniques or in an M. Braun inert atmosphere drybox containing an atmosphere of purified nitrogen. Solvents for air- and moisture-sensitive manipulations were initially dried and deoxygenated using literature procedures.[25] Benzene-d_6 was distilled from sodium metal under an atmosphere of argon and stored over 4 Å molecular sieves or titanocene. Argon and hydrogen gas were purchased from Airgas Incorporated and passed through a column containing manganese oxide on vermiculite and 4 Å molecular sieves before admission to the high vacuum line. Me_2NHBH_3 was purchased from Aldrich and sublimed at 30 ºC before use. H_3NBH_3 was prepared according to literature procedure[5] and recrystallized from a THF/Et_2O mixture at low temperature prior to use. Carbon monoxide was passed through a liquid nitrogen cooled trap immediately before use.

^{1}H NMR spectra were recorded on a Varian Inova 400 Spectrometer operating at 399.779 MHz (^{1}H), while ^{13}C spectra were collected on a Varian Inova 500 spectrometer operating at 125.704 MHz. ^{11}B NMR spectra were recorded on a Bruker ARX 300 MHz Spectrometer operating at 96.294 MHz (^{11}B). In some cases, reactions catalytic reactions were monitored in THF solution by ^{11}B NMR spectroscopy. Chemical shifts are reported relative to $SiMe_4$ using ^{1}H (residual) or ^{13}C NMR chemical shifts of the solvent as secondary standard or external $BF_3 \cdot Et_2O$ (^{11}B). **1**,[13a]

2,[13c] **3**,[13b] **4**,[13d] **7**,[13e] **8**[18] **9**,[15a] **10**,[15b] **11**[19] and **12**[19] were all prepared according to literature procedures.

Single crystals suitable for X-ray diffraction were coated with polyisobutylene oil in a drybox and were quickly transferred to the goniometer head of a Siemens SMART CCD Area detector system equipped with a molybdenum X-ray tube (δ = 0.71073 A). Preliminary data revealed the crystal system. A hemisphere routine was used for data collection and determination of lattice constants. The space group was identified and the data were processed using the Bruker SAINT program and corrected for absorption using SADABS. The structures were solved using direct methods (SHELXS) completed by subsequent Fourier synthesis and refined by full-matrix least-squares procedures. Infrared spectra were collected on a Thermo Nicolet spectrometer. Elemental analyses were performed at Robertson Microlit Laboratories, Inc., in Madison, NJ.

General Procedure for Catalytic Dehydrogenation of Me_2NHBH_3. A J. Young NMR tube was charged with 0.018 g (305 μmol) of Me_2NHBH_3 and 0.003 g (6 μmol) of the desired catalyst. Approximately 0.5 mL of benzene-d_6 was added to the tube, sealed with a Teflon valve and heated to 65 ºC in a temperature controlled oil bath if necessary. Conversion to $[Me_2NBH_2]_2$ was monitored as a function of time by ^{11}B NMR and ^{1}H NMR spectroscopy. ^{11}B NMR (benzene-d_6): δ = 5.0 (t, J_{BH} = 113 Hz, $[Me_2NBH_2]_2$); δ = 1.5 (t, J_{BH} = 113 Hz, $[Me_2NBH_2]_3$), δ = 37.8 (t, J_{BH} = 130 Hz, $Me_2N{=}BH_2$). A similar procedure was used for the dehydrogenation of NH_3BH_3 with THF as the solvent.

Quantification of H_2 Gas by Toepler Pump. A J. Young NMR tube was charged with 0.011 g (187 μmol) of Me_2NHBH_3 and 7 μmol of the desired catalyst.

Approximately 0.5 mL of benzene was added either by vacuum transfer or via pipette. The catalytic reaction was stirred until it reached the known time for completion after which time all of the gases were collected by a Toepler pump and quantified. The gases were exposed to combustion conditions by heating to 75 ºC under vacuum and the non-condensable gas recollected and the amount of hydrogen liberated determined by difference.

Preparation of (η^5-C_9H_5-1,3-$^i Pr_2$)(η^5-C_9H_9-1,3-$^i Pr_2$)Zr(BH_4)H (14). A thick walled glass vessel was charged with 0.050 g of (0.102 mmol) of **10** and approximately 5 mL of toluene was added. To the burgundy solution, 0.301 g (5.10 mmol) of Me_2NHBH_3 dissolved in approximately 15 mL of toluene was added, resulting in an immediate color change to yellow. The reaction mixture was stirred and heated to 65 ºC for one week, after which time the dihydrogen byproduct, solvent, amineborane product and unreacted starting material were removed *in vacuo*. Recrystallization from pentane at 35 ºC yielded 0.082 g (79.0%) of a white solid identified as **14**. Anal. Calcd. for $C_{30}H_{47}ZrB$: C, 70.59; H,9.22. Found: C, 70.59; H, 9.38. ^{1}H NMR (benzene-d_6): δ = 0.03 (br , 4H, BH_4), 1.02 (d, 8Hz, 3H, THI CHMe_2), 1.06 (d, 4Hz, 3H, THI CHMe_2), 1.13 (d, 7Hz, 3H, Ind CHMe_2), 1.16 (d, 7Hz, 3H, Ind CHMe_2), 1.21 (d, 7Hz, 3H, THI CHMe_2), 1.24 (d, 8Hz, 3H, THI CHMe_2), 1.37 (m, 1H, THI), 1.41 (m, 1H, THI), 1.51 (d, 7Hz, 3H, Ind CHMe_2), 1.62 (d, 7Hz, 3H, Ind CHMe_2), 1.92 (m, 2H, THI), 2.42 (m, 4H, 2 THI/2 THI CHMe$_2$), 2.72 (s, 1H, Zr-H), 2.81 (m, 1H, THI), 3.02 (m, 1H, THI), 3.36 (m, 1H, Ind CHMe$_2$), 3.85 (m, 1H, Ind CHMe$_2$), 5.45 (s, 1H, CpH), 6.34 (s, 1H, CpH), 6.70 (m, 1H, benzo), 6.77 (m, 1H, benzo), 7.25 (m, 2H, benzo). ^{11}B NMR (benzene-d_6): δ = 6.00 (br, Zr-BH$_4$). ^{13}C NMR (benzene-d_6): δ = 21.99, 22.22, 22.61, 23.17, 23.37, 24.09, 24.83, 25.49, 25.59, 25.73, 25.96, 25.97, 26.96, 27.41, 28.77, 29.74 (CHMe$_2$/THI), 108.5, 112.07, 117.34, 117.97, 120.10, 122.04, 123.08, 123.35,

124.20, 124.61, 124.85, 124.94, 126.18, 131.48 (Cp/Benzo). IR (KBr): ν = 2106 (w), 1966 (m), 1634 (w), 1456 (m), 1376 (m), 1142 cm^{-1} (w).

Preparation of (η^5-C_9H_9-1,3-^{i}Pr$_2$)$_2$Zr(BH_4)H (15). This compound was prepared in a similar manner to **14** with 0.070 g of (0.140 mmol) of **12** and 0.160 g (2.71 mmol) of Me_2NHBH_3 with heating at 65 ºC for three weeks. ^{1}H NMR (benzene-d_6): δ = -0.02 (br , 4H, B*H*$_4$), 1.16 (d, 3H, THI CH*Me*$_2$), 1.17 (d, 3H, THI CH*Me*$_2$), 1.20 (d, 3H, THI CH*Me*$_2$), 1.21 (d, 3H, THI CH*Me*$_2$), 1.48 (m, 2H, THI), 1.65 (m, 2H, THI), 1.98 (m, 2H, THI), 2.10 (m, 2H, THI), 2.49 (m, 2H, THI), 2.60 (m, 2H, THI), 2.80 (m, 2H, THI C*H*Me$_2$), 2.98 (m, 2H, THI), 3.02 (m, 2H, THI C*H*Me$_2$), 5.16 (s, 2H, Cp*H*), 5.44 (s, 1H, Zr*H*). ^{11}B NMR (benzene-d_6): δ = 7.90 (br, Zr-*B*H$_4$). ^{13}C NMR (benzene-d_6): δ = 23.33, 23.35, 24.08, 24.12, 24.38, 24.54, 25.89, 28.55, 28.77 (CHMe$_2$/THI), 98.35, 123.29, 123.45 (Cp). One CHMe$_2$/THI and two Cp resonances not located. IR (KBr): ν = 1965 (m), 1624 (w), 1450 (m), 1362 (m), 1143 cm^{-1} (w).

Preparation of (η^5-C_5Me_4H)$_2$Zr(BH_4)H (13). Prepared in a similar manner as **14** using 0.003 g of (.009 mmol) of **8** and 0.026 g (1.53 mmol) of Me_2NHBH_3, heating at 65 ºC for one week. ^{1}H NMR (benzene-d_6): δ = -0.03 (br , 4H, B*H*$_4$), 1.85 (s, 6H, Cp*Me*), 1.93 (s, 6H, Cp*Me*), 2.02 (s, 6H, Cp*Me*), 2.07 (s, 6H, Cp*Me*), 4.89 (s, 2H, Cp*H*), 5.34 (s, 1H, Zr-*H*). ^{11}B NMR (benzene-d_6): δ = 10.63 (br, Zr-*B*H$_4$). ^{13}C NMR (benzene-d_6): δ = 1.20, 1.38 (Si*Me*$_3$), 95.11, 123.04, 123.40, 124.10 (Cp/Benzo). Five Cp/Benzo resonances not located.

Preparation of (η^5-C_5H_3-1-Me-3-^{i}Pr)$_2$TiCl. A 250 mL round bottomed flask was charged with 1.495 g (11.67 mmol) of Li[C_5H_3-1-Me-3-^{i}Pr] and 2.14 g (5.84 mmol) of $TiCl_3(THF)_3$. Approximately 100 mL of THF was added by vacuum transfer. The

solution was heated to reflux overnight after which the solvent was removed *in vacuo*. The resulting solid was dissolved in pentane and filtered through Celite. Removal of the pentane *in vacuo* yielded a brown solid, which was recrystallized from pentane at –35 ºC. Anal. Calcd. for $C_{18}H_{26}TiCl$: C, 66.37; H, 8.05. Found: C, 65.97; H, 8.22.

Preparation of [(η^5-C_5H_3-1-Me,3-^{i}Pr)$_2$Ti]$_2$(μ_2, η^2, η^2-N_2) (5). A 100 mL round bottom flask was charged with 28.10 g of mercury and approximately 5 mL of toluene was added. To the stirring solution, 0.141 g (6.13 mmol) of sodium was added and the mixture was stirred for 20 minutes. 0.387 g (1.19 mmol) of (η^5-C_5H_3-1-Me,3-^{i}Pr)$_2$TiCl dissolved in 20 mL of toluene was added and the reaction was stirred vigorously for three days. Filtration of the blue solution through Celite followed by solvent removal *in vacuo* produced a blue oil. Recrystallization from pentane at –35 ºC yielded 0.10 g (13.8 %) of a blue solid identified as **5**. Anal. Calcd. for $C_{36}H_{52}Ti_2N_2$: C, 71.05; H, 8.61; N, 4.60. Found: C, 70.85; H, 9.06; N, 4.34.

REFERENCES

[1] Clark, T. J.; Lee, K.; Manners, I. *Chem. Eur. J.* **2006**, *12*, 8634.

[2] Hamilton, C. W.; Baker, R. T.; Staubitz, A.; Manners, I. *Chem. Soc. Rev.* **2009**, *38*, 279.

[3] (a) Jaska, C. A.; Temple, K.; Lough, A. J.; Manners, I. *Chem. Commun.* **2001**, 962. (b) Jaska, C. A.; Temple, K.; Lough, A. J.; Manners, I. *J. Am. Chem. Soc.* **2003**, *125*, 9424.

[4] Denney, M. C.; Pons, V.; Hebden, T. J.; Heinekey, D. M.; Goldberg, K. I. *J. Am. Chem. Soc.* **2006**, *128*, 12048.

[5] Keaton, R. J.; Blacquiere, M.; Baker, R. T. *J. Am. Chem. Soc.* **2006**, *127*, 1844.

[6] Zimmerman, P. M.; Paul, A.; Zhang, Z.; Musgrave, C. B. *Angew. Chem., Int. Ed.* **2009**, *48*, 2201.

[7] Zimmerman, P. M.; Paul, A.; Musgrave, C. B.; *Inorg. Chem.* **2009**, *48*, 5418.

[8] Yoon, C. W.; Sneddon, L. G. *J. Am. Chem. Soc.* **2006**, *128*, 13992.

[9] Clark, T. J.; Russell, C. A.; Manners, I. *J. Am. Chem. Soc.* **2006**, *128*, 9582.

[10] Brintzinger, H. H.; Bercaw, J. E. *J. Am. Chem. Soc.* **1970**, *92*, 6182.

[11] Fischer, A. K.; Wilkinson, G. *J. Inorg. Nuc. Chem.* **1956**, *2*, 149.

[12] Dioumaev, V. K.; Harrod, J. F. *Organometallics* **1997**, *16*, 1452.

[13] (a) Bercaw, J. E.; Brintzinger, H. H. *J. Am. Chem. Soc.* **1971**, *93*, 2045. (b) de Wolf, J. M.; Blaauw, R.; Meetsma, A.; Teuben J. H.; Gyepes, R.; Varga, V.; Mach, K.; Veldman, N.; Spek, A. L. *Organometallics* **1996**, *15*, 4977. (c) Hanna, T. E.; Lobkovsky, E.; Chirik, P. J. *J. Am. Chem. Soc.* **2004**, *126*, 14688. (d) Hanna, T. E.; Keresztes, I.; Bernskoetter, W. H.; Lobkovsky, E.; Chirik, P. J. *Organometallics* **2004**, *23*, 3448. (e) Hanna, T. E.; Bernskoetter, W. H.; Bouwkamp, M. W.; Lobkovsky, E.; Chirik, P. J. *Organometallics* **2007**, *26*, 2431.

[14] Hitchcock, P. B.; Kerton, F.; Lawless, G. A. *J. Am. Chem. Soc.* **1998**, *120*, 10264.

[15] (a) Bradley, C. A.; Lobkovsky, E.; Chirik, P. J. *J. Am. Chem. Soc.* **2003**, *125*, 8110. (b) Bradley, C. A.; Keresztes, I.; Lobkovsky, E.; Young, V. G.; Chirik, P. J. *J. Am. Chem. Soc.* **2004**, *126*, 16937.

[16] In the situations where the catalyst is a dimer, 2 mol % of titanium was used.

[17] Luo, Y.; Ohno, K. *Organometallics* **2007**, *26*, 3597.

[18] Weigold, H.; Bell, A. P.; Willing, R. I. *J. Organomet. Chem.* **1974**, *73*, C23.

[19] Chirik, P. J.; Day, M. W.; Bercaw, J. E. *Organometallics* **1999**, *18*, 1873.

[20] Bradley, C.A.; Lobkovsky, E.; Keresztes, I. Chirik, P. J. *J. Am. Chem. Soc.* **2006**, *128*, 6454.

[21] Chirik, P. J.; Henling, L. M.; Bercaw, J. E.; *Organometallics*. **2001**, *20*, 534.

[22] Marks, T. J.; Kolb, J. R.; *J. Am. Chem. Soc.* **1975**, *97*, 3397.

[23] Liu, F.-C.; Chen, J.-H.; Chen, S.-C.; Chen, K.-Y.; Lee, G.-H.; Peng, S.-M. *J. Organomet. Chem.* **2005**, *690*, 291.

[24] James, B. D.; Nanda, R. K.; Wallbridge, M. G. H. *Inorg. Chem.* **1967**, *6*, 1979.

[25] Pangborn, A. B.; Giardello, M. A.; Grubbs, R. H.; Rosen, R. K.; Timmers, F. J. *Organometallic.* **1996**, *15*, 1518.

APPENDIX A: EPR Data

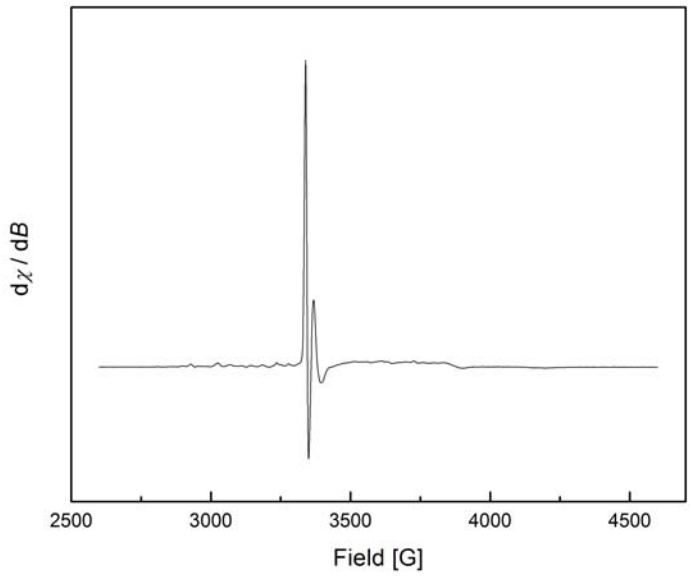

Figure A1. Toluene glass EPR spectrum of **5-Cl** (Chapter 2) collected at 5 K. g_x = 1.98, g_y = 1.96 and g_z = 1.70.

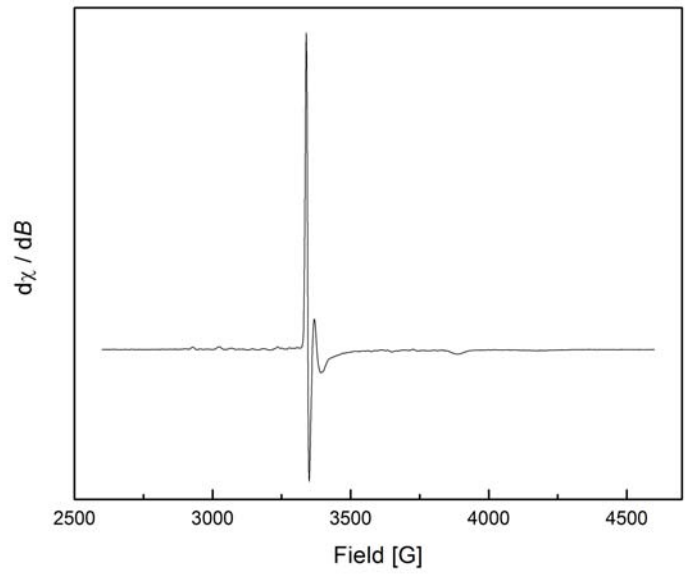

Figure A2. Toluene glass EPR spectrum of **5-Cl** (Chapter 2) collected at 26 K. g_x = 1.98, g_y = 1.96 and g_z = 1.70.

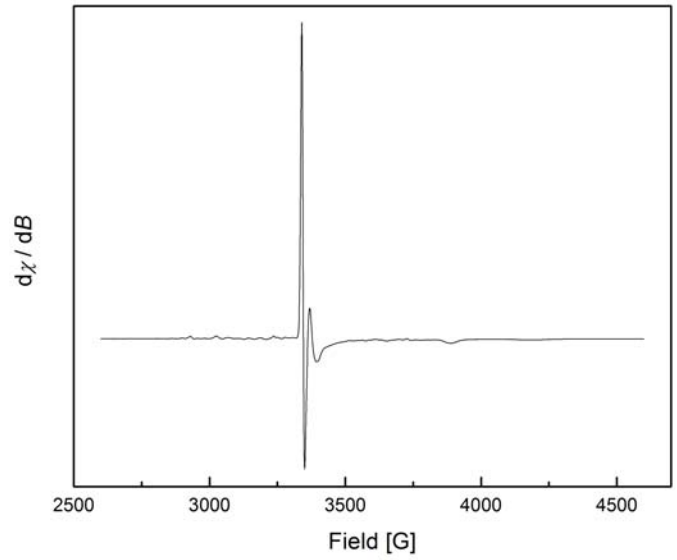

Figure A3. Toluene glass EPR spectrum of 5-Cl (Chapter 2) collected at 50 K. g_x = 1.98, g_y = 1.96 and g_z = 1.70.

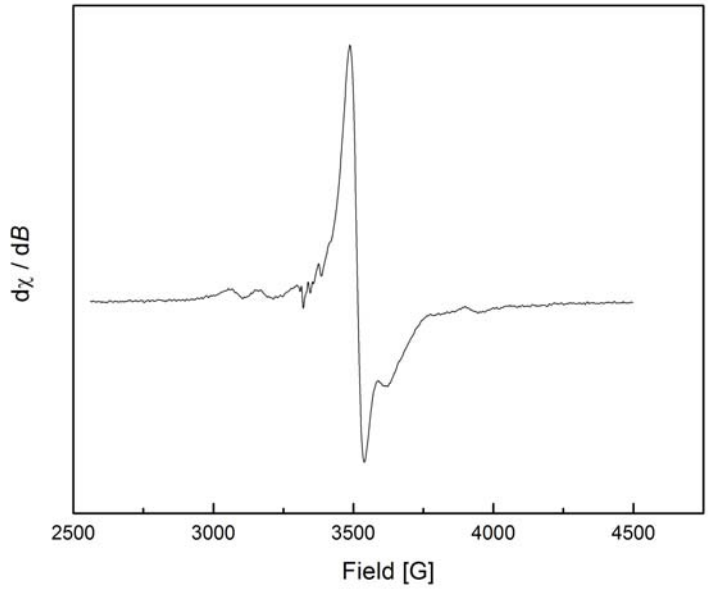

Figure A4. EPR spectrum of **5-Cl** (Chapter 2) in toluene collected at 293 K.

APPENDIX B: Kinetic Data

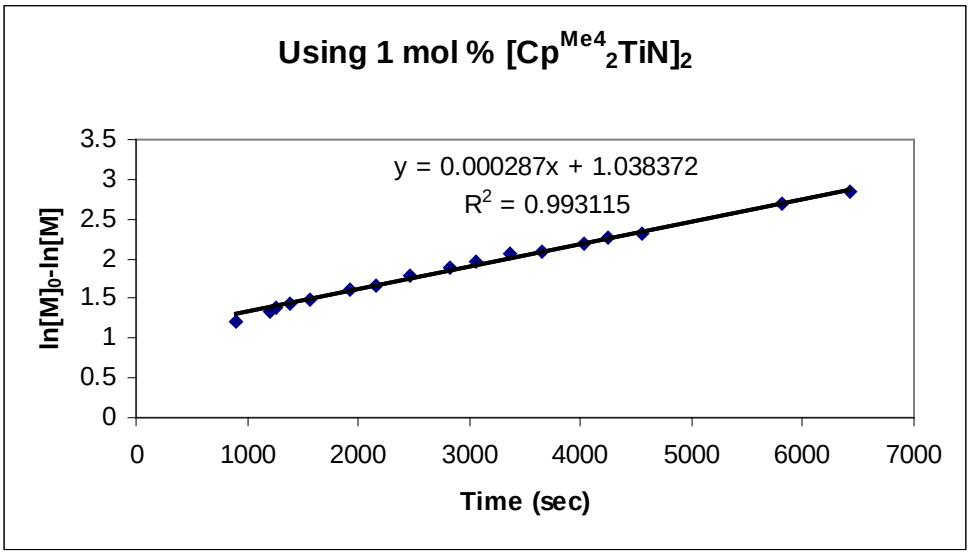

Figure B1. Plot of ln(Me_2NHBH_3) vs time (sec) for the catalytic dehydrogenation of Me_2NHBH_3 at 22 ºC using 1 mol % cat. loading of **[Cp^{Me4}_2TiN]$_2$**.

APPENDIX C: Crystal Structure Data

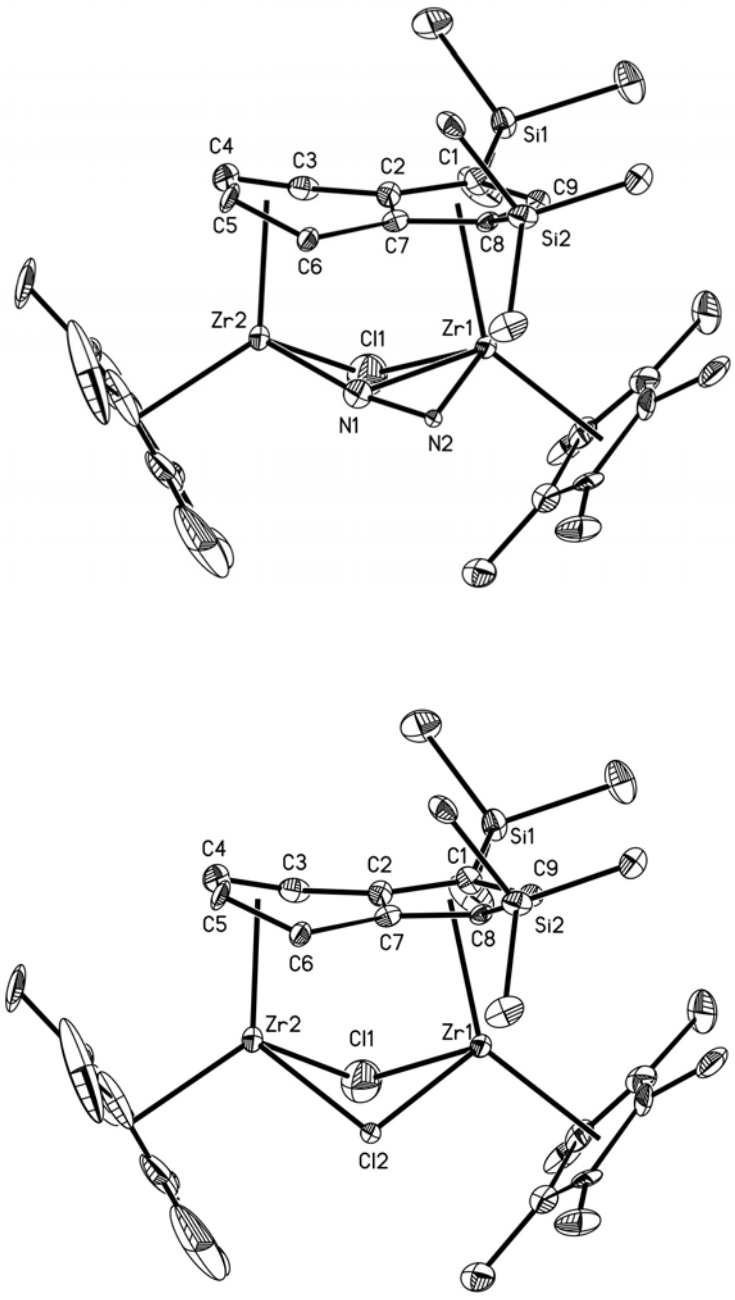

Figure C.1. Molecular structure of (a) **18-N_2Cl** and (b) **18-Cl_2** at 30 % probability ellipsoids. Both molecules were co-crystallized in the same unit cell. Hydrogen atoms omitted for clarity.

Table C.1. Compiled X-ray data on compounds discussed in thesis.

Compound	CU X-ray ID	Location
14 (Chapter 5)	dp1	CCDC 642675
6_2-N_2 (Chapter 1)	dp7	CCDC 695050
18-N_2Cl & **18-Cl_2** (Chapter 1)	dp8	Appendix B
16-N_2Cl (Chapter 1)	dp9	CCDC 708549
8 (Chapter 1)	dp10	CCDC 695047
[13-NaI]$_2$$N_2$ (Chapter 1)	dp11	CCDC 712779
[13-Cl]$_2$(N_2)(Na){Na(crown-ether)}$_{1.5}$ (Chapter 1)	dp12	CCDC 730316
[5-Cl]$_2$Na{Na(DME)$_3$} (Chapter 2)	dp13	CCDC 733697
1-(CH_2CHCH_2)$_2$N^{t}Bu (Chapter 3)	dp14	Appendix B
5-Cl (Chapter 2)	dp15	CCDC 733695
1-(O^{c}Pent)$_2$-1,4 (Chapter 3)	dp16	CCDC 756463
[*meso*-3]$_2$-HI (Chapter 4)	dp19	Appendix B
3-(O^{c}Pent)$_2$-1,4 (Chapter 3)	dp20	CCDC 756464
[*rac*-4]$_2$-N_2 (Chapter 4)	dp24	Appendix B
[*meso*-3]$_2$-N_2 (Chapter 4)	dp26	Appendix B
1-(Ofluorenyl)$_2$ (Chapter 3)	dp28	Appendix B
1-(OMe_2)$_2$-4,7 (Chapter 3)	dp31	Appendix B

Table C.2. Crystal data and structure refinement for **18-N_2Cl** & **18-Cl_2** (Chapter 1).

Identification code	**18-N_2Cl** & **18-Cl_2**	
Empirical formula	C35 H53 Cl1.38 N1.25 Si2 Zr2	
Formula weight	778.76	
Temperature	173(2) K	
Wavelength	0.71073 Å	
Crystal system	Monoclinic	
Space group	P2(1)	
Unit cell dimensions	a = 9.4060(5) Å	α= 90°.
	b = 17.2333(11) Å	β= 110.745(3)°.
	c = 11.7355(7) Å	γ = 90°.
Volume	1778.95(18) $Å^3$	
Z	2	
Density (calculated)	1.454 Mg/m^3	
Absorption coefficient	0.782 mm^{-1}	
F(000)	806	
Crystal size	0.30 x 0.20 x 0.03 mm^3	
Theta range for data collection	1.86 to 26.43°.	
Index ranges	-11<=h<=11, 0<=k<=21, 0<=l<=14	
Reflections collected	6734	
Independent reflections	6734 [R(int) = 0.0000]	
Completeness to theta = 26.43°	99.9 %	
Absorption correction	Semi-empirical from equivalents	
Max. and min. transmission	0.9807 and 0.7992	
Refinement method	Full-matrix least-squares on F^2	
Data / restraints / parameters	6734 / 459 / 384	
Goodness-of-fit on F^2	1.017	
Final R indices [I>2sigma(I)]	R1 = 0.0427, wR2 = 0.0981	
R indices (all data)	R1 = 0.0623, wR2 = 0.1137	
Absolute structure parameter	0.16(10)	
Largest diff. peak and hole	0.656 and -0.747 $e.Å^{-3}$	

Table C.3. Atomic coordinates (x 10^4) and equivalent isotropic displacement parameters (Å^2 x 10^3) for **18-N_2Cl** & **18-Cl_2**. U(eq) is defined as one third of the trace of the orthogonalized U^{ij} tensor.

	x	y	z	U(eq)
Zr(1)	1645(1)	4009(1)	7665(1)	19(1)
Zr(2)	3242(1)	4000(1)	10710(1)	22(1)
Cl(1)	3364(3)	3023(1)	9083(2)	68(1)
Si(1)	-1274(2)	2312(1)	7609(2)	29(1)
Si(2)	-1294(2)	5709(1)	7596(2)	25(1)
N(2)	2691(6)	5174(3)	8381(5)	11(1)
N(1)	3081(8)	4685(5)	9376(7)	31(2)
Cl(2)	3466(4)	5020(2)	9120(3)	15
C(1)	-555(7)	3307(3)	7979(6)	23(1)
C(2)	211(6)	3607(3)	9178(5)	22(1)
C(3)	923(6)	3206(4)	10279(6)	29(1)
C(4)	1193(6)	3621(4)	11388(6)	33(1)
C(5)	1177(7)	4410(4)	11397(6)	30(1)
C(6)	1036(7)	4856(4)	10330(5)	24(1)
C(7)	238(7)	4449(4)	9143(6)	19(1)
C(8)	-549(7)	4687(4)	7936(6)	18(1)
C(9)	-1019(4)	4071(4)	7223(3)	19(1)
C(10)	1118(7)	4439(4)	5470(5)	34(1)
C(11)	1085(8)	3607(5)	5433(7)	38(1)
C(12)	2473(7)	3344(4)	6141(6)	32(1)
C(13)	3492(4)	4007(7)	6597(3)	27(1)
C(14)	2654(6)	4683(4)	6138(6)	27(1)
C(15)	-109(7)	4974(5)	4684(6)	54(2)
C(16)	-254(9)	3155(5)	4669(7)	58(3)
C(17)	3136(8)	2531(4)	6223(6)	46(2)
C(18)	5171(4)	3954(6)	7355(4)	35(1)
C(19)	3128(8)	5518(4)	6296(8)	48(2)
C(20)	5455(6)	3373(4)	12340(7)	44(2)

Table C.3. (continued)

C(21)	4822(5)	3914(6)	12930(4)	48(1)
C(22)	4975(8)	4642(5)	12517(8)	68(2)
C(23)	5793(8)	4584(5)	11825(8)	77(2)
C(24)	6079(5)	3835(6)	11613(5)	60(2)
C(25)	5622(9)	2540(4)	12471(8)	89(3)
C(26)	4252(7)	3900(17)	13923(5)	223(6)
C(27)	4561(12)	5363(6)	13101(9)	179(5)
C(28)	6313(10)	5287(6)	11287(10)	216(5)
C(29)	7000(7)	3512(8)	10897(7)	174(6)
C(30)	-2824(8)	2212(5)	5981(7)	47(2)
C(31)	183(7)	1564(4)	7724(7)	54(3)
C(32)	-2132(8)	2024(4)	8698(7)	47(2)
C(33)	213(7)	6440(4)	7690(6)	33(2)
C(34)	-2235(7)	5943(4)	8745(6)	30(2)
C(35)	-2760(7)	5708(4)	6112(6)	27(2)

Table C.4. Bond lengths [Å] and angles [°] for **18-N_2Cl** & **18-Cl_2**.

Zr(1)-N(2)	2.262(6)	C(10)-C(11)	1.435(7)
Zr(1)-N(1)	2.301(8)	C(10)-C(14)	1.441(8)
Zr(1)-C(9)	2.375(3)	C(10)-C(15)	1.509(9)
Zr(1)-C(12)	2.471(7)	C(11)-C(12)	1.353(9)
Zr(1)-C(13)	2.476(4)	C(11)-C(16)	1.482(10)
Zr(1)-C(8)	2.487(6)	C(12)-C(13)	1.466(11)
Zr(1)-Cl(1)	2.523(2)	C(12)-C(17)	1.522(10)
Zr(1)-C(1)	2.533(6)	C(13)-C(14)	1.402(12)
Zr(1)-C(10)	2.555(6)	C(13)-C(18)	1.516(5)
Zr(1)-C(14)	2.582(7)	C(14)-C(19)	1.498(10)
Zr(1)-C(11)	2.577(7)	C(20)-C(21)	1.413(11)
Zr(1)-Cl(2)	2.610(4)	C(20)-C(24)	1.436(10)
Zr(2)-N(1)	1.924(8)	C(20)-C(25)	1.447(10)
Zr(2)-C(4)	2.421(7)	C(21)-C(22)	1.371(13)
Zr(2)-C(22)	2.435(7)	C(21)-C(26)	1.445(8)
Zr(2)-C(5)	2.456(7)	C(22)-C(23)	1.306(13)
Zr(2)-C(6)	2.454(7)	C(22)-C(27)	1.533(12)
Zr(2)-C(3)	2.470(6)	C(23)-C(24)	1.359(13)
Zr(2)-C(23)	2.501(7)	C(23)-C(28)	1.525(11)
Zr(2)-C(21)	2.505(4)	C(24)-C(29)	1.511(10)
Zr(2)-C(24)	2.514(5)		
Zr(2)-C(20)	2.517(6)	N(2)-Zr(1)-N(1)	35.2(2)
Zr(2)-Cl(1)	2.578(3)	N(2)-Zr(1)-C(9)	109.1(2)
Zr(2)-Cl(2)	2.626(4)	N(1)-Zr(1)-C(9)	114.6(2)
Si(1)-C(32)	1.807(8)	N(2)-Zr(1)-C(12)	118.3(2)
Si(1)-C(1)	1.839(6)	N(1)-Zr(1)-C(12)	128.9(2)
Si(1)-C(31)	1.851(7)	C(9)-Zr(1)-C(12)	116.20(19)
Si(1)-C(30)	1.957(7)	N(2)-Zr(1)-C(13)	84.2(3)
Si(2)-C(35)	1.799(6)	N(1)-Zr(1)-C(13)	98.1(3)
Si(2)-C(33)	1.870(7)	C(9)-Zr(1)-C(13)	139.91(13)
Si(2)-C(8)	1.885(7)	C(12)-Zr(1)-C(13)	34.5(3)
Si(2)-C(34)	1.899(8)	N(2)-Zr(1)-C(8)	78.9(2)
N(2)-N(1)	1.379(9)	N(1)-Zr(1)-C(8)	84.7(2)
C(1)-C(2)	1.431(8)	C(9)-Zr(1)-C(8)	31.6(2)
C(1)-C(9)	1.560(9)	C(12)-Zr(1)-C(8)	143.01(19)
C(2)-C(3)	1.408(8)	C(13)-Zr(1)-C(8)	145.9(3)
C(2)-C(7)	1.452(5)	N(2)-Zr(1)-Cl(1)	105.05(15)
C(3)-C(4)	1.427(9)	N(1)-Zr(1)-Cl(1)	74.0(2)
C(4)-C(5)	1.360(6)	C(9)-Zr(1)-Cl(1)	123.66(16)
C(5)-C(6)	1.435(9)	C(12)-Zr(1)-Cl(1)	82.66(16)
C(6)-C(7)	1.502(9)	C(13)-Zr(1)-Cl(1)	86.1(2)
C(7)-C(8)	1.407(9)	C(8)-Zr(1)-Cl(1)	126.79(16)
C(8)-C(9)	1.327(9)	N(2)-Zr(1)-C(1)	129.8(2)

Table C.4. (continued)

N(1)-Zr(1)-C(1)	111.9(2)	C(11)-Zr(1)-Cl(2)	134.0(2)
C(9)-Zr(1)-C(1)	36.9(2)	N(1)-Zr(2)-C(4)	126.2(3)
C(12)-Zr(1)-C(1)	111.5(2)	N(1)-Zr(2)-C(22)	105.4(3)
C(13)-Zr(1)-C(1)	145.9(3)	C(4)-Zr(2)-C(22)	101.6(3)
C(8)-Zr(1)-C(1)	56.55(13)	N(1)-Zr(2)-C(5)	104.3(3)
Cl(1)-Zr(1)-C(1)	87.02(14)	C(4)-Zr(2)-C(5)	32.37(15)
N(2)-Zr(1)-C(10)	91.2(2)	C(22)-Zr(2)-C(5)	87.0(3)
N(1)-Zr(1)-C(10)	125.3(3)	N(1)-Zr(2)-C(6)	70.5(3)
C(9)-Zr(1)-C(10)	87.38(18)	C(4)-Zr(2)-C(6)	60.1(2)
C(12)-Zr(1)-C(10)	53.4(2)	C(22)-Zr(2)-C(6)	98.5(2)
C(13)-Zr(1)-C(10)	53.9(2)	C(5)-Zr(2)-C(6)	34.0(2)
C(8)-Zr(1)-C(10)	96.8(2)	N(1)-Zr(2)-C(3)	111.4(3)
Cl(1)-Zr(1)-C(10)	135.29(17)	C(4)-Zr(2)-C(3)	33.9(2)
C(1)-Zr(1)-C(10)	114.1(2)	C(22)-Zr(2)-C(3)	134.4(3)
N(2)-Zr(1)-C(14)	68.9(2)	C(5)-Zr(2)-C(3)	58.9(2)
N(1)-Zr(1)-C(14)	97.5(3)	C(6)-Zr(2)-C(3)	70.58(15)
C(9)-Zr(1)-C(14)	116.58(18)	N(1)-Zr(2)-C(23)	87.9(3)
C(12)-Zr(1)-C(14)	54.47(15)	C(4)-Zr(2)-C(23)	131.7(3)
C(13)-Zr(1)-C(14)	32.1(3)	C(22)-Zr(2)-C(23)	30.6(3)
C(8)-Zr(1)-C(14)	113.8(2)	C(5)-Zr(2)-C(23)	115.9(3)
Cl(1)-Zr(1)-C(14)	116.97(15)	C(6)-Zr(2)-C(23)	116.5(3)
C(1)-Zr(1)-C(14)	146.69(19)	C(3)-Zr(2)-C(23)	160.7(2)
C(10)-Zr(1)-C(14)	32.58(19)	N(1)-Zr(2)-C(21)	136.8(3)
N(2)-Zr(1)-C(11)	121.4(2)	C(4)-Zr(2)-C(21)	83.71(19)
N(1)-Zr(1)-C(11)	150.3(3)	C(22)-Zr(2)-C(21)	32.2(3)
C(9)-Zr(1)-C(11)	88.31(19)	C(5)-Zr(2)-C(21)	85.57(19)
C(12)-Zr(1)-C(11)	31.0(2)	C(6)-Zr(2)-C(21)	112.1(2)
C(13)-Zr(1)-C(11)	54.0(2)	C(3)-Zr(2)-C(21)	109.6(2)
C(8)-Zr(1)-C(11)	112.1(2)	C(23)-Zr(2)-C(21)	51.3(3)
Cl(1)-Zr(1)-C(11)	109.99(19)	N(1)-Zr(2)-C(24)	100.3(3)
C(1)-Zr(1)-C(11)	97.8(2)	C(4)-Zr(2)-C(24)	132.9(2)
C(10)-Zr(1)-C(11)	32.46(16)	C(22)-Zr(2)-C(24)	53.2(3)
C(14)-Zr(1)-C(11)	53.7(2)	C(5)-Zr(2)-C(24)	137.7(2)
N(2)-Zr(1)-Cl(2)	21.01(15)	C(6)-Zr(2)-C(24)	147.9(3)
N(1)-Zr(1)-Cl(2)	17.2(2)	C(3)-Zr(2)-C(24)	138.8(3)
C(9)-Zr(1)-Cl(2)	120.69(18)	C(23)-Zr(2)-C(24)	31.4(3)
C(12)-Zr(1)-Cl(2)	118.74(17)	C(21)-Zr(2)-C(24)	53.47(16)
C(13)-Zr(1)-Cl(2)	85.2(2)	N(1)-Zr(2)-C(20)	133.4(3)
C(8)-Zr(1)-Cl(2)	89.14(17)	C(4)-Zr(2)-C(20)	100.1(2)
Cl(1)-Zr(1)-Cl(2)	84.21(7)	C(22)-Zr(2)-C(20)	54.2(2)
C(1)-Zr(1)-Cl(2)	127.17(17)	C(5)-Zr(2)-C(20)	114.3(2)
C(10)-Zr(1)-Cl(2)	108.29(18)	C(6)-Zr(2)-C(20)	144.5(2)
C(14)-Zr(1)-Cl(2)	80.57(18)	C(3)-Zr(2)-C(20)	110.5(2)

Table C.4. (continued)

C(23)-Zr(2)-C(20)	52.7(2)	C(2)-C(1)-Si(1)	125.7(5)
C(21)-Zr(2)-C(20)	32.7(2)	C(9)-C(1)-Si(1)	130.3(4)
C(24)-Zr(2)-C(20)	33.2(2)	C(2)-C(1)-Zr(1)	79.5(4)
N(1)-Zr(2)-Cl(1)	79.0(2)	C(9)-C(1)-Zr(1)	66.0(3)
C(4)-Zr(2)-Cl(1)	108.44(18)	Si(1)-C(1)-Zr(1)	131.5(3)
C(22)-Zr(2)-Cl(1)	138.6(2)	C(3)-C(2)-C(1)	129.4(6)
C(5)-Zr(2)-Cl(1)	132.72(17)	C(3)-C(2)-C(7)	120.6(6)
C(6)-Zr(2)-Cl(1)	120.95(15)	C(1)-C(2)-C(7)	109.9(6)
C(3)-Zr(2)-Cl(1)	75.77(17)	C(3)-C(2)-Zr(1)	123.3(4)
C(23)-Zr(2)-Cl(1)	111.3(2)	C(1)-C(2)-Zr(1)	68.7(4)
C(21)-Zr(2)-Cl(1)	124.5(2)	C(7)-C(2)-Zr(1)	72.8(5)
C(24)-Zr(2)-Cl(1)	85.38(19)	C(3)-C(2)-Zr(2)	59.7(3)
C(20)-Zr(2)-Cl(1)	92.33(18)	C(1)-C(2)-Zr(2)	138.2(5)
N(1)-Zr(2)-Cl(2)	9.5(2)	C(7)-C(2)-Zr(2)	76.0(4)
C(4)-Zr(2)-Cl(2)	133.47(16)	Zr(1)-C(2)-Zr(2)	74.43(15)
C(22)-Zr(2)-Cl(2)	96.7(2)	C(2)-C(3)-C(4)	117.7(6)
C(5)-Zr(2)-Cl(2)	108.23(18)	C(2)-C(3)-Zr(2)	90.8(4)
C(6)-Zr(2)-Cl(2)	75.18(18)	C(4)-C(3)-Zr(2)	71.1(4)
C(3)-Zr(2)-Cl(2)	120.83(16)	C(5)-C(4)-C(3)	120.6(7)
C(23)-Zr(2)-Cl(2)	78.4(2)	C(5)-C(4)-Zr(2)	75.2(5)
C(21)-Zr(2)-Cl(2)	127.7(2)	C(3)-C(4)-Zr(2)	75.0(4)
C(24)-Zr(2)-Cl(2)	91.99(19)	C(4)-C(5)-C(6)	121.8(8)
C(20)-Zr(2)-Cl(2)	125.05(18)	C(4)-C(5)-Zr(2)	72.4(5)
Cl(1)-Zr(2)-Cl(2)	82.82(7)	C(6)-C(5)-Zr(2)	72.9(4)
Zr(1)-Cl(1)-Zr(2)	82.09(7)	C(5)-C(6)-C(7)	114.9(6)
C(32)-Si(1)-C(1)	107.9(3)	C(5)-C(6)-Zr(2)	73.1(4)
C(32)-Si(1)-C(31)	105.2(4)	C(7)-C(6)-Zr(2)	90.0(4)
C(1)-Si(1)-C(31)	115.5(3)	C(8)-C(7)-C(2)	108.2(6)
C(32)-Si(1)-C(30)	107.5(3)	C(8)-C(7)-C(6)	135.2(6)
C(1)-Si(1)-C(30)	113.4(3)	C(2)-C(7)-C(6)	116.6(6)
C(31)-Si(1)-C(30)	106.6(3)	C(8)-C(7)-Zr(1)	68.3(4)
C(35)-Si(2)-C(33)	111.3(3)	C(2)-C(7)-Zr(1)	75.5(5)
C(35)-Si(2)-C(8)	107.6(3)	C(6)-C(7)-Zr(1)	122.8(4)
C(33)-Si(2)-C(8)	113.6(3)	C(9)-C(8)-C(7)	109.9(6)
C(35)-Si(2)-C(34)	107.3(3)	C(9)-C(8)-Si(2)	126.8(4)
C(33)-Si(2)-C(34)	110.4(3)	C(7)-C(8)-Si(2)	120.6(5)
C(8)-Si(2)-C(34)	106.3(3)	C(9)-C(8)-Zr(1)	69.5(3)
N(1)-N(2)-Zr(1)	73.9(4)	C(7)-C(8)-Zr(1)	80.0(4)
N(2)-N(1)-Zr(2)	169.7(6)	Si(2)-C(8)-Zr(1)	132.4(3)
N(2)-N(1)-Zr(1)	70.9(4)	C(8)-C(9)-C(1)	110.7(3)
Zr(2)-N(1)-Zr(1)	104.6(3)	C(8)-C(9)-Zr(1)	78.9(3)
Zr(2)-Cl(2)-Zr(1)	79.0(2)	C(1)-C(9)-Zr(1)	77.1(3)
C(2)-C(1)-C(9)	101.3(5)	C(11)-C(10)-C(14)	108.3(6)

Table C.4. (continued)

C(11)-C(10)-C(15)	126.0(7)		
C(14)-C(10)-C(15)	123.9(7)	C(21)-C(20)-C(25)	130.7(8)
C(11)-C(10)-Zr(1)	74.6(5)	C(24)-C(20)-C(25)	124.2(8)
C(14)-C(10)-Zr(1)	74.7(4)	C(21)-C(20)-Zr(2)	73.2(3)
C(15)-C(10)-Zr(1)	128.8(5)	C(24)-C(20)-Zr(2)	73.3(3)
C(12)-C(11)-C(10)	108.1(7)	C(25)-C(20)-Zr(2)	122.5(4)
C(12)-C(11)-C(16)	128.5(7)	C(22)-C(21)-C(20)	108.4(6)
C(10)-C(11)-C(16)	123.2(7)	C(22)-C(21)-C(26)	114.5(14)
C(12)-C(11)-Zr(1)	70.2(4)	C(20)-C(21)-C(26)	136.5(14)
C(10)-C(11)-Zr(1)	72.9(5)	C(22)-C(21)-Zr(2)	71.1(4)
C(16)-C(11)-Zr(1)	125.4(6)	C(20)-C(21)-Zr(2)	74.1(3)
C(11)-C(12)-C(13)	109.0(6)	C(26)-C(21)-Zr(2)	125.9(3)
C(11)-C(12)-C(17)	129.2(6)	C(23)-C(22)-C(21)	108.0(7)
C(13)-C(12)-C(17)	119.6(6)	C(23)-C(22)-C(27)	129.7(9)
C(11)-C(12)-Zr(1)	78.8(4)	C(21)-C(22)-C(27)	120.6(9)
C(13)-C(12)-Zr(1)	73.0(3)	C(23)-C(22)-Zr(2)	77.5(5)
C(17)-C(12)-Zr(1)	127.5(5)	C(21)-C(22)-Zr(2)	76.7(4)
C(14)-C(13)-C(12)	107.5(3)	C(27)-C(22)-Zr(2)	124.0(5)
C(14)-C(13)-C(18)	127.0(9)	C(22)-C(23)-C(24)	112.6(7)
C(12)-C(13)-C(18)	125.3(9)	C(22)-C(23)-C(28)	122.9(10)
C(14)-C(13)-Zr(1)	78.1(3)	C(24)-C(23)-C(28)	124.5(9)
C(12)-C(13)-Zr(1)	72.6(3)	C(22)-C(23)-Zr(2)	71.9(4)
C(18)-C(13)-Zr(1)	118.4(3)	C(24)-C(23)-Zr(2)	74.8(4)
C(13)-C(14)-C(10)	106.6(6)	C(28)-C(23)-Zr(2)	119.5(5)
Zr(1)-Cl(2)-Zr(2)	79.57(11)	C(23)-C(24)-C(20)	105.6(7)
C(13)-C(14)-C(19)	130.4(6)	C(23)-C(24)-C(29)	129.8(8)
C(10)-C(14)-C(19)	123.0(6)	C(20)-C(24)-C(29)	124.2(9)
C(13)-C(14)-Zr(1)	69.8(3)	C(23)-C(24)-Zr(2)	73.8(4)
C(10)-C(14)-Zr(1)	72.7(4)	C(20)-C(24)-Zr(2)	73.5(3)
C(19)-C(14)-Zr(1)	120.9(5)	C(29)-C(24)-Zr(2)	122.6(4)
C(21)-C(20)-C(24)	104.9(6)		

Table C.5. Anisotropic displacement parameters ($Å^2 x\ 10^3$) for **18-N_2Cl** & **18-Cl_2**. The anisotropic displacement factor exponent takes the form: $-2\pi^2[\ h^2 a^{*2} U^{11} + ... + 2\ h\ k\ a^*\ b^*\ U^{12}\ ]$

	U^{11}	U^{22}	U^{33}	U^{23}	U^{13}	U^{12}
Zr(1)	21(1)	22(1)	16(1)	-1(1)	7(1)	-1(1)
Zr(2)	23(1)	26(1)	15(1)	0(1)	5(1)	-1(1)
Cl(1)	67(1)	77(2)	61(1)	11(1)	23(1)	6(1)
Si(1)	34(1)	21(1)	25(1)	5(1)	3(1)	-6(1)
Si(2)	24(1)	14(1)	36(1)	7(1)	11(1)	-1(1)
C(1)	25(2)	14(2)	26(3)	2(2)	5(2)	-1(2)
C(2)	22(2)	22(2)	22(2)	2(2)	8(2)	6(2)
C(3)	21(2)	24(3)	41(3)	16(2)	11(2)	4(2)
C(4)	24(2)	46(3)	28(3)	23(2)	9(2)	15(3)
C(5)	35(2)	45(3)	13(2)	10(2)	12(2)	9(3)
C(6)	26(3)	29(3)	16(3)	0(2)	8(2)	-8(2)
C(7)	19(2)	16(3)	25(2)	-3(2)	14(2)	7(2)
C(8)	19(2)	18(2)	19(2)	5(2)	10(2)	-1(2)
C(9)	19(2)	13(2)	23(2)	14(2)	5(1)	-1(3)
C(10)	37(3)	53(3)	11(2)	-5(2)	8(2)	1(2)
C(11)	39(3)	54(3)	31(2)	-22(3)	23(2)	-13(3)
C(12)	48(3)	29(3)	26(2)	-11(2)	23(2)	-1(2)
C(13)	31(2)	30(2)	26(2)	-18(4)	17(1)	3(3)
C(14)	23(2)	36(3)	33(3)	-1(2)	24(2)	4(2)
C(15)	42(3)	96(5)	36(3)	29(3)	29(3)	27(4)
C(16)	65(5)	75(5)	28(4)	-30(4)	9(3)	-13(4)
C(17)	83(4)	29(3)	50(4)	-9(3)	53(3)	-14(3)
C(18)	35(2)	35(3)	41(2)	-14(5)	21(2)	-1(4)
C(19)	44(4)	33(4)	80(6)	16(4)	37(4)	-2(3)
C(20)	18(2)	30(3)	61(4)	11(3)	-15(2)	2(2)
C(21)	28(2)	93(4)	20(2)	20(3)	4(2)	15(4)
C(22)	56(3)	40(3)	59(4)	-16(3)	-38(2)	12(3)
C(23)	41(3)	82(4)	69(4)	43(3)	-27(3)	-39(3)

Table C.5. (continued)

C(24)	19(2)	136(5)	22(2)	2(3)	4(2)	-4(3)
C(25)	78(5)	42(4)	87(6)	-15(4)	-44(4)	9(4)
C(26)	54(4)	596(19)	19(3)	77(8)	13(3)	57(11)
C(27)	207(9)	105(5)	96(6)	-72(5)	-106(5)	99(6)
C(28)	144(6)	208(7)	165(8)	141(7)	-105(5)	-156(6)
C(29)	21(3)	442(17)	56(4)	-56(7)	9(3)	20(6)
C(30)	52(4)	35(4)	39(3)	-12(3)	-3(3)	-5(3)
C(31)	36(4)	36(4)	79(6)	-25(4)	4(3)	4(3)
C(32)	52(4)	34(4)	61(4)	4(3)	25(3)	-17(3)
C(33)	52(4)	8(3)	51(4)	-15(3)	33(3)	-5(3)
C(34)	22(3)	30(4)	32(3)	-11(3)	4(2)	-5(3)
C(35)	33(3)	22(3)	29(3)	12(3)	14(2)	20(3)

Table C.6. Hydrogen coordinates (x 10^4) and isotropic displacement parameters ($Å^2$x 10^3) for **18-N_2Cl** & **18-Cl_2**.

	x	y	z	U(eq)
H(3A)	989	2627	10284	35
H(4A)	1427	3329	12170	40
H(5A)	1442	4684	12196	36
H(6A)	1153	5433	10370	29
H(9A)	-1789	4094	6379	23
H(15A)	139	5510	4960	81
H(15B)	-1086	4830	4748	81
H(15C)	-176	4929	3834	81
H(16A)	-190	3069	3863	87
H(16B)	-1185	3444	4582	87
H(16C)	-272	2654	5058	87
H(17A)	2338	2170	5754	69
H(17B)	3540	2366	7078	69
H(17C)	3956	2534	5891	69
H(18A)	5731	3777	6841	53
H(18B)	5321	3585	8023	53
H(18C)	5545	4467	7691	53
H(19A)	4060	5571	7012	72
H(19B)	2319	5831	6409	72
H(19C)	3317	5697	5570	72
H(25A)	5572	2310	11694	133
H(25B)	4803	2328	12711	133
H(25C)	6606	2417	13098	133
H(26A)	5107	3913	14700	335
H(26B)	3661	3425	13876	335
H(26C)	3600	4353	13865	335
H(27A)	3850	5217	13505	269
H(27B)	4085	5750	12469	269
H(27C)	5484	5582	13702	269

Table C.6. (continued)

H(28A)	6875	5113	10773	324
H(28B)	6973	5612	11948	324
H(28C)	5424	5588	10794	324
H(29A)	6865	3843	10186	261
H(29B)	6654	2985	10624	261
H(29C)	8077	3500	11415	261
H(30A)	-3632	2593	5884	71
H(30B)	-3256	1687	5880	71
H(30C)	-2361	2304	5365	71
H(31A)	953	1571	8546	82
H(31B)	668	1674	7127	82
H(31C)	-299	1052	7560	82
H(32A)	-1385	2075	9526	71
H(32B)	-2468	1483	8551	71
H(32C)	-3008	2358	8610	71
H(33A)	681	6315	7088	49
H(33B)	990	6431	8509	49
H(33C)	-244	6959	7522	49
H(34A)	-2635	6474	8611	44
H(34B)	-1485	5898	9572	44
H(34C)	-3069	5578	8644	44
H(35A)	-2310	5598	5493	41
H(35B)	-3256	6217	5952	41
H(35C)	-3513	5308	6081	41

Table C.7. Crystal data and structure refinement for ***cis*-1-$(CH_2CHCH_2)_2N^tBu$** (Chapter 3).

Identification code	***cis*-1-$(CH_2CHCH_2)_2N^tBu$**	
Empirical formula	C45 H69 N Zr	
Formula weight	715.23	
Temperature	173(2) K	
Wavelength	0.71073 Å	
Crystal system	Monoclinic	
Space group	P2(1)/c	
Unit cell dimensions	a = 13.2599(4) Å	α= 90°.
	b = 17.5475(6) Å	β= 92.942(2)°.
	c = 17.0737(6) Å	γ= 90°.
Volume	3967.4(2) $Å^3$	
Z	4	
Density (calculated)	1.197 Mg/m^3	
Absorption coefficient	0.308 mm^{-1}	
F(000)	1544	
Crystal size	0.45 x 0.40 x 0.35 mm^3	
Theta range for data collection	1.93 to 30.51°.	
Index ranges	-18<=h<=18, -23<=k<=25, -24<=l<=24	
Reflections collected	54861	
Independent reflections	12109 [R(int) = 0.0643]	
Completeness to theta = 30.51°	100.0 %	
Absorption correction	Semi-empirical from equivalents	
Max. and min. transmission	0.9000 and 0.8740	
Refinement method	Full-matrix least-squares on F^2	
Data / restraints / parameters	12109 / 0 / 531	
Goodness-of-fit on F^2	1.073	
Final R indices [I>2sigma(I)]	R1 = 0.0414, wR2 = 0.0942	
R indices (all data)	R1 = 0.0612, wR2 = 0.1024	
Largest diff. peak and hole	0.797 and -0.472 $e.Å^{-3}$	

Table C.8. Atomic coordinates (x 10^4) and equivalent isotropic displacement parameters (Å^{2}x 10^3) for ***cis*-1-$(CH_2CHCH_2)_2N^tBu$**. U(eq) is defined as one third of the trace of the orthogonalized U^{ij} tensor.

	x	y	z	U(eq)
Zr(1)	1857(1)	4712(1)	2587(1)	16(1)
N(1)	3077(1)	6155(1)	247(1)	26(1)
C(1)	2169(1)	3373(1)	2085(1)	19(1)
C(2)	1900(1)	3312(1)	2869(1)	20(1)
C(3)	880(1)	3508(1)	2954(1)	19(1)
C(4)	475(1)	3688(1)	2185(1)	18(1)
C(5)	-507(1)	3886(1)	1875(1)	23(1)
C(6)	-673(1)	3983(1)	1089(1)	25(1)
C(7)	109(1)	3899(1)	569(1)	24(1)
C(8)	1059(1)	3716(1)	837(1)	20(1)
C(9)	1269(1)	3607(1)	1651(1)	18(1)
C(10)	2358(1)	4914(1)	4022(1)	21(1)
C(11)	1335(1)	5135(1)	3906(1)	20(1)
C(12)	1245(1)	5801(1)	3446(1)	19(1)
C(13)	2249(1)	6023(1)	3295(1)	19(1)
C(14)	2618(1)	6665(1)	2901(1)	23(1)
C(15)	3631(1)	6770(1)	2883(1)	28(1)
C(16)	4315(1)	6246(1)	3241(1)	29(1)
C(17)	3991(1)	5620(1)	3616(1)	25(1)
C(18)	2940(1)	5485(1)	3654(1)	20(1)
C(19)	3118(1)	3088(1)	1741(1)	22(1)
C(20)	3980(1)	2990(1)	2349(1)	29(1)
C(21)	2909(1)	2332(1)	1316(1)	34(1)
C(22)	349(1)	3345(1)	3698(1)	22(1)
C(23)	341(2)	2494(1)	3853(1)	44(1)
C(24)	-722(1)	3647(1)	3723(1)	41(1)
C(25)	2734(1)	4333(1)	4619(1)	25(1)
C(26)	2820(2)	4714(1)	5425(1)	41(1)
C(27)	3724(1)	3940(1)	4460(1)	36(1)
C(28)	326(1)	6278(1)	3273(1)	24(1)
C(29)	-617(1)	5824(1)	3072(1)	39(1)
C(30)	161(1)	6811(1)	3958(1)	38(1)
C(31)	1152(1)	5441(1)	1601(1)	20(1)
C(32)	1875(1)	5479(1)	923(1)	21(1)
C(33)	2249(1)	6274(1)	763(1)	24(1)
C(34)	3618(1)	5476(1)	541(1)	31(1)
C(35)	2880(1)	5025(1)	1034(1)	21(1)
C(36)	3229(1)	4953(1)	1896(1)	21(1)

Table C.8. (continued)

C(37)	3704(1)	6826(1)	89(1)	32(1)
C(38)	4274(2)	7139(1)	816(1)	47(1)
C(39)	3006(2)	7453(1)	-246(1)	54(1)
C(40)	4444(2)	6608(1)	-515(1)	52(1)
C(1S)	7342(2)	6054(2)	1082(2)	101(1)
C(2S)	6624(2)	5693(2)	1618(1)	70(1)
C(3S)	6946(2)	4978(1)	2012(2)	57(1)
C(4S)	6203(2)	4614(1)	2521(1)	57(1)
C(5S)	6547(2)	3922(1)	2909(2)	74(1)

Table C.9. Bond lengths [Å] and angles [°] for ***cis*-1-$(CH_2CHCH_2)_2N^tBu$**.

Zr(1)-C(36)	2.2589(15)	C(22)-C(24)	1.518(2)
Zr(1)-C(31)	2.2765(14)	C(25)-C(27)	1.521(2)
Zr(1)-C(11)	2.5021(14)	C(25)-C(26)	1.528(2)
Zr(1)-C(2)	2.5034(14)	C(28)-C(29)	1.508(2)
Zr(1)-C(10)	2.5300(13)	C(28)-C(30)	1.522(2)
Zr(1)-C(1)	2.5426(14)	C(31)-C(32)	1.542(2)
Zr(1)-C(12)	2.5657(14)	C(32)-C(33)	1.512(2)
Zr(1)-C(3)	2.5717(14)	C(32)-C(35)	1.555(2)
Zr(1)-C(9)	2.6063(13)	C(34)-C(35)	1.543(2)
Zr(1)-C(4)	2.6318(13)	C(35)-C(36)	1.525(2)
Zr(1)-C(18)	2.6367(14)	C(37)-C(40)	1.509(3)
Zr(1)-C(13)	2.6376(13)	C(37)-C(38)	1.523(2)
N(1)-C(33)	1.457(2)	C(37)-C(39)	1.529(3)
N(1)-C(34)	1.466(2)	C(1S)-C(2S)	1.495(4)
N(1)-C(37)	1.474(2)	C(2S)-C(3S)	1.477(4)
C(1)-C(2)	1.406(2)	C(3S)-C(4S)	1.491(3)
C(1)-C(9)	1.4319(19)	C(4S)-C(5S)	1.446(3)
C(1)-C(19)	1.503(2)		
C(2)-C(3)	1.411(2)	C(36)-Zr(1)-C(31)	79.62(5)
C(3)-C(4)	1.4281(19)	C(36)-Zr(1)-C(11)	133.01(5)
C(3)-C(22)	1.511(2)	C(31)-Zr(1)-C(11)	112.10(5)
C(4)-C(5)	1.4233(19)	C(36)-Zr(1)-C(2)	105.84(5)
C(4)-C(9)	1.435(2)	C(31)-Zr(1)-C(2)	134.27(5)
C(5)-C(6)	1.360(2)	C(11)-Zr(1)-C(2)	97.08(5)
C(6)-C(7)	1.407(2)	C(36)-Zr(1)-C(10)	107.51(5)
C(7)-C(8)	1.356(2)	C(31)-Zr(1)-C(10)	135.59(5)
C(8)-C(9)	1.4156(19)	C(11)-Zr(1)-C(10)	32.66(5)
C(10)-C(11)	1.415(2)	C(2)-Zr(1)-C(10)	87.12(5)
C(10)-C(18)	1.429(2)	C(36)-Zr(1)-C(1)	81.23(5)
C(10)-C(25)	1.509(2)	C(31)-Zr(1)-C(1)	109.74(5)
C(11)-C(12)	1.409(2)	C(11)-Zr(1)-C(1)	129.43(5)
C(12)-C(13)	1.423(2)	C(2)-Zr(1)-C(1)	32.36(5)
C(12)-C(28)	1.495(2)	C(10)-Zr(1)-C(1)	114.66(5)
C(13)-C(14)	1.413(2)	C(36)-Zr(1)-C(12)	116.51(5)
C(13)-C(18)	1.4307(19)	C(31)-Zr(1)-C(12)	82.75(5)
C(14)-C(15)	1.359(2)	C(11)-Zr(1)-C(12)	32.25(4)
C(15)-C(16)	1.409(2)	C(2)-Zr(1)-C(12)	128.75(5)
C(16)-C(17)	1.352(2)	C(10)-Zr(1)-C(12)	54.35(4)
C(17)-C(18)	1.419(2)	C(1)-Zr(1)-C(12)	160.52(5)
C(19)-C(20)	1.514(2)	C(36)-Zr(1)-C(3)	135.25(5)
C(19)-C(21)	1.529(2)	C(31)-Zr(1)-C(3)	116.66(5)
C(22)-C(23)	1.518(2)	C(11)-Zr(1)-C(3)	81.87(5)

Table C.9. (continued)

C(2)-Zr(1)-C(3)	32.24(5)	C(33)-N(1)-C(37)	116.47(13)
C(10)-Zr(1)-C(3)	89.44(5)	C(34)-N(1)-C(37)	116.14(13)
C(1)-Zr(1)-C(3)	54.25(5)	C(2)-C(1)-C(9)	105.66(12)
C(12)-Zr(1)-C(3)	107.11(5)	C(2)-C(1)-C(19)	127.23(13)
C(36)-Zr(1)-C(9)	92.42(5)	C(9)-C(1)-C(19)	125.85(13)
C(31)-Zr(1)-C(9)	82.29(5)	C(2)-C(1)-Zr(1)	72.29(8)
C(11)-Zr(1)-C(9)	133.24(5)	C(9)-C(1)-Zr(1)	76.32(8)
C(2)-Zr(1)-C(9)	52.50(4)	C(19)-C(1)-Zr(1)	126.41(9)
C(10)-Zr(1)-C(9)	138.93(4)	C(1)-C(2)-C(3)	111.73(12)
C(1)-Zr(1)-C(9)	32.26(4)	C(1)-C(2)-Zr(1)	75.35(8)
C(12)-Zr(1)-C(9)	144.19(4)	C(3)-C(2)-Zr(1)	76.54(8)
C(3)-Zr(1)-C(9)	53.14(4)	C(2)-C(3)-C(4)	106.05(12)
C(36)-Zr(1)-C(4)	124.06(5)	C(2)-C(3)-C(22)	122.10(12)
C(31)-Zr(1)-C(4)	86.37(5)	C(4)-C(3)-C(22)	130.17(13)
C(11)-Zr(1)-C(4)	102.50(5)	C(2)-C(3)-Zr(1)	71.22(8)
C(2)-Zr(1)-C(4)	52.34(4)	C(4)-C(3)-Zr(1)	76.41(8)
C(10)-Zr(1)-C(4)	119.56(5)	C(22)-C(3)-Zr(1)	128.51(9)
C(1)-Zr(1)-C(4)	53.43(4)	C(5)-C(4)-C(3)	133.61(14)
C(12)-Zr(1)-C(4)	114.89(4)	C(5)-C(4)-C(9)	118.33(12)
C(3)-Zr(1)-C(4)	31.83(4)	C(3)-C(4)-C(9)	108.00(12)
C(9)-Zr(1)-C(4)	31.80(4)	C(5)-C(4)-Zr(1)	122.83(10)
C(36)-Zr(1)-C(18)	80.78(5)	C(3)-C(4)-Zr(1)	71.76(8)
C(31)-Zr(1)-C(18)	114.20(5)	C(9)-C(4)-Zr(1)	73.12(7)
C(11)-Zr(1)-C(18)	52.53(5)	C(6)-C(5)-C(4)	119.80(14)
C(2)-Zr(1)-C(18)	111.48(4)	C(5)-C(6)-C(7)	121.43(13)
C(10)-Zr(1)-C(18)	32.03(5)	C(8)-C(7)-C(6)	120.95(14)
C(1)-Zr(1)-C(18)	128.06(4)	C(7)-C(8)-C(9)	119.69(14)
C(12)-Zr(1)-C(18)	53.07(4)	C(8)-C(9)-C(1)	131.56(13)
C(3)-Zr(1)-C(18)	121.18(4)	C(8)-C(9)-C(4)	119.78(12)
C(9)-Zr(1)-C(18)	160.32(4)	C(1)-C(9)-C(4)	108.54(12)
C(4)-Zr(1)-C(18)	151.49(4)	C(8)-C(9)-Zr(1)	122.65(9)
C(36)-Zr(1)-C(13)	86.07(5)	C(1)-C(9)-Zr(1)	71.42(8)
C(31)-Zr(1)-C(13)	84.98(5)	C(4)-C(9)-Zr(1)	75.08(8)
C(11)-Zr(1)-C(13)	52.09(4)	C(11)-C(10)-C(18)	106.39(12)
C(2)-Zr(1)-C(13)	139.96(4)	C(11)-C(10)-C(25)	124.05(13)
C(10)-Zr(1)-C(13)	52.98(4)	C(18)-C(10)-C(25)	127.18(13)
C(1)-Zr(1)-C(13)	158.28(4)	C(11)-C(10)-Zr(1)	72.59(8)
C(12)-Zr(1)-C(13)	31.71(4)	C(18)-C(10)-Zr(1)	78.10(8)
C(3)-Zr(1)-C(13)	133.96(4)	C(25)-C(10)-Zr(1)	128.37(10)
C(9)-Zr(1)-C(13)	167.25(4)	C(12)-C(11)-C(10)	110.99(13)
C(4)-Zr(1)-C(13)	146.39(4)	C(12)-C(11)-Zr(1)	76.36(8)
C(18)-Zr(1)-C(13)	31.48(4)	C(10)-C(11)-Zr(1)	74.75(8)
C(33)-N(1)-C(34)	106.26(12)	C(11)-C(12)-C(13)	105.89(12)

Table C.9. (continued)

C(11)-C(12)-C(28)	128.31(13)	C(23)-C(22)-C(24)	108.87(15)
C(13)-C(12)-C(28)	124.81(13)	C(10)-C(25)-C(27)	116.34(13)
C(11)-C(12)-Zr(1)	71.39(8)	C(10)-C(25)-C(26)	108.64(13)
C(13)-C(12)-Zr(1)	76.93(8)	C(27)-C(25)-C(26)	109.51(14)
C(28)-C(12)-Zr(1)	125.65(9)	C(12)-C(28)-C(29)	113.97(13)
C(14)-C(13)-C(12)	130.85(13)	C(12)-C(28)-C(30)	109.89(12)
C(14)-C(13)-C(18)	119.98(13)	C(29)-C(28)-C(30)	110.40(14)
C(12)-C(13)-C(18)	109.11(12)	C(32)-C(31)-Zr(1)	109.36(9)
C(14)-C(13)-Zr(1)	122.82(10)	C(33)-C(32)-C(31)	113.48(12)
C(12)-C(13)-Zr(1)	71.36(8)	C(33)-C(32)-C(35)	101.94(12)
C(18)-C(13)-Zr(1)	74.23(8)	C(31)-C(32)-C(35)	116.65(12)
C(15)-C(14)-C(13)	119.10(14)	N(1)-C(33)-C(32)	104.01(12)
C(14)-C(15)-C(16)	121.11(15)	N(1)-C(34)-C(35)	106.90(13)
C(17)-C(16)-C(15)	121.51(15)	C(36)-C(35)-C(34)	113.57(13)
C(16)-C(17)-C(18)	119.62(14)	C(36)-C(35)-C(32)	112.11(12)
C(17)-C(18)-C(10)	133.72(14)	C(34)-C(35)-C(32)	103.58(12)
C(17)-C(18)-C(13)	118.67(13)	C(35)-C(36)-Zr(1)	107.85(9)
C(10)-C(18)-C(13)	107.54(12)	N(1)-C(37)-C(40)	108.38(15)
C(17)-C(18)-Zr(1)	123.78(10)	N(1)-C(37)-C(38)	113.59(13)
C(10)-C(18)-Zr(1)	69.87(8)	C(40)-C(37)-C(38)	109.59(15)
C(13)-C(18)-Zr(1)	74.30(8)	N(1)-C(37)-C(39)	107.83(14)
C(1)-C(19)-C(20)	112.81(12)	C(40)-C(37)-C(39)	109.27(16)
C(1)-C(19)-C(21)	109.80(12)	C(38)-C(37)-C(39)	108.10(16)
C(20)-C(19)-C(21)	109.84(13)	C(3S)-C(2S)-C(1S)	117.5(2)
C(3)-C(22)-C(23)	109.94(13)	C(2S)-C(3S)-C(4S)	116.4(2)
C(3)-C(22)-C(24)	115.81(13)	C(5S)-C(4S)-C(3S)	115.1(2)

Symmetry transformations used to generate equivalent atoms:

Table C.10. Anisotropic displacement parameters ($Å^2 x\ 10^3$) for ***cis*-1-$(CH_2CHCH_2)_2N^tBu$**. The anisotropic displacement factor exponent takes the form: $-2\pi^2[\ h^2\ a^{*2}U^{11} + ...\ + 2\ h\ k\ a^*\ b^*\ U^{12}\ ]$

	U^{11}	U^{22}	U^{33}	U^{23}	U^{13}	U^{12}
Zr(1)	15(1)	15(1)	17(1)	0(1)	1(1)	0(1)
N(1)	26(1)	28(1)	23(1)	6(1)	4(1)	-5(1)
C(1)	18(1)	15(1)	24(1)	-1(1)	2(1)	0(1)
C(2)	20(1)	16(1)	22(1)	2(1)	-1(1)	1(1)
C(3)	18(1)	17(1)	22(1)	1(1)	3(1)	-2(1)
C(4)	16(1)	15(1)	23(1)	-1(1)	1(1)	-2(1)
C(5)	16(1)	24(1)	28(1)	-2(1)	3(1)	-2(1)
C(6)	18(1)	27(1)	29(1)	1(1)	-4(1)	0(1)
C(7)	26(1)	24(1)	22(1)	-1(1)	-3(1)	-3(1)
C(8)	21(1)	19(1)	21(1)	-3(1)	4(1)	-4(1)
C(9)	18(1)	14(1)	22(1)	-1(1)	2(1)	-1(1)
C(10)	22(1)	22(1)	18(1)	-1(1)	0(1)	1(1)
C(11)	21(1)	20(1)	19(1)	-1(1)	4(1)	-1(1)
C(12)	20(1)	18(1)	20(1)	-3(1)	1(1)	1(1)
C(13)	20(1)	17(1)	20(1)	-3(1)	1(1)	0(1)
C(14)	29(1)	18(1)	22(1)	-2(1)	-1(1)	-2(1)
C(15)	33(1)	24(1)	28(1)	-1(1)	3(1)	-12(1)
C(16)	20(1)	34(1)	31(1)	-7(1)	0(1)	-8(1)
C(17)	21(1)	27(1)	26(1)	-2(1)	-3(1)	-2(1)
C(18)	20(1)	21(1)	19(1)	-3(1)	0(1)	-1(1)
C(19)	19(1)	20(1)	28(1)	-2(1)	4(1)	2(1)
C(20)	19(1)	33(1)	36(1)	0(1)	1(1)	7(1)
C(21)	29(1)	27(1)	45(1)	-12(1)	7(1)	3(1)
C(22)	22(1)	23(1)	21(1)	1(1)	4(1)	-5(1)
C(23)	66(1)	27(1)	41(1)	6(1)	21(1)	-8(1)
C(24)	26(1)	63(1)	34(1)	12(1)	11(1)	4(1)
C(25)	27(1)	26(1)	23(1)	3(1)	-1(1)	1(1)
C(26)	57(1)	44(1)	21(1)	2(1)	-1(1)	12(1)
C(27)	36(1)	37(1)	34(1)	6(1)	-4(1)	12(1)
C(28)	23(1)	24(1)	25(1)	1(1)	3(1)	7(1)
C(29)	22(1)	40(1)	54(1)	-13(1)	-2(1)	7(1)
C(30)	40(1)	31(1)	43(1)	-11(1)	1(1)	14(1)
C(31)	19(1)	20(1)	22(1)	2(1)	2(1)	0(1)
C(32)	20(1)	23(1)	19(1)	3(1)	0(1)	-1(1)
C(33)	23(1)	24(1)	25(1)	5(1)	2(1)	-2(1)
C(34)	27(1)	32(1)	34(1)	6(1)	10(1)	0(1)
C(35)	20(1)	21(1)	24(1)	1(1)	6(1)	-1(1)
C(36)	18(1)	20(1)	25(1)	-1(1)	2(1)	-1(1)
C(37)	33(1)	35(1)	28(1)	8(1)	3(1)	-12(1)

Table C.10. (continued)

C(38)	52(1)	47(1)	41(1)	1(1)	4(1)	-26(1)
C(39)	58(1)	43(1)	63(1)	29(1)	4(1)	-11(1)
C(40)	54(1)	59(1)	44(1)	1(1)	24(1)	-24(1)
C(1S)	93(2)	122(2)	88(2)	-2(2)	8(2)	-62(2)
C(2S)	68(2)	88(2)	54(1)	-6(1)	2(1)	10(2)
C(3S)	33(1)	58(1)	81(2)	-22(1)	4(1)	-9(1)
C(4S)	37(1)	74(2)	61(1)	-5(1)	1(1)	6(1)
C(5S)	58(2)	64(2)	97(2)	-8(2)	-14(1)	-7(1)

Table C.11. Hydrogen coordinates (x 10^4) and isotropic displacement parameters (Å^{2}x 10^3) for ***cis*-1-$(CH_2CHCH_2)_2N^tBu$**.

	x	y	z	U(eq)
H(2)	2357(12)	3142(9)	3270(9)	19(4)
H(5)	-1019(13)	3954(9)	2190(9)	22(4)
H(6)	-1336(12)	4087(9)	894(9)	22(4)
H(7)	-23(12)	3974(9)	56(10)	27(4)
H(8)	1546(12)	3651(8)	505(9)	18(4)
H(11)	810(13)	4858(9)	4118(9)	19(4)
H(14)	2177(13)	7024(9)	2669(9)	24(4)
H(15)	3873(13)	7156(9)	2647(10)	26(4)
H(16)	5037(14)	6352(10)	3244(10)	38(5)
H(17)	4475(14)	5282(9)	3847(10)	30(5)
H(19)	3344(11)	3463(8)	1354(8)	9(3)
H(20A)	4100	3473	2628	43
H(20B)	4592	2841	2089	43
H(20C)	3807	2594	2723	43
H(21A)	2714	1947	1695	51
H(21B)	3520	2164	1066	51
H(21C)	2361	2401	916	51
H(22)	715(12)	3542(9)	4119(9)	19(4)
H(23A)	-44	2235	3426	66
H(23B)	27	2394	4350	66
H(23C)	1036	2301	3884	66
H(24A)	-738	4183	3564	61
H(24B)	-951	3601	4258	61
H(24C)	-1169	3350	3364	61
H(25)	2243(13)	3953(10)	4664(9)	29(5)
H(26A)	3320	5125	5420	61
H(26B)	3033	4336	5823	61
H(26C)	2162	4925	5549	61
H(27A)	3728	3801	3904	54
H(27B)	3796	3479	4783	54
H(27C)	4288	4286	4591	54
H(28)	473(12)	6587(9)	2836(9)	19(4)
H(29A)	-504	5492	2623	58
H(29B)	-1177	6172	2938	58
H(29C)	-783	5512	3524	58
H(30A)	-2	6511	4419	57
H(30B)	-399	7158	3819	57
H(30C)	776	7107	4077	57
H(31B)	543(13)	5234(9)	1437(10)	25(4)

Table C 11. (continued)

H(31A)	975(13)	5947(10)	1779(10)	29(5)
H(32)	1503(13)	5295(8)	431(10)	26(4)
H(33B)	1724(11)	6591(8)	521(8)	11(4)
H(33A)	2469(13)	6513(9)	1293(10)	29(4)
H(34B)	4208(13)	5601(9)	848(10)	25(4)
H(34A)	3872(16)	5161(11)	92(12)	51(6)
H(35)	2800(11)	4520(8)	805(9)	13(4)
H(36B)	3797(14)	4630(9)	1973(10)	27(5)
H(36A)	3425(13)	5439(9)	2067(10)	28(5)
H(38A)	3791	7303	1197	70
H(38B)	4687	7575	669	70
H(38C)	4712	6741	1049	70
H(39A)	2584	7249	-685	82
H(39B)	3412	7877	-430	82
H(39C)	2573	7634	164	82
H(40A)	4919	6229	-291	77
H(40B)	4817	7061	-670	77
H(40C)	4077	6392	-976	77
H(1SA)	7041	6521	859	152
H(1SB)	7482	5699	658	152
H(1SC)	7973	6179	1378	152
H(2SA)	6474	6069	2028	84
H(2SB)	5984	5591	1311	84
H(3SA)	7571	5082	2337	69
H(3SB)	7120	4606	1605	69
H(4SA)	6020	4986	2926	69
H(4SB)	5582	4498	2196	69
H(5SA)	6014	3725	3232	110
H(5SB)	7153	4030	3243	110
H(5SC)	6706	3540	2514	110

Table C.12. Crystal data and structure refinement for **[*meso*-3]$_2$(HI)** (Chapter 4).

Identification code	**[*meso*-3]$_2$(HI)**	
Empirical formula	C40 H60 I Si2 Zr2	
Formula weight	906.40	
Temperature	173(2) K	
Wavelength	0.71073 Å	
Crystal system	Monoclinic	
Space group	P2(1)/c	
Unit cell dimensions	a = 12.0178(8) Å	α= 90°.
	b = 18.8884(10) Å	β= 94.298(2)°.
	c = 18.2398(11) Å	γ= 90°.
Volume	4128.7(4) Å^3	
Z	4	
Density (calculated)	1.458 Mg/m^3	
Absorption coefficient	1.336 mm^{-1}	
F(000)	1844	
Crystal size	0.40 x 0.20 x 0.03 mm^3	
Theta range for data collection	1.70 to 24.99°.	
Index ranges	-14<=h<=14, -22<=k<=18, -21<=l<=21	
Reflections collected	30328	
Independent reflections	7079 [R(int) = 0.0727]	
Completeness to theta = 24.99°	97.3 %	
Absorption correction	Semi-empirical from equivalents	
Max. and min. transmission	0.9674 and 0.6171	
Refinement method	Full-matrix least-squares on F^2	
Data / restraints / parameters	7079 / 0 / 422	
Goodness-of-fit on F^2	1.074	
Final R indices [I>2sigma(I)]	R1 = 0.0735, wR2 = 0.1951	
R indices (all data)	R1 = 0.1115, wR2 = 0.2165	
Largest diff. peak and hole	1.886 and -2.178 e.Å^{-3}	

Table C.13. Atomic coordinates (x 10^4) and equivalent isotropic displacement parameters (Å^{2}x 10^3) for **[*meso*-3]$_2$(HI)**. U(eq) is defined as one third of the trace of the orthogonalized U^{ij} tensor.

	x	y	z	U(eq)
I(1)	4206(1)	1172(1)	4193(1)	39(1)
Zr(1)	2729(1)	2368(1)	3867(1)	17(1)
Zr(2)	5572(1)	2435(1)	4387(1)	21(1)
Si(1)	1146(2)	3694(1)	3361(1)	27(1)
Si(2)	7190(2)	3789(1)	4780(1)	26(1)
C(1)	1344(7)	3224(4)	4272(4)	24(2)
C(2)	2304(7)	3294(4)	4780(4)	26(2)
C(3)	2391(6)	2679(4)	5198(4)	23(2)
C(4)	1494(7)	2201(4)	4981(4)	24(2)
C(5)	877(6)	2550(4)	4393(4)	22(2)
C(6)	1823(6)	3009(4)	2813(4)	21(2)
C(7)	1354(7)	2317(4)	2758(4)	24(2)
C(8)	2150(6)	1811(4)	2557(4)	22(2)
C(9)	3148(7)	2200(4)	2506(4)	23(2)
C(10)	2932(7)	2932(4)	2665(4)	22(2)
C(11)	6958(7)	3260(4)	3918(4)	24(2)
C(12)	5984(6)	3296(4)	3423(4)	23(2)
C(13)	5873(7)	2658(4)	3034(4)	22(2)
C(14)	6758(6)	2193(4)	3272(4)	21(2)
C(15)	7396(7)	2571(5)	3828(5)	28(2)
C(16)	6514(6)	3146(4)	5382(4)	22(2)
C(17)	6972(7)	2456(4)	5489(4)	26(2)
C(18)	6170(7)	1985(5)	5725(4)	31(2)
C(19)	5158(7)	2382(5)	5741(4)	28(2)
C(20)	5363(7)	3098(4)	5532(4)	26(2)
C(21)	1154(7)	1550(5)	5379(5)	31(2)
C(22)	2161(8)	1222(5)	5834(5)	46(3)
C(23)	328(8)	1790(6)	5923(5)	46(3)
C(24)	650(11)	1012(6)	4883(6)	68(4)

Table C.13. (continued)

C(25)	1908(7)	1060(4)	2321(4)	24(2)
C(26)	1286(8)	665(5)	2901(5)	35(2)
C(27)	1131(8)	1084(5)	1608(5)	37(2)
C(28)	2938(8)	663(5)	2180(5)	41(3)
C(29)	7086(6)	1495(4)	2919(4)	26(2)
C(30)	6092(8)	1173(5)	2466(5)	45(3)
C(31)	7955(8)	1690(5)	2370(6)	49(3)
C(32)	7540(10)	984(5)	3461(5)	56(3)
C(33)	6398(7)	1242(5)	6029(5)	32(2)
C(34)	6917(9)	771(5)	5445(5)	44(3)
C(35)	7268(8)	1307(6)	6698(5)	47(3)
C(36)	5365(8)	901(5)	6286(6)	48(3)
C(37)	-355(8)	3797(5)	3058(5)	41(3)
C(38)	1926(9)	4543(5)	3357(6)	49(3)
C(39)	6435(8)	4640(5)	4705(5)	39(2)
C(40)	8690(7)	3904(6)	5080(5)	43(3)

Table C.14. Bond lengths [Å] and angles [°] for **[*meso*-3]$_2$(HI)**.

I(1)-Zr(2)	2.9032(10)	C(9)-C(10)	1.441(11)
I(1)-Zr(1)	2.9075(10)	C(11)-C(15)	1.418(11)
Zr(1)-C(6)	2.457(7)	C(11)-C(12)	1.426(11)
Zr(1)-C(10)	2.466(7)	C(12)-C(13)	1.399(11)
Zr(1)-C(1)	2.472(8)	C(13)-C(14)	1.422(11)
Zr(1)-C(2)	2.494(8)	C(14)-C(15)	1.418(11)
Zr(1)-C(5)	2.512(8)	C(14)-C(29)	1.530(11)
Zr(1)-C(7)	2.516(7)	C(16)-C(17)	1.422(11)
Zr(1)-C(3)	2.558(7)	C(16)-C(20)	1.433(11)
Zr(1)-C(9)	2.590(7)	C(17)-C(18)	1.403(12)
Zr(1)-C(4)	2.622(8)	C(18)-C(19)	1.431(12)
Zr(1)-C(8)	2.656(7)	C(18)-C(33)	1.527(12)
Zr(1)-Si(1)	3.237(2)	C(19)-C(20)	1.432(12)
Zr(2)-C(16)	2.463(7)	C(21)-C(24)	1.463(13)
Zr(2)-C(20)	2.466(7)	C(21)-C(23)	1.523(12)
Zr(2)-C(12)	2.472(8)	C(21)-C(22)	1.545(12)
Zr(2)-C(11)	2.480(8)	C(25)-C(28)	1.485(12)
Zr(2)-C(15)	2.499(8)	C(25)-C(26)	1.532(12)
Zr(2)-C(17)	2.523(8)	C(25)-C(27)	1.544(11)
Zr(2)-C(13)	2.554(7)	C(29)-C(32)	1.457(13)
Zr(2)-C(19)	2.559(8)	C(29)-C(30)	1.527(12)
Zr(2)-C(14)	2.609(8)	C(29)-C(31)	1.545(12)
Zr(2)-C(18)	2.633(8)	C(33)-C(36)	1.504(13)
Si(1)-C(6)	1.860(8)	C(33)-C(34)	1.553(12)
Si(1)-C(38)	1.858(10)	C(33)-C(35)	1.551(12)
Si(1)-C(37)	1.857(9)		
Si(1)-C(1)	1.882(8)	Zr(2)-I(1)-Zr(1)	73.57(3)
Si(2)-C(39)	1.845(9)	C(6)-Zr(1)-C(10)	32.7(3)
Si(2)-C(40)	1.857(9)	C(6)-Zr(1)-C(1)	69.1(3)
Si(2)-C(16)	1.864(8)	C(10)-Zr(1)-C(1)	95.6(3)
Si(2)-C(11)	1.867(8)	C(6)-Zr(1)-C(2)	94.4(3)
C(1)-C(5)	1.416(11)	C(10)-Zr(1)-C(2)	109.3(3)
C(1)-C(2)	1.431(11)	C(1)-Zr(1)-C(2)	33.5(3)
C(2)-C(3)	1.388(11)	C(6)-Zr(1)-C(5)	83.0(2)
C(3)-C(4)	1.439(11)	C(10)-Zr(1)-C(5)	115.5(3)
C(4)-C(5)	1.420(11)	C(1)-Zr(1)-C(5)	33.0(3)
C(4)-C(21)	1.500(12)	C(2)-Zr(1)-C(5)	54.4(3)
C(6)-C(10)	1.387(11)	C(6)-Zr(1)-C(7)	33.2(3)
C(6)-C(7)	1.424(11)	C(10)-Zr(1)-C(7)	53.4(3)
C(7)-C(8)	1.420(11)	C(1)-Zr(1)-C(7)	81.3(3)
C(8)-C(9)	1.415(11)	C(2)-Zr(1)-C(7)	114.1(3)
C(8)-C(25)	1.506(11)	C(5)-Zr(1)-C(7)	76.4(2)

Table C.14. (continued)

C(6)-Zr(1)-C(3)	122.5(3)	C(2)-Zr(1)-Si(1)	60.18(19)
C(10)-Zr(1)-C(3)	141.1(3)	C(5)-Zr(1)-Si(1)	58.98(18)
C(1)-Zr(1)-C(3)	53.8(3)	C(7)-Zr(1)-Si(1)	57.6(2)
C(2)-Zr(1)-C(3)	31.9(3)	C(3)-Zr(1)-Si(1)	87.79(18)
C(5)-Zr(1)-C(3)	53.0(2)	C(9)-Zr(1)-Si(1)	88.52(18)
C(7)-Zr(1)-C(3)	129.1(2)	C(4)-Zr(1)-Si(1)	87.69(18)
C(6)-Zr(1)-C(9)	54.3(3)	C(8)-Zr(1)-Si(1)	86.62(17)
C(10)-Zr(1)-C(9)	33.0(3)	I(1)-Zr(1)-Si(1)	175.07(5)
C(1)-Zr(1)-C(9)	123.4(3)	C(16)-Zr(2)-C(20)	33.8(3)
C(2)-Zr(1)-C(9)	142.3(3)	C(16)-Zr(2)-C(12)	93.4(3)
C(5)-Zr(1)-C(9)	128.6(2)	C(20)-Zr(2)-C(12)	107.9(3)
C(7)-Zr(1)-C(9)	52.3(3)	C(16)-Zr(2)-C(11)	68.2(3)
C(3)-Zr(1)-C(9)	173.5(3)	C(20)-Zr(2)-C(11)	95.0(3)
C(6)-Zr(1)-C(4)	115.0(3)	C(12)-Zr(2)-C(11)	33.5(3)
C(10)-Zr(1)-C(4)	147.2(3)	C(16)-Zr(2)-C(15)	82.9(3)
C(1)-Zr(1)-C(4)	54.2(3)	C(20)-Zr(2)-C(15)	116.2(3)
C(2)-Zr(1)-C(4)	54.0(3)	C(12)-Zr(2)-C(15)	54.1(3)
C(5)-Zr(1)-C(4)	32.0(2)	C(11)-Zr(2)-C(15)	33.1(3)
C(7)-Zr(1)-C(4)	104.0(3)	C(16)-Zr(2)-C(17)	33.1(3)
C(3)-Zr(1)-C(4)	32.2(2)	C(20)-Zr(2)-C(17)	54.6(3)
C(9)-Zr(1)-C(4)	152.8(3)	C(12)-Zr(2)-C(17)	113.5(3)
C(6)-Zr(1)-C(8)	54.5(3)	C(11)-Zr(2)-C(17)	80.8(3)
C(10)-Zr(1)-C(8)	53.7(2)	C(15)-Zr(2)-C(17)	76.7(3)
C(1)-Zr(1)-C(8)	113.0(3)	C(16)-Zr(2)-C(13)	122.1(3)
C(2)-Zr(1)-C(8)	145.7(3)	C(20)-Zr(2)-C(13)	139.9(3)
C(5)-Zr(1)-C(8)	102.6(2)	C(12)-Zr(2)-C(13)	32.3(3)
C(7)-Zr(1)-C(8)	31.7(2)	C(11)-Zr(2)-C(13)	54.3(3)
C(3)-Zr(1)-C(8)	153.5(2)	C(15)-Zr(2)-C(13)	53.0(3)
C(9)-Zr(1)-C(8)	31.3(2)	C(17)-Zr(2)-C(13)	129.2(3)
C(4)-Zr(1)-C(8)	121.6(2)	C(16)-Zr(2)-C(19)	54.7(3)
C(6)-Zr(1)-I(1)	140.41(18)	C(20)-Zr(2)-C(19)	33.1(3)
C(10)-Zr(1)-I(1)	114.67(19)	C(12)-Zr(2)-C(19)	140.9(3)
C(1)-Zr(1)-I(1)	149.52(19)	C(11)-Zr(2)-C(19)	122.8(3)
C(2)-Zr(1)-I(1)	124.14(19)	C(15)-Zr(2)-C(19)	129.6(3)
C(5)-Zr(1)-I(1)	124.96(18)	C(17)-Zr(2)-C(19)	53.0(3)
C(7)-Zr(1)-I(1)	119.22(19)	C(13)-Zr(2)-C(19)	172.1(3)
C(3)-Zr(1)-I(1)	97.04(18)	C(16)-Zr(2)-C(14)	115.0(2)
C(9)-Zr(1)-I(1)	86.58(18)	C(20)-Zr(2)-C(14)	147.8(3)
C(4)-Zr(1)-I(1)	96.91(18)	C(12)-Zr(2)-C(14)	53.9(3)
C(8)-Zr(1)-I(1)	89.44(17)	C(11)-Zr(2)-C(14)	54.6(2)
C(6)-Zr(1)-Si(1)	34.83(19)	C(15)-Zr(2)-C(14)	32.1(2)
C(10)-Zr(1)-Si(1)	60.51(19)	C(17)-Zr(2)-C(14)	104.7(3)
C(1)-Zr(1)-Si(1)	35.40(19)	C(13)-Zr(2)-C(14)	32.0(2)

Table C.14. (continued)

C(19)-Zr(2)-C(14)	154.5(3)	C(39)-Si(2)-C(16)	112.2(4)
C(16)-Zr(2)-C(18)	54.2(3)	C(40)-Si(2)-C(16)	111.1(4)
C(20)-Zr(2)-C(18)	54.3(3)	C(39)-Si(2)-C(11)	111.2(4)
C(12)-Zr(2)-C(18)	144.7(3)	C(40)-Si(2)-C(11)	113.0(4)
C(11)-Zr(2)-C(18)	112.3(3)	C(16)-Si(2)-C(11)	95.9(3)
C(15)-Zr(2)-C(18)	103.0(3)	C(5)-C(1)-C(2)	107.0(7)
C(17)-Zr(2)-C(18)	31.5(3)	C(5)-C(1)-Si(1)	122.4(6)
C(13)-Zr(2)-C(18)	154.1(3)	C(2)-C(1)-Si(1)	124.8(6)
C(19)-Zr(2)-C(18)	32.0(3)	C(5)-C(1)-Zr(1)	75.1(4)
C(14)-Zr(2)-C(18)	122.6(3)	C(2)-C(1)-Zr(1)	74.1(4)
C(16)-Zr(2)-I(1)	139.66(19)	Si(1)-C(1)-Zr(1)	95.1(3)
C(20)-Zr(2)-I(1)	115.4(2)	C(3)-C(2)-C(1)	107.6(7)
C(12)-Zr(2)-I(1)	126.54(18)	C(3)-C(2)-Zr(1)	76.6(5)
C(11)-Zr(2)-I(1)	149.66(18)	C(1)-C(2)-Zr(1)	72.4(4)
C(15)-Zr(2)-I(1)	122.71(19)	C(2)-C(3)-C(4)	110.5(7)
C(17)-Zr(2)-I(1)	116.60(18)	C(2)-C(3)-Zr(1)	71.5(4)
C(13)-Zr(2)-I(1)	97.90(18)	C(4)-C(3)-Zr(1)	76.3(4)
C(19)-Zr(2)-I(1)	86.4(2)	C(5)-C(4)-C(3)	104.8(7)
C(14)-Zr(2)-I(1)	95.63(17)	C(5)-C(4)-C(21)	126.9(7)
C(18)-Zr(2)-I(1)	87.7(2)	C(3)-C(4)-C(21)	127.4(7)
C(16)-Zr(2)-Zr(1)	127.41(18)	C(5)-C(4)-Zr(1)	69.7(4)
C(20)-Zr(2)-Zr(1)	95.1(2)	C(3)-C(4)-Zr(1)	71.4(4)
C(12)-Zr(2)-Zr(1)	94.29(18)	C(21)-C(4)-Zr(1)	131.7(6)
C(11)-Zr(2)-Zr(1)	126.88(19)	C(4)-C(5)-C(1)	110.1(7)
C(15)-Zr(2)-Zr(1)	140.03(19)	C(4)-C(5)-Zr(1)	78.3(5)
C(17)-Zr(2)-Zr(1)	143.1(2)	C(1)-C(5)-Zr(1)	71.9(4)
C(13)-Zr(2)-Zr(1)	87.13(18)	C(10)-C(6)-C(7)	105.7(7)
C(19)-Zr(2)-Zr(1)	90.19(19)	C(10)-C(6)-Si(1)	130.0(6)
C(14)-Zr(2)-Zr(1)	111.35(16)	C(7)-C(6)-Si(1)	119.3(6)
C(18)-Zr(2)-Zr(1)	115.78(19)	C(10)-C(6)-Zr(1)	74.0(4)
I(1)-Zr(2)-Zr(1)	53.27(2)	C(7)-C(6)-Zr(1)	75.6(4)
C(6)-Si(1)-C(38)	110.9(4)	Si(1)-C(6)-Zr(1)	96.2(3)
C(6)-Si(1)-C(37)	111.5(4)	C(8)-C(7)-C(6)	111.4(7)
C(38)-Si(1)-C(37)	112.8(5)	C(8)-C(7)-Zr(1)	79.6(4)
C(6)-Si(1)-C(1)	96.6(3)	C(6)-C(7)-Zr(1)	71.1(4)
C(38)-Si(1)-C(1)	112.4(4)	C(7)-C(8)-C(9)	105.0(7)
C(37)-Si(1)-C(1)	111.6(4)	C(7)-C(8)-C(25)	126.1(7)
C(6)-Si(1)-Zr(1)	49.0(2)	C(9)-C(8)-C(25)	128.0(7)
C(38)-Si(1)-Zr(1)	112.5(4)	C(7)-C(8)-Zr(1)	68.7(4)
C(37)-Si(1)-Zr(1)	134.7(3)	C(9)-C(8)-Zr(1)	71.8(4)
C(1)-Si(1)-Zr(1)	49.5(2)	C(25)-C(8)-Zr(1)	131.5(5)
C(39)-Si(2)-C(40)	112.4(5)	C(8)-C(9)-C(10)	108.5(7)

Table C.14. (continued)

C(8)-C(9)-Zr(1)	76.9(4)	C(17)-C(18)-C(33)	125.9(8)
C(10)-C(9)-Zr(1)	68.8(4)	C(19)-C(18)-C(33)	127.1(8)
C(6)-C(10)-C(9)	109.3(7)	C(17)-C(18)-Zr(2)	69.9(5)
C(6)-C(10)-Zr(1)	73.3(4)	C(19)-C(18)-Zr(2)	71.2(4)
C(9)-C(10)-Zr(1)	78.2(4)	C(33)-C(18)-Zr(2)	131.5(6)
C(15)-C(11)-C(12)	105.3(7)	C(18)-C(19)-C(20)	109.0(8)
C(15)-C(11)-Si(2)	123.7(6)	C(18)-C(19)-Zr(2)	76.9(5)
C(12)-C(11)-Si(2)	124.9(6)	C(20)-C(19)-Zr(2)	69.9(4)
C(15)-C(11)-Zr(2)	74.2(5)	C(19)-C(20)-C(16)	107.3(7)
C(12)-C(11)-Zr(2)	73.0(4)	C(19)-C(20)-Zr(2)	77.0(4)
Si(2)-C(11)-Zr(2)	96.2(3)	C(16)-C(20)-Zr(2)	73.0(4)
C(13)-C(12)-C(11)	108.8(7)	C(24)-C(21)-C(4)	112.6(7)
C(13)-C(12)-Zr(2)	77.1(5)	C(24)-C(21)-C(23)	110.5(9)
C(11)-C(12)-Zr(2)	73.6(4)	C(4)-C(21)-C(23)	106.7(7)
C(12)-C(13)-C(14)	109.7(7)	C(24)-C(21)-C(22)	108.9(8)
C(12)-C(13)-Zr(2)	70.6(4)	C(4)-C(21)-C(22)	110.9(7)
C(14)-C(13)-Zr(2)	76.1(4)	C(23)-C(21)-C(22)	107.0(7)
C(15)-C(14)-C(13)	105.0(7)	C(28)-C(25)-C(8)	112.3(7)
C(15)-C(14)-C(29)	126.3(7)	C(28)-C(25)-C(26)	109.3(7)
C(13)-C(14)-C(29)	127.9(7)	C(8)-C(25)-C(26)	110.7(6)
C(15)-C(14)-Zr(2)	69.6(4)	C(28)-C(25)-C(27)	109.2(7)
C(13)-C(14)-Zr(2)	71.9(4)	C(8)-C(25)-C(27)	107.7(7)
C(29)-C(14)-Zr(2)	130.6(5)	C(26)-C(25)-C(27)	107.5(7)
C(14)-C(15)-C(11)	111.0(7)	C(32)-C(29)-C(14)	112.3(7)
C(14)-C(15)-Zr(2)	78.2(5)	C(32)-C(29)-C(30)	110.0(8)
C(11)-C(15)-Zr(2)	72.7(5)	C(14)-C(29)-C(30)	110.7(7)
C(17)-C(16)-C(20)	106.6(7)	C(32)-C(29)-C(31)	111.1(8)
C(17)-C(16)-Si(2)	119.8(6)	C(14)-C(29)-C(31)	105.9(7)
C(20)-C(16)-Si(2)	128.5(6)	C(30)-C(29)-C(31)	106.5(7)
C(17)-C(16)-Zr(2)	75.7(4)	C(36)-C(33)-C(18)	112.2(7)
C(20)-C(16)-Zr(2)	73.2(4)	C(36)-C(33)-C(34)	110.6(8)
Si(2)-C(16)-Zr(2)	96.8(3)	C(18)-C(33)-C(34)	110.3(7)
C(18)-C(17)-C(16)	110.8(7)	C(36)-C(33)-C(35)	108.2(8)
C(18)-C(17)-Zr(2)	78.6(5)	C(18)-C(33)-C(35)	107.7(7)
C(16)-C(17)-Zr(2)	71.2(4)	C(34)-C(33)-C(35)	107.6(7)
C(17)-C(18)-C(19)	106.2(8)		

Symmetry transformations used to generate equivalent atoms:

Table C.15. Anisotropic displacement parameters ($Å^2 x\ 10^3$) for **[*meso*-3]$_2$(HI)**. The anisotropic displacement factor exponent takes the form: $-2\pi^2[\ h^2\ a^{*2}U^{11} + ... + 2\ h\ k\ a^*\ b^*\ U^{12}\ ]$

	U^{11}	U^{22}	U^{33}	U^{23}	U^{13}	U^{12}
I(1)	43(1)	34(1)	40(1)	-2(1)	3(1)	1(1)
Zr(1)	16(1)	21(1)	14(1)	0(1)	3(1)	-1(1)
Zr(2)	20(1)	24(1)	18(1)	1(1)	4(1)	4(1)
Si(1)	36(1)	21(1)	25(1)	2(1)	4(1)	3(1)
Si(2)	26(1)	28(1)	24(1)	-5(1)	3(1)	0(1)
C(1)	22(4)	22(4)	28(4)	-2(4)	8(3)	7(3)
C(2)	30(5)	27(4)	22(4)	-10(4)	5(4)	6(4)
C(3)	14(4)	39(5)	17(4)	-7(4)	5(3)	9(4)
C(4)	24(4)	36(5)	13(4)	1(3)	5(3)	1(4)
C(5)	17(4)	36(5)	13(4)	-5(3)	4(3)	4(3)
C(6)	22(4)	29(4)	12(4)	8(3)	-2(3)	8(3)
C(7)	17(4)	38(5)	15(4)	-1(4)	-4(3)	-5(4)
C(8)	24(4)	29(4)	11(4)	-1(3)	-1(3)	2(4)
C(9)	22(4)	38(5)	9(4)	-6(3)	4(3)	3(4)
C(10)	27(4)	24(4)	15(4)	10(3)	-1(3)	-2(3)
C(11)	24(4)	23(4)	25(4)	-3(3)	13(3)	-2(3)
C(12)	20(4)	28(4)	21(4)	2(3)	8(3)	-2(3)
C(13)	23(4)	31(4)	13(4)	0(3)	6(3)	-4(4)
C(14)	10(4)	31(4)	22(4)	5(3)	-1(3)	-2(3)
C(15)	18(4)	37(5)	30(5)	-3(4)	10(4)	-2(4)
C(16)	21(4)	36(5)	11(4)	-9(3)	3(3)	-3(4)
C(17)	25(4)	29(5)	22(4)	5(4)	-3(3)	1(4)
C(18)	26(5)	43(5)	22(4)	4(4)	-4(4)	8(4)
C(19)	29(5)	41(5)	14(4)	4(4)	7(3)	10(4)
C(20)	35(5)	29(5)	14(4)	-8(3)	3(4)	6(4)
C(21)	29(5)	34(5)	28(4)	6(4)	3(4)	3(4)
C(22)	45(6)	45(6)	51(6)	25(5)	19(5)	13(5)
C(23)	39(5)	58(6)	45(6)	20(5)	25(4)	14(5)

Table C.15. (continued)

C(24)	113(10)	49(7)	39(6)	16(5)	-3(6)	-39(7)
C(25)	23(4)	29(4)	18(4)	-9(3)	-2(3)	-4(4)
C(26)	43(6)	29(5)	32(5)	-8(4)	-9(4)	-8(4)
C(27)	50(6)	29(5)	30(5)	-7(4)	-6(4)	-12(4)
C(28)	47(6)	38(5)	38(5)	-15(5)	3(4)	3(5)
C(29)	15(4)	34(5)	29(4)	-8(4)	9(3)	4(4)
C(30)	44(6)	43(6)	48(6)	-21(5)	3(5)	3(5)
C(31)	49(6)	45(6)	57(6)	-15(5)	28(5)	3(5)
C(32)	89(8)	42(6)	36(6)	-18(5)	-12(6)	12(6)
C(33)	27(5)	35(5)	34(5)	5(4)	6(4)	9(4)
C(34)	61(7)	31(5)	42(6)	9(4)	14(5)	15(5)
C(35)	46(6)	60(6)	33(5)	14(5)	-1(5)	20(5)
C(36)	36(6)	45(6)	63(7)	22(5)	10(5)	15(5)
C(37)	41(5)	45(6)	36(5)	9(5)	1(4)	18(5)
C(38)	73(7)	29(5)	46(6)	-8(5)	9(5)	-15(5)
C(39)	57(6)	30(5)	32(5)	-12(4)	9(5)	3(5)
C(40)	32(5)	60(6)	38(5)	-15(5)	0(4)	-18(5)

Table C.16. Hydrogen coordinates (x 10^4) and isotropic displacement parameters ($Å^2$x 10 ^{3}) for **[*meso*-3]$_2$(HI)**.

	x	y	z	U(eq)
H(2A)	2739	3739	4883	31
H(3A)	2945	2604	5627	27
H(5A)	146	2380	4158	26
H(7A)	541	2214	2781	28
H(9A)	3858	2009	2331	27
H(10A)	3450	3332	2579	26
H(12A)	5545	3736	3301	27
H(13A)	5308	2564	2615	26
H(15A)	8127	2404	4065	33
H(17A)	7782	2340	5471	31
H(19A)	4450	2204	5930	34
H(20A)	4849	3508	5589	31
H(22A)	1923	792	6077	70
H(22B)	2453	1563	6205	70
H(22C)	2745	1105	5507	70
H(23A)	-354	1963	5653	69
H(23B)	662	2170	6231	69
H(23C)	145	1389	6234	69
H(24A)	-36	1199	4631	101
H(24B)	474	591	5166	101
H(24C)	1175	884	4519	101
H(26A)	1752	652	3365	53
H(26B)	1124	181	2732	53
H(26C)	586	912	2975	53
H(27A)	395	1259	1720	55
H(27B)	1056	608	1398	55
H(27C)	1448	1402	1254	55
H(28A)	3307	894	1783	61
H(28B)	2742	176	2036	61

Table C.16. (continued)

H(28C)	3443	658	2627	61
H(30A)	6280	693	2315	67
H(30B)	5911	1465	2029	67
H(30C)	5446	1156	2764	67
H(31A)	8569	1955	2627	74
H(31B)	7601	1983	1976	74
H(31C)	8247	1257	2160	74
H(32A)	8158	1201	3763	84
H(32B)	7812	568	3209	84
H(32C)	6955	841	3777	84
H(34A)	6391	728	5011	66
H(34B)	7079	300	5652	66
H(34C)	7611	988	5305	66
H(35A)	7989	1450	6528	71
H(35B)	7348	849	6949	71
H(35C)	7017	1663	7040	71
H(36A)	5031	1214	6637	72
H(36B)	5563	449	6526	72
H(36C)	4829	817	5863	72
H(37A)	-427	4007	2565	61
H(37B)	-712	4107	3402	61
H(37C)	-718	3333	3045	61
H(38A)	2728	4448	3434	73
H(38B)	1694	4848	3751	73
H(38C)	1768	4779	2882	73
H(39A)	5658	4554	4523	59
H(39B)	6791	4950	4361	59
H(39C)	6454	4865	5189	59
H(40A)	8763	4068	5592	65
H(40B)	9020	4255	4766	65
H(40C)	9078	3451	5042	65

Table C.17. Crystal data and structure refinement for **[*rac*-4]$_2$N$_2$** (Chapter 4).

Identification code	**[*rac*-4]$_2$N$_2$**	
Empirical formula	C38 H60 N2 Si4 Zr2	
Formula weight	839.68	
Temperature	173(2) K	
Wavelength	0.71073 Å	
Crystal system	Orthorhombic	
Space group	Pbcn	
Unit cell dimensions	a = 40.646(3) Å	α= 90°.
	b = 10.1714(9) Å	β= 90°.
	c = 47.152(4) Å	γ = 90°.
Volume	19494(3) Å^3	
Z	16	
Density (calculated)	1.144 Mg/m^3	
Absorption coefficient	0.549 mm^{-1}	
F(000)	7008	
Crystal size	0.45 x 0.30 x 0.08 mm^3	
Theta range for data collection	1.80 to 24.71°.	
Index ranges	-30<=h<=47, -11<=k<=10, -55<=l<=55	
Reflections collected	80153	
Independent reflections	16589 [R(int) = 0.1098]	
Completeness to theta = 24.71°	99.9 %	
Absorption correction	Semi-empirical from equivalents	
Max. and min. transmission	0.9574 and 0.7901	
Refinement method	Full-matrix least-squares on F^2	
Data / restraints / parameters	16589 / 0 / 829	
Goodness-of-fit on F^2	1.026	
Final R indices [I>2sigma(I)]	R1 = 0.0615, wR2 = 0.1437	
R indices (all data)	R1 = 0.0960, wR2 = 0.1574	
Largest diff. peak and hole	0.455 and -2.471 e.Å^{-3}	

Table C.18. Atomic coordinates (x 10^4) and equivalent isotropic displacement parameters ($Å^2$x 10^3) for **[*rac*-4]$_2$N$_2$**. U(eq) is defined as one third of the trace of the orthogonalized U^{ij} tensor.

	x	y	z	U(eq)
Zr(1)	6576(1)	6458(1)	589(1)	23(1)
Zr(2)	5696(1)	5724(1)	885(1)	24(1)
Si(1)	6398(1)	3511(1)	25(1)	35(1)
Si(2)	6433(1)	9617(1)	1091(1)	31(1)
Si(3)	5427(1)	7650(1)	160(1)	39(1)
Si(4)	6177(1)	4661(1)	1619(1)	34(1)
N(1)	6172(1)	6483(3)	867(1)	29(1)
N(2)	6068(1)	6126(4)	589(1)	30(1)
C(1)	7117(1)	5353(4)	499(1)	28(1)
C(2)	6947(1)	4630(4)	716(1)	28(1)
C(3)	6680(1)	3975(4)	593(1)	27(1)
C(4)	6663(1)	4292(4)	299(1)	30(1)
C(5)	6937(1)	5144(4)	245(1)	29(1)
C(6)	7121(1)	7619(4)	606(1)	28(1)
C(7)	6955(1)	7885(4)	868(1)	28(1)
C(8)	6684(1)	8724(4)	823(1)	27(1)
C(9)	6668(1)	8919(4)	522(1)	28(1)
C(10)	6932(1)	8255(4)	392(1)	29(1)
C(11)	5084(1)	5537(5)	847(1)	31(1)
C(12)	5150(1)	6755(4)	975(1)	30(1)
C(13)	5292(1)	7597(4)	770(1)	33(1)
C(14)	5328(1)	6917(4)	513(1)	31(1)
C(15)	5206(1)	5616(4)	563(1)	28(1)
C(16)	5364(1)	3934(4)	1114(1)	30(1)
C(17)	5523(1)	4557(4)	1346(1)	31(1)
C(18)	5870(1)	4339(4)	1329(1)	30(1)
C(19)	5920(1)	3560(4)	1086(1)	32(1)
C(20)	5613(1)	3333(4)	951(1)	33(1)
C(21)	7359(1)	6499(4)	552(1)	30(1)

Table C.18. (continued)

C(22)	7577(1)	6738(5)	294(1)	45(1)
C(23)	7576(1)	6228(5)	808(1)	42(1)
C(24)	5021(1)	4257(4)	1009(1)	34(1)
C(25)	4885(1)	3188(5)	819(1)	46(2)
C(26)	4777(1)	4506(5)	1251(1)	49(2)
C(27)	6391(1)	4602(6)	-295(1)	55(2)
C(28)	6589(2)	1890(5)	-75(1)	62(2)
C(29)	5985(1)	3163(6)	175(1)	51(2)
C(30)	6375(1)	8631(5)	1421(1)	50(2)
C(31)	6032(1)	10073(5)	937(1)	45(1)
C(32)	6663(1)	11162(4)	1188(1)	40(1)
C(33)	5631(2)	6441(6)	-71(1)	64(2)
C(34)	5022(1)	8085(5)	-3(1)	54(2)
C(35)	5682(2)	9165(6)	207(1)	65(2)
C(36)	6018(1)	5973(5)	1859(1)	46(1)
C(37)	6587(1)	5058(5)	1471(1)	42(1)
C(38)	6219(1)	3114(5)	1833(1)	54(2)
Zr(1A)	4383(1)	190(1)	1707(1)	26(1)
Zr(2A)	3421(1)	485(1)	1759(1)	26(1)
Si(1A)	4203(1)	-1185(1)	890(1)	34(1)
Si(2A)	4322(1)	2160(1)	2451(1)	31(1)
Si(3A)	3648(1)	3773(1)	1313(1)	32(1)
Si(4A)	3475(1)	-2395(1)	2350(1)	38(1)
N(1A)	3914(1)	349(3)	1891(1)	29(1)
N(2A)	3899(1)	692(3)	1600(1)	29(1)
C(1A)	4824(1)	-1417(5)	1582(1)	34(1)
C(2A)	4549(1)	-2140(4)	1684(1)	33(1)
C(3A)	4295(1)	-2071(4)	1477(1)	33(1)
C(4A)	4403(1)	-1271(4)	1246(1)	32(1)
C(5A)	4730(1)	-847(4)	1319(1)	33(1)
C(6A)	4958(1)	293(4)	1901(1)	29(1)
C(7A)	4745(1)	311(4)	2136(1)	30(1)
C(8A)	4571(1)	1539(4)	2145(1)	28(1)

Table C.18. (continued)

C(9A)	4669(1)	2256(4)	1899(1)	29(1)
C(10A)	4905(1)	1480(4)	1750(1)	30(1)
C(11A)	2885(1)	1478(4)	1614(1)	35(1)
C(12A)	2987(1)	2134(4)	1864(1)	32(1)
C(13A)	3265(1)	2897(4)	1797(1)	29(1)
C(14A)	3346(1)	2732(4)	1511(1)	30(1)
C(15A)	3110(1)	1825(4)	1398(1)	33(1)
C(16A)	2894(1)	-781(4)	1725(1)	33(1)
C(17A)	2993(1)	-955(4)	2009(1)	36(1)
C(18A)	3285(1)	-1718(4)	2020(1)	32(1)
C(19A)	3369(1)	-2006(4)	1738(1)	32(1)
C(20A)	3138(1)	-1432(4)	1554(1)	35(1)
C(21A)	5114(1)	-935(5)	1769(1)	41(1)
C(22A)	5413(1)	-606(6)	1591(1)	55(2)
C(23A)	5199(2)	-1985(5)	1990(1)	64(2)
C(24A)	2655(1)	282(5)	1615(1)	41(1)
C(25A)	2525(1)	-52(5)	1319(1)	62(2)
C(26A)	2369(1)	481(5)	1821(1)	60(2)
C(27A)	4384(1)	173(5)	677(1)	53(2)
C(28A)	4297(1)	-2756(5)	702(1)	53(2)
C(29A)	3749(1)	-1017(5)	933(1)	45(1)
C(30A)	4180(2)	712(5)	2653(1)	57(2)
C(31A)	3977(1)	3195(5)	2331(1)	54(2)
C(32A)	4594(1)	3208(5)	2679(1)	46(1)
C(33A)	3877(1)	2834(5)	1037(1)	47(2)
C(34A)	3411(1)	5122(5)	1131(1)	50(2)
C(35A)	3935(1)	4503(5)	1577(1)	39(1)
C(36A)	3399(1)	-1233(6)	2650(1)	62(2)
C(37A)	3924(1)	-2703(5)	2294(1)	46(1)
C(38A)	3263(2)	-4003(5)	2433(1)	59(2)

Table C.19. Bond lengths [Å] and angles [°] for **[*rac*-4]$_2$N$_2$**.

Zr(1)-N(2)	2.092(4)	C(1)-C(2)	1.435(6)
Zr(1)-N(1)	2.101(4)	C(1)-C(21)	1.547(6)
Zr(1)-C(2)	2.468(4)	C(2)-C(3)	1.401(6)
Zr(1)-C(7)	2.493(4)	C(3)-C(4)	1.427(6)
Zr(1)-C(1)	2.504(4)	C(4)-C(5)	1.432(6)
Zr(1)-C(10)	2.509(4)	C(6)-C(10)	1.425(6)
Zr(1)-C(6)	2.512(4)	C(6)-C(7)	1.435(6)
Zr(1)-C(9)	2.551(4)	C(6)-C(21)	1.515(6)
Zr(1)-C(3)	2.560(4)	C(7)-C(8)	1.412(6)
Zr(1)-C(5)	2.562(4)	C(8)-C(9)	1.434(6)
Zr(1)-C(8)	2.591(4)	C(9)-C(10)	1.406(6)
Zr(1)-C(4)	2.619(4)	C(11)-C(12)	1.405(6)
Zr(2)-N(1)	2.085(4)	C(11)-C(15)	1.430(6)
Zr(2)-N(2)	2.100(4)	C(11)-C(24)	1.533(6)
Zr(2)-C(20)	2.474(4)	C(12)-C(13)	1.417(6)
Zr(2)-C(12)	2.489(4)	C(13)-C(14)	1.402(6)
Zr(2)-C(11)	2.498(4)	C(14)-C(15)	1.432(6)
Zr(2)-C(15)	2.507(4)	C(16)-C(20)	1.413(6)
Zr(2)-C(16)	2.510(4)	C(16)-C(17)	1.421(6)
Zr(2)-C(19)	2.562(4)	C(16)-C(24)	1.515(6)
Zr(2)-C(13)	2.572(4)	C(17)-C(18)	1.428(6)
Zr(2)-C(17)	2.571(4)	C(18)-C(19)	1.410(6)
Zr(2)-C(14)	2.607(4)	C(19)-C(20)	1.418(6)
Zr(2)-C(18)	2.619(4)	C(21)-C(23)	1.516(6)
Si(1)-C(29)	1.856(5)	C(21)-C(22)	1.523(6)
Si(1)-C(4)	1.861(5)	C(24)-C(25)	1.514(6)
Si(1)-C(27)	1.873(5)	C(24)-C(26)	1.532(6)
Si(1)-C(28)	1.883(5)	Zr(1A)-N(2A)	2.095(4)
Si(2)-C(31)	1.842(5)	Zr(1A)-N(1A)	2.103(4)
Si(2)-C(8)	1.862(4)	Zr(1A)-C(2A)	2.466(4)
Si(2)-C(30)	1.866(5)	Zr(1A)-C(1A)	2.495(4)
Si(2)-C(32)	1.887(5)	Zr(1A)-C(10A)	2.502(4)
Si(3)-C(33)	1.836(6)	Zr(1A)-C(7A)	2.506(4)
Si(3)-C(34)	1.867(5)	Zr(1A)-C(6A)	2.514(4)
Si(3)-C(35)	1.870(6)	Zr(1A)-C(5A)	2.541(4)
Si(3)-C(14)	1.870(5)	Zr(1A)-C(9A)	2.566(4)
Si(4)-C(37)	1.853(5)	Zr(1A)-C(3A)	2.568(4)
Si(4)-C(36)	1.866(5)	Zr(1A)-C(8A)	2.594(4)
Si(4)-C(38)	1.876(5)	Zr(1A)-C(4A)	2.635(4)
Si(4)-C(18)	1.879(5)	Zr(2A)-N(2A)	2.094(4)
N(1)-N(2)	1.423(5)	Zr(2A)-N(1A)	2.102(4)
C(1)-C(5)	1.419(6)	Zr(2A)-C(20A)	2.462(5)

Table C.19. (continued)

Zr(2A)-C(12A)	2.483(4)	C(14A)-C(15A)	1.436(6)
Zr(2A)-C(11A)	2.499(4)	C(16A)-C(17A)	1.410(6)
Zr(2A)-C(16A)	2.504(4)	C(16A)-C(20A)	1.435(6)
Zr(2A)-C(15A)	2.522(4)	C(16A)-C(24A)	1.543(6)
Zr(2A)-C(13A)	2.540(4)	C(17A)-C(18A)	1.418(6)
Zr(2A)-C(19A)	2.545(4)	C(18A)-C(19A)	1.404(6)
Zr(2A)-C(17A)	2.562(4)	C(19A)-C(20A)	1.405(6)
Zr(2A)-C(14A)	2.585(4)	C(21A)-C(22A)	1.516(7)
Zr(2A)-C(18A)	2.616(4)	C(21A)-C(23A)	1.531(7)
Si(1A)-C(27A)	1.861(5)	C(24A)-C(26A)	1.530(7)
Si(1A)-C(29A)	1.864(5)	C(24A)-C(25A)	1.528(7)
Si(1A)-C(4A)	1.865(5)		
Si(1A)-C(28A)	1.868(5)	N(2)-Zr(1)-N(1)	39.68(13)
Si(2A)-C(31A)	1.840(5)	N(2)-Zr(1)-C(2)	118.82(14)
Si(2A)-C(30A)	1.845(5)	N(1)-Zr(1)-C(2)	109.67(14)
Si(2A)-C(32A)	1.875(5)	N(2)-Zr(1)-C(7)	134.77(14)
Si(2A)-C(8A)	1.875(4)	N(1)-Zr(1)-C(7)	98.48(14)
Si(3A)-C(35A)	1.864(5)	C(2)-Zr(1)-C(7)	86.15(14)
Si(3A)-C(33A)	1.864(5)	N(2)-Zr(1)-C(1)	142.50(14)
Si(3A)-C(14A)	1.869(5)	N(1)-Zr(1)-C(1)	142.88(14)
Si(3A)-C(34A)	1.881(5)	C(2)-Zr(1)-C(1)	33.54(14)
Si(4A)-C(36A)	1.867(6)	C(7)-Zr(1)-C(1)	78.97(14)
Si(4A)-C(37A)	1.870(5)	N(2)-Zr(1)-C(10)	133.30(14)
Si(4A)-C(18A)	1.870(5)	N(1)-Zr(1)-C(10)	132.27(14)
Si(4A)-C(38A)	1.890(5)	C(2)-Zr(1)-C(10)	106.64(15)
N(1A)-N(2A)	1.421(5)	C(7)-Zr(1)-C(10)	54.23(14)
C(1A)-C(5A)	1.421(6)	C(1)-Zr(1)-C(10)	76.04(14)
C(1A)-C(2A)	1.422(6)	N(2)-Zr(1)-C(6)	161.13(14)
C(1A)-C(21A)	1.552(6)	N(1)-Zr(1)-C(6)	131.64(14)
C(2A)-C(3A)	1.423(6)	C(2)-Zr(1)-C(6)	78.90(14)
C(3A)-C(4A)	1.429(6)	C(7)-Zr(1)-C(6)	33.32(13)
C(4A)-C(5A)	1.441(6)	C(1)-Zr(1)-C(6)	56.13(14)
C(6A)-C(7A)	1.406(6)	C(10)-Zr(1)-C(6)	32.97(14)
C(6A)-C(10A)	1.421(6)	N(2)-Zr(1)-C(9)	107.65(14)
C(6A)-C(21A)	1.532(6)	N(1)-Zr(1)-C(9)	100.40(14)
C(7A)-C(8A)	1.436(6)	C(2)-Zr(1)-C(9)	132.81(14)
C(8A)-C(9A)	1.424(6)	C(7)-Zr(1)-C(9)	53.39(14)
C(9A)-C(10A)	1.428(6)	C(1)-Zr(1)-C(9)	106.89(14)
C(11A)-C(15A)	1.414(6)	C(10)-Zr(1)-C(9)	32.25(14)
C(11A)-C(12A)	1.420(7)	C(6)-Zr(1)-C(9)	54.05(14)
C(11A)-C(24A)	1.532(6)	N(2)-Zr(1)-C(3)	90.21(14)
C(12A)-C(13A)	1.407(6)	N(1)-Zr(1)-C(3)	97.86(14)
C(13A)-C(14A)	1.400(6)	C(2)-Zr(1)-C(3)	32.29(14)

Table C.19. (continued)

C(7)-Zr(1)-C(3)	117.97(14)	N(2)-Zr(2)-C(11)	133.07(14)
C(1)-Zr(1)-C(3)	54.11(14)	C(20)-Zr(2)-C(11)	78.42(16)
C(10)-Zr(1)-C(3)	128.76(14)	C(12)-Zr(2)-C(11)	32.73(14)
C(6)-Zr(1)-C(3)	108.56(14)	N(1)-Zr(2)-C(15)	136.65(14)
C(9)-Zr(1)-C(3)	160.81(14)	N(2)-Zr(2)-C(15)	100.18(14)
N(2)-Zr(1)-C(5)	118.70(14)	C(20)-Zr(2)-C(15)	85.70(15)
N(1)-Zr(1)-C(5)	148.03(14)	C(12)-Zr(2)-C(15)	54.19(14)
C(2)-Zr(1)-C(5)	53.91(14)	C(11)-Zr(2)-C(15)	33.19(13)
C(7)-Zr(1)-C(5)	106.51(14)	N(1)-Zr(2)-C(16)	141.80(14)
C(1)-Zr(1)-C(5)	32.50(13)	N(2)-Zr(2)-C(16)	144.55(14)
C(10)-Zr(1)-C(5)	79.36(14)	C(20)-Zr(2)-C(16)	32.93(14)
C(6)-Zr(1)-C(5)	76.14(14)	C(12)-Zr(2)-C(16)	75.70(15)
C(9)-Zr(1)-C(5)	110.39(14)	C(11)-Zr(2)-C(16)	56.01(15)
C(3)-Zr(1)-C(5)	52.83(14)	C(15)-Zr(2)-C(16)	78.58(14)
N(2)-Zr(1)-C(8)	108.06(14)	N(1)-Zr(2)-C(19)	90.21(14)
N(1)-Zr(1)-C(8)	81.74(14)	N(2)-Zr(2)-C(19)	98.97(14)
C(2)-Zr(1)-C(8)	117.66(14)	C(20)-Zr(2)-C(19)	32.64(15)
C(7)-Zr(1)-C(8)	32.18(14)	C(12)-Zr(2)-C(19)	128.01(15)
C(1)-Zr(1)-C(8)	108.88(14)	C(11)-Zr(2)-C(19)	108.35(15)
C(10)-Zr(1)-C(8)	54.02(14)	C(15)-Zr(2)-C(19)	117.90(14)
C(6)-Zr(1)-C(8)	54.53(14)	C(16)-Zr(2)-C(19)	53.85(15)
C(9)-Zr(1)-C(8)	32.37(13)	N(1)-Zr(2)-C(13)	107.95(14)
C(3)-Zr(1)-C(8)	147.86(14)	N(2)-Zr(2)-C(13)	100.03(14)
C(5)-Zr(1)-C(8)	129.51(14)	C(20)-Zr(2)-C(13)	131.93(15)
N(2)-Zr(1)-C(4)	89.88(14)	C(12)-Zr(2)-C(13)	32.47(14)
N(1)-Zr(1)-C(4)	116.26(14)	C(11)-Zr(2)-C(13)	53.65(15)
C(2)-Zr(1)-C(4)	53.87(14)	C(15)-Zr(2)-C(13)	52.98(14)
C(7)-Zr(1)-C(4)	133.04(14)	C(16)-Zr(2)-C(13)	106.59(15)
C(1)-Zr(1)-C(4)	54.17(14)	C(19)-Zr(2)-C(13)	160.24(15)
C(10)-Zr(1)-C(4)	109.91(14)	N(1)-Zr(2)-C(17)	117.33(14)
C(6)-Zr(1)-C(4)	107.01(14)	N(2)-Zr(2)-C(17)	147.99(14)
C(9)-Zr(1)-C(4)	137.74(14)	C(20)-Zr(2)-C(17)	53.44(14)
C(3)-Zr(1)-C(4)	31.96(13)	C(12)-Zr(2)-C(17)	78.92(14)
C(5)-Zr(1)-C(4)	32.05(13)	C(11)-Zr(2)-C(17)	75.85(14)
C(8)-Zr(1)-C(4)	161.39(14)	C(15)-Zr(2)-C(17)	106.02(14)
N(1)-Zr(2)-N(2)	39.76(13)	C(16)-Zr(2)-C(17)	32.45(14)
N(1)-Zr(2)-C(20)	119.67(15)	C(19)-Zr(2)-C(17)	52.39(14)
N(2)-Zr(2)-C(20)	111.83(14)	C(13)-Zr(2)-C(17)	110.31(14)
N(1)-Zr(2)-C(12)	132.67(14)	N(1)-Zr(2)-C(14)	109.39(14)
N(2)-Zr(2)-C(12)	132.33(14)	N(2)-Zr(2)-C(14)	82.80(14)
C(20)-Zr(2)-C(12)	105.79(15)	C(20)-Zr(2)-C(14)	117.62(15)
N(1)-Zr(2)-C(11)	161.43(14)	C(12)-Zr(2)-C(14)	53.67(14)

Table C.19. (continued)

C(11)-Zr(2)-C(14)	54.24(14)	N(2)-N(1)-Zr(1)	69.8(2)
C(15)-Zr(2)-C(14)	32.44(14)	Zr(2)-N(1)-Zr(1)	138.34(18)
C(16)-Zr(2)-C(14)	108.56(15)	N(1)-N(2)-Zr(1)	70.5(2)
C(19)-Zr(2)-C(14)	148.43(14)	N(1)-N(2)-Zr(2)	69.6(2)
C(13)-Zr(2)-C(14)	31.41(13)	Zr(1)-N(2)-Zr(2)	137.95(18)
C(17)-Zr(2)-C(14)	128.85(14)	C(5)-C(1)-C(2)	106.2(4)
N(1)-Zr(2)-C(18)	88.96(14)	C(5)-C(1)-C(21)	125.2(4)
N(2)-Zr(2)-C(18)	116.18(14)	C(2)-C(1)-C(21)	125.2(4)
C(20)-Zr(2)-C(18)	53.74(14)	C(5)-C(1)-Zr(1)	76.0(3)
C(12)-Zr(2)-C(18)	109.35(14)	C(2)-C(1)-Zr(1)	71.9(2)
C(11)-Zr(2)-C(18)	106.62(14)	C(21)-C(1)-Zr(1)	101.1(3)
C(15)-Zr(2)-C(18)	132.50(14)	C(3)-C(2)-C(1)	108.7(4)
C(16)-Zr(2)-C(18)	54.01(14)	C(3)-C(2)-Zr(1)	77.5(2)
C(19)-Zr(2)-C(18)	31.56(13)	C(1)-C(2)-Zr(1)	74.6(2)
C(13)-Zr(2)-C(18)	137.73(14)	C(2)-C(3)-C(4)	109.4(4)
C(17)-Zr(2)-C(18)	31.93(14)	C(2)-C(3)-Zr(1)	70.2(2)
C(14)-Zr(2)-C(18)	160.65(14)	C(4)-C(3)-Zr(1)	76.3(2)
C(29)-Si(1)-C(4)	109.9(2)	C(3)-C(4)-C(5)	105.7(4)
C(29)-Si(1)-C(27)	114.0(3)	C(3)-C(4)-Si(1)	127.3(3)
C(4)-Si(1)-C(27)	108.4(2)	C(5)-C(4)-Si(1)	125.9(3)
C(29)-Si(1)-C(28)	107.6(3)	C(3)-C(4)-Zr(1)	71.8(2)
C(4)-Si(1)-C(28)	107.8(2)	C(5)-C(4)-Zr(1)	71.8(2)
C(27)-Si(1)-C(28)	108.9(3)	Si(1)-C(4)-Zr(1)	130.1(2)
C(31)-Si(2)-C(8)	109.8(2)	C(1)-C(5)-C(4)	110.0(4)
C(31)-Si(2)-C(30)	110.7(2)	C(1)-C(5)-Zr(1)	71.5(2)
C(8)-Si(2)-C(30)	112.0(2)	C(4)-C(5)-Zr(1)	76.2(2)
C(31)-Si(2)-C(32)	109.0(2)	C(10)-C(6)-C(7)	105.8(4)
C(8)-Si(2)-C(32)	107.4(2)	C(10)-C(6)-C(21)	124.6(4)
C(30)-Si(2)-C(32)	108.0(2)	C(7)-C(6)-C(21)	125.8(4)
C(33)-Si(3)-C(34)	108.3(3)	C(10)-C(6)-Zr(1)	73.4(2)
C(33)-Si(3)-C(35)	111.9(3)	C(7)-C(6)-Zr(1)	72.6(2)
C(34)-Si(3)-C(35)	110.0(3)	C(21)-C(6)-Zr(1)	101.8(3)
C(33)-Si(3)-C(14)	110.9(2)	C(8)-C(7)-C(6)	110.5(4)
C(34)-Si(3)-C(14)	105.7(2)	C(8)-C(7)-Zr(1)	77.7(3)
C(35)-Si(3)-C(14)	110.0(2)	C(6)-C(7)-Zr(1)	74.1(2)
C(37)-Si(4)-C(36)	112.6(2)	C(7)-C(8)-C(9)	105.6(4)
C(37)-Si(4)-C(38)	107.6(2)	C(7)-C(8)-Si(2)	128.3(3)
C(36)-Si(4)-C(38)	107.8(2)	C(9)-C(8)-Si(2)	125.6(3)
C(37)-Si(4)-C(18)	111.2(2)	C(7)-C(8)-Zr(1)	70.1(2)
C(36)-Si(4)-C(18)	109.7(2)	C(9)-C(8)-Zr(1)	72.3(2)
C(38)-Si(4)-C(18)	107.8(2)	Si(2)-C(8)-Zr(1)	129.1(2)
N(2)-N(1)-Zr(2)	70.7(2)	C(10)-C(9)-C(8)	109.4(4)

Table C.19. (continued)

C(10)-C(9)-Zr(1)	72.2(2)	C(18)-C(19)-Zr(2)	76.4(2)
C(8)-C(9)-Zr(1)	75.4(2)	C(20)-C(19)-Zr(2)	70.3(2)
C(9)-C(10)-C(6)	108.7(4)	C(16)-C(20)-C(19)	108.5(4)
C(9)-C(10)-Zr(1)	75.5(2)	C(16)-C(20)-Zr(2)	74.9(2)
C(6)-C(10)-Zr(1)	73.6(2)	C(19)-C(20)-Zr(2)	77.1(3)
C(12)-C(11)-C(15)	106.8(4)	C(6)-C(21)-C(23)	112.0(4)
C(12)-C(11)-C(24)	124.4(4)	C(6)-C(21)-C(22)	112.6(4)
C(15)-C(11)-C(24)	125.1(4)	C(23)-C(21)-C(22)	109.0(4)
C(12)-C(11)-Zr(2)	73.3(3)	C(6)-C(21)-C(1)	100.8(3)
C(15)-C(11)-Zr(2)	73.7(2)	C(23)-C(21)-C(1)	111.2(4)
C(24)-C(11)-Zr(2)	101.4(3)	C(22)-C(21)-C(1)	111.2(4)
C(11)-C(12)-C(13)	108.4(4)	C(16)-C(24)-C(25)	111.8(4)
C(11)-C(12)-Zr(2)	74.0(3)	C(16)-C(24)-C(26)	112.8(4)
C(13)-C(12)-Zr(2)	77.0(3)	C(25)-C(24)-C(26)	109.0(4)
C(14)-C(13)-C(12)	109.5(4)	C(16)-C(24)-C(11)	101.0(4)
C(14)-C(13)-Zr(2)	75.7(3)	C(25)-C(24)-C(11)	112.0(4)
C(12)-C(13)-Zr(2)	70.5(2)	C(26)-C(24)-C(11)	110.0(4)
C(13)-C(14)-C(15)	106.2(4)	N(2A)-Zr(1A)-N(1A)	39.56(13)
C(13)-C(14)-Si(3)	126.6(3)	N(2A)-Zr(1A)-C(2A)	118.69(15)
C(15)-C(14)-Si(3)	126.1(3)	N(1A)-Zr(1A)-C(2A)	109.85(14)
C(13)-C(14)-Zr(2)	72.9(2)	N(2A)-Zr(1A)-C(1A)	140.92(14)
C(15)-C(14)-Zr(2)	69.9(2)	N(1A)-Zr(1A)-C(1A)	143.07(15)
Si(3)-C(14)-Zr(2)	131.5(2)	C(2A)-Zr(1A)-C(1A)	33.32(15)
C(11)-C(15)-C(14)	109.0(4)	N(2A)-Zr(1A)-C(10A)	133.44(14)
C(11)-C(15)-Zr(2)	73.1(2)	N(1A)-Zr(1A)-C(10A)	134.07(14)
C(14)-C(15)-Zr(2)	77.6(2)	C(2A)-Zr(1A)-C(10A)	106.04(15)
C(20)-C(16)-C(17)	106.5(4)	C(1A)-Zr(1A)-C(10A)	75.78(15)
C(20)-C(16)-C(24)	125.3(4)	N(2A)-Zr(1A)-C(7A)	137.35(14)
C(17)-C(16)-C(24)	125.1(4)	N(1A)-Zr(1A)-C(7A)	101.31(14)
C(20)-C(16)-Zr(2)	72.1(2)	C(2A)-Zr(1A)-C(7A)	85.53(15)
C(17)-C(16)-Zr(2)	76.1(2)	C(1A)-Zr(1A)-C(7A)	78.55(14)
C(24)-C(16)-Zr(2)	101.4(3)	C(10A)-Zr(1A)-C(7A)	53.91(14)
C(16)-C(17)-C(18)	109.8(4)	N(2A)-Zr(1A)-C(6A)	162.14(14)
C(16)-C(17)-Zr(2)	71.4(2)	N(1A)-Zr(1A)-C(6A)	133.67(14)
C(18)-C(17)-Zr(2)	75.9(2)	C(2A)-Zr(1A)-C(6A)	78.57(15)
C(19)-C(18)-C(17)	106.0(4)	C(1A)-Zr(1A)-C(6A)	56.35(14)
C(19)-C(18)-Si(4)	126.5(4)	C(10A)-Zr(1A)-C(6A)	32.90(14)
C(17)-C(18)-Si(4)	125.9(3)	C(7A)-Zr(1A)-C(6A)	32.52(13)
C(19)-C(18)-Zr(2)	72.0(2)	N(2A)-Zr(1A)-C(5A)	116.62(14)
C(17)-C(18)-Zr(2)	72.2(2)	N(1A)-Zr(1A)-C(5A)	146.46(14)
Si(4)-C(18)-Zr(2)	131.8(2)	C(2A)-Zr(1A)-C(5A)	54.43(15)
C(18)-C(19)-C(20)	109.3(4)	C(1A)-Zr(1A)-C(5A)	32.77(14)

Table C.19. (continued)

C(10A)-Zr(1A)-C(5A)	78.76(14)	N(2A)-Zr(2A)-C(20A)	111.90(15)
C(7A)-Zr(1A)-C(5A)	106.03(14)	N(1A)-Zr(2A)-C(20A)	120.66(14)
C(6A)-Zr(1A)-C(5A)	76.31(14)	N(2A)-Zr(2A)-C(12A)	131.53(14)
N(2A)-Zr(1A)-C(9A)	108.11(14)	N(1A)-Zr(2A)-C(12A)	131.44(14)
N(1A)-Zr(1A)-C(9A)	101.63(13)	C(20A)-Zr(2A)-C(12A)	106.29(15)
C(2A)-Zr(1A)-C(9A)	132.75(15)	N(2A)-Zr(2A)-C(11A)	132.13(14)
C(1A)-Zr(1A)-C(9A)	107.18(15)	N(1A)-Zr(2A)-C(11A)	159.97(14)
C(10A)-Zr(1A)-C(9A)	32.71(13)	C(20A)-Zr(2A)-C(11A)	78.69(15)
C(7A)-Zr(1A)-C(9A)	53.73(14)	C(12A)-Zr(2A)-C(11A)	33.11(15)
C(6A)-Zr(1A)-C(9A)	54.30(14)	N(2A)-Zr(2A)-C(16A)	145.25(14)
C(5A)-Zr(1A)-C(9A)	110.08(14)	N(1A)-Zr(2A)-C(16A)	143.10(14)
N(2A)-Zr(1A)-C(3A)	89.15(14)	C(20A)-Zr(2A)-C(16A)	33.57(15)
N(1A)-Zr(1A)-C(3A)	96.71(14)	C(12A)-Zr(2A)-C(16A)	75.71(15)
C(2A)-Zr(1A)-C(3A)	32.75(14)	C(11A)-Zr(2A)-C(16A)	56.22(14)
C(1A)-Zr(1A)-C(3A)	54.09(15)	N(2A)-Zr(2A)-C(15A)	99.73(14)
C(10A)-Zr(1A)-C(3A)	128.46(15)	N(1A)-Zr(2A)-C(15A)	135.60(14)
C(7A)-Zr(1A)-C(3A)	117.85(14)	C(20A)-Zr(2A)-C(15A)	85.86(15)
C(6A)-Zr(1A)-C(3A)	108.71(15)	C(12A)-Zr(2A)-C(15A)	54.12(15)
C(5A)-Zr(1A)-C(3A)	53.22(15)	C(11A)-Zr(2A)-C(15A)	32.70(14)
C(9A)-Zr(1A)-C(3A)	161.03(15)	C(16A)-Zr(2A)-C(15A)	78.75(14)
N(2A)-Zr(1A)-C(8A)	109.92(13)	N(2A)-Zr(2A)-C(13A)	99.22(14)
N(1A)-Zr(1A)-C(8A)	84.16(13)	N(1A)-Zr(2A)-C(13A)	106.29(14)
C(2A)-Zr(1A)-C(8A)	117.55(14)	C(20A)-Zr(2A)-C(13A)	132.52(15)
C(1A)-Zr(1A)-C(8A)	108.86(14)	C(12A)-Zr(2A)-C(13A)	32.50(14)
C(10A)-Zr(1A)-C(8A)	53.73(14)	C(11A)-Zr(2A)-C(13A)	53.95(15)
C(7A)-Zr(1A)-C(8A)	32.66(13)	C(16A)-Zr(2A)-C(13A)	106.75(14)
C(6A)-Zr(1A)-C(8A)	54.10(13)	C(15A)-Zr(2A)-C(13A)	53.21(15)
C(5A)-Zr(1A)-C(8A)	129.00(14)	N(2A)-Zr(2A)-C(19A)	99.40(14)
C(9A)-Zr(1A)-C(8A)	32.02(13)	N(1A)-Zr(2A)-C(19A)	91.45(14)
C(3A)-Zr(1A)-C(8A)	148.34(14)	C(20A)-Zr(2A)-C(19A)	32.54(14)
N(2A)-Zr(1A)-C(4A)	88.05(14)	C(12A)-Zr(2A)-C(19A)	128.36(15)
N(1A)-Zr(1A)-C(4A)	114.30(14)	C(11A)-Zr(2A)-C(19A)	108.58(15)
C(2A)-Zr(1A)-C(4A)	54.12(14)	C(16A)-Zr(2A)-C(19A)	54.10(15)
C(1A)-Zr(1A)-C(4A)	54.11(14)	C(15A)-Zr(2A)-C(19A)	118.00(15)
C(10A)-Zr(1A)-C(4A)	109.68(14)	C(13A)-Zr(2A)-C(19A)	160.66(15)
C(7A)-Zr(1A)-C(4A)	132.57(14)	N(2A)-Zr(2A)-C(17A)	148.51(14)
C(6A)-Zr(1A)-C(4A)	107.23(14)	N(1A)-Zr(2A)-C(17A)	118.20(14)
C(5A)-Zr(1A)-C(4A)	32.27(14)	C(20A)-Zr(2A)-C(17A)	53.80(15)
C(9A)-Zr(1A)-C(4A)	137.71(14)	C(12A)-Zr(2A)-C(17A)	79.16(14)
C(3A)-Zr(1A)-C(4A)	31.84(14)	C(11A)-Zr(2A)-C(17A)	76.38(14)
C(8A)-Zr(1A)-C(4A)	161.11(14)	C(16A)-Zr(2A)-C(17A)	32.31(14)
N(2A)-Zr(2A)-N(1A)	39.58(13)	C(15A)-Zr(2A)-C(17A)	106.19(15)

Table C.19. (continued)

C(13A)-Zr(2A)-C(17A)	110.50(14)	C(36A)-Si(4A)-C(18A)	109.2(2)
C(19A)-Zr(2A)-C(17A)	52.53(15)	C(37A)-Si(4A)-C(18A)	110.3(2)
N(2A)-Zr(2A)-C(14A)	81.83(14)	C(36A)-Si(4A)-C(38A)	108.5(3)
N(1A)-Zr(2A)-C(14A)	107.75(14)	C(37A)-Si(4A)-C(38A)	109.2(3)
C(20A)-Zr(2A)-C(14A)	117.87(15)	C(18A)-Si(4A)-C(38A)	107.6(2)
C(12A)-Zr(2A)-C(14A)	53.86(14)	N(2A)-N(1A)-Zr(2A)	69.9(2)
C(11A)-Zr(2A)-C(14A)	54.28(14)	N(2A)-N(1A)-Zr(1A)	69.9(2)
C(16A)-Zr(2A)-C(14A)	108.96(14)	Zr(2A)-N(1A)-Zr(1A)	138.33(18)
C(15A)-Zr(2A)-C(14A)	32.63(14)	N(1A)-N(2A)-Zr(2A)	70.5(2)
C(13A)-Zr(2A)-C(14A)	31.70(14)	N(1A)-N(2A)-Zr(1A)	70.5(2)
C(19A)-Zr(2A)-C(14A)	148.49(14)	Zr(2A)-N(2A)-Zr(1A)	139.46(17)
C(17A)-Zr(2A)-C(14A)	129.34(14)	C(5A)-C(1A)-C(2A)	107.3(4)
N(2A)-Zr(2A)-C(18A)	116.83(14)	C(5A)-C(1A)-C(21A)	124.8(4)
N(1A)-Zr(2A)-C(18A)	90.32(14)	C(2A)-C(1A)-C(21A)	124.5(4)
C(20A)-Zr(2A)-C(18A)	53.61(15)	C(5A)-C(1A)-Zr(1A)	75.4(3)
C(12A)-Zr(2A)-C(18A)	109.50(14)	C(2A)-C(1A)-Zr(1A)	72.2(2)
C(11A)-Zr(2A)-C(18A)	106.87(15)	C(21A)-C(1A)-Zr(1A)	101.7(3)
C(16A)-Zr(2A)-C(18A)	53.73(14)	C(1A)-C(2A)-C(3A)	108.1(4)
C(15A)-Zr(2A)-C(18A)	132.38(15)	C(1A)-C(2A)-Zr(1A)	74.5(3)
C(13A)-Zr(2A)-C(18A)	137.82(14)	C(3A)-C(2A)-Zr(1A)	77.6(2)
C(19A)-Zr(2A)-C(18A)	31.53(14)	C(2A)-C(3A)-C(4A)	109.3(4)
C(17A)-Zr(2A)-C(18A)	31.76(14)	C(2A)-C(3A)-Zr(1A)	69.7(2)
C(14A)-Zr(2A)-C(18A)	160.94(14)	C(4A)-C(3A)-Zr(1A)	76.6(2)
C(27A)-Si(1A)-C(29A)	112.4(3)	C(3A)-C(4A)-C(5A)	105.8(4)
C(27A)-Si(1A)-C(4A)	110.4(2)	C(3A)-C(4A)-Si(1A)	125.4(3)
C(29A)-Si(1A)-C(4A)	109.8(2)	C(5A)-C(4A)-Si(1A)	127.0(3)
C(27A)-Si(1A)-C(28A)	107.3(3)	C(3A)-C(4A)-Zr(1A)	71.5(2)
C(29A)-Si(1A)-C(28A)	109.4(2)	C(5A)-C(4A)-Zr(1A)	70.3(2)
C(4A)-Si(1A)-C(28A)	107.4(2)	Si(1A)-C(4A)-Zr(1A)	134.6(2)
C(31A)-Si(2A)-C(30A)	112.3(3)	C(1A)-C(5A)-C(4A)	109.4(4)
C(31A)-Si(2A)-C(32A)	107.5(2)	C(1A)-C(5A)-Zr(1A)	71.8(2)
C(30A)-Si(2A)-C(32A)	110.0(2)	C(4A)-C(5A)-Zr(1A)	77.4(2)
C(31A)-Si(2A)-C(8A)	111.5(2)	C(7A)-C(6A)-C(10A)	106.9(4)
C(30A)-Si(2A)-C(8A)	107.3(2)	C(7A)-C(6A)-C(21A)	125.8(4)
C(32A)-Si(2A)-C(8A)	108.2(2)	C(10A)-C(6A)-C(21A)	123.5(4)
C(35A)-Si(3A)-C(33A)	110.9(2)	C(7A)-C(6A)-Zr(1A)	73.4(2)
C(35A)-Si(3A)-C(14A)	107.6(2)	C(10A)-C(6A)-Zr(1A)	73.1(2)
C(33A)-Si(3A)-C(14A)	112.7(2)	C(21A)-C(6A)-Zr(1A)	101.6(3)
C(35A)-Si(3A)-C(34A)	109.5(2)	C(6A)-C(7A)-C(8A)	109.7(4)
C(33A)-Si(3A)-C(34A)	108.2(2)	C(6A)-C(7A)-Zr(1A)	74.1(2)
C(14A)-Si(3A)-C(34A)	107.9(2)	C(8A)-C(7A)-Zr(1A)	77.1(2)
C(36A)-Si(4A)-C(37A)	112.0(2)	C(9A)-C(8A)-C(7A)	106.6(4)

Table C.19. (continued)

C(9A)-C(8A)-Si(2A)	127.2(3)	C(17A)-C(16A)-C(24A)	125.9(4)
C(7A)-C(8A)-Si(2A)	125.6(3)	C(20A)-C(16A)-C(24A)	124.7(4)
C(9A)-C(8A)-Zr(1A)	72.9(2)	C(17A)-C(16A)-Zr(2A)	76.1(3)
C(7A)-C(8A)-Zr(1A)	70.3(2)	C(20A)-C(16A)-Zr(2A)	71.6(3)
Si(2A)-C(8A)-Zr(1A)	129.2(2)	C(24A)-C(16A)-Zr(2A)	101.5(3)
C(8A)-C(9A)-C(10A)	107.8(4)	C(16A)-C(17A)-C(18A)	109.9(4)
C(8A)-C(9A)-Zr(1A)	75.1(2)	C(16A)-C(17A)-Zr(2A)	71.6(3)
C(10A)-C(9A)-Zr(1A)	71.2(2)	C(18A)-C(17A)-Zr(2A)	76.2(3)
C(6A)-C(10A)-C(9A)	108.9(4)	C(19A)-C(18A)-C(17A)	106.4(4)
C(6A)-C(10A)-Zr(1A)	74.0(2)	C(19A)-C(18A)-Si(4A)	127.7(4)
C(9A)-C(10A)-Zr(1A)	76.1(2)	C(17A)-C(18A)-Si(4A)	125.3(4)
C(15A)-C(11A)-C(12A)	107.0(4)	C(19A)-C(18A)-Zr(2A)	71.5(2)
C(15A)-C(11A)-C(24A)	126.4(4)	C(17A)-C(18A)-Zr(2A)	72.0(2)
C(12A)-C(11A)-C(24A)	123.3(4)	Si(4A)-C(18A)-Zr(2A)	128.3(2)
C(15A)-C(11A)-Zr(2A)	74.5(3)	C(20A)-C(19A)-C(18A)	109.5(4)
C(12A)-C(11A)-Zr(2A)	72.8(3)	C(20A)-C(19A)-Zr(2A)	70.5(2)
C(24A)-C(11A)-Zr(2A)	102.0(3)	C(18A)-C(19A)-Zr(2A)	77.0(3)
C(13A)-C(12A)-C(11A)	108.0(4)	C(19A)-C(20A)-C(16A)	107.9(4)
C(13A)-C(12A)-Zr(2A)	76.0(3)	C(19A)-C(20A)-Zr(2A)	77.0(3)
C(11A)-C(12A)-Zr(2A)	74.1(3)	C(16A)-C(20A)-Zr(2A)	74.8(3)
C(14A)-C(13A)-C(12A)	109.8(4)	C(22A)-C(21A)-C(23A)	110.4(4)
C(14A)-C(13A)-Zr(2A)	75.9(2)	C(22A)-C(21A)-C(6A)	112.1(4)
C(12A)-C(13A)-Zr(2A)	71.5(2)	C(23A)-C(21A)-C(6A)	112.7(4)
C(13A)-C(14A)-C(15A)	106.1(4)	C(22A)-C(21A)-C(1A)	111.3(4)
C(13A)-C(14A)-Si(3A)	124.6(3)	C(23A)-C(21A)-C(1A)	109.9(4)
C(15A)-C(14A)-Si(3A)	128.1(3)	C(6A)-C(21A)-C(1A)	100.2(4)
C(13A)-C(14A)-Zr(2A)	72.4(2)	C(26A)-C(24A)-C(11A)	111.0(4)
C(15A)-C(14A)-Zr(2A)	71.3(2)	C(26A)-C(24A)-C(25A)	110.1(4)
Si(3A)-C(14A)-Zr(2A)	130.5(2)	C(11A)-C(24A)-C(25A)	112.6(4)
C(11A)-C(15A)-C(14A)	109.0(4)	C(26A)-C(24A)-C(16A)	111.0(4)
C(11A)-C(15A)-Zr(2A)	72.8(2)	C(11A)-C(24A)-C(16A)	100.1(4)
C(14A)-C(15A)-Zr(2A)	76.1(3)	C(25A)-C(24A)-C(16A)	111.7(4)
C(17A)-C(16A)-C(20A)	106.2(4)		

Symmetry transformations used to generate equivalent atoms:

Table C.20. Anisotropic displacement parameters ($Å^2 x\ 10^3$) for **[*rac*-4]$_2$N$_2$**. The anisotropic displacement factor exponent takes the form: $-2\pi^2[\ h^2\ a^{*2}U^{11} + ... + 2\ h\ k\ a^*\ b^*\ U^{12}\ ]$

	U^{11}	U^{22}	U^{33}	U^{23}	U^{13}	U^{12}
Zr(1)	19(1)	22(1)	28(1)	-1(1)	0(1)	0(1)
Zr(2)	21(1)	23(1)	29(1)	0(1)	1(1)	1(1)
Si(1)	33(1)	39(1)	34(1)	-8(1)	-3(1)	-7(1)
Si(2)	29(1)	24(1)	41(1)	-2(1)	8(1)	1(1)
Si(3)	31(1)	45(1)	40(1)	13(1)	-4(1)	3(1)
Si(4)	30(1)	41(1)	29(1)	6(1)	2(1)	6(1)
N(1)	28(2)	29(2)	31(2)	-1(2)	1(2)	3(2)
N(2)	29(2)	31(2)	30(2)	0(2)	-2(2)	-1(2)
C(1)	20(2)	28(2)	34(2)	-2(2)	3(2)	9(2)
C(2)	31(3)	23(2)	30(2)	1(2)	0(2)	6(2)
C(3)	31(3)	10(2)	39(3)	-1(2)	3(2)	2(2)
C(4)	26(3)	24(2)	38(3)	-6(2)	2(2)	2(2)
C(5)	31(3)	25(2)	30(2)	-4(2)	6(2)	-4(2)
C(6)	20(2)	25(2)	39(3)	-5(2)	-4(2)	-8(2)
C(7)	24(3)	25(2)	33(2)	0(2)	-1(2)	-2(2)
C(8)	26(3)	18(2)	37(3)	-2(2)	4(2)	-4(2)
C(9)	34(3)	11(2)	39(3)	4(2)	0(2)	0(2)
C(10)	30(3)	28(2)	30(2)	1(2)	5(2)	-7(2)
C(11)	16(2)	45(3)	32(2)	2(2)	-1(2)	3(2)
C(12)	21(2)	33(3)	37(3)	-5(2)	-1(2)	6(2)
C(13)	28(3)	22(2)	48(3)	-2(2)	-9(2)	11(2)
C(14)	24(3)	35(3)	34(3)	-3(2)	-3(2)	6(2)
C(15)	20(2)	33(2)	30(2)	-3(2)	-10(2)	-3(2)
C(16)	32(3)	24(2)	34(2)	5(2)	8(2)	-6(2)
C(17)	27(3)	35(3)	30(2)	1(2)	8(2)	5(2)
C(18)	36(3)	23(2)	32(2)	7(2)	5(2)	4(2)
C(19)	33(3)	26(2)	38(3)	8(2)	6(2)	6(2)
C(20)	42(3)	23(2)	35(3)	-1(2)	12(2)	-1(2)
C(21)	12(2)	34(3)	46(3)	-8(2)	-1(2)	-4(2)

Table C.20. (continued)

C(22)	28(3)	41(3)	68(3)	-17(3)	18(3)	-5(2)
C(23)	24(3)	43(3)	60(3)	-20(3)	-13(2)	13(2)
C(24)	23(3)	36(3)	43(3)	0(2)	6(2)	-3(2)
C(25)	38(3)	46(3)	55(3)	7(3)	-1(3)	-15(3)
C(26)	28(3)	73(4)	47(3)	14(3)	9(2)	1(3)
C(27)	49(4)	66(4)	49(3)	4(3)	-1(3)	-9(3)
C(28)	68(4)	43(3)	74(4)	-19(3)	-11(3)	-6(3)
C(29)	43(3)	66(4)	44(3)	-5(3)	0(3)	-23(3)
C(30)	62(4)	39(3)	49(3)	-4(2)	12(3)	-2(3)
C(31)	35(3)	35(3)	65(3)	-6(3)	9(3)	2(2)
C(32)	37(3)	34(3)	48(3)	-10(2)	7(2)	1(2)
C(33)	67(4)	81(4)	44(3)	13(3)	-2(3)	33(3)
C(34)	48(3)	59(3)	54(3)	8(3)	-13(3)	12(3)
C(35)	68(4)	66(4)	61(4)	29(3)	-20(3)	-25(3)
C(36)	46(3)	54(3)	38(3)	2(2)	-1(2)	2(3)
C(37)	36(3)	50(3)	39(3)	9(2)	3(2)	-4(3)
C(38)	58(4)	65(4)	39(3)	12(3)	13(3)	22(3)
Zr(1A)	20(1)	29(1)	29(1)	-5(1)	0(1)	4(1)
Zr(2A)	18(1)	23(1)	39(1)	3(1)	0(1)	1(1)
Si(1A)	31(1)	38(1)	34(1)	-8(1)	-4(1)	-2(1)
Si(2A)	27(1)	36(1)	28(1)	-6(1)	2(1)	7(1)
Si(3A)	26(1)	27(1)	42(1)	3(1)	3(1)	-2(1)
Si(4A)	40(1)	35(1)	39(1)	7(1)	-2(1)	0(1)
N(1A)	31(2)	23(2)	33(2)	-2(2)	1(2)	2(2)
N(2A)	31(2)	33(2)	24(2)	2(2)	-2(2)	-3(2)
C(1A)	23(3)	45(3)	34(3)	-13(2)	-4(2)	12(2)
C(2A)	33(3)	26(2)	40(3)	-5(2)	0(2)	13(2)
C(3A)	35(3)	23(2)	40(3)	-5(2)	0(2)	3(2)
C(4A)	29(3)	30(2)	38(3)	-13(2)	2(2)	4(2)
C(5A)	25(3)	40(3)	33(2)	-16(2)	4(2)	1(2)
C(6A)	14(2)	41(3)	31(2)	-9(2)	-8(2)	5(2)
C(7A)	29(3)	37(3)	23(2)	-6(2)	-5(2)	5(2)
C(8A)	20(2)	35(3)	28(2)	-10(2)	-10(2)	1(2)

Table C.20. (continued)

C(9A)	23(3)	32(3)	31(2)	-4(2)	-3(2)	-5(2)
C(10A)	15(2)	44(3)	32(2)	-5(2)	0(2)	-3(2)
C(11A)	17(2)	25(2)	63(3)	15(2)	-3(2)	6(2)
C(12A)	24(3)	29(2)	43(3)	9(2)	9(2)	6(2)
C(13A)	24(3)	19(2)	45(3)	3(2)	3(2)	0(2)
C(14A)	24(3)	27(2)	38(3)	5(2)	1(2)	2(2)
C(15A)	28(3)	30(2)	40(3)	15(2)	-2(2)	3(2)
C(16A)	24(3)	22(2)	52(3)	5(2)	0(2)	-7(2)
C(17A)	28(3)	21(2)	57(3)	8(2)	6(2)	-2(2)
C(18A)	33(3)	21(2)	43(3)	3(2)	-1(2)	-3(2)
C(19A)	31(3)	21(2)	45(3)	4(2)	-5(2)	0(2)
C(20A)	32(3)	28(3)	44(3)	5(2)	1(2)	-6(2)
C(21A)	28(3)	54(3)	40(3)	-12(2)	-2(2)	18(3)
C(22A)	28(3)	78(4)	60(3)	-23(3)	6(3)	12(3)
C(23A)	62(4)	64(4)	65(4)	-26(3)	-22(3)	29(3)
C(24A)	17(3)	39(3)	67(3)	12(3)	-9(2)	-5(2)
C(25A)	36(3)	45(3)	103(5)	17(3)	-35(3)	-18(3)
C(26A)	18(3)	38(3)	123(5)	31(3)	11(3)	-3(2)
C(27A)	58(4)	54(3)	48(3)	-3(3)	0(3)	-14(3)
C(28A)	44(3)	56(3)	59(3)	-21(3)	-18(3)	10(3)
C(29A)	38(3)	49(3)	47(3)	-5(3)	-5(2)	1(3)
C(30A)	76(4)	48(3)	48(3)	-9(3)	19(3)	-2(3)
C(31A)	48(3)	63(4)	49(3)	-18(3)	1(3)	25(3)
C(32A)	29(3)	56(3)	53(3)	-20(3)	-2(2)	1(3)
C(33A)	40(3)	48(3)	54(3)	-2(3)	7(3)	-4(3)
C(34A)	45(3)	41(3)	64(3)	22(3)	9(3)	0(3)
C(35A)	31(3)	39(3)	46(3)	3(2)	-1(2)	-6(2)
C(36A)	57(4)	75(4)	56(4)	-13(3)	-2(3)	13(3)
C(37A)	40(3)	48(3)	49(3)	9(3)	-1(3)	0(3)
C(38A)	62(4)	51(3)	65(4)	23(3)	-19(3)	-10(3)

Table C.21. Hydrogen coordinates (x 10^4) and isotropic displacement parameters ($Å^2$x 10 ^{3}) for **[*rac*-4]$_2$N$_2$**.

	x	y	z	U(eq)
H(2A)	7035	4457	911	33
H(3A)	6539	3310	691	32
H(5A)	7007	5455	53	34
H(7A)	7045	7654	1060	33
H(9A)	6513	9529	423	33
H(10A)	6997	8345	188	35
H(12A)	5067	7038	1165	36
H(13A)	5338	8555	798	40
H(15A)	5171	4936	413	33
H(17A)	5408	4989	1508	37
H(19A)	6133	3143	1030	39
H(20A)	5575	2688	794	40
H(22A)	7729	7462	334	68
H(22B)	7439	6967	131	68
H(22C)	7702	5939	252	68
H(23A)	7727	6967	836	63
H(23B)	7702	5423	775	63
H(23C)	7438	6120	976	63
H(25A)	4663	3429	756	69
H(25B)	4876	2357	924	69
H(25C)	5028	3085	653	69
H(26A)	4560	4719	1172	74
H(26B)	4855	5242	1367	74
H(26C)	4760	3716	1369	74
H(27A)	6292	5449	-245	82
H(27B)	6261	4185	-445	82
H(27C)	6616	4742	-363	82
H(28A)	6594	1312	91	92
H(28B)	6815	2037	-142	92

Table C.21. (continued)

H(28C)	6460	1477	-226	92
H(29A)	5880	3990	232	76
H(29B)	6007	2591	341	76
H(29C)	5849	2724	32	76
H(30A)	6254	7822	1376	74
H(30B)	6249	9146	1559	74
H(30C)	6590	8407	1501	74
H(31A)	5912	9275	884	67
H(31B)	6068	10616	768	67
H(31C)	5904	10570	1076	67
H(32A)	6699	11693	1017	60
H(32B)	6876	10928	1272	60
H(32C)	6535	11669	1326	60
H(33A)	5490	5665	-91	96
H(33B)	5841	6182	14	96
H(33C)	5670	6831	-258	96
H(34A)	4890	7287	-26	80
H(34B)	5059	8492	-189	80
H(34C)	4906	8703	121	80
H(35A)	5893	8930	294	98
H(35B)	5565	9785	330	98
H(35C)	5721	9573	22	98
H(36A)	5997	6798	1753	69
H(36B)	6171	6095	2017	69
H(36C)	5802	5715	1932	69
H(37A)	6660	4340	1348	63
H(37B)	6745	5171	1627	63
H(37C)	6574	5873	1361	63
H(38A)	6302	2406	1711	81
H(38B)	6004	2865	1909	81
H(38C)	6374	3262	1989	81
H(2AA)	4553	-2759	1849	39
H(3AA)	4085	-2585	1482	39

Table C.21. (continued)

H(5AA)	4881	-354	1189	39
H(7AA)	4747	-351	2293	36
H(9AA)	4607	3185	1855	34
H(10B)	5041	1795	1587	36
H(12B)	2858	2189	2045	39
H(13B)	3371	3544	1928	35
H(15B)	3086	1594	1193	39
H(17B)	2861	-681	2178	43
H(19B)	3548	-2622	1678	39
H(20B)	3116	-1624	1347	42
H(22D)	5591	-299	1714	83
H(22E)	5356	87	1455	83
H(22F)	5485	-1392	1488	83
H(23D)	5383	-1675	2107	95
H(23E)	5263	-2798	1893	95
H(23F)	5008	-2152	2110	95
H(25D)	2383	-829	1331	92
H(25E)	2710	-234	1192	92
H(25F)	2398	693	1246	92
H(26D)	2228	-300	1819	89
H(26E)	2241	1251	1763	89
H(26F)	2455	620	2013	89
H(27D)	4338	1016	770	80
H(27E)	4286	172	487	80
H(27F)	4622	47	661	80
H(28D)	4204	-3496	809	79
H(28E)	4536	-2864	687	79
H(28F)	4200	-2734	512	79
H(29D)	3699	-194	1032	67
H(29E)	3664	-1760	1043	67
H(29F)	3644	-1008	745	67
H(30D)	4049	1002	2816	86
H(30E)	4371	214	2720	86

Table C.21. (continued)

H(30F)	4045	152	2530	86
H(31D)	3852	3504	2495	80
H(31E)	3833	2680	2207	80
H(31F)	4064	3952	2226	80
H(32D)	4468	3541	2841	69
H(32E)	4677	3949	2567	69
H(32F)	4780	2681	2748	69
H(33D)	3999	2115	1127	71
H(33E)	4032	3422	940	71
H(33F)	3722	2471	899	71
H(34D)	3288	5627	1273	75
H(34E)	3258	4737	994	75
H(34F)	3565	5705	1032	75
H(35D)	4057	3799	1672	58
H(35E)	3810	5004	1718	58
H(35F)	4090	5090	1480	58
H(36D)	3162	-1105	2674	94
H(36E)	3504	-386	2608	94
H(36F)	3493	-1597	2824	94
H(37D)	4035	-1870	2252	69
H(37E)	3953	-3307	2134	69
H(37F)	4018	-3094	2465	69
H(38D)	3028	-3844	2465	89
H(38E)	3360	-4391	2604	89
H(38F)	3290	-4609	2273	89

Table C.22. Crystal data and structure refinement for **[*meso*-3]$_2$N$_2$** (Chapter 4).

Identification code	**[*meso*-3]$_2$N$_2$**	
Empirical formula	C40 H60 N2 Si2 Zr2	
Formula weight	807.52	
Temperature	173(2) K	
Wavelength	0.71073 Å	
Crystal system	Triclinic	
Space group	P-1	
Unit cell dimensions	a = 9.8845(15) Å	α=105.559(5)°.
	b = 13.1037(19) Å	β= 90.465(5)°.
	c = 17.466(2) Å	γ =110.485(5)°.
Volume	2028.4(5) Å^3	
Z	2	
Density (calculated)	1.322 Mg/m^3	
Absorption coefficient	0.601 mm^{-1}	
F(000)	844	
Crystal size	0.20 x 0.10 x 0.03 mm^3	
Theta range for data collection	1.73 to 24.71°.	
Index ranges	-8<=h<=11, -15<=k<=14, -19<=l<=20	
Reflections collected	24661	
Independent reflections	6668 [R(int) = 0.1033]	
Completeness to theta = 24.71°	96.3 %	
Absorption correction	Semi-empirical from equivalents	
Max. and min. transmission	0.9851 and 0.8892	
Refinement method	Full-matrix least-squares on F^2	
Data / restraints / parameters	6668 / 0 / 431	
Goodness-of-fit on F^2	0.940	
Final R indices [I>2sigma(I)]	R1 = 0.0532, wR2 = 0.1050	
R indices (all data)	R1 = 0.1232, wR2 = 0.1287	
Largest diff. peak and hole	0.727 and -0.668 e.Å^{-3}	

Table C.23. Atomic coordinates (x 10^4) and equivalent isotropic displacement parameters ($Å^2$x 10^3) for **[*meso*-3]$_2$N$_2$**. U(eq) is defined as one third of the trace of the orthogonalized U^{ij} tensor.

	x	y	z	U(eq)
Zr(1)	5993(1)	3775(1)	1737(1)	22(1)
Zr(2)	5648(1)	6552(1)	3095(1)	23(1)
Si(1)	7104(1)	2625(1)	57(1)	30(1)
Si(2)	3225(1)	7754(1)	3549(1)	31(1)
N(1)	6645(4)	5452(3)	2479(2)	25(1)
N(2)	5270(4)	4824(3)	2631(2)	25(1)
C(1)	7796(5)	2929(4)	1120(3)	27(1)
C(2)	8580(5)	4027(4)	1658(3)	29(1)
C(3)	8360(4)	3967(4)	2449(3)	27(1)
C(4)	7410(5)	2872(4)	2426(3)	27(1)
C(5)	7066(5)	2250(4)	1601(3)	28(1)
C(6)	5392(5)	2906(4)	261(3)	27(1)
C(7)	5246(5)	3988(4)	454(3)	26(1)
C(8)	4030(5)	3935(4)	856(2)	27(1)
C(9)	3387(5)	2846(4)	957(2)	24(1)
C(10)	4244(5)	2226(4)	588(3)	27(1)
C(11)	4405(5)	7738(3)	2724(3)	25(1)
C(12)	5901(5)	8401(4)	2789(3)	29(1)
C(13)	6586(5)	7889(4)	2177(3)	27(1)
C(14)	5492(5)	6864(4)	1724(3)	28(1)
C(15)	4168(5)	6751(4)	2053(3)	30(1)
C(16)	4158(5)	7176(4)	4164(3)	30(1)
C(17)	5635(5)	7775(4)	4494(2)	26(1)
C(18)	6268(5)	7003(4)	4621(2)	25(1)
C(19)	5183(5)	5904(4)	4359(2)	31(1)
C(20)	3896(5)	6019(4)	4058(2)	29(1)
C(21)	6726(6)	1132(4)	-522(3)	53(2)
C(22)	8364(5)	3640(4)	-408(3)	42(2)
C(23)	6999(5)	2417(4)	3134(3)	37(1)

Table C.23. (continued)

C(24)	6724(7)	3288(5)	3821(3)	70(2)
C(25)	8226(6)	2112(5)	3407(3)	55(2)
C(26)	5641(6)	1341(5)	2902(3)	60(2)
C(27)	1993(5)	2400(4)	1334(3)	28(1)
C(28)	751(5)	1732(4)	660(3)	42(2)
C(29)	1648(5)	3379(4)	1881(3)	43(2)
C(30)	2135(5)	1630(4)	1821(3)	46(2)
C(31)	1345(5)	6758(5)	3172(3)	50(2)
C(32)	3301(6)	9207(4)	4095(3)	46(2)
C(33)	8134(5)	8377(4)	1979(3)	34(1)
C(34)	8137(6)	9165(4)	1468(3)	48(2)
C(35)	9200(5)	9063(5)	2724(3)	47(2)
C(36)	8612(6)	7437(5)	1475(4)	65(2)
C(37)	7759(5)	7331(4)	5058(3)	32(1)
C(38)	8843(6)	8363(4)	4896(3)	50(2)
C(39)	7629(6)	7583(5)	5952(3)	46(2)
C(40)	8303(5)	6337(4)	4810(3)	45(2)

Table C.24. Bond lengths [Å] and angles [°] for **[*meso*-3]$_2$N$_2$**.

Zr(1)-N(1)	2.095(3)	C(8)-C(9)	1.405(6)
Zr(1)-N(2)	2.096(3)	C(9)-C(10)	1.415(6)
Zr(1)-C(7)	2.468(5)	C(9)-C(27)	1.526(6)
Zr(1)-C(2)	2.471(4)	C(11)-C(12)	1.414(6)
Zr(1)-C(6)	2.494(4)	C(11)-C(15)	1.440(6)
Zr(1)-C(1)	2.518(4)	C(12)-C(13)	1.413(6)
Zr(1)-C(5)	2.532(5)	C(13)-C(14)	1.413(6)
Zr(1)-C(10)	2.538(4)	C(13)-C(33)	1.521(6)
Zr(1)-C(3)	2.542(4)	C(14)-C(15)	1.410(6)
Zr(1)-C(8)	2.565(5)	C(16)-C(20)	1.405(6)
Zr(1)-C(4)	2.590(5)	C(16)-C(17)	1.421(6)
Zr(1)-C(9)	2.613(4)	C(17)-C(18)	1.423(7)
Zr(2)-N(2)	2.083(3)	C(18)-C(19)	1.411(6)
Zr(2)-N(1)	2.094(4)	C(18)-C(37)	1.517(6)
Zr(2)-C(15)	2.450(5)	C(19)-C(20)	1.442(7)
Zr(2)-C(20)	2.479(4)	C(23)-C(25)	1.513(7)
Zr(2)-C(11)	2.492(5)	C(23)-C(26)	1.521(7)
Zr(2)-C(16)	2.527(4)	C(23)-C(24)	1.517(7)
Zr(2)-C(17)	2.540(4)	C(27)-C(28)	1.527(6)
Zr(2)-C(14)	2.548(5)	C(27)-C(30)	1.524(7)
Zr(2)-C(12)	2.549(5)	C(27)-C(29)	1.526(6)
Zr(2)-C(19)	2.559(5)	C(33)-C(35)	1.517(6)
Zr(2)-C(18)	2.588(4)	C(33)-C(36)	1.533(7)
Zr(2)-C(13)	2.627(5)	C(33)-C(34)	1.534(7)
Si(1)-C(21)	1.847(5)	C(37)-C(38)	1.501(7)
Si(1)-C(22)	1.848(5)	C(37)-C(39)	1.524(6)
Si(1)-C(1)	1.862(5)	C(37)-C(40)	1.538(7)
Si(1)-C(6)	1.871(5)		
Si(2)-C(31)	1.847(5)	N(1)-Zr(1)-N(2)	38.76(13)
Si(2)-C(11)	1.861(5)	N(1)-Zr(1)-C(7)	101.38(14)
Si(2)-C(32)	1.862(5)	N(2)-Zr(1)-C(7)	106.37(15)
Si(2)-C(16)	1.868(5)	N(1)-Zr(1)-C(2)	88.95(14)
N(1)-N(2)	1.390(5)	N(2)-Zr(1)-C(2)	123.46(13)
C(1)-C(5)	1.407(6)	C(7)-Zr(1)-C(2)	103.24(16)
C(1)-C(2)	1.428(6)	N(1)-Zr(1)-C(6)	133.23(15)
C(2)-C(3)	1.419(7)	N(2)-Zr(1)-C(6)	135.79(15)
C(3)-C(4)	1.403(6)	C(7)-Zr(1)-C(6)	33.40(15)
C(4)-C(5)	1.422(6)	C(2)-Zr(1)-C(6)	91.98(15)
C(4)-C(23)	1.512(7)	N(1)-Zr(1)-C(1)	122.02(13)
C(6)-C(10)	1.408(6)	N(2)-Zr(1)-C(1)	154.97(13)
C(6)-C(7)	1.426(6)	C(7)-Zr(1)-C(1)	92.13(15)
C(7)-C(8)	1.387(6)	C(2)-Zr(1)-C(1)	33.24(13)

Table C.24. (continued)

C(6)-Zr(1)-C(1)	67.54(15)	C(7)-Zr(1)-C(9)	53.21(14)
N(1)-Zr(1)-C(5)	132.08(14)	C(2)-Zr(1)-C(9)	145.35(14)
N(2)-Zr(1)-C(5)	138.52(15)	C(6)-Zr(1)-C(9)	54.03(14)
C(7)-Zr(1)-C(5)	114.52(15)	C(1)-Zr(1)-C(9)	114.91(13)
C(2)-Zr(1)-C(5)	53.70(15)	C(5)-Zr(1)-C(9)	108.72(14)
C(6)-Zr(1)-C(5)	82.41(15)	C(10)-Zr(1)-C(9)	31.85(14)
C(1)-Zr(1)-C(5)	32.36(15)	C(3)-Zr(1)-C(9)	160.28(14)
N(1)-Zr(1)-C(10)	147.26(15)	C(8)-Zr(1)-C(9)	31.47(14)
N(2)-Zr(1)-C(10)	121.34(14)	C(4)-Zr(1)-C(9)	129.14(14)
C(7)-Zr(1)-C(10)	53.38(15)	N(2)-Zr(2)-N(1)	38.88(13)
C(2)-Zr(1)-C(10)	115.05(14)	N(2)-Zr(2)-C(15)	98.52(14)
C(6)-Zr(1)-C(10)	32.48(14)	N(1)-Zr(2)-C(15)	104.82(14)
C(1)-Zr(1)-C(10)	83.17(14)	N(2)-Zr(2)-C(20)	87.07(15)
C(5)-Zr(1)-C(10)	80.55(15)	N(1)-Zr(2)-C(20)	121.62(15)
N(1)-Zr(1)-C(3)	79.56(14)	C(15)-Zr(2)-C(20)	103.09(16)
N(2)-Zr(1)-C(3)	101.18(14)	N(2)-Zr(2)-C(11)	130.48(13)
C(7)-Zr(1)-C(3)	135.82(15)	N(1)-Zr(2)-C(11)	135.41(14)
C(2)-Zr(1)-C(3)	32.85(15)	C(15)-Zr(2)-C(11)	33.86(13)
C(6)-Zr(1)-C(3)	121.23(15)	C(20)-Zr(2)-C(11)	92.06(16)
C(1)-Zr(1)-C(3)	54.14(14)	N(2)-Zr(2)-C(16)	119.18(14)
C(5)-Zr(1)-C(3)	52.63(13)	N(1)-Zr(2)-C(16)	153.41(16)
C(10)-Zr(1)-C(3)	132.62(14)	C(15)-Zr(2)-C(16)	91.93(16)
N(1)-Zr(1)-C(8)	95.11(14)	C(20)-Zr(2)-C(16)	32.58(15)
N(2)-Zr(1)-C(8)	81.97(14)	C(11)-Zr(2)-C(16)	67.61(16)
C(7)-Zr(1)-C(8)	31.91(14)	N(2)-Zr(2)-C(17)	132.38(15)
C(2)-Zr(1)-C(8)	134.83(15)	N(1)-Zr(2)-C(17)	140.85(15)
C(6)-Zr(1)-C(8)	53.85(15)	C(15)-Zr(2)-C(17)	114.17(15)
C(1)-Zr(1)-C(8)	120.79(14)	C(20)-Zr(2)-C(17)	53.47(14)
C(5)-Zr(1)-C(8)	132.01(13)	C(11)-Zr(2)-C(17)	81.77(15)
C(10)-Zr(1)-C(8)	52.25(14)	C(16)-Zr(2)-C(17)	32.58(14)
C(3)-Zr(1)-C(8)	165.71(15)	N(2)-Zr(2)-C(14)	93.97(14)
N(1)-Zr(1)-C(4)	103.50(14)	N(1)-Zr(2)-C(14)	81.07(15)
N(2)-Zr(1)-C(4)	108.00(14)	C(15)-Zr(2)-C(14)	32.69(15)
C(7)-Zr(1)-C(4)	145.51(14)	C(20)-Zr(2)-C(14)	135.45(15)
C(2)-Zr(1)-C(4)	54.14(15)	C(11)-Zr(2)-C(14)	54.56(15)
C(6)-Zr(1)-C(4)	114.57(15)	C(16)-Zr(2)-C(14)	121.44(16)
C(1)-Zr(1)-C(4)	54.29(15)	C(17)-Zr(2)-C(14)	132.12(15)
C(5)-Zr(1)-C(4)	32.21(13)	N(2)-Zr(2)-C(12)	146.51(14)
C(10)-Zr(1)-C(4)	108.58(14)	N(1)-Zr(2)-C(12)	122.67(14)
C(3)-Zr(1)-C(4)	31.71(13)	C(15)-Zr(2)-C(12)	53.91(14)
C(8)-Zr(1)-C(4)	159.93(13)	C(20)-Zr(2)-C(12)	115.30(15)
N(1)-Zr(1)-C(9)	118.19(14)	C(11)-Zr(2)-C(12)	32.55(14)
N(2)-Zr(1)-C(9)	89.90(13)	C(16)-Zr(2)-C(12)	83.88(15)

Table C.24. (continued)

C(17)-Zr(2)-C(12)	80.38(15)	C(11)-Si(2)-C(16)	97.0(2)
C(14)-Zr(2)-C(12)	52.54(13)	C(32)-Si(2)-C(16)	112.0(2)
N(2)-Zr(2)-C(19)	79.33(14)	N(2)-N(1)-Zr(2)	70.1(2)
N(1)-Zr(2)-C(19)	100.30(15)	N(2)-N(1)-Zr(1)	70.65(19)
C(15)-Zr(2)-C(19)	135.98(16)	Zr(2)-N(1)-Zr(1)	137.38(17)
C(20)-Zr(2)-C(19)	33.23(15)	N(1)-N(2)-Zr(2)	71.0(2)
C(11)-Zr(2)-C(19)	121.66(15)	N(1)-N(2)-Zr(1)	70.6(2)
C(16)-Zr(2)-C(19)	54.36(16)	Zr(2)-N(2)-Zr(1)	138.11(19)
C(17)-Zr(2)-C(19)	53.06(15)	C(5)-C(1)-C(2)	105.8(4)
C(14)-Zr(2)-C(19)	166.31(14)	C(5)-C(1)-Si(1)	121.9(3)
C(12)-Zr(2)-C(19)	133.03(14)	C(2)-C(1)-Si(1)	126.0(4)
N(2)-Zr(2)-C(18)	105.13(15)	C(5)-C(1)-Zr(1)	74.4(3)
N(1)-Zr(2)-C(18)	109.69(15)	C(2)-C(1)-Zr(1)	71.6(2)
C(15)-Zr(2)-C(18)	145.15(15)	Si(1)-C(1)-Zr(1)	96.85(19)
C(20)-Zr(2)-C(18)	53.95(14)	C(3)-C(2)-C(1)	108.0(4)
C(11)-Zr(2)-C(18)	113.94(14)	C(3)-C(2)-Zr(1)	76.3(2)
C(16)-Zr(2)-C(18)	54.22(15)	C(1)-C(2)-Zr(1)	75.2(2)
C(17)-Zr(2)-C(18)	32.21(15)	C(4)-C(3)-C(2)	109.6(4)
C(14)-Zr(2)-C(18)	159.76(14)	C(4)-C(3)-Zr(1)	76.1(3)
C(12)-Zr(2)-C(18)	108.20(14)	C(2)-C(3)-Zr(1)	70.8(2)
C(19)-Zr(2)-C(18)	31.82(13)	C(3)-C(4)-C(5)	105.6(4)
N(2)-Zr(2)-C(13)	118.84(14)	C(3)-C(4)-C(23)	126.6(4)
N(1)-Zr(2)-C(13)	91.20(15)	C(5)-C(4)-C(23)	127.4(4)
C(15)-Zr(2)-C(13)	53.82(15)	C(3)-C(4)-Zr(1)	72.2(3)
C(20)-Zr(2)-C(13)	145.48(16)	C(5)-C(4)-Zr(1)	71.7(3)
C(11)-Zr(2)-C(13)	54.12(15)	C(23)-C(4)-Zr(1)	126.4(3)
C(16)-Zr(2)-C(13)	115.39(15)	C(1)-C(5)-C(4)	111.0(4)
C(17)-Zr(2)-C(13)	108.46(14)	C(1)-C(5)-Zr(1)	73.3(3)
C(14)-Zr(2)-C(13)	31.65(13)	C(4)-C(5)-Zr(1)	76.1(3)
C(12)-Zr(2)-C(13)	31.65(14)	C(10)-C(6)-C(7)	105.1(4)
C(19)-Zr(2)-C(13)	160.13(13)	C(10)-C(6)-Si(1)	123.5(4)
C(18)-Zr(2)-C(13)	128.68(13)	C(7)-C(6)-Si(1)	126.3(3)
C(21)-Si(1)-C(22)	112.0(2)	C(10)-C(6)-Zr(1)	75.5(2)
C(21)-Si(1)-C(1)	112.2(2)	C(7)-C(6)-Zr(1)	72.3(2)
C(22)-Si(1)-C(1)	110.6(2)	Si(1)-C(6)-Zr(1)	97.45(18)
C(21)-Si(1)-C(6)	111.8(2)	C(8)-C(7)-C(6)	109.1(4)
C(22)-Si(1)-C(6)	112.9(2)	C(8)-C(7)-Zr(1)	77.9(3)
C(1)-Si(1)-C(6)	96.5(2)	C(6)-C(7)-Zr(1)	74.3(3)
C(31)-Si(2)-C(11)	110.4(2)	C(7)-C(8)-C(9)	109.5(4)
C(31)-Si(2)-C(32)	112.1(3)	C(7)-C(8)-Zr(1)	70.2(3)
C(11)-Si(2)-C(32)	113.3(2)	C(9)-C(8)-Zr(1)	76.1(3)
C(31)-Si(2)-C(16)	111.1(2)	C(8)-C(9)-C(10)	105.6(4)

Table C.24. (continued)

C(8)-C(9)-C(27)	127.0(4)	C(18)-C(17)-Zr(2)	75.7(2)
C(10)-C(9)-C(27)	127.2(4)	C(19)-C(18)-C(17)	107.0(4)
C(8)-C(9)-Zr(1)	72.4(2)	C(19)-C(18)-C(37)	126.9(4)
C(10)-C(9)-Zr(1)	71.2(2)	C(17)-C(18)-C(37)	125.7(4)
C(27)-C(9)-Zr(1)	124.4(3)	C(19)-C(18)-Zr(2)	73.0(2)
C(6)-C(10)-C(9)	110.7(4)	C(17)-C(18)-Zr(2)	72.1(2)
C(6)-C(10)-Zr(1)	72.0(2)	C(37)-C(18)-Zr(2)	126.4(3)
C(9)-C(10)-Zr(1)	77.0(2)	C(18)-C(19)-C(20)	107.4(4)
C(12)-C(11)-C(15)	105.3(4)	C(18)-C(19)-Zr(2)	75.2(3)
C(12)-C(11)-Si(2)	126.2(3)	C(20)-C(19)-Zr(2)	70.3(3)
C(15)-C(11)-Si(2)	123.3(3)	C(16)-C(20)-C(19)	109.4(4)
C(12)-C(11)-Zr(2)	75.9(3)	C(16)-C(20)-Zr(2)	75.6(3)
C(15)-C(11)-Zr(2)	71.5(3)	C(19)-C(20)-Zr(2)	76.5(3)
Si(2)-C(11)-Zr(2)	97.3(2)	C(25)-C(23)-C(4)	108.6(4)
C(13)-C(12)-C(11)	111.1(4)	C(25)-C(23)-C(26)	107.8(5)
C(13)-C(12)-Zr(2)	77.2(3)	C(4)-C(23)-C(26)	110.8(4)
C(11)-C(12)-Zr(2)	71.5(3)	C(25)-C(23)-C(24)	109.5(4)
C(12)-C(13)-C(14)	105.9(4)	C(4)-C(23)-C(24)	111.4(4)
C(12)-C(13)-C(33)	127.9(4)	C(26)-C(23)-C(24)	108.7(5)
C(14)-C(13)-C(33)	125.9(4)	C(28)-C(27)-C(9)	108.0(4)
C(12)-C(13)-Zr(2)	71.1(3)	C(28)-C(27)-C(30)	109.8(4)
C(14)-C(13)-Zr(2)	71.1(3)	C(9)-C(27)-C(30)	110.6(4)
C(33)-C(13)-Zr(2)	127.1(3)	C(28)-C(27)-C(29)	108.7(4)
C(15)-C(14)-C(13)	109.4(4)	C(9)-C(27)-C(29)	111.0(4)
C(15)-C(14)-Zr(2)	69.8(3)	C(30)-C(27)-C(29)	108.8(4)
C(13)-C(14)-Zr(2)	77.2(3)	C(35)-C(33)-C(13)	112.1(4)
C(14)-C(15)-C(11)	108.3(4)	C(35)-C(33)-C(36)	110.2(5)
C(14)-C(15)-Zr(2)	77.5(3)	C(13)-C(33)-C(36)	111.2(4)
C(11)-C(15)-Zr(2)	74.6(3)	C(35)-C(33)-C(34)	108.8(4)
C(20)-C(16)-C(17)	106.1(4)	C(13)-C(33)-C(34)	106.9(4)
C(20)-C(16)-Si(2)	125.8(3)	C(36)-C(33)-C(34)	107.4(4)
C(17)-C(16)-Si(2)	121.3(4)	C(38)-C(37)-C(18)	111.6(4)
C(20)-C(16)-Zr(2)	71.8(2)	C(38)-C(37)-C(39)	109.2(4)
C(17)-C(16)-Zr(2)	74.2(3)	C(18)-C(37)-C(39)	108.4(4)
Si(2)-C(16)-Zr(2)	95.91(19)	C(38)-C(37)-C(40)	109.4(4)
C(16)-C(17)-C(18)	110.1(4)	C(18)-C(37)-C(40)	110.4(4)
C(16)-C(17)-Zr(2)	73.2(2)	C(39)-C(37)-C(40)	107.8(4)

Symmetry transformations used to generate equivalent atoms:

Table C.25. Anisotropic displacement parameters ($Å^2 x\ 10^3$) for **[*meso*-3]$_2$N$_2$**. The anisotropic displacement factor exponent takes the form: $-2\pi^2[\ h^2\ a^{*2}U^{11} + ... + 2\ h\ k\ a^*\ b^*\ U^{12}\ ]$

	U^{11}	U^{22}	U^{33}	U^{23}	U^{13}	U^{12}
Zr(1)	20(1)	27(1)	21(1)	6(1)	1(1)	11(1)
Zr(2)	26(1)	27(1)	19(1)	6(1)	3(1)	12(1)
Si(1)	25(1)	40(1)	26(1)	6(1)	6(1)	17(1)
Si(2)	28(1)	35(1)	33(1)	7(1)	6(1)	15(1)
N(1)	19(2)	30(2)	26(2)	10(2)	2(2)	8(2)
N(2)	21(2)	32(2)	26(2)	11(2)	0(2)	11(2)
C(1)	25(2)	34(2)	28(3)	10(2)	4(2)	17(2)
C(2)	15(2)	42(3)	36(3)	18(2)	9(2)	13(2)
C(3)	22(2)	40(3)	25(3)	10(2)	0(2)	18(2)
C(4)	27(2)	30(2)	29(3)	6(2)	0(2)	17(2)
C(5)	33(2)	27(2)	33(3)	10(2)	5(2)	19(2)
C(6)	28(2)	33(2)	15(2)	2(2)	-1(2)	8(2)
C(7)	26(2)	30(2)	18(2)	7(2)	-3(2)	6(2)
C(8)	30(2)	34(2)	22(3)	6(2)	-2(2)	19(2)
C(9)	21(2)	28(2)	18(2)	6(2)	-3(2)	5(2)
C(10)	21(2)	25(2)	29(3)	0(2)	0(2)	9(2)
C(11)	28(2)	30(2)	23(3)	10(2)	3(2)	15(2)
C(12)	33(2)	33(2)	27(3)	8(2)	4(2)	20(2)
C(13)	33(3)	32(2)	24(3)	17(2)	7(2)	13(2)
C(14)	44(3)	28(2)	16(2)	10(2)	1(2)	18(2)
C(15)	32(3)	39(3)	23(3)	10(2)	-5(2)	19(2)
C(16)	33(3)	31(3)	18(3)	3(2)	9(2)	8(2)
C(17)	36(3)	30(2)	14(2)	3(2)	3(2)	18(2)
C(18)	31(2)	36(3)	7(2)	5(2)	10(2)	12(2)
C(19)	47(3)	40(3)	13(2)	13(2)	10(2)	20(2)
C(20)	24(2)	46(3)	18(2)	15(2)	9(2)	11(2)
C(21)	58(3)	57(3)	48(4)	7(3)	17(3)	33(3)
C(22)	30(3)	60(3)	35(3)	16(3)	7(2)	13(2)
C(23)	51(3)	44(3)	28(3)	12(2)	5(2)	29(2)

Table C.25. (continued)

C(24)	124(5)	67(4)	45(4)	26(3)	46(4)	58(3)
C(25)	57(3)	67(3)	54(4)	31(3)	-9(3)	28(3)
C(26)	54(4)	76(4)	59(4)	45(3)	12(3)	16(3)
C(27)	22(2)	33(2)	28(3)	3(2)	-2(2)	14(2)
C(28)	23(3)	62(3)	35(3)	16(3)	5(2)	7(2)
C(29)	23(2)	51(3)	48(3)	0(3)	7(2)	15(2)
C(30)	39(3)	60(3)	50(3)	19(3)	13(3)	29(2)
C(31)	33(3)	65(3)	50(4)	13(3)	9(3)	17(3)
C(32)	43(3)	51(3)	49(3)	15(3)	11(3)	21(2)
C(33)	38(3)	39(3)	28(3)	15(2)	11(2)	14(2)
C(34)	44(3)	47(3)	47(3)	20(3)	3(3)	5(3)
C(35)	35(3)	71(4)	38(3)	28(3)	10(2)	14(3)
C(36)	58(4)	64(4)	79(4)	26(3)	44(3)	24(3)
C(37)	34(3)	44(3)	18(3)	6(2)	2(2)	17(2)
C(38)	41(3)	53(3)	50(4)	16(3)	-6(3)	9(3)
C(39)	43(3)	74(4)	23(3)	9(3)	-3(2)	26(3)
C(40)	43(3)	60(3)	34(3)	9(3)	-3(2)	26(3)

Table C.26. Hydrogen coordinates (x 10^4) and isotropic displacement parameters ($Å^2$x 10 ^{3}) for **[*meso*-3]$_2$N$_2$**.

	x	y	z	U(eq)
H(2A)	9329	4668	1513	35
H(3A)	8891	4581	2947	32
H(5A)	6494	1414	1396	34
H(7A)	5793	4622	230	31
H(8A)	3614	4547	998	32
H(10A)	3989	1392	504	32
H(12A)	6382	9175	3174	34
H(14A)	5610	6351	1211	33
H(15A)	3194	6183	1789	36
H(17A)	6113	8623	4684	31
H(19A)	5251	5194	4436	38
H(20A)	2916	5396	3911	34
H(21A)	6306	996	-1067	79
H(21B)	6038	622	-264	79
H(21C)	7633	985	-543	79
H(22A)	8083	3386	-987	63
H(22B)	9357	3675	-302	63
H(22C)	8320	4396	-183	63
H(24A)	7615	3965	4002	105
H(24B)	6433	2960	4264	105
H(24C)	5947	3501	3640	105
H(25A)	8363	1514	2974	83
H(25B)	7987	1837	3876	83
H(25C)	9124	2787	3546	83
H(26A)	4864	1488	2652	90
H(26B)	5328	1111	3381	90
H(26C)	5855	730	2523	90
H(28A)	675	2228	343	63
H(28B)	-163	1455	888	63

Table C.26. (continued)

H(28C)	943	1083	315	63
H(29A)	2443	3821	2313	65
H(29B)	743	3073	2109	65
H(29C)	1534	3873	1571	65
H(30A)	2388	1011	1480	69
H(30B)	1210	1309	2027	69
H(30C)	2899	2073	2270	69
H(31A)	938	7013	2778	76
H(31B)	752	6739	3619	76
H(31C)	1348	5995	2921	76
H(32A)	2850	9497	3743	69
H(32B)	4317	9715	4264	69
H(32C)	2775	9175	4567	69
H(34A)	7403	8743	1003	72
H(34B)	9098	9443	1286	72
H(34C)	7913	9812	1789	72
H(35A)	8868	9646	3049	71
H(35B)	10162	9430	2570	71
H(35C)	9260	8556	3036	71
H(36A)	8524	6873	1763	98
H(36B)	9626	7769	1377	98
H(36C)	7992	7066	963	98
H(38A)	8887	8221	4318	75
H(38B)	9803	8527	5162	75
H(38C)	8545	9016	5101	75
H(39A)	7299	8223	6128	69
H(39B)	8578	7776	6243	69
H(39C)	6925	6909	6061	69
H(40A)	7609	5668	4929	67
H(40B)	9253	6553	5109	67
H(40C)	8395	6157	4236	67

Table C.27. Crystal data and structure refinement for **1-(Ofluorenyl)$_2$** (Chapter 3).

Identification code	**1-(Ofluorenyl)$_2$**	
Empirical formula	C56 H54 O2 Zr	
Formula weight	850.21	
Temperature	173(2) K	
Wavelength	0.71073 Å	
Crystal system	Tetragonal	
Space group	I4(1)/a	
Unit cell dimensions	a = 28.9514(15) Å	α= 90°.
	b = 28.9514(15) Å	β= 90°.
	c = 27.6145(17) Å	γ = 90°.
Volume	23146(2) Å^3	
Z	16	
Density (calculated)	0.976 Mg/m^3	
Absorption coefficient	0.222 mm^{-1}	
F(000)	7136	
Crystal size	0.15 x 0.10 x 0.10 mm^3	
Theta range for data collection	1.74 to 21.96°.	
Index ranges	-30<=h<=26, -30<=k<=20, -24<=l<=29	
Reflections collected	28230	
Independent reflections	7046 [R(int) = 0.0969]	
Completeness to theta = 21.96°	100.0 %	
Absorption correction	Semi-empirical from equivalents	
Max. and min. transmission	0.9781 and 0.9674	
Refinement method	Full-matrix least-squares on F^2	
Data / restraints / parameters	7046 / 0 / 532	
Goodness-of-fit on F^2	0.998	
Final R indices [I>2sigma(I)]	R1 = 0.0500, wR2 = 0.0995	
R indices (all data)	R1 = 0.0863, wR2 = 0.1074	
Largest diff. peak and hole	0.276 and -0.267 e.Å^{-3}	

Table C.27. Atomic coordinates (x 10^4) and equivalent isotropic displacement parameters ($Å^2$x 10^3) for **1-(Ofluorenyl)$_2$**. U(eq) is defined as one third of the trace of the orthogonalized U^{ij} tensor.

	x	y	z	U(eq)
Zr(1)	2183(1)	8050(1)	53(1)	31(1)
O(1)	2853(1)	7958(1)	-114(1)	38(1)
O(2)	2043(1)	8012(1)	-625(1)	32(1)
C(1)	1745(1)	6869(1)	-316(1)	42(1)
C(2)	2075(1)	6593(1)	-514(2)	50(1)
C(3)	2536(2)	6605(1)	-340(2)	55(1)
C(4)	2659(1)	6880(1)	39(1)	46(1)
C(5)	2322(1)	7149(1)	271(1)	35(1)
C(6)	1860(1)	7165(1)	78(1)	38(1)
C(7)	1591(1)	7473(1)	371(1)	39(1)
C(8)	1880(1)	7599(1)	768(1)	39(1)
C(9)	2329(1)	7424(1)	706(1)	39(1)
C(10)	2321(1)	8592(1)	1247(1)	41(1)
C(11)	1972(1)	8522(1)	1570(1)	41(1)
C(12)	1499(1)	8536(1)	1426(1)	40(1)
C(13)	1385(1)	8607(1)	956(1)	37(1)
C(14)	1729(1)	8678(1)	606(1)	31(1)
C(15)	2208(1)	8682(1)	754(1)	31(1)
C(16)	2475(1)	8833(1)	355(1)	34(1)
C(17)	2165(1)	8913(1)	-36(1)	32(1)
C(18)	1709(1)	8805(1)	108(1)	30(1)
C(19)	1069(1)	7579(1)	364(1)	42(1)
C(20)	802(1)	7200(1)	640(2)	55(1)
C(21)	875(1)	7637(1)	-148(2)	56(1)
C(22)	2703(1)	7432(1)	1097(1)	47(1)
C(23)	2762(2)	6942(1)	1316(2)	69(2)
C(24)	3174(1)	7624(1)	943(2)	59(1)
C(25)	3109(1)	7851(1)	-499(1)	34(1)
C(26)	2989(1)	7713(1)	-959(1)	33(1)

Table C.27. (continued)

C(27)	3415(1)	7660(1)	-1240(1)	37(1)
C(28)	3802(1)	7773(1)	-926(2)	40(1)
C(29)	3623(1)	7894(1)	-471(1)	37(1)
C(30)	2147(1)	7976(1)	-1131(1)	33(1)
C(31)	2281(1)	8441(1)	-1354(1)	33(1)
C(32)	1986(1)	8550(1)	-1736(1)	35(1)
C(33)	1638(1)	8181(1)	-1785(1)	35(1)
C(34)	1718(1)	7856(1)	-1422(1)	33(1)
C(35)	2985(1)	8970(1)	397(1)	45(1)
C(36)	3019(1)	9406(1)	727(2)	66(2)
C(37)	3225(1)	9064(1)	-76(1)	48(1)
C(38)	1268(1)	8898(1)	-176(1)	33(1)
C(39)	1054(1)	9355(1)	-4(1)	52(1)
C(40)	1327(1)	8898(1)	-721(1)	40(1)
C(41)	3907(1)	8020(1)	-87(2)	45(1)
C(42)	4386(1)	8029(1)	-178(2)	59(1)
C(43)	4561(1)	7916(1)	-629(2)	61(1)
C(44)	4278(1)	7788(1)	-1004(2)	50(1)
C(45)	2532(1)	7596(1)	-1185(1)	33(1)
C(46)	2576(1)	7456(1)	-1707(1)	42(1)
C(47)	2978(2)	7422(1)	-1935(2)	53(1)
C(48)	3419(1)	7526(1)	-1704(2)	48(1)
C(49)	2630(1)	8741(1)	-1225(1)	37(1)
C(50)	2673(1)	9163(1)	-1464(1)	44(1)
C(51)	2372(1)	9275(1)	-1842(2)	48(1)
C(52)	2030(1)	8972(1)	-1983(1)	46(1)
C(53)	1281(1)	8128(1)	-2111(1)	44(1)
C(54)	990(1)	7744(1)	-2069(1)	48(1)
C(55)	1062(1)	7428(1)	-1697(1)	45(1)
C(56)	1430(1)	7478(1)	-1380(1)	45(1)

Table C.28. Bond lengths [Å] and angles [°] for **1-(Ofluorenyl)$_2$**.

Zr(1)-O(2)	1.920(2)	C(25)-C(26)	1.376(5)
Zr(1)-O(1)	2.014(2)	C(25)-C(29)	1.495(5)
Zr(1)-C(17)	2.512(3)	C(26)-C(27)	1.463(5)
Zr(1)-C(8)	2.524(4)	C(26)-C(45)	1.501(5)
Zr(1)-C(7)	2.548(4)	C(27)-C(48)	1.339(5)
Zr(1)-C(16)	2.559(3)	C(27)-C(28)	1.454(5)
Zr(1)-C(18)	2.586(3)	C(28)-C(44)	1.394(5)
Zr(1)-C(9)	2.590(4)	C(28)-C(29)	1.404(5)
Zr(1)-C(15)	2.664(3)	C(29)-C(41)	1.391(5)
Zr(1)-C(5)	2.706(3)	C(30)-C(34)	1.522(5)
Zr(1)-C(14)	2.712(3)	C(30)-C(31)	1.530(5)
Zr(1)-C(6)	2.728(3)	C(30)-C(45)	1.575(5)
O(1)-C(25)	1.332(4)	C(31)-C(49)	1.378(5)
O(2)-C(30)	1.432(4)	C(31)-C(32)	1.392(5)
C(1)-C(2)	1.359(5)	C(32)-C(52)	1.406(5)
C(1)-C(6)	1.424(5)	C(32)-C(33)	1.476(5)
C(2)-C(3)	1.420(5)	C(33)-C(53)	1.380(5)
C(3)-C(4)	1.362(5)	C(33)-C(34)	1.392(5)
C(4)-C(5)	1.402(5)	C(34)-C(56)	1.381(5)
C(5)-C(9)	1.442(5)	C(35)-C(37)	1.502(5)
C(5)-C(6)	1.440(5)	C(35)-C(36)	1.562(5)
C(6)-C(7)	1.436(5)	C(38)-C(40)	1.515(5)
C(7)-C(8)	1.427(5)	C(38)-C(39)	1.534(5)
C(7)-C(19)	1.541(5)	C(41)-C(42)	1.409(5)
C(8)-C(9)	1.403(5)	C(42)-C(43)	1.383(6)
C(9)-C(22)	1.530(5)	C(43)-C(44)	1.373(5)
C(10)-C(11)	1.362(5)	C(45)-C(46)	1.501(5)
C(10)-C(15)	1.425(5)	C(46)-C(47)	1.328(5)
C(11)-C(12)	1.424(5)	C(47)-C(48)	1.458(5)
C(12)-C(13)	1.356(5)	C(49)-C(50)	1.394(5)
C(13)-C(14)	1.404(5)	C(50)-C(51)	1.397(5)
C(14)-C(18)	1.427(5)	C(51)-C(52)	1.378(5)
C(14)-C(15)	1.444(5)	C(53)-C(54)	1.400(5)
C(15)-C(16)	1.414(5)	C(54)-C(55)	1.392(5)
C(16)-C(17)	1.423(5)	C(55)-C(56)	1.387(5)
C(16)-C(35)	1.535(5)		
C(17)-C(18)	1.413(4)	O(2)-Zr(1)-O(1)	88.37(9)
C(18)-C(38)	1.521(5)	O(2)-Zr(1)-C(17)	87.56(11)
C(19)-C(21)	1.529(5)	O(1)-Zr(1)-C(17)	97.41(10)
C(19)-C(20)	1.544(5)	O(2)-Zr(1)-C(8)	131.33(11)
C(22)-C(24)	1.534(5)	O(1)-Zr(1)-C(8)	116.46(11)
C(22)-C(23)	1.551(5)	C(17)-Zr(1)-C(8)	125.77(12)

Table C.28. (continued)

O(2)-Zr(1)-C(7)	99.01(11)	C(7)-Zr(1)-C(14)	85.39(11)
O(1)-Zr(1)-C(7)	129.87(11)	C(16)-Zr(1)-C(14)	51.87(11)
C(17)-Zr(1)-C(7)	132.19(11)	C(18)-Zr(1)-C(14)	31.12(10)
C(8)-Zr(1)-C(7)	32.69(11)	C(9)-Zr(1)-C(14)	98.96(11)
O(2)-Zr(1)-C(16)	116.03(11)	C(15)-Zr(1)-C(14)	31.14(10)
O(1)-Zr(1)-C(16)	82.74(10)	C(5)-Zr(1)-C(14)	126.36(11)
C(17)-Zr(1)-C(16)	32.58(11)	O(2)-Zr(1)-C(6)	84.16(10)
C(8)-Zr(1)-C(16)	108.54(12)	O(1)-Zr(1)-C(6)	102.22(10)
C(7)-Zr(1)-C(16)	133.63(12)	C(17)-Zr(1)-C(6)	158.43(11)
O(2)-Zr(1)-C(18)	89.64(10)	C(8)-Zr(1)-C(6)	51.35(12)
O(1)-Zr(1)-C(18)	129.54(10)	C(7)-Zr(1)-C(6)	31.34(11)
C(17)-Zr(1)-C(18)	32.14(10)	C(16)-Zr(1)-C(6)	159.53(12)
C(8)-Zr(1)-C(18)	102.02(11)	C(18)-Zr(1)-C(6)	127.70(11)
C(7)-Zr(1)-C(18)	100.21(11)	C(9)-Zr(1)-C(6)	51.79(11)
C(16)-Zr(1)-C(18)	53.62(11)	C(15)-Zr(1)-C(6)	129.50(11)
O(2)-Zr(1)-C(9)	132.31(11)	C(5)-Zr(1)-C(6)	30.73(10)
O(1)-Zr(1)-C(9)	84.84(11)	C(14)-Zr(1)-C(6)	116.72(11)
C(17)-Zr(1)-C(9)	140.12(12)	C(25)-O(1)-Zr(1)	138.5(2)
C(8)-Zr(1)-C(9)	31.82(11)	C(30)-O(2)-Zr(1)	155.7(2)
C(7)-Zr(1)-C(9)	53.99(12)	C(2)-C(1)-C(6)	119.8(4)
C(16)-Zr(1)-C(9)	109.80(12)	C(1)-C(2)-C(3)	120.6(4)
C(18)-Zr(1)-C(9)	129.60(11)	C(4)-C(3)-C(2)	121.4(4)
O(2)-Zr(1)-C(15)	138.95(10)	C(3)-C(4)-C(5)	119.5(4)
O(1)-Zr(1)-C(15)	103.38(10)	C(4)-C(5)-C(9)	132.7(4)
C(17)-Zr(1)-C(15)	52.30(11)	C(4)-C(5)-C(6)	119.7(3)
C(8)-Zr(1)-C(15)	78.27(12)	C(9)-C(5)-C(6)	107.6(3)
C(7)-Zr(1)-C(15)	102.59(11)	C(4)-C(5)-Zr(1)	122.5(2)
C(16)-Zr(1)-C(15)	31.33(10)	C(9)-C(5)-Zr(1)	69.79(19)
C(18)-Zr(1)-C(15)	52.50(11)	C(6)-C(5)-Zr(1)	75.5(2)
C(9)-Zr(1)-C(15)	88.30(11)	C(1)-C(6)-C(7)	132.7(4)
O(2)-Zr(1)-C(5)	101.09(10)	C(1)-C(6)-C(5)	118.7(3)
O(1)-Zr(1)-C(5)	77.28(10)	C(7)-C(6)-C(5)	108.4(3)
C(17)-Zr(1)-C(5)	169.60(11)	C(1)-C(6)-Zr(1)	128.7(2)
C(8)-Zr(1)-C(5)	51.64(11)	C(7)-C(6)-Zr(1)	67.39(19)
C(7)-Zr(1)-C(5)	52.61(11)	C(5)-C(6)-Zr(1)	73.8(2)
C(16)-Zr(1)-C(5)	137.06(11)	C(8)-C(7)-C(6)	105.8(3)
C(18)-Zr(1)-C(5)	151.78(11)	C(8)-C(7)-C(19)	122.4(3)
C(9)-Zr(1)-C(5)	31.50(11)	C(6)-C(7)-C(19)	130.4(3)
C(15)-Zr(1)-C(5)	119.77(11)	C(8)-C(7)-Zr(1)	72.7(2)
O(2)-Zr(1)-C(14)	119.08(10)	C(6)-C(7)-Zr(1)	81.3(2)
O(1)-Zr(1)-C(14)	133.19(10)	C(19)-C(7)-Zr(1)	121.7(2)
C(17)-Zr(1)-C(14)	51.58(11)	C(9)-C(8)-C(7)	111.0(3)
C(8)-Zr(1)-C(14)	74.85(11)	C(9)-C(8)-Zr(1)	76.7(2)

Table C.28. (continued)

C(7)-C(8)-Zr(1)	74.6(2)	C(9)-C(22)-C(23)	109.9(3)
C(8)-C(9)-C(5)	106.8(3)	O(1)-C(25)-C(26)	131.7(3)
C(8)-C(9)-C(22)	124.4(3)	O(1)-C(25)-C(29)	119.4(3)
C(5)-C(9)-C(22)	127.2(3)	C(26)-C(25)-C(29)	108.8(3)
C(8)-C(9)-Zr(1)	71.5(2)	C(25)-C(26)-C(27)	107.9(3)
C(5)-C(9)-Zr(1)	78.7(2)	C(25)-C(26)-C(45)	132.1(3)
C(22)-C(9)-Zr(1)	126.6(2)	C(27)-C(26)-C(45)	119.9(3)
C(11)-C(10)-C(15)	118.8(3)	C(48)-C(27)-C(28)	128.9(4)
C(10)-C(11)-C(12)	121.8(4)	C(48)-C(27)-C(26)	123.0(4)
C(13)-C(12)-C(11)	120.4(4)	C(28)-C(27)-C(26)	108.1(3)
C(12)-C(13)-C(14)	120.5(3)	C(44)-C(28)-C(29)	119.7(4)
C(13)-C(14)-C(18)	132.3(3)	C(44)-C(28)-C(27)	132.6(4)
C(13)-C(14)-C(15)	119.2(3)	C(29)-C(28)-C(27)	107.7(3)
C(18)-C(14)-C(15)	108.1(3)	C(41)-C(29)-C(28)	121.9(3)
C(13)-C(14)-Zr(1)	129.4(2)	C(41)-C(29)-C(25)	130.6(4)
C(18)-C(14)-Zr(1)	69.54(19)	C(28)-C(29)-C(25)	107.5(3)
C(15)-C(14)-Zr(1)	72.59(19)	O(2)-C(30)-C(34)	111.1(3)
C(16)-C(15)-C(10)	132.5(3)	O(2)-C(30)-C(31)	112.6(3)
C(16)-C(15)-C(14)	107.8(3)	C(34)-C(30)-C(31)	101.2(3)
C(10)-C(15)-C(14)	119.3(3)	O(2)-C(30)-C(45)	107.0(3)
C(16)-C(15)-Zr(1)	70.2(2)	C(34)-C(30)-C(45)	111.6(3)
C(10)-C(15)-Zr(1)	125.1(2)	C(31)-C(30)-C(45)	113.4(3)
C(14)-C(15)-Zr(1)	76.3(2)	C(49)-C(31)-C(32)	120.1(3)
C(15)-C(16)-C(17)	107.3(3)	C(49)-C(31)-C(30)	129.5(3)
C(15)-C(16)-C(35)	123.2(3)	C(32)-C(31)-C(30)	110.4(3)
C(17)-C(16)-C(35)	128.4(3)	C(31)-C(32)-C(52)	120.6(3)
C(15)-C(16)-Zr(1)	78.5(2)	C(31)-C(32)-C(33)	109.0(3)
C(17)-C(16)-Zr(1)	71.90(19)	C(52)-C(32)-C(33)	130.3(3)
C(35)-C(16)-Zr(1)	124.8(2)	C(53)-C(33)-C(34)	121.3(3)
C(18)-C(17)-C(16)	109.8(3)	C(53)-C(33)-C(32)	130.7(4)
C(18)-C(17)-Zr(1)	76.82(19)	C(34)-C(33)-C(32)	108.0(3)
C(16)-C(17)-Zr(1)	75.5(2)	C(56)-C(34)-C(33)	119.8(3)
C(17)-C(18)-C(14)	106.8(3)	C(56)-C(34)-C(30)	128.9(3)
C(17)-C(18)-C(38)	126.9(3)	C(33)-C(34)-C(30)	111.2(3)
C(14)-C(18)-C(38)	125.2(3)	C(37)-C(35)-C(16)	115.3(3)
C(17)-C(18)-Zr(1)	71.04(18)	C(37)-C(35)-C(36)	109.4(3)
C(14)-C(18)-Zr(1)	79.3(2)	C(16)-C(35)-C(36)	108.2(3)
C(38)-C(18)-Zr(1)	124.4(2)	C(40)-C(38)-C(18)	114.7(3)
C(21)-C(19)-C(7)	113.2(3)	C(40)-C(38)-C(39)	110.6(3)
C(21)-C(19)-C(20)	110.5(3)	C(18)-C(38)-C(39)	109.5(3)
C(7)-C(19)-C(20)	110.2(3)	C(29)-C(41)-C(42)	116.8(4)
C(24)-C(22)-C(9)	116.1(3)	C(43)-C(42)-C(41)	121.1(4)
C(24)-C(22)-C(23)	110.1(3)	C(44)-C(43)-C(42)	121.6(4)

Table C.28. (continued)

C(43)-C(44)-C(28)	118.9(4)	C(49)-C(50)-C(51)	120.1(4)
C(26)-C(45)-C(46)	112.7(3)	C(52)-C(51)-C(50)	120.7(4)
C(26)-C(45)-C(30)	115.2(3)	C(51)-C(52)-C(32)	118.8(4)
C(46)-C(45)-C(30)	109.8(3)	C(33)-C(53)-C(54)	119.0(4)
C(47)-C(46)-C(45)	123.3(4)	C(55)-C(54)-C(53)	119.5(4)
C(46)-C(47)-C(48)	122.9(4)	C(56)-C(55)-C(54)	121.0(4)
C(27)-C(48)-C(47)	118.1(4)	C(34)-C(56)-C(55)	119.4(4)
C(31)-C(49)-C(50)	119.7(3)		

Symmetry transformations used to generate equivalent atoms:

Table C.29. Anisotropic displacement parameters ($Å^2 x\ 10^3$) for **1-(Ofluorenyl)$_2$**. The anisotropic displacement factor exponent takes the form: $-2\pi^2[\ h^2\ a^{*2}U^{11} + ... + 2\ h\ k\ a^*\ b^*\ U^{12}\ ]$

	U^{11}	U^{22}	U^{33}	U^{23}	U^{13}	U^{12}
Zr(1)	30(1)	33(1)	30(1)	-1(1)	1(1)	1(1)
O(1)	35(1)	51(2)	30(2)	-4(1)	6(1)	5(1)
O(2)	33(1)	37(1)	26(1)	-2(1)	1(1)	-3(1)
C(1)	44(2)	36(2)	46(3)	4(2)	-4(2)	-4(2)
C(2)	64(3)	41(3)	46(3)	0(2)	1(3)	-6(2)
C(3)	65(3)	41(3)	59(3)	-1(2)	9(3)	9(2)
C(4)	48(2)	36(2)	54(3)	2(2)	0(2)	11(2)
C(5)	41(2)	29(2)	34(2)	8(2)	-2(2)	4(2)
C(6)	45(2)	31(2)	39(3)	8(2)	6(2)	-2(2)
C(7)	39(2)	35(2)	42(3)	-2(2)	3(2)	-6(2)
C(8)	43(2)	37(2)	38(3)	4(2)	5(2)	-1(2)
C(9)	43(2)	36(2)	37(3)	0(2)	-3(2)	3(2)
C(10)	43(2)	42(2)	37(3)	-3(2)	-9(2)	8(2)
C(11)	45(3)	47(3)	31(2)	-8(2)	2(2)	2(2)
C(12)	47(3)	44(2)	30(2)	-3(2)	5(2)	3(2)
C(13)	33(2)	36(2)	41(3)	-10(2)	3(2)	5(2)
C(14)	31(2)	35(2)	27(2)	-6(2)	6(2)	4(2)
C(15)	30(2)	34(2)	28(2)	-8(2)	0(2)	6(2)
C(16)	32(2)	32(2)	38(2)	-6(2)	3(2)	5(2)
C(17)	33(2)	30(2)	33(2)	1(2)	-1(2)	-1(2)
C(18)	29(2)	29(2)	31(2)	-3(2)	2(2)	-3(2)
C(19)	38(2)	41(2)	47(3)	-6(2)	5(2)	-1(2)
C(20)	48(3)	56(3)	60(3)	1(3)	7(2)	-1(2)
C(21)	46(3)	48(3)	73(3)	5(3)	-1(3)	-6(2)
C(22)	57(3)	47(3)	38(3)	3(2)	-5(2)	3(2)
C(23)	80(3)	62(3)	65(3)	15(3)	-18(3)	9(3)
C(24)	52(3)	77(3)	49(3)	8(3)	-7(3)	-5(2)
C(25)	38(2)	30(2)	34(2)	3(2)	1(2)	4(2)
C(26)	32(2)	32(2)	34(2)	6(2)	2(2)	8(2)

Table C.29. (continued)

C(27)	48(3)	24(2)	37(3)	1(2)	12(2)	4(2)
C(28)	37(2)	34(2)	50(3)	-2(2)	5(2)	6(2)
C(29)	34(2)	33(2)	43(3)	5(2)	-1(2)	1(2)
C(30)	39(2)	33(2)	28(2)	3(2)	-6(2)	2(2)
C(31)	38(2)	33(2)	28(2)	-5(2)	3(2)	1(2)
C(32)	38(2)	38(2)	29(2)	-3(2)	1(2)	5(2)
C(33)	41(2)	37(2)	26(2)	-4(2)	3(2)	6(2)
C(34)	33(2)	36(2)	30(2)	-11(2)	-5(2)	1(2)
C(35)	42(2)	40(2)	52(3)	-1(2)	-2(2)	-4(2)
C(36)	57(3)	73(3)	69(3)	-24(3)	5(3)	-21(3)
C(37)	40(2)	60(3)	45(3)	-6(2)	-1(2)	-11(2)
C(38)	28(2)	34(2)	38(2)	0(2)	-2(2)	3(2)
C(39)	50(3)	61(3)	44(3)	-4(2)	-4(2)	15(2)
C(40)	35(2)	45(2)	39(3)	-1(2)	-4(2)	12(2)
C(41)	36(2)	45(2)	54(3)	4(2)	1(2)	5(2)
C(42)	50(3)	54(3)	72(3)	-2(3)	-6(3)	12(2)
C(43)	36(3)	67(3)	79(4)	-3(3)	5(3)	8(2)
C(44)	41(3)	50(3)	58(3)	-8(2)	7(3)	16(2)
C(45)	38(2)	34(2)	27(2)	1(2)	-2(2)	2(2)
C(46)	48(3)	42(2)	35(3)	-6(2)	-3(2)	7(2)
C(47)	73(3)	45(3)	40(3)	-9(2)	3(3)	10(2)
C(48)	50(3)	51(3)	44(3)	-2(2)	10(2)	6(2)
C(49)	36(2)	40(2)	34(2)	-4(2)	5(2)	0(2)
C(50)	40(2)	39(2)	51(3)	-3(2)	12(2)	-6(2)
C(51)	49(3)	48(3)	48(3)	11(2)	2(2)	1(2)
C(52)	46(3)	52(3)	41(3)	5(2)	4(2)	11(2)
C(53)	47(3)	46(3)	39(3)	-3(2)	-7(2)	11(2)
C(54)	41(3)	53(3)	50(3)	-20(2)	-12(2)	3(2)
C(55)	41(2)	47(3)	48(3)	-6(2)	-5(2)	-8(2)
C(56)	52(3)	46(3)	37(3)	-4(2)	-7(2)	-4(2)

Table C.30. Hydrogen coordinates (x 10^4) and isotropic displacement parameters ($Å^2$x 10 ^{3}) for **1-(Ofluorenyl)$_2$**.

	x	y	z	U(eq)
H(1A)	1439	6864	-440	50
H(2A)	1996	6390	-772	60
H(3A)	2763	6417	-490	66
H(4A)	2971	6890	146	55
H(8A)	1765	7743	1074	47
H(10A)	2634	8580	1349	49
H(11A)	2045	8463	1899	49
H(12A)	1263	8495	1661	48
H(13A)	1069	8610	863	44
H(17A)	2247	9083	-339	38
H(19A)	1021	7877	539	50
H(20A)	471	7273	636	82
H(20B)	910	7188	976	82
H(20C)	853	6901	484	82
H(21A)	1044	7882	-316	83
H(21B)	547	7719	-128	83
H(21C)	909	7346	-326	83
H(22A)	2587	7635	1363	57
H(23A)	2997	6951	1571	104
H(23B)	2858	6726	1062	104
H(23C)	2467	6839	1454	104
H(24A)	3385	7620	1220	89
H(24B)	3137	7942	827	89
H(24C)	3302	7433	682	89
H(35A)	3153	8712	562	53
H(36A)	3343	9497	762	100
H(36B)	2890	9336	1047	100
H(36C)	2844	9661	580	100
H(37A)	3209	8788	-281	73

Table C.30. (continued)

H(37B)	3549	9142	-14	73
H(37C)	3072	9322	-240	73
H(38A)	1045	8647	-94	40
H(39A)	1017	9348	349	77
H(39B)	751	9396	-157	77
H(39C)	1257	9612	-94	77
H(40A)	1458	8602	-824	59
H(40B)	1535	9149	-815	59
H(40C)	1025	8943	-875	59
H(41A)	3784	8096	222	54
H(42A)	4592	8114	75	70
H(43A)	4885	7927	-679	73
H(44A)	4403	7712	-1311	60
H(45A)	2416	7317	-1009	40
H(46A)	2302	7389	-1882	50
H(47A)	2979	7324	-2263	63
H(48A)	3701	7501	-1878	58
H(49A)	2840	8660	-975	44
H(50A)	2906	9375	-1369	52
H(51A)	2404	9562	-2004	58
H(52A)	1828	9047	-2242	55
H(53A)	1233	8350	-2360	53
H(54A)	745	7699	-2294	57
H(55A)	857	7175	-1660	54
H(56A)	1484	7253	-1135	54

Table C.31. Crystal data and structure refinement for **1-$(OMe_2)_2$-4,7** (Chapter 3).

Identification code	**1-$(OMe_2)_2$-4,7**	
Empirical formula	C36 H50 O2 Zr	
Formula weight	605.98	
Temperature	173(2) K	
Wavelength	0.71073 Å	
Crystal system	Triclinic	
Space group	P-1	
Unit cell dimensions	a = 9.3205(4) Å	α= 83.079(2)°.
	b = 9.8440(5) Å	β= 84.848(2)°.
	c = 17.9792(8) Å	γ = 71.828(2)°.
Volume	1553.53(12) $Å^3$	
Z	2	
Density (calculated)	1.295 Mg/m^3	
Absorption coefficient	0.384 mm^{-1}	
F(000)	644	
Crystal size	0.40 x 0.20 x 0.05 mm^3	
Theta range for data collection	2.30 to 28.46°.	
Index ranges	-12<=h<=12, -13<=k<=10, -23<=l<=24	
Reflections collected	25944	
Independent reflections	7610 [R(int) = 0.0373]	
Completeness to theta = 28.46°	97.0 %	
Absorption correction	Semi-empirical from equivalents	
Max. and min. transmission	0.9811 and 0.8617	
Refinement method	Full-matrix least-squares on F^2	
Data / restraints / parameters	7610 / 0 / 372	
Goodness-of-fit on F^2	1.081	
Final R indices [I>2sigma(I)]	R1 = 0.0535, wR2 = 0.1383	
R indices (all data)	R1 = 0.0595, wR2 = 0.1410	
Largest diff. peak and hole	1.712 and -0.816 e.$Å^{-3}$	

Table C.32. Atomic coordinates (x 10^4) and equivalent isotropic displacement parameters ($Å^2$x 10^3) for **1-$(OMe_2)_2$-4,7**. U(eq) is defined as one third of the trace of the orthogonalized U^{ij} tensor.

	x	y	z	U(eq)
Zr(1)	984(1)	6306(1)	2496(1)	20(1)
O(1)	2140(2)	4594(3)	3112(2)	51(1)
O(2)	1137(3)	5529(3)	1523(2)	59(1)
C(1)	4647(3)	4807(3)	2740(2)	29(1)
C(2)	5462(4)	4090(4)	2069(2)	44(1)
C(3)	5030(4)	4470(4)	1380(2)	47(1)
C(4)	3672(4)	5674(4)	1146(2)	42(1)
C(5)	3180(3)	6705(4)	1743(2)	30(1)
C(6)	2085(3)	8087(4)	1719(2)	32(1)
C(7)	1919(3)	8487(3)	2459(2)	26(1)
C(8)	2872(3)	7432(3)	2935(2)	23(1)
C(9)	3652(3)	6293(3)	2490(2)	23(1)
C(10)	-1157(3)	6719(3)	3555(2)	21(1)
C(11)	-917(3)	6951(3)	4292(2)	28(1)
C(12)	-1241(4)	8322(4)	4468(2)	36(1)
C(13)	-1750(4)	9507(3)	3929(2)	35(1)
C(14)	-1915(3)	9342(3)	3211(2)	28(1)
C(15)	-1647(3)	7929(3)	3001(2)	22(1)
C(16)	-1888(3)	7405(3)	2330(2)	23(1)
C(17)	-1589(3)	5897(3)	2497(2)	22(1)
C(18)	-1103(3)	5449(3)	3227(2)	21(1)
C(19)	-688(3)	3947(3)	3623(2)	25(1)
C(20)	-359(4)	2813(3)	3080(2)	37(1)
C(21)	-1910(4)	3774(4)	4219(2)	37(1)
C(22)	-2573(4)	8299(3)	1631(2)	30(1)
C(23)	-4177(4)	9223(4)	1800(2)	46(1)
C(24)	-2569(5)	7371(4)	1013(2)	43(1)
C(25)	3681(3)	3918(3)	3237(2)	32(1)
C(26)	3931(5)	3830(4)	4068(2)	50(1)

Table C.32. (continued)

C(27)	4065(4)	2378(4)	3041(3)	48(1)
C(28)	3162(3)	7617(3)	3724(2)	27(1)
C(29)	2239(4)	9062(4)	3968(2)	40(1)
C(30)	2298(4)	5150(4)	958(2)	46(1)
C(31)	4811(4)	7429(5)	3810(2)	55(1)
C(32)	2741(5)	3528(5)	934(2)	59(1)
C(33)	1698(5)	5867(5)	200(2)	58(1)
C(34)	1337(4)	9062(4)	1051(2)	46(1)
C(35)	299(5)	10497(4)	1284(3)	60(1)
C(36)	2509(6)	9328(6)	451(2)	79(1)

Table C.33. Bond lengths [Å] and angles [°] for **1-(OMe_2)$_2$-4,7**.

Zr(1)-O(1)	1.964(2)	C(22)-C(23)	1.514(5)
Zr(1)-O(2)	1.968(3)	C(22)-C(24)	1.520(5)
Zr(1)-C(5)	2.461(3)	C(25)-C(26)	1.520(5)
Zr(1)-C(9)	2.482(3)	C(25)-C(27)	1.523(5)
Zr(1)-C(6)	2.522(3)	C(28)-C(29)	1.509(4)
Zr(1)-C(7)	2.549(3)	C(28)-C(31)	1.509(5)
Zr(1)-C(17)	2.551(3)	C(30)-C(32)	1.525(6)
Zr(1)-C(18)	2.553(3)	C(30)-C(33)	1.525(6)
Zr(1)-C(8)	2.574(3)	C(34)-C(36)	1.525(6)
Zr(1)-C(16)	2.586(3)	C(34)-C(35)	1.524(6)
Zr(1)-C(10)	2.602(3)		
Zr(1)-C(15)	2.625(3)	O(1)-Zr(1)-O(2)	100.88(13)
O(1)-C(25)	1.408(4)	O(1)-Zr(1)-C(5)	95.93(10)
O(2)-C(30)	1.409(4)	O(2)-Zr(1)-C(5)	70.75(10)
C(1)-C(2)	1.495(5)	O(1)-Zr(1)-C(9)	70.53(10)
C(1)-C(9)	1.507(4)	O(2)-Zr(1)-C(9)	96.97(10)
C(1)-C(25)	1.592(4)	C(5)-Zr(1)-C(9)	33.47(9)
C(2)-C(3)	1.313(6)	O(1)-Zr(1)-C(6)	125.28(10)
C(3)-C(4)	1.491(5)	O(2)-Zr(1)-C(6)	82.29(11)
C(4)-C(5)	1.508(5)	C(5)-Zr(1)-C(6)	33.15(10)
C(4)-C(30)	1.597(5)	C(9)-Zr(1)-C(6)	54.99(10)
C(5)-C(6)	1.422(4)	O(1)-Zr(1)-C(7)	114.88(10)
C(5)-C(9)	1.423(4)	O(2)-Zr(1)-C(7)	114.67(11)
C(6)-C(7)	1.415(4)	C(5)-Zr(1)-C(7)	53.57(10)
C(6)-C(34)	1.519(5)	C(9)-Zr(1)-C(7)	53.25(9)
C(7)-C(8)	1.395(4)	C(6)-Zr(1)-C(7)	32.39(10)
C(8)-C(9)	1.425(4)	O(1)-Zr(1)-C(17)	102.35(9)
C(8)-C(28)	1.510(4)	O(2)-Zr(1)-C(17)	78.80(10)
C(10)-C(11)	1.418(4)	C(5)-Zr(1)-C(17)	146.91(10)
C(10)-C(18)	1.431(4)	C(9)-Zr(1)-C(17)	171.08(9)
C(10)-C(15)	1.442(4)	C(6)-Zr(1)-C(17)	131.23(9)
C(11)-C(12)	1.359(5)	C(7)-Zr(1)-C(17)	135.66(9)
C(12)-C(13)	1.411(5)	O(1)-Zr(1)-C(18)	77.65(9)
C(13)-C(14)	1.349(5)	O(2)-Zr(1)-C(18)	102.97(10)
C(14)-C(15)	1.426(4)	C(5)-Zr(1)-C(18)	170.24(10)
C(15)-C(16)	1.429(4)	C(9)-Zr(1)-C(18)	145.05(9)
C(16)-C(17)	1.422(4)	C(6)-Zr(1)-C(18)	155.58(9)
C(16)-C(22)	1.513(4)	C(7)-Zr(1)-C(18)	135.80(9)
C(17)-C(18)	1.401(4)	C(17)-Zr(1)-C(18)	31.87(9)
C(18)-C(19)	1.509(4)	O(1)-Zr(1)-C(8)	83.30(10)
C(19)-C(20)	1.513(4)	O(2)-Zr(1)-C(8)	125.15(10)
C(19)-C(21)	1.527(4)	C(5)-Zr(1)-C(8)	54.48(10)

Table C.33. (continued)

C(9)-Zr(1)-C(8)	32.67(9)	C(3)-C(4)-C(30)	113.4(3)
C(6)-Zr(1)-C(8)	54.18(9)	C(5)-C(4)-C(30)	110.6(3)
C(7)-Zr(1)-C(8)	31.59(9)	C(6)-C(5)-C(9)	108.6(3)
C(17)-Zr(1)-C(8)	154.37(9)	C(6)-C(5)-C(4)	129.4(3)
C(18)-Zr(1)-C(8)	130.78(9)	C(9)-C(5)-C(4)	121.6(3)
O(1)-Zr(1)-C(16)	131.42(9)	C(6)-C(5)-Zr(1)	75.76(17)
O(2)-Zr(1)-C(16)	87.58(10)	C(9)-C(5)-Zr(1)	74.06(16)
C(5)-Zr(1)-C(16)	131.38(10)	C(4)-C(5)-Zr(1)	109.9(2)
C(9)-Zr(1)-C(16)	156.44(9)	C(7)-C(6)-C(5)	105.6(3)
C(6)-Zr(1)-C(16)	103.18(9)	C(7)-C(6)-C(34)	124.4(3)
C(7)-Zr(1)-C(16)	103.89(9)	C(5)-C(6)-C(34)	129.7(3)
C(17)-Zr(1)-C(16)	32.13(9)	C(7)-C(6)-Zr(1)	74.87(17)
C(18)-Zr(1)-C(16)	53.94(9)	C(5)-C(6)-Zr(1)	71.10(17)
C(8)-Zr(1)-C(16)	129.72(9)	C(34)-C(6)-Zr(1)	123.9(2)
O(1)-Zr(1)-C(10)	88.76(10)	C(8)-C(7)-C(6)	111.4(3)
O(2)-Zr(1)-C(10)	130.97(10)	C(8)-C(7)-Zr(1)	75.21(17)
C(5)-Zr(1)-C(10)	156.51(10)	C(6)-C(7)-Zr(1)	72.74(17)
C(9)-Zr(1)-C(10)	131.06(9)	C(7)-C(8)-C(9)	106.2(3)
C(6)-Zr(1)-C(10)	129.77(10)	C(7)-C(8)-C(28)	124.8(3)
C(7)-Zr(1)-C(10)	103.68(9)	C(9)-C(8)-C(28)	128.3(2)
C(17)-Zr(1)-C(10)	52.23(9)	C(7)-C(8)-Zr(1)	73.20(17)
C(18)-Zr(1)-C(10)	32.22(9)	C(9)-C(8)-Zr(1)	70.09(16)
C(8)-Zr(1)-C(10)	103.58(9)	C(28)-C(8)-Zr(1)	128.9(2)
C(16)-Zr(1)-C(10)	53.21(9)	C(8)-C(9)-C(5)	108.2(3)
O(1)-Zr(1)-C(15)	120.70(10)	C(8)-C(9)-C(1)	128.7(3)
O(2)-Zr(1)-C(15)	119.28(10)	C(5)-C(9)-C(1)	122.7(3)
C(5)-Zr(1)-C(15)	136.06(10)	C(8)-C(9)-Zr(1)	77.24(16)
C(9)-Zr(1)-C(15)	135.87(9)	C(5)-C(9)-Zr(1)	72.47(16)
C(6)-Zr(1)-C(15)	103.06(10)	C(1)-C(9)-Zr(1)	110.08(19)
C(7)-Zr(1)-C(15)	87.15(9)	C(11)-C(10)-C(18)	132.1(3)
C(17)-Zr(1)-C(15)	52.16(9)	C(11)-C(10)-C(15)	119.6(3)
C(18)-Zr(1)-C(15)	53.37(9)	C(18)-C(10)-C(15)	108.1(2)
C(8)-Zr(1)-C(15)	103.31(9)	C(11)-C(10)-Zr(1)	122.29(19)
C(16)-Zr(1)-C(15)	31.82(9)	C(18)-C(10)-Zr(1)	72.01(15)
C(10)-Zr(1)-C(15)	32.01(8)	C(15)-C(10)-Zr(1)	74.89(15)
C(25)-O(1)-Zr(1)	135.4(2)	C(12)-C(11)-C(10)	118.8(3)
C(30)-O(2)-Zr(1)	134.2(2)	C(11)-C(12)-C(13)	121.4(3)
C(2)-C(1)-C(9)	109.4(3)	C(14)-C(13)-C(12)	122.0(3)
C(2)-C(1)-C(25)	113.3(3)	C(13)-C(14)-C(15)	118.9(3)
C(9)-C(1)-C(25)	110.4(2)	C(14)-C(15)-C(16)	132.6(3)
C(3)-C(2)-C(1)	124.5(3)	C(14)-C(15)-C(10)	119.0(3)
C(2)-C(3)-C(4)	125.5(3)	C(16)-C(15)-C(10)	108.1(2)
C(3)-C(4)-C(5)	109.8(3)	C(14)-C(15)-Zr(1)	124.3(2)

Table C.33. (continued)

C(16)-C(15)-Zr(1)	72.55(15)	C(16)-C(22)-C(24)	111.9(3)
C(10)-C(15)-Zr(1)	73.10(15)	C(23)-C(22)-C(24)	109.1(3)
C(17)-C(16)-C(15)	106.0(2)	O(1)-C(25)-C(26)	109.5(3)
C(17)-C(16)-C(22)	126.6(3)	O(1)-C(25)-C(27)	107.4(3)
C(15)-C(16)-C(22)	126.7(3)	C(26)-C(25)-C(27)	106.6(3)
C(17)-C(16)-Zr(1)	72.61(15)	O(1)-C(25)-C(1)	108.6(2)
C(15)-C(16)-Zr(1)	75.63(15)	C(26)-C(25)-C(1)	111.7(3)
C(22)-C(16)-Zr(1)	124.4(2)	C(27)-C(25)-C(1)	113.0(3)
C(18)-C(17)-C(16)	111.3(3)	C(29)-C(28)-C(8)	112.5(3)
C(18)-C(17)-Zr(1)	74.13(16)	C(29)-C(28)-C(31)	108.5(3)
C(16)-C(17)-Zr(1)	75.25(16)	C(8)-C(28)-C(31)	111.7(3)
C(17)-C(18)-C(10)	106.4(2)	O(2)-C(30)-C(32)	107.7(3)
C(17)-C(18)-C(19)	128.0(3)	O(2)-C(30)-C(33)	109.4(3)
C(10)-C(18)-C(19)	125.5(3)	C(32)-C(30)-C(33)	108.0(3)
C(17)-C(18)-Zr(1)	74.00(16)	O(2)-C(30)-C(4)	108.4(3)
C(10)-C(18)-Zr(1)	75.77(16)	C(32)-C(30)-C(4)	112.7(3)
C(19)-C(18)-Zr(1)	118.50(17)	C(33)-C(30)-C(4)	110.5(3)
C(18)-C(19)-C(20)	112.2(3)	C(6)-C(34)-C(36)	111.3(3)
C(18)-C(19)-C(21)	111.3(2)	C(6)-C(34)-C(35)	111.6(3)
C(20)-C(19)-C(21)	110.8(3)	C(36)-C(34)-C(35)	109.4(4)
C(16)-C(22)-C(23)	111.2(3)		

Symmetry transformations used to generate equivalent atoms:

Table C.34. Anisotropic displacement parameters ($Å^2 x\ 10^3$) for **1-$(OMe_2)_2$-4,7**. The anisotropic displacement factor exponent takes the form: $-2\pi^2[\ h^2\ a^{*2}U^{11} + ... + 2\ h\ k\ a^*\ b^*\ U^{12}\ ]$

	U^{11}	U^{22}	U^{33}	U^{23}	U^{13}	U^{12}
Zr(1)	22(1)	22(1)	20(1)	-3(1)	2(1)	-11(1)
O(1)	17(1)	29(1)	98(2)	21(1)	1(1)	-6(1)
O(2)	57(1)	106(2)	43(1)	-47(1)	30(1)	-63(1)
C(1)	19(1)	35(2)	35(2)	-6(1)	4(1)	-11(1)
C(2)	24(1)	50(2)	64(2)	-28(2)	15(2)	-16(1)
C(3)	36(2)	71(2)	47(2)	-32(2)	21(1)	-31(2)
C(4)	44(2)	71(2)	25(2)	-18(1)	14(1)	-39(2)
C(5)	32(1)	44(2)	25(1)	-3(1)	3(1)	-26(1)
C(6)	35(1)	41(2)	27(2)	9(1)	-8(1)	-27(1)
C(7)	29(1)	26(1)	28(1)	2(1)	-7(1)	-17(1)
C(8)	24(1)	22(1)	25(1)	0(1)	-2(1)	-12(1)
C(9)	21(1)	32(1)	22(1)	-4(1)	3(1)	-15(1)
C(10)	19(1)	22(1)	21(1)	-1(1)	0(1)	-5(1)
C(11)	29(1)	31(1)	24(1)	-1(1)	-2(1)	-8(1)
C(12)	42(2)	38(2)	27(2)	-10(1)	-5(1)	-9(1)
C(13)	34(2)	28(1)	41(2)	-12(1)	-2(1)	-7(1)
C(14)	27(1)	22(1)	32(2)	-1(1)	-5(1)	-5(1)
C(15)	21(1)	22(1)	22(1)	0(1)	-1(1)	-5(1)
C(16)	23(1)	20(1)	27(1)	0(1)	-6(1)	-5(1)
C(17)	19(1)	21(1)	25(1)	-3(1)	-1(1)	-7(1)
C(18)	16(1)	22(1)	26(1)	-1(1)	1(1)	-7(1)
C(19)	21(1)	23(1)	31(2)	6(1)	-5(1)	-9(1)
C(20)	43(2)	20(1)	46(2)	-1(1)	-1(2)	-10(1)
C(21)	30(2)	39(2)	40(2)	10(1)	1(1)	-15(1)
C(22)	37(2)	29(1)	28(2)	3(1)	-10(1)	-14(1)
C(23)	46(2)	37(2)	50(2)	1(2)	-23(2)	-2(2)
C(24)	59(2)	43(2)	27(2)	0(1)	-18(2)	-14(2)
C(25)	18(1)	25(1)	48(2)	-1(1)	3(1)	-4(1)

Table C.34. (continued)

C(26)	59(2)	48(2)	46(2)	1(2)	12(2)	-27(2)
C(27)	45(2)	31(2)	69(3)	-2(2)	-6(2)	-11(2)
C(28)	33(1)	28(1)	21(1)	-2(1)	-1(1)	-10(1)
C(29)	39(2)	39(2)	44(2)	-16(2)	-7(2)	-8(1)
C(30)	43(2)	78(2)	34(2)	-27(2)	15(1)	-41(2)
C(31)	33(2)	81(3)	48(2)	-32(2)	-15(2)	-3(2)
C(32)	64(2)	86(3)	49(2)	-24(2)	5(2)	-50(2)
C(33)	56(2)	94(3)	45(2)	-23(2)	2(2)	-49(2)
C(34)	61(2)	57(2)	35(2)	21(2)	-21(2)	-43(2)
C(35)	85(3)	42(2)	62(2)	23(2)	-43(2)	-32(2)
C(36)	99(3)	119(3)	41(2)	44(2)	-26(2)	-80(3)

Table C.35. Hydrogen coordinates (x 10^4) and isotropic displacement parameters ($Å^2$x 10 ^{3}) for **1-$(OMe_2)_2$-4,7**.

	x	y	z	U(eq)
H(2A)	6354	3304	2148	53
H(3A)	5634	3933	997	57
H(7A)	1280	9444	2610	31
H(11A)	-537	6162	4654	34
H(12A)	-1121	8487	4966	43
H(13A)	-1985	10451	4076	41
H(14A)	-2204	10154	2851	33
H(17A)	-1825	5261	2164	26
H(19A)	259	3793	3886	30
H(20A)	-1271	2931	2814	55
H(20B)	-52	1858	3357	55
H(20C)	458	2916	2716	55
H(21A)	-2129	4536	4554	55
H(21B)	-1553	2836	4509	55
H(21C)	-2831	3839	3974	55
H(22A)	-1953	8948	1442	36
H(23A)	-4849	8620	1876	69
H(23B)	-4504	9956	1379	69
H(23C)	-4217	9691	2256	69
H(24A)	-3209	6756	1179	64
H(24B)	-1533	6770	901	64
H(24C)	-2963	7988	561	64
H(26A)	3683	4802	4222	75
H(26B)	4992	3308	4159	75
H(26C)	3279	3323	4358	75
H(27A)	3407	1897	3347	73
H(27B)	5124	1864	3141	73
H(27C)	3912	2382	2508	73
H(28A)	2874	6860	4071	33
H(29A)	2425	9111	4491	61

Table C.35. (continued)

H(29B)	1162	9193	3925	61
H(29C)	2529	9822	3647	61
H(31A)	5134	8130	3456	82
H(31B)	5418	6455	3705	82
H(31C)	4954	7580	4323	82
H(32A)	3101	3044	1422	89
H(32B)	3547	3234	544	89
H(32C)	1859	3263	822	89
H(33A)	811	5590	109	87
H(33B)	2486	5559	-197	87
H(33C)	1412	6913	201	87
H(34A)	709	8574	826	56
H(35A)	-450	10327	1672	90
H(35B)	-222	11070	847	90
H(35C)	900	11017	1481	90
H(36A)	3162	9775	665	118
H(36B)	1994	9969	31	118
H(36C)	3125	8412	272	118
H(1)	5380(40)	4870(30)	3064(18)	23(8)
H(4)	3950(40)	6160(40)	710(20)	38(10)

APPENDIX D: Permissions for Figure Reproduction

Figure D.1. Permissions from American Chemical Society for reproduction of figures from *J. Am. Chem. Soc.* **2002**, *124*, 9525.

AMERICAN CHEMICAL SOCIETY LICENSE
TERMS AND CONDITIONS
Oct 13, 2009

This is a License Agreement between Doris Pun ("You") and American Chemical Society ("American Chemical Society") provided by Copyright Clearance Center ("CCC"). The license consists of your order details, the terms and conditions provided by American Chemical Society, and the payment terms and conditions.

All payments must be made in full to CCC. For payment instructions, please see information listed at the bottom of this form.

License Number	2287070580058
License Date	Oct 13, 2009
Licensed content publisher	American Chemical Society
Licensed content publication	Journal of the American Chemical Society
Licensed content title	The Electronic Influence of Ring Substituents and Ansa Bridges in Zirconocene Complexes as Probed by Infrared Spectroscopic, Electrochemical, and Computational Studies
Licensed content author	Cary E. Zachmanoglou et al.
Licensed content date	Aug 1, 2002
Volume number	124
Issue number	32
Type of Use	Thesis/Dissertation
Requestor type	Not specified
Format	Electronic
Portion	Table/Figure/Chart
Number of Table/Figure/Charts	1
Author of this ACS article	No

Order reference number	
Title of the thesis / dissertation	Fundamental Reactivity Studies and Dinitrogen Activation of Reduced Group 4 Metallocenes
Expected completion date	Jan 2010
Estimated size(pages)	250
Billing Type	Invoice
Billing Address	303A Cornell St Ithaca, NY 14850 United States
Customer reference info	
Total	0.00 USD
Terms and Conditions	

Thesis/Dissertation

ACS / RIGHTSLINK TERMS & CONDITIONS
THESIS/DISSERTATION
INTRODUCTION
The publisher for this copyrighted material is the American Chemical Society. By clicking "accept" in connection with completing this licensing transaction, you agree that the following terms and conditions apply to this transaction (along with the Billing and Payment terms and conditions established by Copyright Clearance Center, Inc. ("CCC"), at the time that you opened your Rightslink account and that are available at any time at <http://myaccount.copyright.com>).
LIMITED LICENSE
Publisher hereby grants to you a non-exclusive license to use this material. Licenses are for one-time use only with a maximum distribution equal to the number that you identified in the licensing process; any form of republication must be completed within 60 days from the date hereof (although copies prepared before then may be distributed thereafter).
GEOGRAPHIC RIGHTS: SCOPE
Licenses may be exercised anywhere in the world.
RESERVATION OF RIGHTS
Publisher reserves all rights not specifically granted in the combination of (i) the license details provided by you and accepted in the course of this licensing transaction, (ii) these terms and conditions and (iii) CCC's Billing and Payment terms and conditions.
PORTION RIGHTS STATEMENT: DISCLAIMER
If you seek to reuse a portion from an ACS publication, it is your responsibility to examine each portion as published to determine whether a credit to, or copyright notice of, a third party owner was published adjacent to the item. You may only obtain permission via Rightslink to use material owned by ACS. Permission to use any material published in an

ACS publication, journal, or article which is reprinted with permission of a third party must be obtained from the third party owner. ACS disclaims any responsibility for any use you make of items owned by third parties without their permission.

REVOCATION

The American Chemical Society reserves the right to revoke a license for any reason, including but not limited to advertising and promotional uses of ACS content, third party usage, and incorrect figure source attribution.

LICENSE CONTINGENT ON PAYMENT

While you may exercise the rights licensed immediately upon issuance of the license at the end of the licensing process for the transaction, provided that you have disclosed complete and accurate details of your proposed use, no license is finally effective unless and until full payment is received from you (by CCC) as provided in CCC's Billing and Payment terms and conditions. If full payment is not received on a timely basis, then any license preliminarily granted shall be deemed automatically revoked and shall be void as if never granted. Further, in the event that you breach any of these terms and conditions or any of CCC's Billing and Payment terms and conditions, the license is automatically revoked and shall be void as if never granted. Use of materials as described in a revoked license, as well as any use of the materials beyond the scope of an unrevoked license, may constitute copyright infringement and publisher reserves the right to take any and all action to protect its copyright in the materials.

COPYRIGHT NOTICE: DISCLAIMER

You must include the following copyright and permission notice in connection with any reproduction of the licensed material: "Reprinted (“Adapted” or “in part”) with permission from REFERENCE CITATION. Copyright YEAR American Chemical Society."

WARRANTIES: NONE

Publisher makes no representations or warranties with respect to the licensed material.

INDEMNITY

You hereby indemnify and agree to hold harmless publisher and CCC, and their respective officers, directors, employees and agents, from and against any and all claims arising out of your use of the licensed material other than as specifically authorized pursuant to this license.

NO TRANSFER OF LICENSE

This license is personal to you or your publisher and may not be sublicensed, assigned, or transferred by you to any other person without publisher's written permission.

NO AMENDMENT EXCEPT IN WRITING

This license may not be amended except in a writing signed by both parties (or, in the case of publisher, by CCC on publisher's behalf).

OBJECTION TO CONTRARY TERMS

Publisher hereby objects to any terms contained in any purchase order, acknowledgment, check endorsement or other writing prepared by you, which terms are inconsistent with these terms and conditions or CCC's Billing and Payment terms and conditions. These terms and conditions, together with CCC's Billing and Payment terms and conditions (which are incorporated herein), comprise the entire agreement between you and publisher (and CCC) concerning this licensing transaction. In the event of any conflict between your obligations established by these terms and conditions and those established by CCC's

Billing and Payment terms and conditions, these terms and conditions shall control.
JURISDICTION
This license transaction shall be governed by and construed in accordance with the laws of the District of Columbia. You hereby agree to submit to the jurisdiction of the courts located in the District of Columbia for purposes of resolving any disputes that may arise in connection with this licensing transaction.
THESES/DISSERTATION TERMS
Publishing implications of electronic publication of theses and dissertation material
Students and their mentors should be aware that posting of theses and dissertation material on the Web prior to submission of material from that thesis or dissertation to an ACS journal may affect publication in that journal. Whether Web posting is considered prior publication may be evaluated on a case-by-case basis by the journal's editor. If an ACS journal editor considers Web posting to be "prior publication", the paper will not be accepted for publication in that journal. If you intend to submit your unpublished paper to ACS for publication, check with the appropriate editor prior to posting your manuscript electronically.
If your paper has already been published by ACS and you want to include the text or portions of the text in your thesis/dissertation in **print or microfilm formats**, please print the ACS copyright credit line on the first page of your article: "Reproduced (or 'Reproduced in part') with permission from [FULL REFERENCE CITATION.] Copyright [YEAR] American Chemical Society." Include appropriate information.
Submission to a Dissertation Distributor: If you plan to submit your thesis to UMI or to another dissertation distributor, you should not include the unpublished ACS paper in your thesis if the thesis will be disseminated electronically, until ACS has published your paper. After publication of the paper by ACS, you may release the entire thesis (**not the individual ACS article by itself**) for electronic dissemination through the distributor; ACS's copyright credit line should be printed on the first page of the ACS paper.
Use on an Intranet: The inclusion of your ACS unpublished or published manuscript is permitted in your thesis in print and microfilm formats. If ACS has published your paper you may include the manuscript in your thesis on an intranet that is not publicly available. Your ACS article cannot be posted electronically on a publicly available medium (i.e. one that is not password protected), such as but not limited to, electronic archives, Internet, library server, etc. The only material from your paper that can be posted on a public electronic medium is the article abstract, figures, and tables, and you may link to the article's DOI or post the article's author-directed URL link provided by ACS. This paragraph does not pertain to the dissertation distributor paragraph above.
Other conditions:
v1.301

Gratis licenses (referencing $0 in the Total field) are free. Please retain this printable license for your reference. No payment is required.

If you would like to pay for this license now, please remit this license along with your payment made payable to "COPYRIGHT CLEARANCE CENTER" otherwise you will be invoiced within 30 days of the license date. Payment should be in the form of a check or money order referencing your account number and this license number